

Synthesis and Pharmacological Characterization of Novel N & O Containing Heterocyclic Compounds as Potential Therapeutic Agents

Dissertation

Zur Erlangung des Doktorgrades

(Dr. rer. nat.)

an der Fakultät für Chemie und Pharmazie

der Universität Regensburg



vorgelegt von

Balakrishna Dulla

aus

Rajam (Indien)

Regensburg 2013

Die Arbeit wurde angeleitet von: Prof. Dr. Oliver Reiser und Prof. Dr. Javed Iqbal

Promotionsgesuch eingereicht am: 20.09.2013

Promotionskolloquium am: 11.10.2013

Prüfungsausschuss: Vorsitz: Prof. Dr. Robert Wolf

1. Gutachter: Prof. Dr. Oliver Reiser

2. Gutachter: Prof. Dr. Javed Iqbal

3. Prüfer: Prof. Dr. Joachim Wegener

Der experimentelle Teil der vorliegenden Arbeit wurde unter der Leitung von Herrn Prof. Dr. Oliver Reiser in der Zeit von July 2009 bis July 2013 am Institut für Organische Chemie der Universität Regensburg und am Institute of Life Sciences, Hyderabad, Indien, angefertigt.

Herrn Prof. Dr. Oliver Reiser möchte und Herrn Prof. Dr. Javed Iqbal ich herzlich für die Überlassung des äußerst interessanten Themas, die anregenden Diskussionen und seine stete Unterstützung während der Durchführung dieser Arbeit danken.

Meinen Eltern

“Dream is not what you see in sleep. It is the thing which does not let you sleep.” Dr. A. P. J. Abdul Kalam

Abstract:

The majority of pharmaceuticals and biologically active agrochemicals are heterocyclic compounds; it represents their immense importance in serving mankind. The purpose of this thesis was to investigate feasibility of making potential biological active novel heterocyclic compounds designed based on lead molecules. The work accomplished in this thesis includes five different chapters to explain importance, achieve simple and fused-ring heteropolycyclic systems having potential pharmacological properties.

The **first chapter** briefly explains importance of heterocyclic compounds and research objective.

The **second chapter** of thesis concerns with target-oriented synthesis to access complex dehydro shikimate analogues containing a pyridine/isoquinoline unit with antitubercular activities with MIC: 4-10 μ M. **Third chapter** deals with study of novel synthetic approach to the one pot synthesis of 2*H*-benzo[*b*] [1,4]oxazines with anti inflammatory activities.

In the **fourth chapter** is presented as a series of functionalized phenyl oxazole derivatives were designed, synthesized and screened *in vitro* for their activities against LSD1 and for effects on viability of cervical and breast cancer cells (IC₅₀: 1-10 nM), and *in vivo* for effects using zebrafish embryos. Indeed it also explains the designing and cost effective route to synthesis of LSD1 inhibitors. Finally, **fifth one** is related to the intramolecular 1,3-dipolar cycloaddition of isovanillin derived *N*-aryl hydroxylamines possessing *ortho*-allylic dipolarophiles affords novel benzo analogues of tricyclic isoxazolidines that can be readily transformed into functionalized lactams, γ -aminoalcohols and oxazepines. The corresponding *N*-unsubstituted hydroxylamines give rise to tetrahydroisoquinolines. Anxiogenic properties of these compounds were tested in zebrafish.

Moreover, in all chapters *in silico* docking studies were performed to predict binding interactions of the most potent scaffolds synthesized and reported inhibitors with the selected targets. At the end of each chapter are drawn a series of conclusions, concerning the investigations performed and the results obtained. *Prof. Dr. Oliver Reiser (advisor), Prof. Dr. Javed Iqbal (advisor), Prof. Joachim Wegener, Prof. Dr. Robert Wolf (Committee Members).*

Table of contents

1. General introduction

1.1 Pharmacological significance of Heterocycle scaffolds	1
1.2 Research envision	3
1.3 References	4

2. Design, synthesis & pharmacological evaluation of dehydroshikimate analogues as potential antitubercular agents

2.1 Introduction	5
2.1.1 Definition of Tuberculosis	5
2.1.2 Pathogenesis of Tuberculosis	5
2.1.3 Overview of TB infection and host defence	5
2.1.4 Epidemiology of Tuberculosis	6
2.1.5 Mechanism of action	7
2.1.6 Classification of antitubercular drugs	8
2.1.7 TB Drug Resistances	8
2.2 Shikimate pathway	9
2.3 Design of new and potential antitubercular agents from known DHS analogues.	10
2.4 Results and discussion	13
2.4.1 Chemistry	13
2.4.2 Pharmacology	18
2.4.3 Molecular docking studies	19
2.5 Summary	22
2.6 Experimental section	22
2.6.1 Chemistry general methods	23
2.6.2 Synthesis	24
2.6.3 Single crystal X-ray data for compound 3e , 5a and 5b	36
2.6.4 Pharmacology methods	37
2.6.5 Docking procedure	39
2.7 References	41

3. Novel synthesis of 2*H*-benzo[*b*][1,4]oxazines *via* sequential C-N and C-O bond formation in single pot and their pharmacological evaluation as anti-inflammatory agents

3.1	Introduction	42
3.2	Literature reports for synthesis of 1,4-benzoxazines	43
3.3	Dearomatisation of arenes	47
3.4	Results and discussion	50
3.4.1	Our approach for synthesis of 2 <i>H</i> -benzo[<i>b</i>][1,4]oxazines <i>via</i> one pot sequential C-N, C-O bond formation	50
3.4.2	The single crystal X-ray study of compound 69	55
3.4.3	Pharmacology	56
3.4.2	Molecular docking studies	57
3.5	Summary	60
3.6	Experimental section	60
3.6.1	Chemistry general methods	60
3.6.2	Synthesis	61
3.6.3	Single crystal X-ray data for compound 69	68
3.6.4	Pharmacology methods	68
3.6.5	Docking procedure	70
3.7	References	71

4. Synthesis & pharmacological evolution of substituted phenyl oxazoles as a novel class of LSD1 inhibitors with anti-proliferative properties

4.1	Introduction	74
4.2	Epigenetics	74
4.2.1	Epigenetic alterations in the genesis of cancer	74
4.2.2	Lysine-specific histone demethylase 1 (LSD1)	76
4.3	Design of novel LSD1 inhibitors	78
4.4	Results and discussion	80
4.4.1	Chemistry	80
4.4.2	Pharmacology	82
4.4.2.1	Cell viability	82

Table of Contents

4.4.2.2 <i>In vitro</i> LSD1 activity	84
4.4.2.3 Zebra fish embryo toxicity and apoptosis	84
4.4.3 Molecular docking studies	87
4.5 Summary	92
4.6 Experimental section	92
4.6.1 Chemistry general methods	92
4.6.2 Synthesis	93
4.6.3 Pharmacology methods	106
4.6.3.1 Evaluation of cell viability	106
4.6.3.2 Evaluation of <i>in vitro</i> LSD1 activity	106
4.6.3.3 Evaluation of <i>in vivo</i> apoptosis and toxicity using zebra fish embryos	107
4.6.4 Molecular Modelling studies	108
4.6.4.1 Docking method	108
4.6.4.2 Molecular Dynamics Simulations Protocols	108
4.7 References	110
5. Design, synthesis & pharmacological evolution of isovanillin derived isoxazolidines as potential vanilloid receptors	
5.1 Introduction	113
5.1.1 Importance for Noval Scaffolds to Treat Pain	113
5.1.2 The Transient Receptor Potential (TRP) Super family	114
5.1.2.1 Physiological functions of TRPV1	116
5.1.2.2 TRPV1 Agonists	116
5.1.2.3 TRPV1 Antagonists	117
5.2 Research objective	118
5.3 Results and discussion	120
5.3.1 Chemistry	120
5.3.2 Pharmacology	125
5.3.2.1 Video for anxiogenic acitivity of compound 23	126
5.3.3 Molecular docking	126

Table of Contents

5.4 Summary	127
5.5 Experimental section	130
5.5.1 Chemistry general methods	131
5.5.2 Synthesis	132
5.5.3 Single crystal X-ray data for compound 16a	132
5.5.4 Pharmacology methods	149
5.5.5 Molecular docking studies	149
5.5.5.1 Homology modelling of catalytic site of rat TRPV1 receptor	150
5.5.5.2 Docking procedure	152
5.6 References	154
6. Appendix	
6.1 NMR Spectra	156
6.2 Curriculam Vitae	253
7. Acknowledgements	258
8. Declaration	260

List of Abbreviations

Abs	absolute	M	molar / metal
AIDS	acquired immunodeficiency syndrome	Me	methyl
aq	aqueous	μ M	micro molar
Bn	benzyl	min	minute(s)
Bz	benzoyl	mp	melting point
Bu	butyl	MS	mass spectroscopy
CCDC	cambridge crystallographic data centre	Mtb	mycobacterium tuberculosis
calcd	calculated	NMR	nuclear magnetic resonance
cat	catalytic	nd	not determined
CI	chemical ionization (MS)	no	number
d	day(s)	NOE	nuclear Overhauser effect
DCM	dichloromethane	Nu	nucleophile
DMAP	4-dimethylaminopyridine	ORTEP	oak ridge thermal ellipsoid plot
DMF	dimethylformamide	PDE4B	cAMP-specific 3',5'-cyclic phosphodiesterase 4B
DMSO	dimethyl sulfoxide	PE	hexanes
<i>dr</i>	diastereomeric ratio	ppm	parts per million
EI	electron impact (MS)	Ph	phenyl
<i>ent</i>	enantiomer	PDB	protein data bank
equiv	equivalent(s)	quant	quantitative
ESI	electrospray ionization (MS)	rac	racemic
Et	ethyl	rt	room temperature
EtOAc	ethyl acetate	<i>t</i>	<i>tert</i>
GC	gas chromatography	SDH	shikimate dehydrogenase
h	hour(s)	TBAF	tetra- <i>n</i> -butylammonium fluoride
HPLC	high-pressure liquid chromatography	TBS	<i>tert</i> -butyldimethylsilyl
HRMS	high resolution mass spectrometry	TBSCl	<i>tert</i> -butyldimethylsilyl chloride
Hz	hertz	TFA	trifluoroacetic acid
HIV	human immunodeficiency virus	THF	tetrahydrofuran
<i>i</i>	<i>iso</i>	TLC	thin layer chromatography
IR	infra red spectroscopy	TNF- α	tumor necrosis factor alpha
LAH	lithium aluminium hydride	Ts	tosyl
LSD1	lysine specific demethylase 1	wt	weight
LORA	low oxygen recovery assay		

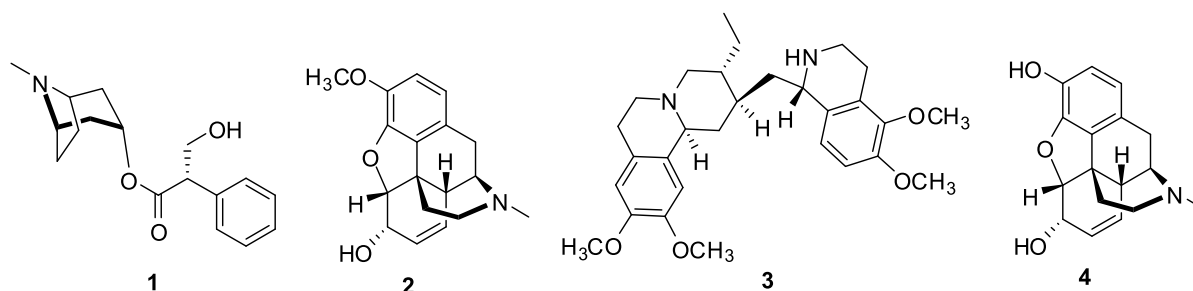
General Introduction

1.1 Pharmacological Significance of Heterocycle Scaffolds

A heterocyclic compound is a cyclic compound that has atoms of at least two different elements as members of its ring(s). Heterocyclic chemistry is the branch of chemistry dealing with synthesis, properties, and applications of heterocycles. The IUPAC recommends the Hantzsch-Widman nomenclature for naming heterocyclic compounds.¹ Heterocycles form by far the largest of the classical divisions of organic chemistry and the majority of pharmaceuticals and biologically active agrochemicals are heterocyclic, as are countless additives and modifiers used in industries as varied as cosmetics, reprography, information storage, and plastics indeed to understanding of life process and to the efforts to improve the quality of life.²

Many natural drugs [5-8]³ such as atropine (1), codeine (2), emetine (3), morphine (4), papaverine (5), procaine (6), quinine (7), theobromine (8), and theophylline (9) are heterocycles. Most of the synthetic drugs such as antipyrine (10), azidothymidine (11), barbiturates (12), chlorpromazine (13), isoniazid (14), diazepam (15), and metronidazole (16) are also heterocycles (Figure 1). Since almost all biological process are chemical in nature and as heterocycles are able to get involved in an extraordinarily wide range of reactions these natural and synthetic heterocyclic compounds can and do participate in chemical reactions in human body.

Synthetic heterocycles have wide spread therapeutic uses such as antibacterial, antifungal, antimycobacterial, trypanocidal, anti-HIV activity, antileishmanial agents, genotoxic, antitubercular, antimalarial, herbicidal, analgesic, anti-inflammatory, muscle relaxants, anticonvulsant, anticancer and lipid peroxidation inhibitor, hypnotics, antidepressant, antitumor, anthelmintic and insecticidal agents.⁴



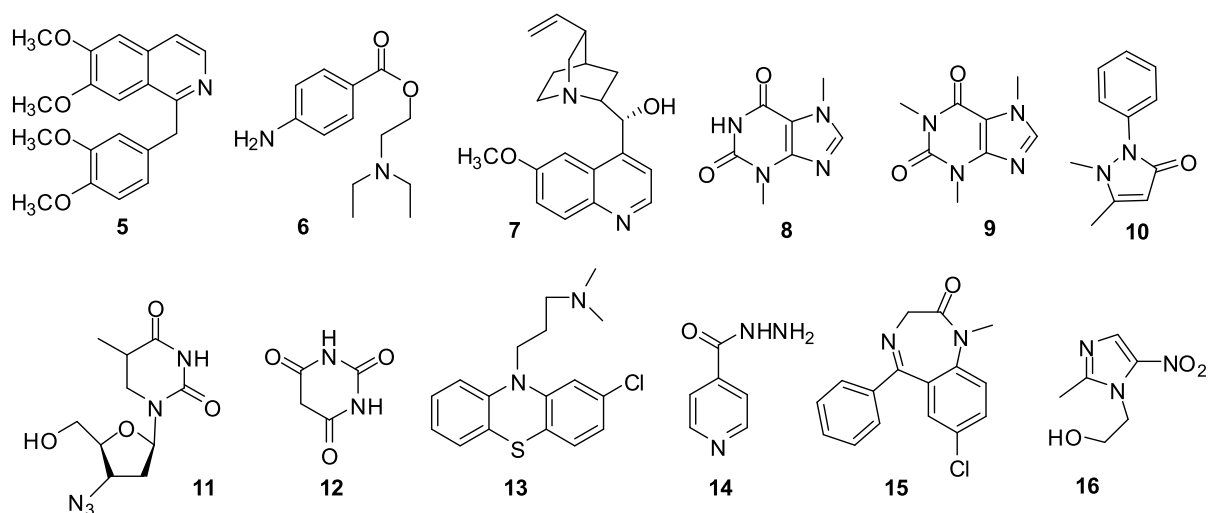


Figure 1: Few natural, synthetic drugs consisting of heterocyclic rings

Prompted by these observations it is clear that heterocycles playing a vital role in serving mankind. But nowadays due to increasing costs of research, development and a simultaneous stagnating number of new chemical entities (NCEs) the entire pharmaceutical industry is facing with the challenge of increasing productivity and innovation. The cause of this innovation deficit is definitively not the biology, because literature precedents showing that 1,000 genes are significantly involved in the emergence and course of disease out of 30000 human genes. Furthermore, because each of these genes is linked to the function of between five and ten proteins, the conclusion is that there might be 5,000 – 10,000 targets for new drugs.³ Hence, the most challenging thing is not only to select drugable targets, but also find corresponding drug-like candidates, substances with specific pharmacokinetic and toxicological properties, that allow them to be developed as a drug.

Even though medicinal chemistry as a scientific discipline has introduced several new techniques to speed up the drug discovery process, such as combinatorial chemistry, microwave-assisted organic synthesis, and high-throughput purification the number of NCEs reaching the market has actually decreased dramatically.⁴ This is probably due to improper selection of drug like molecules.

It has been estimated that the number of possible molecules with a molecular weight of less than 500 Da (Lipinski rule) is 10^{200} , of which only 10^{60} may possess drug-like properties. The issue is therefore the selection of new molecules from this vast universe that have the potential to be biologically active.⁵ The possible options to find biologically active molecules

(drug like candidates) are obtaining hits *via* virtual screening approach (and high-throughput screening) or can be copied from scientific or patent literature. As the main interest of the Laboratory of Medicinal Chemistry lays in the synthesis and biological evaluation of novel heterocycles, we have chosen the later approach of selecting lead molecules of particular target for different diseases from scientific or patent literature and making analogues of that lead molecule without changing pharmacophore responsible for interaction with the specific target to improve potency, selectivity or pharmacokinetic parameters.

In order to improve the hit rate in high-throughput screening campaigns, privileged structures provide an ideal source of lead compounds. A single library based upon privileged substructures⁶ can lead to active compounds in variety of biological assays. Several research groups have utilized these structures in such a manner. For example, Nicolau and co-workers constructed a library based on the benzopyran (**17**) privileged scaffold,⁷ whereas Schultz and co-workers made use of the purine (**18**) scaffold⁸ (Figure 2).

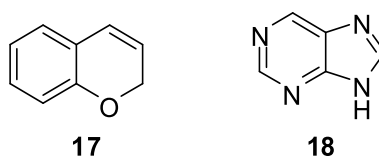


Figure 2: The benzopyran and purine privileged scaffold

1.2 Research Objective

Our interest behind the design of novel heterocyclic compounds based on lead compounds, synthesis and biological evaluation is that all of these compounds are not frequently used (1-hydroxy-2-oxo-1,2-dihydropyridine-4-carboxylicacids (**19a**), 1-hydroxy-2-oxo-1,2-dihydroquinoline-4-carboxylic acids (**19b**), 7-chloro-2,4-dioxo-1,2,3,4,4a,8a-hexahydropyrido [2,3-d]pyrimidine-5-carboxylicacid(**19c**), 1-(3-(4-methyl-5-(2-(methyl thio)ethyl)oxazol-2-yl)phenyl) guanidine (**20**), 7-hydroxy-8-methoxy-1-phenyl-5,5a,6,10b-tetrahydro-1*H*-indeno[1,2-*e*][1,4]oxazepin-2(3*H*)-one (**21**) and 2*H*-Benzo[*b*][1,4]oxazines (**22**) and are totally absent in commercial compound libraries, and having similar pharmacological features as lead compounds, prompted us to elaborate this type of medicinal chemistry approach and to synthesize different novel heterocyclic scaffolds having potential biological activities (Figure 3).

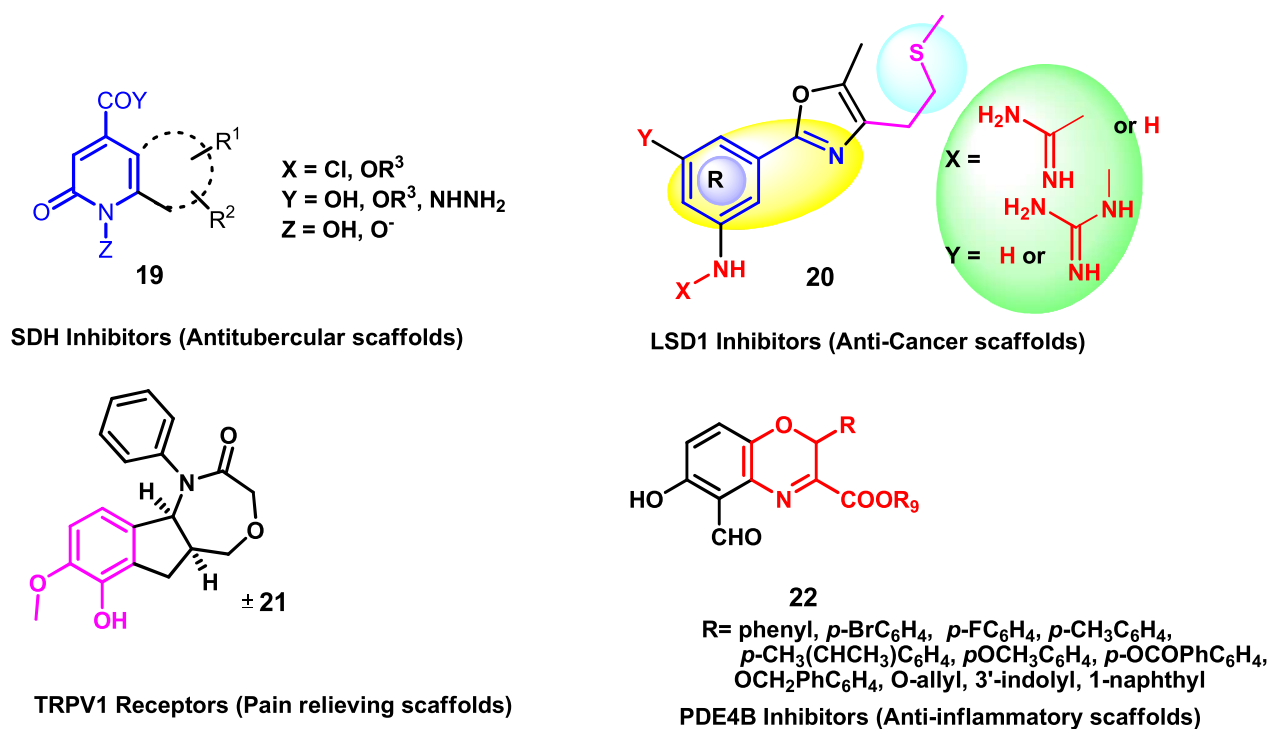


Figure 3: Generalized structures of synthesized novel heterocyclic scaffolds. Highlighted areas of the above novel scaffolds were taken from lead molecules.

References:

1. Panico, R.; Powell, W. H.; Richer, J. C. IUPAC/Blackwell Science. **1993**, *40*, ISBN 0-632-03488-2.
2. Dua, R.; Shrivastava, S.; Sonwane, S. K.; Srivastava, S. K. *Advances in Biological Research*. **2011**, *5*, 120.
3. a) Drews, J. *Science*, **2000**, *287*, 1960. b) Wess, G.; Urmann, M.; Sickenberger, B. *Angew. Chem. Int. Ed.* **2001**, *40*, 3341.
4. Lombardino, J. G.; Lowe, J. A. *Nat. Rev. Drug Discov.* **2004**, *3*, 853.
5. Kolb, H. C.; Finn, M. G.; Sharpless, K. B. *Angew. Chem. Int. Ed.* **2001**, *40*, 2004.
6. Evans, B. E.; Rittle, K. E.; Bock, M. G.; Dipardo, R. M.; Freidinger, R. M.; Whitter, W. L.; Lundell, G. F.; Veber, D. F.; Anderson, P. S.; Chang, R. S. L.; Lotti, V. J.; Cerino, D. J.; Chen, T. B.; Kling, P. J.; Kunkel, K. A.; Springer, J. P.; Hirshfield, J. *J. Med. Chem.* **1988**, *31*, 2235.
7. Nicolaou, K. C.; Pfefferkorn, J. A.; Roecker, A. J.; Cao, G. Q.; Barluenga, S.; Mitchell, H. J. *J. Am. Chem. Soc.* **2000**, *122*, 9939.
8. Ding, S.; Gray, N. S.; Ding, Q.; Schultz, P. G. *Tetrahedron Lett.* **2001**, *42*, 8751.

2. Design, synthesis & pharmacological evolution of dehydroshikimate analogues as potential antitubercular agents

1 Introduction:

1.1 Definition:

Tuberculosis is an infectious disease characterized by the growth of nodules (tubercles) in the tissues, especially in the lungs. *Bacillus Mycobacterium tuberculosis* is the etiological agent of TB belonging to the genus *Mycobacterium*, which is presumed to have originated more than 150 million years ago. Tuberculosis (TB) is one of the leading causes of death due to a single infectious organism in the world. It typically affects the lungs (pulmonary TB) but can affect other sites as well (extrapulmonary TB).¹ The probability of developing TB is much higher among people infected with the Human Immunodeficiency Virus (HIV).

1.2 Pathogenesis of tuberculosis

The primary mode of transmission of *M. tuberculosis* (Mtb) is through the air in an aerosolized form, most commonly when pulmonary TB bacteria are expelled via a cough or sneeze from people who are sick with TB.² The infective droplet nuclei trapped in nasopharynx and the upper respiratory tract enters the alveoli, whereby they are ingested by the alveolar macrophages through the process of phagocytosis. In this early stage of the infection, Mtb is able to replicate within non-activated macrophages.³ However the body subsequently mounts a cell-mediated immune response to the growing mycobacterium via the activation of macrophages with interferon- γ which controls Mtb infection, but not wiped out the bacteria from the host.^{3, 4} In fact, the remaining mycobacterium will enter into the non-replicating persistence phase (latent stage of the infection). Mtb can reside in alveolar macrophages, avoiding the host immune response for an indefinite period of time. Such latent mycobacterium can get activated anytime later, especially when the host has immune deficiency.

1.3 Overview of TB infection and host defence:

There are three potential outcomes of infection of the human host in *M. tuberculosis*.

- a) The frequency of spontaneous healing is unknown, but is assumed to be rare.
- b) Disease progression immediately after infection in the immunocompromised host.

c) In the majority of cases, mycobacteria are initially contained and the disease progresses later due to reactivation.

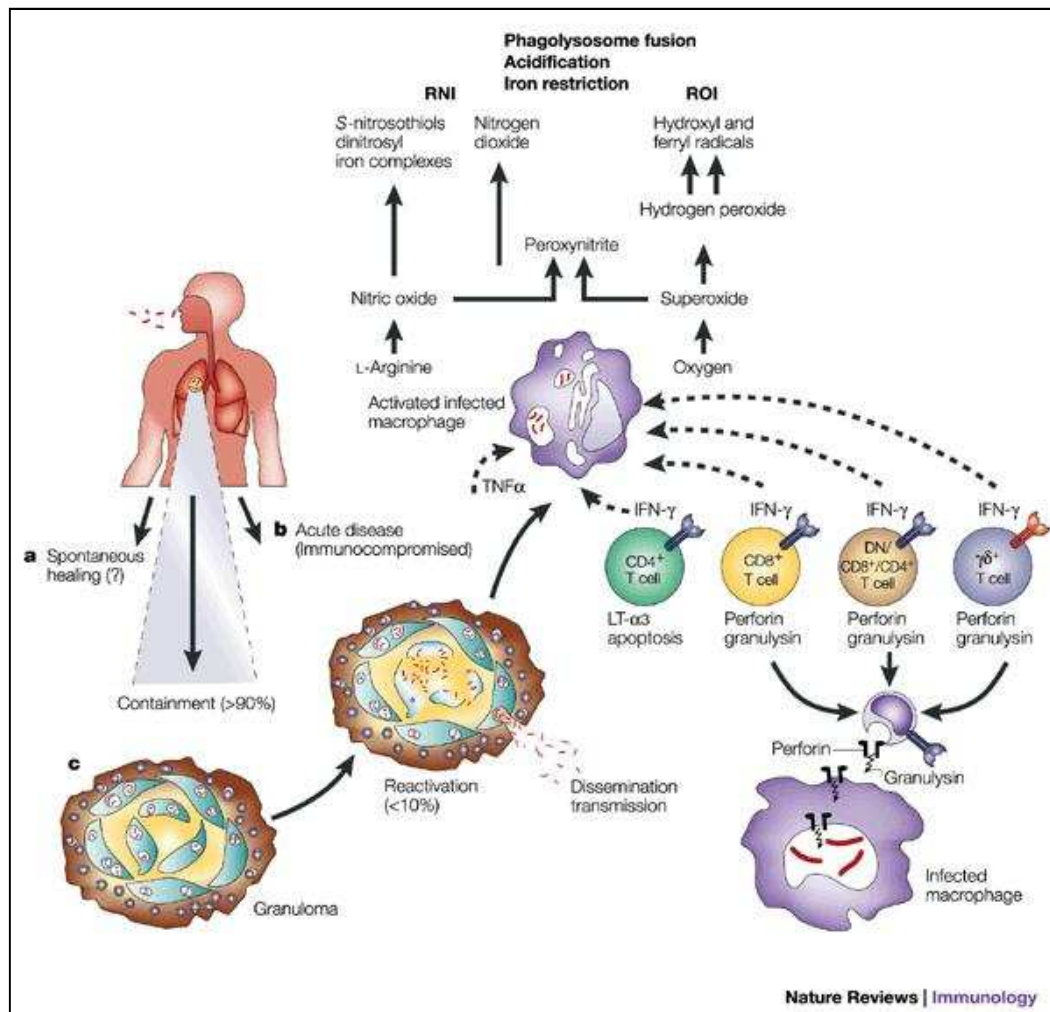


Figure 1: Overview of TB infection and host defence.

The granuloma is the major site of infection, which develops from infected macrophages and becomes surrounded by lymphocytes. Effector T cells (CD4⁺CD8⁺ T cells, and double-negative or CD4/CD8 single-positive T cells that recognize antigen presented by CD1) and macrophages participate in the control of TB. Crucial macrophage activators interferon- γ (IFN- γ) and tumor-necrosis factor- α (TNF- α) are produced by T cell and macrophages respectively. Macrophage activation permits phagosomal maturation and the production of antimicrobial molecules such as reactive nitrogen intermediates (RNI) and reactive oxygen intermediates (ROI). Extracted from *Nature Reviews Immunology* 1, 20-30 (October 2001) with licence.

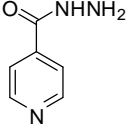
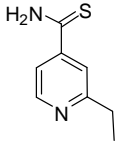
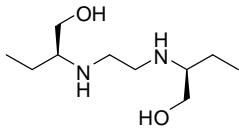
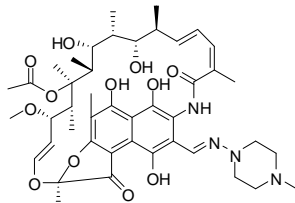
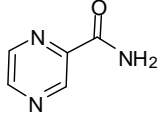
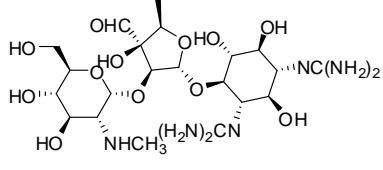
1.4 Epidemiology of tuberculosis

The burden of disease caused by TB can be measured in terms of incidence, prevalence, and mortality. Globally, the absolute number of incident TB cases per year has been falling since 2006, if these trends are sustained; the MDG (Millennium Development Goals) target that TB incidence should be falling by 2015 will be achieved.

1.5 Structure and Mechanism of action of anti tubercular drugs

The available chemotherapies for *M. tuberculosis* are mainly relies on drugs which inhibit bacterial metabolism with a special significance on inhibitors of the cell wall synthesis.

Table 1: Example of anti TB drugs and their mode of action

Drug	Drug mechanism of action
Isoniazid (INH) (1952) 	Inhibition of mycolic acid biosynthesis and other multiple effects on DNA, lipids, carbohydrates and NAD metabolism
Ethionamide (ETH) (1956) 	Inhibition of mycolic acid biosynthesis
Ethambutol (EMB) (1961) 	Inhibition of cell wall arabinogalactan (AG) biosynthesis
Rifampicin (RIF) (1966) 	Inhibition of transcription
Pyrazinamide (PYR) (1952) 	Acidification of cytoplasm and de-energising the membrane
Streptomycin (STREP) (1944) 	Inhibition of protein synthesis

The currently available first and second line TB drugs can be grouped as cell wall

inhibitors (isoniazid (INH), ethambutol, ethionamide), nucleic acid synthesis inhibitors (rifampicin (RIF), quinolones), protein synthesis inhibitors (streptomycin, kanamycin) and inhibitors of membrane energy metabolism (pyrazinamide).

1.6 Classification of antitubercular drugs:

Tuberculosis treatment includes three basic concepts which are as follows: (1) Regimens must contain multiple drugs to which the organism is susceptible. (2) Drugs must be taken regularly. (3) Drug therapy must continue for a sufficient time. Traditionally, antituberculosis drugs are classified as first line drugs are superior in efficacy and possess an acceptable degree of toxicity. If the *M. tuberculosis* organisms are resistant to the first line drugs, second-line drugs will be preferred which are more toxic and less effective and they are indicated only agents.

Table 2: Examples of 1st line and 2nd line drugs with characteristics

	Characteristics	Drugs
First line drugs (Essential anti TB drugs)	High anti TB effect, acceptable degree of toxicity, used routinely	Isoniazid, Ethambutol, Rifampicin, Pyrazinamide, Streptomycin
Second line drugs (Reserved anti TB drugs)	Low anti TB effect, high degree of toxicity, used in special circumstances	PAS, Amikacin, Capreomycin, Ethionamide, Kanamycin, Cycloserine

The common side effects to these antituberculosis drugs include hepatitis, cutaneous reactions, gastrointestinal intolerance, haematological reactions and renal failure which must be adverse effects must be recognised early, to reduce associated morbidity and mortality.

1.3 TB Drug resistance

This disease is complicated by the human immunodeficiency virus (HIV), TB turns out to be most opportunistic co-infection which is growing at an alarming rate with the increase of world human population.^{5,6} The disease poses a major threat to the human life with the recent emergence of multidrug-resistant (MDR) and extensively drug resistant (XDR)-TB. Because of its increasing prevalence MDR-TB is now subdivided into 'basic' MDR-TB, with

resistance only to rifampicin and isoniazid, and 'MDR-TB-plus', with a similar resistance pattern but with resistance to one or more additional first- and/or second-line drugs. The most effective drug regimen is endorsed by the WHO and is called Directly Observed Treatment, Short-course (DOTS), developed to fully supervise those patients deemed high-risk for non-drug adherence.⁷ Since this disease poses a major threat to the human life it requires an immediate attention for the identification and development of novel antitubercular drugs.⁸

2. Shikimate pathway:

The shikimate pathway plays a pivotal role in the biosynthesis of precursors for aromatic amino acids, vitamins, quinones, and a variety of other aromatic compounds in bacteria, plants, fungi, and apicomplexa parasites.⁹ The end product of the shikimate pathway is chorismate, which is converted to precursors of a host of secondary metabolites essential for the survival of these organisms. (Figure 2) Shikimate is the first intermediate identified, isolated from fruit of *Illicium religiosum* (commonly known as the Japanese star anise, shikimi) which gave the name to this pathway.¹⁰

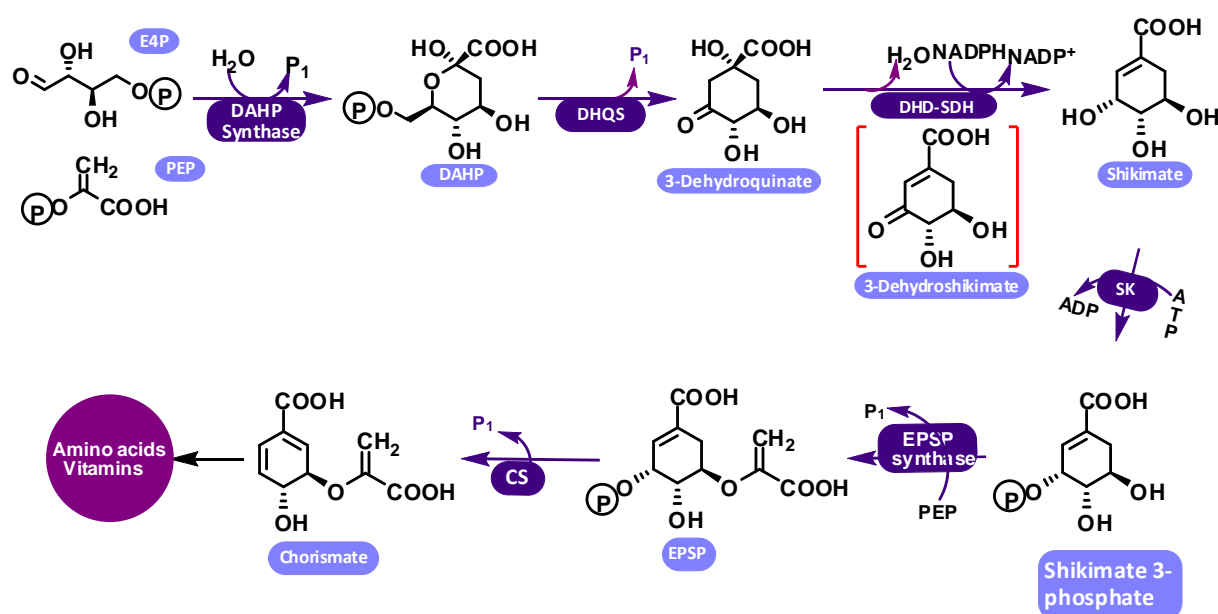


Figure 2: Shikimate pathway ² (self drawn)

1st step: The shikimate pathway begins with the aldol condensation of two phosphorylated 'household metabolites', phosphoenolpyruvate (PEP) and D-erythrose 4-phosphate (E4P) catalyzed by 3-deoxy-D-arabino-heptulosonate-7-phosphate (DAHP) synthase. Based on sequence similarity, DAHP synthases are classified into two types. Type

II DAHP synthases are found in plants and some microbes (e.g., *Mycobacterium tuberculosis*).

2nd step: 3-Deoxy-D-arabino-heptulosonate-7-phosphate undergoes five consecutive chemical reactions: alcohol oxidation, β -elimination of inorganic phosphate, carbonyl reduction, ring opening, and intramolecular aldol condensation performed by 3-dehydro quinate synthase (DHQS) in one active site using a divalent cation (e.g., Co^{2+}) and NAD^+ cofactors to form 3-dehydro quinate.

3rd step: The third enzymatic reaction include the dehydration of 3-dehydroquinate to 3-dehydroshikimate to introduce the first double bond by 3-dehydro dehydratase (DHD).

4th step: Shikimate dehydrogenase plays an important role in catalyzing the fourth step in the shikimate pathway involving the reversible conversion of 3-dehydro shikimate (DHS) and NADPH to yield shikimate, a 3,4,5-trihydroxycyclohexene-1-carboxylic acid and NADP^+ .

5th step: Shikimate kinase (SK) phosphorylates the C3 hydroxyl group of Shikimate using ATP as a co substrate to yield shikimate 3-phosphate.

6th step: 5-Enolpyruvylshikimate-3-phosphate synthase (EPSP) catalyzes the penultimate step of the shikimate pathway, the addition of enolpyruvyl moiety of phospho enolpyruvate (PEP) to the 5-hydroxyl group of shikimate-3-phosphate.

7th step: The last step of the synthesis of aromatic amino acids, vitamins and quinones catalyzed by chorismate synthase (CS) involves a 1,4-trans elimination of phosphoric acid from 5-enolpyruvylshikimate 3-phosphate introducing the second double bond in the ring to produce chorismate.¹¹

Importantly the shikimate pathway has been shown to be essential for the viability of *Mycobacterium tuberculosis*.¹² The absence of the shikimate pathway in humans and its indispensable importance in algae, higher plants, bacteria, and fungi makes it a potential target for the development of novel antitubercular agents.¹³

3. Design of new and potential antitubercular agents from known DHS analogues:

Shikimate dehydrogenase was chosen as the target since it occurs early in the pathway and also due to easy accessibility of its synthetic analogue.

- a. In 1961, D. Balinsky. *et al.* reported studies on shikimate dehydrogenase inhibition with a variety of substituted phenols. They disclosed that both dehydroshikimic acid (**1**)

and shikimic acid (**2**) (figure 3) bind to the enzyme by means of the $-\text{COOH}$ and OH groups at **C4**, **C5** respectively. ¹⁴



Figure 3: Structures of dehydro shikimic acid, shikimic acid

b. In 1972, A. C Baillie. *et al.* reported active site directed inhibitors based on D. Balinsky. *et al* results. They have designed a novel dehydroshikimate analogue 1, 6-dihydroxy-2-oxoinicotinic acid (**3**; R =H) [a tautomeric form of citrazinic acid 1-oxide (**4**)] (figure 4) in which the amide carbonyl should be less susceptible to enzyme reduction than the keto carbonyl of the natural substrate.

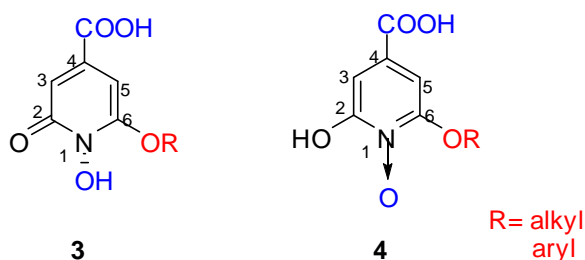
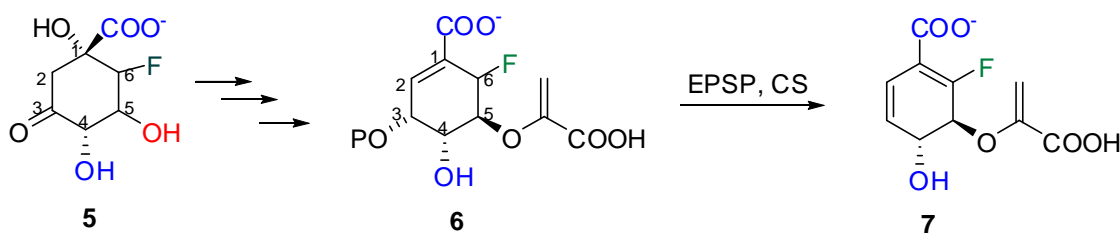


Figure 4: Structures of dehydro shikimate analogues

They found that a hydrophobic area exists near the active site of the enzyme, since a series of 6-O-alkyl derivatives of compound **3** bound almost similarly like the parent compound **1**. Maximum binding was obtained with the isopropyl ether. ¹⁵

c. In 1972, Floss *et al.* demonstrated that the substituent on C-6 of 3-dehydro quinate (**5**) are not directly involved in any reaction until chorismate synthase step. This was further supported by S. Bornemann. *et al.* in 1995,



EPSP: 5-Enolpyruvylshikimate-3-phosphate synthase; CS: chorismate synthase

Figure 5: Synthesis of 6-fluoro chorismic acid

through enzymatic conversion of 6 α -fluoro-5-enolpyruvylshikimate-3-phosphate (**6**) to 6-fluorochorismic acid (**7**) at 0.3% rate with the normal substrate.¹⁶

- d. In 1988, A. B. Chris. *et al.* discussed about the specificity of shikimate dehydrogenase towards analogues of 3-dehydroshikimic acid. Treatment of (**8**) with DHS (Shikimate dehydrogenase) and NADPH rapidly gave (3R, 4S)-3, 4-dihydroxycyclohex-1-enecarboxylic acid (**9**).¹⁷

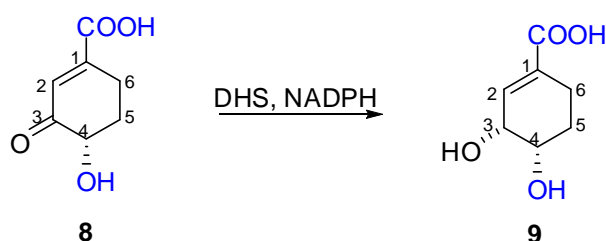


Figure 6: Synthesis of (3R, 4S)-3, 4-dihydroxycyclohex-1-enecarboxylic acid

Moreover, the results indicate that for the C-5 hydroxyl group the apparent binding energy (ΔG_{app}) is 1.8 kJ mol^{-1} , whereas for the C-4 hydroxyl group $\Delta G_{app} = 29 \text{ kJ mol}^{-1}$. This demonstrates that removal of the C-5 hydroxyl group has little effect on specificity, but removal of the C-4 hydroxyl group is very significant. The observed loss of specificity on removal of the C-4 hydroxyl group suggests removal of a hydrogen bonding interaction between substrate and a charged group at the enzyme active site.

Prompted by these observations and due to our continuing interest in the identification of novel small molecules as potential antitubercular agents we became interested in evaluating 1, 6-dihydroxy-2-oxoinicotinic acid (**A**) and a series of pyridine-4-carboxylic acid derivatives (**B** and **C**, Figure 7) for their potential antitubercular properties.

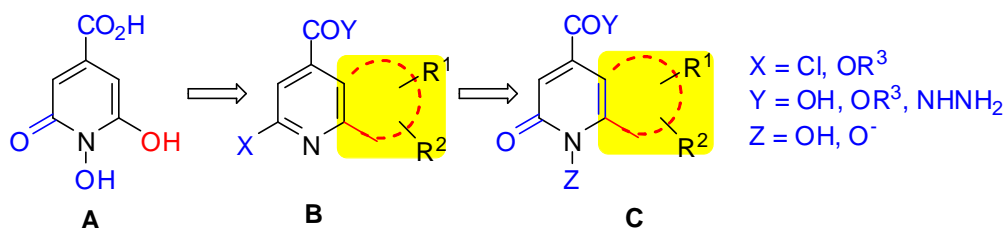


Figure 7: Design pyridine-4-carboxylic acid derivatives from a known DHS analogue **A**

The target compounds were achieved by introducing a fused ring with or without any substituent at C-5 and C-6 positions into the 2-pyridone moiety of **A** and/or converting the carboxylate group into an ester or carbohydrazide moiety (Figure 7).

4. Results and discussion:

4.1 Chemistry: The synthesis of our target molecules based on **B** and **C** primarily consisting of three different classes of protocols known in literature.

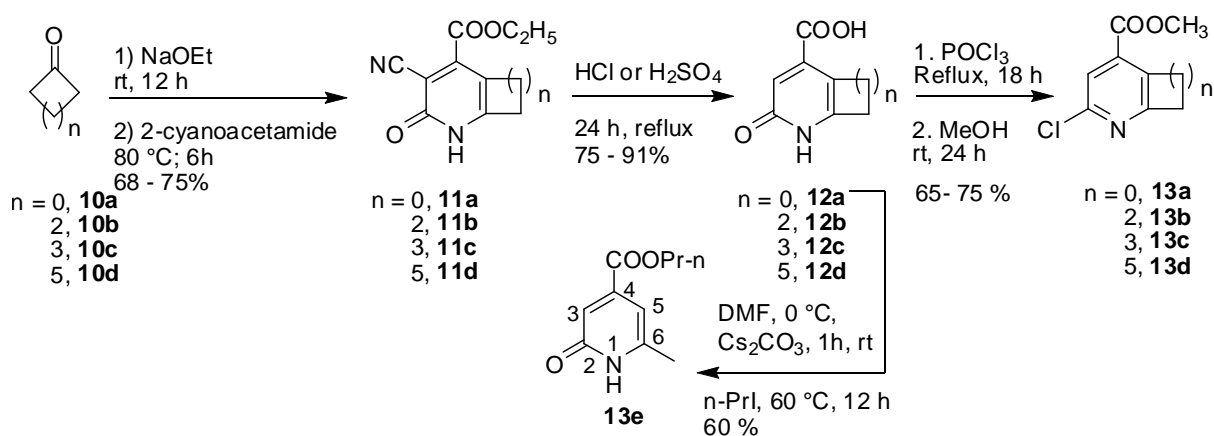
4.1.1. Synthesis of substituted 3-cyano-2-pyridone derivatives from appropriate methyl ketones followed by converting them into corresponding 1-hydroxy-2-pyridone derivatives *via* 5 steps.

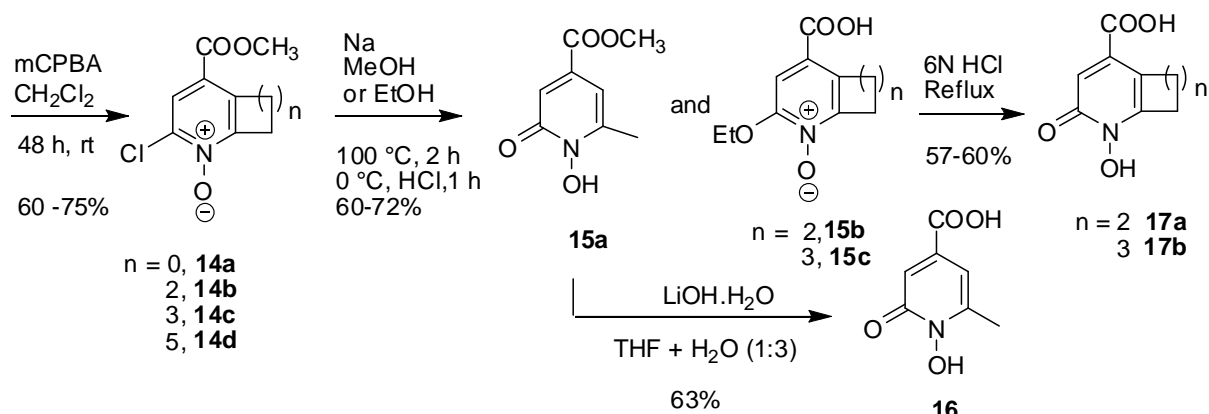
4.1.2 Synthesis of 2-oxo-1, 2-dihydroquinoline-4-carboxylic acids from appropriate indoline-2, 3-diones were converted to the corresponding 1-hydroxy-2-oxo-1, 2-dihydroquinoline-4-carboxylic acid derivatives in 3 steps.

4.1.3 Construction of 1-hydroxy 2-pyridone 4-carboxylic acid ring fused with different substituted uracil derivatives in 5 steps.

4.1.1 Synthesis of 1-hydroxy-2-oxo-1,2-dihydropyridine-4-carboxylic acid derivatives

The 3-cyano-2-pyridone derivatives prepared by treating appropriate ketones with cyanoacetamide in the presence of NaOEt, were converted to 2-pyridonecarboxylic acids and subsequently to 2-chloro ester derivatives (Scheme 1).¹⁸ The acid (**12a**) was also converted to the corresponding ester (**13e**) (synthesized to explore chemistry at C5-C6 double bond like cyclopropanation, epoxidation, which was however unsuccessful) as shown in Scheme 1.¹⁹ Treating the compounds (**13a-d**) with *m*-CPBA provided the corresponding *N*-oxides **14a-d** that were converted to 1-hydroxy-2-pyridone derivative **15a** or 2-ethoxy pyridine *N*-oxides **15b-c** depending on the reaction conditions employed.^{20, 21} Finally, the ester **15a** was hydrolyzed to the corresponding acid **16a** and the acids **15b-c** was transformed into the corresponding 1-hydroxy 2-pyridone derivatives **17a-b**.^{22, 23}

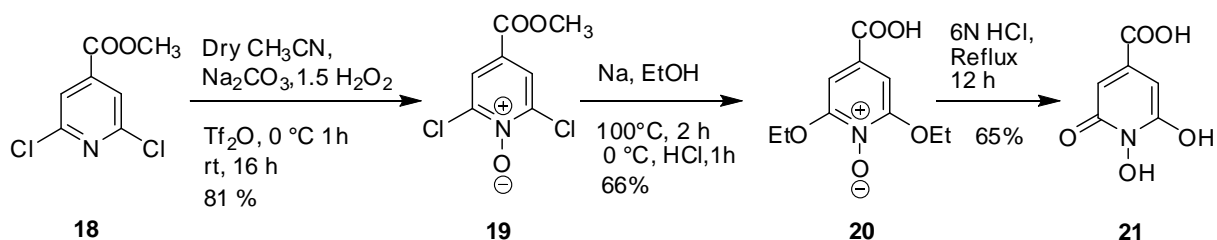




Scheme 1. Synthesis of 1-Hydroxy-2-oxo-1,2-dihydropyridine-4-carboxylic acid derivatives (B)

The dehydro shikimate analogue **A** (or **21**) was prepared according to a known method as shown in Scheme 2. Initially the N-oxide **19** was synthesized from **18** using *m*-CPBA, DCM at rt for 36 h affords 40% of yields. Similarly substitution of chlorides in **19** with NaOEt (commercially available) affording **20** in 35% yield according to the literature protocols²² Yields

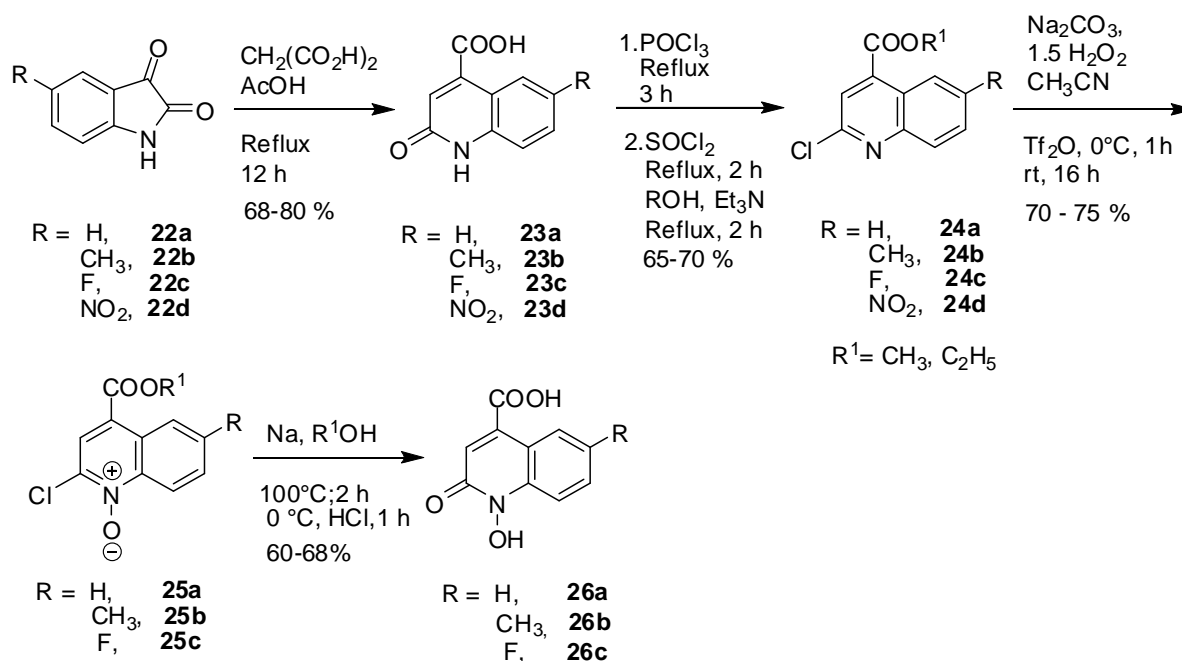
however did not exceed 30% even after 5 times repetition of experiments using above protocols which could be improved to 66% by following the reaction protocol of Zhu *et al.*²⁴



Scheme 2. Synthesis of 1,6-dihydroxy-2-oxoisonicotinic acid **A** (**11**).²²

4.1.2 Synthesis of 1-hydroxy-2-oxo-1,2-dihydroquinoline-4-carboxylic acid derivatives

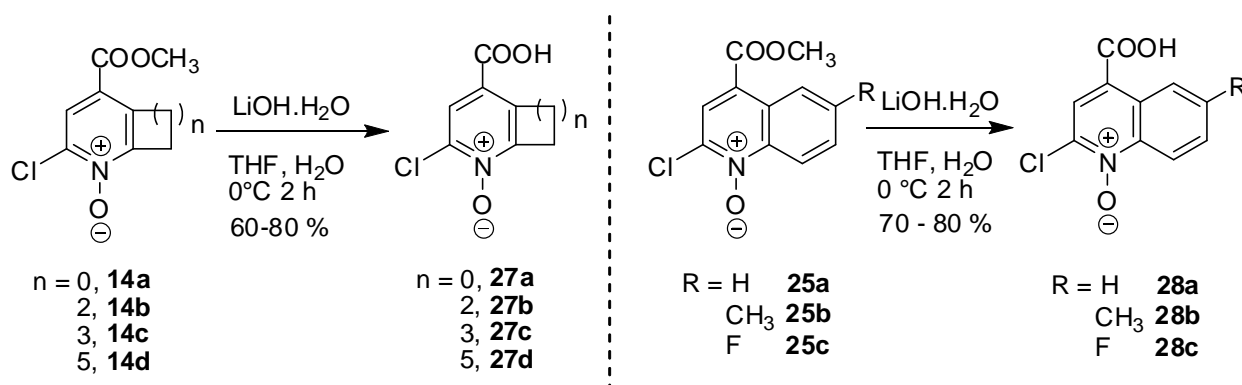
The synthesis of other target molecules based on **B** is shown in Scheme 3. The 2-oxo-1,2-dihydroquinoline-4-carboxylic acid derivatives (**23a-d**)^{25a} prepared from appropriate indoline-2,3-diones (**22a-d**) were converted to the corresponding 2-chloro ester derivatives (**24a-d**).^{25b} Treating these compounds with H_2O_2 provided the corresponding N-oxides (**25a-c**) that were converted to the desired 1-hydroxy-2-oxo-1,2-dihydroquinoline-4-carboxylic acid derivatives (**26a-c**).²²



Scheme 3. Synthesis of 1-hydroxy-2-oxo-1, 2-dihydroquinoline-4-carboxylic acid derivatives

Synthesis of 2-chloro acid derivatives

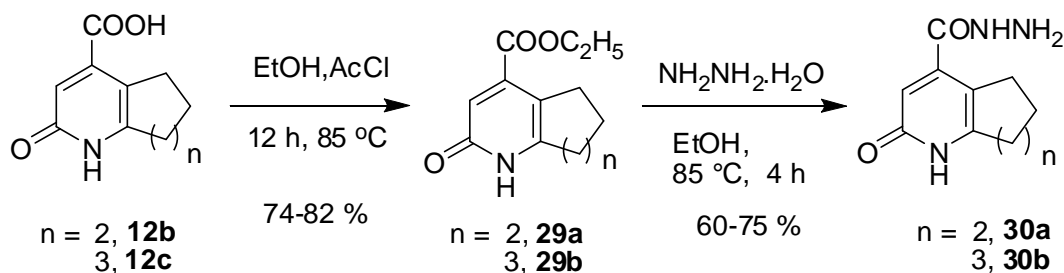
2-chloro acid derivatives (**27a-d**), (**28a-c**) were synthesized from precursors **14a-d**, **25a-c** respectively as shown in Scheme 4. The reactions were carried out in the presence of $\text{LiOH}\cdot\text{H}_2\text{O}$ in these cases.²³



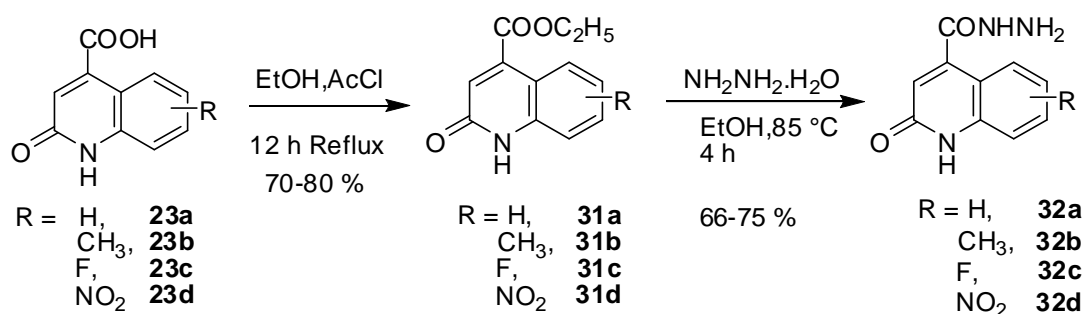
Scheme 4. Synthesis of 2-chloro acid derivatives (**16**)

Synthesis of 2-oxo-1, 2-dihydropyridine/quinoline-4-carbohydrazide derivatives:

The ethyl-2-oxo-1, 2-dihydropyridine-4-carboxylate derivatives (**29a-c** and **31a-d**)²⁶ were prepared from the appropriate 2-oxo-1, 2-dihydroquinoline-4-carboxylic acid derivatives (**12b-d** and **23a-d**). The resulting ethyl esters were treated with hydrazine hydrate to afford 2-oxo-1, 2-dihydropyridine-4-carbohydrazide derivatives (**30a-b** and **32a-d**).²⁷



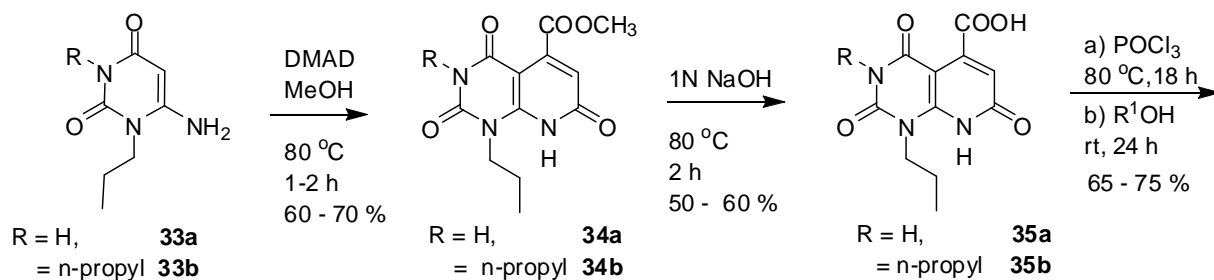
Scheme 5. Synthesis of 2-oxo-1, 2-dihydroquinoline-4-carbohydrazide derivatives

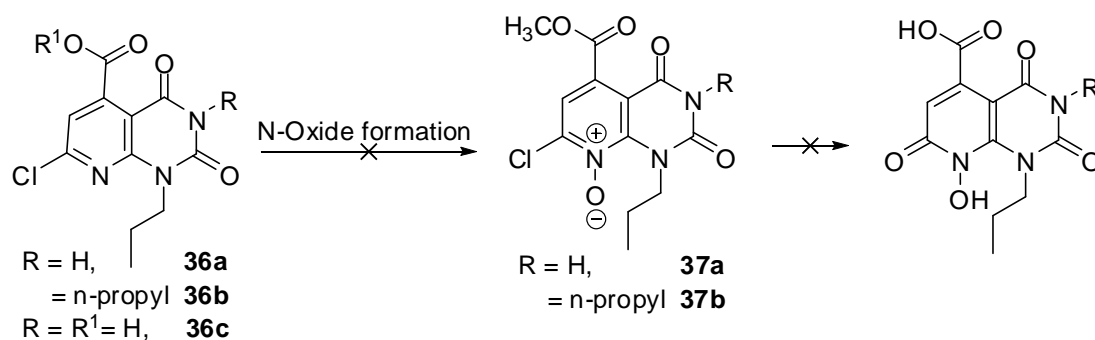


Scheme 6. Synthesis of 2-oxo-1, 2-dihydropyridine-4-carbohydrazide derivatives

4.1.3 Synthesis of 7-chloro-2, 4-dioxo-1-propyl-1, 2, 3, 4-tetrahydropyrido [2, 3-d] pyrimidine derivatives

The 4-methylcarboxylate-2-pyridone derivatives (**34a**, **34b**) were synthesized by refluxing uracil derivatives with dimethyl acetylenedicarboxylate in MeOH²⁸ which were on hydrolysis converted to 2-pyridone carboxylic acids (**35a**, **35b**) and subsequently to 2-chloro ester derivatives (**36a**, **36b**) (Scheme 7). Treating the compounds **36a**, **36b** with several per acids did not provide the corresponding *N*-oxides. Hydrolysis of **36a** with LiOH·H₂O provided the compound **36c**.





Scheme 7. Synthesis of 7-chloro-2,4-dioxo-1-propyl-1,2,3,4-tetrahydropyrido[2,3-*d*]pyrimidine derivatives.

ORTEP diagrams:

While all the compounds synthesized were characterized by spectral (NMR, IR and MS) data the molecular structure of few representative compounds for example, **13e**, **15a**, and **15b** were confirmed unambiguously by single crystal X-ray diffraction (Fig 8, 9 and 10).

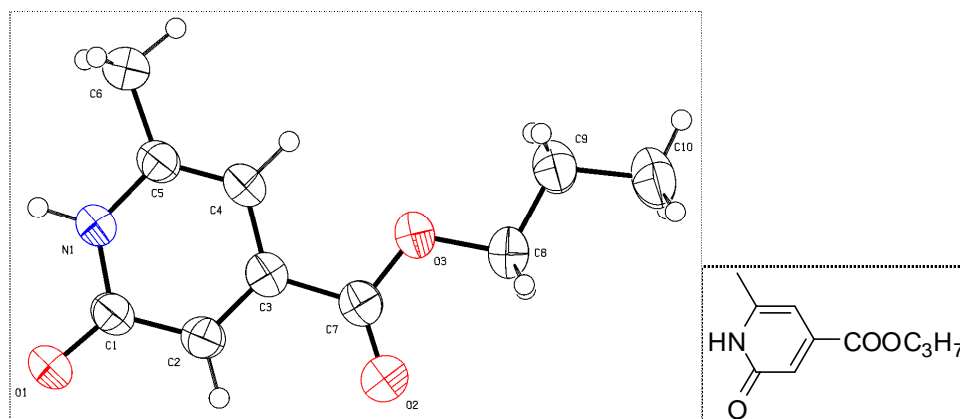


Figure 8: ORTEP representation of the **13e** ($C_{10}H_{13}NO_3$). (Thermal ellipsoids are drawn at 50% probability level).

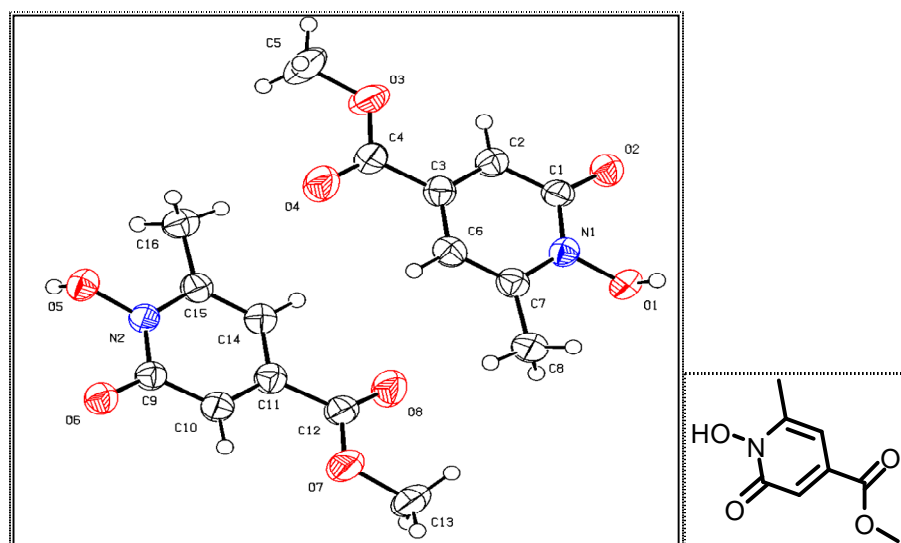


Figure 9: ORTEP representation of the **15a** (C₈H₉NO₄). (Thermal ellipsoids are drawn at 50% probability level).

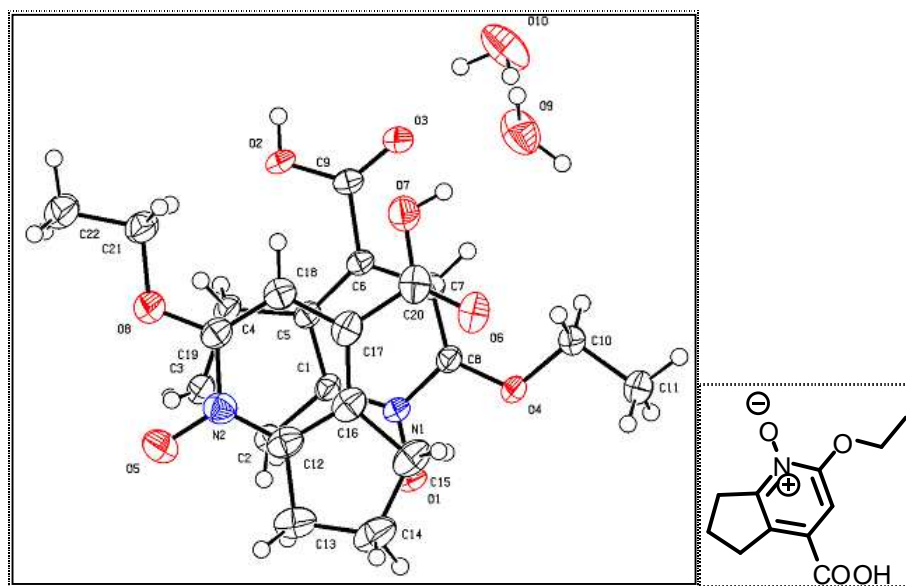


Figure 10: ORTEP representation of the **15b** (C₁₁H₁₃NO₄·H₂O). (Thermal ellipsoids are drawn at 50% probability level).

4.2 Pharmacology:

Pharmacological testing was performed at the Institute for Tuberculosis Research, College of Pharmacy, in the group of Prof. Scott G. Franzblau, University of Illinois at Chicago.

All the compounds synthesized initially were tested for their activity against *M. tuberculosis* H₃₇Rv, which was determined by using fluorescence readout in the Microplate Alamar Blue Assay (MABA).²⁹ The compounds found promising in this assay were then tested for their activity against non-replicating *M. tuberculosis*, which was determined by using the Low-Oxygen Recovery Assay (LORA).³⁰ The well-known agents such as rifampicin (asemisynthetic bactericidal antibiotic drug), isoniazide (or isonicotinylhydrazine, an antitubercular agent) and moxifloxacin (a fluoroquinolone antibacterial agent) were used as reference compounds in these assays. Finally, the cytotoxicity assay³¹ of the most active compound was carried out using Vero cells.

Among all the compounds tested quinoline-1-oxides i.e. **25a**, **25b**, and **25c** were found to be promising in MABA assay (Table 3). Indeed, compound **25b** showed the lowest MIC i.e. 4.33 µg/mL among them. This compound also showed the lowest MIC i.e. 3.65 µg/mL in LORA assay (Table 3). Finally, this compound showed IC₅₀ value < 8.0 µg/mL in the cytotoxicity assay in Vero cells. Among the other compounds **12a-d**, **16**, **15a-c**, and **23a-d** showed MIC ~ 50 µg/mL whereas rest of the compounds showed MIC ~ 100 µg/mL (see

page 35) when tested in MABA assay. Notably, MIC of the known inhibitor of shikimate dehydrogenase **21**²² and citrazinic acid were found to be >50 and 100 µg /mL, respectively, in the same assay.

Table 3. *In vitro* assay results of selected compounds.

Compound	MIC (µg/mL) ^{a,c}		IC ₅₀ (µg/mL) ^b ,
	MABA	LORA	Vero Cell
25a	9.2	7.3	n.d.
25b	4.33	3.65	< 8.0 (96%)
25c	10.9	13.1	n.d.
21	> 50	n.d.	n.d.
Citrazinic acid	> 100	n.d.	n.d.
Rifampicin	0.05	1.47	n.d.
Isoniazide	0.33	> 128 (84%)	n.d.
Moxifloxacin	0.39	15.93	n.d.

n.d. = not determined. ^a MIC value obtained was defined as the lowest concentration inhibiting recovery of luciferase signal, greater or equal to 90% relative to bacteria-only controls. ^b IC₅₀ represent the concentration of compound that causes a 50% growth inhibition to untreated cells using the MABA assay.

Nevertheless, the compound **25b** though found to be less effective than the reference compounds employed in MABA assay but was comparable or better than rifampicin, isoniazide and moxifloxacin in LORA assay. Overall, the compound **25b** appeared as attractive new chemical entity due to its interesting and novel structural features.

4.2 Molecular docking studies

Molecular docking studies were done by K. Ravi Kumar at Institute of Life Sciences, India. To understand the nature of interactions of these molecules with the shikimate dehydrogenase protein of Mycobacterium tuberculosis (SDHmt), *in silico* docking studies were performed using compounds **25a–c** along with the known inhibitor of shikimate dehydrogenase ²² **21**. An SDHmt protein homology model was developed and used for this purpose. The dock scores obtained after docking these molecules into the SDHmt protein are summarized in Table 4. It is evident from Table 4 that in compared to compound **21** these molecules (**25a–c**) bind better with SDHmt the compound **25b** being the best among them. The ligand interaction and binding pose of compound **25a–c** with SDHmt protein is shown in

Figs. 12–14. All these molecules were found to interact with the SDHmt protein through H-bonding. For example, compound **25a** with Arg 29 or **25b** with Lys69 or **25c** with Arg29 residue of the protein used. Additionally, the fused ring (introduced by drug design approach, see Figure 14) that is, the benzene ring fused with the pyridine moiety participated well in hydrophobic interactions in all these cases.

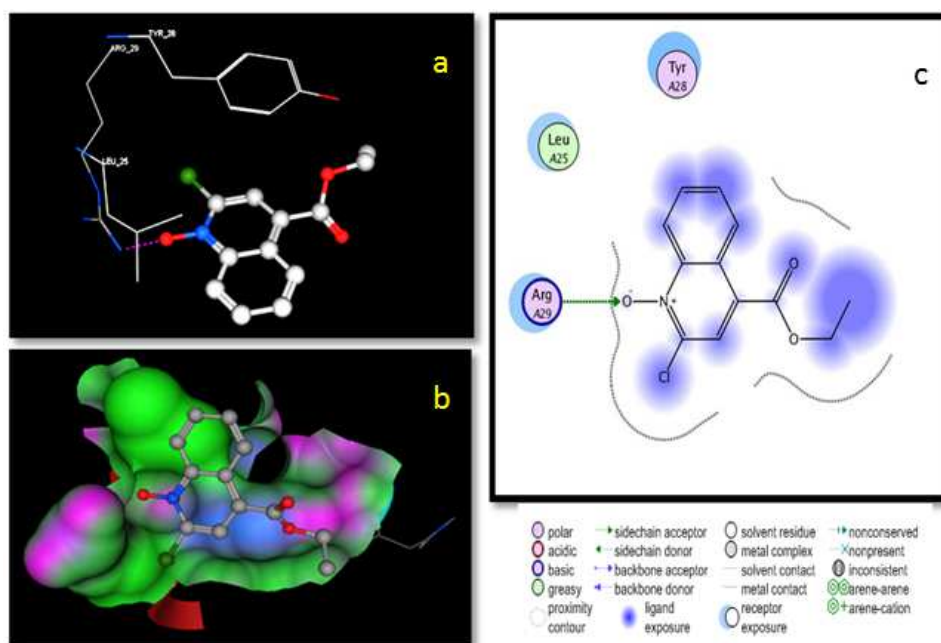


Figure 11: (a) Interaction mode of compound **25a** with SHMDt showing H-bonding (pink dotted line) with Arg 29. (b) Binding pose of compound 25a in SHMDt protein represented in electrostatic potential solid surface. (c) 2D interaction diagram of compound 25a with SHMDt protein

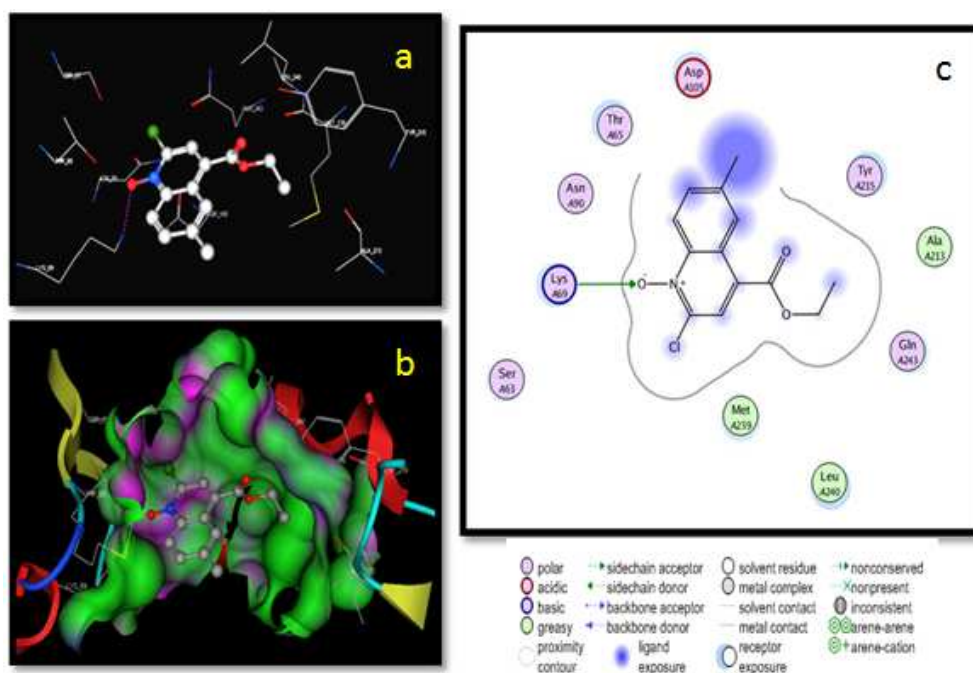


Figure 12: (a) Interaction mode of compound **25b** with SHMDt showing H-bonding (pink dottedline) with Arg 29. (b) Binding pose of compound **25b** in SHMDt protein represented in electrostatic potential solid surface. (c) 2D interaction diagram of compound **25b** with SHMDt protein

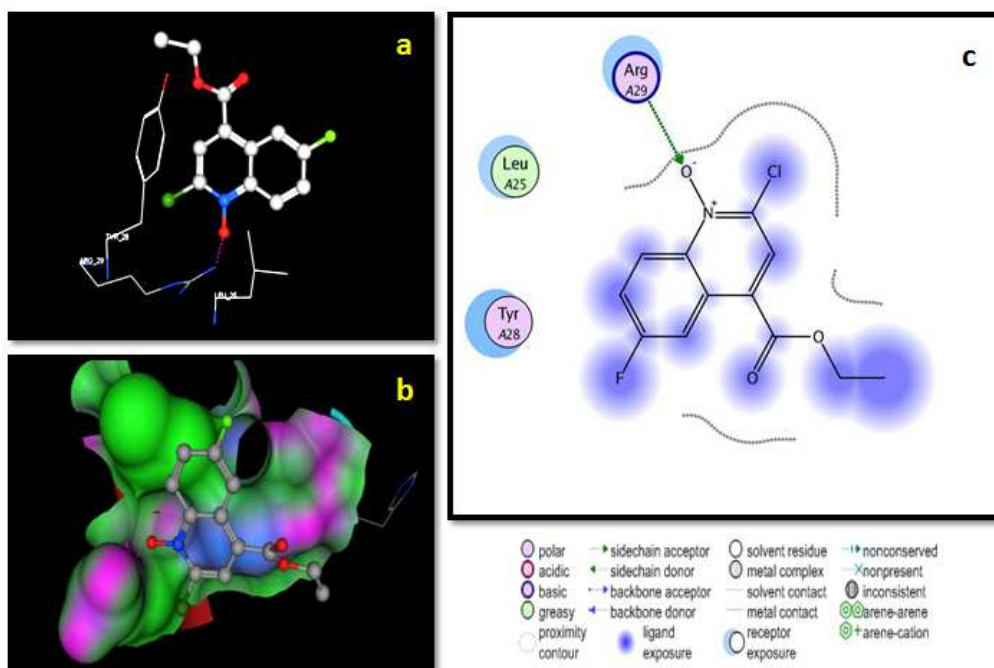


Figure 13: (a) Interaction mode of compound **25c** with SHMDt showing H-bonding (pink dotted line) with Arg 29. (b) Binding pose of compound **25c** in SHMDt protein represented in electrostatic potential solid surface. (c) 2D interaction diagram of compound **25c** with SHMDt protein

Overall, the docking studies indicated that the present N-oxides ²⁹ **25a–c** could be potential inhibitors of shikimate dehydrogenase and are of further interest.

Docking study

The molecular docking simulation was performed using Chemical Computing Group's Molecular Operating Environment (MOE) software 2008.10 Version, "DOCK" application Module. The molecules **25a**, **25b** and **25c** were docked into the Shikimate Dehydrogenase Protein of Mycobacterium tuberculosis (SDHmt) and their respective docking scores (Table 1) and interactions were observed.

Table 4. Dock scores obtained after docking the molecules into the SDHmt protein

Molecules	MOE Dock score (K.cal/mol)
25a	-10.03
25b	-12.84
25c	-10.93
21	-8.87

The purpose of the dock application was to search for favorable binding configurations in macromolecular target, which is usually a protein. For each ligand, a number of configurations called *poses* were generated and scored in an effort to determine favorable binding modes. For all scoring functions, lower scores indicated more favorable poses.

5. Summary

Based on the reported assay results of a novel DHS analogue i.e. 1, 6-dihydroxy-2-oxoisonicotinic acid against shikimate dehydrogenase a series of fused and functionalized pyridine derivatives were designed, synthesized and tested for their potential antitubercular properties. All these pyridine based compounds were prepared by using multistep methods involving the construction of pyridine ring as a key synthetic step followed by further functionalization reactions. The single crystal X-ray diffraction study was used to confirm the

molecular structure of three representative compounds unambiguously. To the best of our knowledge synthesis of the class of designed compounds was not known in the literature. Few of these compounds were found to be interesting when tested *in vitro*. Based on *in vivo* (LORA assay) studies indicated that **25b** better than rifampicin, isoniazide and moxifloxacin. Overall, compound **25b** appeared as an attractive and potential antitubercular agent and its strong binding with SDHmt protein was supported by docking studies.

6. Experimental section

6.1 Chemistry - General methods

All reactions were carried out in oven dried glassware under atmospheric conditions unless otherwise stated. Commercially available chemicals were used as received, without any further purification. The following solvents and reagents were purified prior to use: Dichloromethane (DCM) was distilled from CaCl₂ and stored over molecular sieves (4 Å). Dimethylformamide (DMF) dried with CaH₂, distilled and stored over molecular sieves (4

Å). Ethyl acetate (EA) and hexanes (PE) for chromatographic separations were distilled prior to use.

Chromatography

Analytical thin layer chromatography was performed on Merck TLC aluminium sheets silica gel 60 F₂₅₄. Visualization was accomplished with UV light ($\lambda = 254$ nm). Vaniline, ninhydrin, mostain and permanganate solutions followed by heating or iodine were used for staining. Liquid chromatography was performed using Merck silica gel 60 (0.063 - 0.200 mm) and flash silica gel 60 (0.040 - 0.063 mm).

NMR-Spectroscopy

¹H- and ¹³C-NMR spectra were recorded on a Bruker Avance 300 (300 MHz for ¹H, 75 MHz for ¹³C), Bruker Avance III 400 “Nanobay” (400 MHz for ¹H, 101 MHz for ¹³C) or Avance III 600 (600 MHz for ¹H, 151 MHz for ¹³C) FT-NMR-Spectrometer at ambient temperature. Data are given as follows for ¹H-NMR: Chemical shift in ppm from internal CHCl₃ (7.27 ppm) or CH₃OH (3.31 ppm) as standard on the δ scale, multiplicity (br = broad, s = singlet, d = doublet, t = triplet, q = quartet, dd = doublet of doublet, ddd = doublet of doublet of doublet, dt = doublet of triplet, qd = quartet of doublet, sept = septet and m = multiplet), integration and coupling constant (Hz). Data are as follows for ¹³C-NMR: Chemical shift in ppm from internal CHCl₃ (77 ppm) or CH₃OH (49 ppm) as standard on the δ scale.

Mass spectrometry & IR spectroscopy and melting points

Mass spectrometry was performed using Varian MAT 311A, Finnigan MAT 95, Thermoquest Finnigan TSQ 7000 or Agilent Technologies 6540 UHD Accurate-Mass Q-TOF LC/MS at the analytical department of the University of Regensburg. The percentage set in brackets gives the peak intensity related to the basic peak (I = 100%). High resolution mass spectrometry (HRMS): The molecular formula was proven by the calculated precise mass.

ATR-IR spectroscopy was carried out on a Biorad Excalibur FTS 3000 spectrometer, equipped with a Specac Golden Gate Diamond Single Reflection ATR-System. The melting points were measured on a Büchi SMP-20 apparatus in a silicon oil bath. Values thus obtained were not corrected.

Syntheses of literature-known compounds and reagents

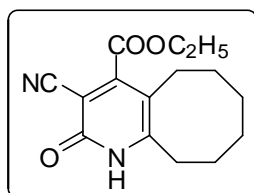
Methyl 2-chloro-6-methyl isonicotinate (**13a**)¹⁸, Methyl 2-chloro-6,7-dihydro-5H-cyclopenta [b] pyridine-4-carboxylate (**13b**)¹⁹, Methyl 2-chloro-5,6,7,8-tetrahydroquinoline-4carboxylate

(**13c**)²⁰, Methyl-2, 6-dichloroisonicotinate (**18**)²², Ethyl 2-chloroquinoline-4-carboxylate (**24a**)¹³, Ethyl 2-chloro-6-methylquinoline-4-carboxylate (**24b**)¹³, Ethyl 2-chloro-6-nitroquinoline-4-carboxylate (**24d**)^{13,14}, 2-Oxo-1,2-dihydroquinoline-4-carbohydrazide (**32a**)^{19,10}, 6-Methyl-2-oxo-1,2-dihydroquinoline-4-carbohydrazide (**32b**)^{19,10}, 6-Nitro-2-oxo-1,2-dihydroquinoline-4-carbohydrazide (**32d**)^{19,18}, 2,4,7-Trioxo-1-propyl-1,2,3,4,7,8-hexahydropyrido [2,3-*d*] pyrimidine-5-carboxylic acid (**35a**)¹⁵, Methyl-2,4,7-trioxo-1,3-dipropyl-1,2,3,4,7,8-hexahydropyrido[2,3-*d*]pyrimidine-5-carboxylate (**35b**)¹⁵. These compounds physical data matching with the literature reports and used as precursors for synthesis of the targeted molecules.

6.2 Syntheses

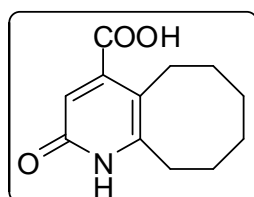
Ethyl-3-cyano-2-oxo-1,2,5,6,7,8,9,10-octahydrocycloocta[*b*]pyridine-4-carboxylate (**11d**):

The compound was prepared in 75% yield according to reported procedure for methyl 2-chloro-6-methyl isonicotinate (**13a**)¹⁸. Mp 278 °C, R_f: (silica gel, 6% MeOH in CH₂Cl₂): 0.60; IR (cm⁻¹): 3444, 2858, 2228 (CN), 1740 (CO ester), 1656 (CO amide), 1247; ¹H NMR (300 MHz, CDCl₃) δ 1.29 - 1.36 (m, 7H), 1.54 - 1.67 (m, 4H), 2.44-2.45 (m, 2H), 2.72-2.76 (m, 2H), 4.41 (q, 2H), 12.85 (s, 1H); ¹³C NMR (75 MHz, CD₃OD) δ 11.6, 23.9, 24.1, 24.3, 28.0, 28.2, 29.2, 60.2, 114.2, 114.8, 121.68, 145.4, 147.6, 162.2, 165.2; MS (EI, 70ev) : m/z (%) [M]⁺ 274.2 (27.56), 245.1 (100%); HRMS [M]⁺ Calcd. for C₁₅H₁₈N₃O₃ 274.1313; Found: 274:1313.



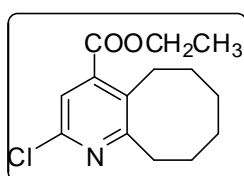
2-Oxo-1,2,5,6,7,8,9,10-octahydrocycloocta[*b*]pyridine-4-carboxylic acid (**12d**):

The title compound was prepared in 75% yield according to the procedure described for Methyl 2-chloro-6-methyl isonicotinate (**13a**)¹⁸; R_f: 0.6 (CH₂Cl₂/ MeOH 1:1), mp 250 °C; IR (cm⁻¹): 3388, 2995, 2915, 1715 (CO acid), 1625 (CO amide), 1442, 1228; ¹H NMR (300 MHz, DMSO-*d*₆) δ 1.30-1.60 (m, 8H), 2.55-2.65 (m, 4H), 6.37 (s, 1H), 12.50 (bs, 1H), 13.00 (bs, 1H); ¹³C NMR (75MHz, CD₃OD) δ 23.9, 24.1, 24.3, 28.2, 29.2, 116.8, 118.4, 134.3, 136.8, 163.2, 166.3; MS (EI, 70ev): m/z (%) [M+H]⁺ 266.6 (100).



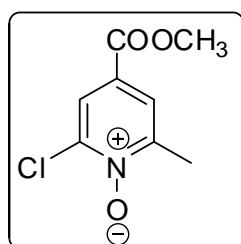
Methyl 2-chloro-5,6,7,8,9,10-hexahydrocycloocta[*b*]pyridine-4-carboxylate (**13d**):

The title compound was prepared in 70% yield according to the general



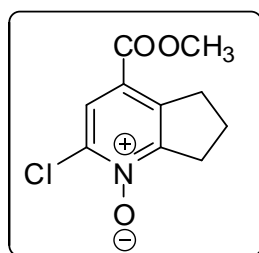
procedure as described above for Methyl 2-chloro-6-methyl isonicotinate (**13a**)¹⁸; R_f : 0.8 (CH_2Cl_2), mp 150 °C; IR (cm^{-1}): 3050, 2944, 1721 (CO ester), 1557, 1458, 1273, 1200; ^1H NMR (300MHz, CDCl_3) δ 1.28 -1.47(m, 7H), 1.73 -1.84 (m, 4H), 3.00 (t, $J = 6.4$ Hz, 4H), 3.91 (s, 3H), 4.38 (q, $J = 4.6$ Hz, 2H), 7.46 (s, 1H); ^{13}C NMR (75MHz, CDCl_3) δ 14.2, 25.8, 26.48, 27.1, 30.7, 31.0, 35.4, 61.9, 121.5, 133.7, 140.8, 148.2, 164.5, 165.9; MS (EI, 70ev): m/z (%) $[\text{M}]^+$. 253.1 (100), 238.1 (88.95); HRMS $[\text{M}]^+$ calcd. for $\text{C}_{13}\text{H}_{16}\text{ClNO}_2$ 253.0870; found: 253.087.

2-Chloro-4 (methoxycarbonyl)-6-methylpyridine-1- oxides (14a):



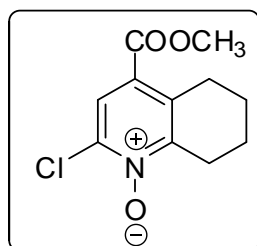
A mixture of (0.5g, 2.7mmol) of 3-chloro-1-methylisoquinoline (**12a**), (0.8 g, 4.6mmol) of m-chloro per benzoic acid, and benzene (8 mL) was stirred until a solution formed and was allowed to stand at room temperature for 2 days. Treatment of the reaction mixture with sodium carbonate solution followed by extraction with dichloromethane afforded 0.35 g (60% yield) of crude product. R_f : 0.4 (30% EtOAc in Petroleum Ether), mp 120 °C; IR (cm^{-1}): 3066, 2928, 1716 (CO ester), 1527, 1439, 1235(N-O), 1176, 935(N-O); ^1H NMR (300 MHz, CDCl_3) δ 2.50 (s, 3H), 3.87 (s, 3H), 7.73 (d, $J = 2.4$ Hz, 1H), 7.93 (d, $J = 2.4$ Hz, 1H) ; ^{13}C NMR (75 MHz, CDCl_3) δ 18.7, 52.9, 124.0, 124.6, 125.1, 142.4, 151.0, 163.6; MS (EI, 70ev): m/z (%) $[\text{M}]^+$ 201(98.75), 184 (100).

2-Chloro-4-(methoxycarbonyl)-6,7-dihydro-5H-cyclopenta[b]pyridine1-oxide(14b):



The title compound was prepared in 70% yield according to the general procedure as described for (**14a**); R_f : 0.38 (30% EtOAc in Petroleum Ether), mp 180 °C; IR (cm^{-1}): 3072, 2958, 1718 (CO ester), 1536, 1439, 1225(N-O), 1136, 940 (N-O); ^1H NMR (300 MHz, CDCl_3) δ 2.16-2.27 (m, 2H), 3.19 (t, $J = 7.8$ Hz, 2H), 3.35 (t, $J = 7.8$ Hz, 2H), 3.92 (s, 1H), 7.92 (s, 1H); ^{13}C NMR (75 MHz, CDCl_3) δ 22.0, 30.4, 32.9, 52.6, 123.1, 125.4, 140.0, 141.2, 155.5, 164.0; MS (EI, 70ev) : m/z (%) $[\text{M}]^+$. 227.03(100).

2-Chloro-4-(methoxycarbonyl)-5,6,7,8-tetrahydroquinoline 1-oxide (14c):

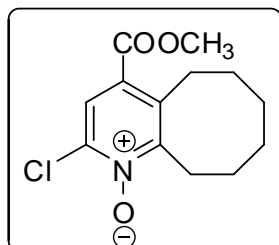


The title compound was prepared in 75% yield according to the general procedure as described for (**14a**); R_f : 0.35 (30% EtOAc in Petroleum Ether), mp 123 °C; IR (cm^{-1}): 3082, 2968, 1720 (CO ester), 1526, 1429, 1238 (N-O), 1166, 936 (N-O); ^1H NMR (300 MHz, CDCl_3) δ 1.73 -1.77 (m, 2H), 1.86 -1.89 (m, 2H), 2.97 (t, $J =$

6.8 Hz, 2H), 3.09 (t, $J = 6.9$ Hz, 2H), 3.90 (s, 3H), 7.92 (s, 1H); ^{13}C NMR (75 MHz, CDCl_3) δ 21.1, 21.4, 26.4, 27.2, 52.6, 124.4, 125.1, 135.7, 138.9, 151.7, 164.5; MS (EI, 70eV): m/z (%) $[\text{M}]^+$ 241.1(37.85), 192.1 (100).

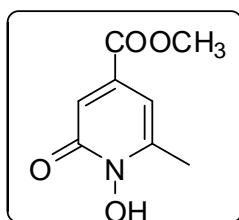
2-Chloro-4-(methoxycarbonyl)-5,6,7,8,9,10-hexahydrocycloocta[b]pyridine 1-oxide (14d):

The title compound was prepared in 72% yield according to the general procedure as



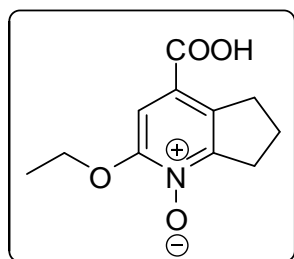
described for (14a); R_f : 0.4 (30% Et OAc in petroleum ether), mp 110 °C; IR (cm^{-1}): 3076, 2966, 1717 (CO ester), 1546, 1419, 1240(N-O), 1166, 948 (N-O); ^1H NMR (300MHz, CDCl_3) δ 1.32 -1.47 (m, 4H), 1.81 -1.85 (m, 4H), 3.12-3.30 (m, 4H), 3.90 (s, 3H), 7.88 (s, 1H); ^{13}C NMR (75MHz, CDCl_3) δ 26.0, 26.7, 26.8, 26.9, 28.3, 30.9, 52.7, 125.1, 138.7, 145.8, 155.0, 158.6, 164.8; MS (EI, 70eV): m/z (%) $[\text{M}]^+$ 269.1(22.96), 252.1 (194.87), 220.1(100); HRMS $[\text{M}]^+$ calcd. for $\text{C}_{13}\text{H}_{16}\text{ClNO}_3$ 269.081, found: 269.0816.

Methyl-1-hydroxy-6-methyl-2-oxo-1,2-dihydropyridine-4-carboxylate (15a):



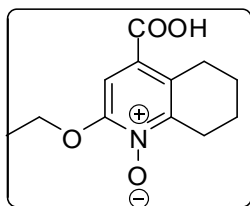
To a solution of (50 mg, 2.17 mmol) of sodium metal dissolved in Methanol (5 ml) was added (200 mg, 0.99mol) of Methyl 1-hydroxy-6-methyl-2-oxo-1, 2-dihydropyridine-4-carboxylate. The solution was heated at reflux for 3 h. The solution was cooled and diluted with Con HCl. Filtered the solid; concentrate the filtrate followed by triturate the filtrate with ether. 100 mg (60 % yield) product obtained. R_f : 0.5 (10% MeOH in EtOAc); ^1H NMR (300 Hz, CDCl_3) δ 2.53 (s, 3H), 3.90 (s, 3H), 6.75 (s, 1H), 7.20 (s, 1H); ^{13}C NMR (75Hz, CDCl_3) δ 22.7, 52.9, 105.5, 114.1, 137.4, 142.4, 157.5, 164.8; MS (EI, 70eV): m/z (%) $[\text{M}]^+$ 183.05 (100); HRMS $[\text{M}]^+$ calcd. for $\text{C}_8\text{H}_9\text{NO}_4$ 183.0532, found: 183.0530.

4-Carboxy-2-ethoxy-6,7-dihydro-5H-cyclopenta[b]pyridine 1-oxide (15b):



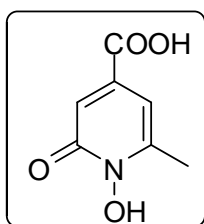
The title compound was prepared in 72% yield according to the general procedure as described for (15a); R_f : 0.4 (50% MeOH in EtOAc); ^1H NMR (250 Hz, CD_3OD) δ 1.57 (t, $J = 6.5$ Hz, 3H), 2.24-2.35 (m, 2H), 3.35 (t, $J = 7.8$ Hz, 4H), 4.55 (q, $J = 6.5$ Hz, 2H), 7.65 (s, 1H); ^{13}C NMR (75Hz, CD_3OD) δ 14.5, 23.4, 31.5, 33.3, 70.2, 109.6, 136.4, 137.6, 157.8, 158.1, 165.8; MS (EI, 70eV) : m/z (%) $[\text{M}]^+$ 223.08.

4-Carboxy-2-ethoxy-5,6,7,8-tetrahydroquinoline 1-oxide (15c): ⁶



The title compound was prepared in 66% yield according to the general procedure as described for (**15a**); R_f : 0.4 (50% MeOH in EtOAc); ¹H NMR (300 MHz, CDCl₃) δ 1.57 (t, J = 6.5 Hz, 3H), 1.70-1.89 (m, 4H), 2.9-2.93 (m, 4H), 4.55 (q, J = 6.5 Hz, 2H), 7.10 (s, 1H), 11.30 (bs, 1H); ¹³C NMR (75 MHz, CD₃OD) δ 14.2, 20.52, 20.9, 26.2, 68.9, 107.7, 128.1, 142.7, 152.6, 156.3, 165.1; MS (EI, 70ev): m/z (%) [M]⁺ 223.08

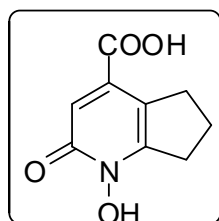
1-Hydroxy-6-methyl-2-oxo-1,2-dihydropyridine-4-carboxylic acid (16):



To a solution of 1-hydroxy-6-methyl-2-oxo-1,2-dihydropyridine-4-carboxylic acid (**15a**) (100 mg, 0.54 mmol) in THF (2.5 mL) was added a solution of LiOH.H₂O (26 mg, 1.08 mmol) in H₂O (7.5 mL) at 0 °C. The reaction was stirred at 23 °C for 2.5 h. After completion of the reaction, solvent was removed under a low vacuum. The solution was cooled in an

ice bath and neutralized with HCl (aq). The excess of HCl was distilled off and CH₃CN was added. The CH₃CN layer was collected and concentrated to give the gel like product (58 mg, 63 % yield). R_f : 0.38 (50% MeOH in EtOAc); IR (cm⁻¹): 3414, 3080, 2956, 1730 (CO acid), 1650 (CO amide), 1556, 1429, 1230(N-O), 1168; ¹H NMR (300MHz, CD₃OD) δ 2.49 (s, 3H), 6.80 (s, 1H), 7.07 (s, 1H); ¹³C NMR (75MHz, CD₃OD) δ 17.6, 107.2, 111.3, 136.4, 146.6, 154.0, 167.2; MS (EI, 70ev): m/z (%) [M]⁺ 169.03(100); HRMS [M]⁺ calcd. for C₇H₇NO₄ 169.0380, found: 169.0380.

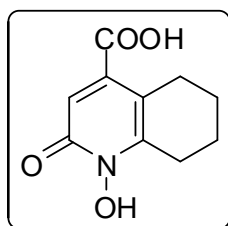
1-Hydroxy-2-oxo-2,5,6,7-tetrahydro-1H-cyclopenta[b]pyridine-4-carboxylic acid (17a):



1-Hydroxy-2-oxo-2,5,6,7-tetrahydro-1H-cyclopenta[b]pyridine-4-carboxylic acid (200 mg, 0.9 m mol) was taken in HCl (8 mL of 10% HCl) and refluxed for 10 h. After completion of the reaction, the excess of HCl was distilled off. The residue was washed with CHCl₃ and dried under high vacuum to give the desired product (100 mg, 57 % yield) as a

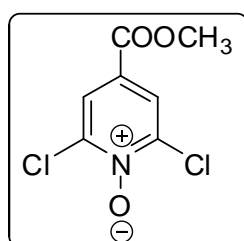
gel like material. R_f : 0.28 (50% MeOH in EtOAc); ¹H NMR (300MHz, CD₃OD) δ 2.14-2.21 (m, 2H), 3.06-3.13 (m, J = 7.8 Hz, 4H), 6.95 (s, 1H); ¹³C NMR (75MHz, CD₃OD) δ 23.5, 31.0, 32.5, 116.7, 122.0, 139.8, 147.0, 151.1, 168.6; MS (EI, 70ev): m/z (%) [M+H]⁺ 196.03 (14.54); HRMS [M]⁺ calcd. for C₈H₉NO₄ 195.0532, Found: 195.0532.

1-Hydroxy-2-oxo-1,2,5,6,7,8-hexahydroquinoline-4-carboxylic acid (17b):



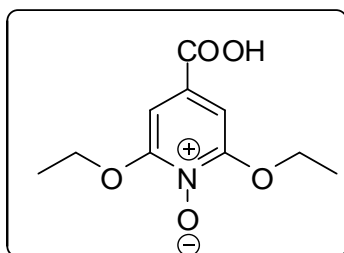
The title compound was prepared in 60% yield according to the general procedure as described above for **17a**; R_f : 0.3 (50% MeOH in EtOAc); ^1H NMR (300MHz, CD_3OD) δ 1.72 -1.82 (m, 4H), 2.75-2.85 (m, 4H), 6.86 (s, 1H); ^{13}C NMR (75MHz, CD_3OD) δ 22.1, 22.7, 26.0, 26.5, 115.1, 117.7, 143.4, 146.3, 158.5, 168.3; MS (EI, 70ev): m/z (%) $[\text{M}-\text{H}]^-$ 208.1(10); HRMS $[\text{M}]^+$ calcd. for $\text{C}_{10}\text{H}_{11}\text{NO}_4$ 209.0632, Found: 209.0631.

2, 6-Dichloro-4-(methoxycarbonyl) pyridine 1-oxide (19):

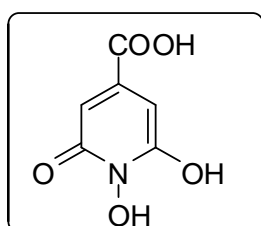


A mixture of methyl 2,6-dichloroisonicotinate (200 mg, 1.0 mmol), sodium per carbonate (157 mg, 1.0 equiv) and anhydrous CH_3CN (5 mL) was cooled to -10°C and trifluoromethanesulfonic anhydride (0.339 ml, 2 equiv) was added drop wise to it. The formations of bubbles were observed during addition. The mixture was stirred at the same temperature for 1 h, then at room temperature for 14 h. Most of the sodium per carbonate disappeared after 4h. The reaction mixture was poured onto mixture of crushed ice and saturated sodium carbonate. After stirred for 1 h the mixture was extracted with EtOAc. The organic layers were collected, combined, washed with 10% $\text{Na}_2\text{S}_2\text{O}_5$ and dried over anhydrous Na_2SO_4 to give the title compound (180 mg, 81% yield). ^1H NMR (300MHz, CDCl_3) δ 3.90 (s, 3H), 7.98 (s, 2H); ^{13}C NMR (75MHz, CDCl_3) δ 53.3, 124.9, 125.4, 143.7, 162.6; MS (EI, 70ev): m/z (%) $[\text{M}-\text{H}]^-$ 220.9 (100).

4-Carboxy-2,6-diethoxy pyridine 1-oxide (20):



The title compound was prepared in 66% yield according to the general procedure as described above for **15a**. R_f : 0.3 (50% MeOH in EtOAc); ^1H NMR (300MHz, CD_3OD) δ 1.58 (t, J = 7.0 Hz, 6H), 4.62 (q, J = 7.0 Hz, 4H), 7.47(s, 2H); ^{13}C NMR (75MHz, CD_3OD) δ 14.5, 71.0, 101.9, 146.5, 159.2, 164.7; MS (EI, 70ev): m/z (%) $[\text{M}]^+$ 228(100).

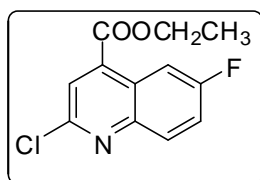


1,6-Dihydroxy-2-oxo-1,2-dihydropyridine-4-carboxylic acid (21):

The title compound was prepared in 65% yield according to the general procedure as described for 1-hydroxy-2-oxo-2,5,6,7-tetrahydro-1*H*-cyclopenta[*b*]pyridine-4-carboxylic acid (**17a**). ^1H

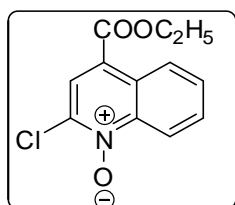
NMR (300 MHz, CD₃OD) δ 6.71(s, 1H), 12.92 (bs, 3H); ¹³C NMR (75 MHz, CD₃OD) δ 130.5, 141.7, 168.4, 169.2, 173.9; MS (EI, 70ev): m/z (%) 171.07 (M+H).

Methyl 2-chloro-6-fluoroquinoline-4-carboxylate (24c):



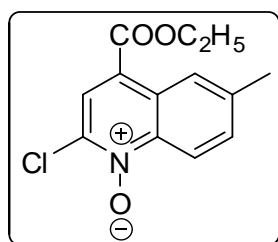
The title compound was prepared in 75% yield according to the literature procedure for (24a). R_f: 0.9 (CH₂Cl₂), mp 120 °C; IR (cm⁻¹): 3090, 2914, 2842, 1710 (CO ester), 1567, 1468, 1243, 1210; ¹H NMR (300 MHz, CDCl₃) δ 1.47 (t, *J* = 7.2 Hz, 3H), 4.5 (q, *J* = 7.2 Hz, 2H), 7.52-7.59 (m, 1H), 7.98 (s, 1H), 8.05- 8.09 (dd, *J*¹ =5.4 Hz, *J*² = 9.3 Hz, 1H), 8.47- 8.52 (dd, *J*¹ =2.7 Hz, *J*² =10.4Hz, 1H); ¹³C NMR (75MHz, CDCl₃) δ 14.3, 62.3, 111.5, 120.6, 122.8, 126.9, 128.0, 137.0, 140.3, 161.7, and 163.5, 164.4; MS (EI, 70ev): m/z (%) [M]⁺ 239.1 (100).

2-Chloro-4 (ethoxycarbonyl) quinoline 1- oxides (25a):



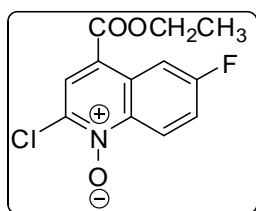
The title compound was prepared in 75% yield according to the general procedure as described for 2,6-dichloro-4-(methoxycarbonyl) pyridine-1-oxide (19). R_f: 0.5 (10% EtOAc in petroleum ether), mp 170 °C; IR (cm⁻¹): 3072, 2968, 1720 (CO ester), 1526, 1429, 1230(N-O), 1166, 930 (N-O); ¹H NMR (300 MHz, CDCl₃) δ 1.46 (t, *J* = 7.2 Hz, 3H), 4.50 (q, *J* = 7.2 Hz, 2H), 7.7-7.83 (m, 2H), 8.17 (s, 1H), 8.76 (dd, *J*¹ =1.1 Hz, *J*² = 8.7 Hz, 1H), 9.03 (dd, *J*¹ = 1.1 Hz, *J*² =8.7 Hz, 1H); ¹³C NMR (75 MHz, CDCl₃) δ 14.3, 62.1, 119.9, 123.3, 125.7, 126.5, 127.0, 129.9, 131.1, 137.4, and 143.2, 163.9; MS (EI, 70ev): m/z (%) [M]⁺ 249.1 (100).

2-Chloro-4 (ethoxycarbonyl)-6-methylquinoline 1-oxides (25b):



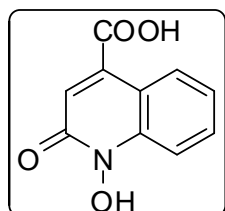
The title compound was prepared in 72% yield according to the general procedure as described for 2,6-dichloro-4-(methoxycarbonyl) pyridine-1-oxide (19). R_f: 0.48 (10% EtOAc in Petroleum Ether), mp 135 °C; IR (cm⁻¹): 3082, 2968, 1720 (CO ester), 1526, 1429, 1238 (N-O), 1166, 936 (N-O); ¹H NMR (300MHz, CDCl₃) δ 1.46 (t, *J* = 7.2 Hz, 3H), 2.56 (s, 1H), 4.48 (q, *J* = 7.2 Hz, 2H), 7.64 (d, *J* = 8.8 Hz, 1H), 8.13(s, 1H), 8.63 (d, *J* = 8.8 Hz, 1H), 8.79(s, 1H); ¹³C NMR (75Hz, CDCl₃) δ 14.3, 22.9, 62.0, 119.7, 122.8, 125.6, 125.9, 126.6, 133.1, 140.5, 141.7, 164.0; MS (EI, 70ev): m/z (%) [M]⁺ 265.1 (100).

2-Chloro-6-fluoro-4-(ethoxycarbonyl) quinoline 1-oxide (25c):



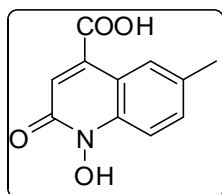
The title compound was prepared in 70% yield according to the general procedure as described for 2, 6-dichloro-4-(methoxycarbonyl) pyridine-1-oxide (**19**). R_f : 0.6 (10% EtOAc in Petroleum Ether), mp 120 °C; IR (cm^{-1}): 3086, 2988, 1717 (CO ester), 1546, 1447, 1291, 1211(N-O), 1136, 933 (N-O); ^1H NMR (300MHz, CDCl_3) δ 1.47 (t, $J = 7.2$ Hz, 3H), 4.50 (q, $J = 7.2$ Hz, 2H), 7.51-7.58 (m, 1H), 8.25(s, 1H), 8.75- 8.80(m, 2H); ^{13}C NMR (75MHz, CDCl_3) δ 14.3, 62.3, 111.5, 120.6, 122.2, 122.8, 123.0, 126.9, 128.1, 137.0, 140.3, 161.0, 163.5; MS (EI, 70ev): m/z (%) $[\text{M}]^+$: 255 (46.72), 239.1(100).

1-Hydroxy-2-oxo-1,2-dihydroquinoline-4-carboxylic acid (26a):



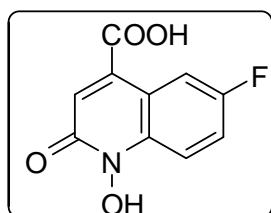
The title compound was prepared in 68% yield according to the general procedure as described for 1-hydroxy-2-oxo-2,5,6,7-tetrahydro-1H-cyclopenta[b]pyridine-4-carboxylic acid (**17a**); R_f : 0.4 (50% MeOH in EtOAc); IR (cm^{-1}): 3424, 3090, 2966, 1732 (CO acid), 1645 (CO amide), 1546, 1419, 1240 (N-O), 1178; ^1H NMR (300 MHz, CD_3OD) δ 7.25 (s, 1H), 7.35 (t, $J = 7.5$ Hz, 1H), 7.7 (t, $J = 7.5$ Hz, 1H), 7.89 (d, $J = 8.2$ Hz, 1H), 8.45 (d, $J = 8.2$ Hz, 1H); ^{13}C NMR (75 MHz, CD_3OD) δ 114.2, 118.3, 123.6, 124.6, 128.1, 132.8, 140.0, 159.1, 167.8; MS (EI): m/z (%) $[\text{M}]^+$: 205.1(100); HRMS $[\text{M}]^+$ calcd. for $\text{C}_{10}\text{H}_7\text{NO}_4$ 205.0375, found: 205.0374.

1-Hydroxy-6-methyl-2-oxo-1,2-dihydroquinoline-4-carboxylic acid (26b):



The title compound was prepared in 60% yield according to the general procedure as described for 1-hydroxy-2-oxo-2, 5, 6, 7-tetrahydro-1H-cyclopenta[b]pyridine-4-carboxylic acid (**17a**). R_f : 0.4 (50% MeOH in EtOAc); ^1H NMR (300MHz, CD_3OD) δ 2.42 (s, 3H), 7.21 (s, 1H), 7.65(d, 2H), 8.22 (s, 1H); ^{13}C NMR (250 Hz, CD_3OD) δ 21.5, 114.1, 118.3, 123.4, 127.5, 134.1, 134.6, 145.8, 158.8, 167.9; MS (EI, 70ev): m/z (%) $[\text{M}]^+$: 219.1 (100); HRMS $[\text{M}]^+$ calcd. For $\text{C}_{11}\text{H}_9\text{NO}_4$ 219.0526, found 219.0532.

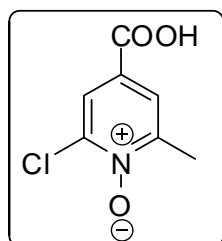
6-Fluoro-1-hydroxy-2-oxo-1,2-dihydroquinoline-4-carboxylic acid (26c):



The title compound was prepared in, 60% yield according to the general procedure as described for 1-hydroxy-2-oxo-2,5,6,7-tetrahydro-1H-cyclopenta[b]pyridine-4-carboxylic acid (**17a**); R_f : 0.4 (50% MeOH in EtOAc), mp 266 °C; ^1H NMR (300MHz, CD_3OD) δ

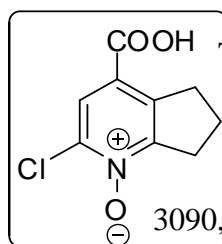
7.25(s, 1H), 7.59-7.65 (m, 1H), 7.79-7.84 (dd, $J^1 = 5.4$ Hz, $J^2 = 9.3$ Hz, 1H), 8.16-8.2 (dd, $J^1 = 2.7$ Hz, $J^2 = 10.4$ Hz, 1H); ^{13}C NMR (75MHz, CD_3OD) δ 113.1, 116.4, 120.6, 121.0, 126.0, 136.9, 138.4, 147.5, 158.6, 161.6, 167.2; MS (EI, Offline, 70ev) : m/z (%) $[\text{M}]^+$ 223.1(100); HRMS $[\text{M}]^+$ calcd. for $\text{C}_{10}\text{H}_6\text{FNO}_4$ 223.0277, found: 223.028.

4-Carboxy-2-chloro-6-methylpyridine 1-oxide (27a):



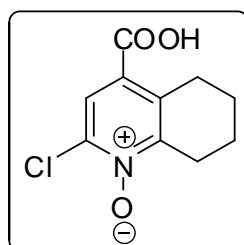
The title compound was prepared in 60% yield according to the general procedure as described for 1-hydroxy-6-methyl-2-oxo-1, 2-dihydropyridine-4-carboxylic acid (**16**); mp 215 °C; IR (cm^{-1}): 3390, 3076, 2968, 1737 (CO acid), 1546, 1447, 1291, 1221(N-O), 1136, 940 (N-O); ^1H NMR (300MHz, $\text{DMSO}-d_6$) δ 2.45 (s, 3H), 7.95(d, $J = 2.0$ Hz, 1H), 7.99 (d, $J = 2.0$ Hz, 1H); ^{13}C NMR (75Hz, $\text{DMSO}-d_6$) δ 17.9, 124.3, 124.3, 125.7, 140.6, 150.4, 164.2; MS (EI, 70ev): m/z (%), 229($[\text{M}+\text{H}]^+ + \text{CH}_3\text{CN}$, 100), 188 (MH^+ , 35); HRMS $[\text{M}]^+$ calcd. for $\text{C}_7\text{H}_6\text{ClNO}_3$ 187.0036, Found: 187.0038.

4-Carboxy-2-chloro-6,7-dihydro-5H-cyclopenta[b]pyridine 1-oxide (27b):



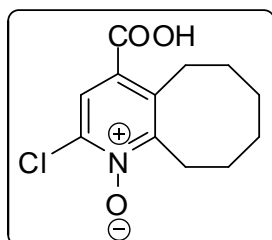
The title compound was prepared in 80% yield according to the general procedure as described for 1-hydroxy-6-methyl-2-oxo-1, 2-dihydropyridine-4-carboxylic acid (**16**); mp 140 °C; IR: (cm^{-1}): 3440, 3090, 2968, 1737 (CO acid), 1556, 1437, 1281, 1241 (N-O), 1136, 918 (N-O); ^1H NMR (300MHz, CD_3OD) δ 2.23 (t, $J = 7.8$ Hz, 2H), 3.15 (t, $J = 7.8$ Hz, 2H), 3.37 (t, $J = 7.8$ Hz, 2H), 7.98 (s, 1H); ^{13}C NMR (75 MHz, CD_3OD) δ 23.1, 31., 33.9, 126.9, 128.7, 140.8, 143.4, 157.4, 166.5; MS (EI, 70ev): m/z (%) $[\text{M}]^+$ 213.1(100); HRMS $[\text{M}]^+$ calcd. for $\text{C}_9\text{H}_8\text{ClNO}_3$ 213.0193, Found: 213.0196.

4-Carboxy-2-chloro-5,6,7,8-tetrahydroquinoline 1-oxide (27c):



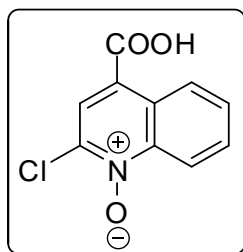
The title compound was prepared in 70% yield according to the general procedure as described for 1-hydroxy-6-methyl-2-oxo-1, 2-dihydropyridine-4-carboxylic acid (**16**); mp 190 °C; IR: (cm^{-1}): 3380, 3086, 2958, 1727 (CO acid), 1546, 1437, 1291, 1231(N-O), 1136, 928 (N-O); ^1H NMR (300Hz, $\text{DMSO}-d_6$) δ 1.62-1.82 (m. 4H), 2.77(t, $J = 6.8$ Hz, 2H), 2.99 (t, $J = 6.8$ Hz, 2H), 7.5(s, 1H), 13.57(s, 1H); ^{13}C NMR (75MHz, $\text{DMSO}-d_6$) δ 20.5, 20.7, 25.9, 26.6, 123.9, 125.8, 134.9, 137.2, 150.5, 165.4; EI Mass: 227.03 (M^+ , 49).

4-Carboxy-2-chloro-5,6,7,8,9,10-hexahydrocycloocta[b]pyridine 1-oxide (27d):



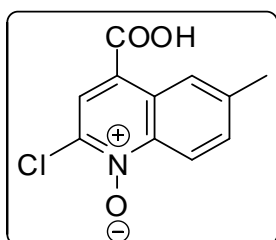
The title compound was prepared in 68% yield according to the general procedure as described for 1-hydroxy-6-methyl-2-oxo-1,2-dihydropyridine-4-carboxylic acid (**16**); mp 219 °C; IR: (cm⁻¹): 3400, 3056, 2960, 1740 (CO acid), 1566, 1437, 1281, 1241(N-O), 1126, 945 (N-O); ¹H NMR (300 MHz, CD₃OD) δ 1.35 -1.49 (m, 4H), 1.77 -1.87 (m, 4H), 3.19-3.34 (m, 4H), 8.00(s, 1H); ¹³C NMR (75 MHz, CD₃OD) δ 27.1, 27.7, 27.9, 28.1, 29.1, 32.1, 126.5, 130.6, 136.4, 140.22, 156.5, 167.2; MS (EI, 70ev): m/z (%), 255.1([M]⁺ 102.88), 238.1(85.97), 196.1(100); HRMS [M]⁺ calcd. for C₁₂H₁₄ClNO₃ 255.0662, Found: 255.0655.

4-Carboxy-2-chloroquinoline 1-oxide (28a):



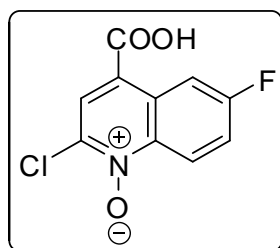
The title compound was prepared in 72% yield according to the general procedure as described for 1-hydroxy-6-methyl-2-oxo-1,2-dihydropyridine-4-carboxylic acid (**6**); mp 197 °C; IR: (cm⁻¹): 3414, 3056, 1730 (CO acid), 1556, 1427, 1281, 1231(N-O), 1126, 935 (N-O); ¹H NMR (300MHz, DMSO-d₆) δ 7.83-7.93 (m, 2H), 8.24(s, 1H), 8.57-8.60 (dd, *J*¹ =1.1Hz, *J*² = 7.3 Hz, 1H), 8.97-8.90 (dd, *J*¹ =2.1Hz, *J*² = 7.3 Hz, 1H), 13.95 (s, 1H); ¹³C NMR (75MHz, DMSO-d₆) δ 119.2, 123.7, 125.7, 126.2, 126.9, 129.9, 131.2, 136.6, 142.4, 165.3; MS (EI, 70ev): m/z (%) [M]⁺ 223.1(100); HRMS [M]⁺ calcd. for C₁₀H₆ClNO₃ 223.0036, found: 223.0032.

4-Carboxy-2-chloro-6-methylquinoline 1-oxide (28b):



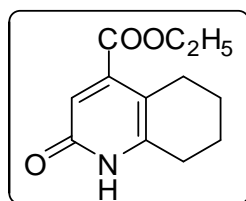
The title compound was prepared in 80% yield according to the general procedure as described for 1-hydroxy-6-methyl-2-oxo-1,2-dihydropyridine-4-carboxylic acid (**6**); mp 172 °C; IR: (cm⁻¹): 3414, 3086, 1736 (CO acid), 1536, 1437, 1271, 1238(N-O), 1126, 929 (N-O) ; ¹H NMR (300 MHz, DMSO-d₆) δ 2.47 (s, 3H), 7.7- 7.74 (d, *J* = 9 Hz, 1H), 8.18 (s, 1H), 8.46(d, *J* = 9 Hz, 1H), 8.74 (s, 1H), 13.75 (s, 1H); ¹³C NMR (75Hz, DMSO-d₆) δ 21.4, 119.1, 123.18, 125.6, 125.7, 126.2, 132.9, 135.7, 139.9, 141.0, 165.4; MS (EI, 70ev): m/z (%) [M]⁺ 237.1(23.52), 221.1(68.33); HRMS [M]⁺ calcd. for C₁₁H₈ClNO₃ 237.019, found: 237.0187.

4-Carboxy-2-chloro-6-fluoroquinoline 1-oxide (28c):



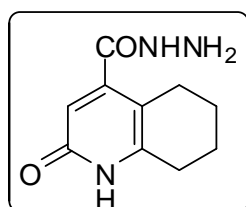
The title compound was prepared in 70% yield according to the general procedure as described for 1-hydroxy-6-methyl-2-oxo-1,2-dihydropyridine-4-carboxylic acid (**6**); mp 222 °C; IR: (cm⁻¹): 3394, 3076, 1728 (CO acid), 1576, 1467, 1261, 1234(N-O), 1116, 937 (N-O); ¹H NMR (300MHz, DMSO-*d*₆) δ 7.79-7.84 (m, 1H), 8.29 (s, 1H), 8.61-8.65 (dd, *J*¹ = 2.9Hz, *J*² = 10.2Hz, 1H), 8.73-8.77 (dd, *J*¹ = 2.9Hz, *J*² = 10.2Hz, 1H); ¹³C NMR (75Hz, DMSO-*d*₆) δ 111.1, 120.5, 122.6, 127.0, 127.7, 136.3, 139.8, 160.5, 162.9, 165.1; MS (EI, 70ev): m/z (%) [M]⁺ 241.1(100); HRMS [M]⁺ calcd. for C₁₀H₅FCINO₃ 240.9942, Found: 240.9943.

Ethyl 2-oxo-1,2,5,6,7,8-hexahydroquinoline-4-carboxylate (29a):



Acetyl chloride (2mL) was added slowly to ethanol (10 mL) at room temperature, stirred it for 10 minutes. To this was added 2-oxo-1,2,5,6,7,8-hexahydroquinoline-4-carboxylic acid (695 mg, 3.59 mmol) and the reaction mixture was heated to reflux for overnight. The reaction mixture was cooled to room temperature and extracted with CHCl₃. The organic layer was collected, washed with 5% NaHCO₃, dried over anhydrous Na₂SO₄, filtered and concentrated under low vacuum to give the titled product (650 mg, 82 % yield). ¹H NMR (300 MHz, DMSO-*d*₆) δ 1.27 (t, *J* = 7.1 Hz, 3H), 1.63-1.67 (m, 4H), 2.43-2.49 (m, 4H), 4.25 (q, *J* = 7.1 Hz, 2H), 6.37 (s, 1H), 11.9 (bs, 1H); ¹³C NMR (75 MHz, DMSO-*d*₆) δ 13.8, 20.7, 21.9, 23.7, 61.2, 111.9, 116.9, 133.8, 144.5, 161.2, 165.9; MS (EI, 70ev): m/z (%) [M]⁺ 221.1 (41.08), 192.1(100).

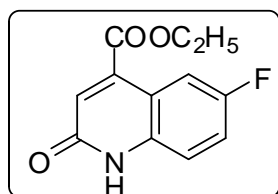
2-Oxo-1,2,5,6,7,8-hexahydroquinoline-4-carbohydrazide (30a):



A mixture of ethyl 2-oxo-1,2,5,6,7,8-hexahydroquinoline-4-carboxylate (71 mg, 0.32 mmol) and N₂H₄·H₂O (0.1 mL) in ethanol (10 mL) was refluxed for 10 h. after completion of the reaction most of the solvent was evaporated. The solid separated was filtered, washed with ether and dried to afford 2-oxo-1,2,5,6,7,8-hexahydroquinoline-4-carbohydrazide (50m g, 75% yield) as a pale yellow solid; mp 258 °C; IR (cm⁻¹): 3348, 2985, 2865, 1685 (CO amide), 1645 (CO amide), 1442, 1228. ¹H NMR (300 MHz, CD₃OD) δ 1.73-1.82 (m, 4H), 2.49-2.53 (t, *J* = 5.9 Hz, 2H), 2.6-2.64 (t, *J* = 5.9 Hz, 2H), 6.35 (s, 1H); ¹³C NMR (75Hz,

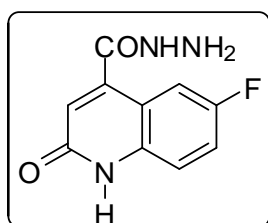
CD₃OD) δ 22.6, 23.3, 24.8, 25.2, 113.7, 116.1, 146.0, 151.1, 163.8, 164.8, 166.1; MS (EI, 70ev): m/z (%) [M]⁺ 207.1(100).

Ethyl 6-fluoro-2-oxo-1,2-dihydroquinoline-4-carboxylate (31c):



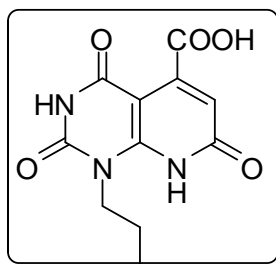
The title compound was prepared in 72% yield according to the general procedure as described for ethyl 2-oxo-1,2,5,6,7,8-hexahydroquinoline-4-carboxylate (**29a**). mp 222 °C; IR: (cm⁻¹): 3394, 3076, 1728 (CO acid), 1576, 1467, 1261, 1234(N-O), 1116, 937 (N-O); ¹H NMR (300MHz, DMSO-*d*₆) δ 1.35(t, *J* = 7.2 Hz, 3H), 4.40 (q, *J* = 7.2 Hz, 2H), 7.02(s, 1H), 7.38-7.50 (m, 2H), 7.9-7.95(dd, *J*¹ = 2.7 Hz, *J*² = 7.7 Hz, 1H), 12.4 (bs, 1H); ¹³C NMR (75Hz, DMSO-*d*₆) δ 13.8, 61.9, 111.1, 116.5, 117.6, 119.1, 136.2, 139.3, 158.6, 160.6, 166.2; MS (EI, 70ev): m/z (%) [M]⁺ 241.1(100); HRMS [M]⁺ calcd. for C₁₀H₅FCINO₃ 240.9942, found: 240.9943.

6-Fluoro-2-oxo-1,2-dihydroquinoline-4-carbohydrazide (32c):



The title compound was prepared according to the general procedure as described in 2-Oxo-1,2,5,6,7,8-hexahydroquinoline-4-carbohydrazide (**30a**) in 70% yield. The physical properties of this material are consistent with previously reported data. mp 321°C; IR (cm⁻¹): 3407, 3265, 3164, 2865, 1661 (CO amide), 1641 (CO amide), 1430, 1252; ¹H NMR (300 MHz, DMSO-*d*₆) δ 4.62 (s, 2H), 7.34 - 7.57 (m, 4H), 9.90 (s, 1H), 12.03 (s, 1H); ¹³C NMR (75MHz, DMSO-*d*₆) δ 110.7, 116.8, 117.4, 119.1, 121.4, 135.8, 143.8, 155.3, 160.8, 164.6; MS (EI, 70ev): m/z (%) [M]⁺ 221.1(72.88), 134.1(100); HRMS [M]⁺ calcd. for C₁₀H₈FN₃O₂ 221.0601, found: 221.0596.

2,4,7-Trioxo-1-propyl-1,2,3,4,7,8-hexahydropyrido[2,3-*d*]pyrimidine-5-carboxylic acid (35a):

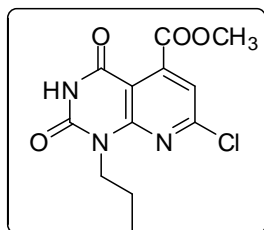


A mixture of methyl-2,4,7-trioxo-1-propyl-1,2,3,4,7,8-hexahydropyrido[2,3-*d*]pyrimidine-5-carboxylate (**22b**) (100 mg, 0.36 mmol) and 1N NaOH (3mL) was refluxed for 2 h. After completion of the reaction the mixture was cooled to 0 °C and acidified with 6N HCl. The solid separated was filtered, washed with cold water and dried to give the desired product (75 mg, 79%). mp 284 °C; IR (cm⁻¹): 3404, 3097, 2962, 2853, 1710 (CO Acid), 1640 (CO amide), 1209; ¹H NMR (300MHz, DMSO-*d*₆) δ 0.89 (t, *J* = 7.3 Hz, 3H), 1.59-1.67 (m, 2H), 4.03 (t, *J* = 7.8 Hz, 2H), 6.4 (s, 1H), 11.50 (s,

1H), 12.31 (s, 1H), 13.45 (s, 1H); ¹³C NMR (75MHz, DMSO-*d*₆) δ 10.9, 20.5, 42.5, 102.3, 115.6, 147.7, 150.2, 152.2, 159.5, 166.5, 167.8; MS (EI, 70ev): m/z (%) [M+H]⁺ 266(100); HRMS [M]⁺ calcd. for C₁₁H₁₁N₃O₅ 265.0699, Found: 265.0700.

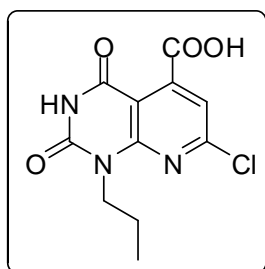
Methyl-7-chloro-2,4-dioxo-1-propyl-1,2,3,4-tetrahydropyrido[2,3-*d*]pyrimidine-5-

carboxylate (36a): The title compound was prepared in 60% yield according to the general



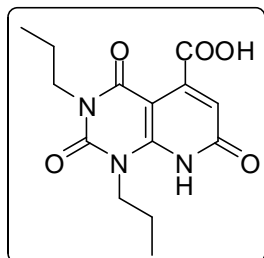
procedure as described for methyl-2-chloro-6-methyl isonicotinate (**3a**). R_f: 0.7 (50% EtOAc in Petroleum Ether); mp 217 °C; IR (cm⁻¹): 3234, 2945, 28513, 1720 (CO ester), 1665 (CO amide), 1550, 1420, 1303, 1258, 1166; ¹H NMR (300 MHz, DMSO-*d*₆) δ 0.89 (t, *J* = 7.3 Hz, 3H), 1.57-1.67 (m, 2H), 3.85 (s, 3H), 4.03 (t, *J* = 7.8Hz, 2H), 7.53 (s, 1H), 11.93(s, 1H); ¹³C NMR (75 MHz, DMSO-*d*₆) δ 10.9, 20.3, 40.3, 52.5, 106.4, 115.8, 145.4, 149.8, 152.2, 153.9, 165.7; MS (EI, 70ev): m/z (%) [M+H]⁺ 298(100).

7-Chloro-2,4-dioxo-1-propyl-1,2,3,4-tetrahydropyrido[2,3-*d*]pyrimidine-5-carboxylic acid (36c):



The title compound was prepared in 60% yield according to the general procedure as described for methyl-2-chloro-6-methyl isonicotinate (**6**). R_f: 0.7 (50% EtOAc in Petroleum Ether). mp 217 °C; IR (cm⁻¹): 3234, 2945, 28513, 1720 (CO ester), 1665(CO amide), 1550, 1420, 1303, 1258, 1166; ¹H NMR (300MHz, DMSO-*d*₆) δ 0.86 (t, *J* = 7.3 Hz, 3H), 1.50-1.60 (m, 2H), 4. 20 (t, *J* = 7.3 Hz, 2H), 7.50 (s, 1H), 11.00 (s, 1H); ¹³C NMR (75MHz, DMSO-*d*₆) δ 10.9, 20.2, 30, 42.5, 112.3, 115.6, 147.7, 150.2, 152.2, 159.5, 166.5, 167.8; MS (EI, 70ev): m/z (%) [M+H]⁺ 284.04 (100); HRMS [M]⁺ calcd. for C₁₁H₁₀ClN₃O₄ 283.114, Found: 283.104.

1-Ethyl-2,4,7-trioxo-3-propyl-1,2,3,4,7,8-hexahydropyrido[2,3-*d*]pyrimidine-5-



carboxylic acid (35b): The title compound was prepared in 60% yield according to the procedure as described for 2,4,7-trioxo-1-propyl-1,2,3,4,7,8-hexahydropyrido[2,3-*d*]pyrimidine-5-carboxylic acid. mp 226 °C; IR (cm⁻¹):3414, 3047, 2972, 2803, 1698 (CO Acid), 1610 (CO amide), 1209; ¹H NMR (300MHz, DMSO-*d*₆) δ 0.83-0.91 (m, 6H), 1.52-1.67 (m, 4H), 3.81 (t, *J* = 7.4 Hz, 2H), 4.10 (t, *J* = 7.8 Hz, 2H), 6.51 (s, 1H), 12.53 (s, 1H), 13.46 (s, 1H);

^{13}C NMR (75 Hz, DMSO- d_6) δ 10.9, 11.2, 20.5, 20.5, 42.2, 43.3, 106.5, 117.7, 142.7, 150.3, 158.7, 166.7, 167.9; MS (EI, 70ev): m/z (%) $[\text{M}+\text{H}]^+$ 294.1 (100).

6.3. Single crystal X-ray data for compound **13e**, **15a** and **15b**.

Single crystals suitable for X-ray diffraction of **13e** and **15a**, **15b**, were grown from 8:2 hexane-ethylacetate and the compound **15b** from MeOH. The crystals were chosen using a stereo zoom microscope supported by a rotatable polarizing stage. The data was collected at room temperature on CrysAlisPro, Oxford Diffraction Ltd, Version 1.171.33.55 with graphite monochromated Cu-K α radiation (1.54814 Å). The crystals were glued to a thin glass fibre using FOMBLIN immersion oil and mounted on the diffractometer. The crystal structure was solved by direct methods using SHELXS-97 and the data was refined by full matrix least-squares refinement on F^2 with anisotropic displacement parameters for non-H atoms, using SHELXL-97.³²

Crystal data of 13e: Molecular formula = $\text{C}_{10}\text{H}_{13}\text{NO}_3$, Formula weight = 195.21, Crystal system = Monoclinic, space group = $\text{P}2(1)/n$, $a = 8.918$ (11) Å, $b = 7.969$ (7)Å, $c = 14.721$ (18)Å, $V = 1009.73$ (2)Å³, $T = 296$ K, $Z = 4$, $D_c = 1.284$ Mg m⁻³, $\mu(\text{Mo-K}\alpha) = 0.79$ mm⁻¹, 5081 reflections measured, 1808 independent reflections, 1612 observed reflections [$I > 2.0 \sigma(I)$], $R_{1_obs} = 0.009$, Goodness of fit = 1.081. Crystallographic data (excluding structure factors) for **13e** have been deposited with the Cambridge Crystallographic Data Center as supplementary publication number CCDC 871206.

Crystal data of 15a: Molecular formula = $\text{C}_8\text{H}_9\text{NO}_4$, Formula weight = 183.16, Crystal system = Orthorhombic, space group = $\text{Pna}2_1$, $a = 23.033$ (6) Å, $b = 4.038$ (10)Å, $c = 18.018$ (5)Å, $V = 1676.2$ (8)Å³, $T = 296$ K, $Z = 8$, $D_c = 1.456$ Mg m⁻³, $\mu(\text{Mo-K}\alpha) = 1.01$ mm⁻¹, 5768 reflections measured, 2506 independent reflections, 2371 observed reflections [$I > 2.0 \sigma(I)$], $R_{1_obs} = 0.026$, Goodness of fit = 1.05. Crystallographic data (excluding structure factors) for **15a** have been deposited with the Cambridge Crystallographic Data Center as supplementary publication number CCDC 871207.

Crystal data of 15b: Molecular formula = $\text{C}_{11}\text{H}_{13}\text{NO}_4 \cdot \text{H}_2\text{O}$, Formula weight = 241.24, Crystal system = Monoclinic, space group = $\text{P}2(1)/n$, $a = 10.413$ (19) Å, $b = 19.895$ (3)Å, $c = 11.164$ (2)Å, $V = 2256.54$ (7)Å³, $T = 296$ K, $Z = 8$, $D_c = 1.387$ Mg m⁻³, $\mu(\text{Mo-K}\alpha) = 0.95$ mm⁻¹, 17064 reflections measured, 4439 independent reflections, 3792 observed reflections [$I > 2.0 \sigma(I)$], $R_{1_obs} = 0.031$, Goodness of fit = 1.05. Crystallographic data (excluding

structure factors) for **15b** have been deposited with the Cambridge Crystallographic Data Center as supplementary publication number CCDC 871209.

6.4 Pharmacology methods

MABA and LORA assay:

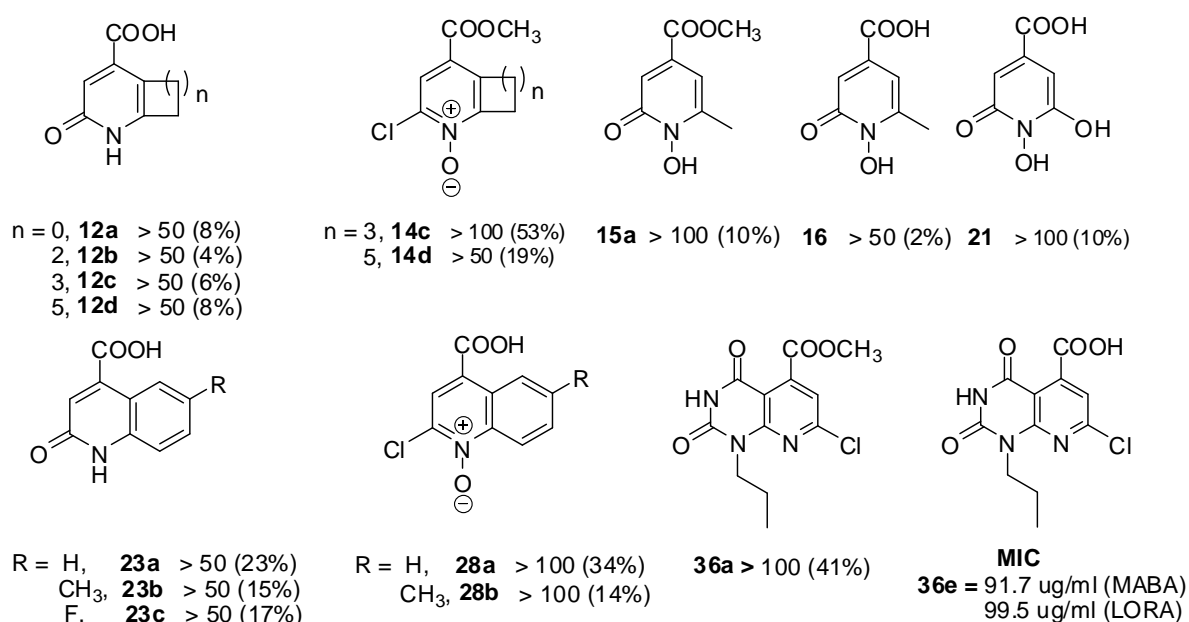
Activity against replicating *M. tuberculosis* H₃₇Rv (ATCC 27294, American Type Culture Collection, Rockville, MD) was determined using a fluorescence readout in the Microplate Alamar Blue Assay (MABA) following incubation for one week with test compounds in glycerol-alanine-salts medium (GAS) as well as in medium without added iron but with Tween 80 (GAST). The MIC was defined as the minimum concentration inhibiting fluorescence by 90% relative to bacteria-only controls. Activity against non-replicating *M. tuberculosis* was determined using the Low-Oxygen Recovery Assay (LORA) by exposing low-oxygen adapted *M. tuberculosis* containing a luciferase gene to test compounds under anaerobic conditions for 10 days. After a 28 h recovery in air, the luciferase signal was measured. MIC was defined as the lowest concentration inhibiting recovery of luciferase signal, greater or equal to 90% relative to bacteria-only controls.

Briefly, the test compound MICs against TB were assessed by the MABA using INH, Moxifloxacin and SM as positive controls. Compound stock solutions were prepared in DMSO at a concentration of 12.8 mM, and the final test concentrations ranged from 100 to 0.5 μ M. 2-fold dilutions of compounds were prepared in Middlebrook 7H12 medium (7H9 broth containing 0.1% w/v casitone, 5.6 μ g/mL palmitic acid, 5 mg/mL bovine serum albumin, 4 mg/mL catalase, filter-sterilized) in a volume of 100 μ L in 96-well microplates (black viewplates). *Mtb* H37RV (100 μ L inoculum of 2×10^5 cfu/mL) was added, yielding a final testing volume of 200 μ L. The plates were incubated at 37 °C. On the 7th day of incubation 12.5 μ L of 20% Tween 80 and 20 μ L of Alamar Blue (Trek Diagnostic, Westlake, OH) were added to the test plate. After incubation at 37 °C for 16–24 h, fluorescence of the wells was measured (ex 530, em 590 nm). The MICs were defined as the lowest concentration effecting a reduction in fluorescence of $\geq 90\%$ relative to the mean of replicate bacteria-only controls.

Cytotoxicity assay:

Vero cells (ATCC CRL-1586) were cultured in 10% fetal bovine serum (FBS) in minimum essential medium Eagle. J774A.1 cells were cultured in 10% FBS in Dulbecco's modified

Eagle's medium (DMEM). The cells were incubated at 37 °C under 5% CO₂ until confluent and then diluted with phosphate-buffered saline to 10⁶ cells/mL. In a transparent 96-well plate (Falcon Microtest 96), threefold serial dilutions of the macrolide stock solutions resulted in final concentrations of 102.4 to 0.42 μM in a final volume of 200 μL. After incubation at 37 °C for 72 h, medium was removed and monolayers were washed twice with 100 μL of warm Hanks' balanced salt solution (HBSS). One hundred microliters of warm medium and 20 μl of freshly made MTS-PMS [3-(4,5-dimethylthiazol-2-yl)-5-(3-carboxymethoxyphenyl)-2-(4-sulfophenyl)-2-tetrazolium and phenylmethasulfazone] (100:20) (Promega) were added to each well, plates were incubated for 3 h, and absorbance was determined at 490 nm.



Foot note: *In vitro* data generated for all the compounds using Microplate Alamar Blue Assay (MABA) with 50 μg/mL, 100 μg/mL concentrations of the compounds. Percentage of inhibition was mentioned in brackets. For potent active molecules MIC values were calculated.

6.5 Docking procedure: The SDHmt Protein Homology Model was used as the receptor for docking. SDHmt Protein was protonated (Addition of Hydrogen atoms) with protonation 3D application in MOE, Connolly Molecular surface was generated around the ligand site of the protein, Gasteiger Partial charges was added to the protein and finally energy minimization was performed to relieve the bad crystallographic contacts. "Active site finder" function of the MOE software was used to denote potential docking pockets within the protein crystal structure. All the molecules were placed in the active site pocket of the protein by the

“Triangle Matcher” method, which generates poses by aligning the ligand triplet of atoms with the triplet of alpha spheres in cavities of tight atomic packing. The dock scoring was performed with London dG method and then finally retaining and scoring the best 10 poses of molecules. The preparation of ligands for docking simulation involved the energy minimization with Molecular Mechanics Force-field MMFF94x (Merck Molecular Force Field) and then molecules were subjected to conformational search in MOE using the Conformations Stochastic search module to find the lowest Energy Conformers. The docking results were appear as docking score in which the docking poses were ranked by the Molecular Mechanics and Generalized Born solvation model (MM/GBVI) binding free energy. RMSD of the docking pose compares the docking poses to the ligand in the co-crystallized structure.^{33, 34, 35}

References:

1. WHO Report http://whqlibdoc.who.int/publications/2011/9789241564380_eng.pdf
2. J. C. Sherris ed., *Medical Microbiology: An Introduction to Infectious Diseases*, Second ed. (Elsevier, New York, 1990).
3. Schroder, K.; Hertzog, P. J.; Ravasi, T. *Journal of Leukocyte Biology*, **2004**, *75*, 163.
4. Bloom, B. R.; Murray, C. J.; *Science*, **1992**, *257*, 1055.
5. (a) Global tuberculosis control: epidemiology, strategy, financing. WHO report 2009, Geneva, World Health Organization, 2009 (WHO/HTM/TB/2009.411). (b) WHO Report. http://www.who.int/tb/publications/global_report/2009/update/en/index.html
6. WHO Report. http://www.who.int/tb/publications/global_report/2009/summary/en/index.html
7. (a) WHO (1996) Guidelines on the Management of Drug-Resistant Tuberculosis. WHO/TB/96.210. Geneva: WHO. (b) Hayward AC, Bennett DE, Herbert J et al. (1996) Risk factors for drug resistance in patients with tuberculosis in England and Wales 1993–4. *Thorax*, *51* (Suppl 3), A8.
8. Mandavilli, A. *Nat. Med.* **2007**, *13*, 271.
9. (a) Singh, S. A.; Christendat, D. *Biochemistry*. **2006**, *45*, 7787-7796. (b) Maeda, H.; Dudareva, N. *Annu. Rev. Plant Biol.* **2012**, *63*, 73–105.
10. Bohm, B. A. Shikimic acid (3, 4, 5-trihydroxy-1-cyclohexene-1-carboxylic acid). *Chem. Rev.* **1965**, *65*, 435–66.

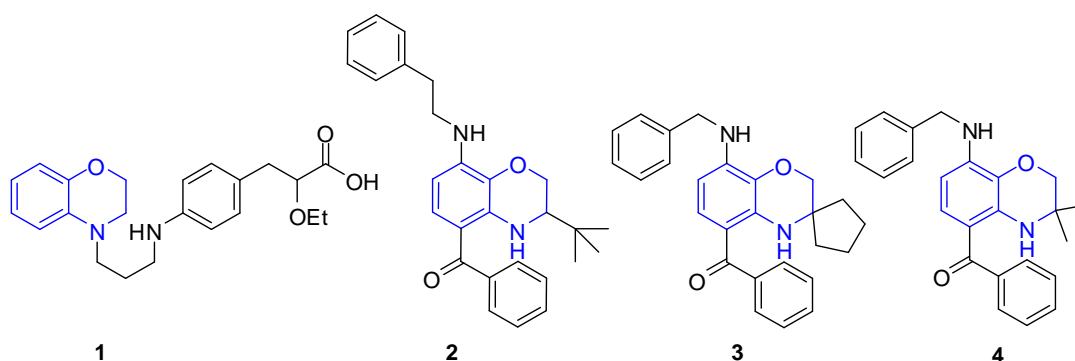
1. Macheroux, P.; Schmidt, J.; Amrhein, N.; Schaller, A. A unique reaction in a common pathway: mechanism and function of chorismate synthase in the shikimate pathway. *Planta*, **1999**, *207*, 325–34.
2. Baillie, A. C.; Corbett, J. R.; Dowsett, J. R.; McCloskey, P. *Biochem. J.* **1972**, *126*, 21P.
3. Stokstad, E. *Science*. **2000**, *287*, 2391.
4. Balinsky, D.; Davies, D. D. *Biochem. J.* **1961**, *80*, 292-296.
5. Baillie, A. C.; Corbett, J. R.; Dowsett, J. R.; McCloskey, P. *Pestic. Sci.* **1972**, *3*, 113.
6. Floss, H. G.; Onderka, D. K.; Carroll, M. J. *Biol. Chem.* **1972**, *247*, 736.
7. Bugg, T. D.H.; Abell, C.; Coggins, J. R. *Tetrahedron Lett.* **1988**, *29*, 6779-6782.
8. Havas, F.; Leygue, N.; Danel, M.; Mestre, B.; Picard, C. G. C. *Tetrahedron*. **2009**, *65*, 7673.
9. Hundscheid, A. F. J.; Engberts, J. B. F. N. *J. Org. Chem.* **1984**, *49*, 3088.
10. Isler, O.; Gutmann, H.; Straub, O.; Fust, B.; Bohni, E.; Studer, A. *Helv. Chim. Acta* **1955**, *38*, 1033.
11. Hirota, K.; Kitade, Y.; Senda, S.; Halat, J. M.; Watanabe, A. K.; Fox, J.J. *J. Org. Chem.* **1981**, *46*, 846.
12. Baillie, A.C.; Dowsett, J.R.; McCloskey, P.; *Pestic.Sci.* **1972**, *3*, 113.
13. Mello, J. V.; Finney, N. S. *J. Am. Chem. Soc.* **2005**, *127*, 10124.
14. Zhu, X.; Kreutter, K.D.; Hu, H.; Player, M.R.; Gaul, M.D. *Tetrahedron Lett.* **2008**, *49*, 832.
15. a) El Ashrya, E. S. H.; Ramadan, E. S.; Hamida, H. A.; Hagara, M. *Synth. Commun.* **2005**, *35*, 2243. b) Feldman, K.S.; Coca, A. *Tetrahedron Lett.* **2008**, *49*, 2136. c) Zhuravleva, A. Y.; Zimichev, A. V.; Zemtsova, M. N.; Klimochkin, Yu. N. *Russian J. Org. Chem.* **2009**, *45*, 609. d) Biichi, J.; Hurni, H.; Lieberherr, R. *Helv. Chim. Acta* **1950**, *114*, 858.
16. (a) Lowe, J. A.; Ewinga, F. E.; Drozda, S. E. *Synth. Commun.* **1989**, *19*, 3027. (b) Feldman, K.S.; Coca, A. *Tetrahedron Lett.* **2008**, *49*, 2136. (c) Isaac, M.; Slassi, A.; Edwards, L.; Dove, P.; Xin, T.; Stefanac, T. World patent application WO 2008041075, Oct 4, 2008. (d) Mei, F.; Wu, S.-Y.; Wang, Y.-Y.; Kao, I-S. *Yaoxue Xuebao.* **1959**, *7*, 311.
17. Li, J.; Zhang, J.; Chen, J.; Luo, X.; Zhu, W.; Shen, J.; Liu, H.; Xu Shen, Jiang,H. *J. Comb. Chem.* **2006**, *8*, 326.
18. Anderson, G. L.; Shim, J. L.; Broom, A. D. *J. Org. Chem.*, **1976**, *41*, 1095.
19. Collins, L. A.; Franzblau, S. G. *Antimicrob. Agents Chemother.* **1997**, *41*, 1004.

20. Cho, S.H.; Warit, S.; Wan, B.; Hwang, C. H.; Pauli, G. F.; Franzblau, S. G. *Antimicrob. Agents Chemother.* **2007**, *51*, 1380.
21. Macabeo, A. P. G.; Vidar, W .S.; Chen, X.; Decker, M; Heilmann, J.; Wan, B.; Franzblau, S .G.; Galvez, E .V.; Aguinaldo, M .A .M.; Cordell, G .A. *Eur. J. Med. Chem.* **2011**, *46*, 3118.
22. Sheldrick, G. M.; SHELX-97, Program for Crystal Structure Determination, University of Göttingen, **1997**.
23. El-Azab, A. S.; Al-Omar, M. A.; Abdel-Aziz, A. A.-M.; Abdel-Aziz, N, I.; El-Sayed, M. A.-A.; Aleisa, A. M.; Sayed-Ahmed, M. M.; Abdel-HamideS. G.; *Eur. J. Med. Chem.***2010**, 4188.
24. Galal, S. A.; Abdelsamie, A. S.; Tokuda, H.; Suzuki, N.; Lida, A.; ElHefnawi, M. M.; Ramadan , R. A.; Atta, M. H.E.; El Diwani, H. I.; *Eur. J. Med. Chem.* **2011**, *42*, 327.
25. Levital, J.; Istyastono, E. P.; Nawawi, A.; Mutholib, A.; Iwan J.P. de Esch.; Ibrahim, S.; *ITB J. Sci.* **2009**, *41 A*, 110.

3. Novel synthesis of 2*H*-benzo[*b*][1,4]oxazines via sequential C-N and C-O bond formation in single pot & their pharmacological evaluation as anti inflammatory agents

3.1 Introduction

1,4-Benzoxazine is a heterocyclic scaffold of paramount importance to human race. Several 1,4-Benzoxazine derivatives isolated from natural resources or prepared synthetically are significant with respect to medicinal chemistry and biomedical use. Indeed, 1,4-Benzoxazines have been part of molecular skeletons for the design of biologically active compounds, ranging from herbicides and fungicides to therapeutically usable drugs (Figure 1).¹ A literature survey provided/identified several 1,4-benzoxazine compounds (Fig. 1) in the development phase as potential new drugs. Novel 1,4-benzoxazine derivative **1**² possesses peroxisome proliferator activated receptor α (PPAR α) and PPAR γ agonist activity and could be used in treating diabetes, hyperlipidemia and other diabetic complications. French investigators recently introduced new 8-arylalkylamino-1,4-benzoxazine neuro-protectants **2**, **3** and **4**.³ Schering has disclosed 1,4-benzoxazines **5**⁴ and **6**⁵ as inhibitors of nitric oxide synthase (NOS) which are potential drugs for treating neurodegenerative, inflammatory, autoimmune and cardio-vascular disorders. 1,4-Benzoxazine **7**⁶ inhibits the coagulation serine proteases factor Xa. 2*H*-benzo[*b*][1,4] oxazine **8**⁷ as hypoxia targeted compounds for cancer therapeutics.⁷



The research results suggested that 1,4-Benzoxazine and related compounds are a plentiful source of potential anti-cancer, anti diabetic, anti inflammatory drugs deserving further study.

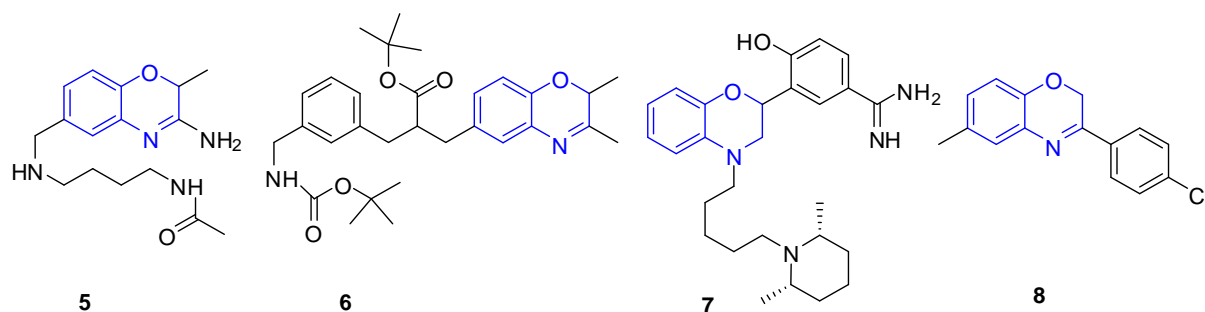
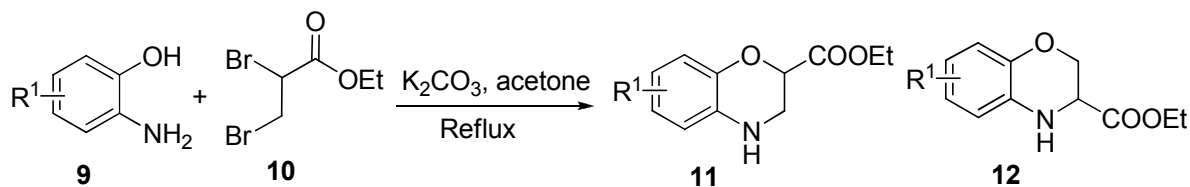


Figure 1: Therapeutically usable drugs with 1,4-benzoxazine core structures

3.2 Literature reports for synthesis of 1,4-benzoxazines

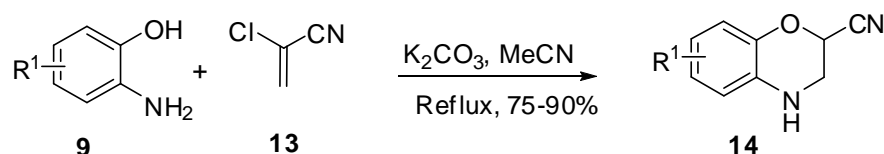
Substituted 2-aminophenols are classical starting compounds for the synthesis of 3, 4-dihydro-2*H*-1,4-benzoxazines.

J. Y. Me´rouer et al. described an environmentally friendly and highly efficient procedure for the synthesis of substituted 3,4-dihydro-2*H*-1,4-benzoxazines as shown in Scheme 1. The reaction of substituted 2-aminophenols **9** with ethyl 2,3-dibromopropionate (**10**) affords, depending on the substituent's on the aromatic ring, ethyl 3,4-dihydro-2*H*-1,4-benzoxazine-2-carboxylates (**11**) as the main, and ethyl 3,4-dihydro-2*H*-1,4-benzoxazine-3-carboxylates (**12**) as the minor, isomers. In the case of the unsubstituted 2-aminophenol, the ratio between the isomers is 20:1.⁸



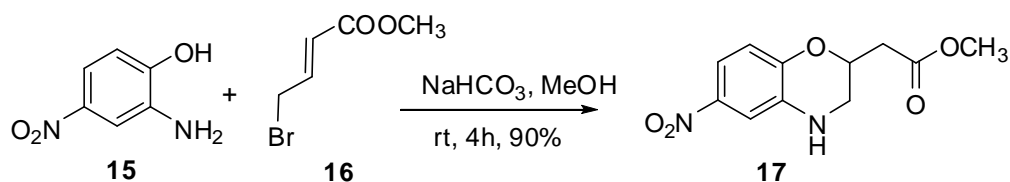
Scheme 1

J. Y. Merour et al. demonstrated that 2-cyano-3,4-dihydro-2*H*-1,4-benzoxazines **14**⁹ can be obtained by a ring-closure reaction following the pathway presented in Scheme 2. The reaction of substituted 2-aminophenols **9** and 2-chloroacrylonitrile (**13**) under reflux in acetonitrile for 18 h in the presence of K_2CO_3 provided 2-cyano-3,4-dihydro-2*H*-1,4-benzoxazine derivatives (**14**) in good yield.⁹



Scheme 2

M. Varasi et al. reported synthesis of integrin receptor antagonists; the key intermediate **17**¹⁰ was prepared in a reaction of methyl (2*E*)-4-bromobut-2-enoate (**16**)

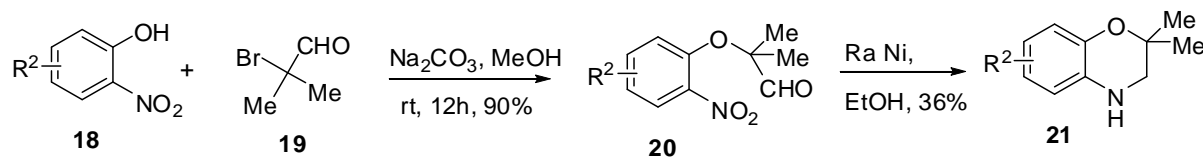


Scheme 3

with 2-amino-phenol **15** via an intramolecular Michael addition (Scheme 3).

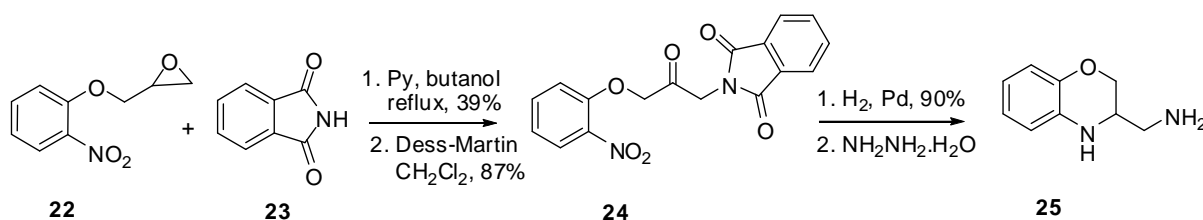
In the recent times several 2-Nitro Phenols have been successfully used for ring closure to 3,4-dihydro-2H-1,4-benzoxazines by a reductive amination reaction.¹¹

T. Fujikura et al. reported that, 2-bromo-2-methylpropanal (**19**) can be used for O-alkylation of 2-nitrophenols (**18**) to give the phenolic ethers (**20**) which are reduced, with concomitant intermolecular reductive amination, yielding 3,4-dihydro-2H-1,4-benzoxazines **21** (Scheme 4).¹¹



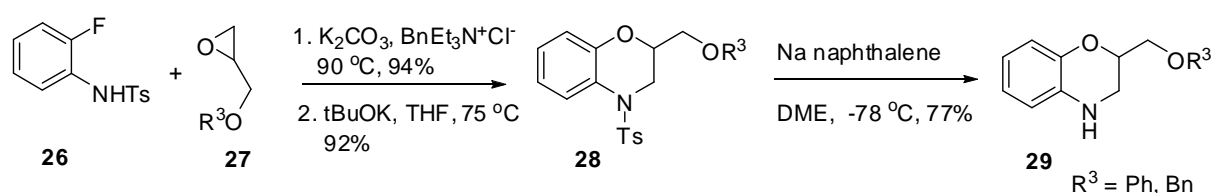
Scheme 4

1-(3,4-Dihydro-2H-1,4-benzoxazin-3-yl) methanamine **25** is used as intermediate in the synthesis of pyrazino [2,1-c]-1,4-benzoxazines, ligands for the α_1 -adrenergic receptor reported by Minneman, K. P and co-workers.¹² Epoxide **22** is opened by Phthalimide **23**, giving the alcohol, which is oxidized by the Dess–Martin reagent to the ketone **24**. Reduction of the nitro group of **24** and concomitant cyclization by reductive amination subsequently deprotection by hydrazinolysis to afford the amine **25** (Scheme 5).



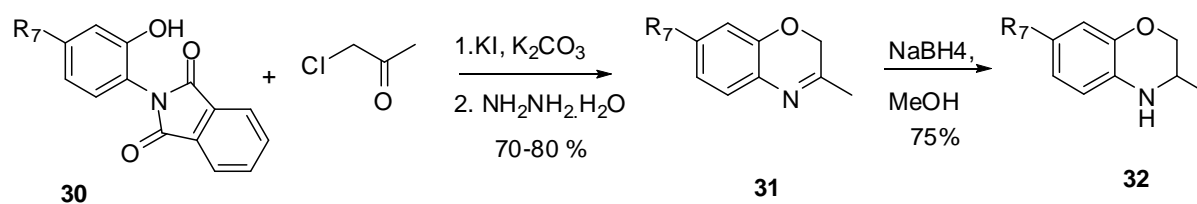
Scheme 5

A novel synthesis of 2-phenoxyethyl-3,4-dihydro-2*H*-1,4-benzoxazine (**29**; R₃ = Bn, Ph), through formation of the C–O and C–N bonds, involves ring-opening of glycidol **27** with the N-nucleophile formed from 2-fluoro-*N*-tosylaniline (**26**) under phase-transfer catalysis, and subsequent intramolecular nucleophilic substitution of fluoride promoted by a non-nucleophilic strong base. Cleavage of the *N*-tosyl protecting group of **28** with sodium/naphthalene in dimethyl ether (DME) affords the 2-substituted 1,4-benzoxazines **29** (Scheme 6).¹³



Scheme 6

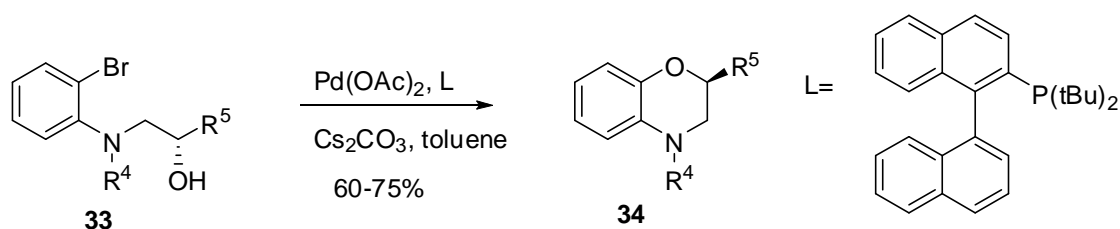
G. E. Zurenko and co workers disclosed that O-alkylation of the 2,5-diaminophenol derivative (**30**) with 1-chloroacetone affords the phenoxyacetate as intermediate in which the protecting groups are removed by hydrazinolysis and the obtained phenylenediamine intermediate undergoes cyclization, yielding the 2*H*-1,4-benzoxazine derivative (**31**), which was reduced to 3-methyl-3, 4-dihydro-2*H*-1,4-benzoxazin-7-amine (**32**), an intermediate in the synthesis of antibacterial agents.¹⁴



Scheme 7

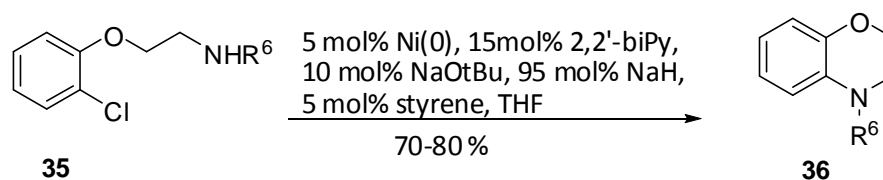
More recently, the formation of aryl C–X bonds (X = N, O, S, etc) by metal mediated coupling was successfully extended to the preparation of many such heterocycles.

S. L. Buchwald and co workers demonstrated Pd-mediated synthesis of 2*H*-1,4-benzoxazines. 3,4-Dihydro-2*H*-1,4-benzoxazines (**34**)¹⁴ were synthesized by intramolecular C–O bond formation using palladium-catalyzed intramolecular etherification of aryl halides (**33**) employing di-*tert*-butyl phospho biaryl ligands (L) and palladium (II) acetate (Scheme 8).



Scheme 8

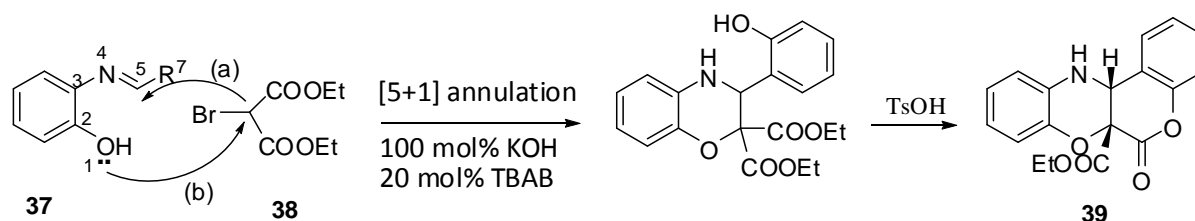
Y. Fort. et al. reported that Nickel-mediated intramolecular amination of aryl chlorides **35** yields 3,4-dihydro-2H-1,4-benzoxazines **36** as shown in Scheme 9 by the in situ-generated Ni (0) catalyst associated with 2,2'-bipyridine.¹⁵



Scheme 9

A series of functionalized 2,3-dihydro-1,4-benzoxazines were obtained in moderate to excellent yields *via* domino [5 + 1] annulations.

W. D. Zhu and co workers revealed the domino [5 + 1] annulations of imines **37** with 2-halo-1,3-dicarbonyl compounds **38** under mild conditions (scheme 10). They have applied this method in the synthesis of bioactive analogues, such as functionalized tetracyclic-1,4-benzoxazines (**39**) which contain two new heterocyclic rings and quaternary carbon centers has also been developed.¹⁶



(a) Mannich reaction; (b) Alkylation; R⁷ : 2-hydroxy phenol

Scheme 10

3.3 Dearomatization of arenes

Despite the high resonance energy of the benzene ring, a number of examples of dearomatization by microorganisms either through oxidation (oxygenases) or reduction (reductases) exist in nature.¹⁷

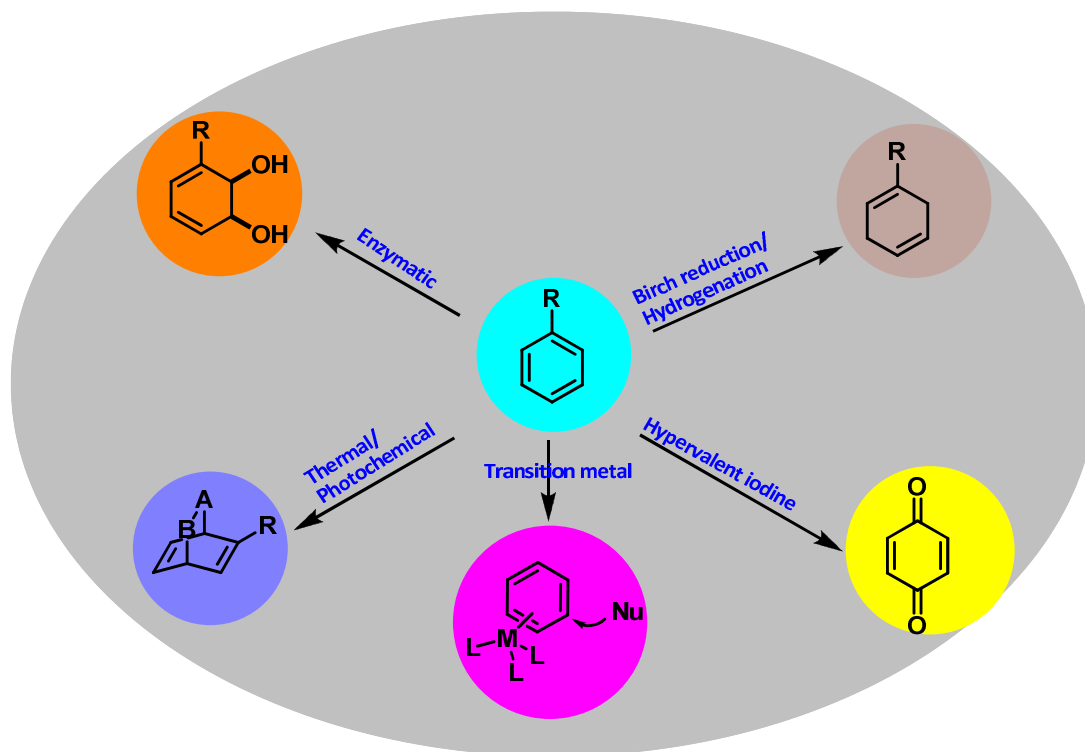
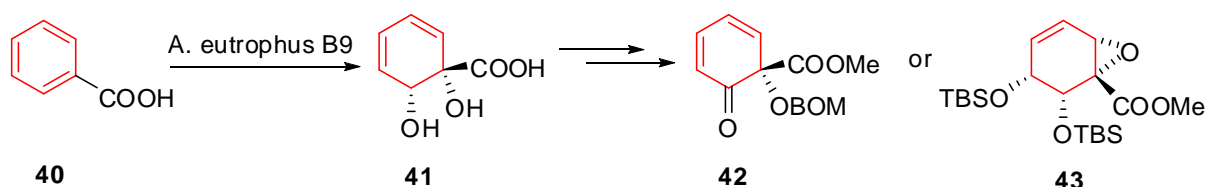


Figure 2: Back ground of dearomatization reactions

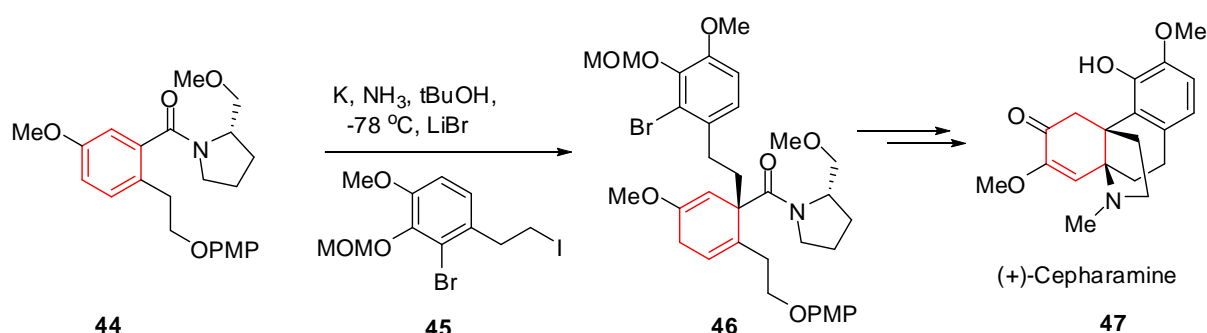
Upon dearomatization of aromatic and heteroaromatic derivatives, highly reactive intermediates are generally produced leading to facile formation of carbon–carbon and carbon–heteroatom bonds, spontaneous cycloadditions, and cascade reactions. As shown in figure 2, a number of strategies for dearomatization have been utilized by organic chemists during the course of complex total syntheses.

Myers and co-workers applied a chemo enzymatic method for arene dearomatization by the dihydroxylation of benzoic acid (**40**) using the bacterium *A. eutrophus* affording 1, 2-dihydroxycyclohexadiene (**41**) with high enantioselectivity (Scheme 11).¹⁸ The simple, dearomatized dihydroxycyclohexadiene (**41**) was parlayed into a number of useful chiral building blocks (e.g. **42** and **43**) for use in total synthesis and demonstrates the utility of enzymatic dearomatization.



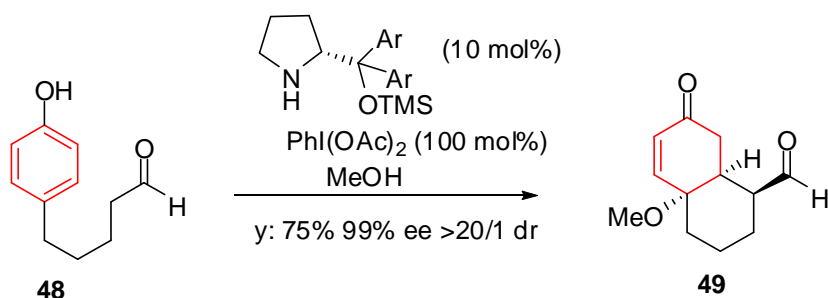
Scheme 11

Schultz and co-workers, pioneers of the diastereoselective Birch reduction/alkylative dearomatization process, reported the first enantioselective synthesis of the alkaloid (+) - Cepharamine (**47**; scheme 12).¹⁹ Their route employed a diastereoselective Birch reduction of chiral benzamide **44** to access a chiral enolate intermediate which was alkylated in situ with iodide **45** to afford 1, 4-cyclohexadiene **46** in 95% yield as a single diastereomer.



Scheme 12

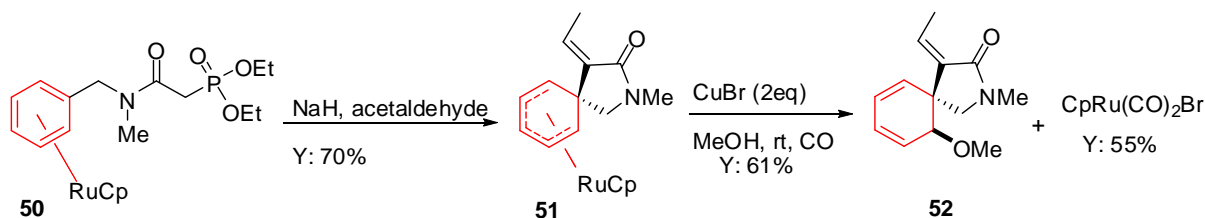
M J. Gaunt et al discussed a process that directly converts a para-substituted phenol (**48**) to a highly functionalized chiral molecule via oxidative dearomatization and amine-catalyzed enantioselective desymmetrizing Michael reaction (Scheme 13). This one-step transformation reveals a complex structure (**49**) formed with control of three new stereogenic centers and an array of exploitable orthogonal functionality directly from a flat molecule that is devoid of architectural complexity.²⁰



Scheme 13

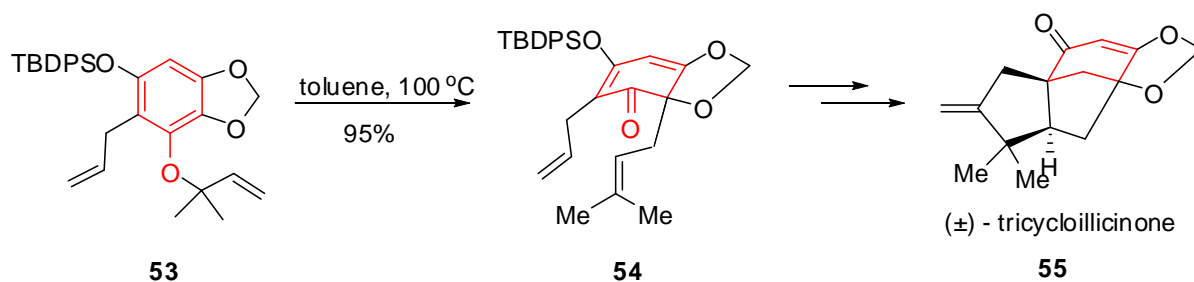
F. Christopher Pigge and co workers reported about the transition metal mediated dearomatization reactions dearomatization through η^6 coordination. Gratifyingly, treatment of **50** in THF (or DMF) with excess NaH at room temperature for 30 min followed by addition of aldehyde afforded the desired azaspirocyclic ruthenium complexes. Deprotonation

of the activated methylene group in the arene ruthenium side chain presumably leads to rapid spirocyclization with nucleophilic aromatic addition occurring exclusively from the face opposite the RuCp fragment.²¹



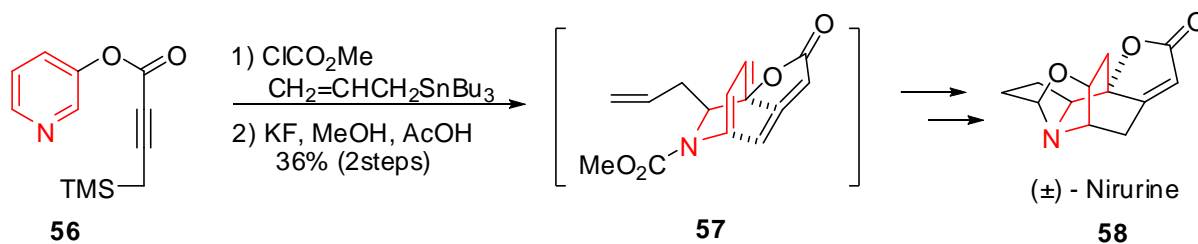
Scheme 14

Danishefsky and co-workers employed a dearomatization strategy involving an *ortho*-Claisen rearrangement (Scheme 15). The rearrangement was conducted using the reverse O-prenylated derivative **53** to furnish the desired dearomatized cyclohexadienone **54**, a precursor of the natural product of tricycloillicinone (**55**).²²



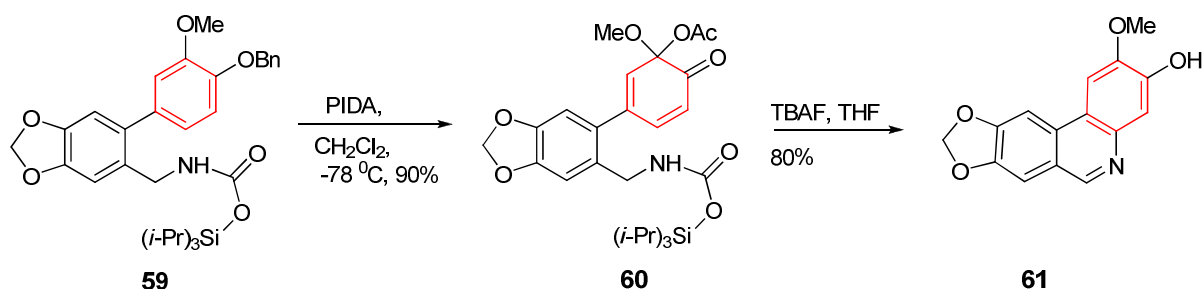
Scheme 15

Finally, an impressive example of pyridinium dearomatization was reported in the early 1990s by Magnus and co-workers in their total synthesis of the pentacyclic alkaloid nirurine (**58**; scheme 16).²³ Synthesis of the azabicyclo-[2.2.2] octane (isoquinuclidine) core of **58** commenced with the alkylative dearomatization at the C₂ position of an acylpyridinium derived from pyridine **56** to introduce an allyl side chain.²⁴ Further desilylation generated allenolate intermediate **57** which participated in intramolecular [4+2] cyclo-addition to furnish the nirurine core structure in two steps as shown in Scheme 16.



Scheme 16

Oxidative dearomatization has been previously adapted to nitrogen-tethered ortho-quinol acetates (**60**) from biphenyl **59** for azacyclization reactions (Scheme 17) for the synthesis of Phenanthridine Alkaloid Motifs (**61**).²⁵



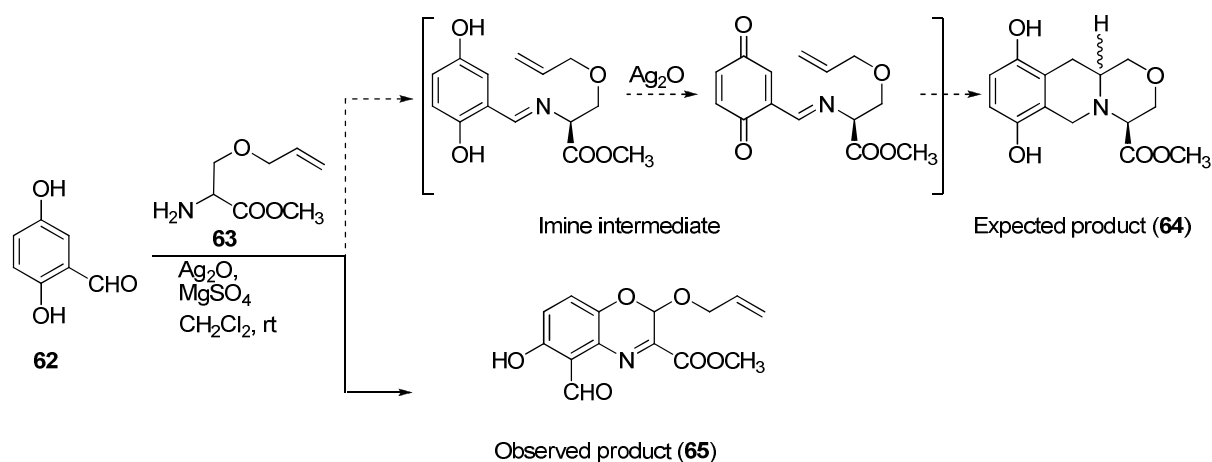
Scheme 17

Prompted by above observations it is evident that, oxidative dearomatization of phenols has been long perceived as an attractive tactic in the design of the syntheses of complex natural products of various kinds. Nevertheless, several previous reports highlighted dearomatization as a powerful strategy for the total synthesis of architecturally complex molecules wherein planar, aromatic scaffolds are converted to three dimensional molecular architectures.²⁶

3.4.1 Our approach for synthesis of 2*H*-benzo[*b*][1,4]oxazines via one pot sequential C-N, C-O bond formation:

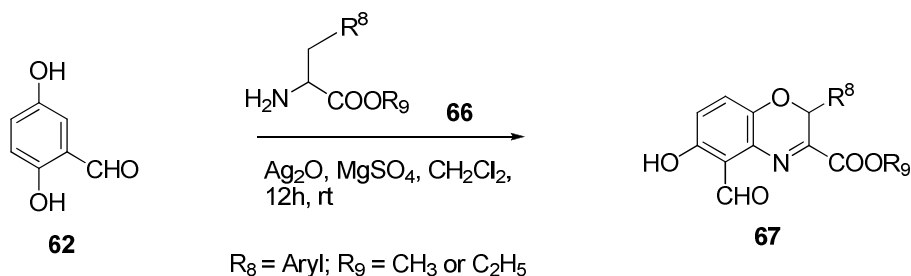
In the light of above classical and elaborated examples, the present report puts forward an application of oxidative dearomatization of 2,5-dihydroxy carbonyl compounds using silver oxide²⁷ for synthesis of 2*H*-benzo[*b*][1,4]oxazines that provides an easy access to nitrogen–carbon (N–Cx) and Oxygen–carbon (O–Cy) strategic bonds in a single operation.

In an experiment designed to synthesize the naphthoxazine cycloadduct **64** by intramolecular Diels-Alder cyclisation from an imine precursor of 2,5-dihydroxy benzaldehyde (**62**) and O-allyl serine ester derivative (**63**), we observed that 2*H*-benzo[*b*][1,4]oxazine **65** was obtained as the only product, in good yields (Scheme 18).



Scheme 18: Noval approach for synthesis of *2H*-benzo[*b*][1,4]oxazines

This new finding lead us to apply the similar reaction conditions to esters of other natural amino acids (**66**) which contain a β -aryl substituent like phenylalanine and tryptophan esters. We were pleased to obtain *2H*-benzo[*b*][1,4] oxazines in good to excellent yields in all the cases (Table 1).



Scheme 19: Generalised scheme for synthesis of *2H*-benzo[*b*][1,4] oxazines

However tyrosine ester did not cyclize to a similar product (entry 1, Table 2). We have attributed this observation to oxidation of hydroxyl moiety in tyrosine in presence of silver oxide. Thus we chose to prepare different derivatives of tyrosine with an electron-releasing and electron withdrawing groups and apply the same reaction conditions. Quantitative yields of *2H*-benzo[*b*][1,4]oxazines were obtained from aminoester derivatives possessing electron donating groups (entry 2, Table 2) and no such product was observed with the electron withdrawing counterparts (entry 3, Table 2). Therefore we presumed that the reaction mechanism is influenced by the electronic factors of the β -aryl ring which merits further validation.

Table 1. Synthesis of 1,4- benzoxazines from quinol and natural amino acid derivatives

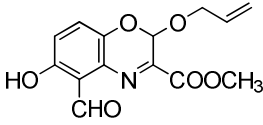
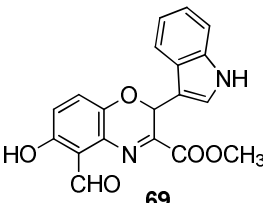
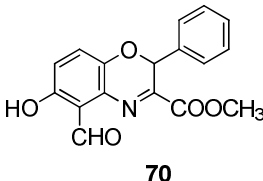
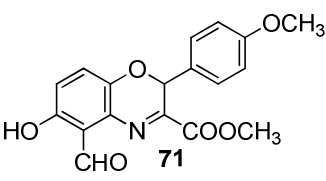
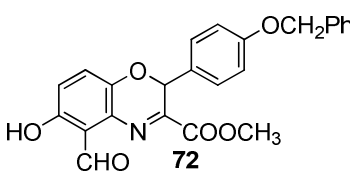
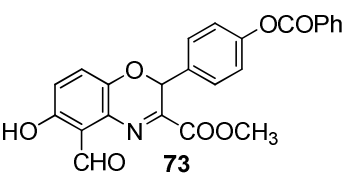
Entry	R ⁸	product	yield (%)
1	O-CH ₂ -CH=CH ₂	 68	52
2	3'-indolyl	 69	70
3	phenyl	 70	75 ^a

Table 2. Synthesis 2*H*-benzo[*b*][1,4]oxazine from quinol and tyrosine derivatives

Entry	R ⁸	product	yield (%)
1	<i>p</i> -OH C ₆ H ₄ ,	—	NR ^a
2	<i>p</i> -H ₃ CO C ₆ H ₄ ,	 71	92
3	<i>p</i> -H ₃ COCC ₆ H ₄ ,	—	NR
4	<i>p</i> -PhCH ₂ O C ₆ H ₄ ,	 72	10
5	<i>p</i> -OCOPh C ₆ H ₄ ,	 73	50

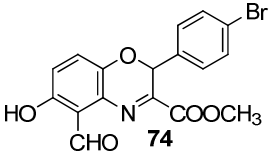
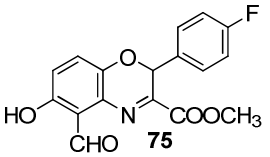
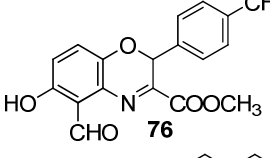
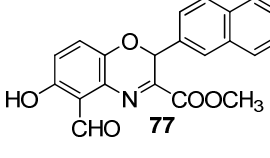
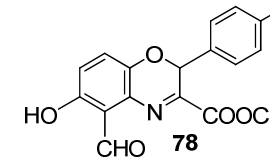
^a No reaction in acetonitrile, methanol and 10% yield in THF with 4 equiv silver oxide; product obtained in 70% yield with THF and 2 equiv silver oxide. b NR: No Reaction

The initial cyclization studies using 4 equiv of silver oxide and dichloromethane as solvent provided the 2*H*-benzo[*b*][1,4]oxazines in good yields. We then attempted further optimization of the reaction conditions using 2 equivalents of silver oxide and CH₂Cl₂, which failed to afford products, except in the case of phenyl alanine (footnote, Table 1). Further, methanol, acetonitrile and THF too have either decreased the yield drastically or failed to afford products. Therefore, we continued using 2 equivalents of silver oxide for the synthesis of 2*H*-benzo[*b*][1,4]oxazines.

We then attempted further optimization of the reaction conditions using 2 equivalents of silver oxide and CH₂Cl₂, which failed to afford products, except in the case of phenyl alanine (footnote, Table 1). Further, methanol, acetonitrile and THF too have either decreased the yield drastically or failed to afford products. Therefore, we continued using 2 equivalents of silver oxide for the synthesis of 2*H*-benzo[*b*][1,4]oxazines. After these optimization studies, we now set out to validate our results using esters of amino acids having withdrawing groupshave been synthesized using the method described in Aldrich.²⁸ These unnatural aminoesters were also subjected to similar reaction conditions and the results are summarized in Table 3.

The observations demonstrated a striking influence of electronic factors in aryl moiety on this transformation. 1,4-benzoxazines were obtained in good yields from aminoesters containing electron-donating moieties (entries 9-14, Table 3). Aminoesters with *p*-CF₃ and *p*-NO₂ substituents on phenyl did not afford the desired 1,4-benzoxazines, thus validating our assumption. We have further observed that 4'-azaphenylalanine ester too did not result in 1,4-benzoxazine formation (footnote, Table 3).

Table 3. Synthesis of 2*H*-benzo[*b*][1,4]oxazines from unnatural amino acid derivatives

Entry	R ⁸	product	yield (%)
1	<i>p</i> -Br C ₆ H ₄ ,	 74	66
2	<i>p</i> -FC ₆ H ₄ ,	 75	58
3	<i>p</i> -CH ₃ C ₆ H ₄ ,	 76	47 ^c
4	1-naphthyl,	 77	70
5	<i>p</i> -CH(CH ₃) ₂ C ₆ H ₄ ,	 78	72
6	<i>p</i> -NO ₂ C ₆ H ₄ ,	---	NR ^d
7	<i>p</i> -CF ₃ C ₆ H ₄ ,	---	NR ^d
8	4'-C ₆ H ₄ N.	---	NR ^d

^c 2 equiv silver oxide in CH₂Cl₂ resulted in only 10% yield, ^d no Reaction

3.4.2 Plausible mechanism:

The most plausible mechanistic pathway delineated for the reaction to account for the formation of the product, is shown in Figure 3. The initial event may be considered as the nucleophilic attack of amine (**66**) in a Michael fashion on the transient enone to generate an intermediate **79**. The intermediate **79** may undergo benzylic oxidation leading to **81** which on dearomatisation provides enone **82** and subsequent electrocyclicization of the latter and eventual re-aromatisation leads to **83** via **82** which further undergoes oxidation to final product **84** (Figure 3).

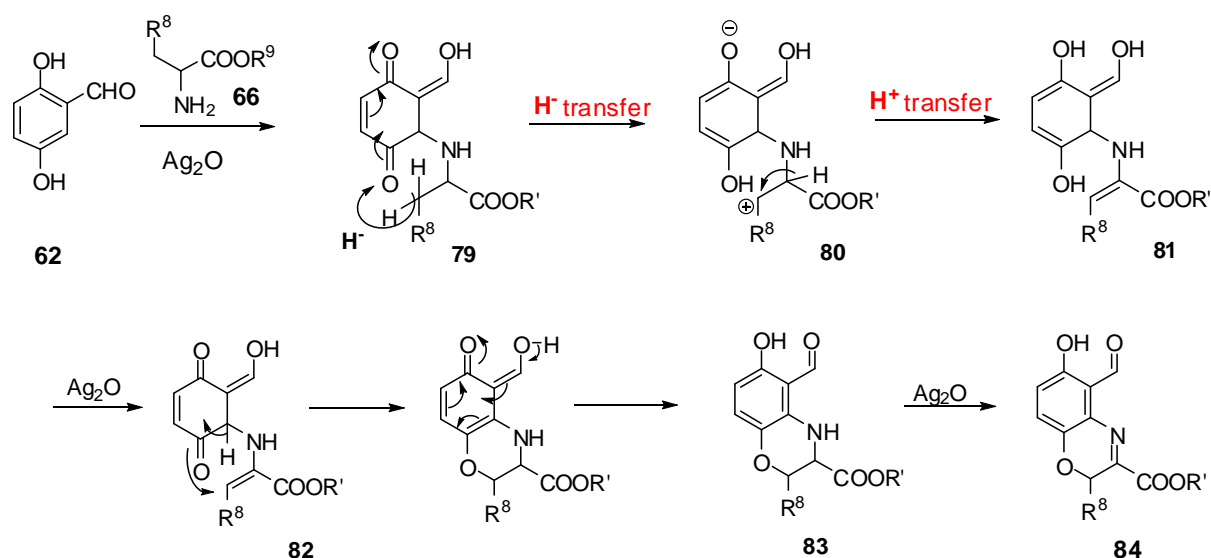


Figure 3. Plausible mechanism for oxidative-dehydrogenation, C-N and C-O bond generation

An electron-rich aryl group can significantly enhance the yield of 2H-benzo[b][1,4]oxazines by an apparent stabilization of benzylic cation (**80**) that may be destabilized by electron-withdrawing substituents on R_8 . The mechanism (formation of **81**) further supported by formation of racemic compounds which is evidenced from the optical rotation $[\alpha]$ value of one of the derivative i.e, **69** found to be zero.

3.4.3 The single crystal X-ray study of 2H-benzo[b][1,4] oxazine **69** :

While all the eleven novel 2H-benzo[b][1,4] oxazines synthesized were characterized by spectral (NMR, IR, MS and HRMS) data the molecular structure of one of the 2H-benzo[b][1,4]oxazines **69** was isolated as bright yellow solid that crystallized well, whose structure was solved by single crystal X-ray diffraction studies (Figure 4).

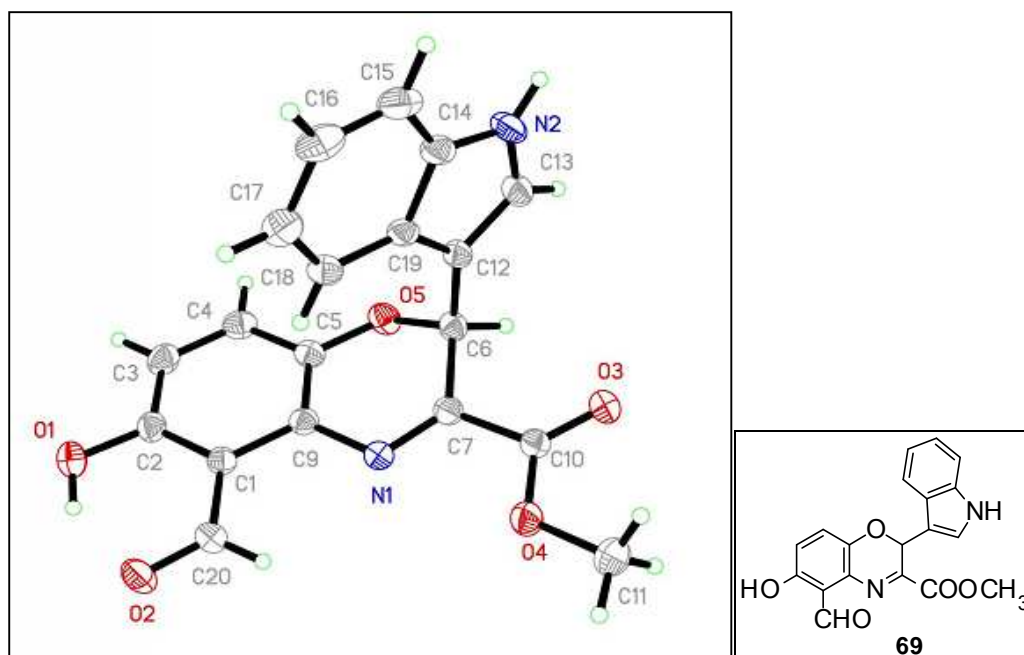


Figure 4. The ORTEP diagram of 2*H*-benzo[*b*][1,4]oxazine **69**

3.4.4 Pharmacology:

Pharmacological testing was performed at the Institute of Life Sciences, in the group of Dr. Kishore V.L. Parsa, University of Hyderabad, India.

All the compounds synthesized were tested for their PDE4B inhibitory activity *in vitro*.¹³ In inflammatory and immune cells, the inhibition of cellular responses, including the production and/or release of proinflammatory mediators, cytokines, and active oxygen species, is associated with elevated levels of cAMP. Since PDE4 (that exists in four different isoforms e.g., PDE4A, B, C and D) plays a key role in the hydrolysis of cAMP to AMP²⁹ hence inhibition of PDE4 should result in elevated levels of cAMP in the air-way tissues and cells thereby suppressing inflammatory cell function. This is supported by the fact that PDE4 inhibitors have been found to be beneficial for the treatment of inflammatory and immunological diseases including asthma and chronic obstructive pulmonary disease (COPD).

Notably, rolipram³⁰ the first-generation PDE4 inhibitor showed adverse effects such as nausea and vomiting. More recently, cardiovascular effects of PDE4 inhibitors have been reported.³¹ While these dose-limiting side effects were reduced by second generation inhibitors like cilomilast³² (Ariflo) and roflumilast, their therapeutic index has delayed

market launch so far. It is therefore necessary to devote a continuing effort in exploring new class of compounds for their PDE4 inhibitory potential.

Moreover, identification of novel small molecules possessing balanced inhibitory properties could be useful in minimizing the adverse side effects. Accordingly, our compounds were evaluated against PDE4B by using PDE4B enzyme isolated from Sf9 cells. Rolipram, a well known inhibitor of PDE4 was used as a reference compound.³³ Among all compounds **74** showed significant inhibition of PDE4B in compared to other molecules when tested at 30 μ M (Table 4).

Table 4: % of inhibition of PDE4B by compounds at 30 μ M

Compound (30 μ M)	% PDE4B Inhibition				% Luciferase Inhibition
	Exp1	Exp2	Exp3	Average	
68	47.53	58.50	30.25	45.42	11.64
69	76.72	70.65	73.68	34.52	28.07
70	70.48	58.70	32.25	53.81	16.13
71	51.87	43.34	47.60	47.58	17.04
72	43.92	78.69	32.37	51.66	13.61
74	65.49	65.64	65.56	65.56	13.55

3.4. 5 Molecular docking studies

Molecular docking studies were done by D. Giridhar Singh at Institute of Life Sciences, India. The docking studies were performed to predict the interactions and binding mode of synthesized molecules with the binding site of human Phosphodiesterase (PDB ID: 3O0J) enzyme. The docking results obtained after docking of these molecules with PDE4B protein is summarized in Table 5 which clearly suggests that these molecules bind well with PDE4B.

Table 5: Glide XP-Parameter contribution to docking score.

Molecule	GScore	LipophilicEvdW	HBond	Electro	PhobEn	LowMW
69	-7.1	-3.9	-0.7	-0.9	-1.3	-0.3
71	-7.0	-4.2	-0.9	-0.6	-1.0	-0.4
74	-7.1	-4.3	-0.9	-0.5	-1.2	-0.2

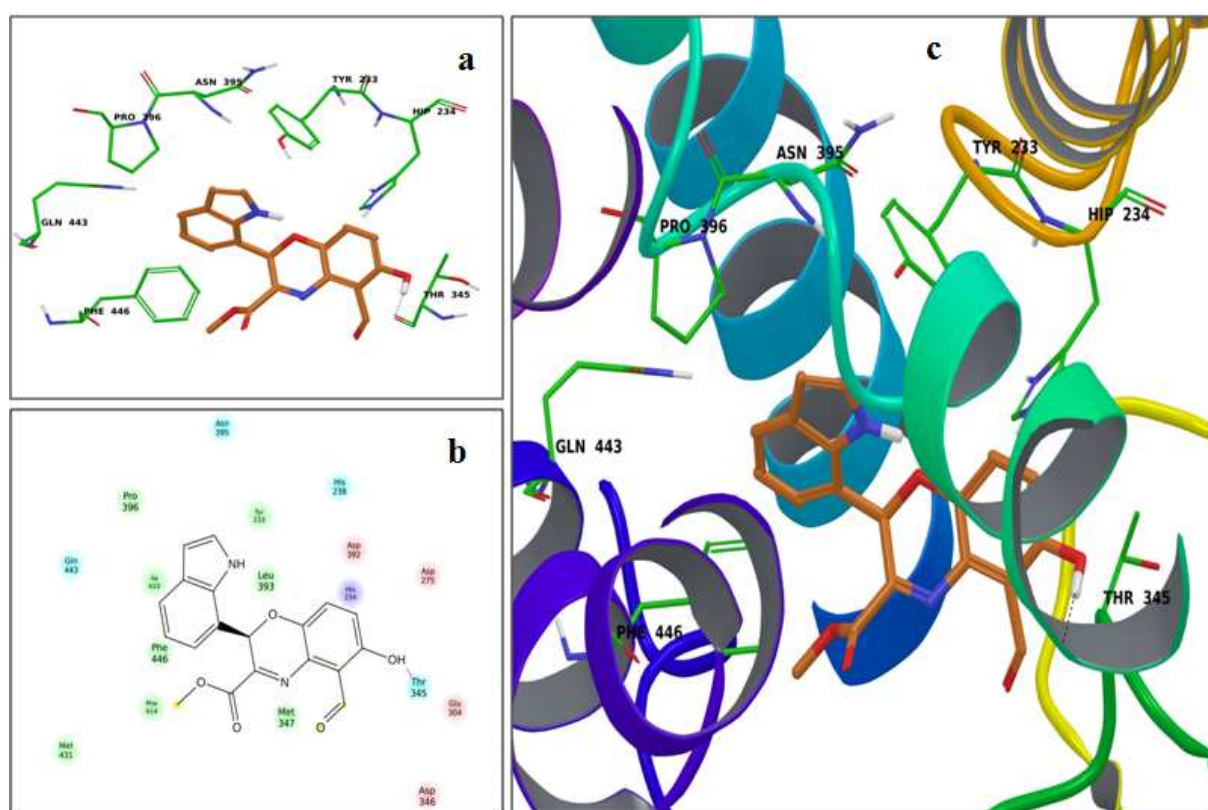


Figure 11: (a) Interaction mode of compound **69** at the binding site of human Phosphodiesterase enzyme showing H-bonding (pink dotted line) with threonine-345. (b) 2D interaction diagram of compound **69** with PDE4B. (c) Binding pose of compound **69** at the binding site of PDE4B protein represented in ribbon form.

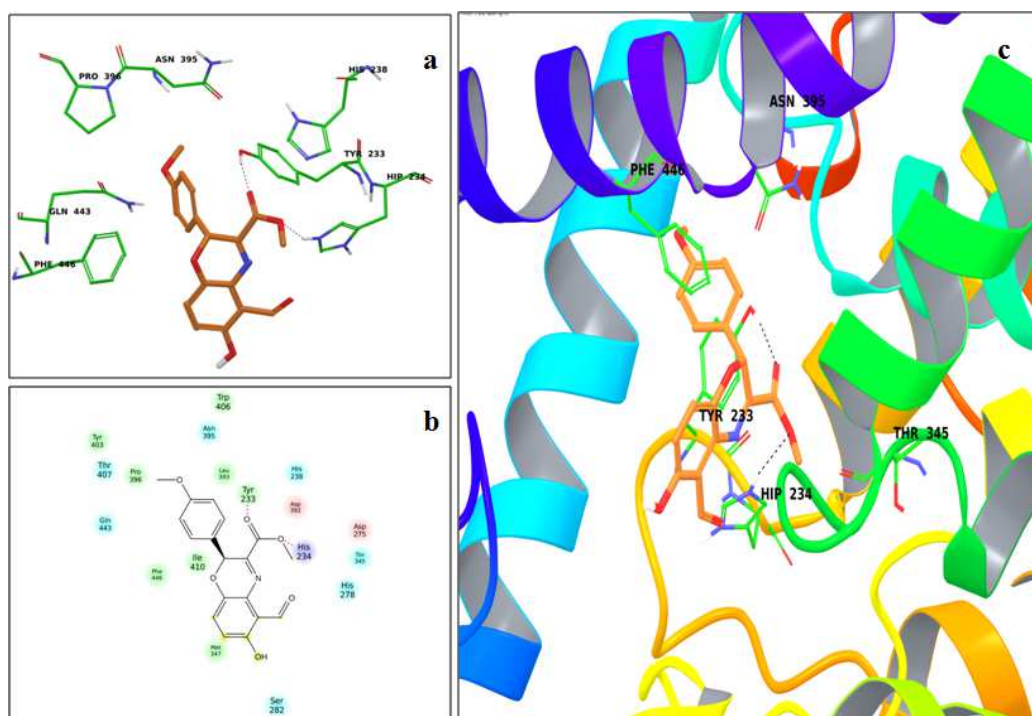


Figure 12: (a) Interaction mode of compound **71** at the binding site of human Phosphodiesterase enzyme showing H-bonding (pink dotted line) with tyrosine-233. (b) 2D interaction diagram of compound **71** with PDE4B. (c) Binding pose of compound **71** at the binding site of PDE4B protein represented in ribbon form

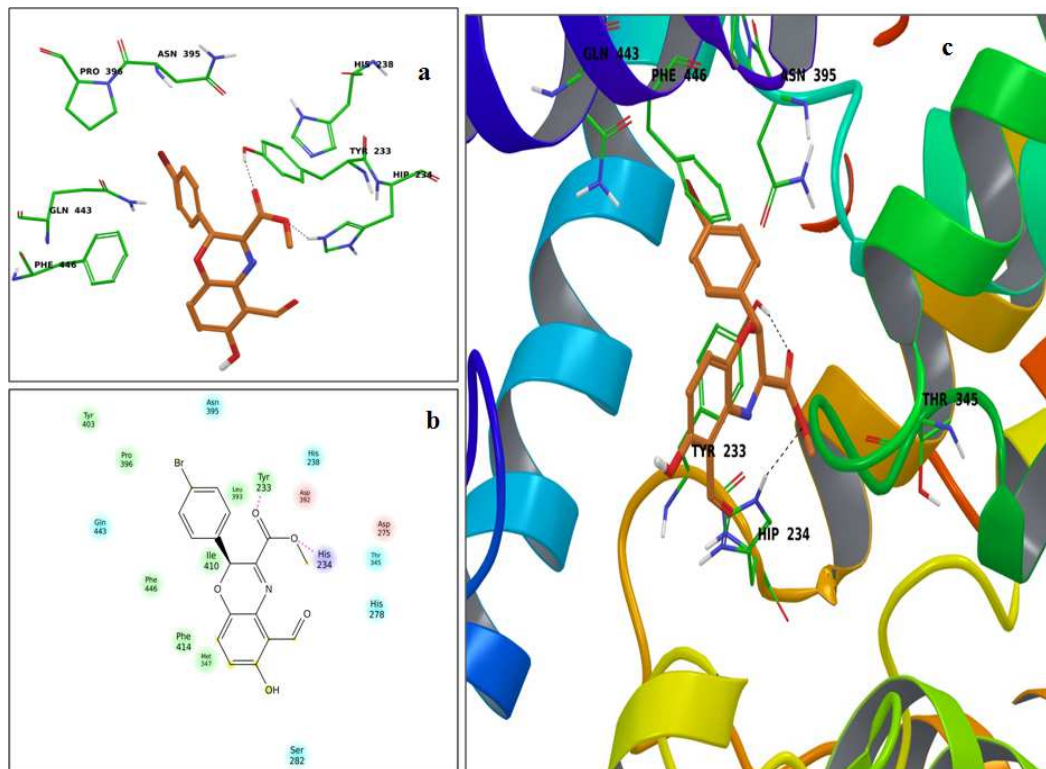


Figure 13: (a) Interaction mode of compound **74** at the binding site of human Phosphodiesterase enzyme showing H-bonding (pink dotted line) with tyrosine-233. (b) 2D interaction diagram of compound **74** with PDE4B. (c) Binding pose of compound **74** at the binding site of PDE4B protein represented in ribbon form.

In case of **69** hydroxyl group of 2*H*-1,4-benzoxazine ring is making perfect H-Bonding with threonine-345 (figure 11). In both the molecules (**71** and **74**) oxygen atom of carbonyl-group is well interacting by H-Bonding with tyrosine-233 and histidine-234 (figure 12 and 13). We also docked the *S*-isomers of **69**, **71** and **74** and the glide docking score (GScore) was found to be -6.9, -6.4 and -5.0, respectively.

3.5 Summary

In conclusion we have demonstrated a facile synthesis of 2*H*-benzo[*b*][1,4]oxazines by sequential generation of C-N, C-O bonds in a single pot *via* oxidative dearomatization of quinols in presence of functionalized amino ester derivatives. Further mechanistic studies of this reaction are underway. All the compounds synthesized were tested for PDE4B inhibitory properties *in vitro* and many of them showed significant inhibition. The docking results suggested that these molecules interact well with PDE4B protein where the ester moiety played a key role in all cases, while the OH of **69** was extended into a hydrophobic pocket.

Overall, novel method for synthesis of 2*H*-benzo[*b*][1,4]oxazines has been identified and further 2*H*-benzo[*b*][1,4]oxazines proved as a new template for the identification of small molecule based novel inhibitors of PDE4B.

3.6. Experimental section

3.6.1 Chemistry - General methods

All reactions were carried out under an inert atmosphere with dry solvents, unless otherwise stated. Reactions were monitored by thin layer chromatography (TLC) on silica gel plates (60 F254), using UV light detection. Visualization of the spots on TLC plates was achieved either by UV light or by staining the plates in 2, 4 Dinitro phenyl hydrazine and Ninhydrin stains charring on hot plate. Flash chromatography was performed on silica gel (230-400 mesh) using distilled hexane, ethyl acetate, dichloromethane.

NMR-Spectroscopy

¹H NMR and ¹³C NMR spectra were recorded in CDCl₃ or acetone-*d*₆ solution by using VARIAN 400 MHz spectrometers. Deuterium exchange studies were done in CD₃OD, DMSO-*d*₆ and D₂O. Chemical shifts are reported as δ values relative to internal CDCl₃ δ 7.26 or TMS δ 0.0 DMSO-*d*₆ δ 2.50 and CD₃OD δ 3.34 for ¹H NMR and CDCl₃ δ 77.0 and CD₃OD δ 49.05 for ¹³C NMR. ¹H NMR data was recorded as follows: chemical shift [multiplicity, coupling constant(s) *J* (Hz), relative integral] where multiplicity is defined as: s

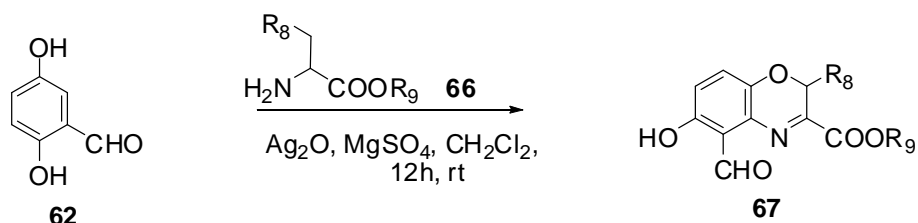
(singlet), d (doublet), t (triplet), q (quartet), dd (doublet of doublet), m (multiplet), bs (broad singlet).

IR spectroscopy, mass spectrometry and melting points

FTIR spectra were recorded on Bruker (Alpha) spectrometer. Mass spectra were recorded on Micro Mass VG-7070H mass spectrometer for ESI and are given in mass units (m/z). High resolution mass spectra (HRMS) [ESI+] were obtained using either a TOF or a double focusing spectrometer. Melting points were determined by using a Buchi melting point B-540 apparatus. Values thus obtained were not corrected.

3.6.2 Syntheses

Typical experimental procedure for synthesis of 2*H*-Benzo [*b*][1,4]oxazines:

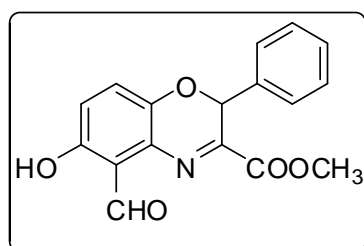


$$\text{R}_8 = \text{phenyl, } p\text{-BrC}_6\text{H}_4, \text{ } p\text{-FC}_6\text{H}_4, \text{ } p\text{-CH}_3\text{C}_6\text{H}_4, \text{ } p\text{-CH}_3(\text{CHCH}_3)\text{C}_6\text{H}_4, \text{ } p\text{-OCH}_3\text{C}_6\text{H}_4, \text{ } p\text{-OCOPhC}_6\text{H}_4, \text{ } \text{OCH}_2\text{PhC}_6\text{H}_4, \text{ } \text{O-allyl}, \text{ } 3'\text{-indolyl}, \text{ } 1\text{-naphthyl}$$

A suspension of **66** (0.179 g, 1 mmol) in anhydrous dichloromethane is cooled in ice bath to 0 °C and neutralised with 1 equiv. triethylamine (if amino acid is HCl salt) (0.15mL, 1 mmol) under constant stirring. 2, 5 dihydroxy benzaldehyde (**62**) (0.138 g, 1 mmol) and Ag₂O (0.924 g, 4 mmol) and anhydrous MgSO₄ (0.120g, 1 mmol), were added consecutively, and stirred at rt for 12h. The mixture was filtered through celite and washed with CH₂Cl₂. Removal of the solvent under reduced pressure followed by column chromatography (10% EtOAc/Hexane) yielded pure 2*H*-benzo[*b*][1,4]oxazines.

2) SPECTRAL DATA FOR NEW COMPOUNDS:

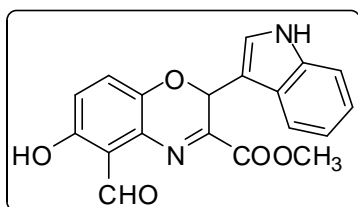
Methyl 5-formyl-6-hydroxy-2-phenyl-2*H*-benzo[*b*][1,4]oxazine-3-carboxylate (**68**):



Yellow oil, Yield(75%), $R_f = 0.5$ (10% EtOAc/Hexane); ¹H NMR (400 MHz, CDCl₃): δ 3.93 (s, 3H), 6.31 (s, 1H), 6.89 (d, $J = 8.8\text{Hz}$, 1H), 7.09 (d, $J = 9\text{Hz}$, 1H), 7.29-7.33 (m, 5H), 10.81(s, 1H), 11.46 (s, 1H); ¹³C NMR (100 MHz, CDCl₃): δ 53.24, 71.87, 114.29, 121.10, 126.10, 127.25, 128.98, 129.58,

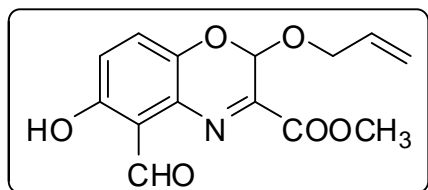
131.59, 134.66, 137.31, 152.88, 157.53, 162.95, 195.87. IR (neat, cm^{-1}): 3426, 2952, 2925, 2855, 1742, 1644, 1251, 1024. Mass (ES) m/z 334.06 ($M+\text{Na}$, 100%); HRMS (ESI): calcd for $\text{C}_{17}\text{H}_{13}\text{NO}_5\text{Na}$ ($M+\text{Na}$)⁺ 334.0691 found 334.0679.

Methyl 5-formyl-6-hydroxy-2-(1*H*-indol-3-yl)-2*H*-benzo[*b*][1,4]oxazine-3-carboxylate (69):



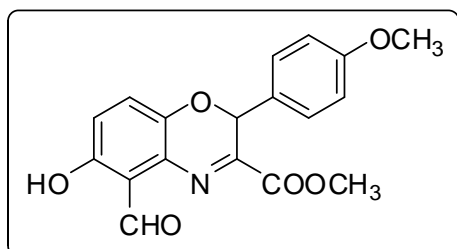
Light yellow solid (mp: 186.0 °C), Yield (70%), R_f = 0.48 (10% EtOAc/Hexane); ^1H NMR (400 MHz, CDCl_3): δ 3.90 (s, 3H), 6.71 (s, 1H), 6.81 (s, 1H), 6.83 (s, 1H), 6.95 (d, J = 2.4Hz, 1H), 7.09 (d, J = 8Hz, 1H), 7.22 (d, J = 2.4Hz, 1H), 7.32 (d, J = 2.4Hz, 1H), 7.87 (d, J = 2.4Hz, 1H), 8.15 (bs, 1H), 10.88 (s, 1H), 11.46 (s, 1H); ^{13}C NMR (100 MHz, CDCl_3): δ 53.22, 65.67, 111.48, 119.24, 120.58, 123.17, 124.97, 126.73, 132.23, 136.57, 152.68, 157.46, 162.34, 195.97. IR (neat, cm^{-1}): 3402, 3049, 2923, 2851, 1737, 1649, 1262, 1021. Mass (ES) m/z 373.07 ($M+\text{Na}$, 100%); HRMS (ESI): calcd for $\text{C}_{19}\text{H}_{14}\text{N}_2\text{O}_5\text{Na}$ ($M+\text{Na}$)⁺ 373.0800 found 373.0788.

Methyl 2-(allyloxy)-5-formyl-6-hydroxy-2*H*-benzo[*b*][1,4]oxazine-3-carboxylate (70):



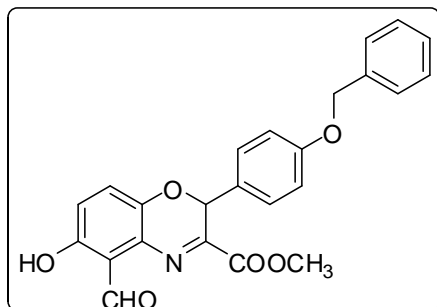
Colorless oil, Yield (52%), R_f = 0.42 (10% EtOAc/Hexane); ^1H NMR (400 MHz, CDCl_3): δ 3.98 (s, 3H), 4.28 (d, J = 5.6 Hz, 2H), 5.24-5.33 (m, 2H), 5.81-5.91 (m, 1H), 6.04 (s, 1H), 7.04 (d, J = 8.8Hz, 1H), 7.3 (d, J = 8.8Hz, 1H), 10.83 (s, 1H), 11.59 (s, 1H); ^{13}C NMR (100 MHz, CDCl_3): δ 53.19, 69.83, 118.97, 121.27, 126.19, 131.75, 132.74, 136.19, 147.49, 158.11, 162.68, 195.85. IR (neat, cm^{-1}): 3421, 3078, 2923, 2854, 1723, 1654, 1294, 1063. Mass (ES) m/z 292.08 ($M+\text{H}$, 100%); HRMS (ESI): calcd for $\text{C}_{14}\text{H}_{14}\text{NO}_6$ ($M+\text{H}$)⁺ 292.0821, found 292.0818.

Methyl 5-formyl-6-hydroxy-2-(4-methoxyphenyl)-2*H*-benzo[*b*][1,4]oxazine-3-carboxylate (71):



Colorless resin, Yield (92%), R_f = 0.46 (10% EtOAc/Hexane); ^1H NMR (400 MHz, CDCl_3): δ 3.76 (s, 3H), 3.9 (s, 3H), 6.24 (s, 1H), 6.88 (d, J = 9.2Hz, 2H), 6.91 (d, J = 9Hz, 1H), 7.06 (d, J = 9Hz, 1H), 7.20 (d, J = 10Hz, 2H), 10.83 (s, 1H), 11.46 (s, 1H); ^{13}C NMR (100 MHz, CDCl_3): δ 53.22, 55.23, 71.72, 114.39, 120.98, 126.24, 128.97, 131.65, 137.30, 153.05, 157.48, 160.61, 162.91, 195.91. IR (neat, cm^{-1}): 3398, 2924, 2855, 1711, 1649, 1291, 1012. Mass (ES) m/z 364.07 ($M+\text{Na}$, 100%); HRMS (ESI): calcd for $\text{C}_{18}\text{H}_{15}\text{NO}_6\text{Na}$ ($M+\text{Na}$)⁺ 364.0797, found 364.0796.

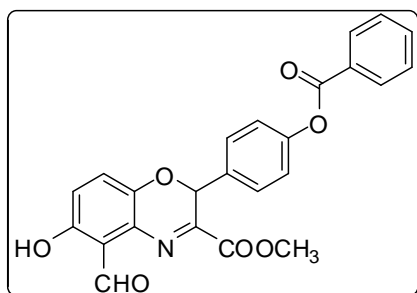
Methyl 2-(4-(benzyloxy) phenyl)-5-formyl-6-hydroxy-2H-benzo[*b*][1,4] oxazine-3-carboxylate (72):



Light brown resin, Yield (10%), $R_f = 0.4$ (15% EtOAc/Hexane); $^1\text{H NMR}$ (400 MHz, CDCl_3): δ 4.2 (s, 3H), 5.05 (s, 2H), 6.94 (d, $J = 8.4\text{Hz}$, 2H), 7.13 (d, $J = 9.2\text{Hz}$, 1H), 7.3-7.4 (m, 9H), 10.84 (s, 1H), 11.82 (s, 1H); $^{13}\text{C NMR}$ (100 MHz, CDCl_3): δ 39.81, 70.02, 115.08, 115.13, 121.08, 125.14, 126.93, 127.44, 127.96, 128.57, 130.74, 131.98, 136.87, 138.82, 152.28, 158.56,

159.99, 195.63. IR (neat, cm^{-1}): 3441, 2924, 2855, 1734, 1649, 1601, 1257, 1018. Mass (ES) m/z 418.14 (M+H, 100%).

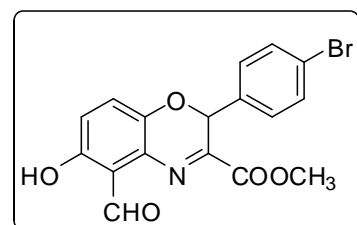
Methyl 2-(4-(benzyloxy)-phenyl)-5-formyl-6-hydroxy-2H-benzo[*b*][1,4]oxazine-3-carboxylate (73):



Colorless resin, Yield (50%), $R_f = 0.5$ (10% EtOAc/Hexane); $^1\text{H NMR}$ (400 MHz, CDCl_3): δ 3.9 (s, 3H), 6.34 (s, 1H), 7.14-7.2 (m, 1H), 7.35-7.65 (m, 8H), 8.17(m, 2H), 10.85 (s, 1H), 11.48 (s, 1H); $^{13}\text{C NMR}$ (100 MHz, CDCl_3): δ 54.47, 69.96, 115.50, 121.08, 125.05, 127.50, 128.03, 128.57, 128.62, 130.38, 136.65, 148.61,

158.61, 164.47, 169.31, 191.63. IR (neat, cm^{-1}): 3433, 3070, 2943, 2844, 1723, 1654, 1620, 1284, 1080. Mass (ES) m/z : 432.10 (M+H, 100%); HRMS (ESI): calcd for $\text{C}_{24}\text{H}_{18}\text{NO}_7$ (M+H) $^+$ 432.1083, found 432.1065.

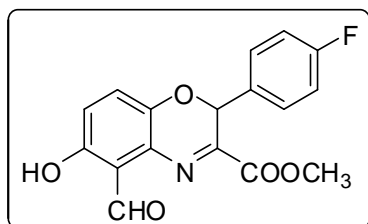
Methyl 2-(4-bromophenyl)-5-formyl-6-hydroxy-2H-benzo[*b*][1,4]oxazine-3-carboxylate (74):



Light brown oil, Yield (66%), $R_f = 0.48$ (10% EtOAc/Hexane); $^1\text{H NMR}$ (CDCl_3): δ $^1\text{H NMR}$ (400 MHz, CDCl_3): δ 3.95 (s, 3H), 6.26 (s, 1H), 6.91 (d, $J = 9.2\text{ Hz}$, 1H), 7.1 (d, $J = 9.2\text{ Hz}$, 1H), 7.15 (d, $J = 7.6\text{ Hz}$, 2H), 7.46 (d, $J = 8\text{ Hz}$, 2H), 10.79 (s, 1H), 11.47 (s, 1H); $^{13}\text{C NMR}$ (100 MHz,

CDCl_3): δ 53.35, 71.18, 121.39, 123.91, 126.02, 128.87, 132.20, 132.40, 133.68, 138.72, 152.24, 157.70, 162.85, 195.71. IR (neat, cm^{-1}): 3364, 2957, 2860, 1722, 1684, 1641, 1311, 1285, 1123. Mass (ES) m/z : 389.99 (M+H, 100%); HRMS (ESI): calcd for $\text{C}_{17}\text{H}_{13}\text{NO}_5\text{Br}$ (M+H) $^+$ 389.9977, found 389.9964.

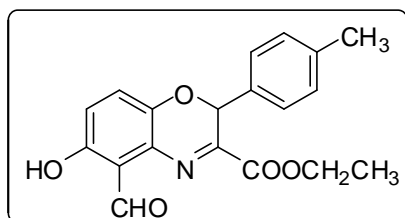
Methyl 2-(4-fluorophenyl)-5-formyl-6-hydroxy-2H-benzo[*b*][1,4]oxazine-3-carboxylate (75):



Light yellow oil, Yield (58%), $R_f = 0.46$ (10% EtOAc/Hexane); $^1\text{H NMR}$ (400 MHz, CDCl_3): δ 3.93 (s, 3H), 6.27 (s, 1H), 6.9 (d, $J = 9.2$ Hz, 1H), 7.08 (m, 2H), 7.11 (d, $J = 9.2$ Hz, 1H), 7.28 (dd, $J = 7.46, 4.19$ Hz, 2H), 10.81 (s, 1H), 11.47 (s, 1H). $^{13}\text{C NMR}$ (100 MHz, CDCl_3): δ 53.30,

71.20, 115.97, 116.18, 117.53, 119.12, 121.28, 126.08, 129.25, 129.35, 135.65, 137.02, 152.57, 157.63, 162.85, 164.56, 195.76. IR (neat, cm^{-1}): 3430, 2924, 2856, 1718, 1648, 1289, 1010. Mass (ES) m/z 352.05 (M+Na, 100%); HRMS (ESI): calcd for $\text{C}_{17}\text{H}_{12}\text{NO}_5\text{FNa}$ (M+Na) $^+$ 352.0597, found 352.0587.

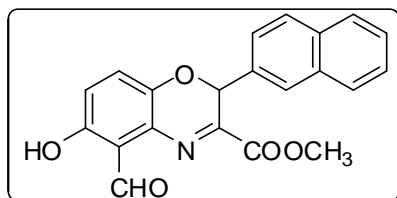
Ethyl 5-formyl-6-hydroxy-2-p-tolyl-2H-benzo[*b*][1,4]oxazine-3-carboxylate (76):



Colourless oil, Yield (47%), $R_f = 0.5$ (10% EtOAc/Hexane): $^1\text{H NMR}$ (400 MHz, CDCl_3): δ 1.36 (t, $J = 7.12$ Hz, 3H), 2.3 (s, 3H), 4.37 (q, $J = 7.12$ Hz, 2H), 6.26 (s, 1H), 6.87 (d, $J = 9.09$ Hz, 1H), 7.18-7.06 (m, 5H), 10.83 (s, 1H), 11.45 (s, 1H). $^{13}\text{C NMR}$ (100 MHz, CDCl_3):

δ 14.03, 21.19, 62.56, 71.92, 114.31, 120.82, 126.11, 127.28, 129.65, 131.73, 137.34, 139.66, 153.48, 157.44, 162.47, 196.04. IR (neat, cm^{-1}): 2954, 2854, 1729, 1651, 1641, 1261, 1123. Mass (ES) m/z : 340.11 (M+H, 100%); HRMS (ESI): calcd for $\text{C}_{19}\text{H}_{18}\text{NO}_5$ (M+H) $^+$ 340.1184, found 340.1182.

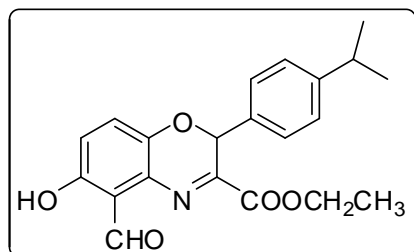
Methyl 5-formyl-6-hydroxy-2-(naphthalen-2-yl)-2H-benzo[*b*][1,4]oxazine-3-carboxylate (77):



Colourless resin, Yield (70%), $R_f = 0.5$ (20% EtOAc/Hexane); $^1\text{H NMR}$ (400 MHz, CDCl_3): δ 3.90 (s, 3H), 6.84-6.69 (m, 1H), 6.92 (d, $J = 9.11$ Hz, 1H), 7.09 (s, 1H), 7.15 (s, $J = 7.2$ Hz, 1H), 7.36-7.21 (m, 1H), 7.58 (t,

$J = 7.2$ Hz, 1H), 7.69 (t, $J = 7.2$ Hz, 1H), 7.87 (dd, $J = 16.19, 8.21$ Hz, 2H), 8.47 (d, $J = 8.53$ Hz, 1H), 10.92 (s, 1H), 11.46 (s, 1H). $^{13}\text{C NMR}$ (100 MHz, CDCl_3): δ 53.30, 68.97, 117.55, 119.14, 120.87, 123.92, 124.76, 125.91, 126.31, 127.19, 128.47, 128.89, 130.85, 131.99, 134.35, 137.07, 152.90, 157.63, 162.78, 195.87. IR (neat, cm^{-1}): 3636, 3053, 2922, 2853, 1724, 1652, 1287, 1051. Mass (ES) m/z 384.08 (M+Na, 100%); HRMS (ESI): calcd for $\text{C}_{21}\text{H}_{15}\text{NO}_5\text{Na}$ (M+Na) $^+$ 384.0847, found 384.0847.

Ethyl 5-formyl-6-hydroxy-2-(4-isopropylphenyl)-2H-benzo[*b*][1,4]oxazine-3-carboxylate (78):



Yellow resin, Yield (72%), $R_f = 0.5$ (10% EtOAc/Hexane); ^1H NMR (400 MHz, CDCl_3 ppm): δ 1.18(d, $J = 6.8\text{Hz}$, 6H), 1.37 (t, $J = 7.2\text{Hz}$, 3H), 2.90-2.79 (m, 1H), 4.37 (q, $J = 7.2$ Hz, 2H), 6.27 (s, 1H), 6.9-6.86 (m, 1H), 7. 2-7.15 (m, 2H), 7.45 (t, $J = 8$ Hz, 1H), 7.84 (d, $J = 7.90$ Hz, 1H), 10.75 (s, 1H), 11.45 (s, 1H). ^{13}C

NMR (100 MHz, CDCl_3): δ 14.03, 23.72, 33.82, 62.55, 71.91, 120.80, 126.13, 127.05, 127.28, 131.70, 132.10, 137.43, 150.40, 153.45, 157.42, 162.53, 196.06. IR (neat, cm^{-1}): 3311, 2960, 2863, 1722, 1652, 1254, 1020. Mass (ES) m/z : 368.14 (M+H, 100%); HRMS (ESI): calcd for $\text{C}_{21}\text{H}_{22}\text{NO}_5$ (M+H) $^+$ 368.1497, found 368.1512.

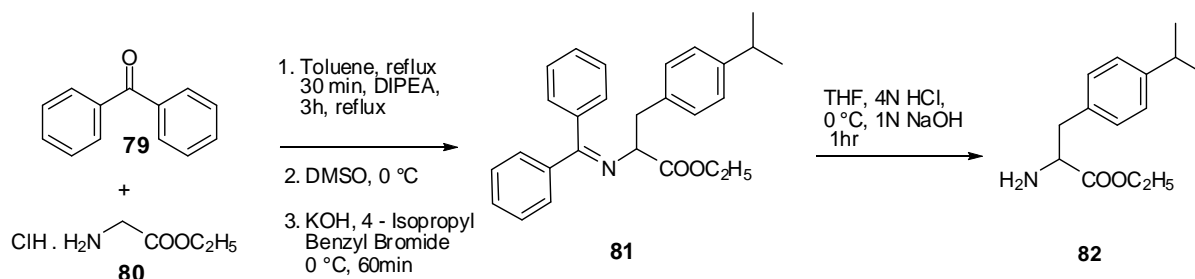
3) EXPERIMENTAL PROCEDURE FOR SYNTHESIS OF UNNATURAL AMINOACID ESTERS

Ethyl 2-amino-3-(4-isopropylphenyl) propanoate (82)

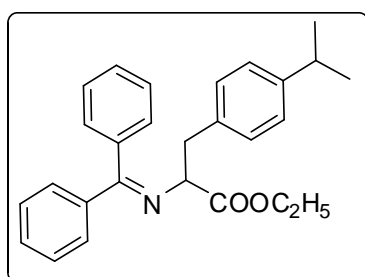
Benzophenone (**79**) (29.0 g, 0.16 mol), glycine ethyl ester hydrochloride (**80**) (11.0g, 0.08 mol) and toluene (50 mL) were charged in a 250 mL, 2-necked round bottomed flask equipped with a Dean-Stark apparatus, heated to reflux for 30 min. DIEA (28 mL, 0.159 mol) was added drop wise over three hours using a dropping funnel at same temperature. Solution was refluxed the pale yellow color solution until it turns to brownish color (3h). After completion of reaction, the mixture was cooled to room temperature followed by addition of water. The layers were separated and the organic solution was washed with water (50 mL) and concentrated in vacuum at 45-50 °C to give (Benzhydrylideneamino)-acetic acid ethyl ester (40g).

A solution of *N*-(diphenylmethylene) glycine ethyl ester (0.800g, 3 mmol) in dimethyl sulfoxide (5 mL) was cooled to 0 °C, potassium hydroxide (0.505g, 9 mmol) was added and stirred for 5 min then treated with *p*-isopropyl benzyl halide (0.636g, 3 mmol) at 0 °C and stirred for 60 min at room temperature. The reaction mixture was neutralized with 1 N hydrochloric acid and extracted with EtOAc several times. The combined organic layers were washed with water and brine, dried over MgSO_4 , filtered and concentrated to obtain **81**.

A solution of above imine **81** (1 mmol) in tetrahydrofuran (10mL) was adjusted to pH ~ 4 with 10mL 4N hydrochloric acid and stirred for 2h. DCM was added to remove benzophenone, neutralize with 1N sodium hydroxide solution and extracted with ethyl acetate several times. The combined organic layers were washed with water and brine, dried over MgSO₄, filtered and concentrated to afford **82** as racemic amino ester.⁴ The amino esters **83**, **84**, **85** and **86** were obtained by similar procedure from the corresponding suitably substituted benzyl halides.

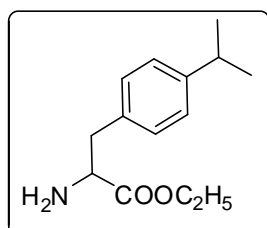


Ethyl 2-(diphenyl methylene amino)-3-(4-isopropylphenyl) propanoate (81):

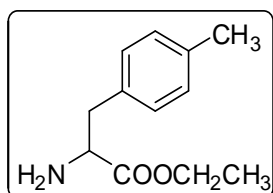


Colorless resin, Yield (80%), $R_f = 0.8$ (10% EtOAc/Hexane); ¹H NMR (400 MHz, CDCl₃): δ 1.25 (m, 9H), 2.84 (Septet, 1H), 3.18 (dd, $J = 13.33, 6.73$ Hz, 1H), 3.28 (dd, $J = 13.33, 6.73$ Hz, 1H), 4.2 (q, $J = 7.16$ Hz, 1H), 6.94 (d, $J = 7.6$ Hz, 2H), 7.25 (m, 2H), 7.599 (m, 4H), 7.81 (d, $J = 7.37$ Hz, 4H).

Ethyl 2-amino-3-(4-isopropylphenyl) propanoate (82):



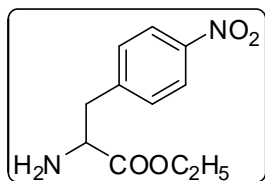
Light brown resin, Yield (80%), $R_f = 0.4$ (40% EtOAc/Hexane); ¹H NMR (400 MHz, CDCl₃): δ 1.24 (m, 9H), 2.61 (bs, 1H), 2.83 (m, 1H), 3.03-3.08 (m, 1H), 3.74 (m, 1H), 4.17 (q, $J = 7.16$ Hz, 2H), 7.1-7.22 (m, 4H).



Ethyl 2-amino-3-p-tolylpropanoate (83):

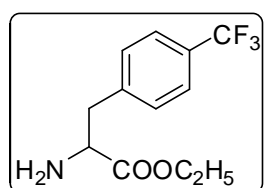
The title compound was synthesized as colourless resin in 88% yield according to general procedure as described above for **82**, $R_f = 0.5$ (40% EtOAc/Hexane); ¹H NMR (400 MHz, CDCl₃): δ 1.19 (t, $J = 7.08$ Hz, 3H), 2.30 (s, 3H), 2.73-2.64 (m, 1H), 3.02-3.06 (m, 1H), 3.66-3.7 (m, 1H), 4.16 (q, $J = 7.16$ Hz, 2H), 7.1-7.19 (m, 4H).

Ethyl 2-amino-3-(4-nitrophenyl) propanoate (84):



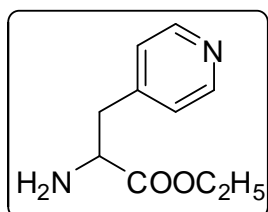
The title compound was synthesized as light yellow resin in 70% yield according to general procedure as described above for **82**, $R_f = 0.4$ (30% EtOAc/Hexane); $^1\text{H NMR}$ (400 MHz, CDCl_3): δ 1.25 (t, $J = 7.08$ Hz, 3H), 2.98 (dd, $J = 13.61, 7.78$ Hz, 1H), 3.17 (dd, $J = 13.63, 5.45$ Hz, 1H), 3.74 (dd, $J = 7.59, 5.69$ Hz, 1H), 4.18 (q, $J = 7.16$ Hz, 2H), 7.47-7.08 (m, 2H), 8.17 (d, $J = 8.43$ Hz, 2H).

Ethyl 2-amino-3-(4-(trifluoromethyl) phenyl) propanoate (85):



The title compound was synthesized as yellow oil in 80% yield according to general procedure as described above for **82**, $R_f = 0.4$ (40% EtOAc/Hexane); $^1\text{H NMR}$ (400 MHz, CDCl_3): δ 1.24 (t, $J = 7.13$ Hz, 3H), 2.07 (bs, 2H), 2.95 (dd, $J = 13.59, 7.6$ Hz, 1H), 3.14 (dd, $J = 13.53, 7.6$ Hz, 1H), 3.75 (m, 1H), 4.17 (q, $J = 7.13$ Hz, 2H), 7.33 (d, $J = 8.4$ Hz, 2H), 7.565 (d, $J = 8.2$ Hz, 2H).

Ethyl 2-amino-3-(pyridin-4-yl) propanoate (86):



The title compound was synthesized as colourless oil in 70% yield according to general procedure as described above for **82**, $R_f = 0.35$ (40% EtOAc/Hexane); $^1\text{H NMR}$ (400 MHz, CDCl_3): δ 1.24 (t, $J = 7.13$ Hz, 3H), 2.86 (dd, $J = 13.8, 7.6$ Hz, 1H), 3.08 (dd, $J = 13.8, 7.6$ Hz, 1H), 3.73 (m, 1H), 4.17 (q, $J = 7.13$ Hz, 2H), 7.15 (d, $J = 5.6$ Hz, 2H), 8.52 (d, $J = 6$ Hz, 2H).

The following amino ester derivatives have been prepared from tyrosine by methods reported in literature.³⁴

Methyl 2-amino-3-(4-hydroxyphenyl) propanoate hydrochloride (**87**), 4-(2-Amino-3-methoxy-3-oxopropyl) phenyl benzoate (**88**), Methyl 2-amino-3-(4-methoxyphenyl) propanoate (**23**), Methyl 2-amino-3-(4-(benzyloxy) phenyl) propanoate (**89**). The following amino ester derivatives have been prepared by simple esterification from the corresponding commercially available amino acids.³⁴ Ethyl 2-amino-3-(4-bromophenyl) propanoate (**90**), Ethyl 2-amino-3-(4-fluorophenyl) propanoate (**91**), Methyl 2-amino-3-(4-(naphthalen-1-yl) phenyl) propanoate (**92**).

3.6.3 Single crystal X-ray data for compound 69

Single crystals suitable for X-ray diffraction of **69** were grown from 2:8 hexane-ethylacetate. The crystals were carefully chosen using a stereo zoom microscope supported by a rotatable polarizing stage. X-ray data was collected at room temperature using a Bruker Smart Apex CCD diffractometer with graphite monochromated MoK α radiation ($\lambda=0.71073\text{\AA}$) with ω -scan method.¹ Integration and scaling of intensity data were accomplished using SAINT program.³⁵ The structures were solved by Direct Methods using SHELXS97³⁶ and refinement was carried out by full-matrix least-squares technique using SHELXL97.

Formula $\text{C}_{19}\text{H}_{14}\text{N}_2\text{O}_5$, $M = 350.32$, monoclinic, space group $P2_1/c$, $a = 9.0334(6)\text{\AA}$, $b = 7.3253(5)\text{\AA}$, $c = 23.9981(15)\text{\AA}$, $\beta = 99.161(1)^\circ$, $V = 1567.76(18)\text{\AA}^3$, $Z = 4$, $D_c = 1.484\text{ g cm}^{-3}$, $\mu(\text{Mo K}) = 0.109\text{ mm}^{-1}$, $F(000) = 728$, $T = 294(2)\text{ K}$, $R1(I > 2\sigma(I)) = 0.0335$, $wR2(\text{all data}) = 0.0937$ for 2535 independent reflections with a goodness-of-fit of 1.058.

3.6.4 Pharmacology methods:

Materials and Methods

Cells and Reagents: HEK 293 and Sf9 cells were obtained from ATCC (Washington D.C., USA). HEK 293 cells were cultured in DMEM supplemented with 10% fetal bovine serum (Invitrogen Inc., San Diego, CA, USA). Sf9 cells were routinely maintained in Grace's supplemented medium (Invitrogen) with 10% FBS. RAW 264.7 cells (murine macrophage cell line) were obtained from ATCC and routinely cultured in RPMI 1640 medium with 10% fetal bovine serum (Invitrogen Inc.). cAMP was purchased from SISCO Research Laboratories (Mumbai, India). PDElight HTS cAMP phosphodiesterase assay kit was procured from Lonza (Basel, Switzerland). PDElight HTS cAMP phosphodiesterase assay kit was procured from Lonza (Basel, Switzerland). PDE4B1, PDE4A4 and PDE4D3 cDNA clones were from OriGene Technologies (Rockville, MD, USA). PDE4D2 enzyme was purchased from BPS Bioscience (San Diego, CA, USA). Lipopolysaccharide (LPS) was from *Escherichia coli* strain 0127:B8 obtained from Sigma (St. Louis, MO, USA). Mouse TNF- α ELISA kit was procured from R&D Systems (Minneapolis, MN, USA).

PDE4B protein production and purification

PDE4B cDNA was sub-cloned into pFAST Bac HTB vector (Invitrogen) and transformed into DH10Bac (Invitrogen) competent cells. Recombinant bacmids were tested for integration by PCR analysis. Sf9 cells were transfected with bacmid using Lipofectamine 2000 (Invitrogen) according to manufacturer's instructions. Subsequently, P3 viral titer was amplified, cells were infected and 48 h post infection cells were lysed in lysis buffer (50 mM Tris-HCl pH 8.5, 10 mM 2-Mercaptoethanol, 1 % protease inhibitor cocktail (Roche), 1 % NP40). Recombinant His-tagged PDE4B protein was purified as previously described elsewhere (Wang et al., 1997). Briefly, lysate was centrifuged at 10,000 rpm for 10 min at 4 °C and supernatant was collected. Supernatant was mixed with Ni-NTA resin (GE Life Sciences) in a ratio of 4:1 (v/v) and equilibrated with binding buffer (20 mM Tris-HCl pH 8.0, 500 mM-KCl, 5 mM imidazole, 10 mM 2-mercaptoethanol and 10 % glycerol) in a ratio of 2:1 (v/v) and mixed gently on rotary shaker for 1 hour at 4°C. After incubation, lysate-Ni-NTA mixture was centrifuged at 4,500 rpm for 5 min at 4°C and the supernatant was collected as the flow-through fraction. Resin was washed twice with wash buffer (20 mM Tris-HCl pH 8.5, 1 M KCl, 10 mM 2-Mercaptoethanol and 10% glycerol). Protein was eluted sequentially twice using elution buffers (Buffer I: 20 mM Tris-HCl pH 8.5, 100 mM KCl, 250 mM imidazole, 10 mM 2-mercaptoethanol, 10% glycerol, Buffer II: 20 mM Tris-HCl pH 8.5, 100 mM KCl, 500 mM imidazole, 10 mM 2-mercaptoethanol, 10% glycerol). Eluates were collected in four fractions and analyzed by SDS-PAGE. Eluates containing PDE4B protein were pooled and stored at -80°C in 50% glycerol until further use.

PDE4B enzymatic assay

The inhibition of PDE4B enzyme was measured using PDElight HTS cAMP phosphodiesterase assay kit (Lonza) according to manufacturer's recommendations. Briefly, 10 ng of PDE4B enzyme was pre-incubated either with DMSO (vehicle control) or compound for 15 min before incubation with the substrate cAMP (5 µM) for 1 h. The reaction was halted with stop solution followed by incubation with detection reagent for 10 minutes in dark. Luminescence values (RLUs) were measured by a Multilabel plate reader (Perkin Elmer 1420 Multilabel counter). The percentage of inhibition was calculated using the following formula:

$$\% \text{ inhibition} = \frac{(\text{RLU of vehicle control} - \text{RLU of inhibitor})}{\text{RLU of vehicle control}} \times 100$$

3.6.5 Docking study

Method: We docked all the molecules by using schrodinger 2011 software. The results are compared with the cocrystal ligand and In vitro activity. The PDB ID 3O0J was used for the docking study. The protein was prepared by giving preliminary treatment like adding hydrogen, adding missing residues, refining the loop with prime and finally minimized by using OPLS 2005 force field. The search grid was generated by picking the cocrystal ligand upto 20 Å search area. The hydroxyl groups of search area were allowed to move.

All the molecules were minimized by using macromodule application. We used 1000 iteration for minimization using OPLS 2005 force field and charges were also added from force field only. The PRCG (Polak-Ribier conjugate gradient) method was used for minimization. All the molecules were docked by using glide XP (extra precision) dock application. We performed flexible docking by allowing sample ring conformations and sample nitrogens to move to possible extent in docking. 10 poses were generated for each ligand. The docking results are documented and analyzed.

3.7 References:

- (a) Ilas̃, J.; Anderluh, P. S.; Dolenc, M. S.; Kikelj, D. *Tetrahedron* **2005**, *61*, 7325.
(b) Cho, S.-D.; Park, Y.-D.; Kim, J.-J.; Lee, S.-G.; Ma, C.; Song, S.-Y.; Joo, W.-H.; Falck, J. R.; Shiro, M.; Shin, D.-S.; Yoon, Y.-J. *J. Org. Chem.* **2003**, *68*, 7918. (c) Chylin´ska, J. B.; Urban´ski, T.; Mordarski, M. *J. Med. Chem.* **1963**, *6*, 484. (d) Largeron, M.; Dupuy, H.; Fleury, M. B. *Tetrahedron* **1995**, *51*, 4953. (e) Adib, M.; Sheibani, E.; Mostofi, M.; Ghanbary, K.; Bijanzadeh, H. R. *Tetrahedron* **2006**, *62*, 3435. (f) Kurz, T. *Tetrahedron* **2005**, *61*, 3091. (g) Zhang, P.; Terefenko, E.A.; Fensome, A.; Wrobel, J.; Winneker, R.; Zhang, Z. *Bioorg. Med. Chem. Lett.* **2003**, *13*, 1313. (g) Bourlot, A.-S.; Sa´nchez, I.; Dureng, G.; Guillaumet, G.; Massingham, R.; Monteil, A.; Winslow, E.; Pujol, M. D.; Me´rour, J.-Y. *J. Med. Chem.* **1998**, *41*, 3142. (h) Combs, D. W.; Rampulla, M. S.; Bell, S. C.; Klaubert, D. H.; Tobia, A. J.; Falotico, R.; Haertlein, R. B.; Lakas-Weiss, C.; Moore, C. J. B. *J. Med. Chem.* **1990**, *33*, 380.
- Madhavan, G. R.; Iqbal, J.; Bhuniya, D.; Chakrabarti, R.; Das, S. K. WO Patent Appl. 03033481, 2003.
- Lestage, P.; Lockhart, B.; Fleury, M. B.; Largeron, M. WO Patent Appl. 9962889, 1999.
- Hoelscher, P.; Jautelat, R.; Rehwinkel, H.; Jaroch, S.; Suelzle, D.; Hillmann, M.; Burton, G. A.; McDonald, F. M. Patent Appl. WO0181324, 2001.
- Burton, G. A.; Rehwinkel, H.; Jaroch, S.; Hoelscher, P.; Suelzle, D.; Hillmann, M.; McDonald, F. M. WO Patent Appl.0017173, 2000.
- Dudley, D. A.; Edmunds, J. J.; Narasimhan, L. S.; Rapundalo, S. T.; Berryman, K. A.; Downing, D. M. WO Patent Appl. 9950257, 1999.
- Das, B. C.; Madhukumar, A. V; Anguiano, J.; Mani, S.; *Bioorg. Med. Chem. Lett.* **2009**, *19*, 4204.
- Mayer, S.; Arrault, A.; Guillaumet, G.; Me´rour, J. Y. *J. Heterocycl. Chem.* **2001**, *38*, 221.
- Touzeau, F.; Arrault, A.; Guillaumet, G.; Scalbert, E.; Pfeiffer, B.; Rettori, M. C.; Renard, P.; Merour, J. Y. *J. Med. Chem.* **2003**, *46*, 1962–1979.
- Vianello, P.; Bandiera, T.; Varasi, M. US Patent 6,794,385,2004.
- Matsumoto, Y.; Tsuzuki, R.; Matsuhisa, A.; Takayama, K.; Yoden, T.; Uchida, W.; Asano, M.; Fujita, S.; Yanagisawa, I.; Fujikura, T. *Chem. Pharm. Bull. (Tokyo)* **1996**, *44*, 103.
- Romeo, G.; Materia, L.; Manetti, F.; Cagnotto, A.; Mennini, T.; Nicoletti, F.; Botta, M.; Russo, F.; Minneman, K. P. *J. Med. Chem.* **2003**, *46*, 2877.

13. Ciske, F. L.; Barbachyn, M. R.; Genin, M. J.; Grega, K. C.; Lee, C. S.; Dolak, L. A.; Seest, E. P.; Watt, W.; Adams, W. J.; Friis, J. M.; Ford, C. W.; Zurenko, G. E. *Bioorg. Med. Chem. Lett.* **2003**, *13*, 4235.
14. Kuwabe, S-I.; Torraca, K. E.; Buchwald, S.; L. *J. Am. Chem.Soc.* **2001**, *123*, 12202.
15. Omar-Amrani, R.; Thomas, A.; Brenner, E.; Schneider, R.; Fort, Y. *Org. Lett.* **2003**, *5*, 2311.
16. Zhang, Y. R.; Xie, J. W.; Huang, X. J.; Zhu, W. D. *Org. Biomol. Chem.* **2012**, *10*, 6554.
17. a) Boll, M. *J. Mol. Microbiol. Biotechnol.* **2005**, *10*, 132; b) Thiele, B.; Rieder, O.; Golding, B. T.; Miller, M. *J. Am. Chem. Soc.* **2008**, *130*, 14050; c) Kung, J. W.; Baumann, S.; Von Bergen, M.; Miller, P. M.; Hagedoorn, L.; Hagen, W. R.; Boll, M. *J. Am. Chem. Soc.* **2010**, *132*, 9850.
18. a) Myers, A. G.; Siegel, D. R.; Buzard, D. J.; Charest, M. G. *Org. Lett.* **2001**, *3*, 2923; For a recent example, see: b) Mihovilovic, M. D.; Leisch, H. G.; Mereiter, K. *Tetrahedron Lett.* **2004**, *45*, 7087.
19. a) Schultz, A. G.; Wang, A. *J. Am. Chem. Soc.* **1998**, *120*, 8259; For review on asymmetric Birch reduction, see: b) Schultz, A. G. *Chem. Commun.* **1999**, 1263.
20. Vo, N.T.; Pace, R. D.; O'Hara, F.; Gaunt, M. J. *J. Am. Chem. Soc.* **2008**, *130*, 404.
21. Pigge, F.C.; Coniglio, J.J.; Dalvi, R. *J. Am. Chem. Soc.* **2006**, *128*, 3498.
22. a) Pettus, T. R. R.; Chen, X.-T.; Danishefsky, S. J. *J. Am. Chem.Soc.* **1998**, *120*, 12684. b) Pettus, T. R. R.; Inoue, M.; Chen, X-T.; Danishefsky, S. J. *J. Am. Chem. Soc.* **2000**, *122*, 6160. for new developments of prenylic dearomatization, see: c) Lei, X.; Dai, M.; Hua, Z.; Danishefsky, S. J. *Tetrahedron Lett.* **2008**, *49*, 6383.
23. a) Magnus, P.; Rodriguez-Lpez, J; Mulholland, K.; Matthewst, I.; *J. Am. Chem. Soc.* **1992**, *114*, 382. b) Magnus, P.; Rodriguez-Lpez, J; Mulholland, K.; Matthewst, I. *Tetrahedron.* **1993**, *49*, 8059.
24. Yamaguchi, R.; Moriyasu, M.; Yoshioka, M.; Kawanisi, M. *J. Org.Chem.* **1988**, *53*, 3507.
25. (a) Quideau, S.; Pouységu, L.; Deffieux, D. *Synlett* **2008**, *4*, 467.(b) Pouységu, L.; Avellan, A. V.; Quideau, S. *J. Org. Chem.* **2002**, *67*, 3425-3436. Braun, N. A.; Ousmer, M.; Bray, J. D.; Bouchu, D.; Peters, K.; Peters, E. -V.; Ciufolini, M. A. *J. Org. Chem.* **2000**, *65*, 4397.
26. (a) Liao, C. C.; Peddinti, R. K.. *Acc. Chem. Res.*, **2002**, *35*, 856. (b) Lin, K. C. et al. *J. Org. Chem.* **2002**, *67*, 8157. (c) Gao, S.-Y.; Lin, Y.-L.; Rao, P. D.; Liao, C.-C. *Synlett* **2000**, 421. (d) Roche, S. P.; Porco Jr. J. A. *Angew. Chem. Int. Ed.* **2011**, *50*, 4068. (e) Tsai, Y-F.; Peddinti, R. K.; Liao, C-C. *Chem. Commun.*, **2000**, 475. (f) Nicolaou, K. C.;

- Vassilikogiannakis, G.; Simonsen, K. B.; Baran, P. S.; Zhong, Y.-L.; Vidali, V. P.; Pitsinos, E. N.; Couladouros, E. A. *J. Am. Chem. Soc.* **2000**, *122*, 3071.
27. (a) Valderrama, J. A.; González, M. F.; Mahana, D. P.; Tapia, R. A.; Fillio, H.; Pautet, F.; Rodriguez, J. A.; Theoduloz, C.; Schmeda-Hirschmann, G. *Bioorg. Med. Chem.* **2006**, *14*, 5003. (b) Valderrama, J. A.; Colonelli, P.; González, M. F.; Rodriguez, J. A.; Theoduloz, C. *Bioorg. Med. Chem.* **2008**, *16*, 10172.
28. (a) *Aldrichimica ACTA* **2001**, *34(1)*, 1-14. (b) Lee, J.; Kim, S. Y.; Park, S.; Lim, J.-O.; Kim, J.-M.; Kang, M.; Lee, J.; Kang, S. U.; Choi, H.-K.; Jin, M.-K.; Welter, J. D.; Szabo, T.; Tran, R.; Pearce, L. V.; Toth, A.; Blumberg, P. M. *Bioorg. Med. Chem.* **2004**, *12*, 1055.
29. Kodimuthali, A.; Jabarisi, S. S. L.; Pal, M. *J. Med. Chem.* **2008**, *51*, 5471.
30. Cheung, W. Y. *Biochemistry.* **1967**, *6*, 1079.
31. Rao, Y. J.; Xi, L. *Acta Pharmacologica Sinica.* **2009**, *30*, 1.
32. Dastidar, S. G.; Rajagopal, D.; Ray, A. *Curr. Opin. Invest. Drugs.* **2007**, *85*, 364.
33. Gorja, D. R.; Shiva Kumar, K.; Kandale, A.; Meda, C. L.; Parsa, K. V.; Mukkanti, K.; Pal, M. *Bioorg. Med. Chem. Lett.* **2012**, *22*, 2480.
34. (a) Lazarides, E.; Griffiths, R. C.; Connell, S.; Mah, J. R.; Cardarelli, P. M.; Nowlin, D. M.; Teegarden, B. R.; Jayakumar, H.; Nomura, S.; Liang, J.; Martin, R.; Gudmundsson, K. S.; Sircar, I. *Bioorg. Med. Chem.* **2002**, *10*, 2051.
35. SMART & SAINT. Software Reference manuals. Versions 6.28a & 5.625, Bruker Analytical X-ray Systems Inc., Madison, Wisconsin, U.S.A., **2001**.
36. (a) Sheldrick, G. M. SHELXS97 and SHELXL97, Programs for crystal structure solution and refinement; University of Göttingen: Germany, **1997**. (b) Flack, K. & Bernardinelli, G. *J. Appl. Cryst.* **2000**, *33*, 1143.

4. Synthesis & pharmacological evolution of substituted phenyl oxazoles as a novel class of LSD1 inhibitors with anti-proliferative properties

4.1 Introduction

Cancer is traditionally viewed as a primarily genetic disorder. However, it is now increasingly apparent that epigenetic abnormalities play a fundamental role in cancer development.¹ Cancer may affect people at all ages, even fetuses, but risk for the more common varieties tends to increase with age. Cancer causes about 13% of all deaths.²

4.2 Epigenetics

Epigenetics is defined as heritable changes in gene activity and expression that occur without alteration in DNA sequence. Examples of such changes are DNA methylation and histone modification, both of which serve to regulate gene expression without altering the basic DNA sequence. Epigenetic changes are preserved when cells divide.³ Thus, epigenetic is considered a bridge between genotype and phenotype.^{4, 5} Different epigenetic phenomena are linked by the fact that DNA exist as an intimate complex with histones and other chromatin remodeling proteins. Mainly, epigenetic information is stored as chemical modifications to cytosine bases and to the histones protein.^{6, 7 and 8}

4.2.1 Epigenetic alterations in the genesis of cancer

DNA methylation and cancer

The first epigenetic alteration to be observed in cancer cells is DNA methylation.⁹ Hypermethylation of CpG islands at tumour suppressor genes switches off these genes, where as global hypomethylation leads to genome instability and inappropriate activation of oncogenes. The genomic DNA methylation levels are maintained by DNMT enzymes (Figure1), are delicately balanced within cells; Over-expression of DNMTs is linked to cancer in humans, and their deletion from animals capable of causing death. Since, DNA exists as an intimate complex with histones in chromatin, most of the factors that affect DNA methylation levels will also affect histone modifications. For example, methylation of DNA, H3K9 is linked and interruption of DNA methylation is linked to loss of H4K20 methylation.¹⁰

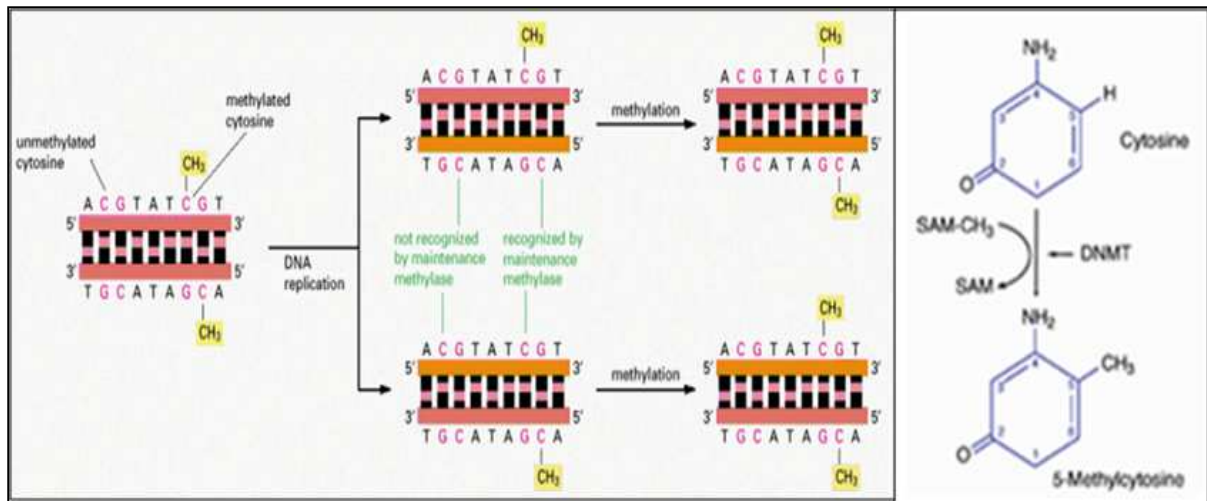


Figure 1: Epigenetic mechanism 1- DNA methylation

Histone modifications and cancer

Histones are proteins which bind to DNA and facilitate efficient ‘packing’ of DNA in eukaryotic cells (Figure 2). Histones are highly basic in nature due to the presence of positively charged amino acids, and this allows them to associate well with DNA and cause the DNA to fold around them into compact structures (nucleosomes). The unwound DNA in chromosomes would be very long (1.8 meters), but wound on the histones it has about 90 micrometers (0.09 mm) of chromatin.

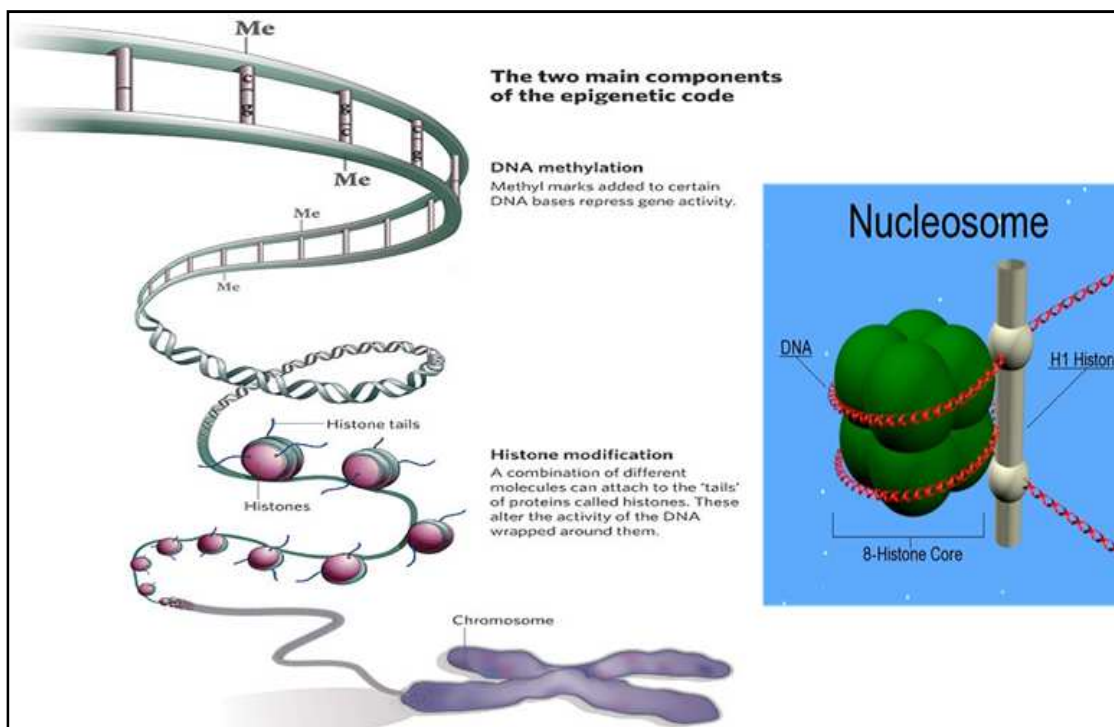


Figure 2: Components of epigenetic code (Taken from *Nature* 2006, 441, 143-5 with licence)

Five major families of histones exist: H1/H5 (linker histones), H2A, H2B, H3, and H4 (core histones).^{11, 12, 13, 14} The ability of histones to regulate gene expression is regulated by post-translational modifications on the N-terminal (and likely C-terminal) “tails” of the core histones which project out of the nucleosome (Figure 2). Modifications including phosphorylation, acetylation, methylation, ubiquitination, sumoylation and biotinylation have been identified on the histone tails.

- **Acetylation:** Histone acetylation tends to open up chromatin structure. Accordingly, histone acetyltransferase (HATs) tend to be transcriptional activators whereas histone deacetylases (HDACs) tend to be repressors. Many HAT genes are altered in some way in a variety of cancers. For instance, the p300 HAT gene is mutated in a number of gastrointestinal tumors. On the other hand, alteration of HDAC genes in cancer seems to be far less common. However, despite this low incidence of genetic mutation in cancer, HDAC inhibitors are performing well in the clinic as anti-cancer drugs.
- **Methylation:** All lysine methyltransferases that target histone N-terminal tails contain a so-called SET domain. This domain possesses lysine methyltransferase activity and numerous SET domain-containing proteins are involved in cancer. One example is the Suv39 family of enzymes that catalyze methylation of H3K9. Although there are clear links to disease¹⁵⁻¹⁸, the role of histone methylation is much less well understood and appears to be context dependent.
- **Phosphorylation:** H3S10 and H3S28 are phosphorylated at mitosis - a crucial part of the cell cycle; misregulation here is often associated with cancers. Indeed, the Aurora kinases that perform this H3 phosphorylation are implicated in cancer.

The large-scale development of small molecule inhibitors of DNA and histone-modifying enzymes is now in full swing. In the clinic, the success of HDAC inhibitors and DNA demethylating agents like aza cytidine as anti-cancer drugs demonstrates 'proof of principle' of this approach and provides great hope for the development of a more comprehensive portfolio of 'epigenetic drugs' in the future.

4.2.2 Lysine-specific histone demethylase 1 (LSD1)

LSD1 (Lysine Specific Demethylase 1) was the first histone demethylase identified.¹⁹ LSD1 is highly conserved in organisms ranging from *Schizosaccharomyces pombe* to human and consists of three major domains: an N-terminal SWIRM (Swi3p/Rsc8p/Moira) domain, a C-terminal AOL (amine oxidase-like) domain, and a central protruding Tower domain. The C-terminal catalytic domain reveals high sequence homology to amine oxidases that belong to

the flavin adenine dinucleotide (FAD)-dependent enzyme family including mono- and polyaminoxidase. The N-terminal SWIRM domain seems to be important for chromatin binding.²⁰ The Tower domain, inserted into the AOL domain, forms a long helix-turn-helix structure and serves as a platform for binding of LSD1 partner proteins such as corepressor element silencing factor, CoREST (Figure 3).

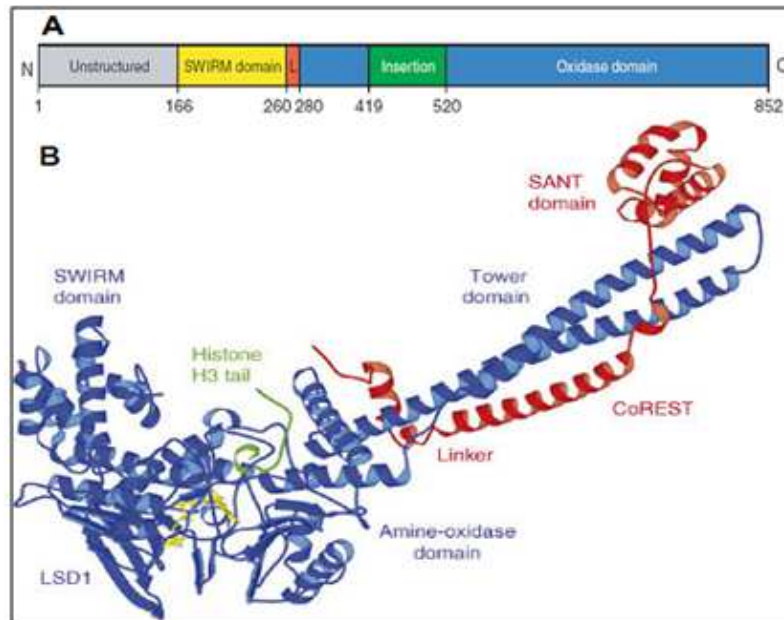


Figure 3: Structure of human LSD1 (A) Domain structure. (B) Structure of LSD1 in complex with CoREST and a peptide substrate.

Its discovery significantly advanced the understanding of epigenetic regulation of gene expression; changing the paradigm that methylation is a non-reversible feature of histones.²¹ Histone methylation/demethylation has since been found to be an important epigenetic modification linked to activation as well as repression of transcription.

Two types of histone demethylases have been discovered. The flavin-dependent demethylase LSD1 acts on lysine 4 and lysine 9 of histone H3 (H3K4 and H3K9). LSD1 acts on mono- and dimethylated H3K4 through a flavin-dependent mechanism. The reaction results in a hybrid transfer with reduction of FAD to FADH₂ which is reoxidized by molecular oxygen, producing hydrogen peroxide. The resulting imine intermediate is hydrolyzed to generate the demethylated H3 tail and formaldehyde (Figure 4).

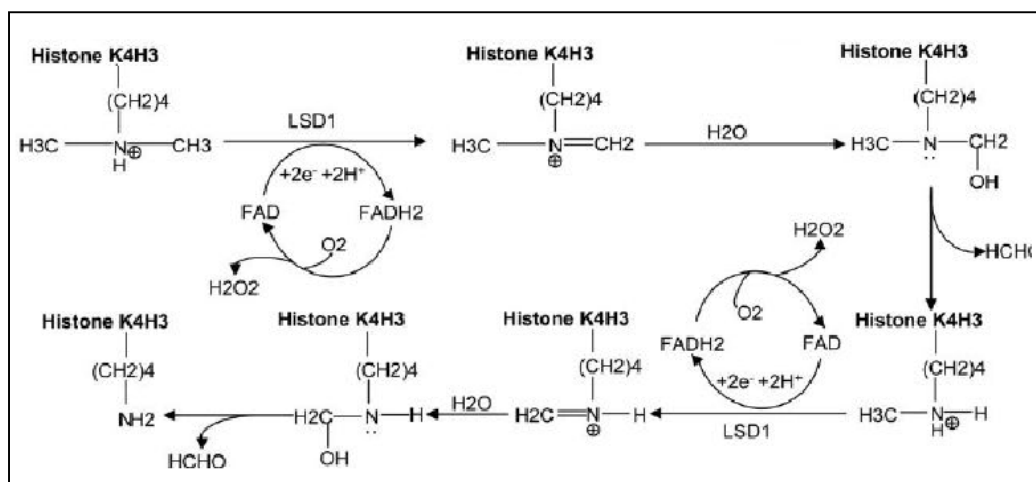


Figure 4: Demethylation of K4H3Me2 by LSD1

LSD1 cannot demethylate trimethylated lysine residues, since a lone pair of electrons in the unprotonated state of N of methylated lysine is required in FAD-mediated reaction. LSD1 requires the first 20 N-terminal amino acids of the histone tail for productive binding in the *in vitro* enzymatic assay.²²

The other major class are Jumonji domain-containing histone demethylases which are Fe(II) and 2-oxoglutarate dependent oxygenases that, act on mono-, di- and trimethylated Lys and methylated Arg residues depending on the particular enzymes.²³ Histone demethylase activity is associated with several pathological states. Increased LSD1 expression in prostate tumors correlates significantly with relapse during therapy.^{24, 25} Suppressed LSD1 expression is associated with vascular smooth muscle cell inflammatory damage in a mouse model of diabetes²⁶. Demethylation of p53 (tumor suppressor) by LSD1 prevents p53 interaction with its co-activator 53BP1.¹⁴ Activation of the telomerase reverse transcriptase (hTERT) gene is known to be dependent on LSD1 levels and recruitment to the hTERT promoter.¹³

4.3 Design of novel LSD1 inhibitors:

Studies on LSD1 have identified a few classes of molecules that exhibit inhibitory activity. Several Monoamine oxidase inhibitors (MAOIs), more commonly used as antidepressants, inhibit LSD1, indicating one possible direction for small molecule design.²⁷ Biguanide and bisguanidine polyamine analogs are another class of molecules that was identified for this process (Figure 5). These molecules have been used in cultured colon cancer cells to demonstrate LSD1 inhibition and resultant activation of silenced genes.¹⁹

Peptides containing methionine as the key structural element also showed LSD1 inhibition. However, none of these molecules are likely to be selective for LSD1 or are druggable. Small molecules which can selectively modulate the activity of LSD1 should therefore hold great promise in two main areas – (1) in laboratory experiments to understand the cellular and physiological effects of LSD1 inhibition and the interaction of histone H3K4 methylation with other epigenetic modifications such as histone acetylation, histone phosphorylation and DNA methylation, (2) in animal studies aimed at defining the potential of clinical therapy as LSD1 inhibitors for the treatment of chronic conditions such as cancer, diabetes and obesity. Herein, we report the synthesis and biological study of a novel class of molecules as probes of LSD1 function, as possible epigenetic modulators or as potential anti-cancer agents.

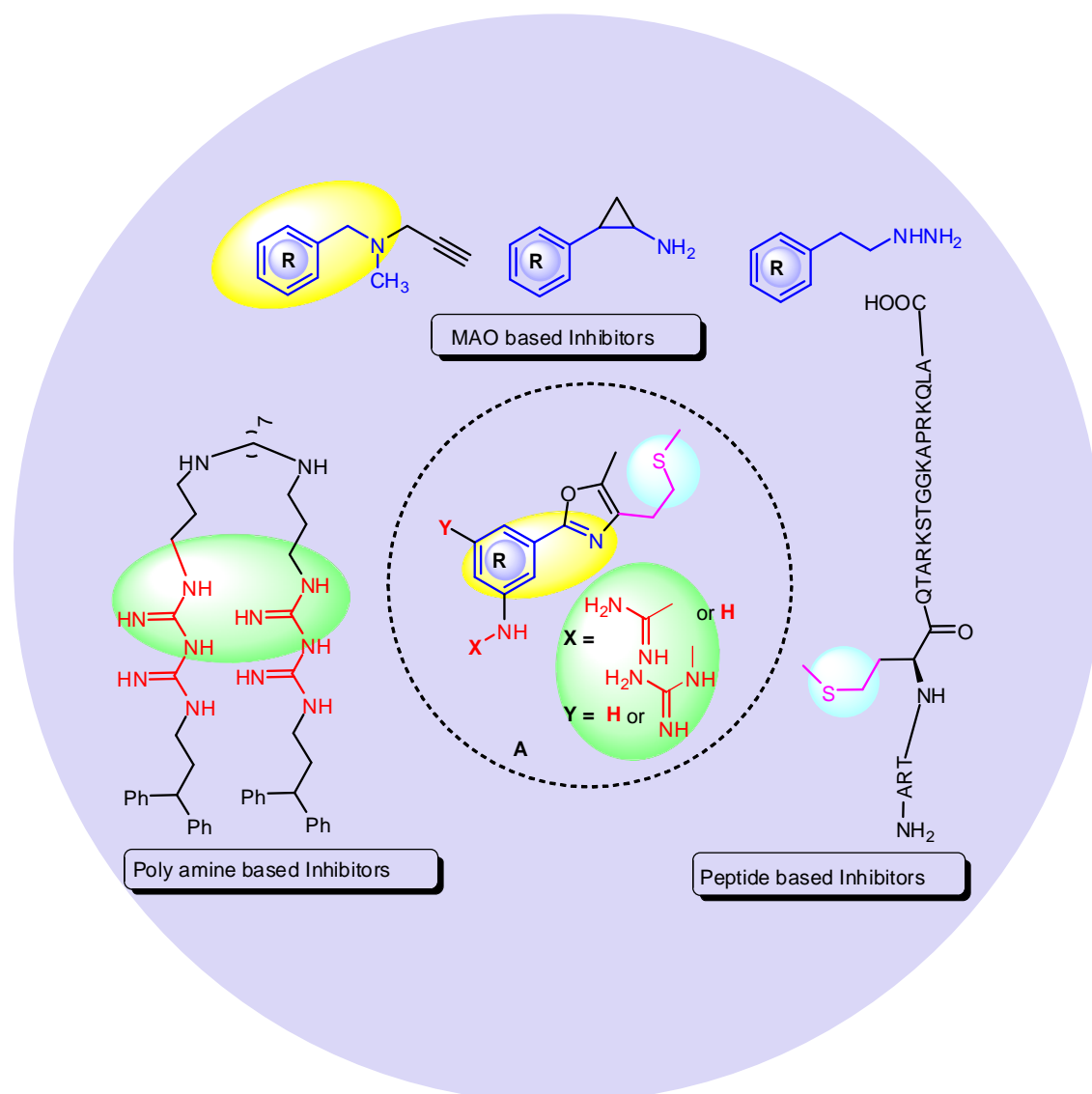


Figure 5: Design of novel LSD1 inhibitors based on pharmacophore similarity with reported inhibitors.

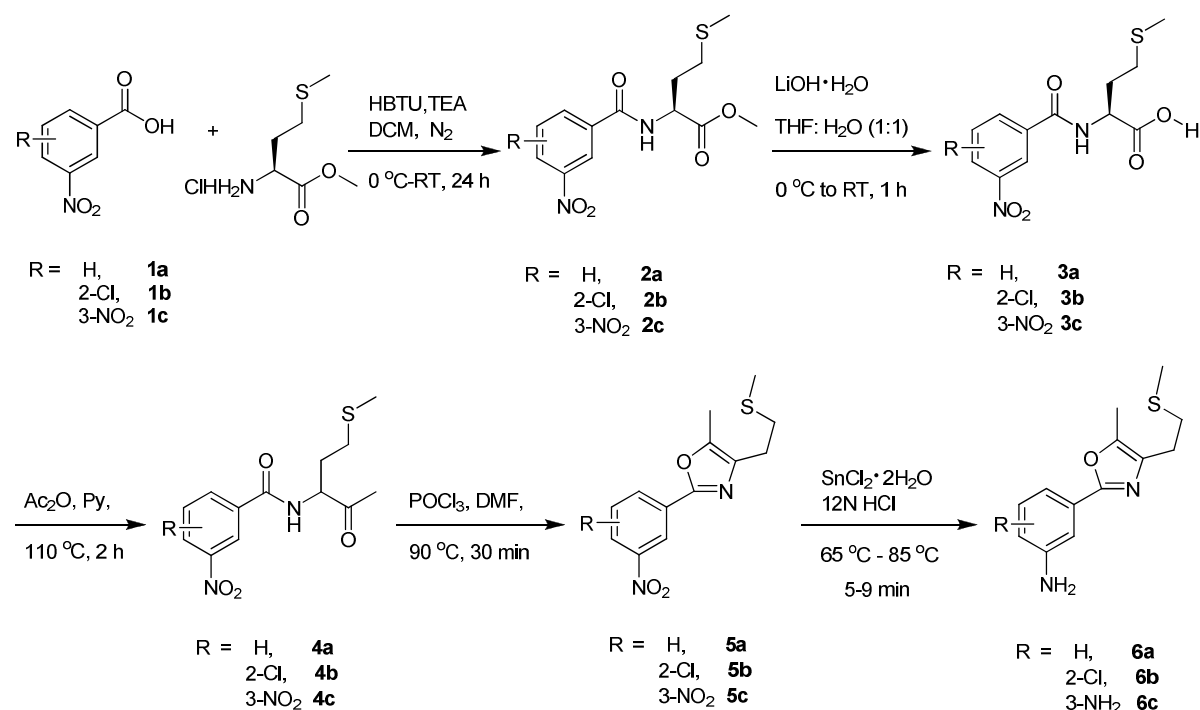
Using the available X-ray diffraction crystal structure of LSD1 as a starting point,²⁸ we designed a series of small molecules as potential inhibitors taking the key pharmacophore features identified for the MAO-, the polyamine/guanidine and methionine based peptide inhibitors into account (Figure 1) being linked through an oxazole moiety.^{19, 27 and 28-34} The Schrodinger molecular modelling suite was used to visualize the three-dimensional structure of LSD1 and predict the docking sites, inhibitory interactions and the theoretical effectiveness of small molecules.

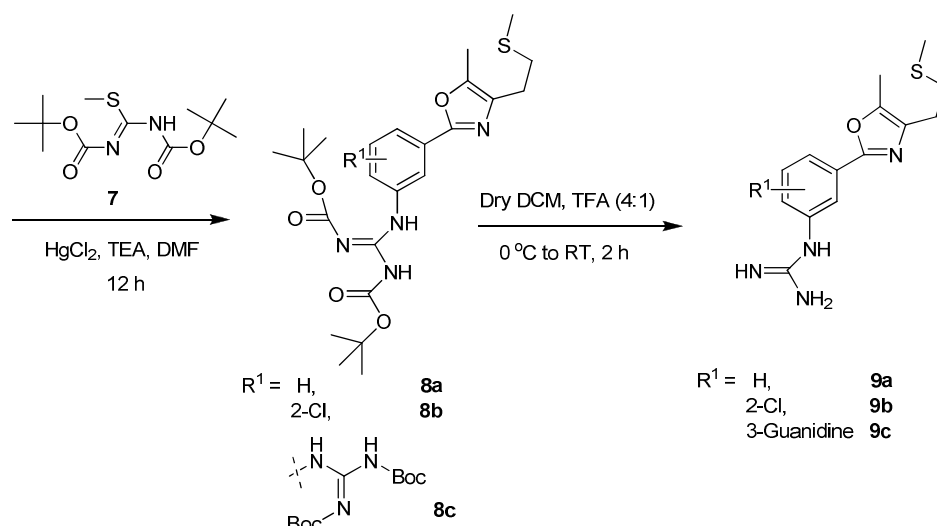
4.4 Results and discussion:

4.4.1 Chemistry:

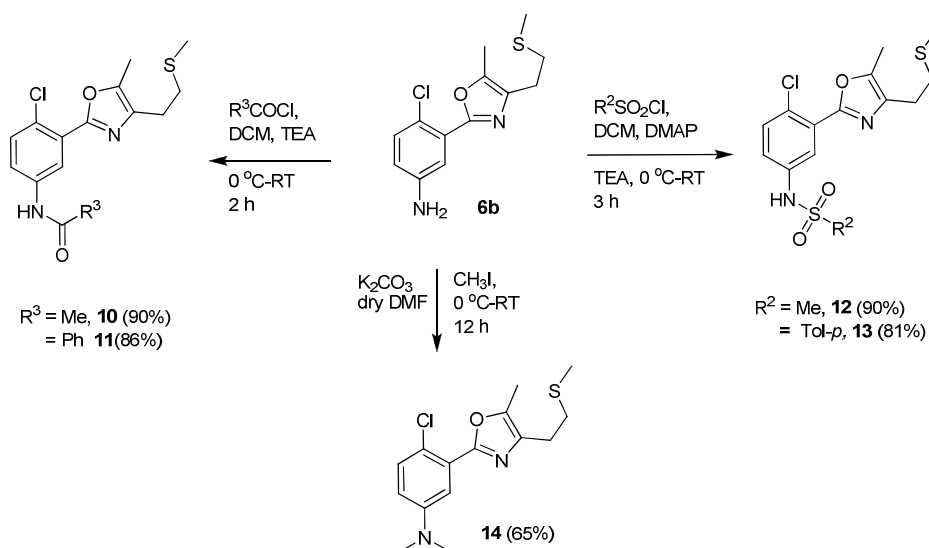
The synthesis of target compounds and their derivatives was efficiently performed using the reaction sequence as shown in Scheme 1.

3-nitrobenzamide derivatives **2**^{35,36} were readily obtained by reacting appropriate 3-nitrobenzoic acids (**1a-c**) with methionine methyl ester hydrochloride in the presence of HBTU, followed by treatment with LiOH•H₂O, to give rise to the corresponding carboxylic acids **3**.³⁷ Those were subsequently converted to keto-amides **4** in the presence of acetic anhydride and pyridine *via* a Dakin-West type reaction.³⁸ After refluxing with POCl₃, the keto-amides **4** cyclized spontaneously to produce the 3-nitro phenyl oxazole derivatives **5a-c**³⁸ which on reduction with SnCl₂•2H₂O afforded 3-amino phenyl oxazole derivatives **6**.³⁹





Scheme 1: Synthesis of substituted 3-guanidine phenyl oxazoles



Scheme 2: Synthesis of analogues **10-14** of **6b**

The installation of a bis-BOC protected 3-guanidine group was achieved by treating **6** with N^1, N^2 -bis-(*tert*-butoxycarbonyl)-*S*-methylisothiourea (**7**),⁴⁰ to give the corresponding 3-guanidine phenyl oxazole derivatives **8**. Finally, on deprotection with trifluoroacetic acid 3-guanidine phenyl oxazole derivatives **9** were obtained. A number of *N*-substituted derivatives (**10-14**) were also prepared via *N*-acylation, *N*-sulfonation or *N*-alkylation of **6b** (Scheme 2). All synthesized compounds were fully characterized by spectroscopic methods (NMR, IR, MS and HRMS).

4.4.2 Pharmacology:

4.4.2.1 Cell viability

Having synthesized the desired target molecules **6** and **9** along with **10-14** we performed their pharmacological evaluation *in vitro* determining cell viability by a MTT assay. Initially, these compounds were subjected to cervical cancer cell line HeLa and breast cancer cell line MDA-MB-231 with concentrations ranging from 0.5 nM to 3.7 nM (log concentrations) for 36h. Among the compounds tested **6a**, **6b**, **9a** and **9c** showed significant inhibitory effects on cell at 1 nM (Table 1). The data was plotted with log (compound concentration) on the x-axis and % viability of cells on the y-axis (Figure 6-10).

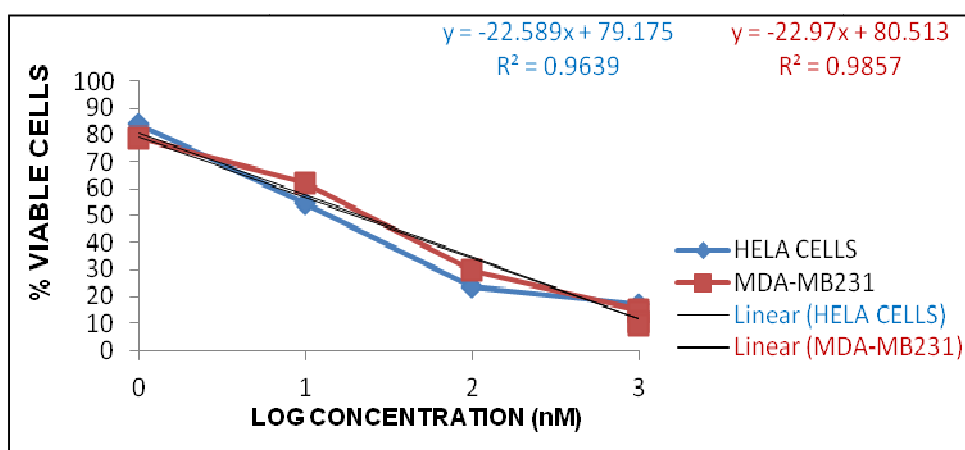


Figure 6: Log Concentration Vs % Viable Cells for Compound 6a against HeLa and MDA-MB231 Cells by MTT assay

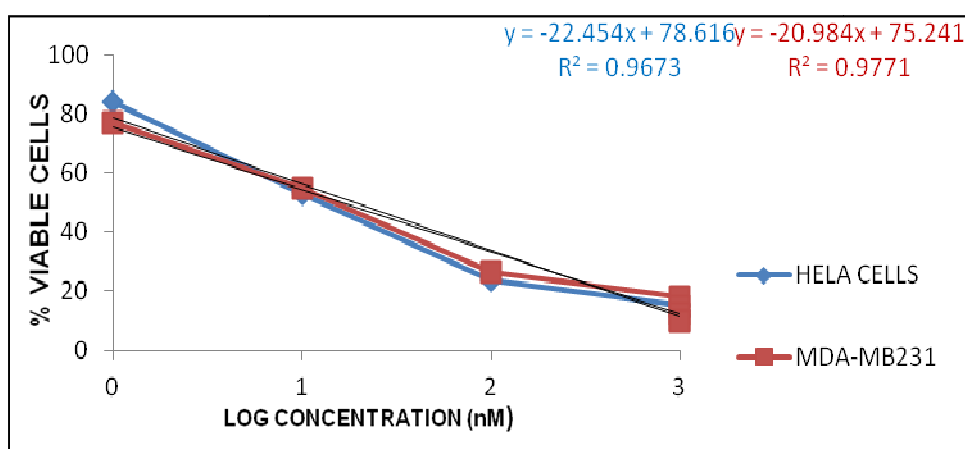


Figure 7: Log Concentration Vs % Viable Cells for Compound 6b against HeLa and MDA-MB231 Cells by MTT assay

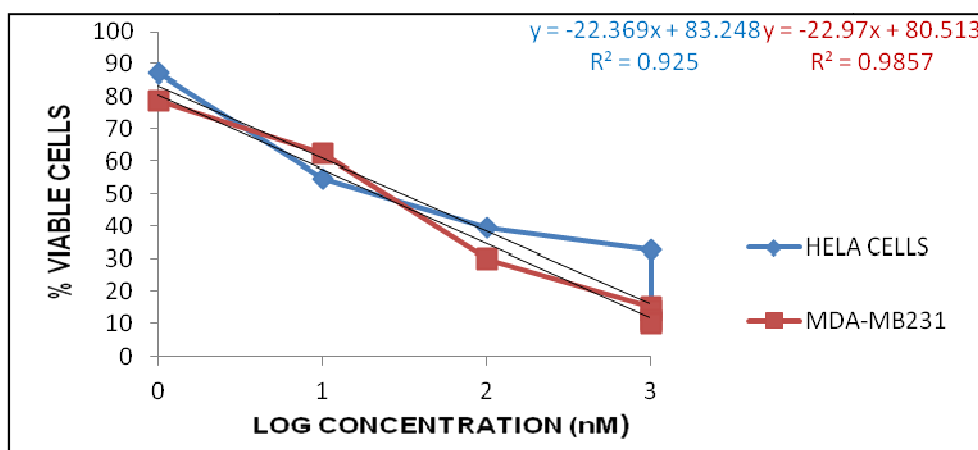


Figure 8: Log Concentration Vs % Viable Cells for Compound **9a** against HeLa and MDA-MB231 Cells by MTT assay

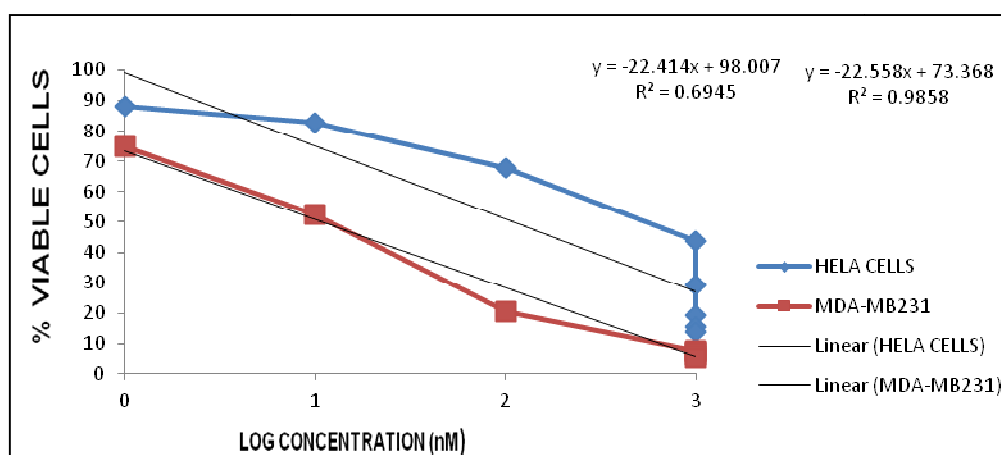


Figure 9: Log Concentration Vs % Viable Cells for Compound **9c** against HeLa and MDA-MB231 Cells by MTT assay

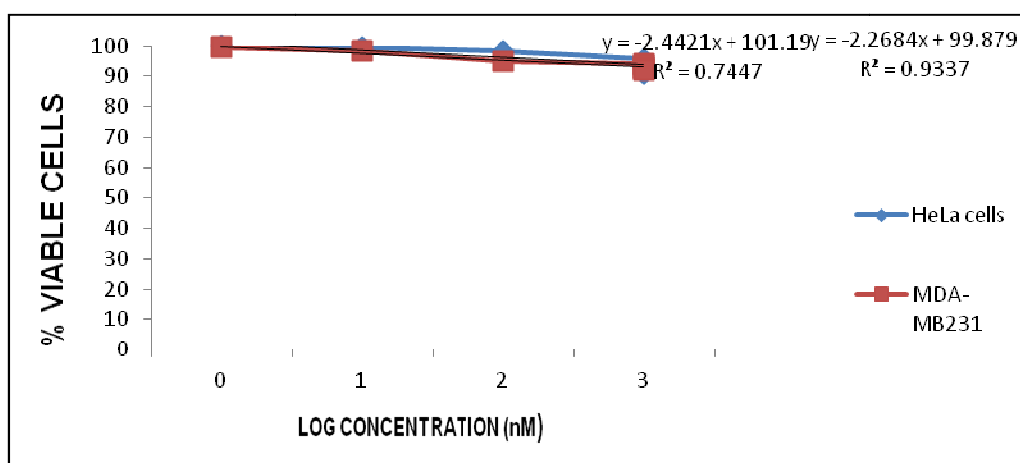


Figure 10: Log Concentration Vs % Viable Cells for 10% DMSO Control against HeLa and MDA-MB231 Cells by MTT assay

From these data it was evident that a guanidine moiety did not offer any significant advantages over an amino group (e.g. **9a** and **9c** vs **6a** and **6b**) with respect to *in vitro* activities. IC₅₀ values were calculated for all test compounds and are shown in table 1. IC₅₀ values for **6a** were 1.29nm for HeLa and 1.328 nm for MDA-MB-231 cells, **6b** were 1.22nm

for HeLa and 1.202nm for MDA-MB-231 cells, **9a** were 1.48nm for HeLa and 1.328nm for MDA-MB-231 cells, **9c** were 2.14nm for HeLa and 1.035nm for MDA-MB-231 cells.

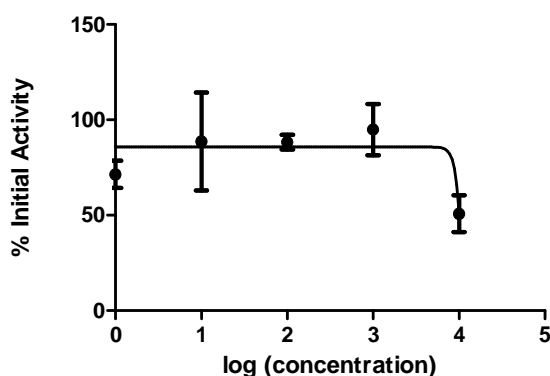
4.4.2.2 *In vitro* LSD1 activity

The *in vitro* LSD1 activity assays showed that compounds **6a**, **6b** and **9a** showed detectable inhibition of *in vitro* LSD1 activity at a concentration of 1 μ M whereas all the other compounds showed no detectable inhibition. A concentration response study of the above compounds was performed using concentrations of 10 μ M, 1 μ M, 0.1 μ M, 0.01 μ M and 0.001 μ M. IC₅₀ values were then calculated with compound **6a** showing 16.1 μ M, **6b** showing 10.2 μ M and **9a** showing 9.5 μ M IC₅₀ values. The data is summarized in table 1.

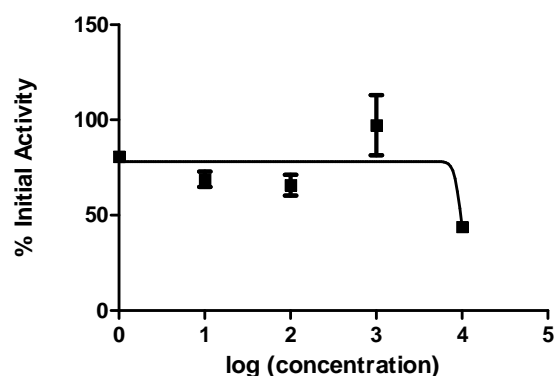
4.4.2.3 Zebrafish embryo toxicity and apoptosis

Developing embryos of the zebrafish *Danio rerio* are excellent animal models for studying specific developmental effects of small molecules, thus allowing effective *in vivo* evaluations of potential drugs before embarking on highly expensive studies on mice and humans.⁴¹ The histone demethylase LSD1 is known to be encoded by the zebrafish genome⁴², and the protein sequence has 85% sequence identity with that of human LSD1 protein. This makes the zebrafish embryo an attractive *in vivo* model to evaluate the effects of small molecules as LSD1 inhibitors as well as *in vivo* toxicity-related effects.

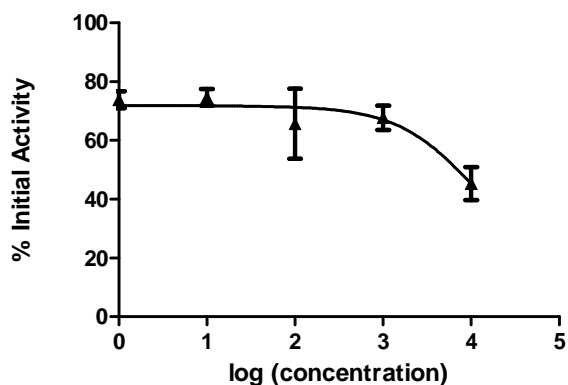
IC₅₀ values calculated using non-linear regression analysis in the software GraphPad Prism. The data was plotted with log (compound concentration) on the x-axis and % initial activity on the y-axis (Figure11).



6a Estimated IC₅₀: 16.1 μ M



9a Estimated IC₅₀: 9.5 μ M

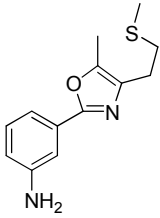
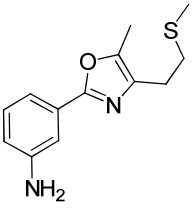
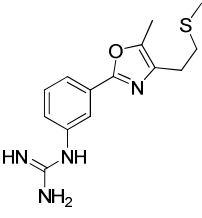
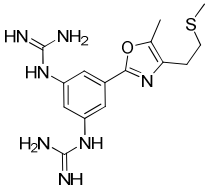


6b Estimated IC₅₀: 10.2 μM

Figure 11: Log Concentration Vs % Initial activity for compounds **6a**, **6b** and **9a** against LSD1

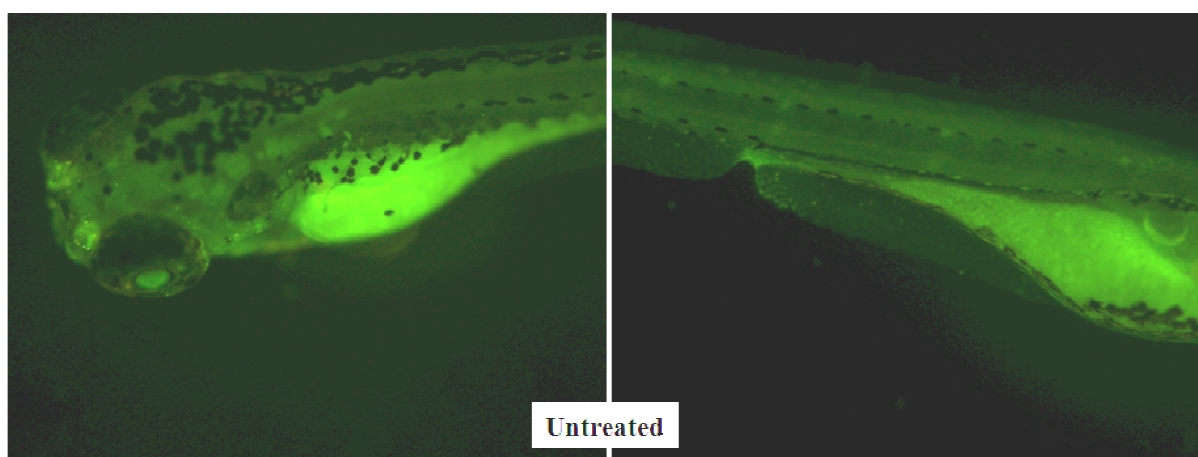
Compounds **5c**, **5b** and **9b** showed general toxicity-related effects in zebrafish embryos, with death resulting after 24h of treatment at 10μM. Compounds **6b**, **9a** and **9c** showed increased apoptosis at 10 μM with no general toxicity-related effects even after 72h of treatment. The data is summarized in table 1 and the microscopy images of treated embryos are shown in figure 2. The data clearly show increased apoptosis as indicated by acridine orange fluorescence, especially in the area of the brain. This observation is consistent with reported brain-related effects of LSD1 inhibition.⁴³

Table 1: Summary of the pharmacological evaluation of compounds.

Pharmacological Activity				
	6a	6b	9a	9c
HeLa cell viability (IC ₅₀)	1.29 nm	1.22 nm	1.48 nm	2.14 nm
MDA-MB-231 cell viability (IC ₅₀)	1.328 nm	1.202 nm	1.328 nm	1.035 nm
<i>In vitro</i> LSD1 inhibition (IC ₅₀)	16.1 μM	10.1 μM	9.5 μM	>50μM
Zebrafish embryo apoptosis	Insignificant	Yes (10 μM)	Yes (10 μM)	Yes (10 μM)
Zebrafish embryo toxicity	None	None	Not done	None

Our results indicate that compounds **6a**, **6b**, **9a** and **9c** possess biological activity related to mechanisms involved in cell viability. The data from *in vitro* LSD1 inhibition is consistent with compounds **6a**, **6b** and **9a** possessing LSD1 inhibition properties, although the IC₅₀ values are higher by an order of 10⁴. This suggests that the activity of the compounds on the cells tested is mediated by additional effects apart from LSD1 inhibition. Possible effects include those on epigenetic modifications other than histone methylation, such as histone acetylation and DNA methylation leading to a significant suppression of cell viability. Such non-specific epigenetic effects are plausible because the compounds were designed based on structural features of the LSD1 protein and that of other known inhibitors of LSD1.

The data from studies with zebrafish embryos shows that compounds **6b**, **9a** and **9c** result in a significant increase in apoptosis (Figure 12), with no general toxicity-related effects. The treatment was done at a concentration of 10 μM, which is in the range of *in vitro* LSD1 inhibition IC₅₀ values. The significant difference in activity shown by the compounds in cells and in zebrafish embryos suggests that the cancer cells used may possess features (such as specific mutations or epigenetic targets) which make them more sensitive to the effects of LSD1 inhibition, compared to the developing zebrafish embryos which represent a non-diseased, living organism. This is plausible since cancer cells are known to have several accumulated defects compared to normal cells. Our data thus support the possibility that the compounds are selective for cancer cells over normal cells. Overall, the results of our detailed pharmacological analysis suggest that compounds **6b** and **9a** possess biological activity consistent across *in vitro*, cell culture and *in vivo* systems.



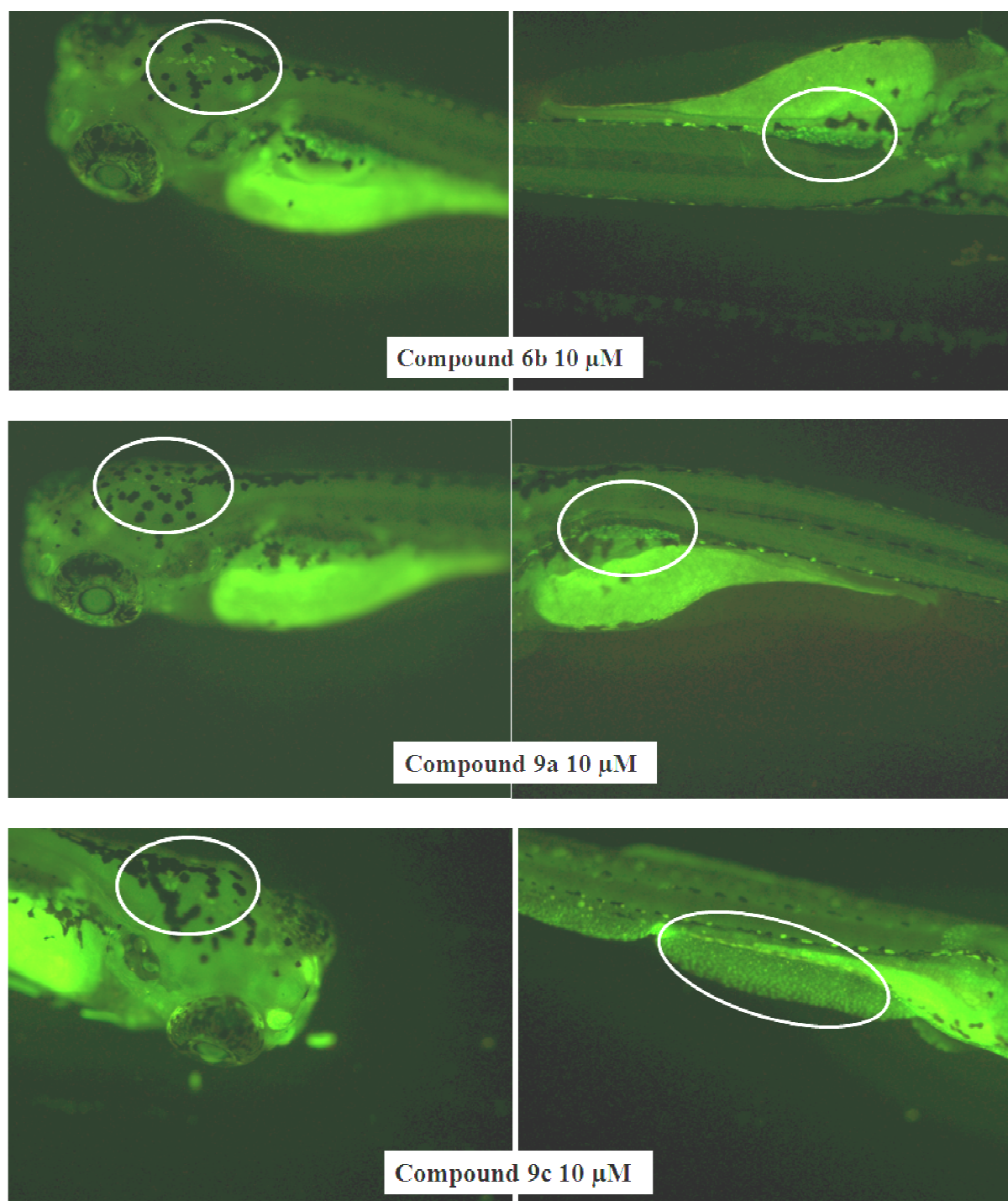


Figure 12: Zebrafish embryos treated with compounds and stained with acridine orange. Brightly stained spots, highlighted with a circle represent apoptotic cells with fragmented nuclei.

4.4.3 Molecular modeling

To understand the binding mode and stability of ligand receptor complexes we performed molecular modeling studies (Docking analysis and Molecular dynamics simulations) using

6a, **6b** and **9a** against LSD1 (Figure 13-15). Docking studies predicted good binding interaction with the LSD1 enzyme. The amino group of molecule **9a** was perfectly locked with Thr-335, Tyr-571 and His-812 by hydrogen bonding whereas the oxazole ring participated in a π stacking with Tyr-761. The sulfur atom of molecule **6b** was involved in H-bonding with Met-332 and Val-333. In case of molecule **6a**, the oxazole and the phenyl ring showed a good π stacking with Tyr-761 and Trp-751, respectively. The docking score and LSD1 inhibition data has a nice correlation with each other.

Table 2: Contribution of glide XP terms in docking score

Comp.	GScore	LipophilicEvdW	HBond	Electro	PhobEn	LowMW
6a	-5.43	-3.9	-0.7	-0.2	-0.5	-0.5
6b	-6.50	-4.8	-0.8	-0.4	-0.3	-0.5
9a	-6.74	-5.0	-0.7	-0.5	-0.5	-0.5

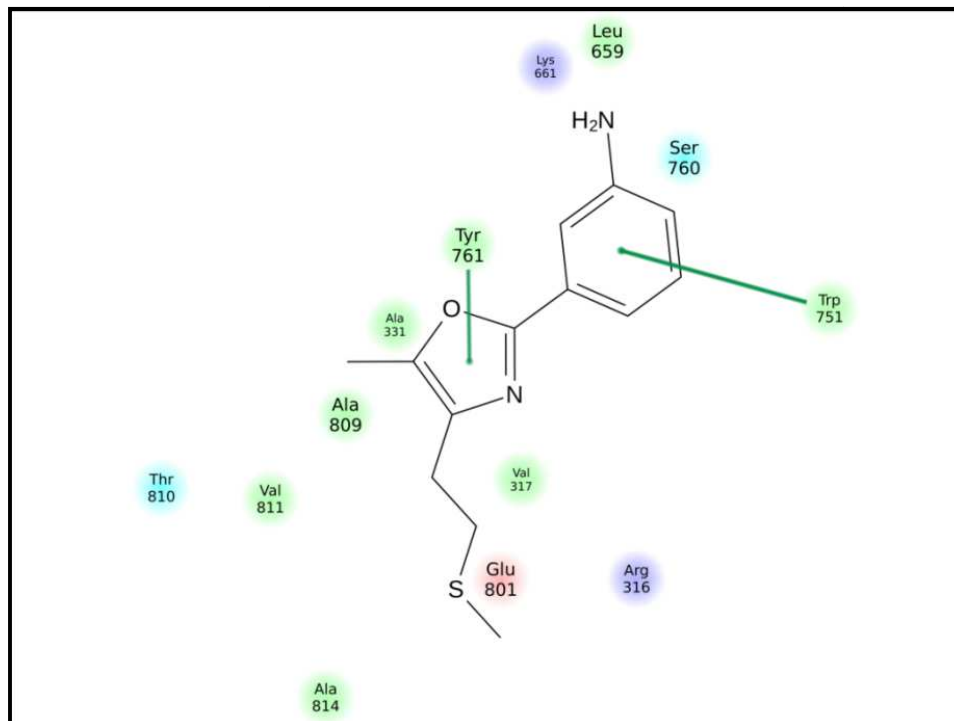
LipophilicEvdW: Chemscore lipophilic pair term and fraction of the total protein-ligand vdw energy

HBond: Rewards for hydrogen bonding interaction between ligand and protein

Electro: Electrostatic reward

PhobEn: Hydrophobic enclosure reward

LowMW: Reward for ligands with low molecular weight



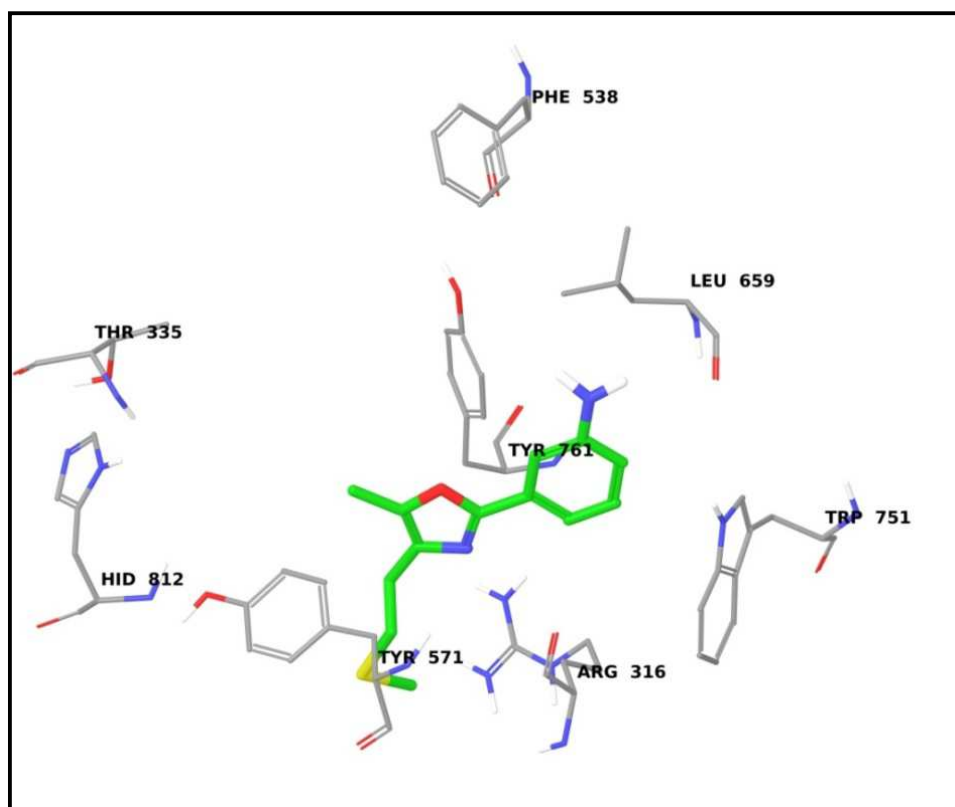
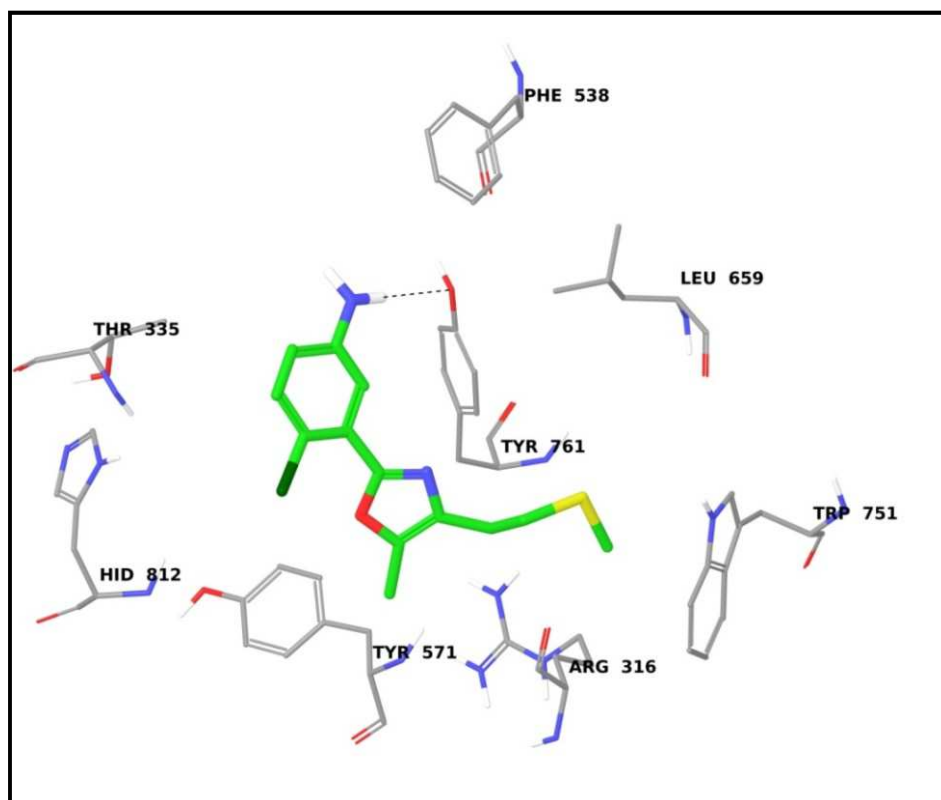


Figure 13: Binding orientation and interactions of **6a** at the LSD1 inhibitors binding site.



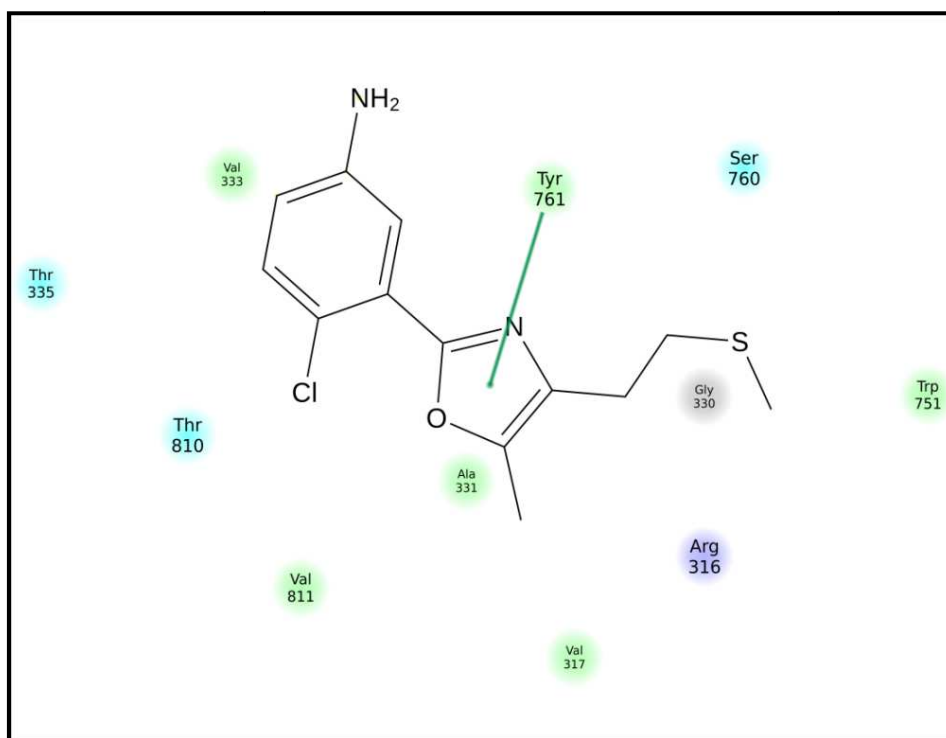
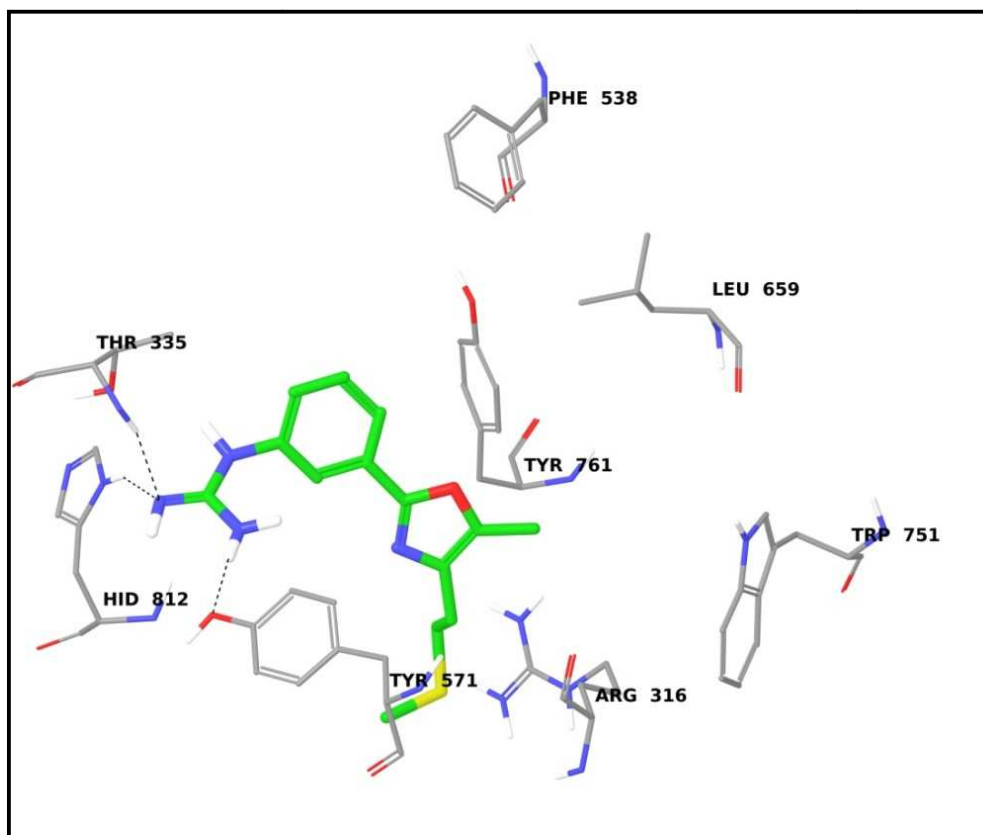


Figure 14: Binding orientation and interactions of **6b** at the LSD1 inhibitors binding site.



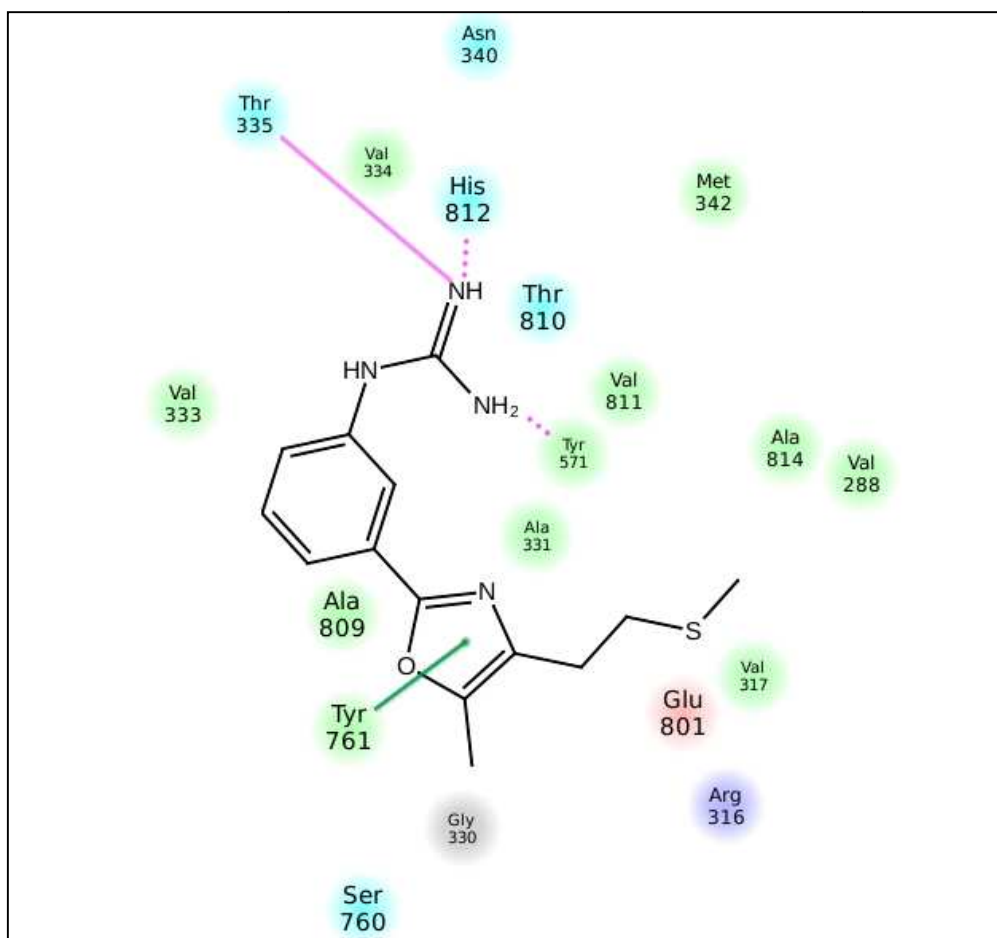


Figure 15: Binding orientation and interactions of **9a** at the LSD1 inhibitors binding site.

Furthermore, the molecular dynamics (MD) simulations of **9a** at the binding site of protein were also performed using the Desmond package incorporated in Maestro. To evaluate stability of the MD trajectories and the differences in the stability of the MD simulations, the total energy of ligand-protein complex and RMSD values for the protein backbone atoms relative to the initial minimized structure through the phase of the simulation were calculated. There was no significant change in the total energy of system observed during entire simulation period. The RMSD values remained within 6.0 Å for the system after reaching at equilibrium, which demonstrated the conformational stabilities of the protein structures. Throughout MD simulations the studied compound maintained binding pose in the expected orientation.

4.5 Summary:

In summary, we have designed, synthesized and performed detailed pharmacological analysis of 3-amino / guanidine substituted phenyl oxazoles as a novel class of LSD1 inhibitors and likely epigenetic modulators. These molecules were conveniently prepared via a multistep sequence involving an amide bond formation, construction of oxazole ring and introduction of guanidine moiety as key steps. Among all the compounds tested **6a**, **6b** and **9a** showed promising activities against LSD1 and cancer cells *in vitro*. Additionally, the compounds **6b** and **9a** were found to increase apoptosis in zebrafish embryos in the brain area when evaluated in a phenotype-based zebrafish assay. All these compounds showed good binding interactions with the LSD1 enzyme *in silico* as indicated by docking studies. Overall, our study provides the basis for future research which can be directed at elucidating the details of the mechanisms of action of the compounds presented, and the contribution of specific structural features to their activity.

4.6 Experimental section

4.6.1 Chemistry - General methods

All reactions were carried out under an inert atmosphere with dry solvents, unless otherwise stated. Reactions were monitored by thin layer chromatography (TLC) on silica gel plates (60 F254), using UV light detection. Visualization of the spots on TLC plates was achieved either by UV light or by staining the plates in 2, 4 Dinitro phenyl hydrazine and Ninhydrin stains charring on hot plate. Flash chromatography was performed on silica gel (230-400 mesh) using distilled hexane, ethyl acetate, dichloromethane.

NMR-Spectroscopy

¹H NMR and ¹³C NMR spectra were recorded in CDCl₃ or acetone-*d*₆ solution by using VARIAN 400 MHz spectrometers. Deuterium exchange studies were done in CD₃OD, DMSO-*d*₆ and D₂O. Chemical shifts are reported as δ values relative to internal CDCl₃ δ 7.26 or TMS δ 0.0 DMSO-*d*₆ δ 2.50 and CD₃OD δ 3.34 for ¹H NMR and CDCl₃ δ 77.0 and CD₃OD δ 49.05 for ¹³C NMR. ¹H NMR data was recorded as follows: chemical shift [multiplicity, coupling constant(s) *J* (Hz), relative integral] where multiplicity is defined as: s (singlet), d (doublet), t (triplet), q (quartet), dd (doublet of doublet), m (multiplet), bs (broad singlet).

IR spectroscopy, mass spectrometry and melting points

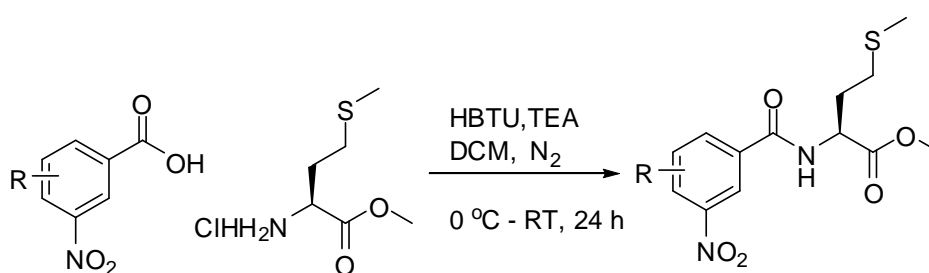
FTIR spectra were recorded on Bruker (Alpha) spectrometer. Mass spectra were recorded on Micro Mass VG-7070H mass spectrometer for ESI and are given in mass units (m/z). High

resolution mass spectra (HRMS) [ESI+] were obtained using either a TOF or a double focusing spectrometer. Melting points were determined by using a Buchi melting point B-540 apparatus. Values thus obtained were not corrected.

4.6.2 Synthesis:

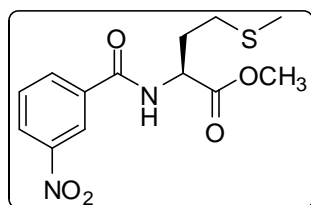
1a, 1b, 1c were commercially available, whereas methionine ester (**1d**) was synthesized from natural amino acid methionine and **7** from thiourea using literature protocols in quantitative yield.

General procedure for synthesis of 2a-c:



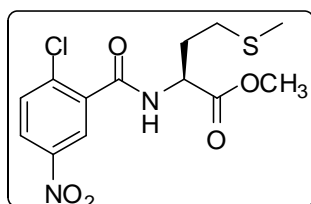
HBTU (1.5 mmol) was added to a mixture of benzoic acid (**1a, 1b, 1c**) (1 mmol), methionine methyl ester hydrochloride (1.2 mmol) in dry DCM (10 mL) at 0 °C. The reaction mixture was stirred for 1 hr followed by drop wise addition of dry triethylamine (10.0 mmol) at 0 °C and stirring was continued at room temperature for 12 h. A clear solution of the reaction mixture was cooled in an ice bath and acidified with 2N HCl. The residue was dissolved in ethyl acetate (750 mL), washed with water (2 x 250 mL), brine (1 x 100 mL), dried over Na₂SO₄, filtered and the solvent evaporated. The residue was purified by flash chromatography (n-hexane/ ethylacetate 4:1) to afford the desired products (**2a, 2b, 2c**).

(S)-Methyl 4-(methylthio)-2-(3-nitrobenzamido) butanoate (**2a**):



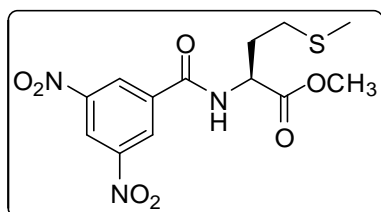
White semi solid; yield (87 %); $R_f = 0.60$ (30% EtOAc-n-Hexane); IR (cm⁻¹): 3325, 3056, 2956, 2876, 1735 (C=O of ester), 1690 (C=O of amide), 1540, 1340; ¹H NMR (300 MHz, CDCl₃) δ 2.13 (s, 3H), 2.16-2.22 (m, 1H), 2.27-2.34 (m, 1H), 2.62 (t, $J = 7.2$ Hz, 1H), 3.81 (s, 3H), 4.92- 4.97 (m, 1H), 7.33 (d, $J = 7.6$ Hz, 1H), 7.66 (d, $J = 8.0$ Hz, 1H), 8.17-8.22 (dd, $J^1 = 7.4$ Hz, $J^2 = 1.6$ Hz, 1H), 8.36- 8.39 (dd, $J^1 = 7.4$ Hz, $J^2 = 1.6$ Hz, 1H), 8.67 (s, 1H); ¹³C NMR (75 MHz, CDCl₃) δ 15.5, 30.2, 31.1, 52.4, 52.8, 122.1, 126.3, 126.3, 129.8, 133.2, 135.2, 148.2, 164.7 ; MS (EI, 70ev): m/z (%) [M]⁻ 311.1 (100%).

(S)-Methyl 2-(2-chloro-5-nitrobenzamido)-4-(methylthio) butanoate (2b):



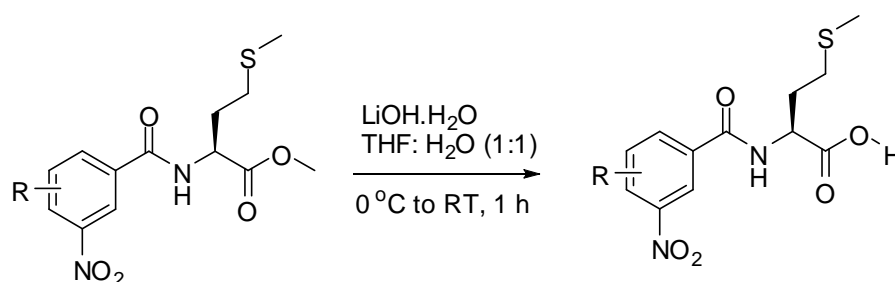
The title compound was prepared in 80% yield according to the general procedure as described above; Brown solid; $R_f = 0.55$ (30% EtOAc-n-Hexane); mp 265-267 °C; IR (cm^{-1}): 3295, 3042, 2955, 2865, 1728 (C=O of ester), 1678 (C=O of amide), 1520, 1334; ^1H NMR (300 MHz, CDCl_3) δ 2.13-2.2 (m, 4H), 2.31-2.38 (m, 1H), 2.56-2.67 (m, 2H), 3.82 (s, 3H), 4.93- 4.98 (m, 1H), 7.02 (d, $J = 7.2$ Hz, 1H), 7.62 (d, $J = 8.8$ Hz, 1H), 8.22-8.25 (dd, $J^1 = 8.8$ Hz, $J^2 = 2.6$ Hz, 1H), 8.53 (d, $J = 3.2$ Hz, 1H); ^{13}C NMR (75 MHz, CDCl_3) δ 15.5, 29.9, 31.3, 52.3, 52.8, 125.2, 125.8, 131.4, 135.7, 137.6, 146.4, 163.8, 171.6; MS (EI, 70ev): m/z (%) $[\text{M}]^+$ 347.1 (100%).

(S)-Methyl 2-(3, 5-dinitrobenzamido)-4-(methylthio)butanoate (2c):



The title compound was prepared in 82% yield according to the general procedure as described above and isolated as yellow solid; $R_f = 0.7$ (30% EtOAc-n-Hexane); mp 285-288 °C; IR (cm^{-1}): 3310, 3010, 2975, 2855, 1732 (C=O of ester), 1660 (C=O of amide), 1515, 1324; ^1H NMR (300 MHz, CDCl_3) δ 2.16 (s, 3H), 2.17- 2.37 (m, 2H), 2.6-2.68 (m, 2H), 3.84 (s, 3H), 4.99 (td, $J^1 = 7.2$ Hz, $J^2 = 4.8$ Hz, 1H), 7.56 (d, $J = 7.2$ Hz, 1H), 9.00(d, $J = 2.0$ Hz, 1H), 9.18 (d, $J = 2.0$ Hz, 1H). ^{13}C NMR (75MHz, CDCl_3) δ 15.5, 30.2, 30.7, 38.6, 52.8, 52.9, 121.3, 127.3, 137.0, 148.6, 162.4, 172.2; MS (EI, 70ev): m/z (%) $[\text{M}]^+$ 358.2 (100%).

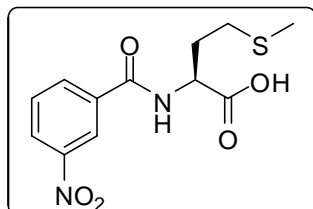
General procedure for synthesis of 3a-c:



LiOH·H₂O (1.5 mmol) was added to the solution of (S)-Methyl 4-(methylthio)-2-(3-nitrobenzamido) butanoate **2a** (1.0 mmol) in THF (6 mL), H₂O (5 mL) at 0 °C. The reaction was stirred at 23 °C for 1 h. After completion of the reaction, the reaction mixture was concentrated to remove THF. The solution was cooled in an ice bath and acidified with 2N HCl, extracted with EtOAc, followed by brine wash then dried over anhydrous Na₂SO₄,

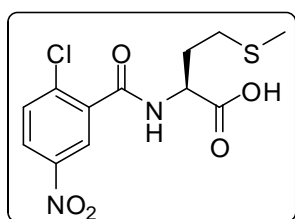
filtered and the solvent evaporated. The residue was purified by flash chromatography (n-hexane/ ethylacetate 3:2) to afford the desired product **3a**.

(S)-4-(Methylthio)-2-(3-nitrobenzamido) butanoic acid (3a):



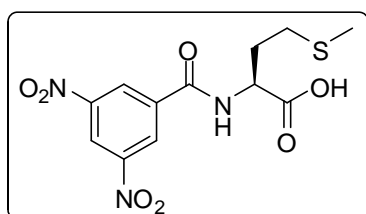
White solid; yield (88 %); $R_f = 0.4$ (30% EtOAc-n-Hexane); mp 276-278 °C; IR (cm^{-1}): 3302, 2989, 2866, 1712 (C=O of acid), 1650 (C=O of amide), 1525, 1314; $^1\text{H NMR}$ (300 MHz, CDCl_3) δ 2.12 (s, 3H), 2.15 -2.34 (m, 2H), 2.65 (t, $J = 7.2$ Hz, 1H), 4.92-4.97 (m, 1H), 7.28 (bs, 1H), 7.61-7.69 (m, 2H), 8.15 (d, $J = 7.8$ Hz, 1H), 8.33 (d, $J = 7.8$ Hz, 1H), 8.65 (s, 1H); $^{13}\text{C NMR}$ (75 MHz, CDCl_3) δ 15.4, 30.2, 30.6, 52.5, 122.2, 126.5, 129.9, 133.4, 134.9, 148.1, 165.6, 175.3; MS (EI, 70ev): m/z (%) $[\text{M}]^+$ 297.0 (100%)

(S)-2-(2-chloro-5-nitrobenzamido)-4-(methylthio) butanoic acid (3b):



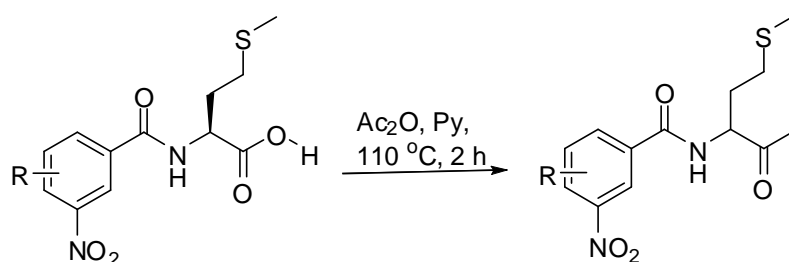
The title compound was synthesized in 94% yield according to the general procedure as described above for **3a** and isolated as brown solid; $R_f = 0.42$ (30% EtOAc-n-Hexane); mp 231-235 °C; IR (cm^{-1}): 3299, 3050, 2979, 2856, 1722 (C=O of acid), 1650 (C=O of amide), 1515, 1324; $^1\text{H NMR}$ (300 MHz, CDCl_3) δ 2.14 (s, 3H), 2.16-2.4 (m, 2H), 2.65-2.69 (m, 4H), 4.13-5.11 (m, 3H), 7.10 (d, $J = 7.6$ Hz, 1H), 7.62 (d, $J = 8.4$ Hz, 1H), 8.22-8.25 (dd, $J^1 = 8.4$ Hz, $J^2 = 2.8$ Hz, 1H), 8.53 (d, $J = 2.4$ Hz, 1H); $^{13}\text{C NMR}$ (75 MHz, CDCl_3) δ 15.5, 29.7, 30.1, 30.9, 52.4, 125.3, 126.0, 131.5, 135.4, 137.7, 146.5, 164.4, 175.2 MS (EI, 70ev): m/z (%) $[\text{M}]^+$ 333.1 (100%).

(S)-2-(3, 5-dinitrobenzamido)-4-(methyl thio) butanoic acid (3c):



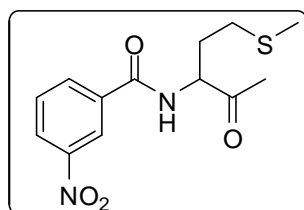
The title compound was synthesized in 90% yield according to the general procedure as described for **3a** as light brown solid; $R_f = 0.42$ (30% EtOAc-n-Hexane); mp 268-270 °C; IR (cm^{-1}): 3301, 3060, 2985, 2862, 1718 (C=O of acid), 1660 (C=O of amide), 1525, 1334; $^1\text{H NMR}$ (300 MHz, $\text{DMSO}-d_6$) δ 2.12 (s, 3H), 2.13- 2.33 (m, 2H), 2.57-2.70 (m, 2H), 4.80-4.86 (m, 2H), 9.11(d, $J = 2.0$ Hz, 1H), 9.21 (d, $J = 7.6$ Hz, 1H), 9.31(d, $J = 2.0$ Hz, 2H). $^{13}\text{C NMR}$ (75MHz, $\text{DMSO}-d_6$) δ 15.3, 30.4, 30.9, 52.6, 120.8, 127.8, 137.4, 148.3, 162.6, 173.3; MS (EI, 70ev): m/z (%) $[\text{M}]^+$ 344.1 (100%).

General procedure for synthesis of 4a-c:



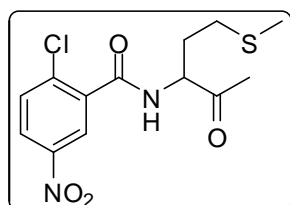
To a solution of (S)-4-(Methylthio)-2-(3-nitrobenzamido) butanoic acid **3a** (4.9 mmol) in acetic anhydride (30.4 mmol, 3 mL), pyridine (58.8 mmol, 5 mL) was added and heated at 90 °C for 2 h. The reaction mixture was concentrated to remove excess acidic anhydride and pyridine, extracted with EtOAc (150 mL). EtOAc layer was washed successively with 1.0 N HCl (50 mL), water (50 mL) and brine then dried over anhydrous Na₂SO₄, filtered and the solvent evaporated. The residue was purified by column chromatography (EtOAc/hexanes) to provide of the desired product **4a**.

N-(1-(Methyl thio)-4-oxopentan-3-yl)-3-nitrobenzamide (4a):



Light brown semi solid; R_f = 0.6 (30% EtOAc-n-Hexane); IR (cm⁻¹): 3100, 3060, 2985, 2862, 1720 (C=O of ketone), 1665 (C=O of amide), 1515, 1314; ¹H NMR (300 MHz, CDCl₃) δ 2.13 (s, 3H), 2.14 -2.17 (m, 2H), 2.34 (s, 3H), 2.41 -2.64 (m, 2H), 4.96 - 4.99 (m, 1H), 7.35 (d, J = 6.4 Hz, 1H), 7.67 (t, J = 7.8 Hz, 1H), 8.17 (d, J = 7.8 Hz, 1H), 8.37- 8.39 (dd, J^1 = 8.0 Hz, J^2 = 1.6 Hz, 1H), 8.67 (s, 1H); ¹³C NMR (75 MHz, CDCl₃) δ 15.7, 27.3, 30.1, 30.5, 58.9, 122.1, 126.4, 129.8, 133.1, 135.4, 148.3, 164.8, 205.7; MS (EI, 70ev): m/z (%) [M]⁺ 295.0 (100%).

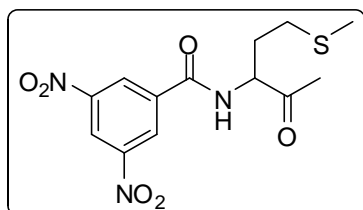
2-chloro-N-(1-(methylthio)-4-oxopentan-3-yl)-5-nitrobenzamide (4b):



The title compound was synthesized as yellow semi solid in 78% yield according to the general procedure as described above for **4a**; R_f = 0.65 (30% EtOAc-n-Hexane); IR (cm⁻¹): 3200, 3050, 2976, 2862, 1710 (C=O of ketone), 1655 (C=O of amide), 1518, 1323; ¹H NMR (300 MHz, CDCl₃) : 2.00- 2.07 (m, 1H), 2.13 (s, 3H), 2.34 (s, 3H), 2.39- 2.46 (m, 1H), 2.53-2.61 (m, 2H), 4.96-5.00 (m, 1H), 7.16 (d, J = 4.8 Hz, 1H), 7.62 (d, J = 7.2 Hz, 1H), 8.22-8.25 (dd, J^1 = 7.2 Hz, J^2 = 2.4 Hz, 1H), 8.51 (d, J = 2.8 Hz, 1H); ¹³C

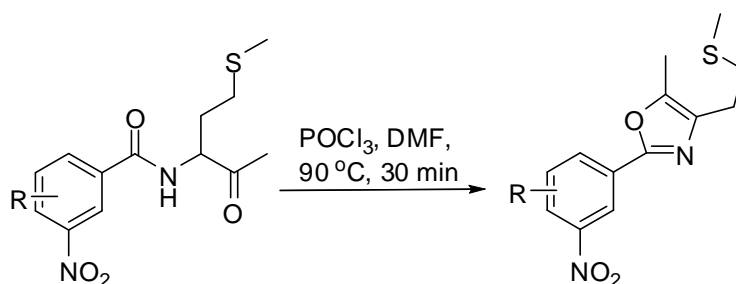
NMR (75 MHz, CDCl₃):15.5, 25.0, 30.9, 33.3, 126.7, 128.2, 131.7, 133.2, 140.2, 146.9, 156.4, 208.2 ; MS (EI, 70ev): m/z (%) [M]⁺ 333.1 (100%).

***N*-(1-(methylthio)-4-oxopentan-3-yl)-3,5-dinitrobenzamide (4c):**



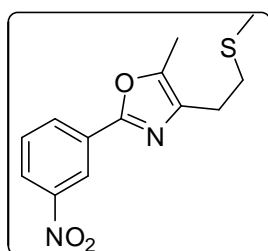
The title compound was synthesized as colorless semi solid in 74% yield according to the general procedure as described above for 4a; $R_f = 0.7$ (30% EtOAc-n-Hexane); IR (cm⁻¹): 3233, 3040, 2978, 2872, 1718 (C=O of ketone), 1656 (C=O of amide), 1520, 1321; ¹H NMR (300 MHz, CDCl₃) δ 2.03- 2.19 (m, 5H), 2.25-2.36 (m, 2H), 2.55-2.64 (m, 2H), 4.90-5.00 (m, 1H), 7.85 (bs, 1H), 9.03 (d, $J = 1.6$ Hz, 2H), 9.17 (d, $J = 1.6$ Hz, 1H). ¹³C NMR (75MHz, CDCl₃) δ 15.7, 27.3, 29.6, 59.1, 121.2, 127.5, 137.1, 148.5, 162.6, 205.6; MS (EI, 70ev): m/z (%) [M]⁺ 288.4 (100%).

General procedure for synthesis of 5a-c:



Phosphorus oxychloride (1 mL, 10 mmol) was added dropwise to a solution of *N*-(1-(Methylthio)-4-oxopentan-3-yl)-3-nitrobenzamide **4a** (3.3 mmol) in DMF (10 mL) at 0 °C. The mixture was heated to 90°C for 45 min and then cooled to 0 °C before being quenching with water and extracted with EtOAc. The combined organic phases were washed with water and brine (15 mL), dried over anhydrous Na₂SO₄, filtered and the solvent evaporated. The residue was purified by column chromatography (EtOAc/hexanes) to provide of the desired products.

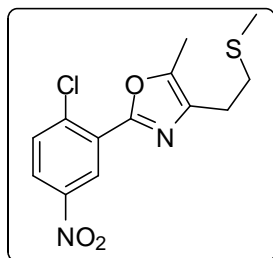
5-Methyl-4-(2-(methylthio) ethyl)-2-(3-nitrophenyl) oxazole (5a):



Brownish semi solid; $R_f = 0.7$ (30% EtOAc-n-Hexane); Yield 84 % ; IR (cm⁻¹): 3060, 2955, 2862, 1520, 1321; ¹H NMR (300 MHz, CDCl₃) δ 2.15 (s, 3H), 2.39 (s, 3H), 2.78 -2.87 (m, 4H), 7.59 - 7.63 (t, $J = 8.0$ Hz, 1H), 8.23 (d, $J = 8.0$ Hz, 1H), 8.25 (d, $J = 1.6$ Hz, 1H), 8.8 (s, 1H) ; ¹³C NMR (75 MHz, CDCl₃) δ 10.3, 15.7, 26.1, 33.5, 120.7, 124.0,

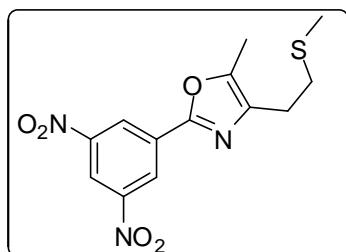
129.3, 129.8, 131.4, 135.4, 145.5, 148.6, 157.1; MS (EI, 70ev): m/z (%) $[M]^+$ 279.0 (100%).

2-(2-chloro-5-nitrophenyl)-5-methyl-4-(2-(methylthio) ethyl) oxazole (5b):



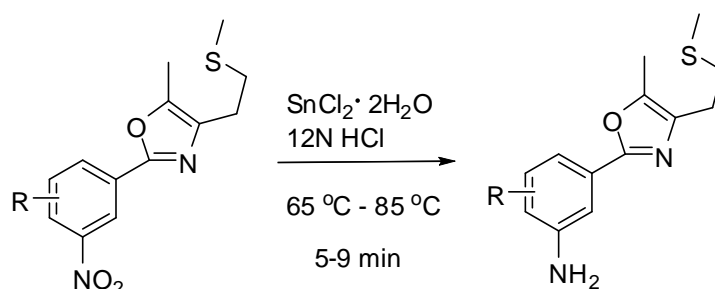
The title compound was synthesized as brown color semi solid in 80% yield according to the general procedure as described above for **5a**; R_f = 0.7 (30% EtOAc-n-Hexane); IR (cm^{-1}): 3070, 2978, 2856, 1510, 1318; ^1H NMR (300 MHz, CDCl_3) δ 2.15 (s, 3H), 2.41(s, 3H), 2.80-2.89 (m, 4H), 7.65 (d, J = 8.4 Hz, 1H), 8.14-8.16 (dd, J^1 = 8.4 Hz, J^2 = 2.8 Hz, 1H), 8.85 (d, J = 2.8 Hz, 1H); ^{13}C NMR (75 MHz, CDCl_3) δ 10.3, 15.7, 26.0, 33.5, 124.3, 125.8, 127.7, 132.3, 135.5, 138.4, 145.9, 146.4, 155.1MS (EI, 70ev): m/z (%) $[M]^+$ 313.1 (100%).

2-(3,5-Dinitrophenyl)-5-methyl-4-(2-(methylthio) ethyl) oxazole (5c):



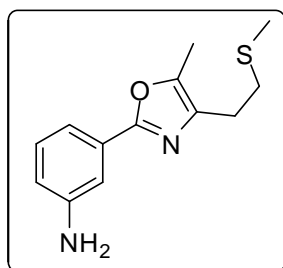
The title compound was synthesized as brown color semi solid in 88% yield according to the general procedure as described above for **5a**; R_f = 0.72 (30% EtOAc-n-Hexane); IR (cm^{-1}): 3048, 2978, 2856, 1530, 1325; ^1H NMR (300 MHz, CDCl_3) δ 2.15 (s, 3H), 2.43 (s, 3H), 2.80-2.89 (m, 4H), 9.02 (d, J = 2.0 Hz, 1H), 9.10 (d, J = 2.0 Hz, 2H). ^{13}C NMR (75MHz, CDCl_3) δ 10.4, 15.7, 25.9, 33.5, 118.6, 125.3, 130.9, 136.4, 146.9, 148.9, 155.2; MS (EI, 70ev): m/z (%) $[M]^+$ 324.2 (96%), 294.2(100%).

General procedure for synthesis of 6a-c:



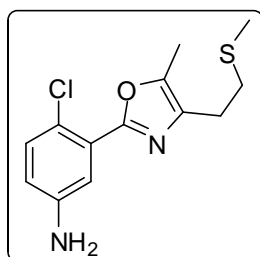
To a solution of 5-Methyl-4-(2-(methylthio) ethyl)-2-(3-nitrophenyl) oxazole (**5a**) (2.5 mmol) in 36% HCl (6 mL), stannouschloride monohydrate (12.5 mmol) was added. The mixture was heated to 100 °C for 15min, cooled to 0 °C the aqueous solution was basified with 2N NaOH and extracted three times with dichloromethane. The organic layers were combined, washed with brine solution and dried over anhydrous Na_2SO_4 and concentrated to give desired product **6a**.

3-(5-Methyl-4-(2-(methylthio) ethyl) oxazol-2-yl) aniline (6a):



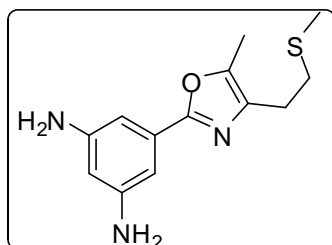
Brown solid; $R_f = 0.4$ (30% EtOAc-n-Hexane); mp 292-294 °C; Yield (65 %); IR (cm^{-1}): 3390, 3350 (NH_2), 3020, 2910, 2858, 1650, 1110; ^1H NMR (300 MHz, CDCl_3) δ 2.12 (s, 3H), 2.33 (s, 3H), 2.74 - 2.85 (m, 4H), 6.70 - 6.73 (dd, $J^1 = 7.8$ Hz, $J^2 = 2.2$ Hz, 1H), 7.18 - 7.22 (m, 2H), 7.31 (t, $J = 1.6$ Hz, 1H), 7.32 - 7.37 (dt, $J^1 = 8.6$ Hz, $J^2 = 1.2$ Hz, 1H), 8.8 (s, 1H); ^{13}C NMR (75 MHz, CDCl_3) δ 10.2, 15.7, 26.1, 33.7, 112.1, 116.6, 116.9, 128.3, 129.7, 134.2, 144.4, 146.2, 159.6; MS (EI, 70ev): m/z (%) $[\text{M}]^+$ 249.3 (100%). HRMS $[\text{M}]^+$ Calcd. for $\text{C}_{13}\text{H}_{17}\text{N}_2\text{O}_5\text{S}$ 249.1062; Found: 249.1056.

4-chloro-3-(5-methyl-4-(2-(methylthio) ethyl) oxazol-2-yl) aniline (6b):



The title compound was synthesized as yellow color semi solid in 76% yield according to the general procedure as described above for **6a**; $R_f = 0.42$ (30% EtOAc-n-Hexane); IR (cm^{-1}): 3400, 3375 (NH_2), 3010, 2962, 2892, 1620, 1220; ^1H NMR (300 MHz, CDCl_3) δ 2.14 (s, 3H), 2.36 (s, 3H), 2.77-2.86 (m, 4H), 3.5 (bs, 2H), 6.63-6.66 (dd, $J^1 = 8$ Hz, $J^2 = 2.8$ Hz, 1H), 7.22-7.26 (dd, $J^1 = 8.0$ Hz, $J^2 = 2.8$ Hz, 2H). ^{13}C NMR (75MHz, CDCl_3) δ 10.23, 15.6, 26.1, 33.6, 116.5, 117.6, 121.2, 126.8, 131.6, 134.3, 144.7, 157.6; MS (EI, 70ev): m/z (%) $[\text{M}]^+$ 283.1 (100%). HRMS $[\text{M}]^+$ Calcd. for $\text{C}_{13}\text{H}_{16}\text{N}_2\text{OSCl}$ 283.0672; Found: 283.0675.

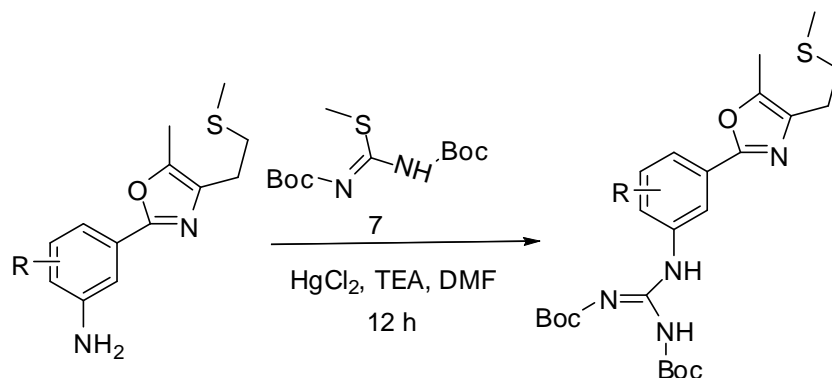
5-(5-Methyl-4-(2-(methylthio) ethyl) oxazol-2-yl) benzene-1,3-diamine (6c):



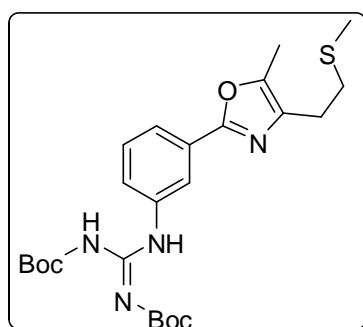
The title compound was synthesized as dark brown color semi solid in 76% yield according to the general procedure as described above for **6a**; $R_f = 0.2$ (30% EtOAc-n-Hexane); IR (cm^{-1}): 3425, 3396 (NH_2), 3030, 2954, 2892, 1600, 1550, 1190; ^1H NMR (300 MHz, CDCl_3) δ 2.12 (s, 3H), 2.32 (s, 3H), 2.73-2.83 (m, 4H), 3.69-3.78 (bs, 4H), 6.07 (t, $J = 2.0$ Hz, 1H), 6.74 (d, $J = 2.0$ Hz, 2H). ^{13}C NMR (75MHz, CDCl_3) δ 15.7, 26.2, 29.7, 33.7, 40.9, 58.8, 71.63, 87.1, 103.1, 103.6, 125.9, 128.4, 128.5, 129.4, 134.3, 143.8, 147.7, 159.7; MS (EI, 70ev): m/z (%) $[\text{M}]^+$ 264.1 (100%), 216.2 (78%) HRMS $[\text{M}]^+$ Calcd. for $\text{C}_{13}\text{H}_{18}\text{N}_3\text{OS}$ 264.1171; Found: 264.1174.

General procedure for synthesis of 8a-c:

To a solution of 3-(5-Methyl-4-(2-(methylthio) ethyl) oxazol-2-yl) aniline **6a** (0.4 mmol) in dryDMF (6 mL), N_1, N_2 -bis (*tert*-butoxycarbonyl)-*S*-methylisothiourea (0.45 mmol), triethylamine (0.1 mL, 0.4 mmol) and HgCl₂ (or AgNO₃) (0.48 mmol) was added. The suspension was stirred at room temperature for 12 h then concentrated in vacuo. The crude reaction mixture was taken up in DCM (20 mL), filtered through a pad of celite on a sintered glass funnel, washed with saturated aqueous NH₄Cl (5 mL) and organic layer was washed with brine (50 mL), and dried over Na₂SO₄, filtered and concentrated to give desired product (**8a**).

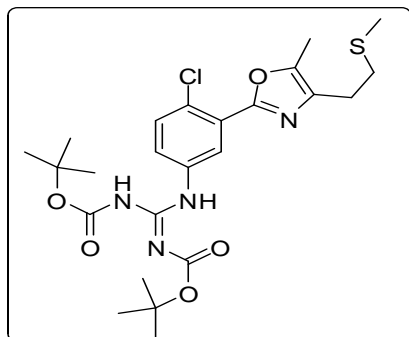


(E)-*tert*-butyl (*tert*-butoxycarbonylamino) (3-(5-methyl-4-(2-(methylthio) ethyl) oxazol-2-yl) phenylamino) methylenecarbamate (8a**):**



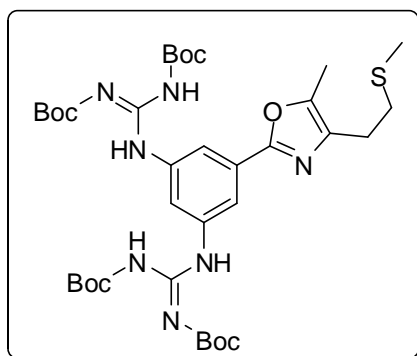
Colorless semi solid; $R_f = 0.8$ (30% EtOAc-n-Hexane); Yield (78%); IR (cm⁻¹): 3261(NH), 3154, 2978, 2926, 1721(amide), 1644 (C=N); ¹H NMR (300 MHz, CDCl₃) δ 1.52(s, 9H), 1.53(s, 9H), 2.14 (s, 3H), 2.35 (s, 3H), 2.75 -2.85 (m, 4H), 7.40 (t, $J = 8.0$ Hz, 1H), 7.71(d, $J = 8.0$ Hz, 1H), 7.92 (t, $J = 2.2$ Hz, 1H), 8.06 (s, 1H), 10.45(bs, 1H), 11.63(bs, 1H); ¹³C NMR (75 MHz, CDCl₃) δ 10.2, 15.7, 26.2, 33.7, 112.3, 116.3, 116.6, 128.5, 129.6, 134.4, 143.9, 146.5, 159.6; MS (EI, 70ev): m/z (%) [M]⁺ 491.23 (100%). HRMS [M]⁺ Calcd. for C₂₄H₃₅N₄O₅S 491.2328; Found: 491.2316.

(E)-tert-butyl (tert-butoxycarbonylamino) (4-chloro-3-(5-methyl-4-(2 (methylthio) ethyl) oxazol-2-yl) phenylamino) methylenecarbamate (8b):



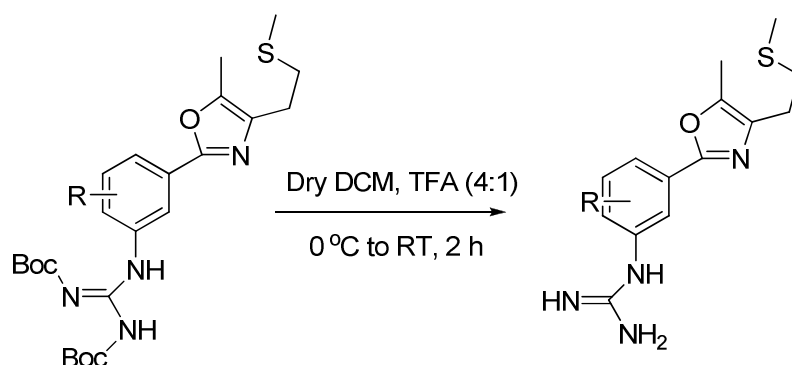
The title compound was synthesized as colorless solid in 72% yield according to the general procedure as described above for **8a**; $R_f = 0.8$ (30% EtOAc-n-Hexane); mp 310-312 °C. IR (cm^{-1}): 3321(NH), 3124, 2978, 2862, 1700 (amide), 1665 (C=N); ^1H NMR (300 MHz, CDCl_3) δ 1.51 (s, 9H), 1.53 (s, 9H), 2.14 (s, 3H), 2.37 (s, 3H), 2.80-2.86 (m, 4H), 7.43 (d, $J = 8.8$ Hz, 1H), 7.87-7.90 (dd, $J^1 = 8.8$ Hz, $J^2 = 2.4$ Hz, 1H), 8.04 (d, $J = 2.4$ Hz, 1H). ^{13}C NMR (75MHz, CDCl_3) δ 10.3, 15.7, 26.2, 28.0, 28.1, 29.7, 33.6, 79.9, 84.0, 123.2, 124.2, 126.7, 127.4, 131.6, 134.7, 135.8, 144.9, 153.2, 153.4, 156.9, 163.2; MS (EI, 70ev): m/z (%) $[\text{M}]^+$: 542.3 (10%), 525.3 (100%) HRMS $[\text{M}]^+$ Calcd. for $\text{C}_{24}\text{H}_{34}\text{N}_4\text{O}_6\text{SCl}$ 541.1874; Found: 541.1865.

Tert-butyl(5-(5-methyl-4-(2-(methylthio)ethyl)oxazol-2-yl)-1,3-phenylene)bis(azanediyl) bis ((tert-butoxycarbonylamino) methan-1-yl-1-ylidene) dicarbamate (8c):



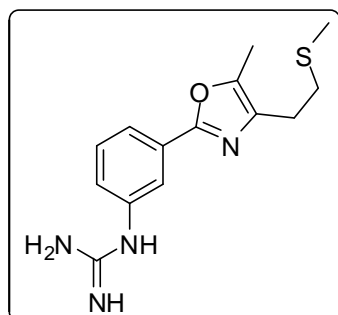
The title compound was synthesized as colorless solid in 80% yield according to the general procedure as described above for **8a**; $R_f = 0.85$ (30% EtOAc-n-Hexane); mp 369-372 °C. IR (cm^{-1}): 3361(NH), 3133, 2958, 2862, 1710(amide), 1660 (C=N); ^1H NMR (300 MHz, CDCl_3): 1.52 (s, 3H), 2.13 (s, 3H), 2.34 (s, 3H), 2.74-2.85 (m, 4H), 8.12 (d, $J = 1.6$ Hz, 2H), 8.16 (s, 1H), 10.48 (s, 2H), 11.54 (bs, 2H). ^{13}C NMR (75MHz, CDCl_3): 10.1, 15.7, 26.2, 28.1, 33.6, 79.6, 83.8, 115.4, 116.5, 128.7, 134.7, 137.9, 144.3, 153.3, 158.8, 163.2; MS (EI, 70ev): m/z (%) $[\text{M}]^+$: 748.36 (68%), 348.15 (100%).

General procedure for synthesis of 9a-c:



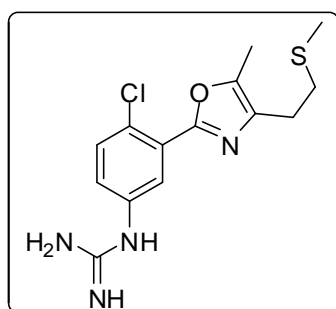
A solution containing (E)-*Tert*-butyl (*tert*-butoxycarbonylamino) (3-(5-methyl-4-(2-(methylthio)ethyl)oxazol-2-yl) phenylamino) methylenecarbamate **8a** (0.023 mmol) in DCM (1 ml), 1mL of TFA was added at 0 °C, and then stirred at RT for 1 h. The solvent was removed under high vacuum to generate the trifluoroacetate salt. This salt was redissolved in 20 mL of an aqueous solution of NaHCO₃ and washed with DCM (3 × 15 mL). The organic layer was washed with water (2 × 10 mL), followed by brine wash, dried over anhydrous Na₂SO₄ and concentrated to give the corresponding free guanidine (**9a**).

1-(3-(5-Methyl-4-(2-(methylthio) ethyl) oxazol-2-yl) phenyl) guanidine (**9a**):



Color less semi solid; $R_f = 0.3$ (5% MeOH-CH₂Cl₂); Yield (85%); IR (cm⁻¹): 3340(NH), 3178, 2963, 2854, 1680 (C=N); ¹H NMR (300 MHz, CDCl₃) δ 2.15 (s, 3H), 2.33 (s, 3H), 2.74 -2.84 (m, 4H), 2.86- 3.40(bs, 4H), 6.98 (d, $J = 8.0$ Hz, 1H), 7.33 (t, $J = 8.0$ Hz, 1H), 7.56 (s, 1H), 7.61 (d, $J = 8.0$ Hz, 1H); ¹³C NMR (75 MHz, CDCl₃) δ 8.6, 14.3, 29.3, 33.1, 122.2, 124.4, 126.6, 128.7, 130.4, 134.5, 135.7, 145.7, 156.6, 158.6; MS (EI, 70ev): m/z (%) [M]⁺ 291.3 (100%). HRMS [M]⁺ Calcd. for C₁₄H₁₈N₄OS 291.3228; Found: 291.3216.

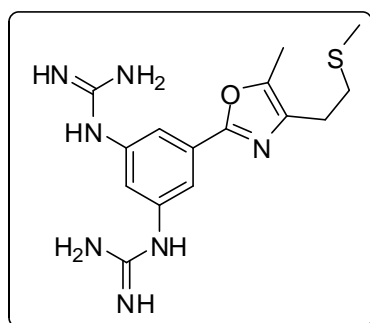
1-(4-chloro-3-(5-methyl-4-(2-(methylthio)ethyl)oxazol-2-yl)phenyl)guanidine (**9b**):



The title compound was synthesized as colorless semi solid in 80% yield according to the general procedure as described above for **9a**; $R_f = 0.3$ (5% MeOH-CH₂Cl₂); Yield (74%); IR (cm⁻¹): 3420(NH), 3178, 2978, 2921, 2834, 1690 (C=N); ¹H NMR (300 MHz, CDCl₃) δ 2.18 (s, 3H), 2.38 (s, 3H), 2.71 -2.89 (m, 4H), 7.10-7.30 (m, 2H), 7.52 (d, $J = 8.0$ Hz, 1H), 7.78 (s,

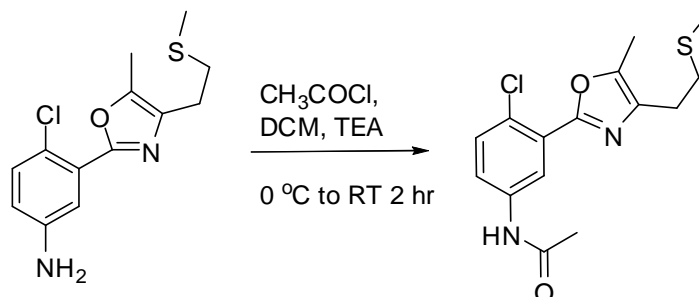
1H), 10.00 (s, 1H), 10.29 (bs, 2H) ; ^{13}C NMR (75 MHz, CDCl_3) δ 10.2, 15.5, 29.7, 33.4, 126.7, 127.2, 128.2, 131.7, 132.9, 133.2, 146.9, 156.4; MS (EI, 70ev): m/z (%) $[\text{M}]^+$ 291.3 (100%). MS (EI, 70ev): m/z (%) $[\text{M}]^+$ 324.3 (100%). HRMS $[\text{M}]^+$ Calcd. for $\text{C}_{14}\text{H}_{17}\text{ClN}_4\text{OS}$ 324.3134; Found: 324.3146.

1,1'-(5-(5-methyl-4-(2-(methylthio)ethyl)oxazol-2-yl)-1,3-phenylene)diguandine (9c):



The title compound was synthesized as white color solid in 80% yield according to the general procedure as described above for **9a**; mp 308-311 °C; R_f = 0.3 (15% MeOH- CH_2Cl_2); Yield (80%); IR (cm^{-1}): 3390 (NH), 3156, 2985, 2911, 2865, 1676 (C=N); ^1H NMR (300 MHz, CD_3OD) δ 2.06 (s, 3H), 2.33 (s, 3H), 2.74-2.77 (m, 4H), 7.24 (s, 1H), 7.79 (s, 2H); ^{13}C NMR (75MHz, CD_3OD) δ 10.1, 15.5, 26.6, 34.4, 121.7, 124.0, 131.8, 136.5, 138.7, 147.6, 158.1, 158.9; MS (EI, 70ev): m/z (%) $[\text{M}]^+$ 348.1 (100%) HRMS $[\text{M}]^+$ Calcd. for $\text{C}_{15}\text{H}_{22}\text{N}_7\text{OS}$ 348.1607; Found: 348.1612.

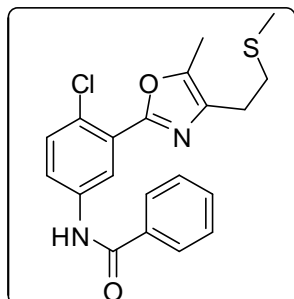
N-(4-chloro-3-(5-methyl-4-(2-(methylthio)ethyl)oxazol-2-yl)phenyl)acetamide (10):



Acetyl chloride (1.2 mmol) was added to a mixture of 4-chloro-3-(5-methyl-4-(2-(methylthio)ethyl)oxazol-2-yl) aniline (**6b**) (1 mmol), triethylamine (2.4 mmol) in dry dichloromethane (10 mL) at 0 °C. The reaction mixture was stirred for 2 hr followed by drop wise addition of 2N HCl. The residue was dissolved in dichloromethane (50 mL), washed with water (2 x 250 mL), brine (1 x 100 mL), dried over Na_2SO_4 , filtered and the solvent evaporated. The residue was purified by flash chromatography (n-hexane/ ethylacetate 4:1) to afford the desired product (**10**) as yellow colour semi solid in 90% yield; R_f = 0.42 (30% EtOAc-n-Hexane); IR (cm^{-1}): 3345, 3066, 2966, 2866, 1685 (C=O of amide), 1340; ^1H NMR (300 MHz, CDCl_3) δ 1.88 (s, 3H), 2.15 (s, 3H), 2.50 (s, 3H), 2.87-2.98 (m, 4H), 7.12 (d, J = 8.1 Hz, 1H), 7.64 (dd, J^1 = 8.1 Hz, J^2 = 2.8 Hz, 2H), 7.82 (s, 1H), 9.86 (bs, 1H) . ^{13}C NMR (75MHz, CDCl_3) δ 10.3,

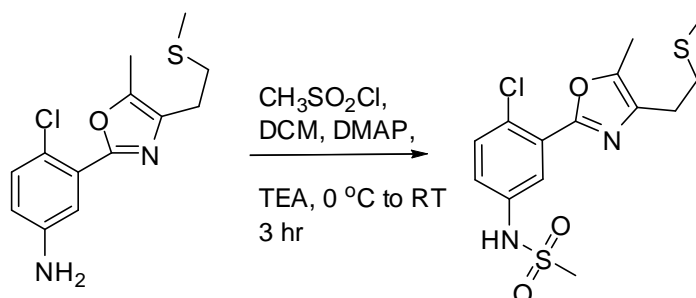
15.6, 23.6, 29.6, 33.6, 119.8, 127.6, 131.8, 131.9, 134.9, 138.0, 145.3, 156.1, 169.6; MS (EI, 70ev): m/z (%) [M]⁺ 323.15 (100%).

N-(4-chloro-3-(5-methyl-4-(2-(methyl thio)ethyl)oxazol-2-yl)phenyl)benzamide (11):



The title compound was synthesized as colourless semi solid in 86% yield according to the procedure as described above for **10** (instead of acetyl chloride benzoyl chloride was taken); $R_f = 0.42$ (10% EtOAc-n-Hexane); IR (cm⁻¹): 3195, 3052, 2965, 2875, 1679 (C=O of amide), 1314; ¹H NMR (300 MHz, CDCl₃) δ 2.16 (s, 3H), 2.48 (s, 3H), 2.96-3.08 (m, 4H), 7.36 (d, $J = 8.2$ Hz, 1H), 7.47-7.52 (m, 2H), 7.63-7.74 (m, 2H), 8.06 (d, $J = 7.2$ Hz, 1H), 8.85 (bs, 1H). ¹³C NMR (75MHz, CDCl₃) δ 11.2, 15.1, 29.8, 33.8, 121.1, 125.1, 126.9, 127.9, 128.6, 130.7, 132.0, 136.9, 138.8, 158.6, 166.6; MS (EI, 70ev): m/z (%) [M]⁺ 385.27 (100%).

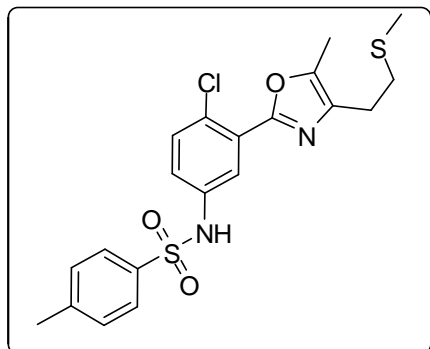
N-(4-chloro-3-(5-methyl-4-(2-(methylthio)ethyl)oxazol-2-yl)phenyl)methane sulfonamide (12):



Methane sulfonyl chloride (1.2 mmol) was added to a mixture of 4-chloro-3-(5-methyl-4-(2-(methylthio) ethyl) oxazol-2-yl) aniline (**6b**) (1 mmol), triethylamine (2.4 mmol) and DMAP (0.1 mmol) in dry dichloromethane (10 mL) at 0 °C. The reaction mixture was stirred for 3 hr followed by drop wise addition of 2N HCl. The residue was dissolved in dichloromethane (50 mL), washed with water (2 x 150 mL), brine (1 x 50 mL), dried over Na₂SO₄, filtered and the solvent evaporated. The residue was purified by flash chromatography (n-hexane/ ethylacetate 3.5:1.5) to afford the desired product (**12**) as brown colour semi solid in 90% yield; $R_f = 0.30$ (30% EtOAc-n-Hexane); IR (cm⁻¹): 3290, 3050, 2985, 2865, 1680 (C=O of amide), 1326; ¹H NMR (300 MHz, CDCl₃) δ 2.25 (s, 3H), 2.35 (s, 3H), 2.75 (s, 3H), 2.87-3.02 (m, 4H), 5.96 (bs, 1H), 6.85 (d, $J = 8.4$ Hz, 1H), 7.13 (d, $J = 8.6$ Hz, 1H), 7.40-7.46 (m, 1H). ¹³C NMR

(75MHz, CDCl₃) δ 11.5, 15.6, 28.6, 36.6, 39.3, 115.5, 121.1, 125.0, 130.4, 136.7, 138.6, 144.5, 158.6; MS (EI, 70ev): m/z (%) [M]⁺: 360.97 (100%).

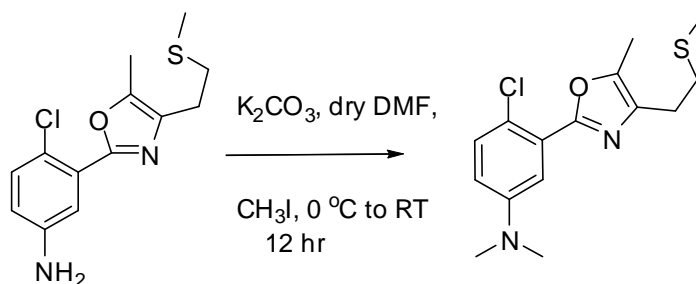
N-(4-chloro-3-(5-methyl-4-(2-(methylthio)ethyl)oxazol-2-yl)phenyl)-4-methylbenzene sulphonamide (13):



The title compound was synthesized as yellow colour semi solid in 86% yield according to the procedure as described above for **12** (instead of methane sulfonyl chloride 4-toluene sulfonyl chloride was taken); R_f = 0.6 (10% EtOAc-n-Hexane); IR (cm⁻¹): 3210, 3010, 2965, 2875, 1690 (C=O of amide), 1314; ¹H NMR (300 MHz, CDCl₃) δ 2.20 (s, 3H), 2.32 (s, 3H), 2.41(s, 3H), 2.85-2.96

(m, 4H), 6.15 (bs, 1H), 6.91 (d, J = 8.4 Hz, 1H), 6.98 (d, J = 7.2 Hz, 1H), 7.21-7.26 (m, 1H), 7.41 (d, J = 8.2 Hz, 2H), 7.62 (d, J = 8.2 Hz, 1H). ¹³C NMR (75MHz, CDCl₃) δ 10.3, 15.6, 20.9, 25.9, 35.9, 110.5, 121.7, 124.5, 128.7, 130.2, 130.9, 136.2, 136.9, 139.9, 157.7; MS (EI, 70ev): m/z (%) [M]⁺: 437.23 (100%).

4-chloro-N,N-dimethyl-3-(5-methyl-4-(2-(methylthio)ethyl)oxazol-2-yl)aniline (14):



Methyl iodide (6.0 mmol) was added to a mixture of 4-chloro-3-(5-methyl-4-(2-(methylthio)ethyl) oxazol-2-yl) aniline (**6b**) (1 mmol), anhydrous K₂CO₃ (6.0 mmol) in dry dimethyl formamide (10 mL) at 0 °C. The reaction mixture was stirred for 12 hr followed by drop wise addition of 1N HCl at 0 °C. The residue was dissolved in dichloromethane (2 x 50 mL), washed with water (2 x 150 mL), brine (1 x 50 mL), dried over Na₂SO₄, filtered and the solvent evaporated. The residue was purified by flash chromatography (n-hexane/ ethylacetate 3:2) to afford the desired product (**14**) as brown colour semi solid in 65% yield; R_f = 0.20 (40% EtOAc-n-Hexane); IR (cm⁻¹): 3050, 2972, 2872, 1630, 1290; ¹H NMR (300 MHz, CDCl₃) δ 2.14 (s, 3H), 2.45 (s, 3H), 3.05-3.16 (m, 4H), 3.55 (s, 6H), 6.82 (d, J = 8.4 Hz, 1H),

6.96 (d, $J= 7.8$ Hz, 1H), 7.15 (m,1H). ^{13}C NMR (75MHz, CDCl_3) δ 10.3, 15.6, 26.0, 31.8, 45.9, 111.7, 117.5, 124.5, 125.2, 128.7, 136.9, 145.3, 148.2, 155.6; MS (EI, 70ev): m/z (%) $[\text{M}]^+$ 311.17 (100%).

4.6.3 Pharmacology

4.6.3.1 Evaluation of cell viability

The MTT assay was used for evaluating the effect of the compounds on cell viability. RPMI medium supplemented with 10% FBS and antibiotics was used to culture HeLa and MDA-MB-231 cells. MTT dye prepared in 1X PBS was used for cell viability assays. HeLa and MDA-MB-231 cells in monolayer were trypsinised and the cell count was adjusted to 3×10^6 cells/ml using medium containing 10% fetal calf serum. Cells were pre-incubated at a concentration of 1×10^6 cells/ml in culture medium for 3h at 37°C and 6.5% CO_2 . Cells were then seeded at a concentration of 5×10^4 cells/well in 100 μl culture medium and the plates incubated at 37°C in 5% CO_2 incubator for 24 h. After 24h, 100 μl of previously diluted compounds of different concentrations of test compounds in media were added and incubated at 37°C in 5% CO_2 for 72h and cells were periodically checked for granularity, shrinkage and swelling. After 72h, 10ml of MTT dye was added to each well. The plates were gently shaken and incubated for 4h at 37°C in 5% CO_2 . The supernatant was removed and 100 μl of 1:1 DMSO: Ethanol was added and the plates were gently shaken to solubilize the formed formazan. The absorbance was measured using a microplate reader at a wavelength of 550 nm.

4.6.3.2 Evaluation of *in vitro* LSD1 activity

The effect of the compounds was evaluated in an *in vitro* LSD1 enzyme assay. The compounds were dissolved in 100% DMSO to a stock concentration of 10mM and used in the assay as per the manufacturer's instructions (Cayman Chemical Company, LSD1 screening kit Catalog # 700120). Briefly, the assay is based on the generation of the product Resorufin by the enzyme Horse radish peroxidase in the presence of hydrogen peroxide, which is produced by the demethylation of a methylated histone H3K4 peptide by LSD1. The amount of Resorufin generated is measured spectrophotometrically at 595/60 nm and is an indicator of LSD1 activity.

The assay was performed in a 96-well plate format with triplicates of all samples. Absorbance values were normalized to background (lacking the substrate peptide) and % initial activity was calculated using the formula $100 - [(I-S)/S] * 100$, where I was the absorbance of the Initial

activity samples (without inhibition) and S was the absorbance of the test samples (with various compounds).

4.6.3.3 Evaluation of *in vivo* apoptosis and toxicity using zebrafish embryos⁴⁴

All procedures using zebrafish were in accordance with ethical guidelines for animal use and followed those published by the NIH. An indigenous wild type adult zebrafish strain from India was used for this study (obtained from Vikrant Aquaculture, Mumbai, India). They were maintained in a recirculation system using purified ELIX System (Millipore, Billerica, US) grade water containing 200mg/l sea salt at 28 °C under a 14:10 h light and dark cycle. Fish were fed three times daily with a combination of freshly hatched live brine shrimp and dry food. Males and females were kept in separate tanks for four days before they were allowed to spawn. On day five, 300-400 embryos were obtained by natural mating of both adult sexes (3:2 female and male ratios) in a breeding tank setup. Embryos were collected and raised in 60 mm Petri dishes containing E3 medium (5 mM NaCl, 0.17 mM KCl, 0.33 mM CaCl₂, and 0.33 mM MgSO₄) for 24h. Compound stocks were diluted in E3 medium to obtain final concentrations of 10µM in 0.1% DMSO. Zebrafish embryos at 24h post fertilization were dechorionated with 500µg/ml Pronase K for 10 minutes. Six embryos per well were placed in 24-well plates containing E3 medium and compounds added to a final concentration of 10µM (in 0.1% DMSO). The embryos were grown in the presence of the compounds for 24h, 48h and 72h. Control embryos were incubated in 0.1% DMSO. Apoptosis was assessed at the respective time points using acridine orange staining. Briefly, embryos were washed twice with 1X PBS (phosphate buffer saline) for 5min each, followed by incubation in acridine orange solution (5µg/ml in E3 medium) for 1h at room temperature. Embryos were then washed with 1X PBS three times for 5min each and visualized under an upright fluorescence microscope (Zeiss Axioscope) at an excitation wavelength of 502nm and an emission wavelength of 525nm. Acridine orange is a fluorescent dye that binds to DNA and exhibits increased fluorescence in fragmented nuclei, a hallmark of apoptosis^[1-2]. Embryos were also observed using visible light microscopy at regular intervals after compound treatment to document general toxicity-related effects such as developmental delays, deformations, edema and death.

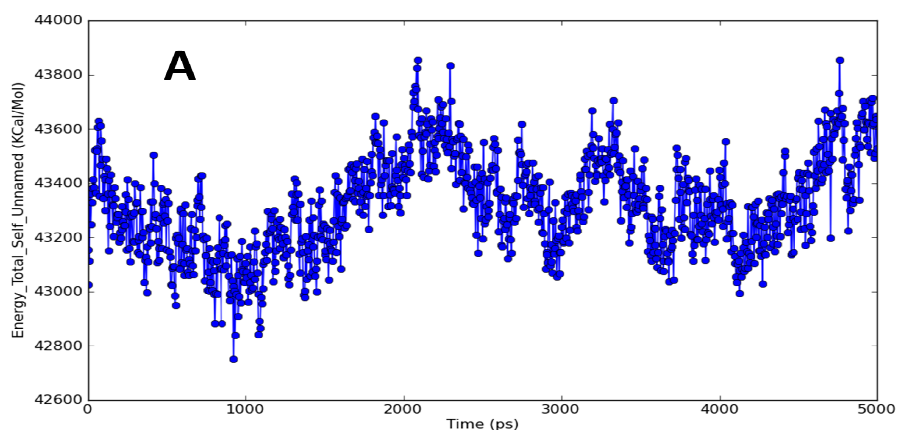
4.6.4 Molecular Modeling Studies

4.6.4.1 Docking method

We carried out Molecular modeling (Docking analysis and Molecular dynamics simulations) studies to reveal the binding mode and ligand receptor complex stability. The docking studies of most potent molecules were performed using the Schrodinger software suite (Maestro, version 9.2, Schrodinger, LLC: New York, NY 2012). The compounds were sketched in 3D format using build panel and were prepared for docking using ligprep application. The Protein (PDB ID: 2Z3Y)⁴⁵ for docking study was retrieved from protein data bank (PDB). The protein was prepared by giving preliminary treatment like adding hydrogen, adding missing residues, refining the loop with prime and finally minimized by using OPLS 2005 force field. Grids for molecular docking were generated with bound co-crystallized ligand. Compounds were docked using Glide (Glide version 5.7, Schrodinger, LLC: New York, NY 2012) in extra-precision mode, with up to three poses saved per molecule.

4.6.4.2 Molecular Dynamics Simulations Protocols:

Molecular dynamics (MD) simulations of **9a** at the binding site of protein were performed using the Desmond package incorporated in the Maestro⁴⁶. The system was built by applying OPLS-AA force field in an explicit solvent with the single point charges (SPC) water model (OPLS-AA/SPC). The initial coordinates for the MD calculations were taken from the docking experiments. The SPC water molecules were then added and system was neutralized by adding Na⁺ counter-ion to balance the net charges of the system. After the construction of the solvent environment, the complex system was composed of approximately 126117 atoms. Before equilibration and long production MD simulations, the systems were minimized and pre-equilibrated using the default relaxation routine implemented in Desmond.



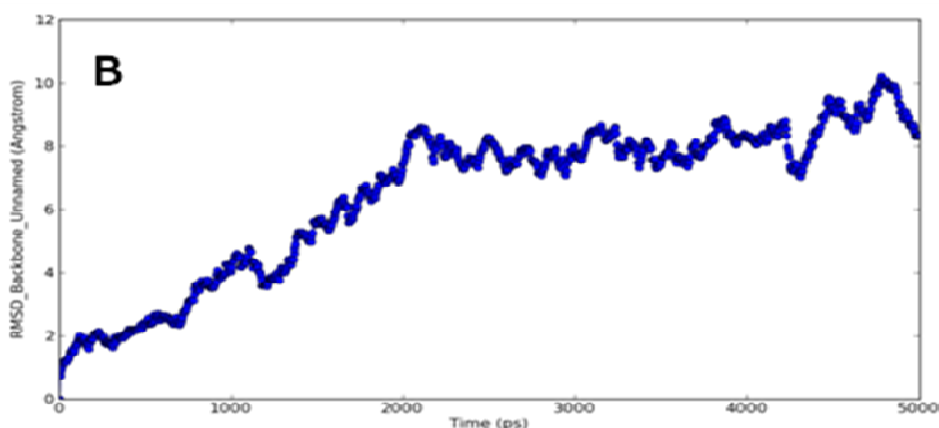


Figure 16: Time dependence of the total energy (A) and protein backbone RMSD (B) relative to the initial minimised complex of **9a** during MD simulations.

The MD simulations were run for 5 ns and during the MD simulations, the equations of motion were integrated with a 2 fs time step in the NVT ensemble. The SHAKE algorithm was applied to all hydrogen atoms; the van der Waals (VDW) cutoff was set to 9 Å. The temperature was maintained at 300 K, employing the Nosé–Hoover thermostat method with a relaxation time of 1ps. The trajectory recording interval was kept for every 10 ps during entire MD runs.

4.7 References:

1. Lim, S.; Metzger, E.; Schüle, R.; Kirfel, J.; Buettner, R. *Int. J. Cancer*. **2010**, *127*, 1991.
2. WHO (February 2006); Cancer World Health Organization, Retrieved on 2007-06-25.
3. Jaenisch, R.; Bird, A. *Nat Genet*. **2003**, *33*, Suppl. 245.
4. Bernstein, B. E.; Meissner, A.; Lande, E. S. *Cell*, **2007**, *128*, 669.
5. Reik, W. *Nature*, **2007**, *447*, 425.
6. Ozanne, S. E.; Constância, M. *Nat Clin Pract Endocrinol Metab*, **2007**, *3*, 539.
7. Feinberg, A. P.; Tycko, B. *Nat Rev Cancer*, **2004**, *4*, 143.
8. Esteller, M. *N Engl J Med*, **2008**, *358*, 1148.
9. Feinberg, A. P.; Tycko, B. *Nat. Rev. Cancer*, **2004**, *4*, 143.
10. Fraga, M. F.; Ballestar, E.; Villar-Garea, A.; Boix-Chornet, M.; Espada, J.; Schotta, G.; Bonaldi, T.; Haydon, C.; Ropero, S.; Petrie, K.; Iyer, N. G.; Pérez-Rosado, A.; Calvo, E.; Lopez, J. A.; Cano, A.; Calasanz, M. J.; Colomer, D.; Piris, M. A.; Ahn, N.; Imhof, A.; Caldas, C.; Jenuwein, T.; Estelle, M.; *Nat. Genet*. **2005**, *37*, 391.
11. Thomas, J.O. *J Cell Sci Suppl*. **1984**, *1*, 1-20.
12. Gelato, K. A.; Fischle, W. *Biol Chem*. **2008**, *389*, 353.
13. Zhu, Q.; Liu, C.; Ge, Z.; Fang, X.; Zhang, X.; Strååt, K.; Björkholm, M.; and Xu, D. *PLoS One*. **2008**, *3*, p. e1446.
14. Huang, J.; Sengupta, R.; Espejo, A. B.; Lee, M. G.; Dorsey, J. A.; Richter, M.; Opravil, S.; Shiekhatar, R.; Bedford, M. T.; Jenuwein, T.; Berger, S. L. *Nature*. **2007**, *449*, 105.
15. Reik, W. *Nature*, **2007**, *447*, 425.
16. Ozanne, S. E.; Constância, M. *Nat Clin Pract Endocrinol Metab*. **2007**, *3*, 539.
17. Feinberg, A. P.; Tycko, B. *Nat Rev Cancer*, **2004**, *4*, 143.
18. Esteller, M. *N. Engl. J. Med*. **2008**, *358*, 1148.
19. Huang, Y.; Greene, E.; Murray, S. T.; Goodwin, A. C.; Baylin, S. B.; Woster, P. M.; Casero, R. A. Jr. *Proc Natl Acad Sci U S A*. **2007**, *104*, 8023.
20. Anand, R.; Marmorstein, R. *J. Biol. Chem*. **2007**, *282*, 35425.
21. Shi, Y.; Lan, F.; Matson, C.; Mulligan, P., Whetstine, J. R.; Cole, P. A.; Casero, R. A.; Shi, Y. *Cell*. **2004**, *119*, 941.
22. Culhane, J. C.; Cole, P. A. *Curr Opin Chem Biol*. **2007**, *11*, 561.
23. Loenarz, C.; Schofield, C. J. *Nat Chem Biol*. **2008**, *4*, 152.

24. Wissmann, M.; Yin, N.; Müller, J. M.; Greschik, H.; Fodor, B. D.; Jenuwein, T.; Vogler, C.; Schneider, R.; Günther, T.; Buettner, R.; Metzger, E.; Schüle, R. *Nat Cell Biol.* **2007**, *9*, 347.
25. Kahl, P.; Gullotti, L.; Heukamp, L. C.; Wolf, S.; Friedrichs, N.; Vorreuther, R.; Solleder, G.; Bastian, P. J.; Ellinger, J.; Metzger, E.; Schüle, R.; Buettner, R. *Cancer Res.* **2006**, *66*, 11341.
26. Reddy, A.; Villeneuve, L. M.; Wang, M.; Lanting, L.; Natarajan, R. *Circ Res.* **2008**, *103*, 615.
27. Szewczuk, L. M.; Culhane, J. C.; Yang, M.; Majumdar, A.; Yu, H.; Cole, P. A. *Biochemistry.* **2007**, *46*, 6892.
28. Forneris, F.; Binda, C.; Adamo, A.; Battaglioli, E.; Mattevi, A. *J Biol Chem.* **2007**, *282*, 20070.
29. Forneris, F.; Binda, C.; Vanoni, M. A.; Mattevi, A.; Battaglioli, E. *FEBS Lett.* **2005**, *579*, 2203.
30. Dallman, J. E.; Allopenna, J.; Bassett, A.; Travers, A.; Mandel, G. *J Neurosci.* **2004**, *24*, 7186.
31. Wissmann, M.; Yin, N.; Müller, J. M., Greschik, H.; Fodor, B. D.; Jenuwein, T.; Vogler, C.; Schneider, R.; Günther, T.; Buettner, R.; Metzger, E.; Schüle, R. *Nat. Cell Biol.* **2007**, *9*, 347.
32. Hu, Q.; Kwon, Y. S.; Nunez, E.; Cardamone, M. D.; Hutt, K. R.; Ohgi, K. A.; Garcia-Bassets, I.; Rose, D. W.; Glass, C. K.; Rosenfeld, M. G.; Fu, X. D. *Proc Natl Acad Sci U S A.* **2008**, *105*, 19199.
33. Katz, D. J.; Edwards, T. M.; Reinke, V.; Kelly, W. G. *Cell.* **2009**, *137*, 308.
34. Forneris, F.; Binda, C.; Battaglioli, E.; Mattevi, A. *Trends. Biochem. Sci.* **2008**, *33*, 181.
35. Donelson, J. L.; Hodges, H. B.; Macdougall, D. D.; Henriksen, B. S.; Hrycyna, C. A.; Gibbs, R. A. *Bioorg Med Chem Lett.* **2006**, *16*, 4420.
36. Ettmayer, P.; Chloupek, S.; Weigand, K. *J Comb Chem.* **2003**, *5*, 253.
37. Dulla, B.; Wan, B.; Franzblau, S. G.; Kapavarapu, R.; Reiser, O.; Iqbal, J.; Pal, M. *Bioorg Med Chem Lett.* **2012**, *22*, 4629.
38. Godfrey, A. G.; Brooks, D. A.; Hay, L. A.; Peters, M.; McCarthy, J. R.; Mitchell, D. *J Org Chem.* **2003**, *68*, 2623.
39. Tahtaoui, C.; Parrot, I.; Klotz, P.; Guillier, F.; Galzi, J. L.; Hibert, M.; Ilien, B. *J Med Chem.* **2004**, *47*, 4300.

40. Powell, D. A.; Ramsden, P. D.; Batey, R. A. *J Org Chem.* **2003**, *68*, 2300.
41. McGrath, P.; Li, C.Q. *Drug Discov Today.* **2008**, *13*, 394.
42. Zhou, X.; Ma, H. *BMC Evol Biol.* **2008**, *8*, 294.
43. Neelamegam, R.; Ricq, E. L.; Malvaez, M.; Patnaik, D.; Norton, S.; Carlin, S. M.; Hill, I. T.; Wood, M. A.; Haggarty, S. J.; Hooker, J. M. *ACS Chem Neurosci.* **2012**, *3*, 120.
44. Tucker, B.; Lardelli, M. *Zebrafish.* **2007**, *4*, 113.
45. Mimasu, S.; Sengoku, T.; Fukuzawa, S.; Umehara, T.; Yokoyama, S. *Biochem Biophys Res Commun.* 2008, *366*, 15.
46. Desmond Molecular Dynamics System, version 3.0, D. E. Shaw Research, New York, NY 2011. Maestro-Desmond Interoperability Tools, version 3.0, Schrödinger, New York, NY 2011.

5. Design, synthesis & pharmacological evolution of isovanillin derived Isoxazolidines as potential vanilloid receptors

5.1 Introduction:

5.1.1 Importance for Noval Scaffolds to Treat Pain:

International Association for the Study of Pain (IASP) define pain as unpleasant sensory and emotional experience associated with actual or potential tissue damage. It has been observed as a major symptom in many disease conditions, which can lead to significant changes in a patient's lifestyle, functional ability and overall quality of life. Based on the nature of impact on body, pain has been classified into two types acute pain that stops without a major treatment pain that is no longer considered a symptom but an illness by itself termed as chronic pain (Figure 1), latter is a major health problem for both individuals and society. Nociception (sensation of pain) can be regulated by a number of chemical (e.g. low pH) or physical stimuli (e.g. mechanical, thermal) that have the potential to damage tissue. The receptors (sensory neurons) which can detect and respond to these harmful stimuli above a set of threshold are known as "nociceptors" (also called pain receptors) which are found in many areas of the body like skin, cornea, mucosa, muscle, joint, bladder, gut and along the digestive track that can sense pain either externally or internally. As soon as nociceptor stimulated it will transmit a signal along the spinal cord, to the brain thereby triggering a variety of autonomic responses followed by pain.

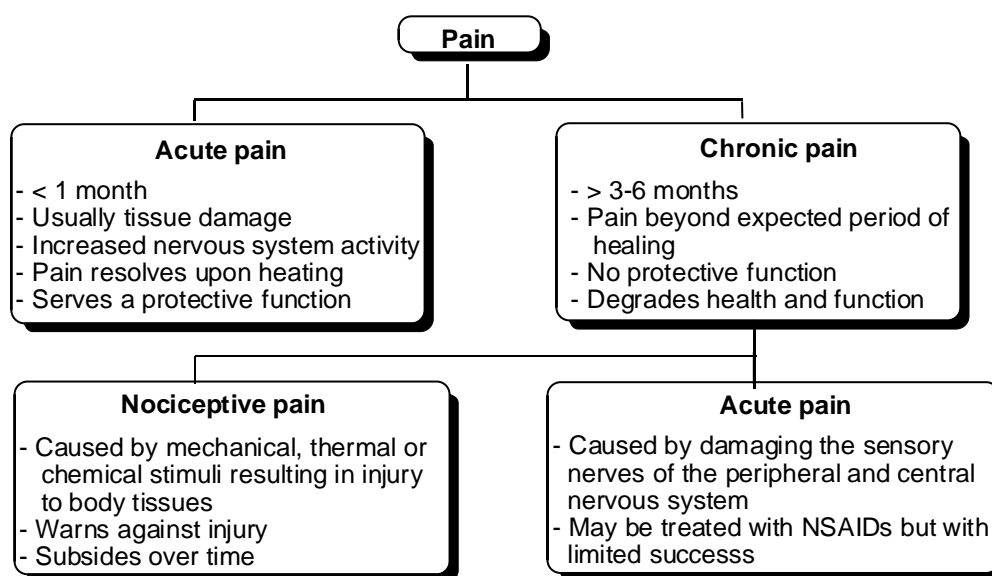


Figure 1: Classification of pain

There is often no satisfactory treatment for chronic pain whereas neuropathic pain, in particular, poorly standard therapies such as NSAIDs, opioids, and tricyclic antidepressants, which reduce approximately 30-50% pain in about 50% of patients, along with producing undesired side effects such as dizziness and somnolence in some patients. Thus, there remains a great medical need for new medicines to treat pain.

Neuropathic pain affecting 26 million patients worldwide resulting healthcare cost over \$ 3 billion per year. While little is known about the proteins that detect noxious stimuli (especially those of a physical nature), vanilloid receptor, an excitatory ion channel expressed by nociceptors, has been identified as molecular target for the development of recent therapies to treat pain.

5.1.2 The Transient Receptor Potential (TRP) Super family:

The vanilloid receptor subtype 1 (VR1) or transient receptor potential vanilloid 1 (TRPV1), also as cation channel on C-fiber sensory neurons that stimulate many organs, including the skin, bladder and gut), can found in the peripheral and central nervous system. TRPV1 not only involved in the transmission and modulation of pain, but also act as the integration of diverse painful stimuli.

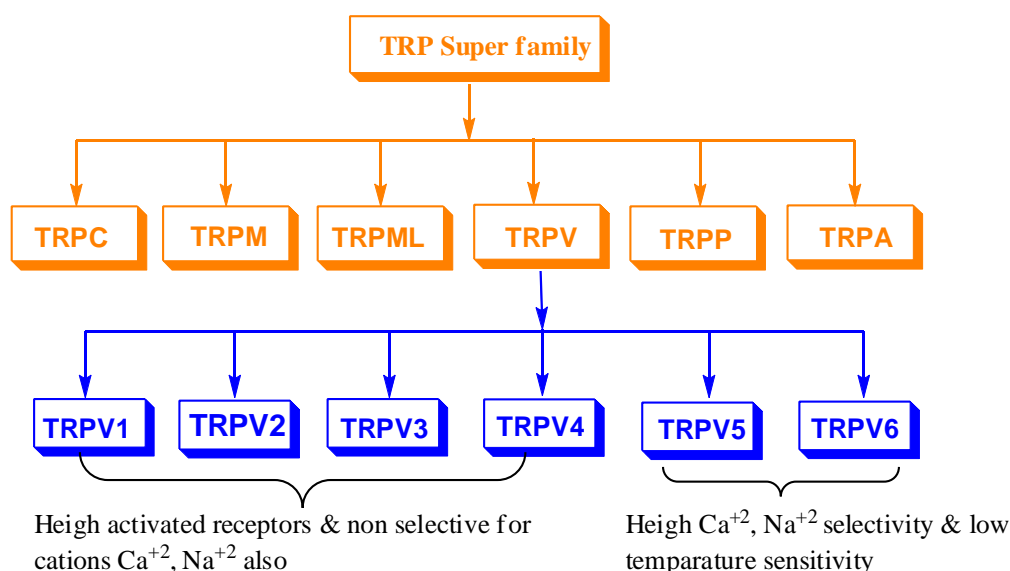


Figure 2: Classification of transient receptor potential (TRP) super family

The TRPV1 is a member of the transient receptor potential (TRP) super family, a group of ion channels currently containing >30 members which are widely expressed in mammalian tissues and playing a vital role in sensory processes.^{1a} Based on sequences homology and functional behaviour the TRP family believed to constitute six different subfamilies: C

(canonical or classical), M (melastatin-related), P (PKD type), ML (mu-colipin), A (ankyrin) and V (vanilloid).^{1b} It is important to notice that this classification is not based on activating stimuli because both V and M subfamilies have members that respond to temperature. TRPV1 was the first and best characterized member of the transient receptor potential vanilloid receptor, while the physiological functions of most of these channels were unrevealed. This receptor is a nonspecific cation channel which can be activated by a variety of exogenous and endogenous physical and chemical stimuli. Exogenous stimuli are protons (pH 5, chemical stimuli), heat (> 42 °C, physical stimuli), where as endogeneous substances, such as endocannabinoid anandamide, lipoxygenase & arachidonic acid metabolites etc. can stimulate it.

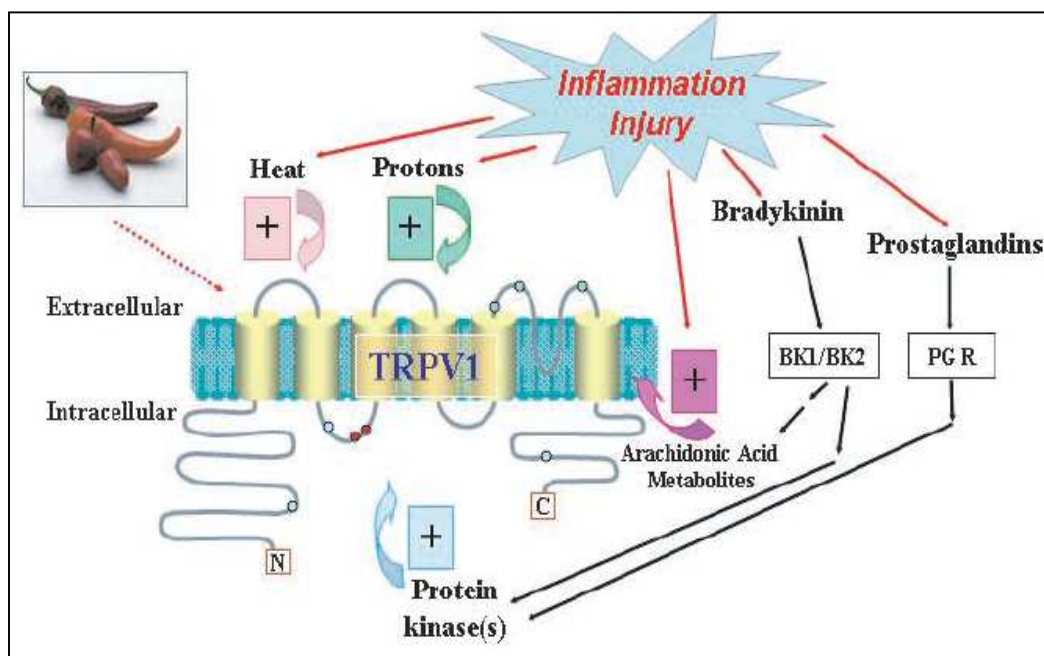


Figure 3: TRPV1 is an integer of inflammatory pain path ways. The figure shows a schematic of TRPV1 and its activators. It is directly activated by a multiplicity of stimuli including vanilloids, such as capsaicin, low pH, elevated temperature and arachidonic acid metabolites such as anandamide. It can also indirectly activate by prostaglandin and bradykinin receptors via protein kinase activity. Filled circles represents amino acids required for TRPV1 activation, red circles corresponds to residues important for capsaicin activation, green circles for low pH and blue circles for protein kinase phosphorylation sites.

Activation of TRPV1 can also be achieved by some natural ligands such as capsaicin (the pungent principle of chili peppers) and other vanilloids (a group of compounds, structurally related to capsaicin) and resiniferatoxin (RTX, an extreme irritant and natural diterpene

isolated from the sap of *Euphorbia resinifera*) and hence, it has been classified as a ligand-gated ion channel.^{2,3}

5.1.2.1 Physiological functions of TRPV1:

As soon as the TRPV1 stimulated, it results in influx of calcium in to cells and also releases calcium from the endoplasmic reticulum to a lesser extent. Due to high permeability of calcium, the extracellular calcium (and also sodium) enters through the channel pore, resulting in depolarization of cell membrane. This increases excitation of primary sensory neurons, leading to action of potential firing and transmission of a noxious nerve impulse to the spinal cord, thereby increase the perception of pain.^{4,5} Besides this the process can lead to release of a short chain poly peptide P that functions as a neurotransmitter and as a neuro modulator and CGRP, resulting to enhanced peripheral sensitization of tissue. It also observed that TRPV1 can following inflammation and nerve damage which directly confirms TRPV1 as a key regulator of pain response.^{6,7} Hence, a clinically effective therapeutic method to treat pain can be *via* blockade of the TRPV1 thereby inhibiting the transmission of painful signals from periphery to the CNS.

5.1.2.2 TRPV1 Agonists:

A chemical substrate or scaffold which can binds to some receptor of a cell and triggers a response by that cell known as Agonists. In general agonists mimic the action of a naturally occurring substance. The vanilloid receptors were named after the presence of vanillyl (i.e. 4-hydroxy-3-methoxybenzyl) moiety in capsaicin (**1**) & resiniferatoxin (**2**), which is responsible for the interactions with the receptor (see Figure 4).

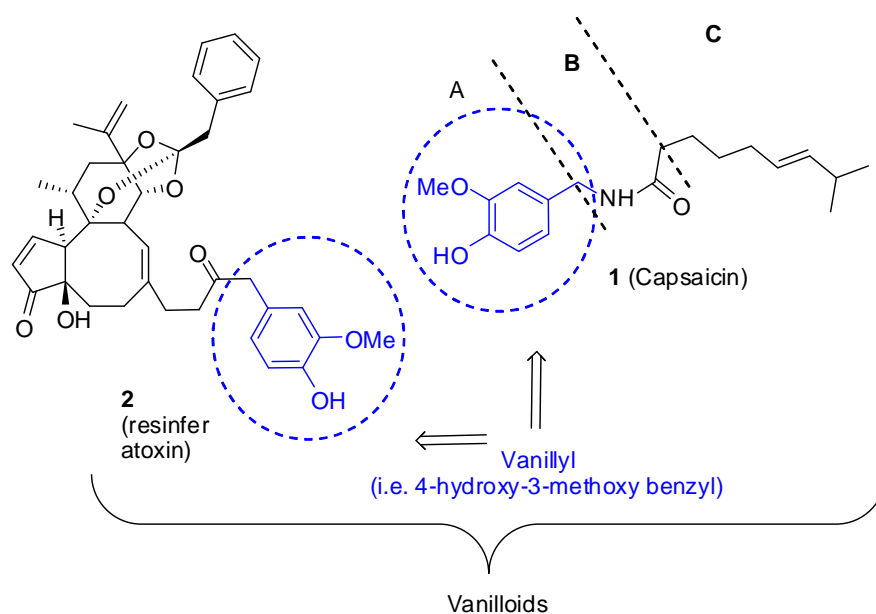


Figure 4: TRPV1 agonists with vanillyl moiety

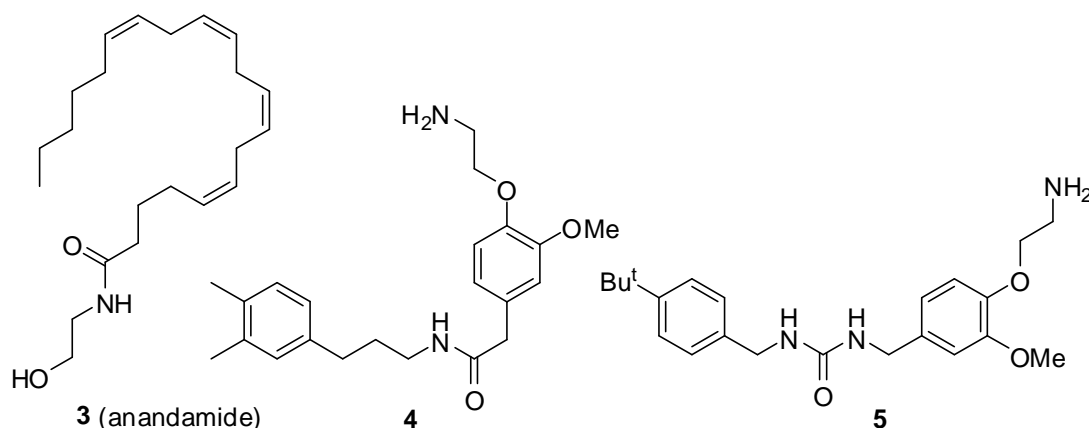


Figure 5: TRPV1 agonists with lack of vanillyl moiety

However, there several reports of vanilloid receptor agonists which lacked any recognizable vanillyl moiety e.g. (3-5). Nevertheless, compound 2 showed binding potency ($K_i = 0.13$ nM in CHO/VR1) approximately 4 orders of magnitude greater than that of 1 ($K_i = 1,700$ nM in CHO/VR1). Vanilloid agonist such as 1 has an analgesic effect, due to the rapid calcium influx leads to stimulation of the sensory neurons and release of neurotransmitter such as substance P. Upon continued stimulation, the neurotransmitters undergo depletion leads to selective damage of the nerves and, thereby, desensitizing them toward further stimulations. There by TRPV1 receptors become less sensitive to subsequent application of painful stimuli including noxious stimuli such as heat and acid or to additional agonist challenges. Therefore repeated exposure to large amounts of capsaicin results in insensitivity to further activation by this agent. Both 1 and 2 have been used to treat the pain associated with diabetic neuropathy and arthritis.⁸ While a number of agonists e.g. 4 and 5 (see Figure 5) along with 2 progressed into clinical trials, these agonists were limited due to side effects of a burning sensation, irritation and neurotoxicity.⁵ To avoid this persisting side effect found in TRPV1 agonists, the focus of drug discovery research was shifted towards the development of competitive antagonists which can be obtained through blockade of the pain-signalling pathway.

5.1.2.3 TRPV1 Antagonists:

Antagonist is defined as an inverse agonist causes an action opposite to that of the agonist. Capsazepine (6) was the first antagonist of TRPV1 and was discovered during the investigation of structure activity relationship of capsaicin (1), in order to predict the effect of conformational constraint on lipophilic C-region (see Figure 4). It has blocked the capsaicin-

induced uptake of Ca^{2+} in neonatal rat dorsal root ganglion (DRG) with a reported $\text{IC}_{50} = 0.420 (\pm 0.046) \mu\text{M}$. And also has shown anti-hyperalgesic effects not only against capsaicin challenge but also against other inflammatory stimuli indicating that analgesic effects were common to both TRPV1 agonists and antagonists.^{9,10} Other classes of TRPV1 antagonists structurally unrelated to the exogenous agonist capsaicin have been discovered during the past few years, some of them are listed in figure 6.¹¹

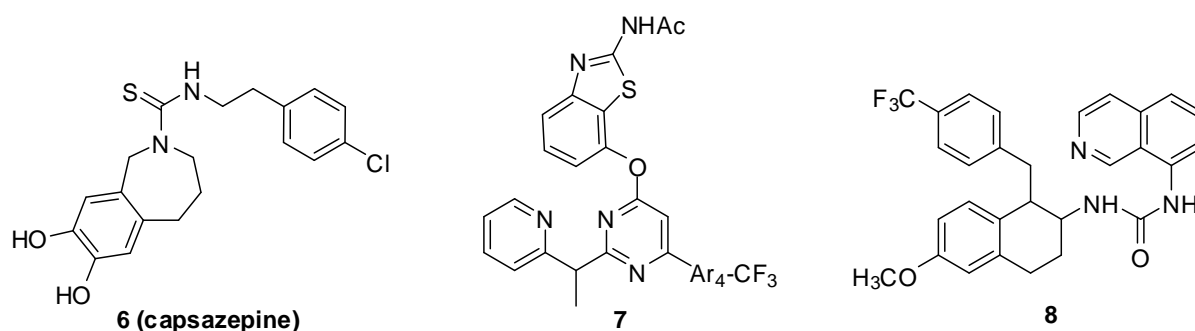


Figure 6: Few examples of TRPV1 antagonists

5.2 Research objective:

In view of the therapeutic value of such vanilloids, as a part of our drug discovery program we were interested in generation of novel molecular scaffolds from vanilloid precursors. In this context, Isoxazolidines (**A**, Fig. 7) are important heterocycles¹² commonly found in a diverse array of bioactive natural products (e.g. cycloserin, acivicine). They are also valuable intermediates in organic synthesis.¹³ Compounds such as capsaicin, the main capsaicinoid in chili peppers containing a vanillyl moiety (**B**, Fig. 7) on the other hand have attracted considerable interest as they target TRPV1 (transient receptor potential vanilloid 1), a molecular integrator for a broad variety of seemingly unrelated noxious stimuli.¹⁴ This and our longstanding interest on bioactive fused heterocycles prompted us to design novel molecular scaffolds by combining the isovanillyl moiety and isoxazolidine ring in a single framework **C** (Fig. 1). We anticipated that isovanilloid based tricyclic drug-like molecules derived from **C** might show pharmacological properties similar to capsaicin as well as vanilloid receptors.

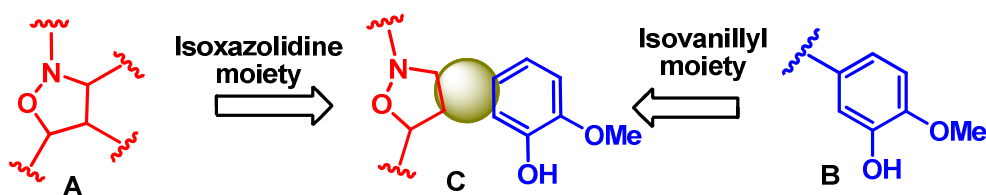
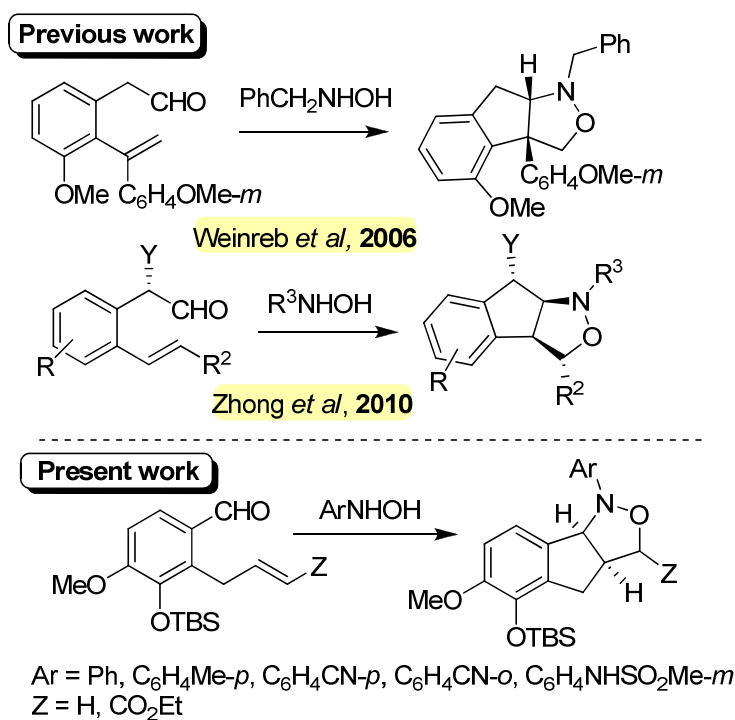


Figure 7: Design of **C** by combining **A** and **B**

While several methods have been reported for the synthesis of isoxazolidines, the dipolar cycloaddition of nitrile oxides/hydroxylamines to allyl dipolarophiles appears to be attractive.¹⁵ The intramolecular version of 1,3-dipolar cycloadditions of hydroxylamines to simple allylic or N/O-allylic dipolarophiles has also been reported.¹⁶ For example benzo analogues of tricyclic isoxazolidines have been prepared by using this strategy¹⁷⁻¹⁹ (Scheme 1). While all these methods were not precisely suitable for our purpose these findings however provided a valuable lead to develop a strategically related but unique approach to **C** (Scheme 1).



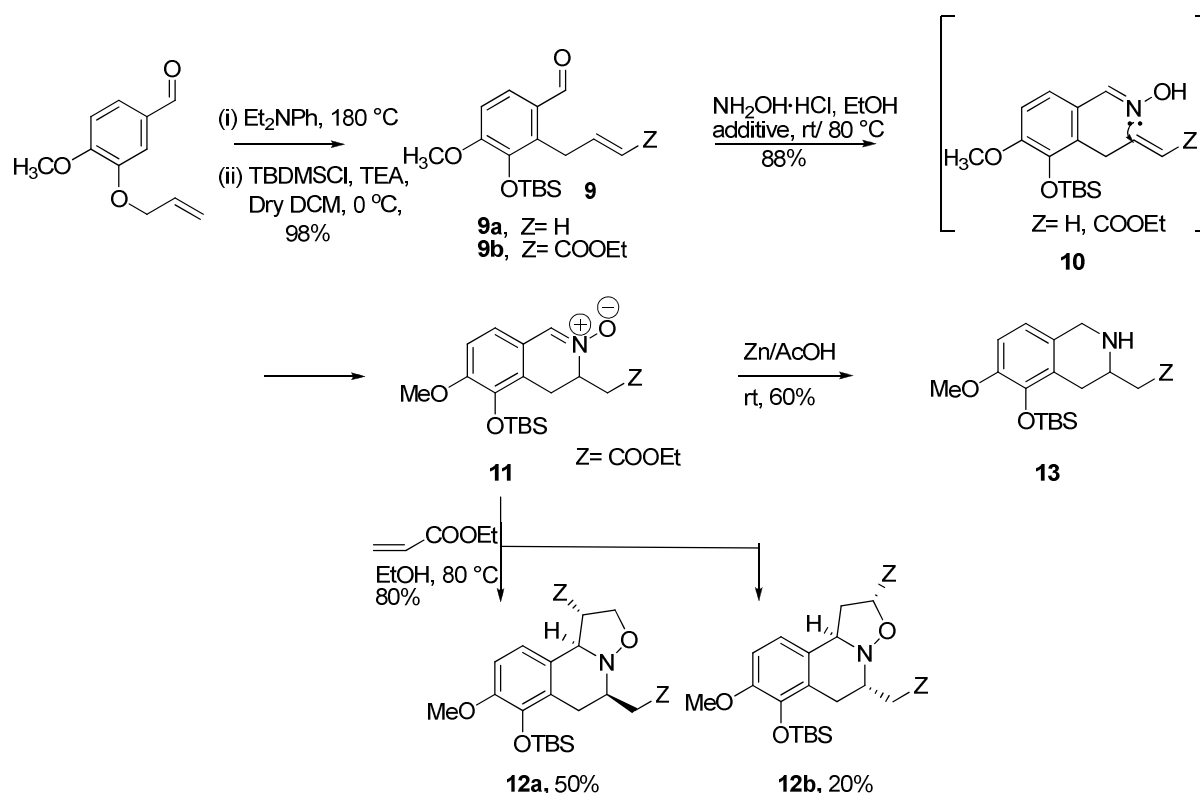
Scheme 1. Synthesis of benzo analogues of tricyclic isoxazolidine

Herein we report the intramolecular 1-3-dipolar cycloaddition of isovanillin derived *N*-substituted hydroxylamines possessing allylic dipolarophiles at the *o*-position. In extension of this approach the corresponding *N*-unsubstituted hydroxyl amines give rise to tetrahydroisoquinolines. Further synthetic applications and pharmacological properties of some of these compounds synthesized are presented.

5.3 Results and Discussion:

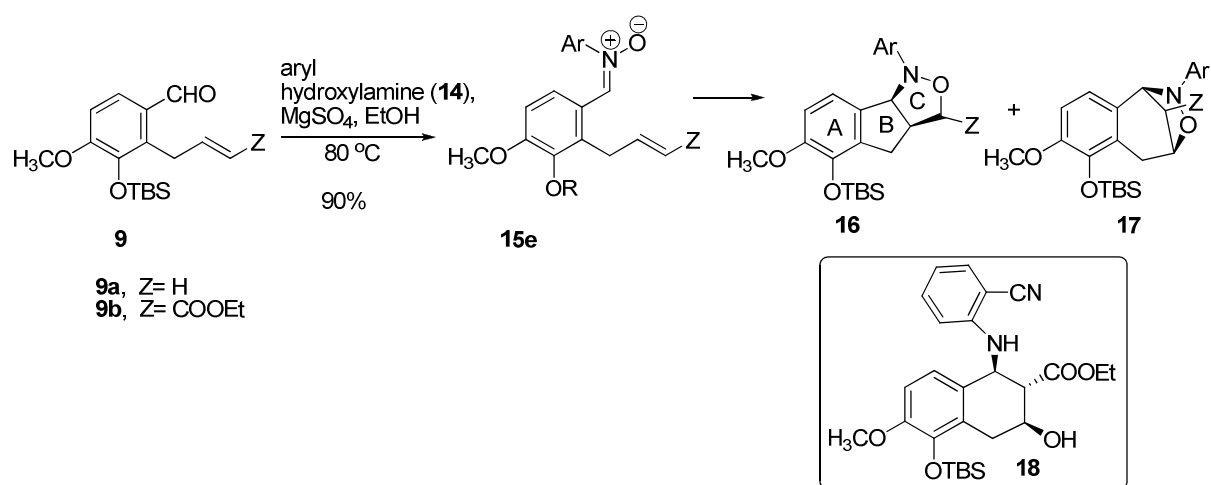
5.3.1 Chemistry

As a starting point the *O*-allyl isovanillin **9a** was prepared by sequential *O*-allylation of isovanillin followed by Claisen rearrangement.²⁰ In an experiment designed to synthesize isoxazolidines by 1,3 dipolar cycloaddition of the nitrones obtained from unsubstituted hydroxylamine hydrochloride on allylic dipolarophile in the adjacent position, we observed the formation of tetrahydroisoquinoline **13** as the only product in 88% yield. We visualized this possibility through the formation of nitron **11** by an apparently favourable intramolecular aza-Michael addition over the expected [3+2] cycloaddition. The formation of **11** was further supported by the generation of two regioisomers **12a** and **12b** obtained as major products *via* intermolecular [3+2] cycloaddition with ethyl acrylate. There was no noticeable change in conversions in the presence of additives like sodium acetate or triethylamine or higher temperatures (Scheme 2).



Scheme 2. Formation of tetrahydroisoquinolines *via* intramolecular aza-michael addition on allyl carboxylate

However when the same reaction conditions were applied to phenyl hydroxylamine, we observed intramolecular cyclization to form isoxazolidines with both simple and activated allyl dipolarophiles (Scheme 3; entry 1, Table 1, see footnote). We were pleased to find that stirring an equimolar mixture of phenyl hydroxylamine and aldehyde **9** in the presence of magnesium sulphate in ethanol under reflux conditions afforded a 1:2 mixture of the two regioisomers **16** and **17** each one in racemic form *via* an apparent formation of nitron. The structure of one of the isomers **16a** was unequivocally characterized by single crystal X-ray diffraction studies (See supporting information).



Scheme 3. Intramolecular 1,3-dipolar cyclo additions on simple and activated allyl dipolarophiles

We then focused our attention to the influence of electronic factors of the phenyl ring. For this, a range of substituted phenyl hydroxyl amines with electron-donating and electron-withdrawing groups were synthesized²¹ and were applied under similar reaction conditions. The observations demonstrated that there is a negligible influence of electronic factors on the favorability of cycloaddition (Table 1).

Table 1. Influence of electronic factors of the aryl substituent on reaction mechanism

Entry	14 ; Ar =	9 ; Z	Products	Yield ^b (%)
1	14a ; Ph	9a ; H	16a:17a (1:2) ^c	96
2	14b ; 4-MeC ₆ H ₄	9a ; H	16b:17b (1:2) ^c	100
3	14c ; 4-NCC ₆ H ₄	9a ; H	16c:17c (1:2) ^c	94
4	14d ; 3-(MeSO ₂ NH)C ₆ H ₄	9a ; H	16d:17d (1:2) ^c	95
5	14e ; 2-NCC ₆ H ₄	9a ; H	15e	88
6	14a	9b ; CO ₂ Et	16f	78
7	14e	9b ; CO ₂ Et	18	58

a) At 80 °C, the ratios of **16a: 17a**, **16b: 17b**, **16c: 17c** and **16d:17d** were 1: 2 where as at 130 °C, the ratios of **16a: 17a**, **16b: 17b**, **16c: 17c** and **16d:17d** were 2:1 b). Regioisomers (**16**, **17**) cannot be separable without TBS protection on column chromatography.

The reaction well accommodated both electron withdrawing and electron releasing substituent on N-phenyl moiety. The presence of methyl and cyano groups in *para* position of N-phenyl substituent led to the formation of isoxazolidines **16b** and **16c** respectively with simple allyl dipolarophiles (entries 2 and 3, Table 1). An electron withdrawing group -NHSO₂CH₃ in *meta*-position had no significant effect on the yields (entry 4). The presence of cyano substituent in *ortho*-position did not afford isoxazolidine with simple allyl dipolarophile and nitrone **15e** was recovered. While the reason for this observation was not clear an intramolecular interaction between the -N⁺-O⁻ moiety and -CN group could prevent the reaction to proceed further. However, the presence of ethyl carboxylate was sufficient to make the reaction facile and afforded **16f** as a major product. The oxime not only cyclised but also underwent further cleavage to afford the corresponding amino alcohol **18** in 58% yield, in a single pot (entry 4). In all the cases, the intramolecular 1, 3-dipolar cycloaddition of nitrones and allylic dipolarophiles was observed to be facile and in many cases preceded with remarkable acceleration. The favorability and origin of the acceleration could be attributed to proximity of the functionalities within the cyclization precursor.

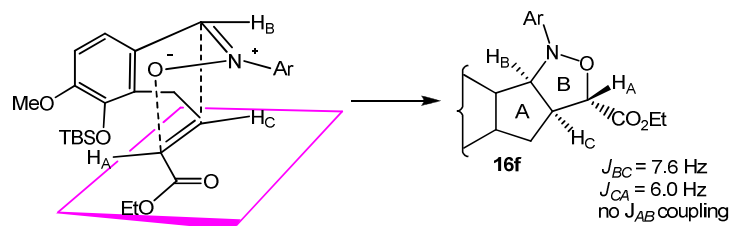
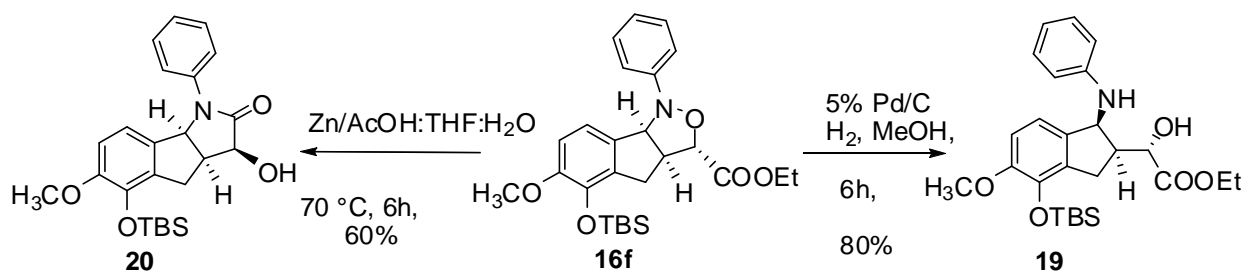


Figure 7. Endo approach of the C=C moiety to the Z-nitrone leading to **16f** with *trans*-relationship of H_A with H_B and H_C from NOESY spectrum.

The regiochemistry of all the four pairs of regioisomers was deduced from NMR spectra. X-ray diffraction analysis confirmed the *cis*-fusion (H_B and H_C) of rings A and B in **16a** (see Figure 8). The proton H_A coupled with the vicinal proton H_C but no long range coupling with the H_B was observed in the NOESY spectrum thus confirming the relative *trans*-relationship of H_A with H_B and H_C in **16f**. An endo approach of the C=C moiety to the Z-nitrone aided by the secondary orbital interactions between the nitrone nitrogen *p* orbitals and the –C=O group^{21e} possibly favored the formation of this particular diastereomer (Figure 7).

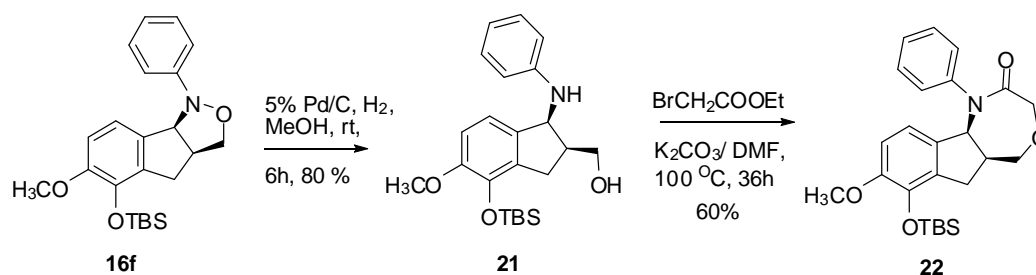
The presence of electron withdrawing group in the form of ethyl carboxylate ester on the allyl moiety of aldehyde **9** led to complete stereo selectivity to afford **16f** in quantitative yields. The polycyclic lactam **20** was also accessible from isoxazolidine **16f** on treatment with Zn/acetic acid. Interestingly, **16f** afforded an amino alcohol **19** on treatment with Pd/C (Scheme 3).



Scheme 3. Exposing the Latent functionalities of isoxazolidines

Finally we were inclined to create further molecular complexity from the synthesized isoxazole derived amino alcohols. Simple transformations were carried out on each regioisomer to construct viable highly functionalized tricyclic scaffold containing oxazepine core. The amino and hydroxyl appendages in γ -amino alcohol **21** obtained on reductive cleavage of **16a** respectively was readily elaborated. The γ -amino alcohol **21** on

stirring with ethylbromoacetate in DMF in presence of potassium carbonate afforded oxazepine **22** (Scheme 4).



Scheme 4. Synthesis of Oxazepine containing tricyclic scaffold

Finally –OTBS in all the compounds was deprotected using *tetra*-butyl ammonium iodide (TBAF) in presence of THF at 0 °C afforded the required compounds **23-36**.

ORTEP diagrams:

While all the compounds synthesized were characterized by spectral (NMR, IR, MS and HRMS) data the molecular structure of one of the representative compounds for example, **16a** was confirmed unambiguously by single crystal X-ray diffraction (Figure 8).

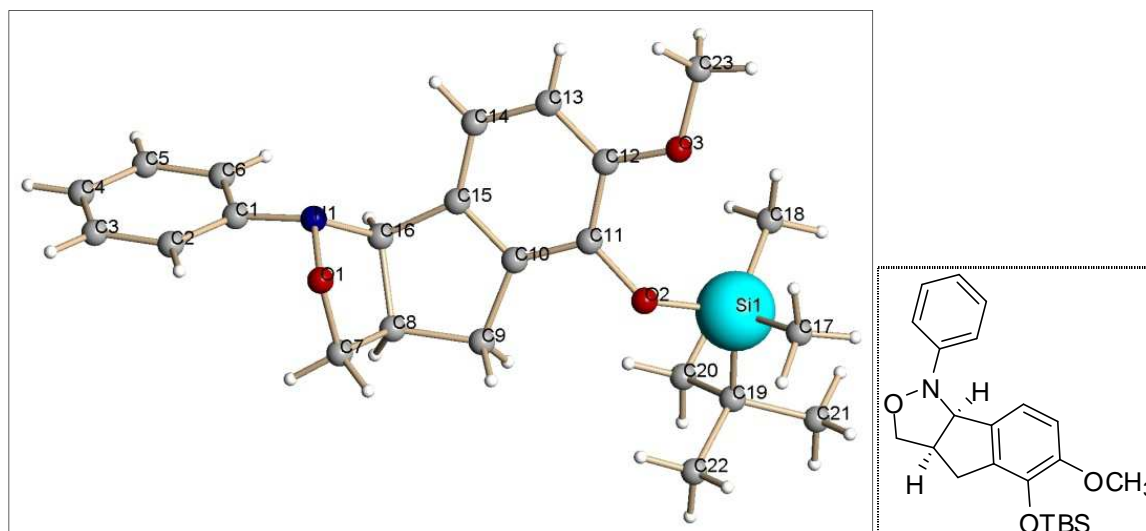


Figure 8: ORTEP representation of the **16a** (C₂₃H₃₁NO₃Si). (Thermal ellipsoids are drawn at 50% probability level).

5.3.2 Pharmacology

EVALUATION OF TEST COMPOUNDS FOR CAPSAICIN LIKE ACTIVITY IN ZEBRAFISH MODEL OF ANXIETY

The compounds synthesised were inspired from Capsaicin and hence were assessed to evaluate their Capsaicin like activity (after removal of TBS protecting group, see Experimental section). Capsaicin is known to show anxiogenic activity in various animal models²³ and therefore, was expected to show the same in zebrafish model of anxiety. We used the adult zebrafish model of light/dark box anxiety test to assess the activity²². This method was used as it is simple and does not require invasive procedures or euthanasia²². We first tested the hypothesis that Capsaicin administration results in anxiogenic behaviour in adult zebrafish. Thereafter, test compounds were tested in this model to identify the most potent anxiogenic compounds.

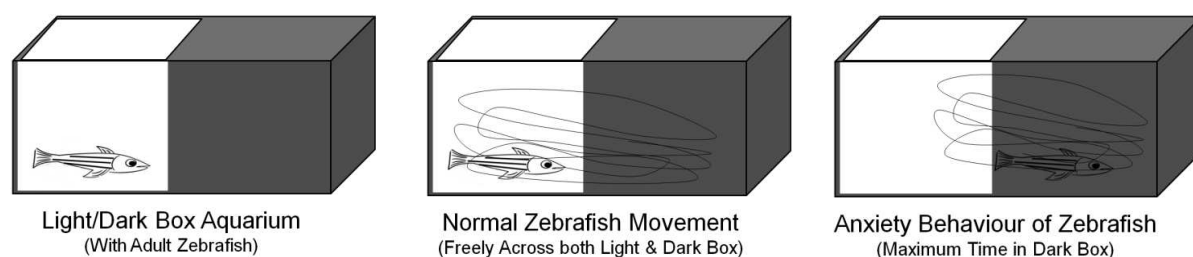
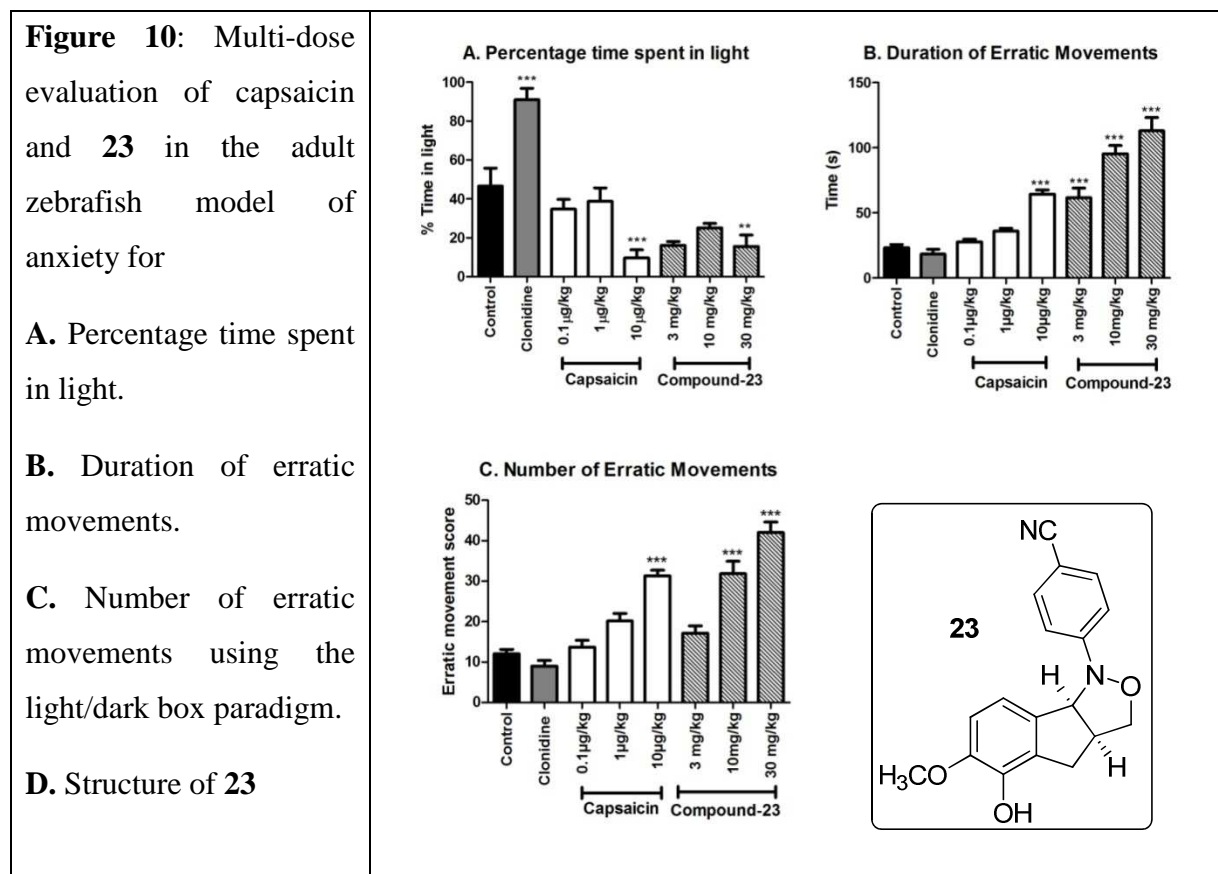


Figure 9: The figure shows the evaluation of anxiety like behaviours in the adult zebrafish using light/dark box paradigm. Normal fish move across freely in both light and dark environments, however, when anxious their movements and higher in the dark environment as compared to light.

Results:

Capsaicin when tested in the adult zebrafish model of anxiety using the dark light box paradigm showed clear anxiogenic behaviour, which was evident from the fact that the percentage time spent in light box was significantly lower in the Capsaicin treated fish as compared to control at 10 $\mu\text{g}/\text{kg}$ dose and the effect was dose dependent (Figure 10 A). The erratic movement (number and duration) were also observed and they increased in a dose dependent manner in Capsaicin treated fish (Figure 10 B & 10 C). This concludes that Capsaicin shows anxiogenic effect in adult zebrafish that is similar to the effect seen in other mammalian species. Screening of test compound in a single dose screening was performed and screening suggested that compound -**23** was the most potent anxiogenic compound (Figure 11). Multi-dose evaluation of Compound-**23** confirmed the anxiogenic activity as the

fish administered with this compound showed significant reduction in the percentage time spent in the light as compared to control fish (Figure 10 A).

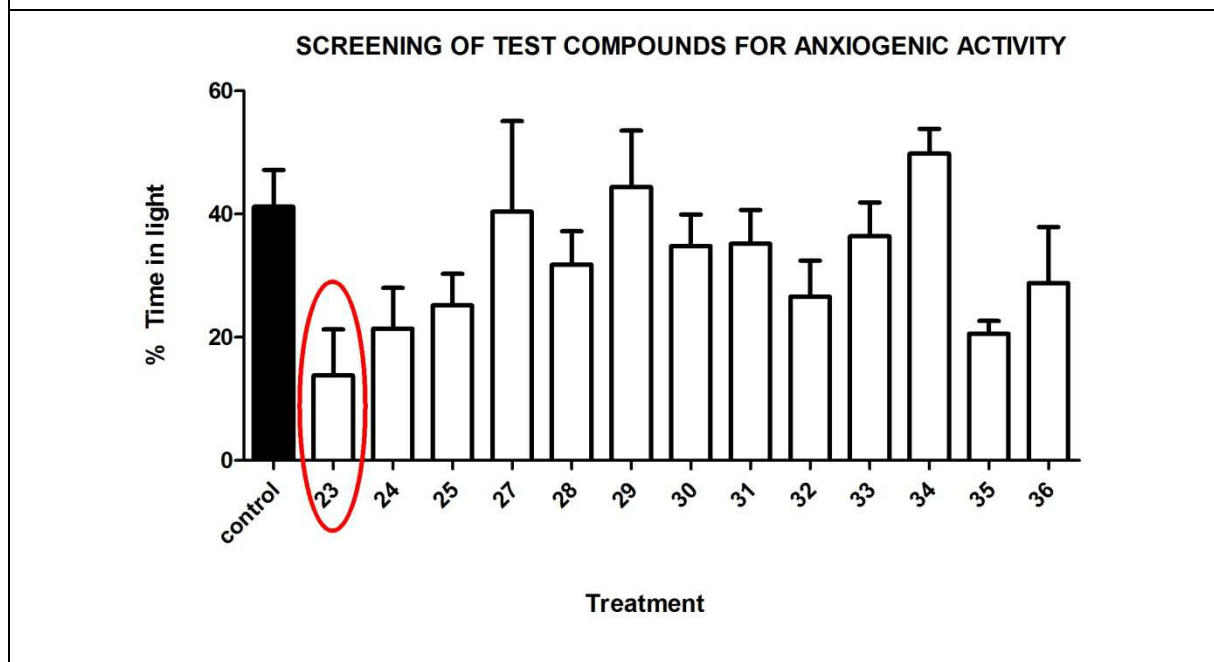


The erratic movement (number and duration) were also observed and there is dose-dependent increase in Compound-**23** group (Figure 10 B & 10 C). This verifies that Compound -**23** has anxiogenic activity which is an activity similar to Capsaicin.

5.3.2.1 Video for anxiogenic activity of compound **23**

This study was done by Swapna Yellanki, Raghavender Medishetti, and Pushkar Kulkarni at Zephase Therapeutics, Dr Reddy's Institute of Life Sciences, University of Hyderabad Campus, and Hyderabad. Video was recorded for the anxiogenic activity of compound **23** (Video attached to this thesis as separate file).

Figure 11: Screening of compounds for anxiolytic activity. Effect of compounds was assessed at 10 mg/kg) in the light/dark box paradigm to evaluate the parameter of percentage time spent in light. Compound-23 was found have maximum effect in this study.



5.3.3 Molecular docking studies

Molecular docking studies were done by K. Lalith Kumar at Institute of Life Sciences, India. To understand the nature of interactions of these molecules with the TRPV1 (Transient receptor potential vanilloid 1) in silico docking studies were performed with compounds **23**, **24** and **35** along with the known inhibitor of TRPV1 using Surflex-Dock (SFXC) programme of Sybyl software.

Till date, the complete crystal structure of the transient receptor potential vanilloid subtype1 (TRPV1) is not reported. Therefore a TRPV1 homology model was developed and used for this purpose. The docking results for capsaicin were in close relevance with the earlier reported docking studies. As reported earlier the vanillyl moiety of capsaicin occupied the deep pocket surrounded by Tyr511, Tyr565, and Lys571.²⁴ The hydrophobic tail region occupied the upper hydrophobic pocket formed at the interface of two monomers **Figure 12**. Using the above docking parameters we performed a docking study of synthesized compounds **23**, **24** and **35**. The dock scores and their contributing factors are represented in Table 2.

Table 2: Surflex dock score of the compounds

Compound	Total_Score ^a	Crash ^b	Polar ^c	Strain ^d	Total ^e
Capsaicin	5.9	-1.4	0	2.2	3.74
23	5.8	-0.7	1.1	0.28	5.6
24	5.0	-1.7	0.98	1.57	3.5
35	4.6	-1.8	1.1	1.6	3.0

^a The total Surflex-Dock score

^b The degree of inappropriate penetration by the ligand in to protein.

^c Contributions of polar interactions to the total score

^d Normal ligand strain relative to the local minimum

^e Ligands score corrected for strain energy

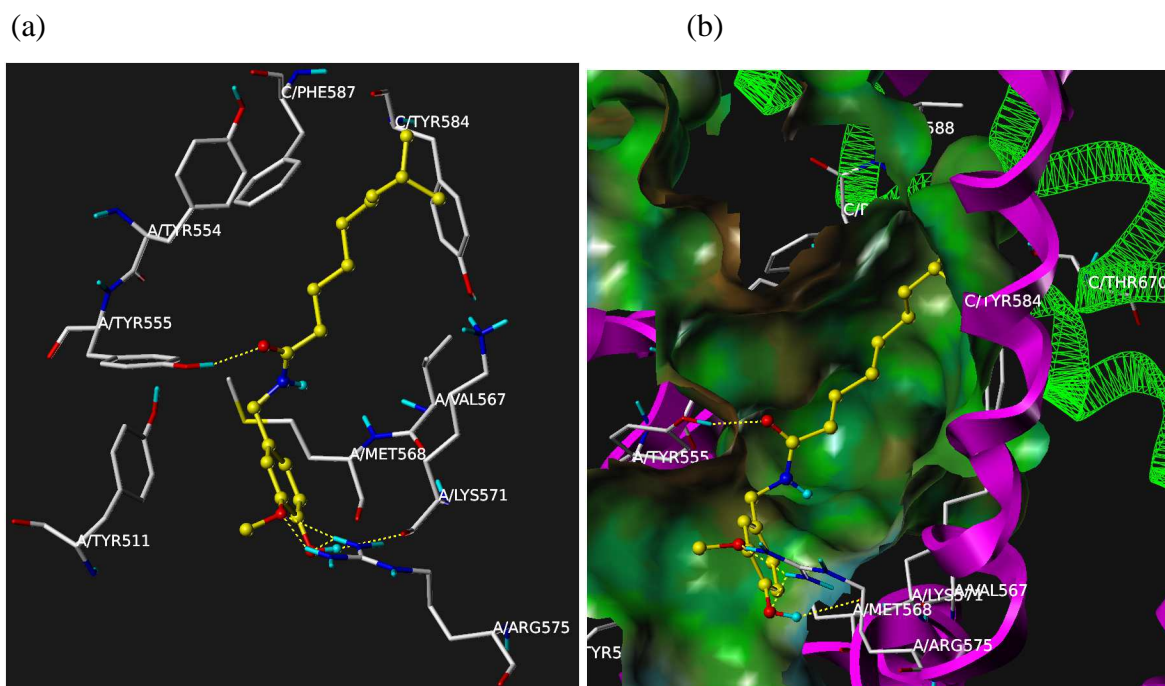


Figure 12: a) Binding mode of capsaicin in rTRPV1 b) MOLCAD surface of rTRPV1 with solid and mesh type representation of two monomers forming active site occupied by capsaicin.

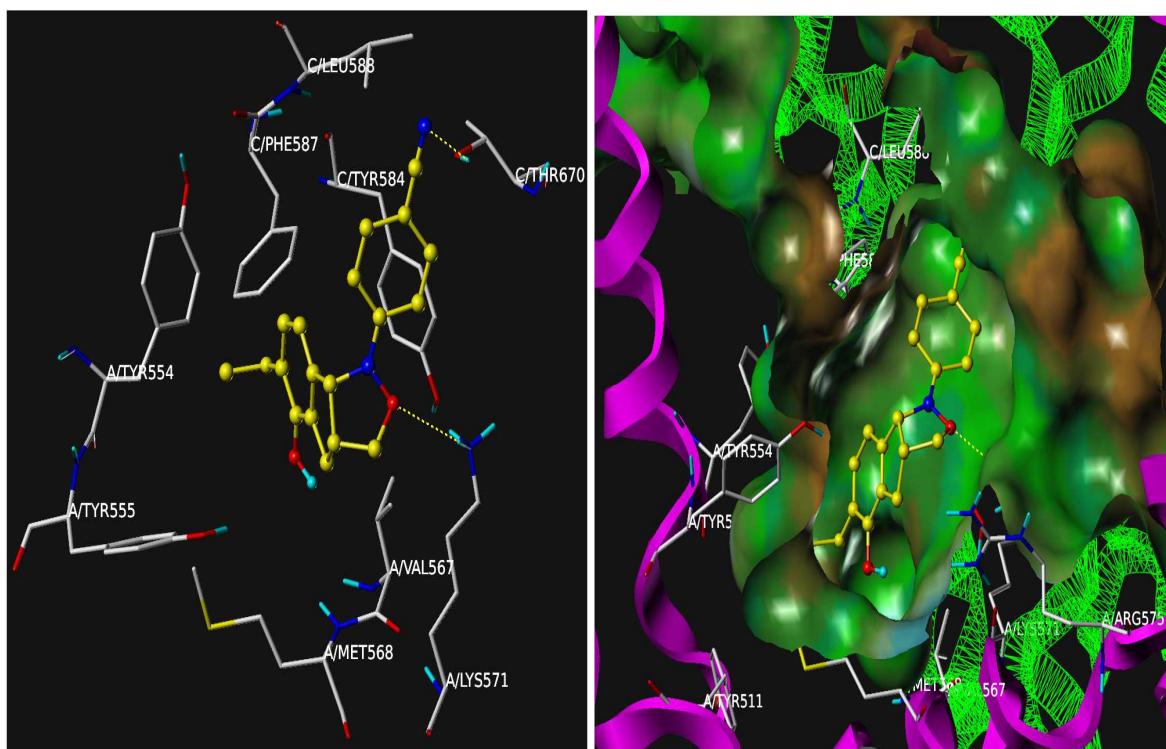


Figure 13: a) Binding mode of **23** in rTRPV1 b) MOLCAD surface of rTRPV1 with solid and mesh type representation of two monomers forming active site occupied by **23**.

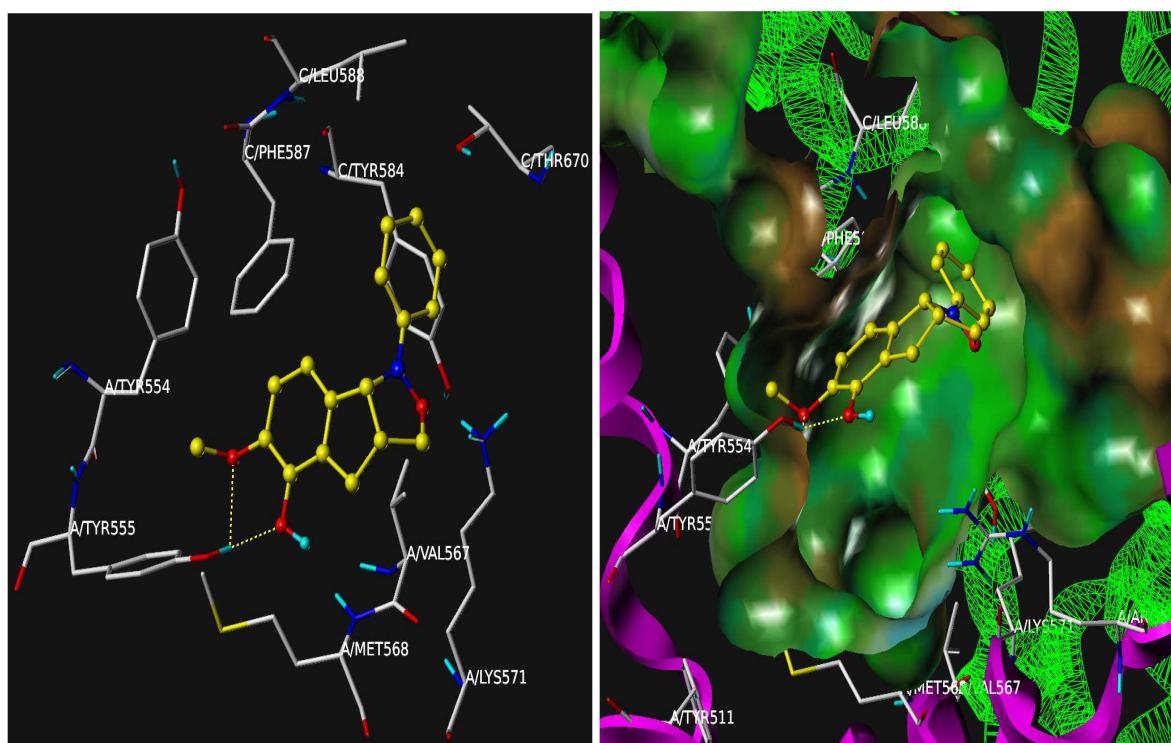


Figure 14: a) Binding mode of **24** in rTRPV1 b) MOLCAD surface of rTRPV1 with solid and mesh type representation of two monomers forming active site occupied by **24**.

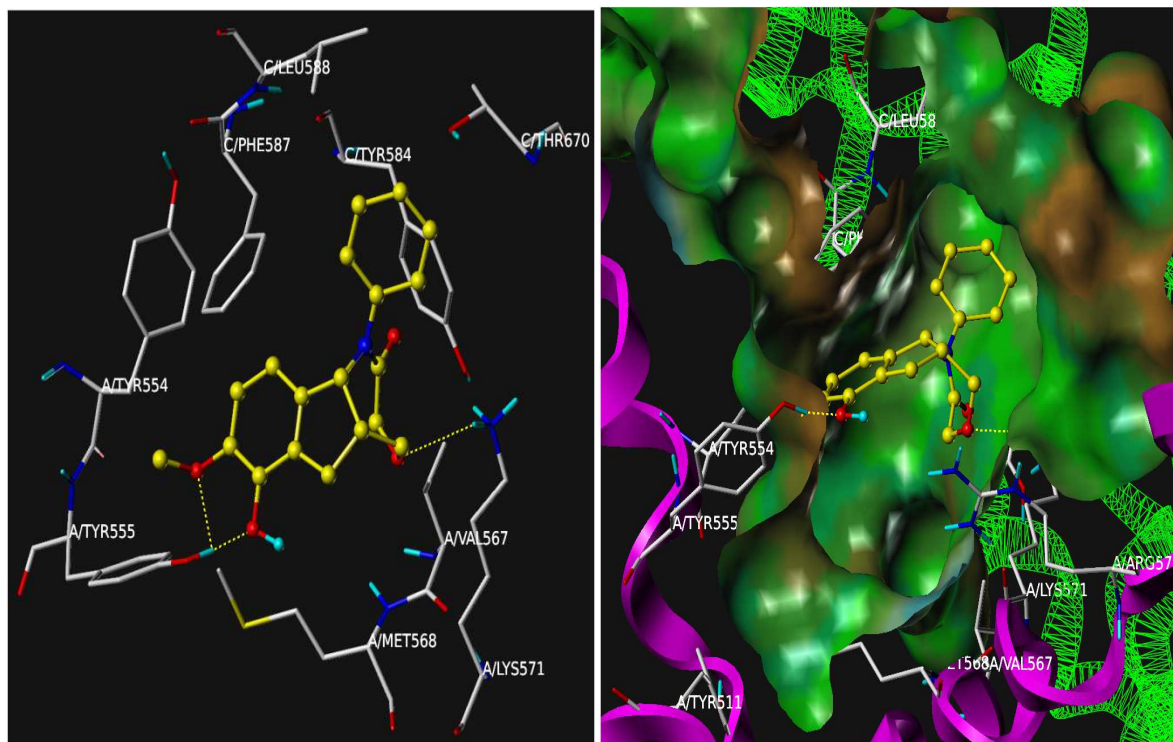


Figure 15: a) Binding mode of **35** in rTRPV1 b) MOLCAD surface of rTRPV1 with solid and mesh type representation of two monomers forming active site occupied by **35**.

As shown in Figure 12, the vanillyl moiety of **23** has also occupied close to the binding site where capsaicin vanillyl moiety interacts. The 4-cyano phenyl substituent of **23** replaces the lipophilic tail of capsaicin and occupies the upper hydrophobic pocket. Also, the nitrogen of the cyano group makes hydrogen bond interaction with the side chain hydroxyl group of Thr 670 from the adjacent ‘C’ chain. Removal of this cyano group in **24** resulted slight decrease in the dock score (Figure 14). Whereas, introducing of hydrophobicity through ring extension (from oxazole to oxazepine) in the compound **35** has increased the dock score (Figure 15).

5.4 Summary:

In conclusion, we have demonstrated an intramolecular 1,3-dipolar cycloaddition of isovanillin derived nitrones to activated and inactivated allylic dipolarophiles. The reaction was highly regioselective, afforded highly functionalized tricyclic isoxazolidines and tolerated electronically different N-substituents well. The utility of the reported methodology was also demonstrated by exploiting the latent functionality of resulting isoxazolidines to unique tricyclic system with an oxazepine core. The single crystal X-ray diffraction study was used to confirm the molecular structure of one of the representative compounds

unambiguously. To the best of our knowledge synthesis of the class of designed compounds was not known in the literature. Few of these compounds were found to be interesting when tested for anxiogenicity. Based on *in vivo* (anxiogenic assay) studies indicated that **23** found to be similar activity with capsaicin. Moreover, our efforts to elucidate the biological activities of all these vanilloid scaffolds containing isoxazolidine, amino alcohol and oxazepine core against the vanilloid receptors are underway.

5.5 Experimental Sections:

5.5.1 Chemistry - General methods

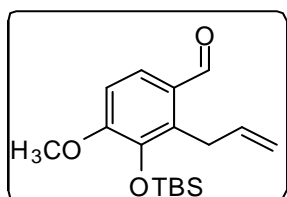
All reactions were carried out under an inert atmosphere with dry solvents, unless otherwise stated. Reactions were monitored by thin layer chromatography (TLC) on silica gel plates (60 F254), using UV light detection. Visualization of the spots on TLC plates was achieved either by UV light or by staining the plates in 2, 4 Di-Nitro Phenyl hydrazine stain, Ninhydrin stain and charring on hot plate. Flash chromatography was performed on silica gel (230-400 mesh) using distilled hexane, ethyl acetate, dichloromethane. ^1H NMR, ^{13}C NMR, 1D- NOE, and 2D-NOE spectra were recorded in CDCl_3 solution by using VARIAN 400 MHz spectrometers. Chemical shifts are reported as δ values relative to internal CDCl_3 δ 7.26 or TMS δ 0.0 for ^1H NMR and CDCl_3 δ 77.0 for ^{13}C NMR. ^1H NMR data is furnished as follows: chemical shift [multiplicity, coupling constant(s) J (Hz), relative integral] where multiplicity is defined as: s (singlet), d (doublet), t (triplet), q (quartet), dd (doublet of doublet), m (multiplet), bs (broad singlet). FTIR spectra were recorded on Bruker (Alpha) spectrometer. Mass spectra were recorded on Micro Mass VG-7070H mass spectrometer for ESI and are given in mass units (m/z). High resolution mass spectra (HRMS) [ESI+] were obtained using either a TOF or a double focusing spectrometer.

5.5.2 Synthesis

General procedure for 1,3 dipolar Cyclo addition

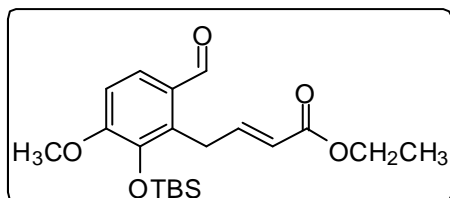
To a solution of aldehyde (1 mmol) in ethanol (5 mL) substituted phenyl hydroxyl amine (2 mmol), MgSO_4 (5 mmol) were added. The reaction mixture was refluxed for 3-5 h (for inversion in the yields of regio isomers reaction heated at $130\text{ }^\circ\text{C}$ for 12 h); ethanol was removed under high vacuum followed by column chromatography on silica gel yields the products. The yields are observed at $80\text{ }^\circ\text{C}$.

2-Allyl-3-(*tert*-butyldimethylsilyloxy)-4-methoxybenzaldehyde (9a):



To a solution of 2-allyl-3-hydroxy-4-methoxybenzaldehyde (1.92 g, 10 mmol) and imidazole (1.36 g, 20 mmol) in *N,N*-dimethylformamide (6 mL) *tert*-butyldimethylsilyl chloride (3 g, 20 mmol) was added under N₂, and the solution was stirred for overnight. The resulting mixture was diluted with saturated NH₄Cl solution and extracted with CH₂Cl₂. The organic layer was collected, washed with saturated aqueous sodium bicarbonate solution and water, dried over Na₂SO₄, filtered and concentrated under low vacuum to give the desired product (2.99 g, 98%). R_f = 0.7 (1:9 EtOAc : Hex); ¹H NMR (400 MHz, CDCl₃) δ 10.10 (s, 1H), 7.52 (d, *J* = 14.6 Hz, 1H), 6.87 (d, *J* = 14.6 Hz, 1H), 6.10-5.92 (m, 1H), 4.99 (d, *J* = 10.2 Hz, 1H), 4.86 (d, *J* = 17.2 Hz, 1H), 3.95 (s, 3H), 1.07 (s, 9H), 0.18 (s, 6H); ¹³C NMR (100 MHz, CDCl₃) δ 191.3, 154.5, 143.1, 136.8, 133.1, 128.2, 126.1, 115.3, 108.9, 54.8, 28.6, 26.1 (3C), 18.9, -3.7 (2C); Mass (ES): *m/z* 307.05 (M+H, 100%).

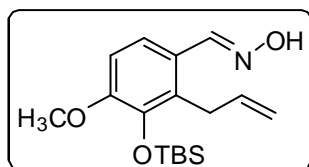
(E)-Ethyl 4-(2-(*tert*-butyldimethylsilyloxy)-6-formyl-3-methoxyphenyl)but-2-enoate (9b):



An oven dried round bottomed flask fitted with a rubber septum containing a stir bar was charged with 2-allyl-3-(*tert*-butyldimethylsilyloxy)-4-methoxybenzaldehyde (0.95 g, 3.10 mmol), ethyl acrylate (0.99 mL, 9.10 mmol), freshly distilled CH₂Cl₂ (25 mL), Grubbs-2 catalyst (0.079 g, 9.10 μmol), and CuI (0.011 g, 9.10 μmol) under an N₂ atmosphere. The rubber septum was then replaced with a reflux condenser under an N₂ atmosphere. The solution was then heated at 50 °C (oil bath temperature) for 3h. After cooling to room temperature, the reaction mixture was concentrated under vacuum and the residue was purified by using column chromatography on silica gel (eluting with 30% EtOAc/Hexanes) to afford the desired product as a colorless oil (1.0 g, 86%); R_f = 0.3 (1:9 EtOAc: Hex); IR (cm⁻¹): 3010, 2957, 2858, 2720 (CH aldehyde), 1720 (CO aldehyde), 1700 (CO ester), 1600, 1247; ¹H NMR (400 MHz, CDCl₃) δ 9.93 (s, 1H), 7.45 (d, *J* = 8.5 Hz, 1H), 7.15-7.05 (td, *J* = 15.7, 5.8 Hz, 1H), 6.90 (d, *J* = 8.5 Hz, 1H), 5.59 (d, *J* = 15.6 Hz, 1H), 4.12 (q, *J* = 7.2 Hz, 3H), 4.09-4.01 (m, 2H), 3.90 (s, 3H), 1.26 (t, *J* = 7.2 Hz, 4H), 1.03 (s, 9H), 0.20 (s, 6H); ¹³C NMR (100 MHz, CDCl₃) δ 191.3, 166.5, 154.5,

147.0, 143.6, 130.4, 128.6, 128.1, 121.6, 109.2, 60.0, 54.9, 27.6, 26.0 (3C), 18.9, 14.2, -3.7 (2C); Mass (ES): m/z 379.15 (M+H, 100%).

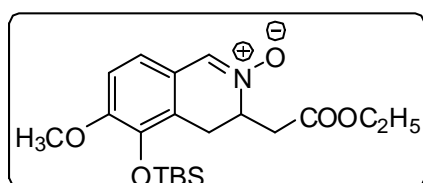
(E)-2-allyl-3-(*tert*-butyldimethylsilyloxy)-4-methoxybenzaldehyde oxime (10):



To a solution of 2-allyl-3-(*tert*-butyldimethylsilyloxy)-4-methoxybenzaldehyde (0.612 g, 2 mmol) in MeOH (5 mL) was added $\text{NH}_2\text{OH}\cdot\text{HCl}$ (0.207 g, 3 mmol) and NaOAc (0.246 g, 3 mmol) and the mixture was refluxed for 1.0 h. After completion of

the reaction, MeOH was removed using high vacuum and the residue was treated with water. The mixture was extracted with ethyl acetate. The organic layer was collected, dried over anhydrous Na_2SO_4 , filtered, and concentrated to afford the desired product as a light yellow oil (0.60 g, 88%); $R_f = 0.75$ (1:9 EtOAc: Hex); IR (cm^{-1}): 3430, 3029, 2975, 2852, 1728 (CO, ester), 1612, 1583, 1456, 1255; ^1H NMR (400 MHz, CDCl_3) δ 8.30 (s, 1H), 7.62 (d, $J = 14.8$ Hz, 1H), 6.90 (d, $J = 14.8$ Hz, 1H), 6.14-5.94 (m, 1H), 5.01 (d, $J = 10.4$ Hz, 1H), 4.92 (d, $J = 17.2$ Hz, 1H), 3.96 (s, 3H), 1.08 (s, 9H), 0.19 (s, 6H); ^{13}C NMR (100 MHz, CDCl_3) δ 154.7, 148.1, 143.1, 136.9, 133.1, 128.3, 126.0, 115.3, 108.8, 56.7, 28.7, 26.1 (3C), 18.9, -3.5 (2C); Mass (ES): m/z 322.08 (M+H, 100%).

5-(*tert*-butyldimethylsilyloxy)-3-(2-ethoxy-2-oxoethyl)-6-methoxy-3,4 dihydro isoquinoline 2-oxide (11):



To a solution of (*E*)-ethyl-4-(2-(*tert*-butyldimethylsilyloxy)-6-formyl-3-methoxyphenyl)but-2-enoate (0.758 g, 2 mmol) in MeOH (5 mL) was added $\text{NH}_2\text{OH}\cdot\text{HCl}$ (0.207 g, 3 mmol) and NaOAc (0.246 g, 3

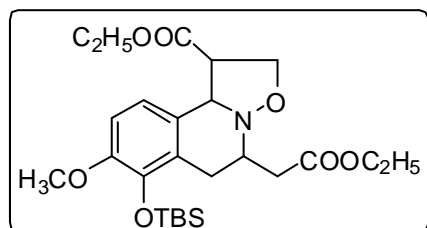
mmol) and the mixture was refluxed for 1.0 h. After completion of the reaction MeOH was removed using high vacuum and the residue was treated with water. The mixture was extracted with ethyl acetate. The organic layer was collected, dried over anhydrous Na_2SO_4 , filtered and concentrated. The residue was purified by column chromatography on silica gel (eluting with 100% EtOAc) to afford the desired product as a colorless oil (0.69 g, 88%); $R_f = 0.7$ (8:2 EtOAc: Hex); IR (cm^{-1}): 3030, 2965, 2862, 1728 (CO, ester), 1610, 1587, 1468, 1247; ^1H NMR (400 MHz, CDCl_3) δ 7.67 (s, 1H), 6.75 (s, 2H), 4.50-4.60 (m, 1H), 4.24-4.11 (m, 2H), 3.82 (s, 3H), 3.35-3.05 (m, 4H), 2.55-2.65 (dd, $J = 16.3, 9.3$ Hz, 1H), 1.33 (t, $J = 7.4$ Hz, 3H), 1.03 (s, 9H), 0.17 (s, 6H); ^{13}C NMR (100 MHz, CDCl_3) δ 170.2, 151.8, 142.5,

134.0, 121.5, 119.9, 119.1, 110.1, 63.5, 60.9, 54.9, 35.6, 29.6, 27.1, 25.9 (3C), 18.7, 14.1, -3.9, -4.0; Mass (ES): m/z 394.20 (M+H, 10%), 192.17 (100%); HRMS (ESI): calcd for $C_{20}H_{32}NO_5Si$ (M+H)⁺ 394.2049 found 394.2035.

Procedure for 1,3 dipolar addition on 11:

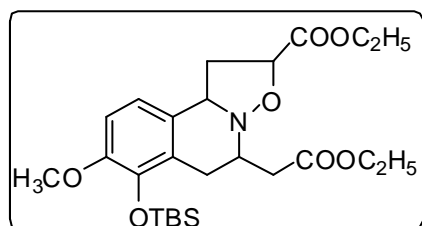
To a solution of 5-(*tert*-butyldimethylsilyloxy)-3-(2-ethoxy-2-oxoethyl)-6-methoxy-3,4-dihydroisoquinoline 2-oxide (0.393 g, 1 mmol) in ethanol (5 mL) was added ethylacrylate (0.5 g, 5 mmol) and the mixture was refluxed for 3.5 h. After completion of the reaction, solvent was removed under high vacuum and the residue was purified by column chromatography on silica gel (eluting with 10% EtOAc/Hexanes) to afford the desired product(s).

Ethyl 7-(*tert*-butyldimethylsilyloxy)-5-(2-ethoxy-2-oxoethyl)-8-methoxy-2,5,6,10b-tetrahydro-1*H*-isoxazolo [3,2-*a*] isoquinoline-1-carboxylate (12a):



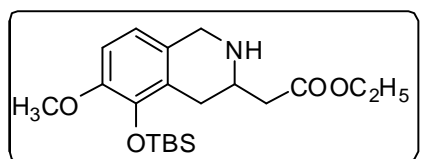
Colorless viscous oil; Yield: 50%; R_f = 0.6 (2:8 EtOAc: Hex); IR (cm^{-1}): 3050, 2966, 2862, 1735 (CO ester), 1725 (CO ester), 1620; 1H NMR (400 MHz, $CDCl_3$) δ 6.76 (s, 2H), 4.76 (d, J = 8.9 Hz, 1H), 4.40-4.35 (dd, J = 9.7, 8.4 Hz, 1H), 4.32-4.23 (m, 2H), 4.22-4.11 (m, 2H), 4.10-4.06 (dd, J = 8.1, 6.4 Hz, 1H), 3.77 (s, 3H), 3.44-3.33 (m, 2H), 3.17-3.12 (dd, J = 16.7, 3.7 Hz, 1H), 2.95-2.89 (dd, J = 15.4, 6.5 Hz, 1H), 2.54-2.41 (ddd, J = 21.1, 16.0, 8.5 Hz, 2H), 1.30 (m, 6H), 0.99 (s, 9H), 0.20 (s, 3H), 0.14 (s, 3H); ^{13}C NMR (100 MHz, $CDCl_3$) δ 172.7, 172.1, 148.6, 141.6, 126.6, 124.4, 119.3, 110.2, 69.3, 67.4, 61.3, 60.5, 55.0, 54.9, 53.0, 39.5, 30.6, 26.0 (3C), 18.8, 14.2, 14.2, -3.8, -4.0; Mass (ES): m/z 494.25 (M+H, 100%); HRMS (ESI): calcd for $C_{25}H_{40}NO_7Si$ (M+H)⁺ 494.2574 found 494.2595.

Ethyl 7-(*tert*-butyldimethylsilyloxy)-5-(2-ethoxy-2-oxoethyl)-8-methoxy-2,5,6,10b-tetrahydro-1*H*-isoxazolo [3,2-*a*] isoquinoline-2-carboxylate (12b):



Colorless viscous oil; Yield: 20%; $R_f = 0.6$ (2:8 EtOAc: Hex); IR (cm^{-1}): 3050, 2966, 2862, 1735 (CO ester), 1725 (CO ester), 1620; ^1H NMR (400 MHz, CDCl_3) δ 6.75 (t, $J = 7.4$ Hz, 1H), 6.69 (d, $J = 8.4$ Hz, 1H), 4.75 (dd, $J = 10.0, 3.4$ Hz, 1H), 4.63 (dd, $J = 10.6, 7.5$ Hz, 1H), 4.29-4.12 (m, 4H), 3.78 (s, 3H), 3.45-3.37 (m, 1H), 3.11 (dd, $J = 16.7, 3.5$ Hz, 1H), 2.98 (dd, $J = 15.5, 6.75$ Hz, 1H), 2.83-2.75 (m, 1H), 2.62-2.41 (m, 3H), 1.34-1.27 (m, 7H), 0.99 (s, 9H), 0.21 (s, 3H), 0.15 (s, 3H); ^{13}C NMR (100 MHz, CDCl_3) δ 172.3, 171.3, 148.3, 141.7, 127.3, 124.5, 119.3, 110.3, 75.7, 63.1, 61.4, 60.5, 54.9, 53.8, 40.8, 39.5, 30.8, 26.0 (3C), 18.8, 14.2, 14.1, -3.8, -4.0; Mass (ES): m/z 494.25 (M+H, 100%); HRMS (ESI): calcd for $\text{C}_{25}\text{H}_{40}\text{NO}_7\text{Si}$ (M+H) $^+$ 494.2574 found 494.2595.

Ethyl 2-(5-(*tert*-butyldimethylsilyloxy)-6-methoxy-1,2,3,4 tetrahydroisoquinolin-3-yl) acetate (13):

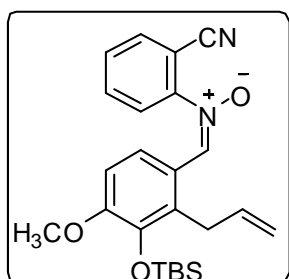


To a solution of 5-(*tert*-butyldimethylsilyloxy)-3-(2-ethoxy-2-oxoethyl)-6-methoxy-3,4 dihydroisoquinoline 2-oxide (0.393 g, 1 mmol) in acetic acid (5 mL) was added activated zinc (0.64 g, 10 mmol) and the mixture was stirred at room temperature for 0.5 h. After completion of the reaction $\text{NaOAc} \cdot \text{H}_2\text{O}$ was added followed by water. The mixture was extracted with ethyl acetate. The organic layer was dried over anhydrous Na_2SO_4 , filtered, and concentrated. The residue was purified by column chromatography on silica gel (eluting with 100% EtOAc) to afford the desired product as a colorless oil (0.228 g, 60%); $R_f = 0.5$ (8:2 EtOAc: Hex); IR (cm^{-1}): 3300, 3040, 2956, 2872, 1740 (CO ester), 1620; ^1H NMR (400 MHz, CDCl_3) δ 6.68 (d, $J = 8.3$ Hz, 1H), 6.59 (d, $J = 8.3$ Hz, 1H), 4.17 (q, $J = 7.1$ Hz, 2H), 3.99 (q, $J = 15.4$ Hz, 2H), 3.75 (s, 3H), 3.32-3.18 (m, 1H), 2.92-2.86 (dd, $J = 16.7, 4.1$ Hz, 1H), 2.64-2.51 (m, 2H), 2.37-2.30 (dd, $J = 16.6, 10.5$ Hz, 1H), 2.00 (s, 1H), 1.27 (t, $J = 7.2$ Hz, 3H), 0.99 (s, 9H), 0.16 (d, $J = 20.0$ Hz, 6H); ^{13}C NMR (100 MHz, CDCl_3) 172.2, 147.8, 142.3, 128.0, 125.9, 118.2, 109.3, 60.5, 54.9, 50.4, 47.2, 40.9, 30.5, 26.1 (3C), 18.9, 14.2, -3.8, -3.9; Mass (ES): m/z 380.22 (M+H, 100%); HRMS (ESI): calcd for $\text{C}_{20}\text{H}_{34}\text{NO}_4\text{Si}$ (M+H) $^+$ 380.2257 found 380.2249.

General procedure for 1,3 dipolar Cyclo addition

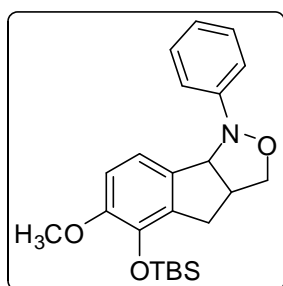
To a solution of aldehyde (1 mmol) in ethanol (5 mL) was added aryl hydroxyl amine (2 mmol) and MgSO₄ (5 mmol) under N₂ atmosphere. The reaction mixture was refluxed for 3-5 h (for inversion in the yields of regio isomers the reaction mixture was heated at 130 °C for 12 h). After completion of the reaction, ethanol was removed under high vacuum and the residue was purified by column chromatography on silica gel to give the desired product.

(E)-N-(2-allyl-3-(tert-butyldimethylsilyloxy)-4-methoxybenzylidene)-2-cyanoaniline oxide (15e):



The title compound was synthesized by using the general procedure; colorless solid; m.p : 176-178 °C; Yield (88%), R_f = 0.5 (2:8 EtOAc: Hex); IR (cm⁻¹): 3277, 2935, 2857, 2120 (CN), 1725, 1662, 1600, 1247; ¹H NMR (400 MHz, CDCl₃) δ 7.96 (d, *J* = 8.6 Hz, 1H), 7.36 (d, *J* = 8.6 Hz, 1H), 7.34-7.28 (m, 1H), 6.88 (t, *J* = 7.5 Hz, 1H), 6.84 (t, *J* = 6.6 Hz, 1H), 6.62 (d, *J* = 8.0 Hz, 1H), 6.06-5.93 (m, 2H), 5.06-5.03 (dd, *J* = 10.2, 1.5 Hz, 1H), 4.84-4.78 (dd, *J* = 17.2, 1.6 Hz, 1H), 3.82 (s, 3H), 3.69-3.51 (m, 2H), 1.04 (s, 9H), 0.19 (s, 6H); ¹³CNMR (100 MHz, CDCl₃) δ 165.0, 150.2, 147.5, 142.9, 137.4, 133.7 (2C), 129.5, 128.9, 128.5, 120.2, 119.1, 115.5, 115.2, 114.4, 109.6, 54.5, 29.7, 26.1 (3C), 18.8, -3.8, -3.82; Mass (ES): m/z 423.2 (M+H, 100%).

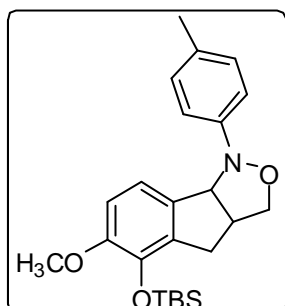
5-(tert-butyldimethylsilyloxy)-6-methoxy-1-phenyl-3,3a,4,8b-tetrahydro-1H-indeno[1,2-c] isoxazole (16a):



The title compound was synthesized by using the general procedure; colorless solid; m.p : 210-212 °C; Yield (36%), R_f = 0.7(1:9 EtOAc: Hex); IR (cm⁻¹): 3050, 2967, 2847, 1620, 1575, 1465, 1280; ¹H NMR (400 MHz, CDCl₃) δ 7.34 (t, *J* = 7.6 Hz, 2H), 7.20 (d, *J* = 7.9 Hz, 2H), 7.06 (d, *J* = 8.1 Hz, 1H), 7.02 (dd, *J* = 17.3, 10.1 Hz, 1H), 6.85 (d, *J* = 8.2 Hz, 1H), 5.36 (d, *J* = 7.5 Hz, 1H), 4.18 (t, *J* = 7.9 Hz, 1H), 3.89-3.77 (m, 4H), 3.49-3.38 (m, 1H), 3.25-3.18 (dd, *J* = 16.8, 8.6 Hz, 1H), 3.08-2.98 (m, 1H), 1.03 (s, 9H), 0.20 (t, *J* = 5.6 Hz, 6H); ¹³C NMR (100MHz, CDCl₃) δ 150.9, 150.1, 140.6, 135.1, 134.4, 128.9 (2C), 121.6, 117.6 (2C), 114.6, 111.8, 76.3, 74.1, 55.4, 46.4, 35.6, 25.9 (2C), 18.6, -4.1, -4.15; Mass (ES): m/z

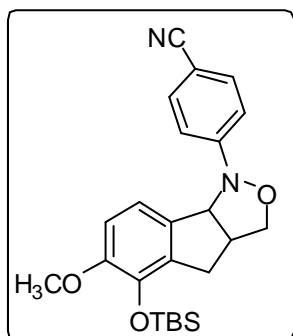
398.21 (M+H, 100%), 292.13 (30%); HRMS (ESI): calcd for C₂₃H₃₂NO₃Si (M+H)⁺ 398.2151 found 398.2165.

5-(*tert*-butyldimethylsilyloxy)-6-methoxy-1-*p*-tolyl-3,3a,4,8b-tetrahydro-1*H*-indeno[1,2-*c*] isoxazole (16b):



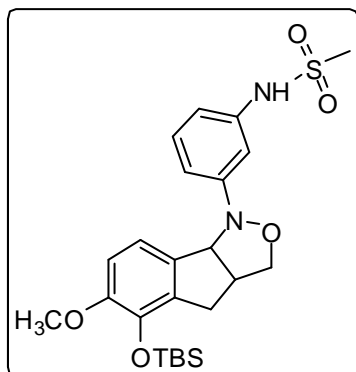
The title compound was synthesized by using the general procedure; yellow color solid; mp: 180-183 °C; Yield (32%), R_f = 0.9 (1:9 EtOAc: Hex); IR (cm⁻¹): 3030, 2953, 2868, 1609, 1576, 1456, 1278; ¹H NMR (400 MHz, CDCl₃) δ 7.13 (m, 4H), 7.09-7.01 (m, 1H), 6.85 (d, *J* = 8.2 Hz, 1H), 5.32 (d, *J* = 7.5 Hz, 1H), 4.19 (t, *J* = 8.0 Hz, 1H), 3.87-3.78 (m, 4H), 3.48-3.36 (m, 1H), 3.25-3.15 (dd, *J* = 16.8, 8.5 Hz, 1H), 3.05-2.95 (dd, *J* = 16.8, 2.7 Hz, 1H), 2.34 (s, 3H), 1.09 (s, 9H), 0.19 (d, *J* = 5.1 Hz, 6H); ¹³CNMR (100 MHz, CDCl₃) δ 150.2, 148.7, 140.7, 135.2, 134.4, 131.1, 129.5, 117.7, 114.9 (2C), 111.9, 76.5, 74.2, 55.5, 46.4, 35.7, 25.9 (3C), 20.6, 18.7, -4.1, -4.0. Mass (ES): *m/z* 412.22 (M+H 100%); HRMS (ESI): calcd for C₂₄H₃₄NO₃Si (M+H)⁺ 412.2307 found 412.2297.

4-(5-(*tert*-butyldimethylsilyloxy)-6-methoxy-3,3a,4,8b-tetrahydro-1*H*-indeno[1,2-*c*]isoxazol-1-yl)benzonitrile (16c):



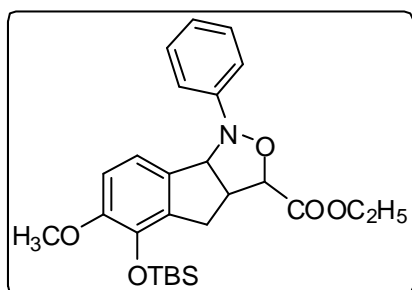
The title compound was synthesized by using the general procedure; white color solid; mp: 210-214 °C; Yield (32%), R_f = 0.9(1:9 EtOAc: Hex); IR (cm⁻¹): 3050, 2967, 2847, 2220, 1615, 1565, 1477, 1269; ¹H NMR (400 MHz, CDCl₃) δ 7.57 (d, *J* = 8.9 Hz, 2H), 7.18 (d, *J* = 8.9 Hz, 2H), 6.98 (d, *J* = 8.2 Hz, 1H), 6.83 (d, *J* = 8.2 Hz, 1H), 5.33 (d, *J* = 7.6 Hz, 1H), 4.12-4.01 (m, 1H), 3.89- 3.86 (dd, *J* = 8.3, 2.6 Hz, 1H), 3.80 (s, 3H), 3.61-3.49 (m, 1H), 3.33-3.15 (dd, *J* = 16.9, 8.7 Hz, 1H), 3.11-2.99 (dd, *J* = 16.9, 3.1 Hz, 1H), 1.07 (s, 9H), 0.18 (d, *J* = 6.4 Hz, 6H); ¹³CNMR (100 MHz, CDCl₃) δ 154.1, 150.4, 140.8, 134.5, 133.9 (2C), 133.4, 119.5, 117.5, 114.0 (2C), 111.9, 103.7, 75.2, 74.5, 55.4, 46.6, 35.4, 25.9 (2C), 18.6, -4.0, -4.1; Mass (ES):*m/z* 423.20 (M+H 80%), 307.16 (100%); HRMS (ESI): calcd for C₂₄H₃₁N₂O₃Si (M+H)⁺ 423.2103 found 423.2093.

***N*-(3-(5-(*tert*-butyldimethylsilyloxy)-6-methoxy-3,3a,4,8b-tetrahydro-1*H*-indeno[1,2-*c*]isoxazol-1-yl) phenyl)methanesulfonamide (16d):**



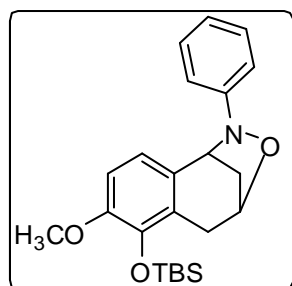
The title compound was synthesized by using the general procedure; yellow color solid; mp: 190-193 °C; Yield (30%), $R_f = 0.2$ (1:9 EtOAc: Hex); IR (cm^{-1}): 3247, 3078, 2928, 2856, 1713, 1598, 1489, 1320, 1277; ^1H NMR (400 MHz, CDCl_3) δ 7.28-7.24 (dd, $J = 9.21, 6.90$ Hz, 1H), 7.09-6.93 (m, 3H), 6.87-6.78 (m, 2H), 6.64 (s, 1H), 5.30 (d, $J = 7.53$ Hz, 1H), 4.13 (t, $J = 7.96$ Hz, 1H), 3.91-3.74 (m, 5H), 3.48-3.38 (m, 1H), 3.22-3.16 (dd, $J = 16.8, 8.6$ Hz, 1H), 3.01 (s, 3H), 1.03 (s, 10H), 0.19 (d, $J = 8.8$ Hz, 6H); ^{13}C NMR (100 MHz, CDCl_3) δ 152.4, 150.2, 140.7, 137.6, 134.5, 130.2 (2C), 117.6, 113.3, 111.8 (2C), 111.4, 106.5, 76.11, 74.2, 55.4, 46.5, 39.3, 35.4, 25.9 (2C), 18.6, -4.1; Mass (ES): m/z 513.18 ($\text{M}+\text{Na}$, 100%), 491.20 ($\text{M}+\text{H}$ 90%); HRMS (ESI): calcd for $\text{C}_{24}\text{H}_{35}\text{N}_2\text{O}_5\text{SiS}$ ($\text{M}+\text{H}$) $^+$ 491.2035 found 491.2021.

Ethyl 5-(*tert*-butyldimethylsilyloxy)-6-methoxy-1-phenyl-3,3a,4,8b-tetrahydro-1*H*-indeno[1,2-*c*]isoxazole-3-carboxylate (16f):



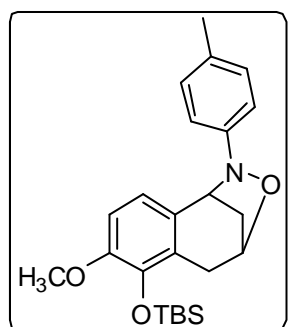
The title compound was synthesized by using the general procedure; Colorless oil: yield (78%), $R_f = 0.6$ (1: 9 EtOAc: Hex); IR (cm^{-1}): 3011, 2925, 2854, 1737, 1610, 1578, 1449, 1247; ^1H NMR (400 MHz, CDCl_3) δ 7.36-7.22 (m, 4H), 7.07-6.96 (m, 1H), 6.89 (d, $J = 8.2$ Hz, 1H), 6.78 (t, $J = 6.6$ Hz, 1H), 5.37 (d, $J = 7.2$ Hz, 1H), 4.31 (d, $J = 5.9$ Hz, 1H), 4.18 (q, $J = 7.1$ Hz, 2H), 3.79 (s, 3H), 3.74-3.63 (m, 1H), 3.15 (d, $J = 3.8$ Hz, 2H), 1.27 (q, $J = 7.2$, 3H), 1.05 (s, 9H), 0.19 (d, $J = 9.5$ Hz, 6H); ^{13}C NMR (100 MHz, CDCl_3) δ 170.7, 150.6, 150.5, 141.3, 134.3, 133.2, 128.6, 122.2, 117.8, 115.8 (2C), 111.7, 83.4, 75.4, 61.4, 55.4, 50.1, 33.2, 29.7, 25.9 (3C), 18.6, 14.0, -4.0, -4.1; Mass (ES): m/z 470.23 ($\text{M}+\text{H}$, 100%), 366.18 (40%); LC Mass: 470.2 (13.13% at 9.067 rt, 72.3% at 9.213 RT respectively. We failed to isolate minor isomer, where as major isomer **16f** was well characterised as mentioned above); HRMS (ESI): calcd for $\text{C}_{26}\text{H}_{36}\text{NO}_5\text{Si}$ ($\text{M}+\text{H}$) $^+$ 470.2362 found 470.2348.

Compound (17a):



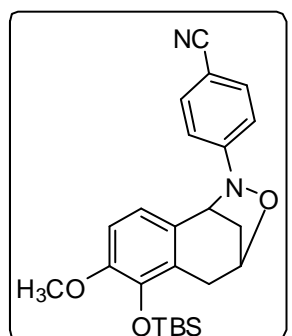
The title compound was synthesized by using the general procedure; Colorless oil; yield (60%), $R_f = 0.5$ (1:9 EtOAc: Hex); IR (cm^{-1}): 3060, 2977, 2857, 1610, 1567, 1455, 1291; $^1\text{H NMR}$ (400 MHz, CDCl_3) δ 7.26 (m, 3H), 7.13 (d, $J = 7.6$ Hz, 2H), 6.97 (d, $J = 7.3$ Hz, 1H), 6.84 (d, $J = 8.2$ Hz, 1H), 6.70 (d, $J = 8.2$ Hz, 1H), 5.12-5.03 (m, 1H), 4.59 (d, $J = 4.2$ Hz, 1H), 3.77 (s, 3H), 3.09 (d, $J = 2.4$ Hz, 1H), 2.83-2.78 (dd, $J = 17.8, 1.8$ Hz, 1H), 2.31 (m, 1H), 1.99 (d, $J = 11.1$ Hz, 2H), 1.00 (s, 9H), 0.18 (d, $J = 9.6$ Hz, 6H); $^{13}\text{CNMR}$ (100 MHz, CDCl_3) δ 151.6, 149.2, 143.2, 130.4, 128.1, 124.9, 121.9, 119.4, 116.2 (2C), 108.8, 73.7, 66.1, 54.5, 34.3, 32.6, 25.8 (3C), 25.3, 18.5, -3.9, -4.2; Mass (ES): m/z 398.21 (M+H, 100%), 292.13 (30%); HRMS (ESI): calcd for $\text{C}_{23}\text{H}_{32}\text{NO}_3\text{Si}$ (M+H) + 398.2151 found 398.2152.

Compound (17b):



The title compound was synthesized by using the general procedure; Light yellow oil; yield (68%), $R_f = 0.6$ (1:9 EtOAc: Hex); IR (cm^{-1}): 3025, 2978, 2856, 1580, 1495, 1268; $^1\text{H NMR}$ (400 MHz, CDCl_3) δ 7.15-7.01 (m, 4H), 6.86 (d, $J = 8.2$ Hz, 1H), 6.72 (d, $J = 8.2$ Hz, 1H), 5.14-5.02 (m, 1H), 4.55 (d, $J = 4.2$ Hz, 1H), 3.87 (s, 3H), 3.22-3.06 (m, 1H), 2.81 (d, $J = 17.7$ Hz, 1H), 2.38-2.23 (m, 4H), 1.98 (d, $J = 11.1$ Hz, 1H), 1.05 (s, 9H), 0.20 (d, $J = 10.9$ Hz, 6H); $^{13}\text{CNMR}$ (100 MHz, CDCl_3) δ 149.6, 149.4, 143.5, 131.5, 130.8, 128.9 (2C), 125.2, 119.6, 116.6 (2C), 109.1, 73.9, 66.6, 54.7, 34.6, 32.6, 26.0 (3C), 20.5, 18.8, -3.7 -3.9; Mass (ES): m/z 412.23 (M+H 100%); HRMS (ESI): calcd for $\text{C}_{24}\text{H}_{34}\text{NO}_3\text{Si}$ (M+H)⁺ 412.2307 found 412.2309.

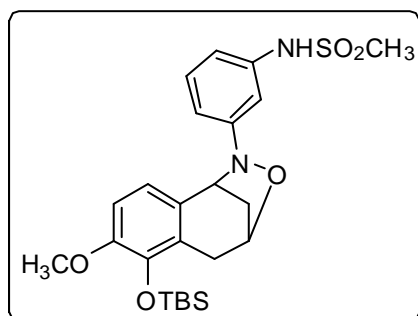
Compound (17c):



The title compound was synthesized by using the general procedure; Colorless oil; yield (62%), $R_f = 0.55$ (1:9 EtOAc: Hex); IR (cm^{-1}): 3060, 2987, 2869, 2198, 1605, 1545, 1487, 1277; $^1\text{H NMR}$ (400 MHz, CDCl_3) δ 7.49 (d, $J = 8.8$ Hz, 2H), 7.09 (d, $J = 8.8$ Hz, 2H), 6.76 (d, $J = 8.2$ Hz, 1H), 6.65 (d, $J = 8.3$ Hz, 1H), 5.12-5.01 (m, 1H), 4.76 (d, $J = 4.4$ Hz, 1H), 3.75 (s, 3H), 3.15-3.05 (dd, $J = 18.1, 1.9$ Hz, 1H), 2.90-2.80 (dd, $J = 18.0, 2.2$ Hz, 1H), 2.37 (td, $J = 10.7, 5.4$ Hz, 1H), 2.15 (d, $J = 8.8$ Hz, 1H), 0.99 (s, 9H), 0.17 (d, $J = 4.9$ Hz, 6H); $^{13}\text{CNMR}$ (100 MHz, CDCl_3) δ 154.2,

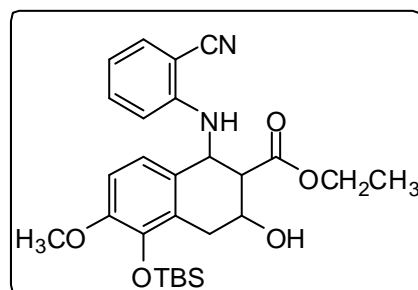
149.7, 143.6, 132.8 (2C), 129.3, 124.7, 119.8, 119.6, 115.8 (2C), 108.9, 103.81, 74.3, 64.5, 54.8, 34.6, 26.1 (3C), 18.9, -3.7, -3.8; Mass (ES): m/z 445.18 (M+Na 100%), 423.20 (M+H 80%), 307.16 (100%); HRMS (ESI): calcd for $C_{24}H_{31}N_2O_3Si$ (M+H)⁺ 423.2103 found 423.2085.

Compound (17d):



The title compound was synthesized by using the general procedure; Brown color oil; yield (65%), R_f = 0.2 (1:9 EtOAc: Hex); IR (cm^{-1}): 3233, 3063, 2954, 2854, 1713, 1595, 1479, 1310, 1257; 1H NMR (400 MHz, $CDCl_3$) δ 7.17 (t, J = 8.0 Hz, 1H), 6.88-6.98 (dd, J = 8.0, 6.0 Hz, 1H), 6.91-6.83 (m, 2H), 6.82-6.74 (m, 2H), 6.64 (d, J = 8.2 Hz, 1H), 5.03 (dd, J = 5.9, 2.5 Hz, 1H), 4.63 (d, J = 4.2 Hz, 1H), 3.75 (d, J = 15.5 Hz, 3H), 3.14-3.00 (m, 1H), 3.00-2.88 (m, 3H), 2.78-2.81 (dd, J = 17.9, 1.9 Hz, 1H), 2.30-2.35 (td, J = 10.7, 5.3 Hz, 1H), 0.97 (s, 9H), 0.23 (s, 6H); ^{13}C NMR (100 MHz, $CDCl_3$) 152.8, 149.6, 143.5, 137.2, 130.1, 129.7 (2C), 125.0, 120.0, 114.00, 113.4, 108.9, 106.6, 74.1, 65.8, 54.8, 39.0, 34.7, 26.1 (3C), 18.9, -3.70, -3.77; Mass (ES): m/z 513.18 (M+Na, 100%), 491.20 (M+H 90%); HRMS (ESI): calcd for $C_{24}H_{35}N_2O_5SiS$ (M+H)⁺ 491.2035 found 491.2015.

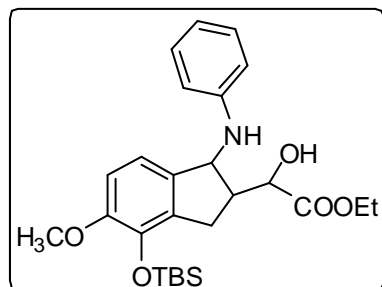
Ethyl 5-(tert-butyldimethylsilyloxy)-1-(2-cyanophenylamino)-3-hydroxy-6-methoxy-1,2,3,4-tetrahydronaphthalene-2-carboxylate (18):



The title compound was synthesized by using the general procedure; white color solid; mp: 180-183 °C, Yield (58%), R_f = 0.4 (2:8 EtOAc: Hex); IR (cm^{-1}): 3311, 2934, 2856, 2140 (CN), 1729, 1620, 1600, 1489, 1247; 1H NMR (400 MHz, $CDCl_3$) δ 7.99 (d, J = 7.9 Hz, 1H), 7.32 (d, J = 7.5 Hz, 1H), 6.94 (t, J = 8.1 Hz, 2H), 6.86 (d, J = 8.3 Hz, 1H), 6.76 (d, J = 7.9 Hz, 1H), 5.83 (s, 1H), 5.46 (d, J = 5.9 Hz, 1H), 4.27 (s, 1H), 4.16-4.02 (m, 2H), 3.83 (s, 3H), 3.20 (d, J = 16.3 Hz, 1H), 2.94 (d, J = 5.4 Hz, 1H), 2.45 (d, J = 6.8 Hz, 1H), 2.35 (d, J = 7.9 Hz, 1H), 1.22 (t, J = 8.4 Hz, 3H), 1.00 (s, 9H), 0.22 (s, 3H), 0.14 (s, 3H); ^{13}C NMR (100 MHz, $CDCl_3$) δ 170.8, 163.8, 149.9, 146.8, 142.9, 133.1, 129.0, 124.9, 124.8, 119.9, 118.5, 117.8, 115.2, 110.1, 64.6, 60.6, 54.8, 44.2, 36.4, 27.3, 25.8 (3C),

18.7, 13.9, -3.9, -4.2; Mass (ES): m/z 519.22 (M+Na, 100%), 497.24 (M+H, 80%); HRMS (ESI): calcd for $C_{27}H_{37}N_2O_5Si$ (M+H)⁺ 497.2471 found 497.2459.

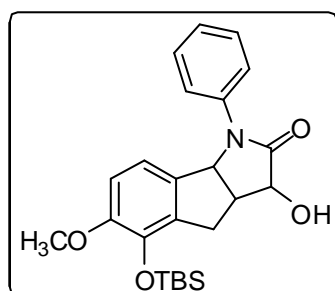
(R)-Ethyl-2-((1R,2R)-4-(*tert*-butyldimethylsilyloxy)-5-methoxy-1-(phenylamino)-2,3-dihydro-1*H*-inden-2-yl)-2-hydroxyacetate (19):



To a solution of (3*R*,3*aR*,8*bR*)-ethyl 5-(*tert*-butyldimethylsilyloxy)-6-methoxy-1-phenyl-3, 3*a*,4,8*b*-tetrahydro-1*H*-indeno [1,2-*c*] isoxazole-3-carboxylate (**8f**) (0.470 g, 1.0 mmol) in MeOH (5 mL) was added 5% Pd/C (47 mg) under balloon pressure of H₂. TLC shows completion of reaction after 6h. The Pd was filtered through celite, and

the filtrate was concentrated under high vacuum. The residue was purified by column chromatography with EtOAc/Hexane (2:8) as eluent to yield the desired product; yield (80%). R_f = 0.4 (2:8 EtOAc: Hex); IR (cm⁻¹): 3340, 3079, 2930, 2847, 1681, 1650, 1585; ¹H NMR (400 MHz, CDCl₃) δ 7.18 (t, J = 7.93 Hz, 2H), 6.82-6.65 (m, 5H), 7H), 5.15 (d, J = 7.3 Hz, 1H), 4.34 (d, J = 4.7 Hz, 1H), 3.96 (dd, J = 10.7, 7.2 Hz, 1H), 3.77 (s, 3H), 3.63 (dd, J = 10.7, 7.1 Hz, 1H), 3.28-2.96 (tdd, J = 37.6, 16.4, 6.3 Hz, 4H), 1.11 (t, J = 7.1 Hz, 3H), 1.01 (s, 9H), 0.17 (d, J = 6.3 Hz); ¹³C NMR (100 MHz, CDCl₃) δ 172.7, 150.8, 141.2, 136.6, 135.9, 132.7, 128.8 (2C), 126.7, 125.3 (2C), 118.7, 109.9 (2C), 71.1, 65.6, 55.1, 42.7, 28.2, 25.9 (3C), 18.6, 14.4, -4.1 (2C); Mass (ES): m/z 494.23 (M+Na, 100%), 379.19 (100%); HRMS (ESI): calcd for $C_{26}H_{37}NO_5SiNa$ (M+Na)⁺ 494.2338 found 494.2341.

(3*S*,3*aR*,8*bR*)-5-(*tert*-butyldimethylsilyloxy)-3-hydroxy-6-methoxy-1-phenyl-1,3*a*,4,8*b*-tetrahydroindeno[1,2-*b*]pyrrol-2(3*H*)-one (20):

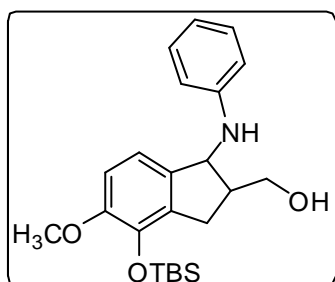


To a solution of (3*R*,3*aR*,8*bR*)-ethyl 5-(*tert*-butyldimethylsilyloxy)-6-methoxy-1-phenyl-3, 3*a*,4,8*b*-tetrahydro-1*H*-indeno [1,2-*c*] isoxazole-3-carboxylate (0.470 g, 1.0 mmol) in AcOH: THF:H₂O (2:1:1, 40 mL) was added Zn dust (0.4 g, 6.1 mmol) at 60 °C. The reaction mixture was stirred for 5h. After completion of the reaction the mixture was cooled

to room temperature and Zn was filtered off. The filtrate was concentrated to remove THF, and neutralized with saturated NaHCO₃ solution. The reaction mixture was extracted with

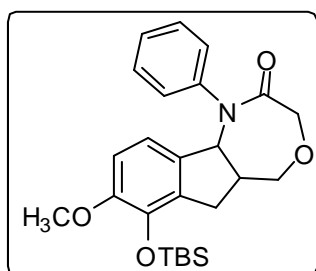
CH₂Cl₂. The organic layer was washed with brine, dried over Na₂SO₄, filtered and concentrated. The residue was purified by column chromatography using EtOAc/Hexane (3:7) as eluent to yield a colorless solid (0.255 g, 60%); mp: 160-163 °C R_f = 0.4 (3:7 EtOAc: Hex); IR (cm⁻¹): 3450, 3088, 2965, 2874, 1700, 1630, 1565; ¹H NMR (400 MHz, CDCl₃) δ 7.40-7.33 (m, 2H), 7.26-7.20 (m, 3H), 6.46 (q, *J* = 8.2 Hz, 2H), 5.30 (d, *J* = 6.30 Hz, 1H), 4.73 (d, *J* = 8.3 Hz, 1H), 3.70 (s, 3H), 3.59-3.50 (m, 1H), 3.30 (s, 1H), 3.24-3.03 (m, 2H), 1.00 (s, 9H), 0.15 (d, *J* = 1.5 Hz, 6H); ¹³CNMR (100 MHz, CDCl₃) δ 173.3, 150.7, 141.2, 136.6, 132.8, 128.8 (2C), 126.7, 125.4 (2C), 118.7, 109.9, 71.0, 65.6, 55.1, 42.6, 28.3, 26.0 (3C), 18.6, -4.04, -4.07; Mass (ES): *m/z* 448.19 (M+Na, 20%), 371.23 (40%), 313.19 (100%); HRMS (ESI): calcd for C₂₄H₃₁NO₄SiNa (M+Na)⁺ 448.1920 found 448.1909.

(4-(*tert*-butyldimethylsilyloxy)-5-methoxy-1-(phenylamino)-2,3-dihydro-1*H*-inden-2-yl)methanol (21):



The title compound was synthesized by using a procedure similar to synthesis of **11**; brown viscous oil, yield (88%), R_f = 0.4 (1:9 EtOAc: Hex); IR (cm⁻¹): 3373, 3079, 2930, 2854, 1600, 1494, 1443; ¹H NMR (400 MHz, CDCl₃) δ 7.27-7.22 (m, 1H), 6.89-6.80 (m, 3H), 6.73 (q, *J* = 8.1 Hz, 2H), 5.06 (d, *J* = 6.6 Hz, 1H), 3.84-3.77 (m, 4H), 3.72 (dd, *J* = 11.2, 4.6 Hz, 1H), 3.40-3.27 (bs, 1H), 3.05-2.86 (m, 3H), 1.02 (s, 9H), 0.19 (d, *J* = 12.2 Hz, 6H); ¹³CNMR (100 MHz, CDCl₃) δ 150.1, 148.0, 141.1, 137.3, 133.1, 129.4 (2C), 118.1, 116.1, 113.6 (2C), 110.8, 63.4, 61.0, 55.3, 44.5, 31.1, 25.9 (3C), 18.6, -4.0, -4.2; Mass (ES): *m/z* 422.21 (M+H, 40%), 400.23 (35%), 307.17 (100%); HRMS (ESI): calcd for C₂₃H₃₄NO₃Si (M+H)⁺ 400.2307 found 400.2313.

7-(*tert*-butyldimethylsilyloxy)-8-methoxy-1-phenyl-5,5a,6,10b-tetrahydro-1*H*-indeno[1,2-*e*][1,4]oxazepin-2(3*H*)-one (22):

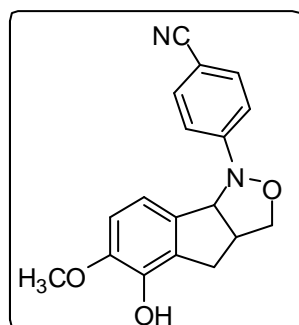


To a solution of (4-(*tert*-butyldimethylsilyloxy)-5-methoxy-1-(phenylamino)-2,3-dihydro-1*H*-inden-2-yl)methanol (0.422 g, 1.0 mmol) in dry DMF (10 mL), was added ethylbromo acetate (0.2 g, 1.2 mmol) and oven dried K₂CO₃ (0.548 g, 4.0 mmol). The mixture was refluxed for 36 h. After completion of the reaction, the mixture was diluted with saturated NH₄Cl solution and extracted with CH₂Cl₂. The

organic layer was collected, washed with 2N HCl and water, then dried over anhydrous Na_2SO_4 , filtered and concentrated. The residue was purified by column chromatography on silica gel using EtOAc/Hexane (3:7) as eluent to afford the desired product as a brown solid (0.228 g, 60%); mp: 280-282 °C; Yield (60%), $R_f = 0.4$ (3:7 EtOAc: Hex); IR (cm^{-1}): 3021, 2973, 2877, 1720, 1615, 1585; ^1H NMR (400 MHz, CDCl_3) δ 7.41 (t, $J = 7.7$ Hz, 2H), 7.34 (d, $J = 7.3$ Hz, 2H), 7.31-7.23 (m, 1H), 6.92 (d, $J = 8.0$ Hz, 1H), 6.75 (d, $J = 8.0$ Hz, 1H), 5.30 (d, $J = 7.1$ Hz, 1H), 4.34 (d, $J = 15.5$ Hz, 1H), 4.11 (dd, $J = 12.6, 3.9$ Hz, 1H), 3.91 (d, $J = 15.5$ Hz, 1H), 3.79 (s, 3H), 3.72 (dd, $J = 12.7, 4.8$ Hz, 1H), 2.94 (dd, $J = 20.0, 13.3$ Hz, 3H), 1.00 (s, 9H), 0.20 (s, 3H), 0.13 (s, 3H); ^{13}C NMR (100 MHz, CDCl_3) 172.6, 150.2, 144.5, 141.3, 134.8, 131.8, 129.2 (2C), 126.9, 126.5 (2C), 114.7, 110.5, 72.5, 71.7, 68.8, 55.2, 43.5, 32.0, 25.8 (3C), 18.5, -4.2, -4.4; Mass (ES): m/z 462.20 (M+Na, 100%), 440.22 (M+H, 10%), 289.16 (80%); HRMS (ESI): calcd for $\text{C}_{25}\text{H}_{33}\text{NO}_4 \text{NaSi}$ (M+Na) $^+$ 462.2076 found 462.2060.

A typical procedure for the deprotection of *tert*-butyldimethylsilyloxy group of compound 16c:

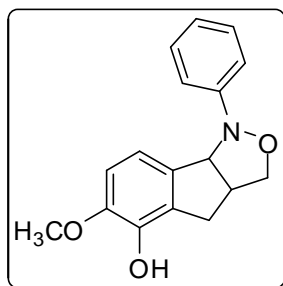
To a solution of 4-(5-(*tert*-butyldimethylsilyloxy)-6-methoxy-3,3a,4,8b-tetrahydro-1*H*-indeno[1,2-*c*]isoxazol-1-yl) benzonitrile (**16c**) (1 mmol) in dry THF (5 mL), was added *tetra*-butyl ammonium iodide (1.5 mmol) at 0 °C. The reaction mixture was stirred at the same temperature for 0.5 h, THF was removed under high vacuum followed by extraction with DCM. The DCM layer was collected, dried over anhydrous Na_2SO_4 , filtered and concentrated. The residue was purified by using column chromatography over silica gel to give the product 4-(5-hydroxy-6-methoxy-3,3a,4,8b-tetrahydro-1*H*-indeno[1,2-*c*]isoxazol-1-yl)benzonitrile (**23**).



White color solid; m.p: 180 °C; Yield (88%), $R_f = 0.2$ (1:9 EtOAc: Hex); IR (cm^{-1}): 3430, 3256, 3060, 2973, 2868, 2205, 1620, 1555, 1486, 1276; ^1H NMR (400 MHz, CDCl_3) δ 7.58 (d, $J = 8.9$ Hz, 2H), 7.19 (d, $J = 8.9$ Hz, 2H), 6.93 (d, $J = 8.1$ Hz, 1H), 6.84 (d, $J = 8.2$ Hz, 1H), 5.67 (s, 1H), 5.35 (d, $J = 7.6$ Hz, 1H), 4.10-4.05 (m, 1H), 3.98-3.85 (m, 4H), 3.56-3.48 (m, 1H), 3.30-3.22 (m, 1H), 3.03

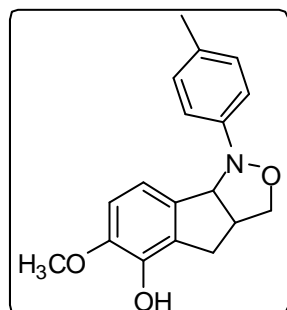
(dd, $J = 16.9, 3.1$ Hz, 1H); ^{13}C NMR (100 MHz, CDCl_3) δ 154.0, 146.6, 141.4, 134.5 (2C), 133.4, 128.6, 119.5, 116.1, 114.0 (2C), 110.7, 103.8, 75.0, 74.6, 56.4, 46.7, 34.2, 29.7; Mass (ES): m/z 309.13 (M+H 100%).

6-methoxy-1-phenyl-3,3a,4,8b-tetrahydro-1H-indeno[1,2-c]isoxazol-5-ol (24):



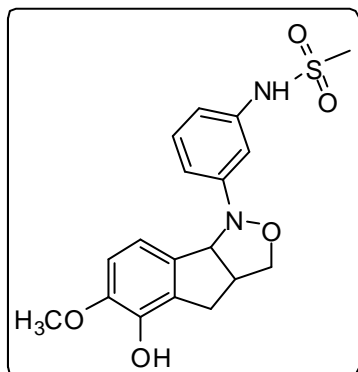
The title compound was synthesized by following the typical procedure for synthesis of compound **15**; colorless solid; m.p: 180 °C; Yield (90%), $R_f = 0.2$ (1:9 EtOAc: Hex); IR (cm^{-1}): 3360, 3040, 2957, 2832, 1620, 1565, 1445, 1290; ^1H NMR (400 MHz, CDCl_3) δ 7.34 (t, $J = 7.6$ Hz, 2H), 7.20 (d, $J = 7.9$ Hz, 2H), 7.03 (d, $J = 8.1$ Hz, 2H), 6.83 (d, $J = 8.1$ Hz, 1H), 5.65 (s, 1H), 5.35 (d, $J = 7.5$ Hz, 1H), 4.17 (t, $J = 7.9$ Hz, 1H), 3.83 (s, 3H), 3.84-3.82 (m, 1H), 3.48-3.42 (m, 1H), 3.25-3.18 (dd, $J = 16.8, 8.6$ Hz, 1H), 3.08-2.98 (m, 1H); ^{13}C NMR (100 MHz, CDCl_3) δ 148.1, 145.0, 141.6, 135.1, 134.4, 128.9 (2C), 121.6, 117.6 (2C), 114.6, 111.8, 76.3, 74.1, 55.4, 46.4, 25.9; Mass (ES): m/z 284.21 (M+H, 100%).

6-Methoxy-1-*p*-tolyl-3,3a,4,8b-tetrahydro-1H-indeno [1, 2-c] isoxazol-5-ol (25):



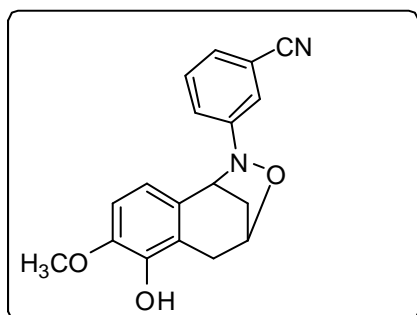
The title compound was synthesized by following the typical procedure for synthesis of compound **15**; light yellow solid; m.p: 170 °C; Yield (86%), $R_f = 0.2$ (1:9 EtOAc: Hex); IR (cm^{-1}): 3296, 3050, 2963, 2878, 1619, 1567, 1476, 1286; ^1H NMR (400 MHz, CDCl_3) δ 7.19-7.09 (m, $J = 8.7$ Hz, 4H), 6.97 (d, $J = 8.2$ Hz, 1H), 6.81 (d, $J = 8.2$ Hz, 1H), 5.30 (d, $J = 7.5$ Hz, 1H), 4.16 (t, $J = 8.0$ Hz, 1H), 3.85 (s, 3H), 3.79-3.68 (dd, $J = 8.4, 2.7$ Hz, 1H), 3.47-3.37 (m, 1H), 3.19 (dd, $J = 16.8, 8.6$ Hz, 1H), 2.99 (dd, $J = 16.8, 2.6$ Hz, 1H), 2.30 (s, 3H); ^{13}C NMR (100 MHz, CDCl_3) δ 148.6, 146.4, 141.4, 135.9, 131.21, 129.5, 116.2, 114.9 (2C), 110.7, 76.3, 74.2, 56.4, 46.6, 34.4, 20.5. Mass (ES): m/z 298.13 (M+H 100%).

N-(3-(5-(*tert*-butyldimethylsilyloxy)-6-methoxy-3,3a,4,8b-tetrahydro-1*H*-indeno[1,2-*c*]isoxazol-1-yl) phenyl) methanesulfonamide (26):



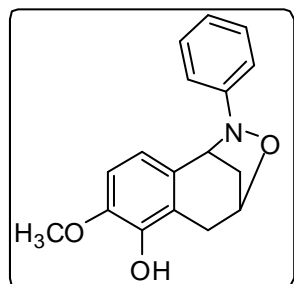
The title compound was synthesized by following the typical procedure for synthesis of compound **15**; yellow solid; mp: 190-193 °C; Yield (70%), $R_f = 0.2$ (3:7 EtOAc: Hex); IR (cm^{-1}): 3437, 3068, 2948, 2856, 1711, 1588, 1482, 1310, 1287; ^1H NMR (400 MHz, CDCl_3) δ 7.25-7.21 (dd, $J = 9.21, 6.90$ Hz, 1H), 7.11-6.95 (m, 3H), 6.89-6.79 (m, 2H), 6.54 (s, 1H), 5.32 (d, $J = 7.5$ Hz, 1H), 4.15 (t, $J = 7.9$ Hz, 1H), 3.93-3.77 (m, 5H), 3.51-3.41 (m, 1H), 3.24-3.19 (dd, $J = 16.8, 8.6$ Hz, 1H), 3.09 (s, 3H); ^{13}C NMR (100 MHz, CDCl_3) δ 153.4, 151.2, 141.2, 138.2, 135.1, 130.9 (2C), 118.5, 113.6, 112.2, 111.9 (2C), 105.7, 77.41, 75.2, 56.4, 47.5, 39.8, 36.4, 26.9; Mass (ES): m/z 377.10 (M+H 100%).

Compound 27:



The title compound was synthesized by following the typical procedure for synthesis of compound **15**; colorless viscous oil; Yield (72%), $R_f = 0.15$ (1:9 EtOAc: Hex); IR (cm^{-1}): 3423, 3070, 2992, 2876, 2198, 1615, 1565, 1497, 1287; ^1H NMR (400 MHz, CDCl_3) δ 7.48 (d, $J = 8.8$ Hz, 2H), 7.09 (d, $J = 8.8$ Hz, 2H), 6.72 (d, $J = 8.1$ Hz, 1H), 6.66 (d, $J = 8.1$ Hz, 1H), 5.72 (s, 1H), 5.11-5.02 (m, 1H), 4.78 (d, $J = 4.40$ Hz, 1H), 3.84 (s, 3H), 3.11 (dd, $J = 18.0, 1.8$ Hz, 1H), 2.88 (dd, $J = 18.0, 2.2$ Hz, 1H), 2.47-2.31 (m, 1H), 2.17 (d, $J = 11.1$ Hz, 1H); ^{13}C NMR (100 MHz, CDCl_3) δ 154.3, 149.7, 143.6, 140.3, 132.8 (2C), 124.7 (2C), 119.7, 119.6, 115.8, 108.9, 103.6, 74.2, 64.5, 54.8, 41.0, 24.3; Mass (ES): m/z 309.16 (M+H 100%).

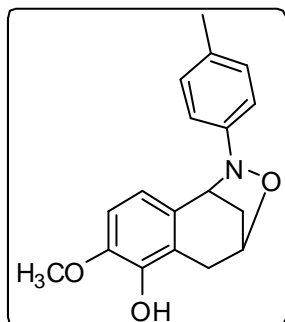
Compound (28):



The title compound was synthesized by following the typical procedure for synthesis of compound **15**; brown semi solid, Yield (80%), $R_f = 0.2$ (1:9 EtOAc: Hex); IR (cm^{-1}): 3345, 3050, 2967, 2875, 1620, 1566, 1465, 1298; ^1H NMR (400 MHz, CDCl_3) δ 7.24 (t, $J = 7.9$ Hz, 2H), 7.12 (d, $J = 7.7$ Hz, 2H), 6.93 (t, $J = 7.3$ Hz, 1H), 6.76 (d, $J = 8.1$ Hz, 1H), 6.67 (d, $J = 8.1$ Hz, 1H), 5.79 (s, 1H), 5.12-5.00 (m, 1H), 4.59 (d, $J = 4.3$ Hz, 1H), 3.84-3.74 (m, 3H), 3.10 (dd, $J = 17.7, 2.0$ Hz,

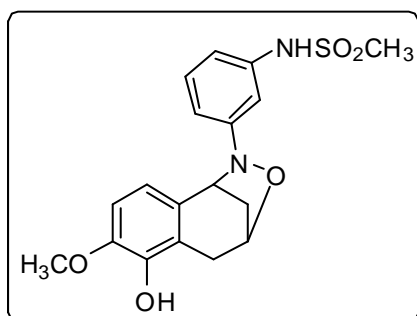
1H), 2.80 (dd, $J = 17.8, 1.7$ Hz, 1H), 2.32 (td, $J = 10.9, 5.3$ Hz, 1H), 2.04-1.96 (m, 1H); ^{13}C NMR (100 MHz, CDCl_3) δ 153.6, 146.7, 141.8, 132.8, 129.3, 124.7, 119.8, 119.6, 115.9, 108.9, 103.8, 74.2, 64.5, 54.8, 48.9, 34.6, 26.1; Mass (ES): m/z 284.21 (M+H, 100%).

Compound 29:



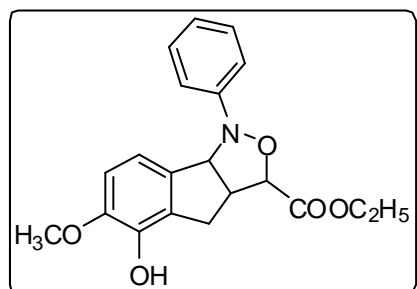
The title compound was synthesized by following the typical procedure for synthesis of compound **15**; colorless semi solid; Yield (90%), $R_f = 0.8$ (1:9 EtOAc: Hex); IR (cm^{-1}): 3346, 3053, 2987, 2867, 1590, 1505, 1286; ^1H NMR (400 MHz, CDCl_3) δ 7.07-7.01 (m, 4H), 6.77 (d, $J = 8.1$ Hz, 1H), 6.69 (d, $J = 8.1$ Hz, 1H), 5.12-4.98 (m, 1H), 5.98-5.45 (m, 1H), 4.53 (d, $J = 4.3$ Hz, 1H), 3.82 (s, 3H), 3.10 (dd, $J = 17.7, 1.8$ Hz, 1H), 2.80 (dd, $J = 17.7, 1.6$ Hz, 1H), 2.38-2.29 (m, 1H), 2.29 (d, $J = 11.0$ Hz, 3H), 1.99 (d, $J = 11.1$ Hz, 1H); ^{13}C NMR (100 MHz, CDCl_3) δ 149.6, 146.1, 144.1, 131.7, 131.2 (2C), 129.1, 119.8, 118.4, 116.7 (2C), 108.3, 73.9, 66.6, 56.1, 33.2, 33.0, 20.6; Mass (ES): m/z 298.13 (M+H 100%).

Compound (30):



The title compound was synthesized by following the typical procedure for synthesis of compound **15**; colorless semi solid; yield (85%), $R_f = 0.2$ (3:7 EtOAc: Hex); IR (cm^{-1}): 3420, 3253, 3083, 2965, 2874, 1713, 1585, 1489, 1320, 1267; ^1H NMR (400 MHz, CDCl_3) δ 7.20 (t, $J = 8.0$ Hz, 1H), 6.97 (s, 1H), 6.90 (d, $J = 8.1$ Hz, 1H), 6.80-6.73 (m, 2H), 6.67 (d, $J = 8.2$ Hz, 1H), 5.12-5.03 (m, 1H), 4.66 (d, $J = 4.3$ Hz, 1H), 5.93-5.46 (m, 1H), 3.85 (s, 3H), 3.11 (dd, $J = 17.9, 1.7$ Hz, 1H), 2.95 (s, 3H), 2.85 (dd, $J = 17.8, 1.8$ Hz, 1H), 2.45-2.35 (m, 1H), 2.10 (d, $J = 11.2$ Hz, 1H); ^{13}C NMR (100 MHz, CDCl_3) 152.8, 146.1, 144.0, 137.1, 130.4, 129.7 (2C), 119.5, 118.6 (2C), 113.9, 113.4, 108.6, 108.1, 74.0, 65.6, 56.0, 39.1, 33.9; Mass (ES): m/z 513.18 (M+Na, 100%), 377.20 (M+H 90%).

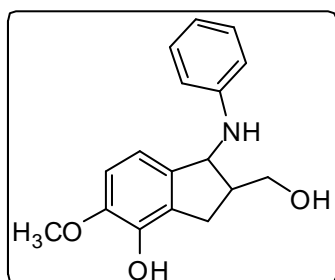
Ethyl-5-hydroxy-6-methoxy-1-phenyl-3,3a,4,8b-tetrahydro-1H-indeno[1,2-c]isoxazole-3-carboxylate (31):



The title compound was synthesized by following the typical procedure for synthesis of compound **15**; Light yellow color oil; yield (88%), $R_f = 0.2$ (1:9 EtOAc: Hex); IR (cm^{-1}): 3367, 3067, 2954, 2874, 1742, 1620, 1565,

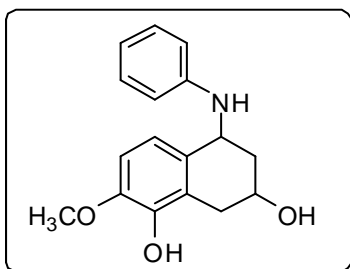
1435, 1255; ^1H NMR (400 MHz, CDCl_3) δ 7.33-7.23 (m, 4H), 7.00 (ddd, $J = 8.3, 6.9, 3.6$ Hz, 1H), 6.84-6.73 (m, 2H), 5.70 (s, 1H), 5.37 (d, $J = 7.3$ Hz, 1H), 4.33 (d, $J = 5.8$ Hz, 1H), 4.17 (q, $J = 7.1$ Hz, 2H), 3.85 (d, $J = 11.8$ Hz, 4H), 3.73 (ddd, $J = 13.4, 6.4, 3.4$ Hz, 1H), 3.23-3.08 (m, 2H), 1.25 (t, $J = 7.14$ Hz, 4H); ^{13}C NMR (100 MHz, CDCl_3) δ 170.7, 150.4, 146.2, 141.9, 134.8, 128.6 (2C), 127.4, 122.2, 116.3, 115.9 (2C), 110.5, 83.4, 75.1, 61.4, 56.3, 50.2, 32.2, 14.0; Mass (ES): m/z 355.24 (M+H, 100%).

2-(Hydroxyl methyl)-5-methoxy-1-(phenylamino)-2,3-dihydro-1H-inden-4-ol (32):



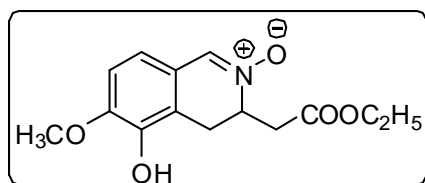
The title compound was synthesized by following the typical procedure for synthesis of compound **15**; yellow color viscous oil, Yield (88%), $R_f = 0.3$ (3:7 EtOAc: Hex); IR (cm^{-1}): 3383, 3089, 2950, 2864, 1610, 1534, 1484, 1453; ^1H NMR (400 MHz, CDCl_3) δ 7.27-7.12 (m, 2H), 6.80-6.69 (m, 5H), 5.05 (d, $J = 6.8$ Hz, 1H), 3.83 (s, 3H), 3.79-3.72 (m, 1H), 3.65 (dd, $J = 11.2, 4.8$ Hz, 1H), 3.04-2.92 (m, 2H), 2.87 (d, $J = 12.2$ Hz, 1H); ^{13}C NMR (100 MHz, CDCl_3) δ 148.0, 146.4, 141.8, 137.9, 129.4 (2C), 127.4, 118.2, 114.5, 113.7 (2C), 109.8, 63.4, 61.0, 56.3, 44.6, 29.9; Mass (ES): m/z 285.21 (M+H, 100%).

2-Methoxy-5-(phenylamino)-5,6,7,8-tetrahydronaphthalene-1,7-diol (33):



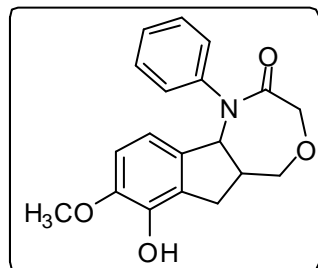
The title compound was synthesized by following the typical procedure for synthesis of compound **15**; yellow color viscous oil, Yield (88%), $R_f = 0.3$ (3:7 EtOAc: Hex); IR (cm^{-1}): 3383, 3089, 2950, 2864, 1610, 1534, 1484, 1453; ^1H NMR (400 MHz, CDCl_3) δ 7.25-7.15 (m, 2H), 6.95 (d, $J = 8.5$ Hz, 1H), 6.77-6.68 (m, 4H), 6.16-6.15 (m, 1H), 6.13-5.50 (m, 1H), 4.66 (t, $J = 5.9$ Hz, 1H), 4.33-4.19 (m, 1H), 3.85 (s, 3H), 3.03 (dd, $J = 17.1, 4.9$ Hz, 1H), 2.83 (dd, $J = 17.1, 6.4$ Hz, 1H), 2.28-2.20 (m, 1H), 2.06-1.95 (m, 1H); ^{13}C NMR (100 MHz, CDCl_3) δ 147.0, 145.4, 143.1, 131.0, 129.4 (2C), 121.0, 118.9, 117.9, 113.6 (2C), 108.9, 65.9, 56.1, 36.4, 32.4; Mass (ES): m/z 285.21 (M+H, 100%).

3-(2-Ethoxy-2-oxoethyl)-5-hydroxy-6-methoxy-3,4-dihydroisoquinoline-2-oxide (34):



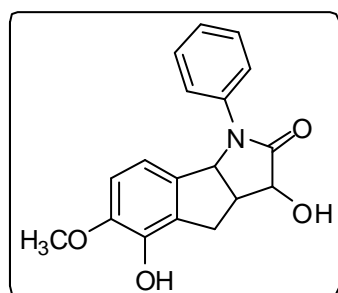
The title compound was synthesized by following the typical procedure for synthesis of compound **15**; colorless oil (88%); $R_f = 0.4$ (8:2 EtOAc: Hex); IR (cm^{-1}): 3326, 3060, 2985, 2872, 1720 (CO, ester), 1621, 1575, 1474, 1257; ^1H NMR (400 MHz, CDCl_3) δ 7.66 (s, 1H), 6.75 (s, 1H), 6.70 (s, 1H), 6.12-5.99 (m, 1H), 4.53-4.48 (m, 1H), 4.22-4.15 (m, 2H), 3.92 (s, 5H), 3.20-3.13 (m, 3H), 3.12-3.06 (m, 1H), 2.65-2.56 (m, 1H), 1.28 (d, $J = 7.1$ Hz, 4H); ^{13}C NMR (100 MHz, CDCl_3) δ 173.8, 152.0, 142.5, 135.1, 121.3, 119.9, 109.8, 63.5, 60.9, 55.0, 35.8, 27.1, 14.1; Mass (ES): m/z 280.20 (M+H, 100%).

7-Hydroxy-8-methoxy-1-phenyl-5,5a,6,10b-tetrahydro-1H-indeno[1,2-e][1,4]oxazepin-2(3H)-one (35):



The title compound was synthesized by following the typical procedure for synthesis of compound **15**; Brown solid (90%); mp: 250 °C; Yield (90%), $R_f = 0.2$ (3:7 EtOAc: Hex); IR (cm^{-1}): 3345, 3051, 2983, 2867, 1710, 1625, 1575; ^1H NMR (400 MHz, CDCl_3) δ 7.42 (t, $J = 7.7$ Hz, 2H), 7.35 (d, $J = 7.6$ Hz, 2H), 7.27 (dd, $J = 12.8, 4.8$ Hz, 1H), 6.88 (d, $J = 8.0$ Hz, 1H), 6.75 (d, $J = 8.0$ Hz, 1H), 5.82 (s, 1H), 5.29 (d, $J = 6.9$ Hz, 1H), 4.33 (d, $J = 15.7$ Hz, 1H), 4.11 (dd, $J = 12.6, 3.2$ Hz, 1H), 3.93 (d, $J = 15.7$ Hz, 1H), 3.89 (d, $J = 18.5$ Hz, 3H), 3.79 (dd, $J = 12.6, 3.3$ Hz, 1H), 3.08-2.89 (m, 3H); ^{13}C NMR (100 MHz, CDCl_3) 172.3, 146.4, 144.9, 141.9, 136.0, 129.3 (2C), 127.0 (2C), 126.6 (2C), 112.9, 109.4, 72.7, 72.1, 68.8, 56.2, 43.8, 31.2; Mass (ES): m/z 326.20.

3,5-Dihydroxy-6-methoxy-1-phenyl-1,3a,4,8b-tetrahydroindeno[1,2-b]pyrrol-2(3H)-one (36):



The title compound was synthesized by following the typical procedure for synthesis of compound **15**; Colorless solid (80%); mp: 168 °C $R_f = 0.25$ (3:7 EtOAc: Hex); IR (cm^{-1}): 3434, 3085, 2975, 2864, 1718, 1628, 1576; ^1H NMR (400 MHz, CDCl_3) δ 7.40-7.33 (m, 2H), 7.26-7.20 (m, 3H), 6.46 (q, $J = 8.2$ Hz, 2H), 5.30 (d, $J = 6.3$ Hz, 1H), 4.73 (d, $J = 8.3$ Hz, 1H), 3.70

(s, 3H), 3.59-3.50 (m, 1H), 3.30 (s, 1H), 3.24-3.03 (m, 2H); ^{13}C NMR (100 MHz, CDCl_3) δ 173.3, 146.5, 144.7, 141.2, 136.6, 136.0, 132.8, 128.8 (2C), 126.7, 125.4 (2C), 118.7, 109.9, 71.0, 65.6, 55.1, 42.6, 28.3, 26.0; Mass (ES): m/z 312.18 (M+H, 100%).

5.5.3 X-ray crystallographic studies

Crystal data for 16a: $\text{C}_{23}\text{H}_{31}\text{NO}_3\text{Si}$, $M = 397.58$, colorless block, $0.15 \times 0.08 \times 0.05 \text{ mm}^3$, monoclinic, space group $P2_1/c$ (No. 14), $a = 12.368(12)$, $b = 13.474(14)$, $c = 13.097(13) \text{ \AA}$, $\beta = 102.866(17)^\circ$, $V = 2128(4) \text{ \AA}^3$, $Z = 4$, $D_c = 1.241 \text{ g/cm}^3$, $F_{000} = 856$, CCD Area Detector, MoK α radiation, $\gamma = 0.71073 \text{ \AA}$, $T = 294(2)\text{K}$, $2\theta_{\text{max}} = 50.0^\circ$, 19940 reflections collected, 3744 unique ($R_{\text{int}} = 0.0237$). Final $\text{Goof} = 1.033$, $RI = 0.0506$, $wR2 = 0.1381$, R indices based on 3243 reflections with $I > 2\sigma(I)$ (refinement on F^2), 259 parameters, 0 restraints, $\mu = 0.134 \text{ mm}^{-1}$. **CCDC 909838** contains the supplementary crystallographic data for this paper. These data can be obtained free of charge at www.ccdc.cam.ac.uk/conts/retrieving.html [or from the Cambridge Crystallographic Data Centre (CCDC), 12 Union Road, Cambridge CB2 1EZ, UK; fax: +44(0) 1223 336 033; email: deposit@ccdc.cam.ac.uk].

5.5.4 Pharmacology methods

Materials and Methods:

Wild type Zebrafish (*Danio rerio*) were maintained as per the procedure mentioned in Zebrafish Book.²⁵ The studies on anxiety assessment using the light/dark box paradigm were conducted based on a published protocol.²¹ Drug administration was carried out by a procedure reported earlier.²⁶ Clonidine, an anxiolytic agent was used as a positive control to ascertain the validity of the experiments.

5.5.5 Molecular docking studies:

Till date, the complete crystal structure of the transient receptor potential vanilloid subtype 1 (TRPV1) is not reported. However, many homology modeling studies were performed to explore the three dimensional structure of TRPV1.^{24, 27} As reported earlier by Autiero *et al.*, the modeling of transmembrane regions (that accommodates capsaicin binding site) of rat TRPV1 (rTRPV1) was performed using MODELLER programme.^{28, 29} This model was used to perform molecular docking studies of the synthesised molecules by using Surflex-dock module implemented in the Sybyl program.³⁰

5.5.5.1 Homology modeling of catalytic site of rat TRPV1 receptor: The homology modeling of catalytic site of rTRPV1 was performed as discussed earlier.²⁷ The amino acid sequence of rTRPV1 (Uniprot ID: O35433) was obtained from Uniprot protein knowledgebase. The sequence corresponding to the six transmembrane regions (431-690) were considered and a three dimensional model was developed based on the procedure reported previously.²⁷ As TRPV1 belongs to class of voltage gated ion channels, the sequence similarity of its transmembrane regions is compared with the other ion gated channels under the same class. With the criteria of the presence of crystallized structure voltage-dependent shaker family K⁺ channel (PDB ID: 2R9R) was chosen as a template.³¹ The sequences are aligned by CLUSTALW2 algorithm as specified in the reference article (Figure 16). MODELLER version 9.11^{28, 29} was used to build homology models based on specified sequence alignment and template.

Homology modeling studies: The homology model of rTRPV1 containing all the six transmembrane regions was developed by employing the procedure as reported earlier by Lee et al.²⁷ The sequence alignment of rTRPV1 with 2R9R was copied as represented in figure 1. and 10 models of the rTRPV1 were developed using MODELLER 9v11.^{28, 29} The best model with lowest PDF score was selected for further optimization and validation studies. The stereochemical quality of the final model was assessed by PDBsum, a web based tool for Procheck.³² The homology model shows 85% residues are in most favoured region which could be taken as a parameter to perform further docking studies (Figure 17).

_aln.pos	10	20	30	40	50	60
2R9R B	SSGPARIIAIVSVMVILISIVSFC	--LETLPIFRDENE	MHGGGVTFHTYSQSTIGYQQS			
035433	KRIFYFNFFVYCLYMIIFTAAAYR	PVEGLPPYKLN	-----	TVG	---	
_consvrd		*	**	*		**
_aln.p	70	80	90	100	110	120
2R9R B	TSFTDPFFIVETLCIIWFSFEFLV	RFFACPSKAGFF	--TN	IMNIIDIVAIIPYYVTIFL		
035433	DYFR-VTGEILSVSGGVYFFFRGI	QYFLQRRPSLKSLFVDSYSEIL	FFVQSLFMLVSVVL			
_consvrd	*	*	*	*	*	*
_aln.pos	130	140	150	160	170	180
2R9R B	TESNKSVLQFQNVRRVVQIFRIMRI	-LR-IFKLSRHSKGLQILGQTLK	ASMRELGLLIFF			
035433	YFSQRKE-----YVASMVFLAMG	WTNMLYYTRGFQQMGIYAVMIEK	MILRDLCRFMFVY			
_consvrd		*	*			
_aln.pos	190	200	210	220	230	240
2R9R B	LFIGVILFSSAVYFAEADERDS	----QFP-----SIPD-----	AFWWAVVSMTTVGY			
035433	LVFLFGFSTAVVTLLIEDGKNN	SLPMESTPHKCRGSACKPGNSYN	SLYSTCLELKFFTIGM			
_consvrd	*	*	*	*	*	**
_aln.pos	250	260				
2R9R B	GDMVPTTIGG-KIVGSLCAIAGV	-LTIALPVPVIVSNFNFYFHRET				
035433	GDLEFTENYDFKAVFIILLLAY	VILTYILLNMLIALMGETVNKIA				
_consvrd	**	*	**	*	**	*

Figure 16: Sequence alignment of rat TRPV1 and the voltage dependent shaker family K⁺ channel (PDBID: 2R9R).

The final monomer model was duplicated in to four entries and superimposed with the reported tetramer model.²⁴ The generated tetramer model was energy minimized with the gradient convergence of 0.05 K. cal. To check the clashes from atom contacts, the quality of tetramer structure was evaluated through MolProbity.³³ Molprobity evaluates the stereochemical quality of the model and provides a clash score from the all atom (including Hydrogen) contact analysis. The final model has a very least clash score of 1.49 and occupies 99th percentile for PDB structures with same resolution. Molprobity also determines backbone bonds and angles, for which our tetramer model has none of them. The molprobity results are detailed in **Table 3**.

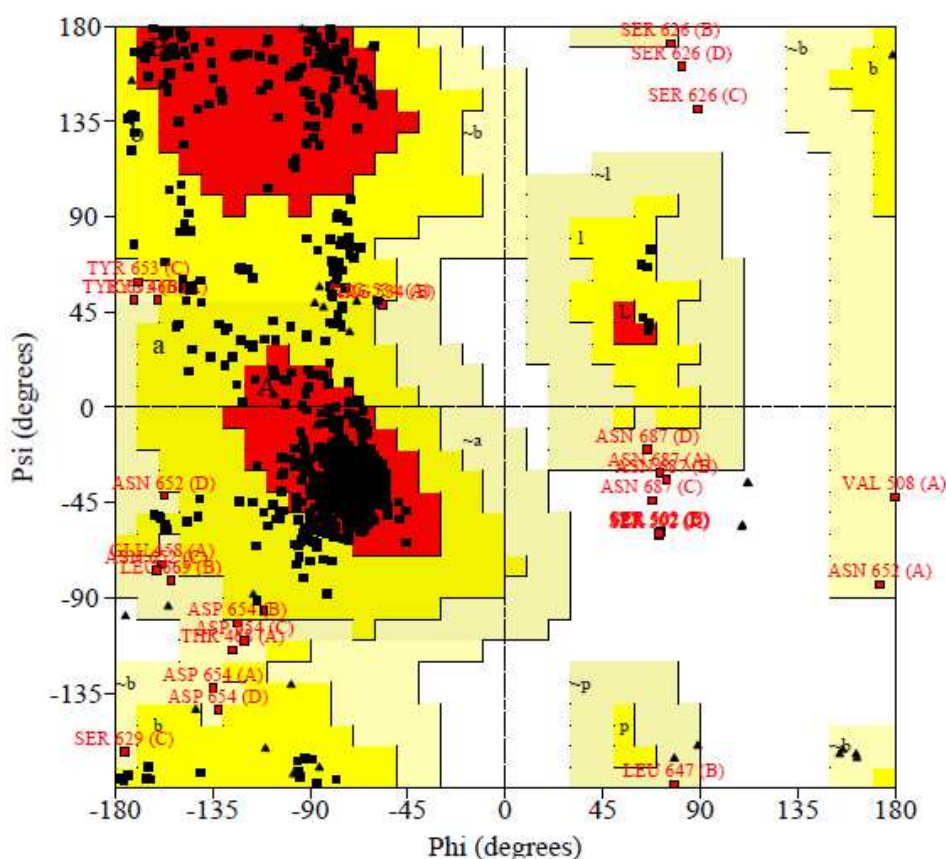


Figure 17. Ramachandran plot of the ϕ - ψ distribution of rTRPV1 produced by PROCHECK after homology modeling. Red [A, B, L] most favored regions; Dark yellow [a, b, l, p] additional allowed regions; Light yellow [\sim a, \sim b, \sim l, \sim p] generously allowed regions; white areas are disallowed regions.

Table 3: Molprobity results of the rTRPV1 homology model

Model	Favored ^a	Outliers ^b	C β -dev. ^c	Bond length ^d	Bond angle ^e	Clash-score ^f	Percentile ^g
rTRPV1	85.6	1.07	10	0	0	1.5	99

^a percentage of residues in favourable region of Ramachandran plot

^b percentage of residues in disallowed region of Ramachandran plot.

^c Number of residues with C β deviation ≥ 0.25 Å

^d Percentage of backbone bond lengths >4 standard deviations from the accepted values

^e Percentage of backbone bond angles >4 standard deviations from the accepted value

^f Number of atomic clashes per 1000 atoms.

^g Percentile rank compared to structures in the PDB within a similar resolution range

5.5.5.2 Docking Procedure:

The docking analysis of molecules was performed using Sybyl, version 1.3 implemented from Tripos package. Synthesized compounds were sketched in 3D format using build module and minimized with gradient convergence of 0.001 K. cal. The protomol (grid) for molecular docking was generated from the centroid of aminoacids accomodating vanilloid (capsaicin) binding site. Molecules were docked using Surflex-dock module.³⁰ The ligands were kept flexible by producing the ring conformations and by penalizing non-polar amide bond conformations, whereas the receptor was kept rigid throughout the docking studies. The most stable pose was selected and the ligand interactions with target protein were determined.

Based on the mutational studies at the vanilloid binding site- LEU515, THR550, SER512, TYR511, MET547, PHE543 and LYS571 are reported as key amino acid residues.²⁷ From the centroid of these aminoacids to 10 angstroms surrounding was considered as a grid for docking studies. To understand the binding mode of the compounds synthesized, molecular docking studies were performed using Surflex-Dock (SFXC) programme of Sybyl software. The docking results for capsaicin were in close relevance with the earlier reported docking studies. As reported earlier the vanillyl moiety of capsaicin occupied the deep pocket surrounded by Tyr511, Tyr565, and Lys571.²⁷ The hydrophobic tail region occupied the upper hydrophobic pocket formed at the interface of two monomers **Figure 3**. Using the above docking parameters we performed a docking study of synthesized compounds **23**, **24** and **35**.

5.6 References:

1. (a) Gunthorpe, M. J.; Benham, C. D.; Randall, A.; Davis, J. B. *Trends Pharmacol Sci*, **2002**, *23*, 183. (b) Birnbaumer, L.; Yidirim, E.; Abramowitz, J. *Cell Calcium*, **2003**, *33*, 419.
2. Kress, M.; Zeihofer, H. U. *Trends Pharmacol Sci*, **1999**, *20*, 112.
3. Di Marzo, V.; Blumberg, P. M.; Szallasi, A. *Curr Opin Neurobiol*. **2002**, *12*, 372.
4. Geppetti, P.; Trevisani, M.; *Br J Pharmacol*. **2004**, *141*, 1313.
5. Caterina, M. J.; Julius, D. *Annu Rev Neurosci*. **2001**, *24*, 487.
6. Hudson, L. J.; Bevan, S.; Wotherspoon, G.; Gentry, C.; Fox, A.; Winter, J.; *Eur J Neurosci*. **2001**, *13*, 2105.
7. Ji R. R, Samad, T. A.; Jin, S. X.; Schmoll, R.; Woolf, C. J. *Neuron*. **2002**, *36*, 57.
8. Pal, M.; Angaru, S.; Kodimuthali, A.; Dhingra, N. *Current Pharmaceutical Design*. **2009**, *15*, 1008.
9. Davis, J. B.; Gray, J.; Gunthorpe, M. J.; Hatcher, J. P.; Davey, P. T.; Over-end, P, et al. *Nature*. **2000**, *405*, 183.
10. Caterina, M. J.; Leffler, A.; Malmberg, A. B.; Martin, W. J.; Trafton, J.; Petersen-Zeitz, K. R, et al. *Science*. **2000**, *288*, 306.
11. (a) Szallasi, A.; Appendino, G. *J Med Chem*. **2004**, *47*, 2717. (b) Rami, H. K.; Gunthorpe, M. J.; **2004**, *1*, 97. (c) Appendino, G.; Szallasi, A. *Med Chem*. **2006**, *44*, 145. (d) Szallasi, A.; Cortright, D. N.; Blum, C. A.; Eid, S. R. *Nat Rev Drug Discov*. **2007**, *6*, 357. (e) Westaway, S. M. *J Med Chem* . **2007**, *50*, 2589.
12. (a) Damien Bonne, Lydie Salat, Jean-Pierre Dulcère, and Jean Rodriguez. *Organic Letters*. **2008**, *10*, 5409-5412. (b) Peng, J.; Jiang, D.; Lin, W.; Chen, Y. *Org. Biomol. Chem*. **2007**, *5*, 1391–1396. (c) Hay, M. B.; Wolfe, J. P. *Angew. Chem., Int. Ed*. **2007**, *46*, 6492–6494. (d) Lemen, G. S.; Giampietro, N. C.; Hay, M. B.; Wolfe, J. P. *J. Org. Chem*. **2009**, *74*, 2533. (e) Evans, D. A.; Song, H. J.; Fandrick, K. R. *Org. Lett*. **2006**, *8*, 3351-3354. (f) Tejero, T.; Dondoni, A.; Rojo, I.; Merchana, F. L.; Merino, P. *Tetrahedron* **1997**, *53*, 3301.
13. (a) Kaliappan, K. P.; Das, P.; Kumar, N. *Tetrahedron Lett*. **2005**, *46*, 3037. (b) Frank, E.; Wolfing, J.; Aukszi, B.; König, V.; Schneider, T. R.; Schneider, G. *Tetrahedron*. **2002**, *58*, 6843–6849. (c) Juan, C. P.; Tan, B.; Yang, L.; Zeng, X.; Zhu, D.; Zhong, G. *Chem. Commun*. **2010**, 7611-7613. (d) Bourke, S.; Hcaney, F. *Tetrahedron Lett*. **1995**, *36*, 7527. (e) Gotoh, M.; Sun, B.; Hirayama, K.; Noguchi, M. *Tetrahedron* **1996**, *52*, 887-900. (f)

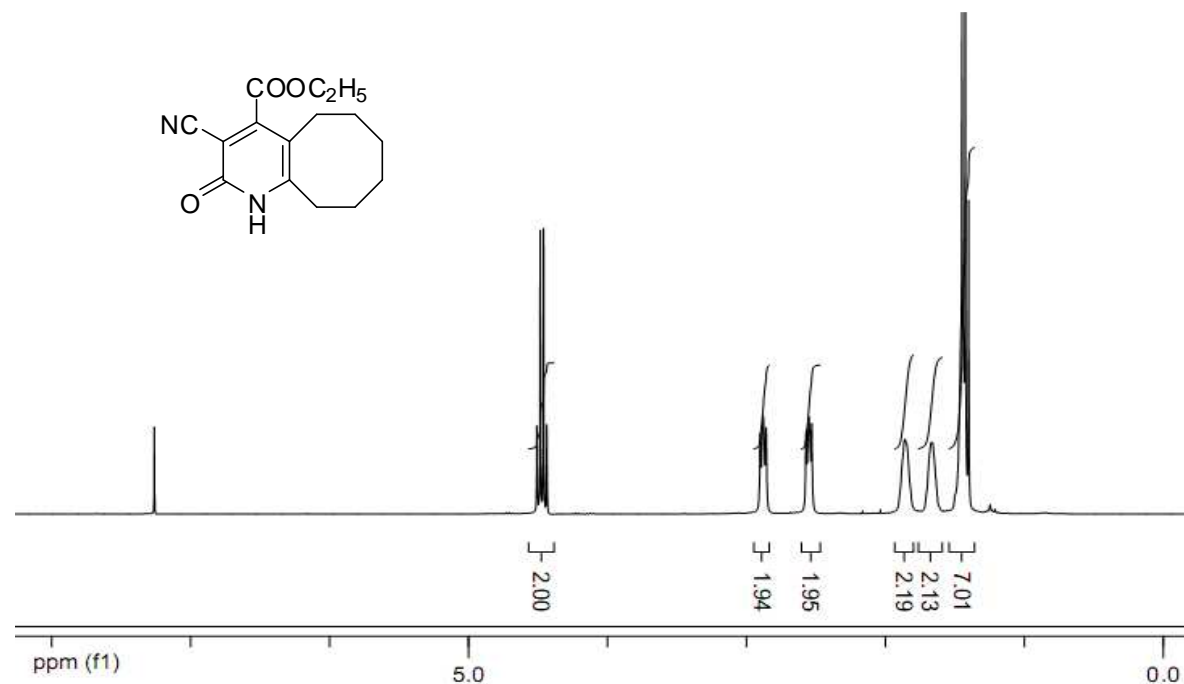
- Heaney, F.; Fenlon, J.; McArdle, P.; Cunningham, D. *Org. Biomol. Chem.*, **2003**, 1122.(g)
- Broggini, G.; Rosa, C. L.; Pilati, T.; Terraneo, A.; Zecchi, G. *Tetrahedron*, **2001**, 57, 8323-8332. (h) Nair, V.; Suja, T. D. *Tetrahedron* **2007**, 63, 12247. (i) Shing, T. K. M.; Zhong, Y, L. *Tetrahedron*, **2001**, 57, 1573.
14. a) V. Jäger, P. A. Colinas in *Synthetic Applications of 1,3-Dipolar Cycloaddition Chemistry Toward Heterocycles and Natural Products*, Wiley, New Jersey, **2003**, p. 416; b) A. A. Akhrem, F. A. Lakhvich, V. A. Khripach, *Chem. Heterocycl. Compd.* **1981**, 17, 853–868; *Khim. Geterotsikl. Soedin.* **1981**, 17, 1155.
15. (a)Curran, D. P.; Scanga, S. A.; Fenk, C. J. *J. Org. Chem.* **1984**, 49, 3474. (b) Gothelf, K.; Thomsen, I.; Torssell, K. B. G. *Acta Chem. Scand.* **1992**, 46, 494. (c) Bode, J. W.; Fraefel, N.; Muri, D.; Carreira, E.M. *Angew. Chem., Int. Ed.* **2001**, 40, 2082. (d) Jiang, D.; Chen, Y. *J. Org. Chem.* **2008**, 73, 9181.
16. Wade, E A.; Bereznak, J. E; Palfey, B. A.; Carroll, P. J.; Dailey, W. E; Sivasubramanian, S. *J. Org. Chem.* **1990**, 55, 3045.
17. (a)Minter, A. R.; Fuller, A. A.;Mapp, A. K. *J. Am. Chem. Soc.* **2003**, 125, 6846. (b) Fuller, A. A.; Chen, B.; Minter, A. R.; Mapp, A. K. *J. Am. Chem. Soc.* **2005**, 127, 5376.
18. (a) Auricchio, S.; Ricca, A. *Tetrahedron* **1987**, 43, 3983. (b) Marotta, E.; Micheloni, L. M.; Scardovi, N.; Righi, P. *Org. Lett.* **2001**, 3, 727. (c) Scott, J. P.; Oliver, S. F.; Brands, K.M. J.; Brewer, S. E.; Davies, A. J.; Gibb, A. D.; Hands, D.; Keen, S. P.; Sheen, F. J.; Reamer, R. A.; Wilson, R. D.; Dolling, U. *J. Org. Chem.* **2006**, 71, 3086. (d) Maimone, T. J.; Shi, J.; Ashida, S.; Baran, P. S. *J. Am. Chem. Soc.* **2009**, 131, 17066.
19. (a) Kumar, K. R. R.; Mallesha, H.; Basappa; Rangappa, K. S. *Eur. J. Med. Chem.* **2003**, 38, 613. (b) Ishiyama, H.; Tsuda, M.; Endo, T.; Kobayashi, J. *Molecules* **2005**, 10, 312. c) Pouilhés, A.; Amado, A. F.; Vidal, A.; Langlois, Y.; Kouklovsky, C. *Org. Biomol. Chem.* **2008**, 6, 1502–1510. (d) Piperno, A.; Chiacchio, U.; Iannazzo, D.; Giofrè, S. V.; Romeo, G.; Romeo, R. *J. Org. Chem.* **2007**, 72, 3958.
20. Huang, K. S.; Wang, E. C. *Tetrahedron Lett.* **2001**, 42, 6155.
21. (a)Beissel, T.; Powers, R. E.; Parac T. N.; Raymond K. N. *J. Am. Chem. Soc.* **1999**, 121, 4200. (b) Sato, M.; Nagano, S.; Seki, T. *Chem. Commun.* **2009**, 3792–3794. (c) Wang, Y.; Guziec Jr., F. S. *J. Org. Chem.* **2001**, 66, 8293-8296.
22. Adam, S.; Caio, M.; Thiago, M.; Manoel, H. A.; Amauri, G.; Silvio, M.; Siddharth, G.; Elegante Marco F., Hart Peter C., Kalueff Allan V. *Neuromethods.* **2011**, 51, 157.
23. Manna, S. S.; Umathe, S. N. *Brain Res.* **2011**, 1425, 75..

24. Brauchi, S.; Orta, G.; Mascayano, C.; Salazar, M.; Raddatz, N.; Urbina, H.; Rosenmann, E.; Gonzalez-Nilo, F.; Latorre, R. *Proc Natl Acad Sci USA*, **2007**, *104*, 10246.
25. Westerfield, M. *The Zebra fish Book. A Guide for the Laboratory Use of Zebrafish (Danio rerio)*. 4th edition. Eugene, OR: University of Oregon Press, 2000.
26. Banote, R. K.; Koutarapu, S.; Chennubhotla, K. S.; Chatti, K.; Kulkarni, P. *Epilepsy Behav.* **2013**, *27*, 212
27. Lee, J. H.; Lee, Y.; Ryu, H.; Kang, D. W.; Lee, J.; Lazar, J.; Pearce, L. V.; Pavlyukovets, V. A.; Blumberg, P. M.; Choi, S. *J Comput Aided Mol Des.* **2011**, *25*, 317.
28. Eswar, N.; Marti-Renom, M. A.; Webb, B.; Madhusudhan, M. S.; Eramian, D.; Shen, M.; Pieper, U.; Sali, A. *Comparative Protein Structure Modeling With MODELLER*. *Current Protocols in Bioinformatics*, John Wiley & Sons, Inc., Supplement 15, 5.6.1-5.6.30, 2006
29. Sali, A.; Blundell, T. L. *J. Mol. Biol.* **1993**, *234*, 779.
30. Jain, A. N. *J. Med. Chem.* **2003**, *46*, 499.
31. Long, S. B.; Tao, X.; Campbell, E. B.; MacKinnon, R. *Nature*, **2007**, *450*, 376.
32. Procheck Server. <http://www.ebi.ac.uk/thornton-srv/databases/pdbsum/Generate.html>
33. Chen, V. B.; Arendall, W.B.; Headd, J. J.; Keedy, D. A.; Immormino, R. M.; Kapral, G. J.; Murray, L. W.; Richardson, J. S.; Richardson, D. C. *Acta Crystallogr. D: Biol. Crystallogr.* **2010**, *66*, 12.

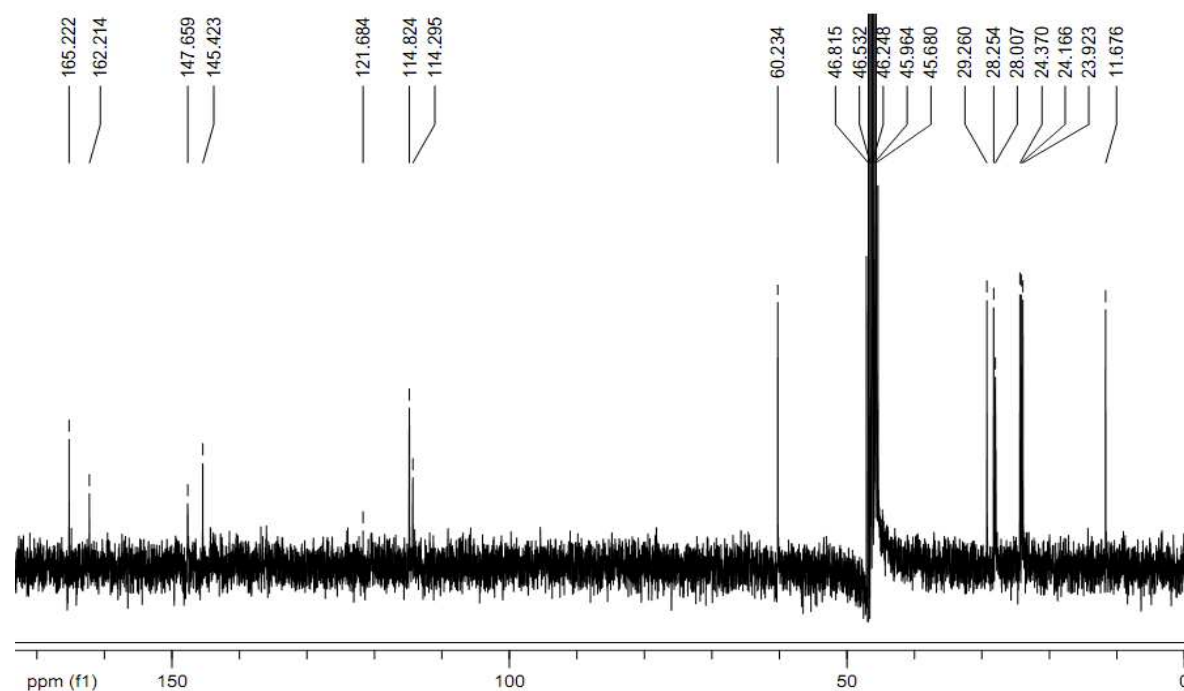
2. Design, synthesis & pharmacological evolution of dehydro shikimate analogues as potential antitubercular agents

^1H & ^{13}C NMR of Selected Compounds:

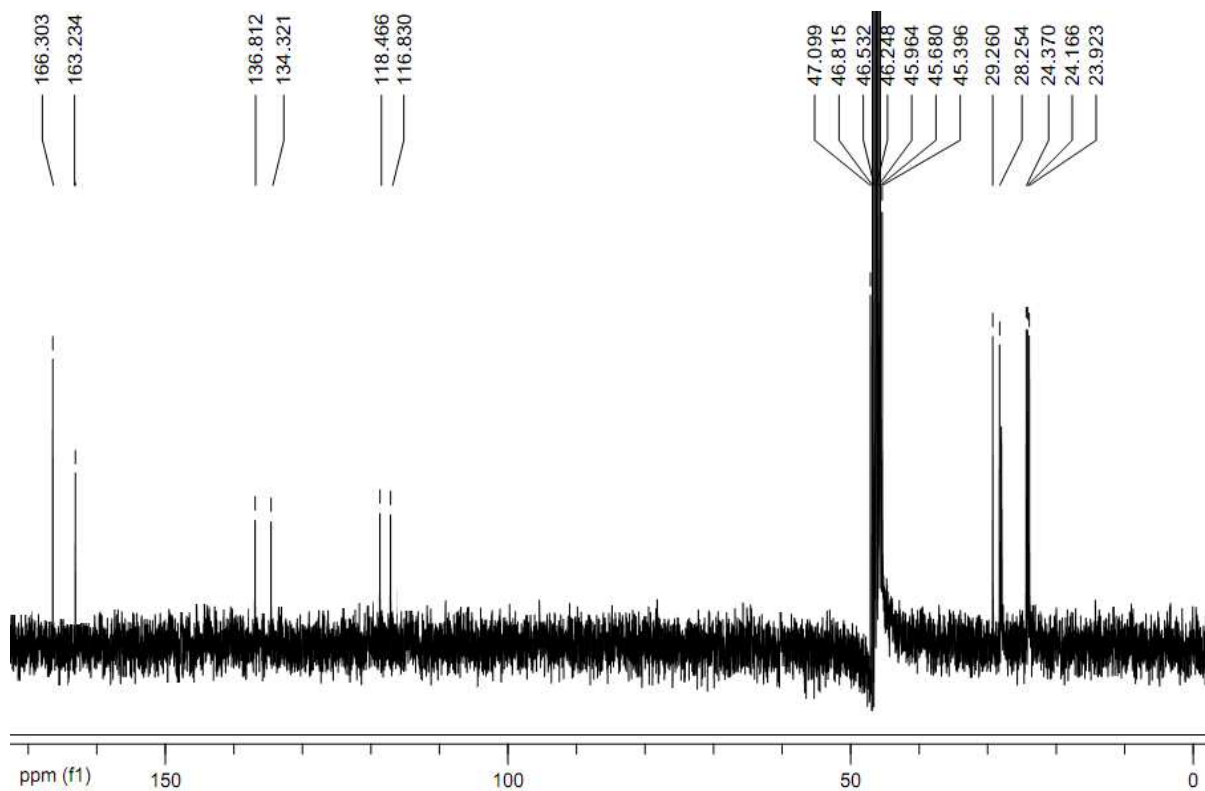
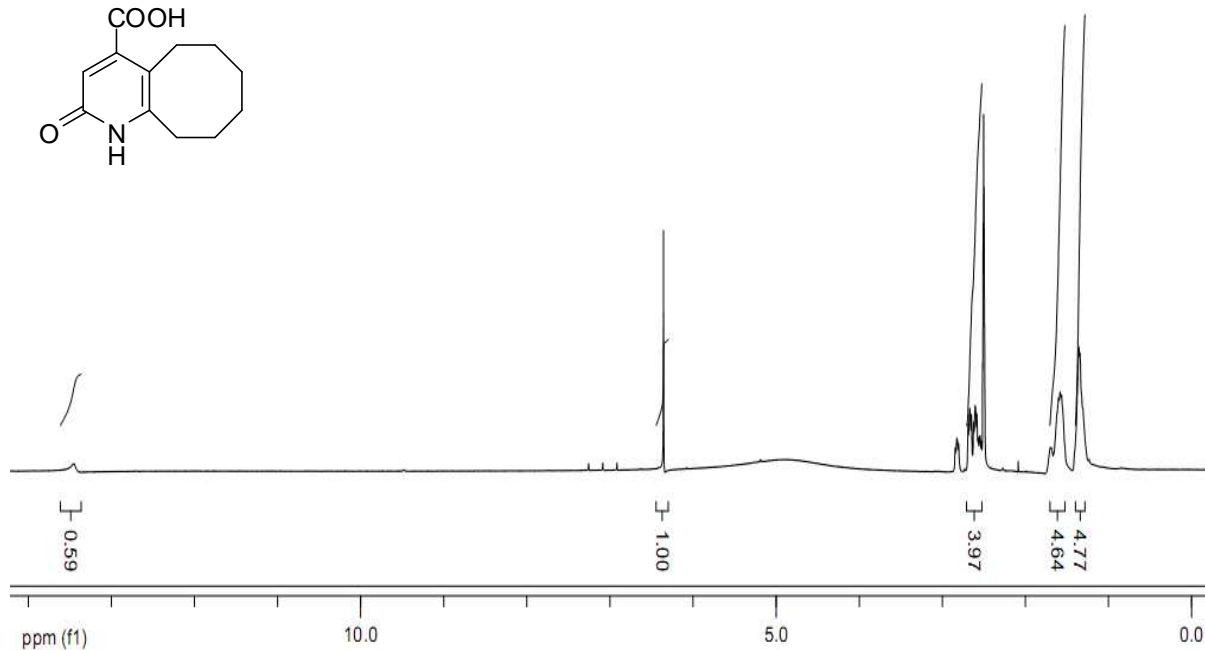
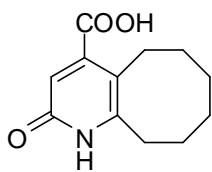
Ethyl -3-cyano-2-oxo-1,2,5,6,7,8,9,10-octahydrocycloocta[b]pyridine-4-carboxylate (11d):

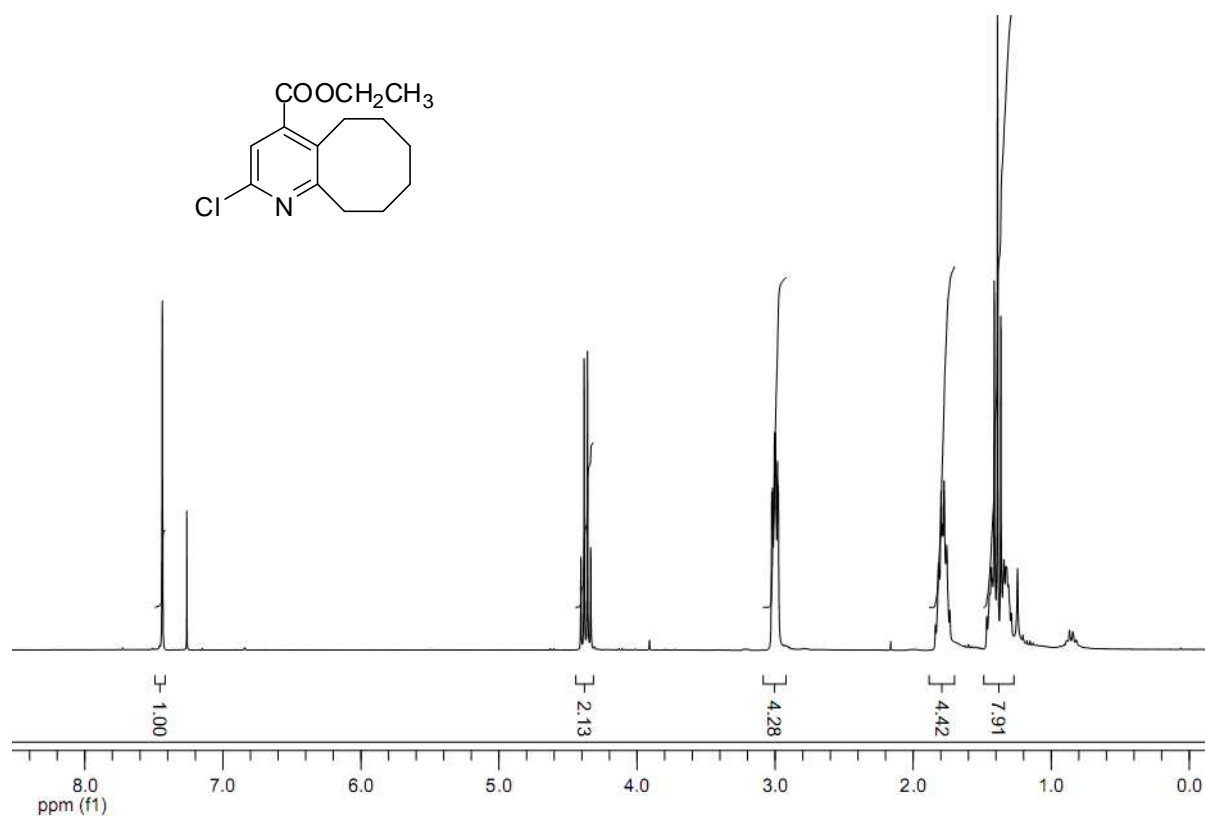
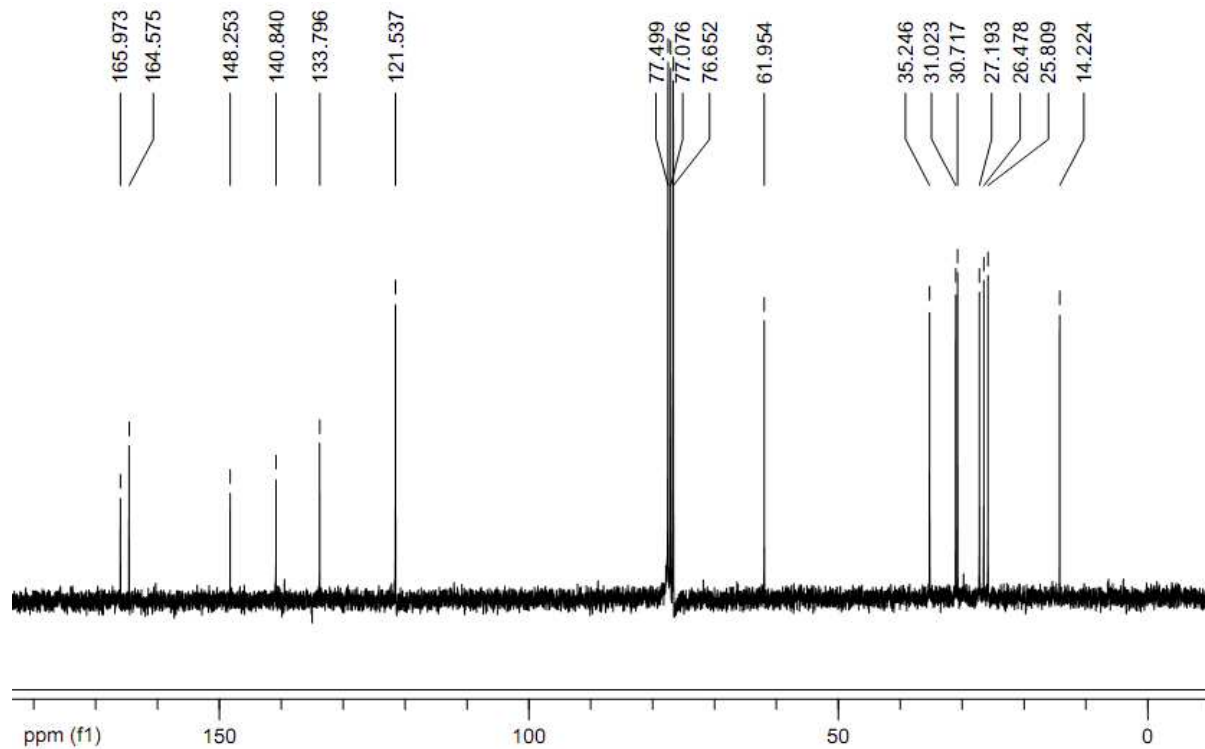


^1H NMR (300 MHz, CDCl₃)

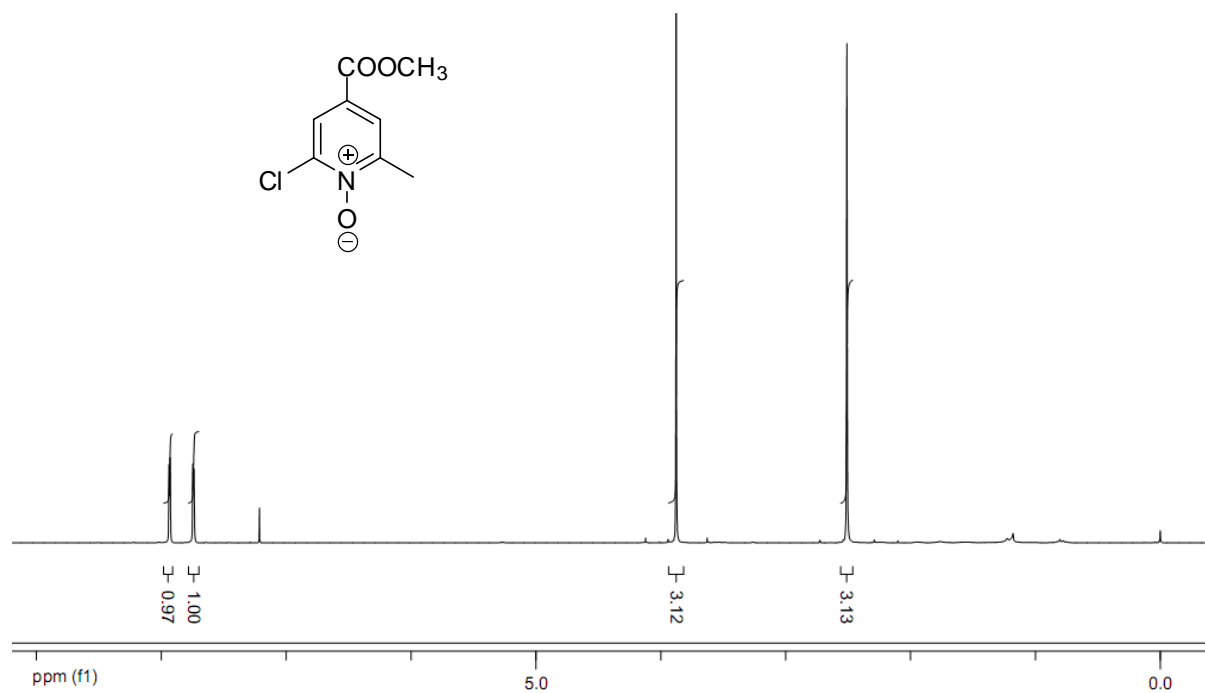
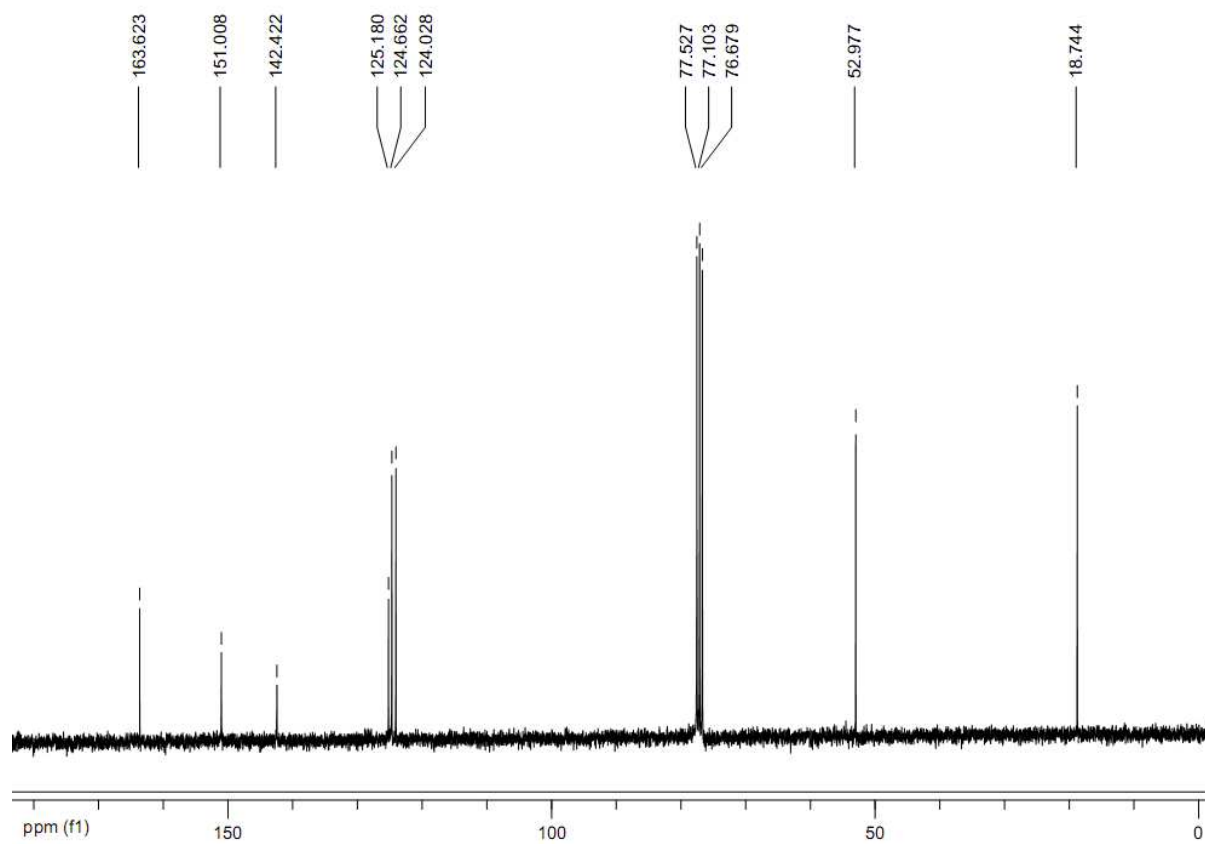


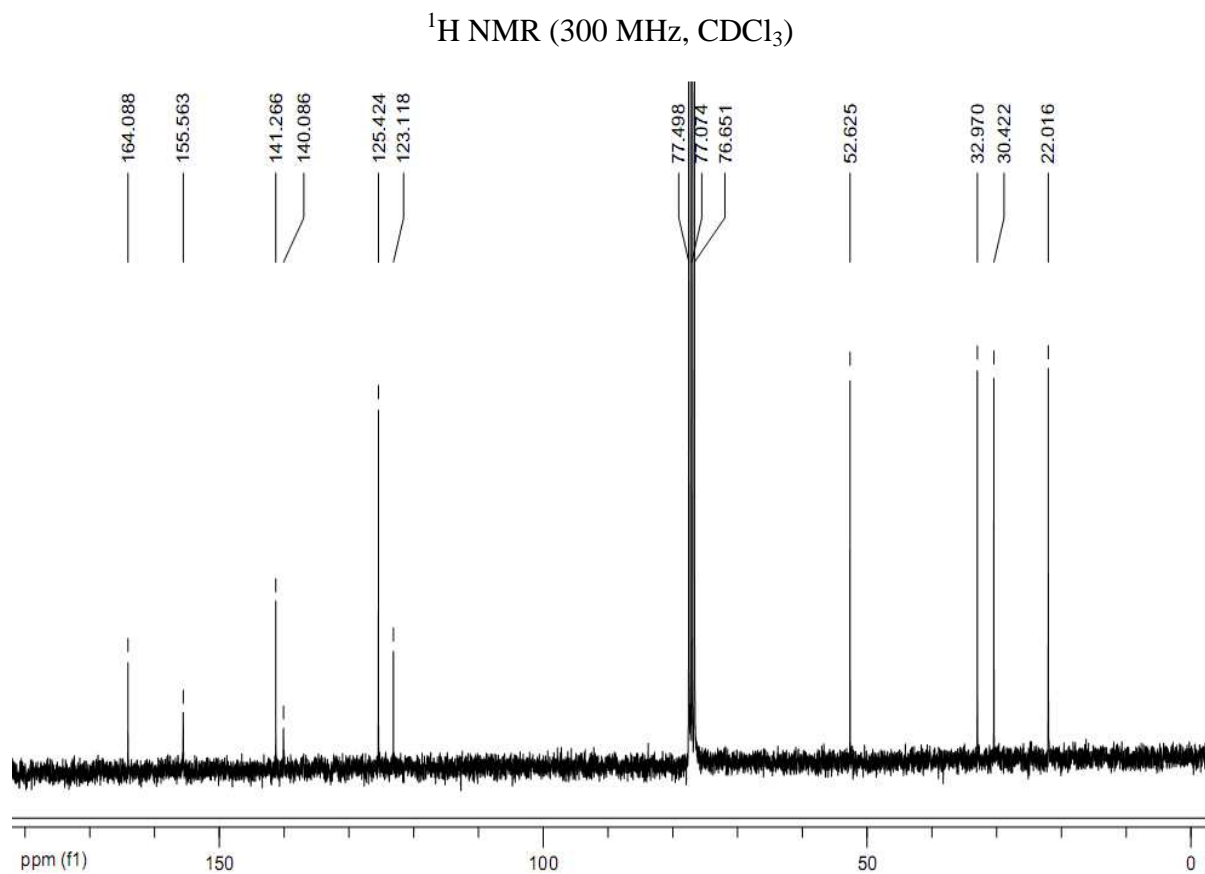
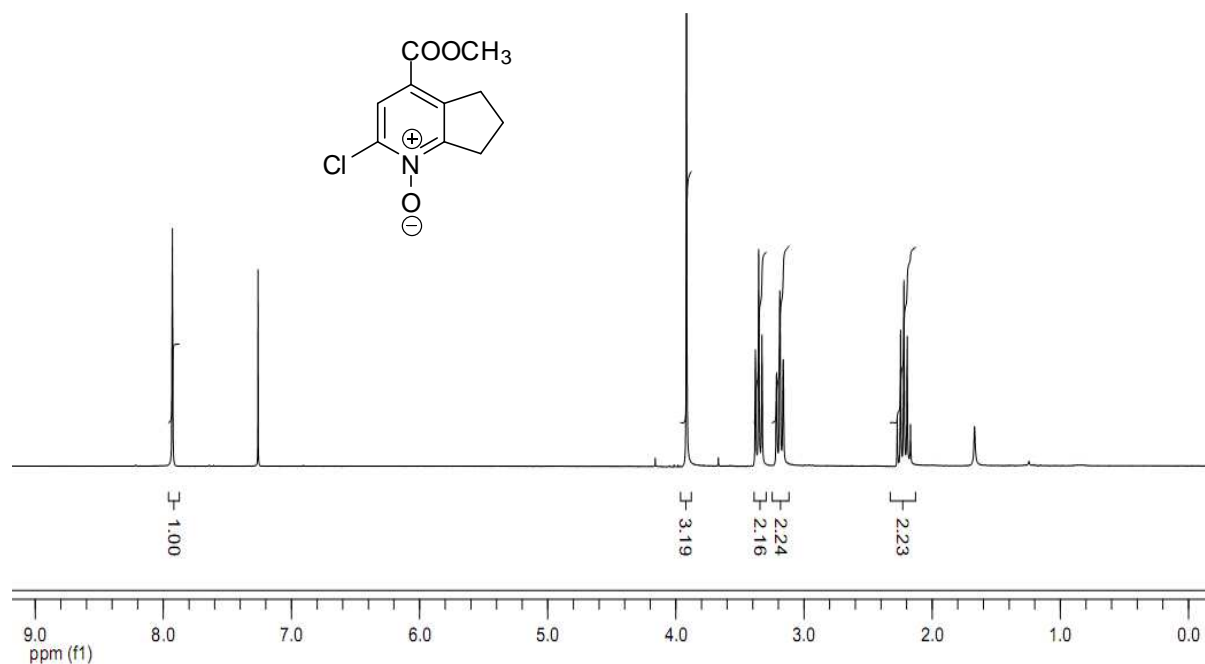
^{13}C NMR (75 MHz, CD₃OD)

2-Oxo-1,2,5,6,7,8,9,10-octahydrocycloocta[*b*]pyridine-4-carboxylic acid (12d):

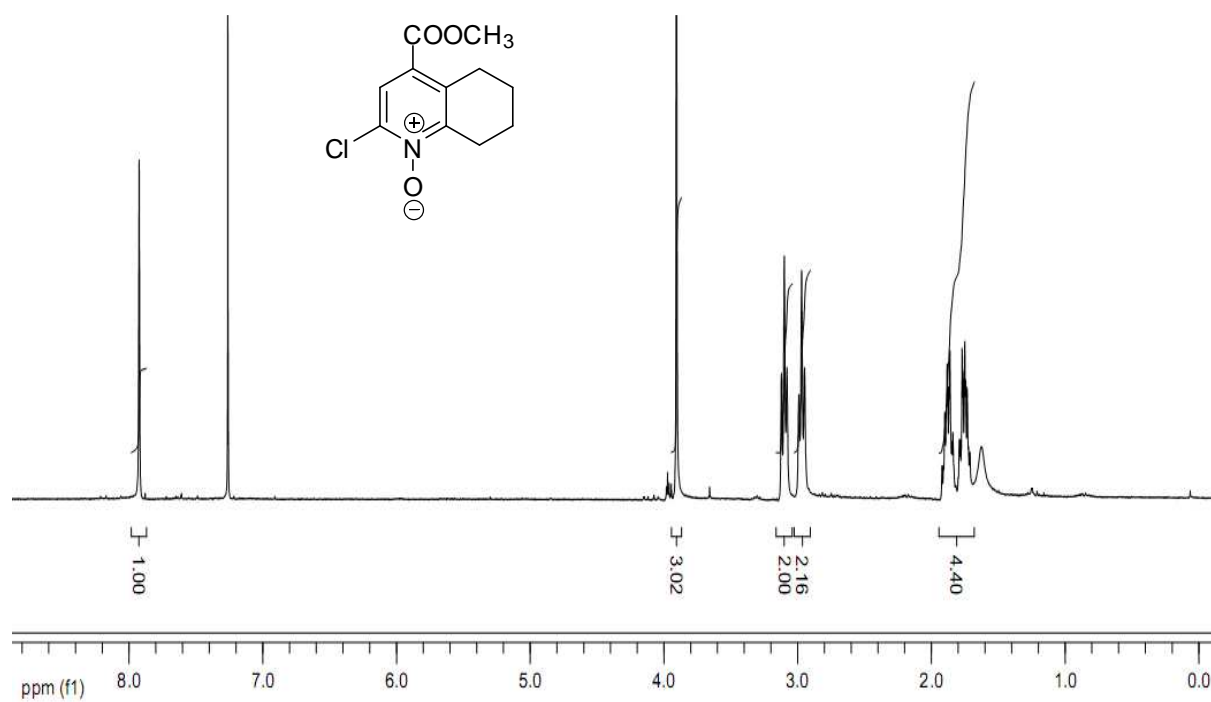
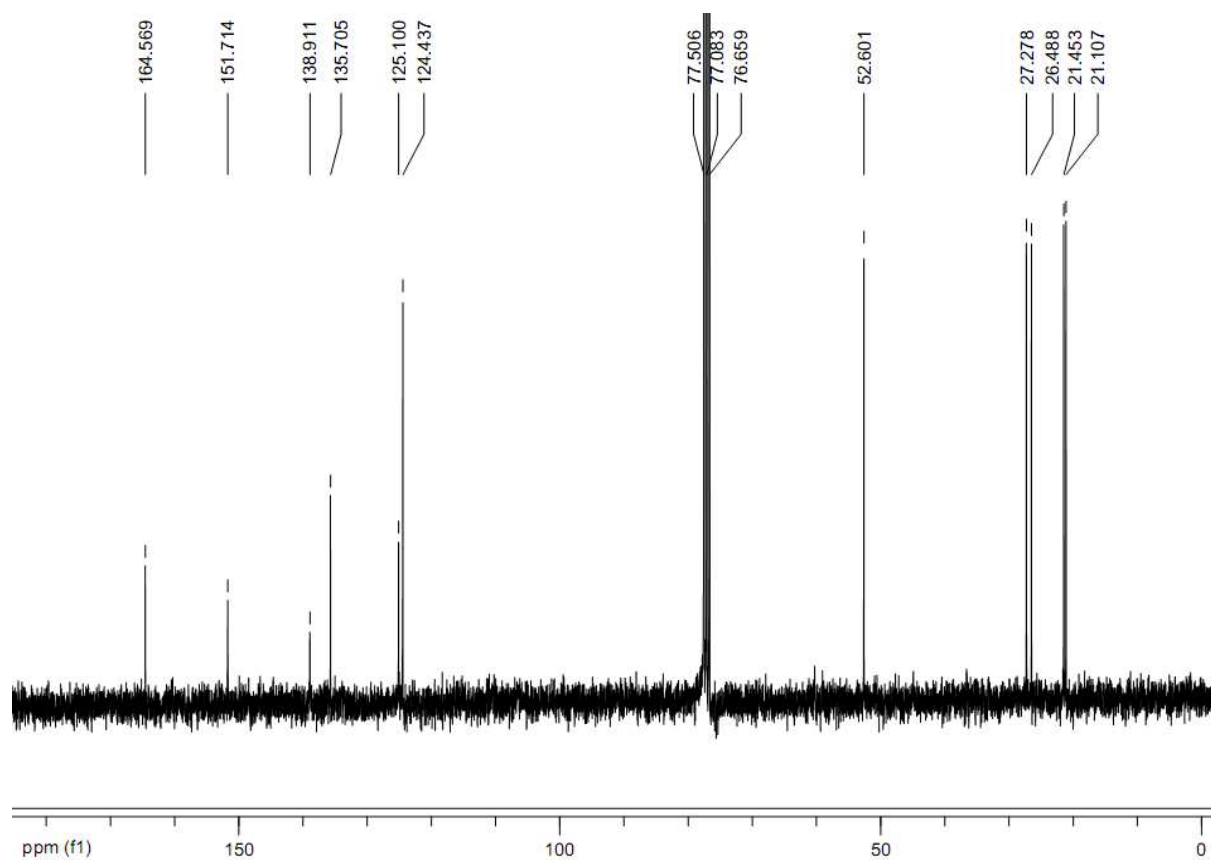
Methyl 2-chloro-5,6,7,8,9,10-hexahydrocycloocta[*b*]pyridine-4-carboxylate (13d): ^1H NMR (300 MHz, CDCl_3) ^{13}C NMR (75 MHz, CDCl_3)

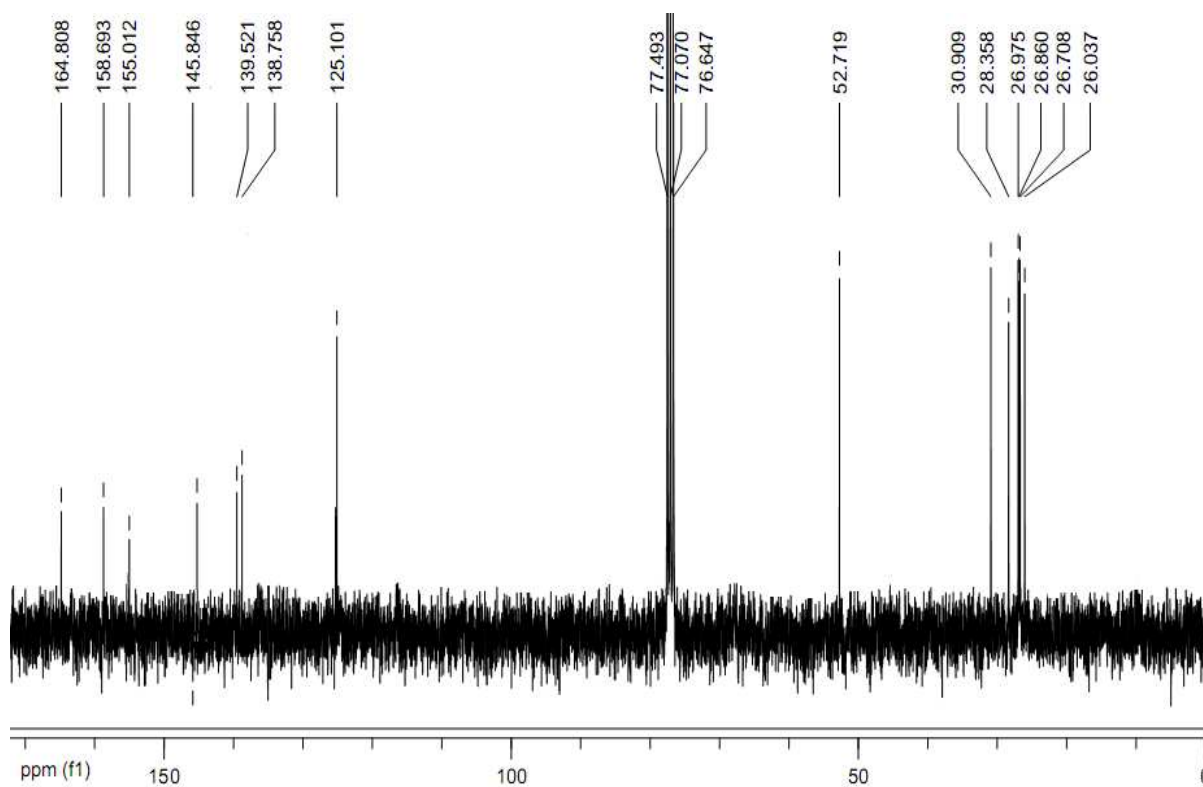
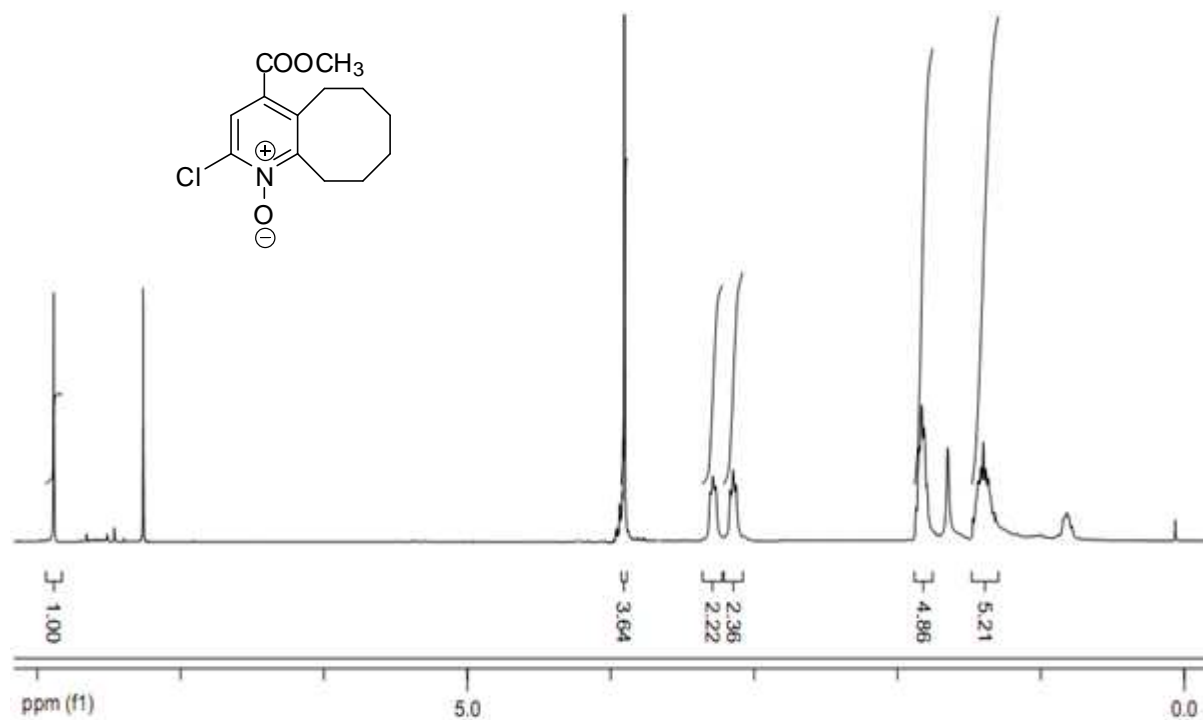
2-Chloro-4 (methoxycarbonyl)-6-methylpyridine-1-oxides (14a):

 ^1H NMR (300 MHz, CDCl_3) ^{13}C NMR (75 MHz, CDCl_3)

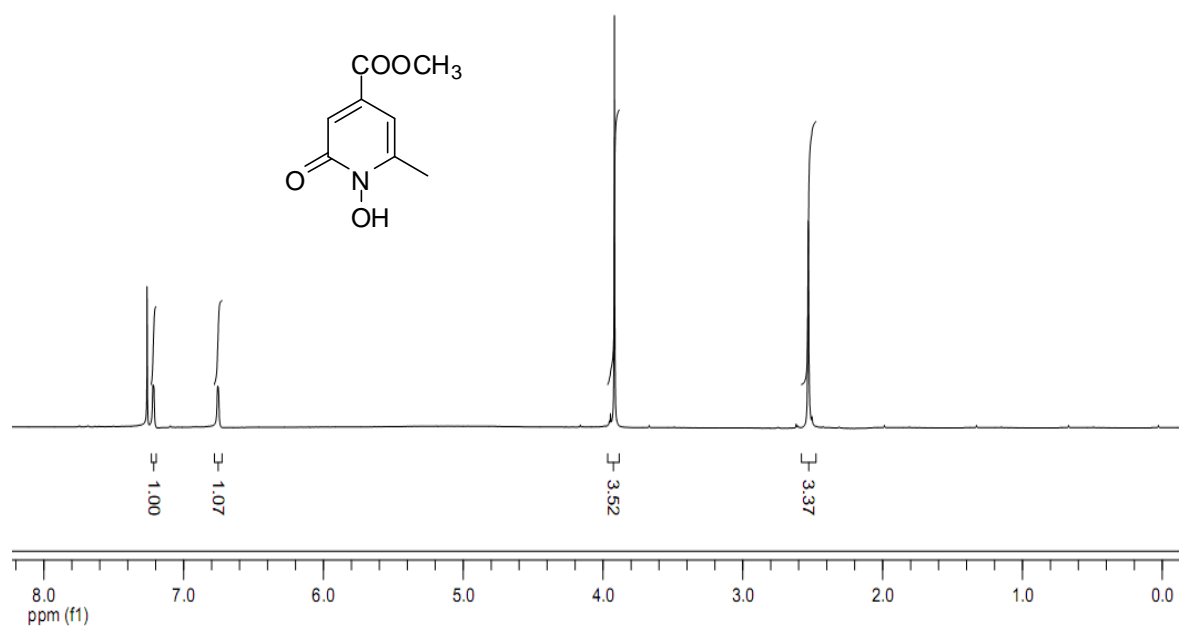
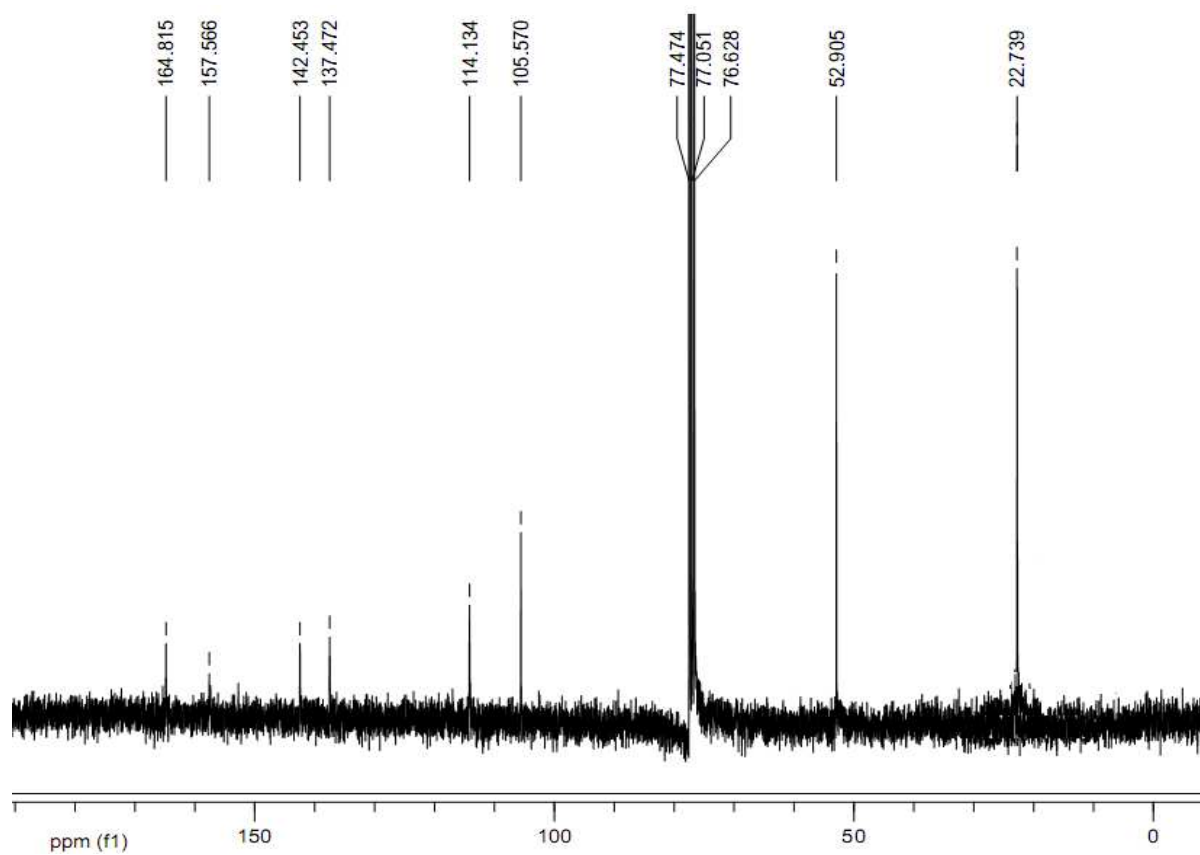
2-Chloro-4-(methoxycarbonyl)-6,7-dihydro-5H-cyclopenta[*b*]pyridine1-oxide(14b):

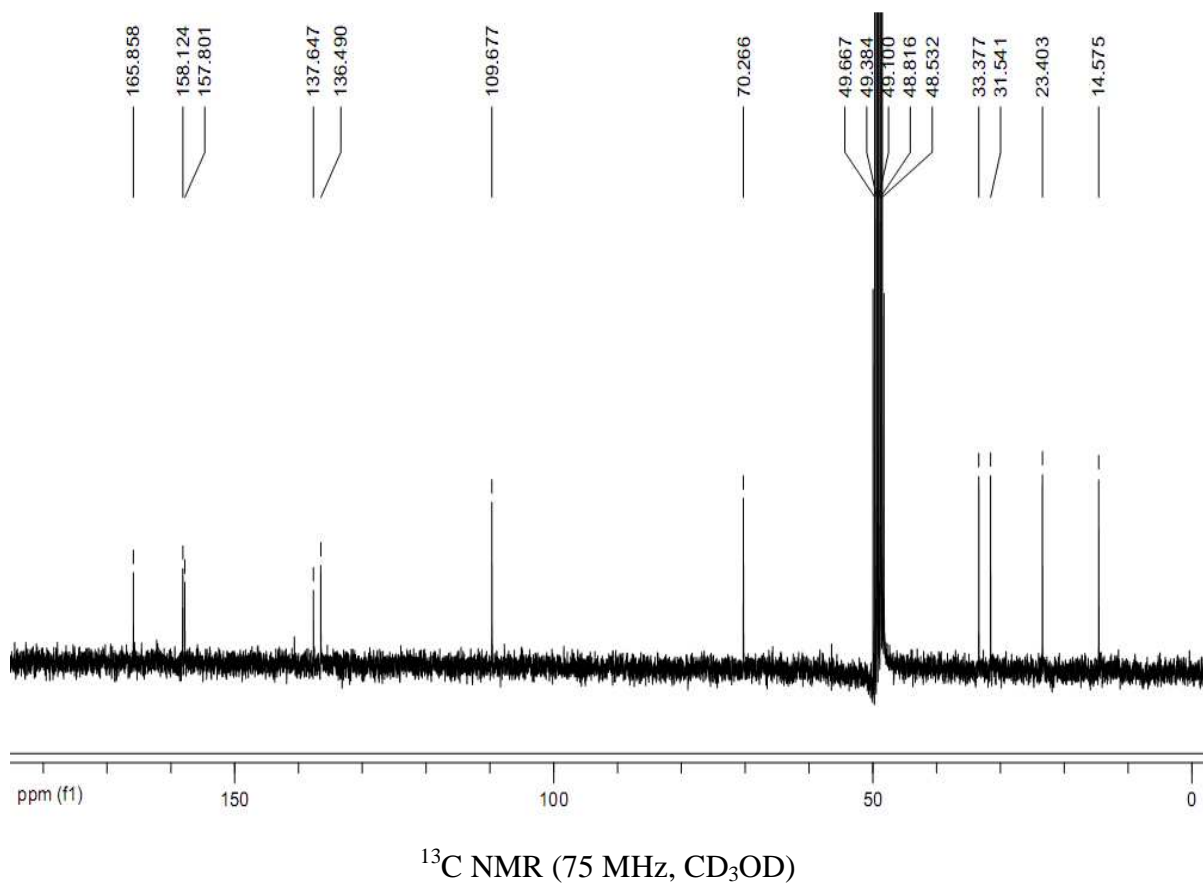
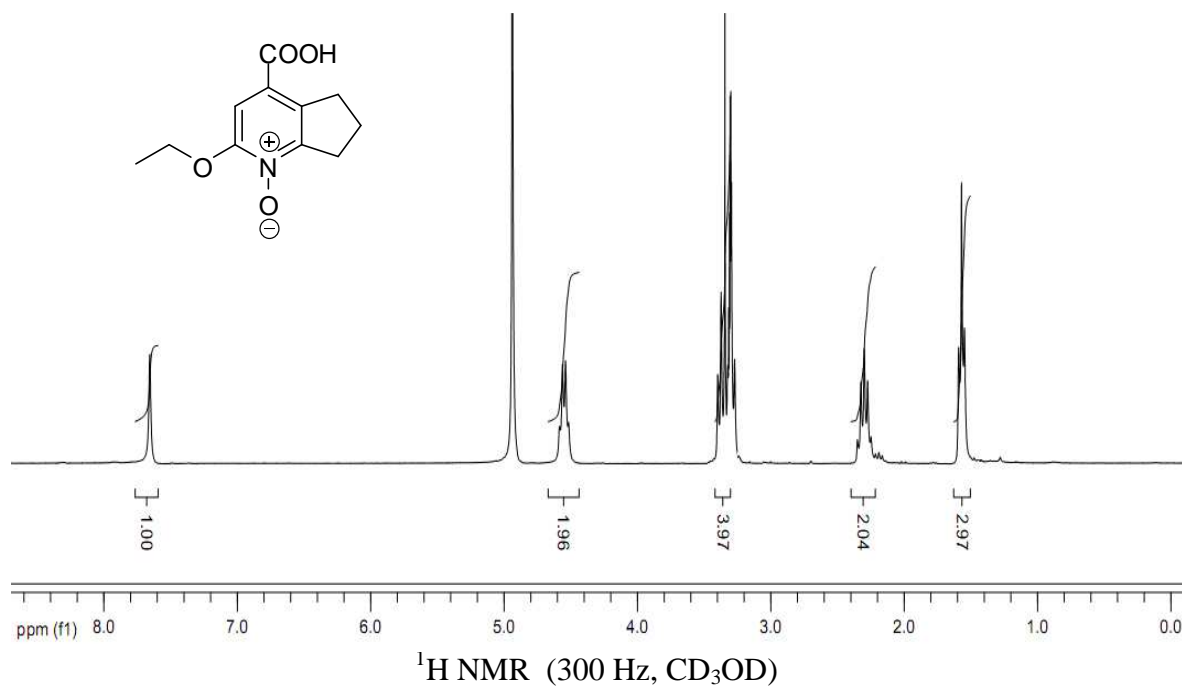
2-Chloro-4-(methoxycarbonyl)-5,6,7,8-tetrahydroquinoline-1-oxide (14c):

 ^1H NMR (300 MHz, CDCl_3) ^{13}C NMR (75 MHz, CDCl_3)

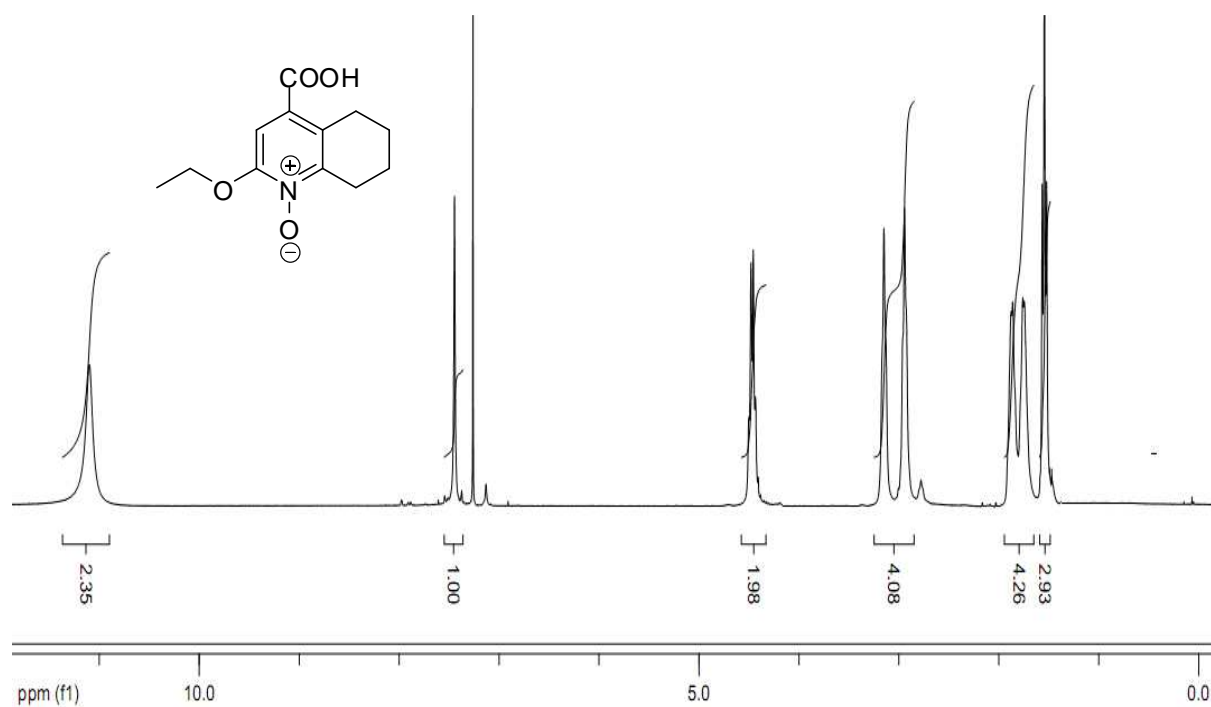
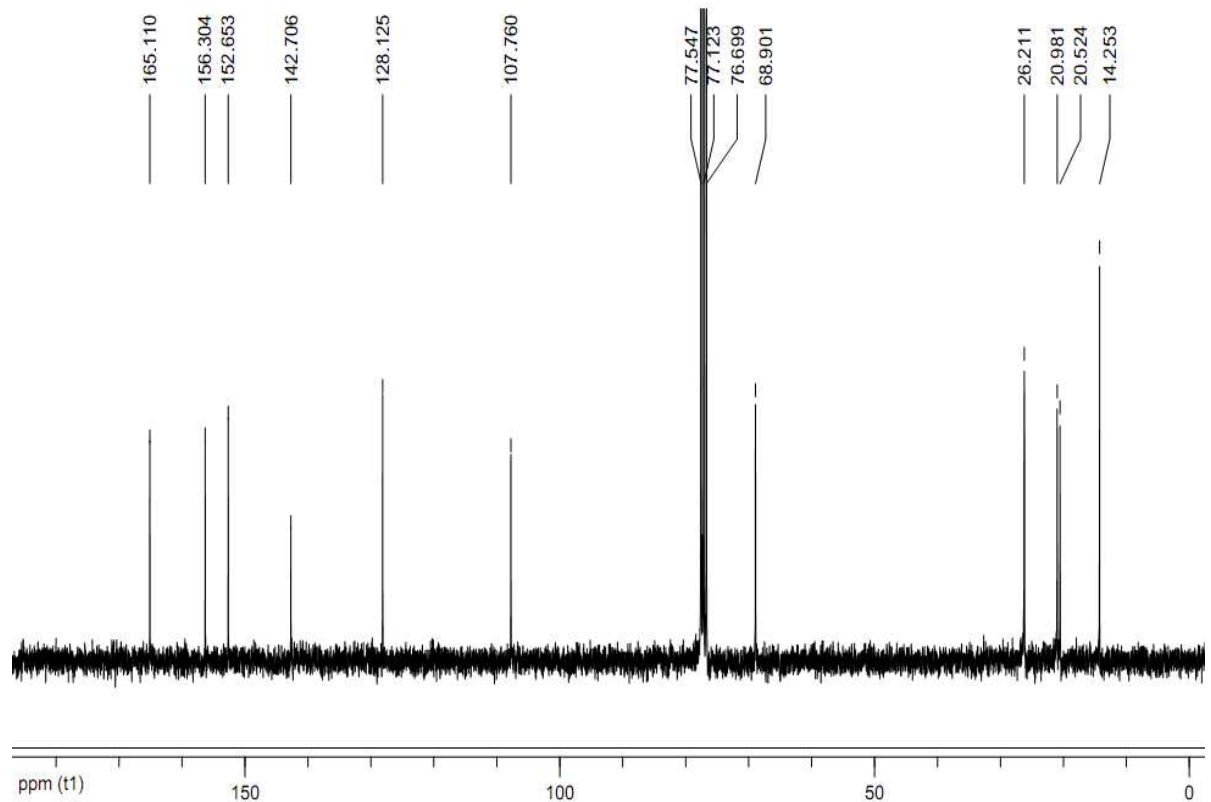
2-Chloro-4-(methoxycarbonyl)-5,6,7,8,9,10-hexahydrocycloocta[b]pyridine1-oxide (14d):

Methyl-1-hydroxy-6-methyl-2-oxo-1,2-dihydropyridine-4-carboxylate (15a):

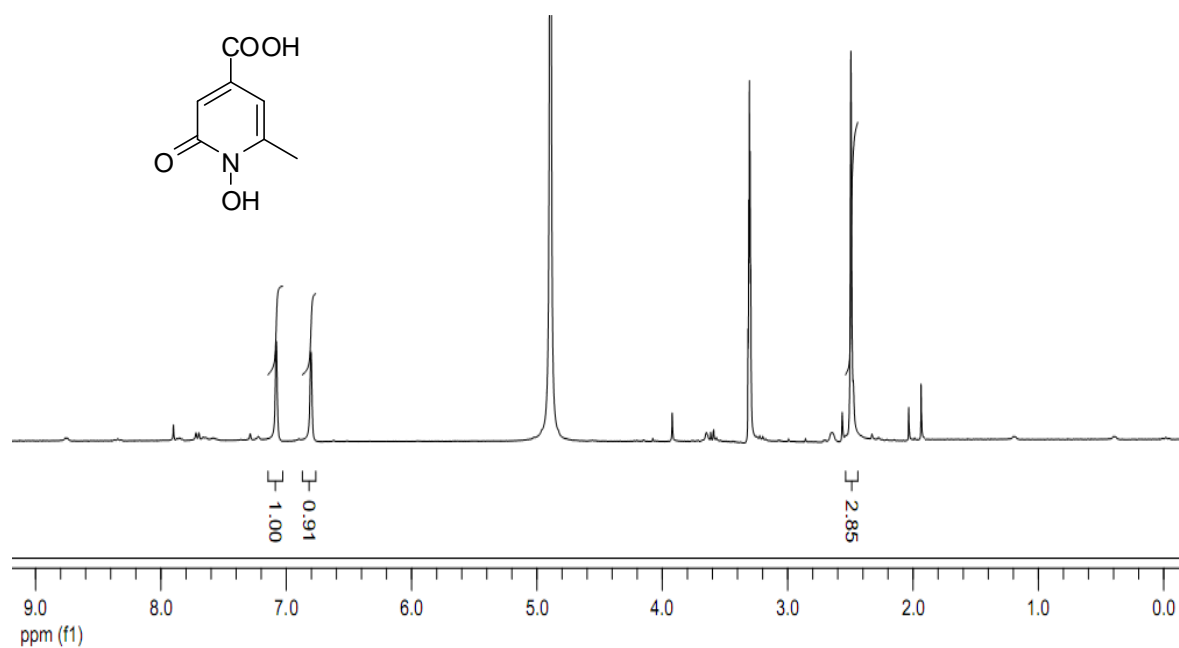
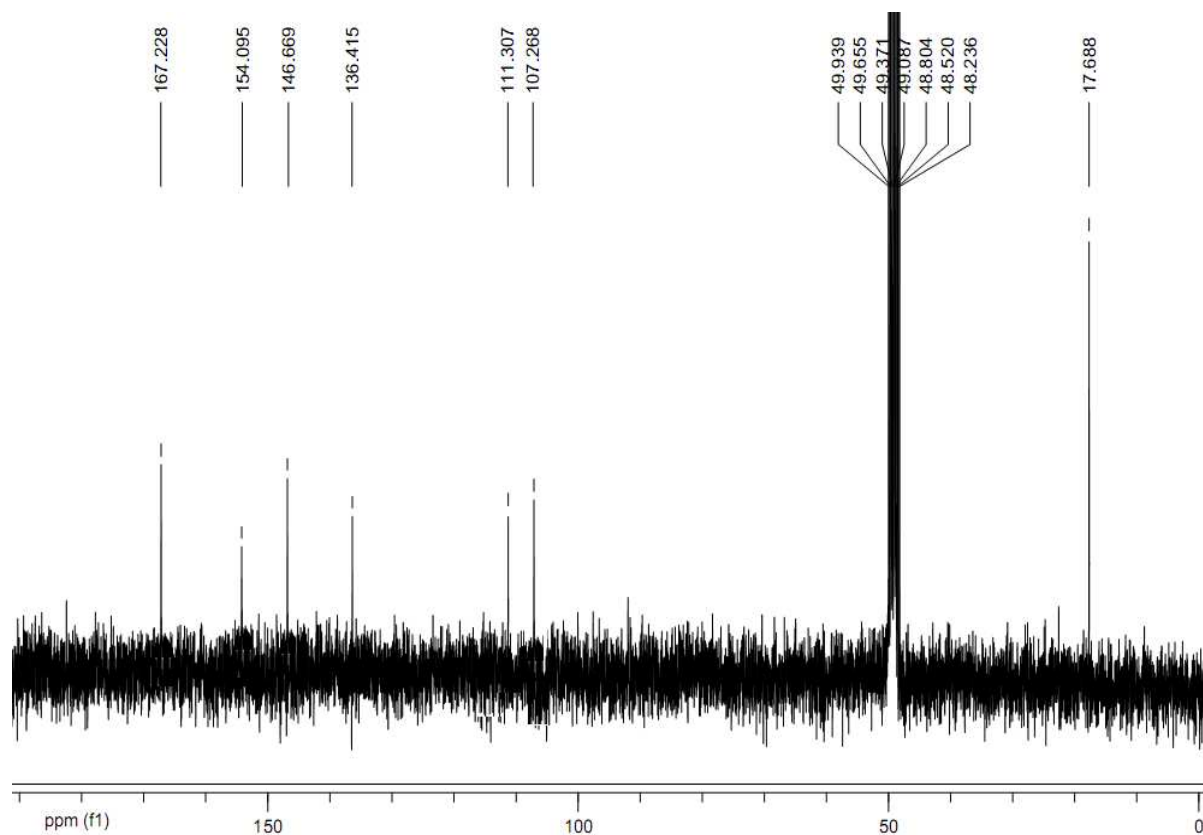
 ^1H NMR (300 MHz, CDCl_3) ^{13}C NMR (75 MHz, CDCl_3)

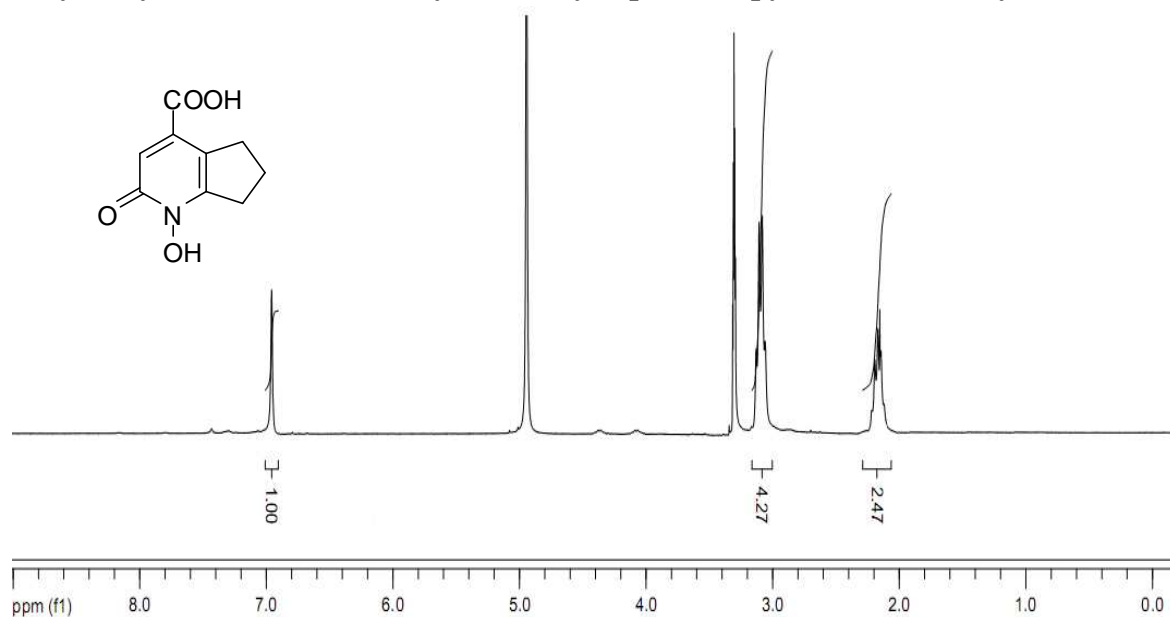
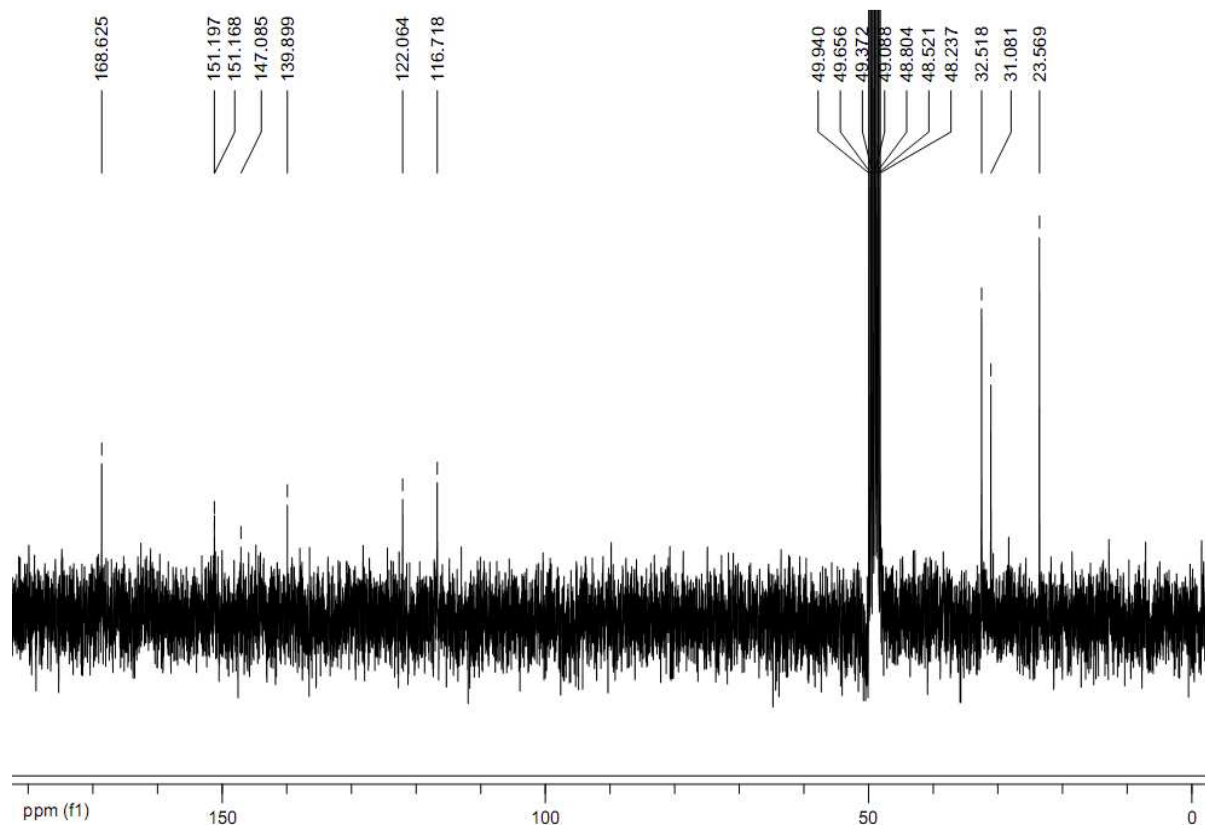
4-Carboxy-2-ethoxy-6,7-dihydro-5H-cyclopenta[*b*]pyridine-1-oxide (15b):

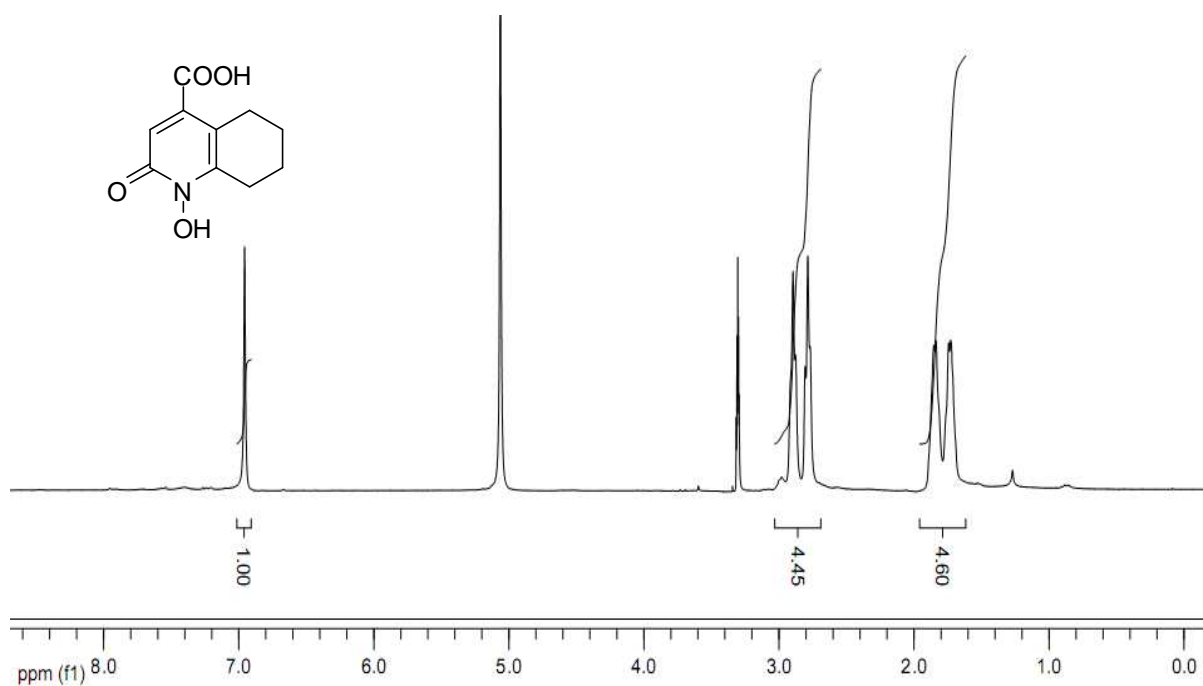
4-Carboxy-2-ethoxy-5,6,7,8-tetrahydroquinoline-1-oxide (15c):

¹H NMR (300 MHz, CDCl₃)¹³C NMR (75 MHz, CDCl₃)

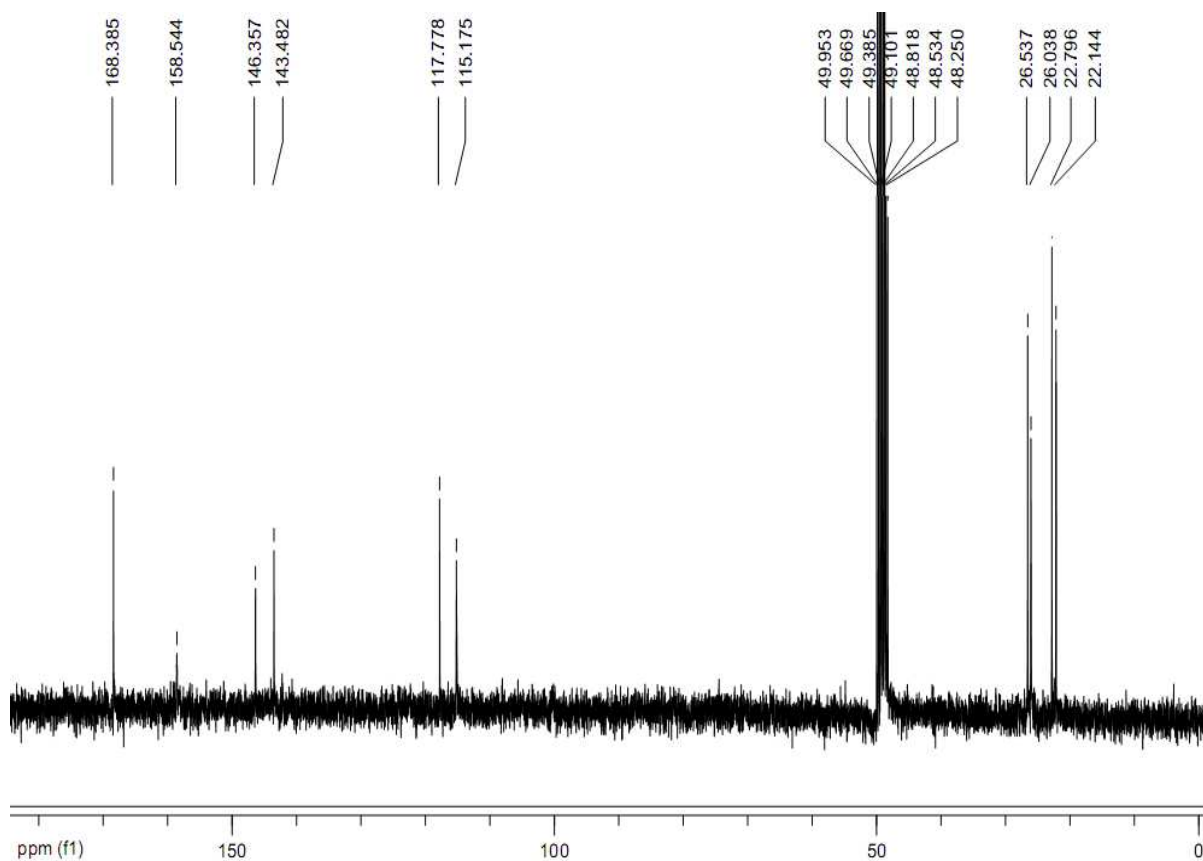
1-Hydroxy-6-methyl-2-oxo-1,2-dihydropyridine-4-carboxylic acid (16):

 ^1H NMR (300 Hz, CD_3OD) ^{13}C NMR (75 MHz, CD_3OD)

1-Hydroxy-2-oxo-2,5,6,7-tetrahydro-1H-cyclopenta[*b*] pyridine-4-carboxylic acid (17a):¹H NMR (300 Hz, CD₃OD)¹³C NMR (75 Hz, CD₃OD)**1-Hydroxy-2-oxo-1,2,5,6,7,8-hexahydroquinoline-4-carboxylic acid (7b):**

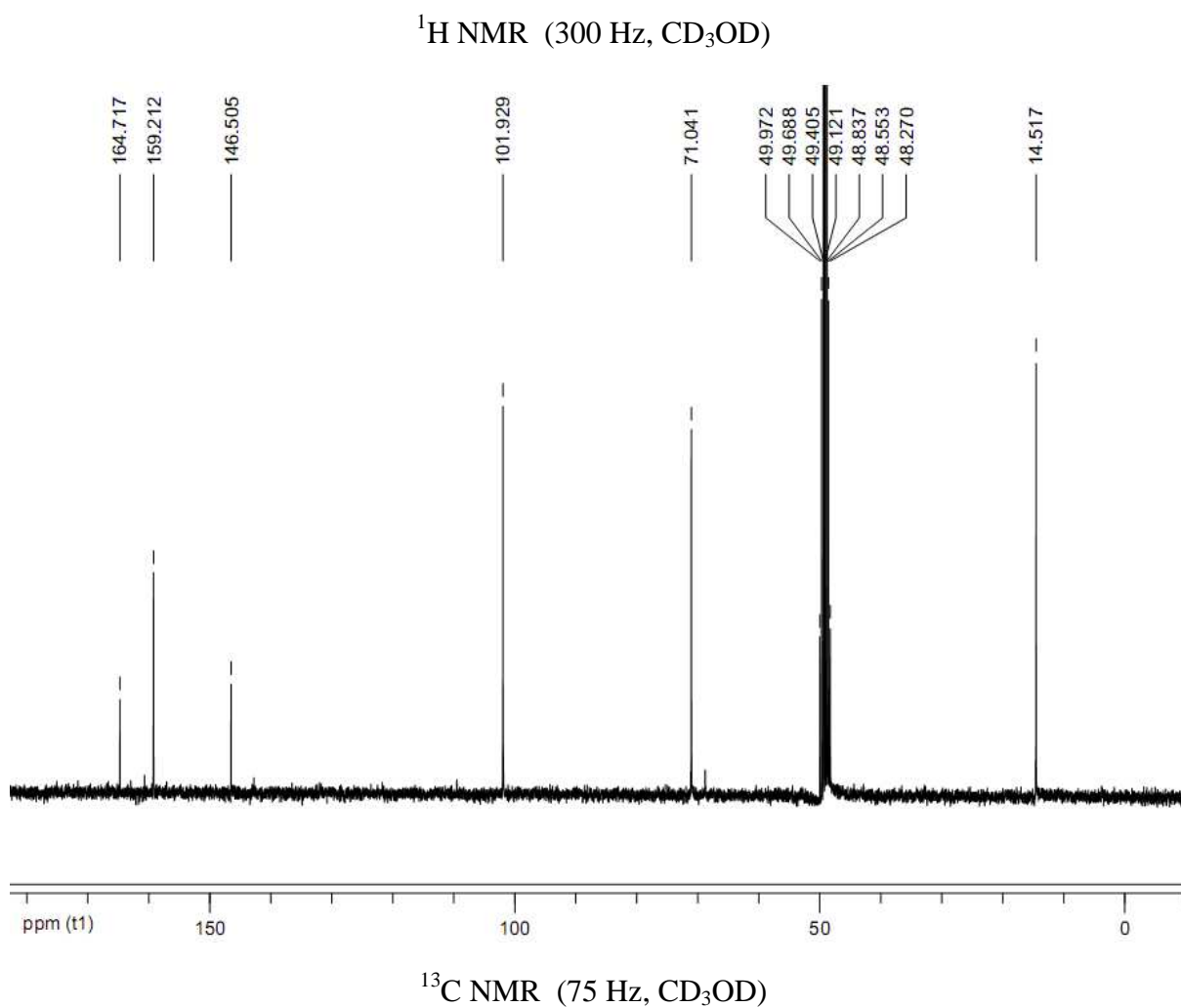
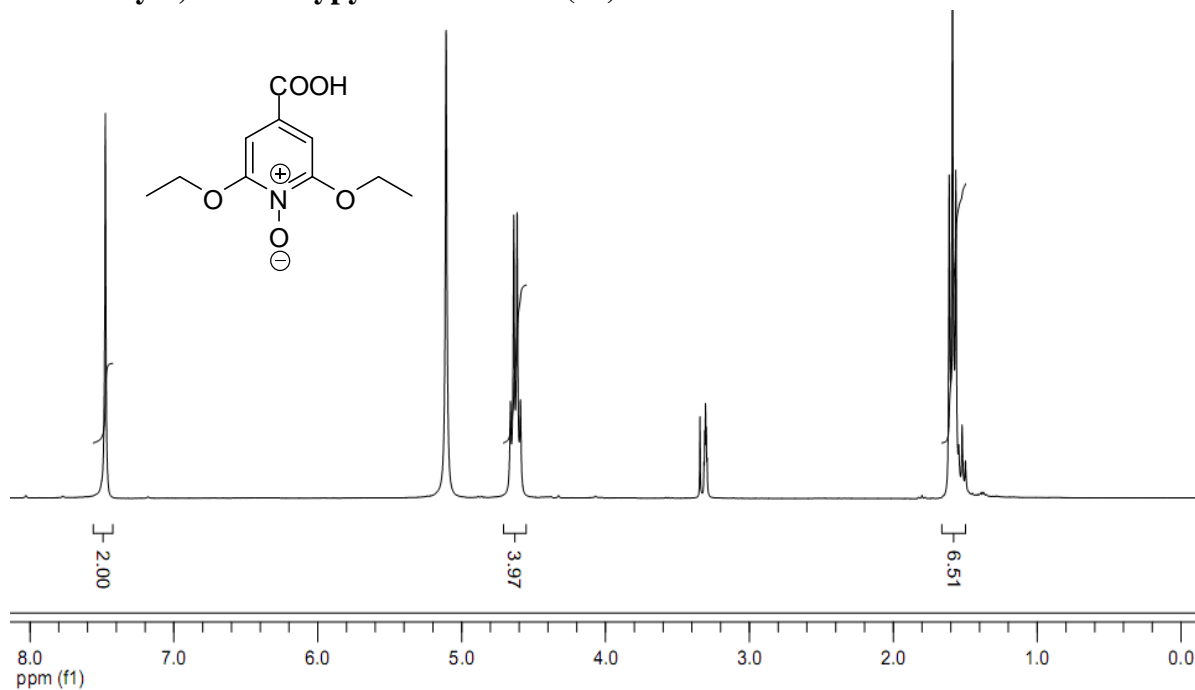


^1H NMR (300 Hz, CD_3OD)

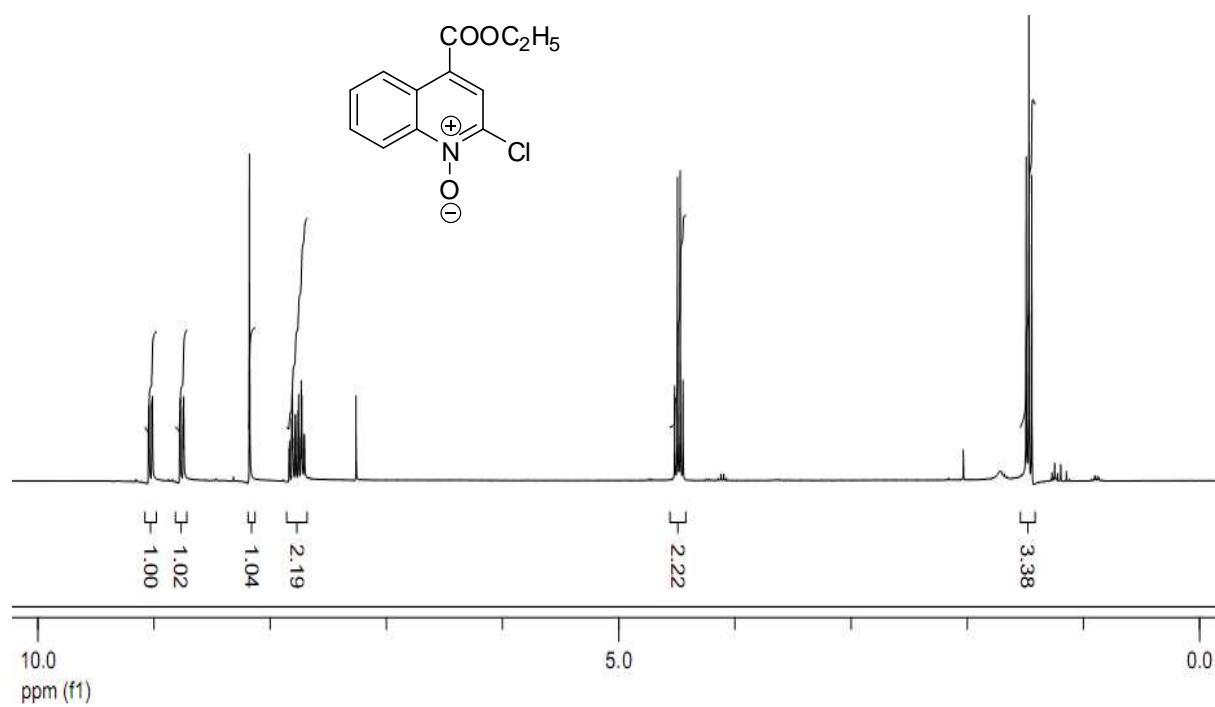
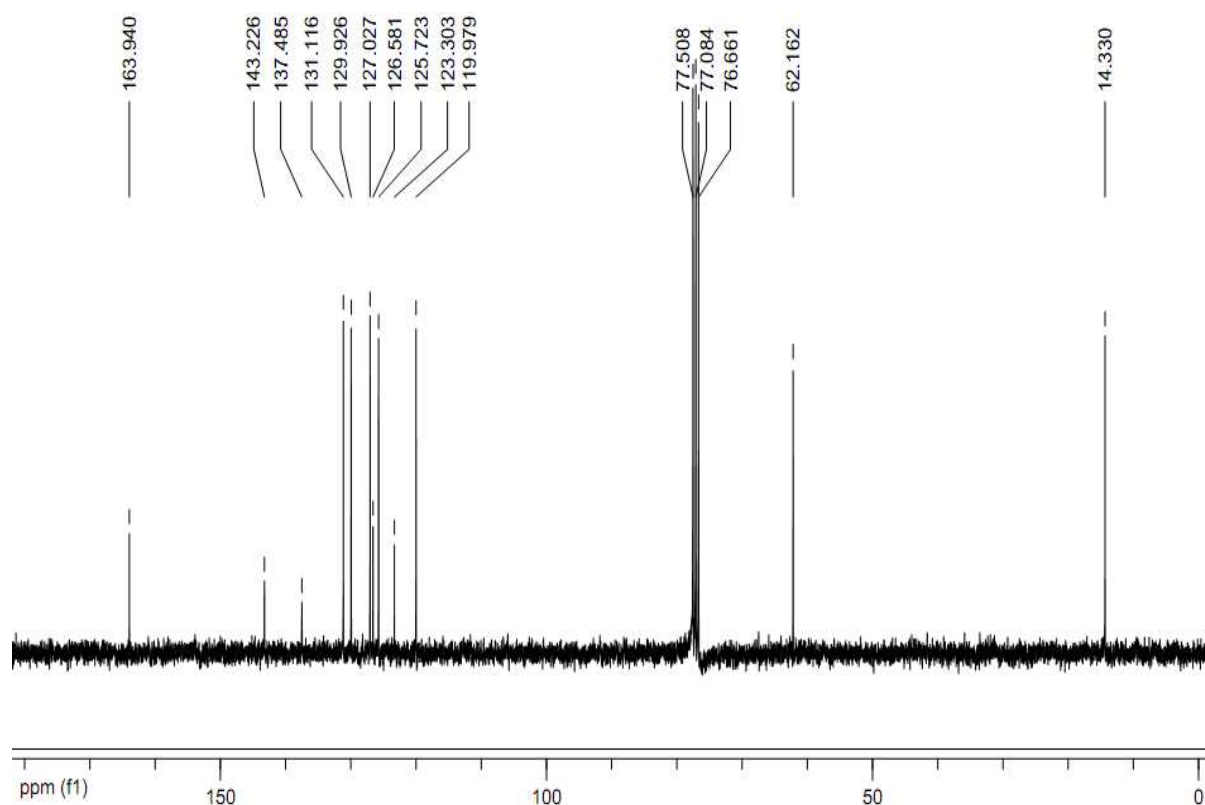


^{13}C NMR (75 Hz, CD_3OD)

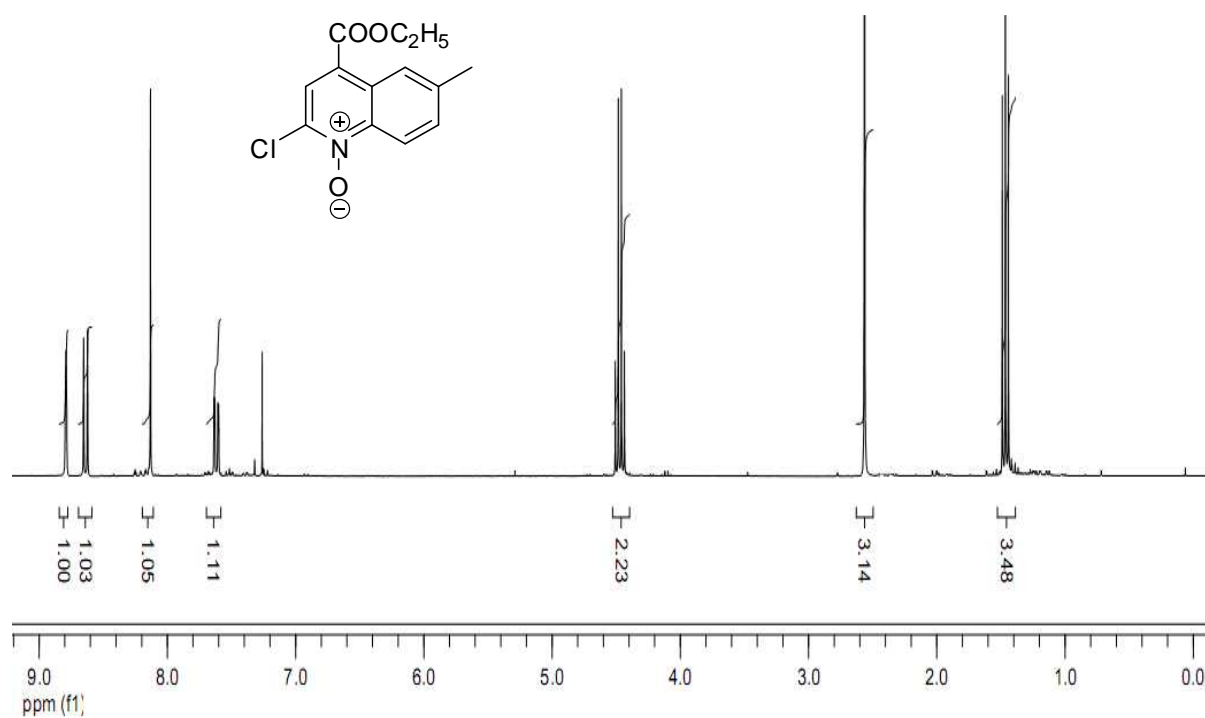
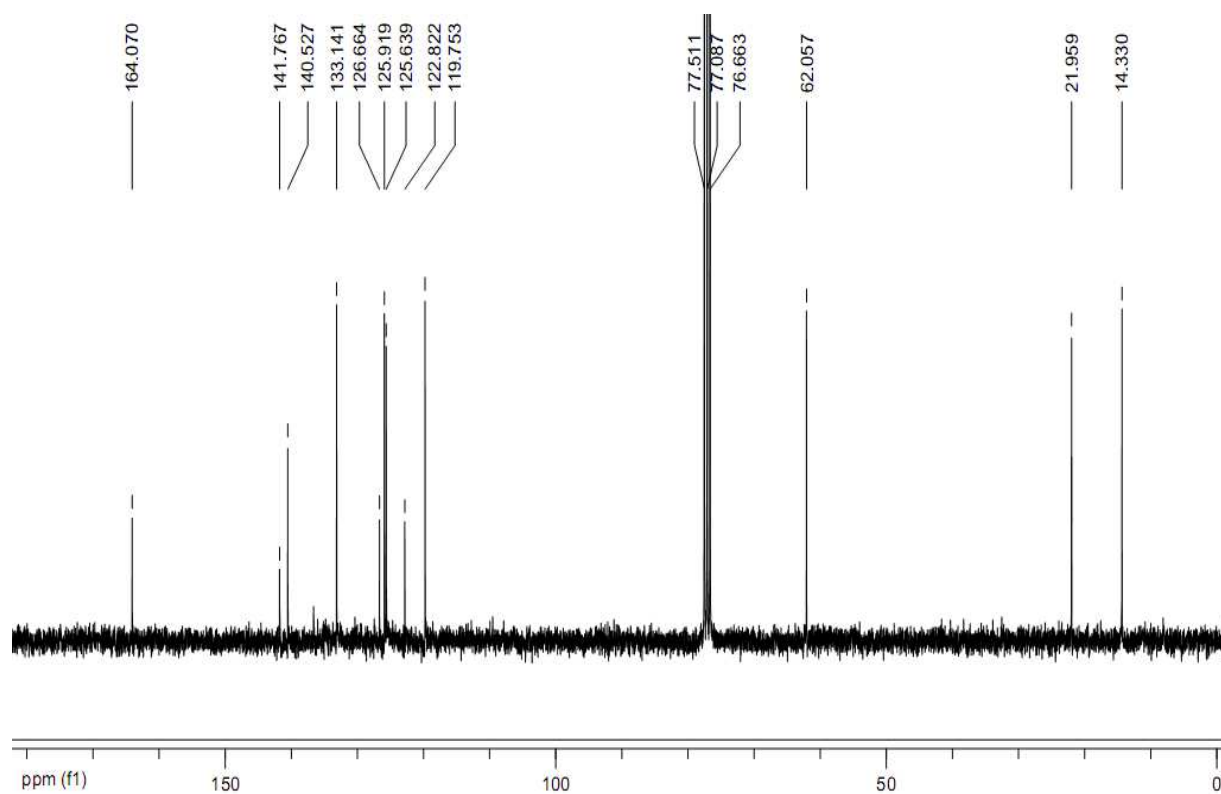
4-Carboxy-2,6-diethoxypyridine-1-oxide (20):



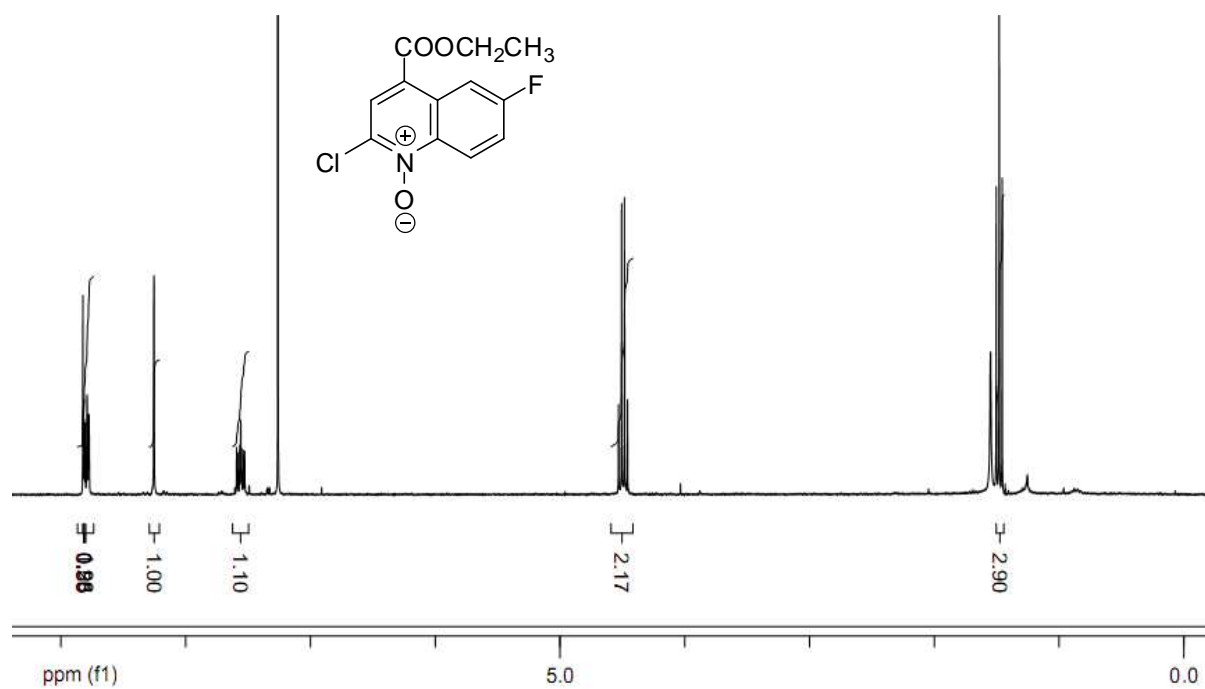
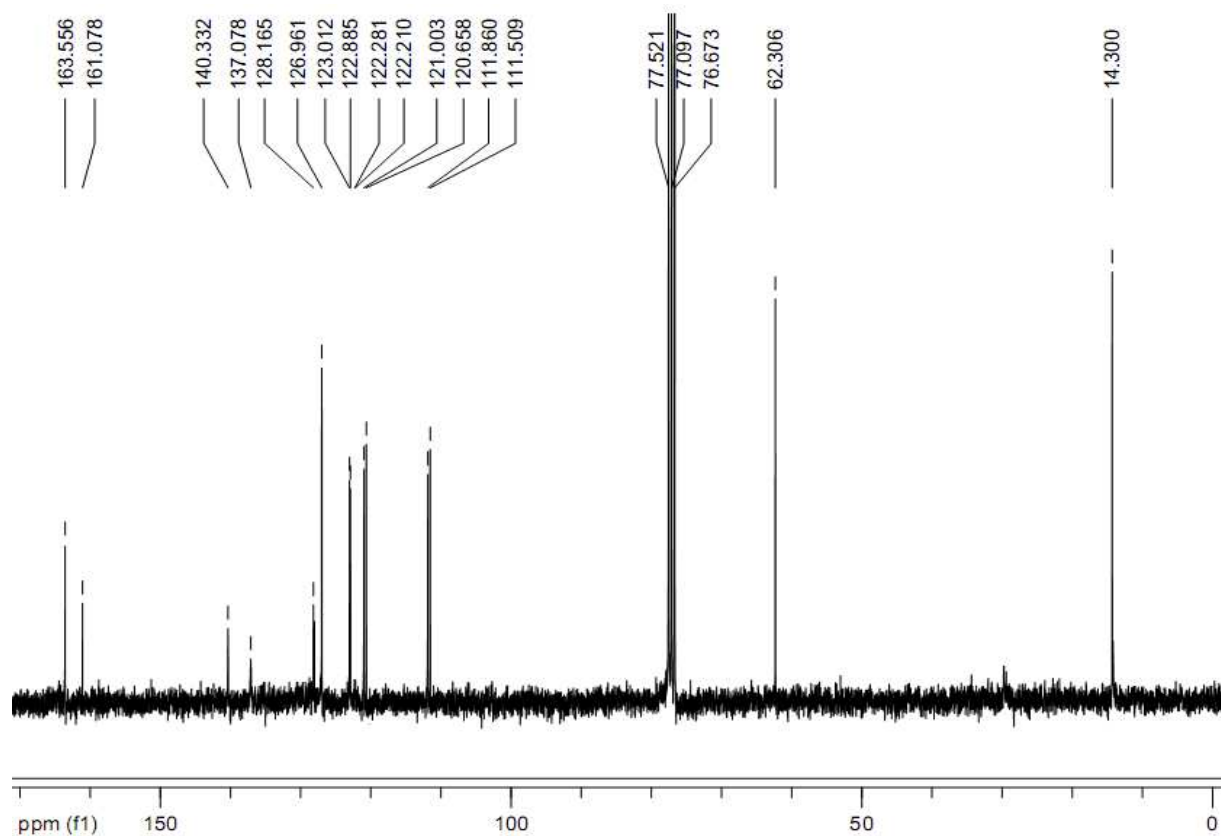
2-Chloro-4 (ethoxycarbonyl quinoline 1-oxides (25a):

 ^1H NMR (300 MHz, CDCl_3) ^{13}C NMR (75 MHz, CDCl_3)

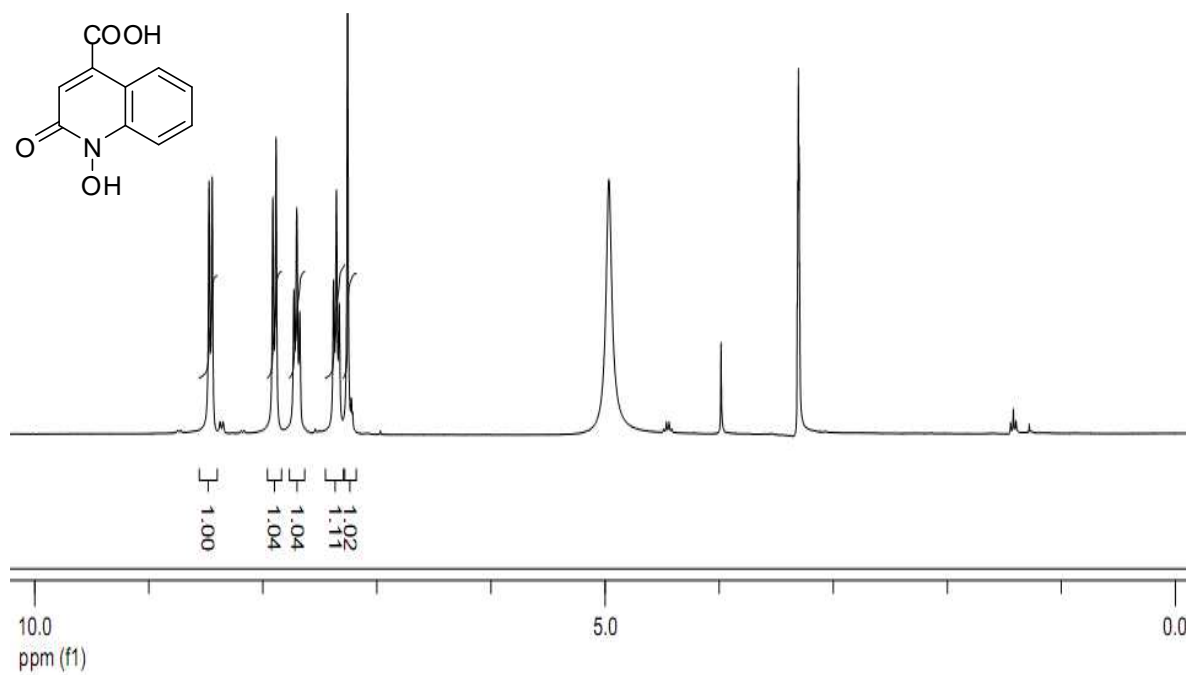
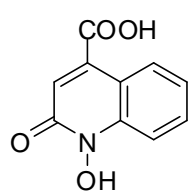
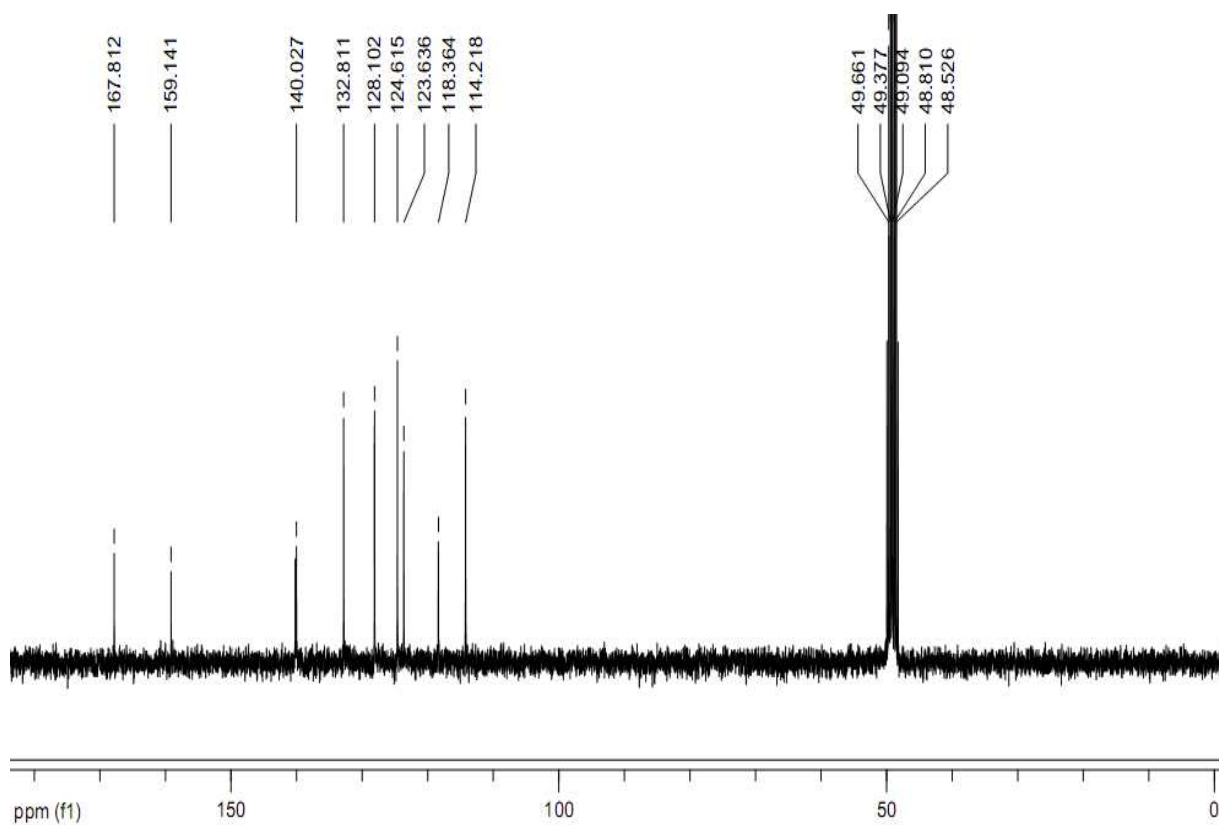
2-Chloro-4 (ethoxycarbonyl)-6-methylquinoline 1-oxides (25b):

¹H NMR (300 MHz, CDCl₃)¹³C NMR (75 MHz, CDCl₃)

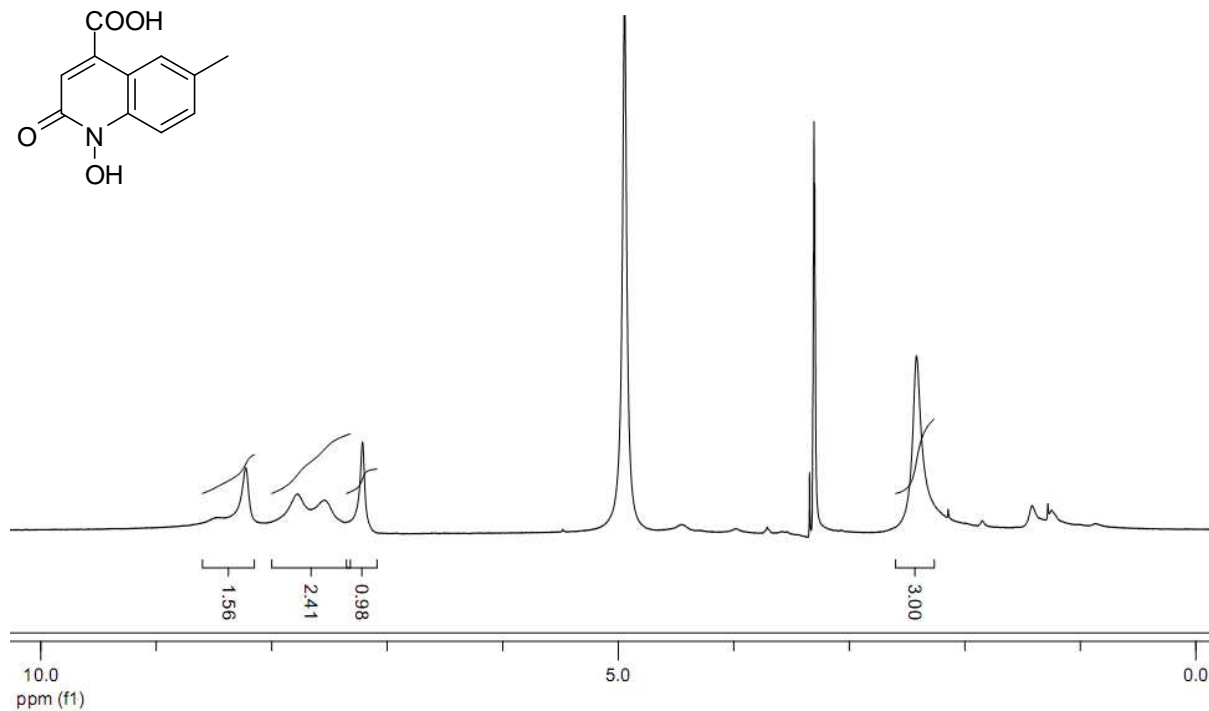
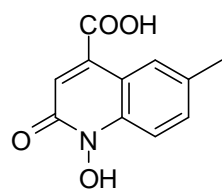
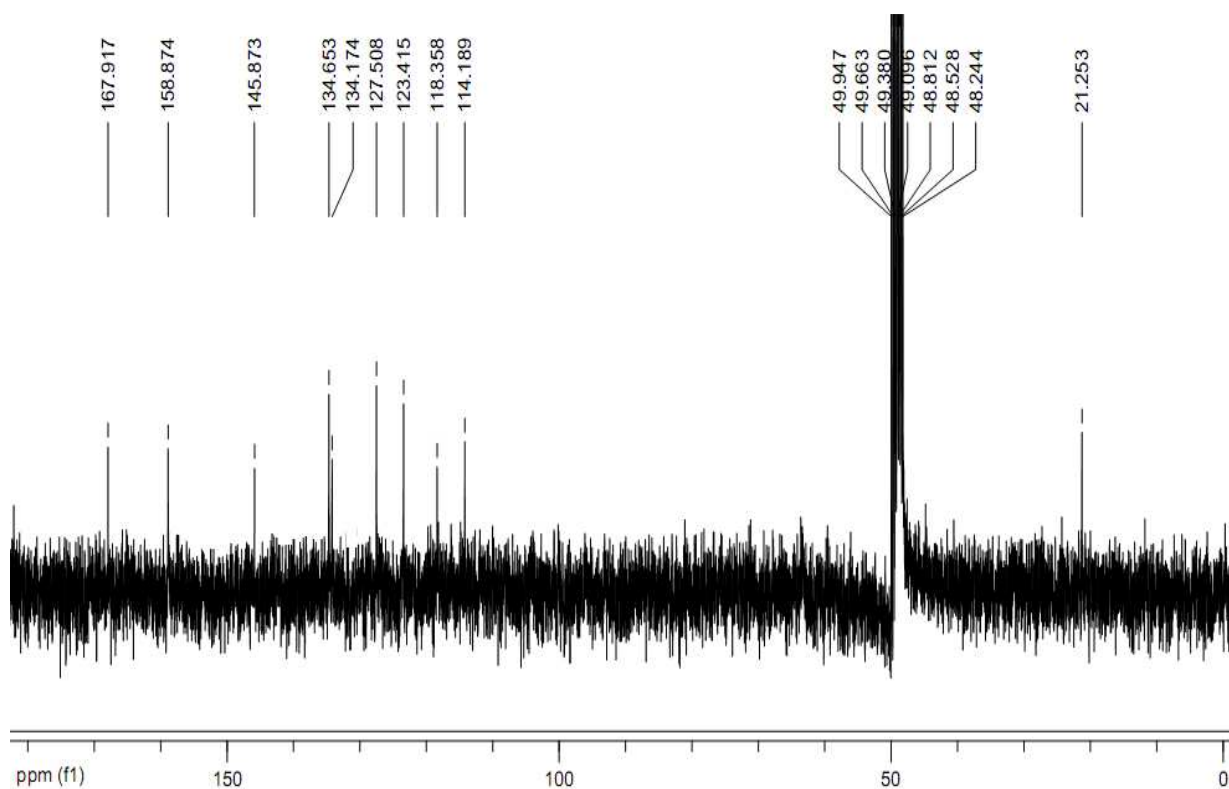
2-Chloro-6-fluoro-4-(ethoxycarbonyl) quinoline 1-oxide (25c):

 ^1H NMR (300 MHz, CDCl_3) ^{13}C NMR (75 MHz, CDCl_3)

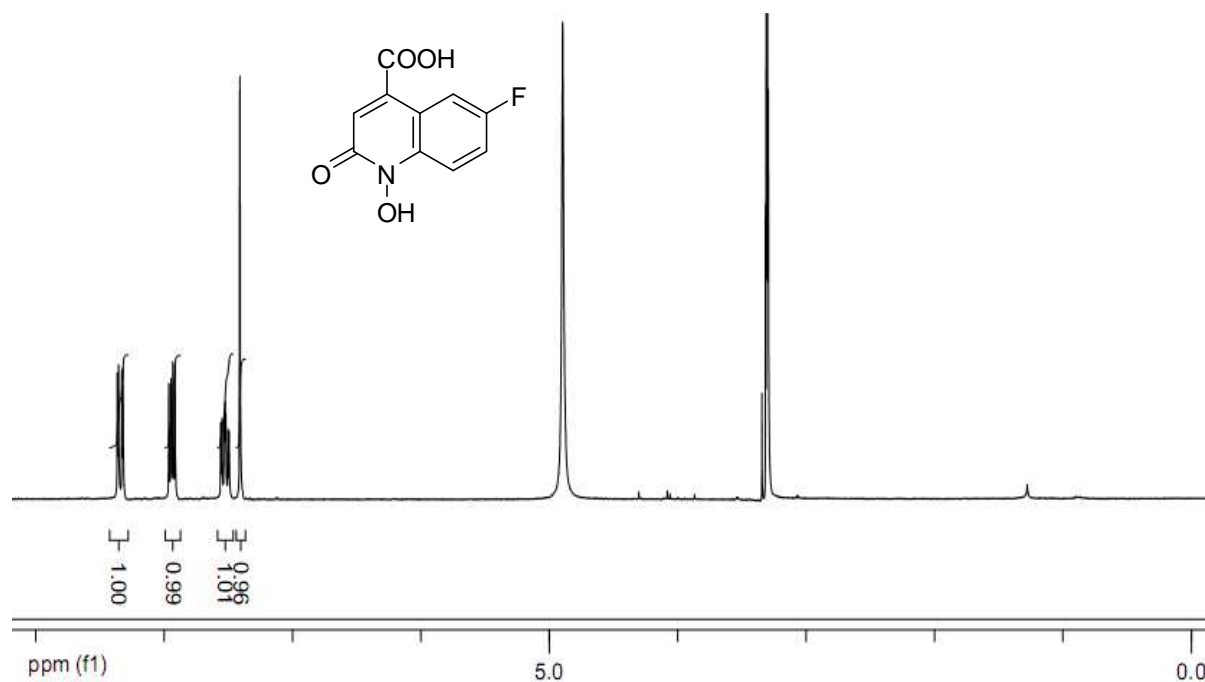
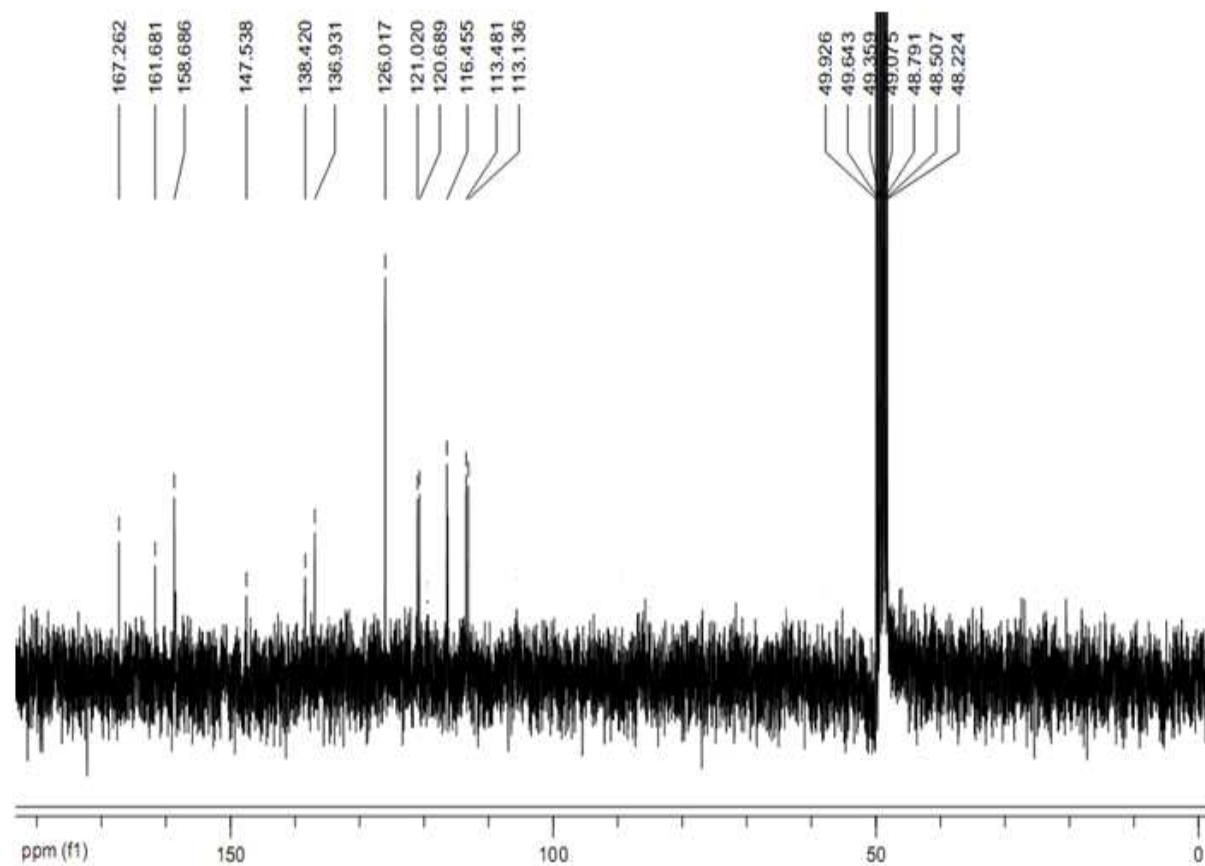
1-Hydroxy-2-oxo-1,2-dihydroquinoline-4-carboxylic acid (26a):

 ^1H NMR (300 Hz, CD_3OD) ^{13}C NMR (75 Hz, CD_3OD)

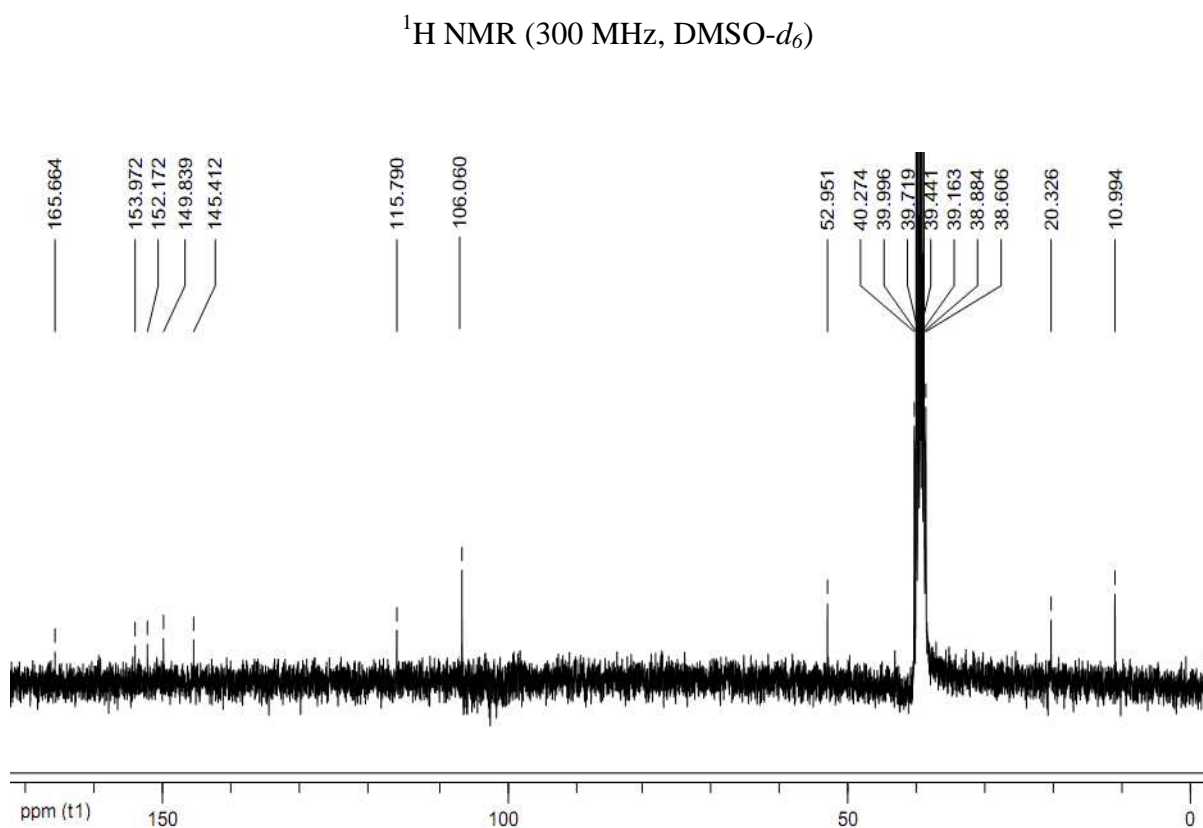
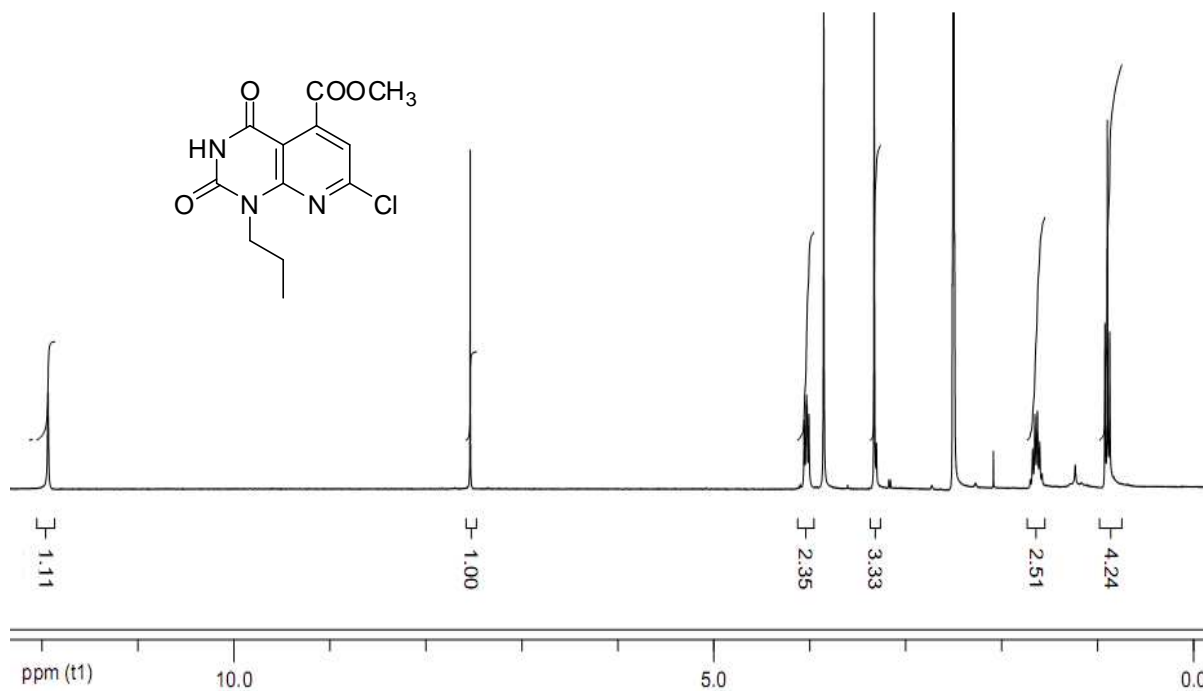
1-Hydroxy-6-methyl-2-oxo-1,2-dihydroquinoline-4-carboxylic acid (26b):

 ^1H NMR (300 Hz, CD_3OD) ^{13}C NMR (75 Hz, CD_3OD)

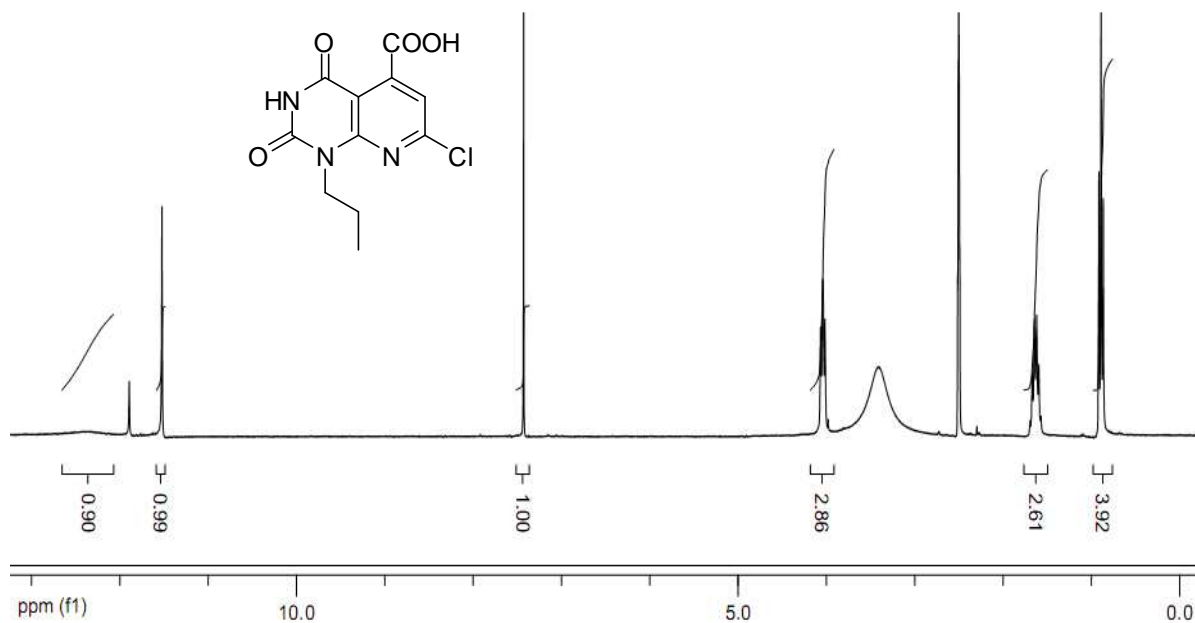
6-Fluoro-1-hydroxy-2-oxo-1,2-dihydroquinoline-4-carboxylic acid (26c):

 ^1H NMR (300 Hz, CD_3OD) ^{13}C NMR (75 Hz, CD_3OD)

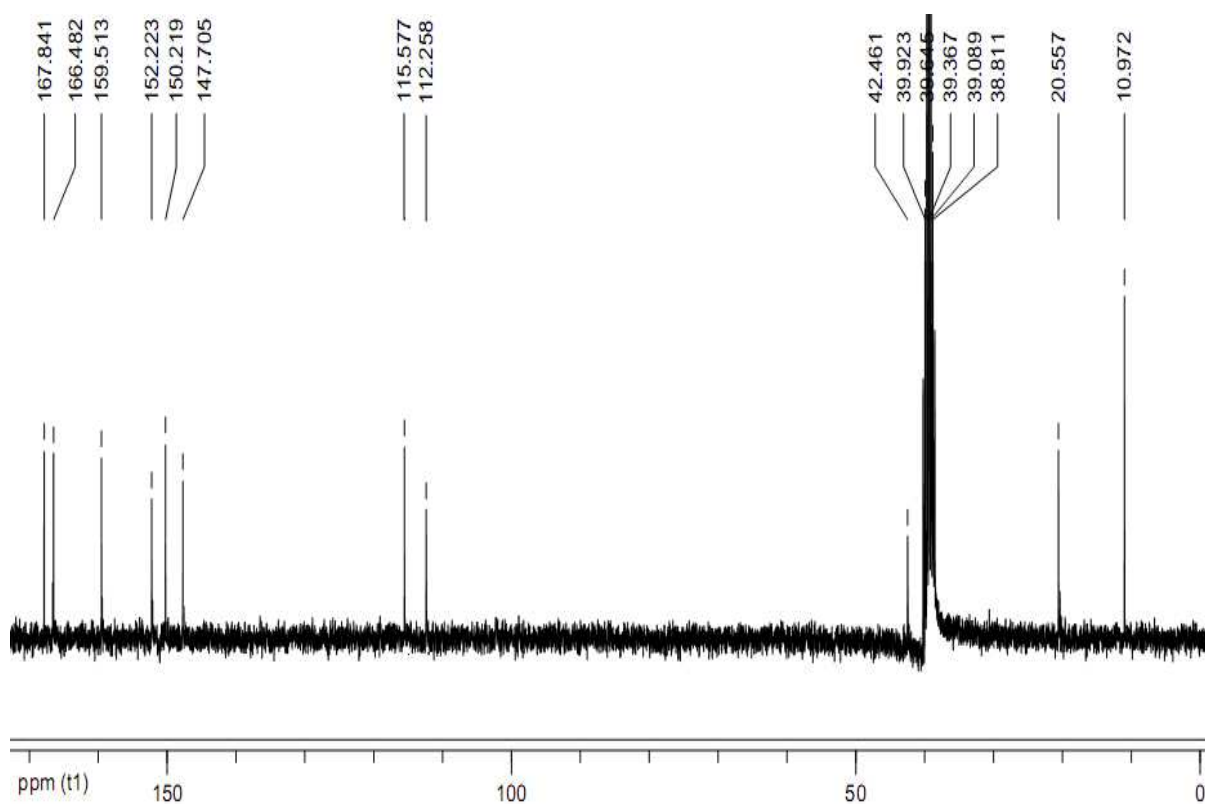
Methyl -7-chloro-2,4-dioxo-1-propyl-1,2,3,4-tetrahydropyrido [2, 3-*d*] pyrimidine-5-carboxylate (36a):



7-Chloro-2,4-dioxo-1-propyl-1,2,3,4-tetrahydropyrido[2,3-*d*]pyrimidine-5-carboxylic acid (36c):



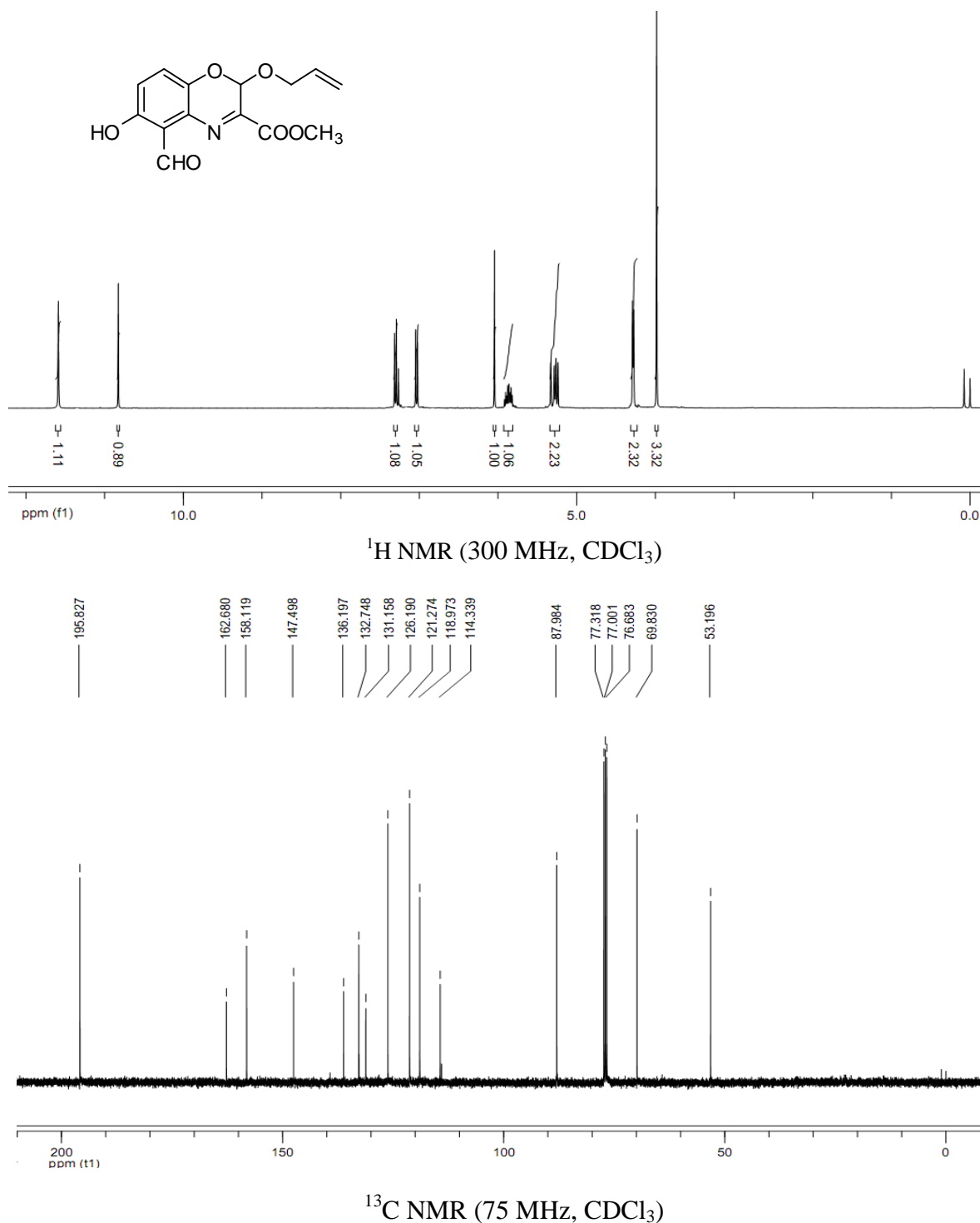
^1H NMR (300 MHz, $\text{DMSO-}d_6$)



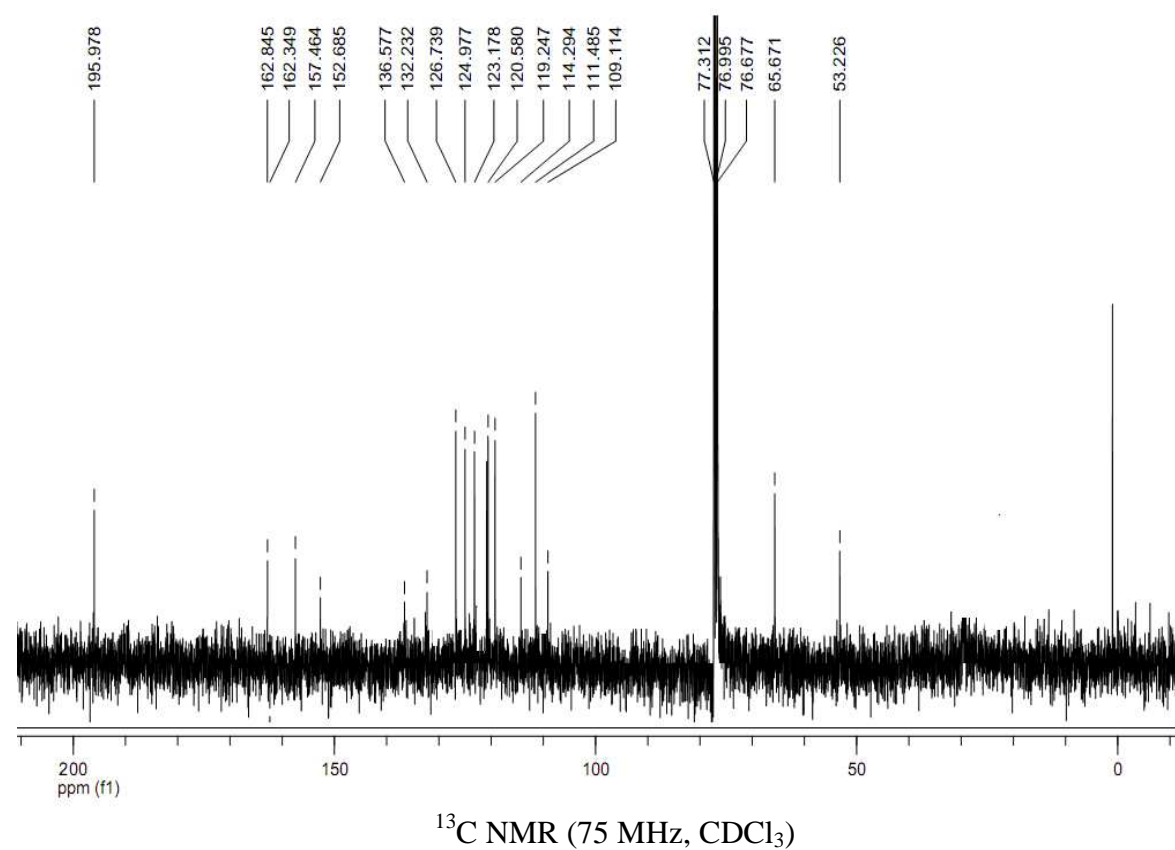
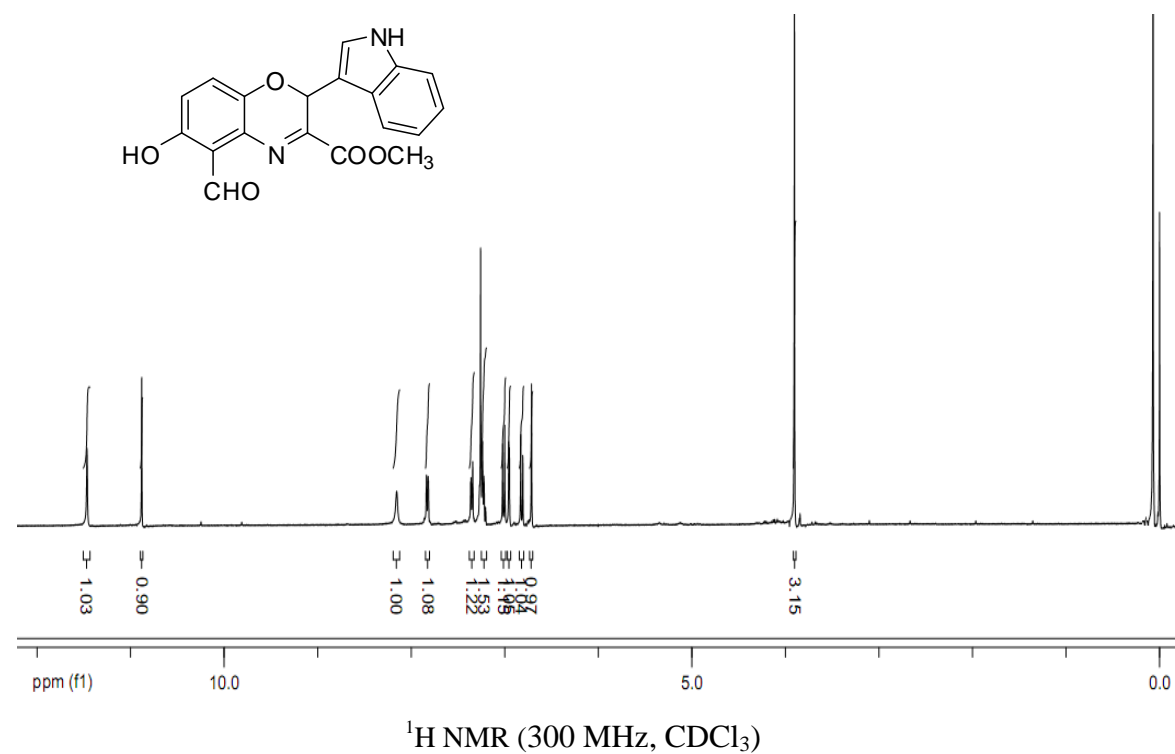
^{13}C NMR (75 MHz, $\text{DMSO-}d_6$)

3. Novel synthesis of 2*H*-benzo[*b*][1,4]oxazines *via* sequential C-N and C-O bond formation in single pot & their pharmacological evaluation as anti-inflammatory agents

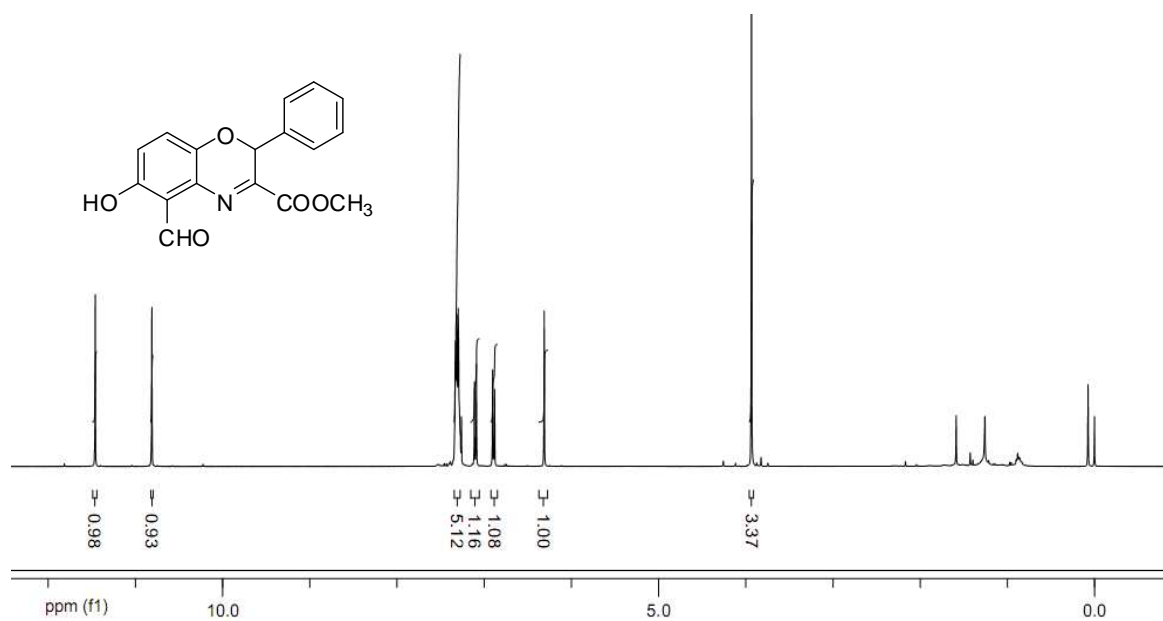
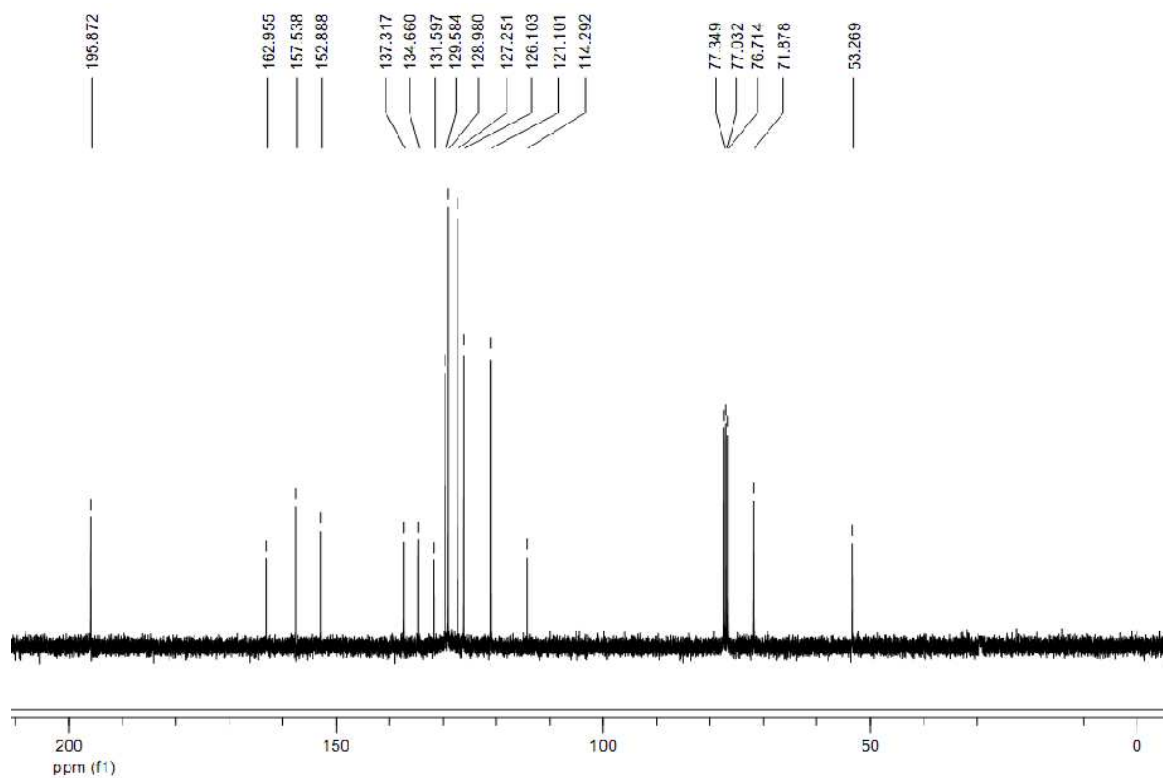
Methyl 2-(allyloxy)-5-formyl-6-hydroxy-2*H*-benzo[*b*][1,4]oxazine-3-carboxylate (**68**):

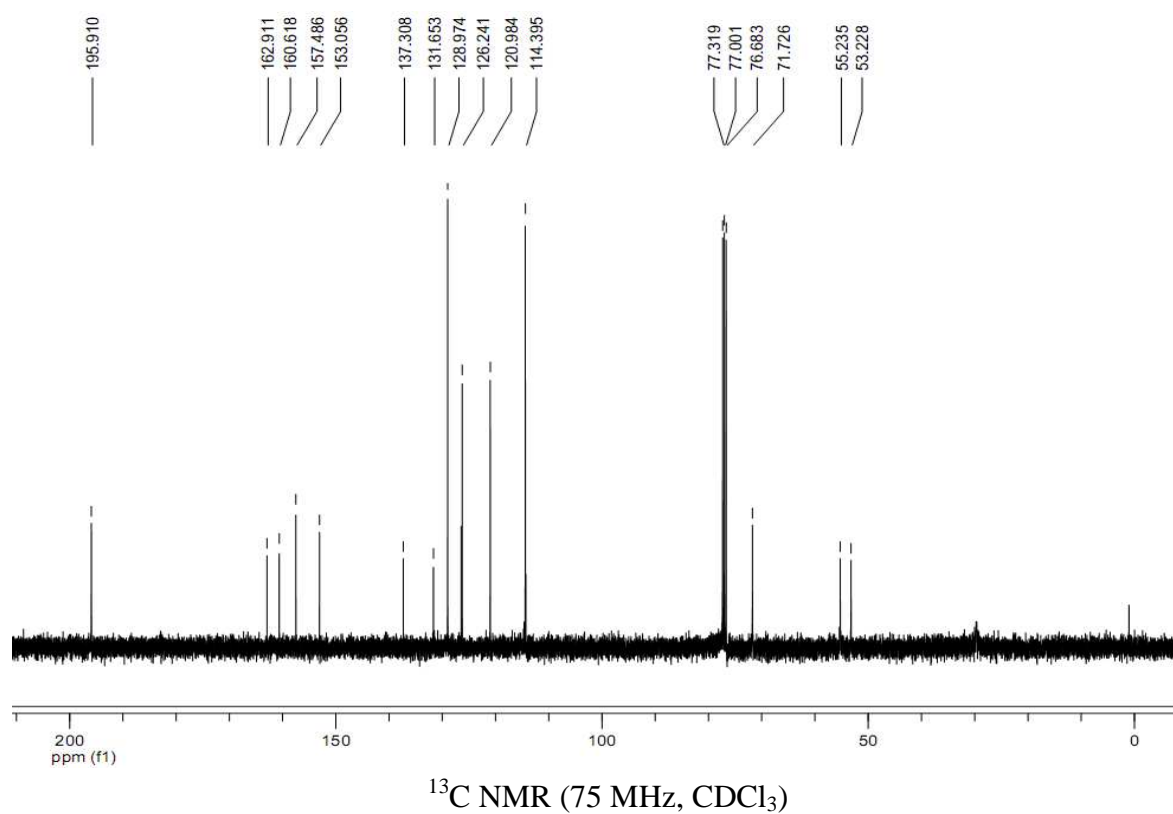
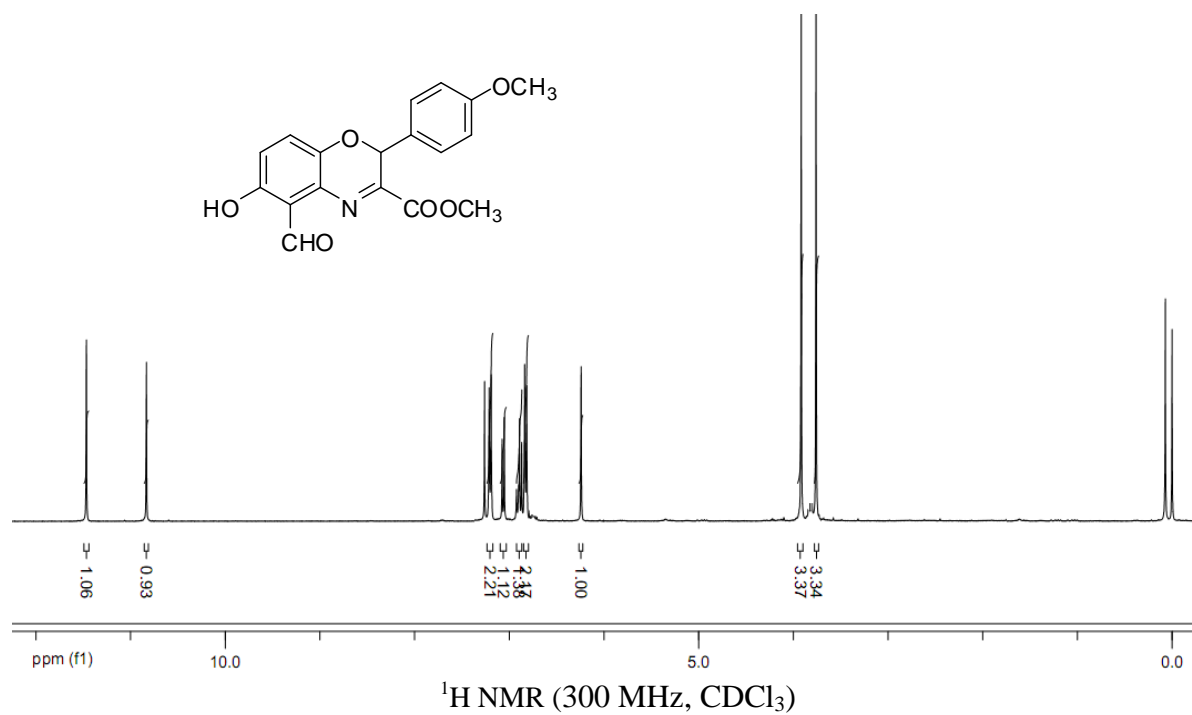


Methyl 5-formyl-6-hydroxy-2-(1*H*-indol-3-yl)-2*H*-benzo[*b*][1,4]oxazine-3-carboxylate (69):

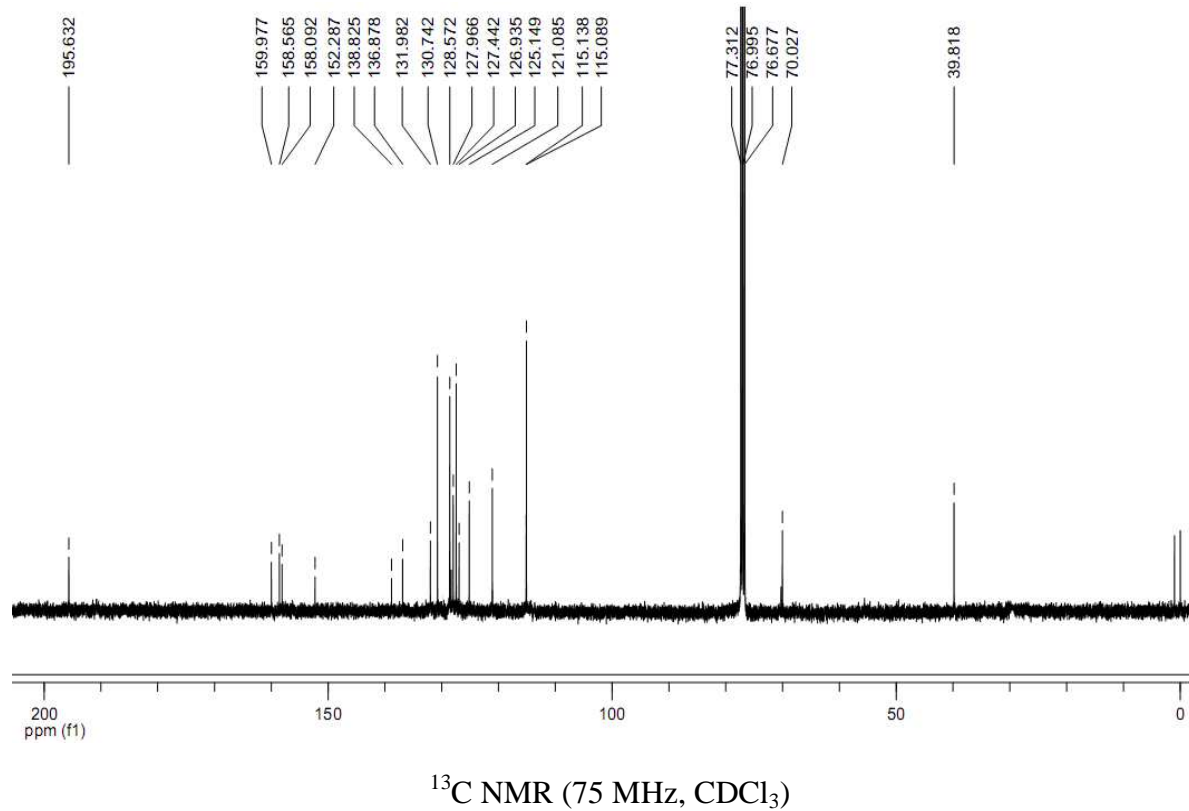
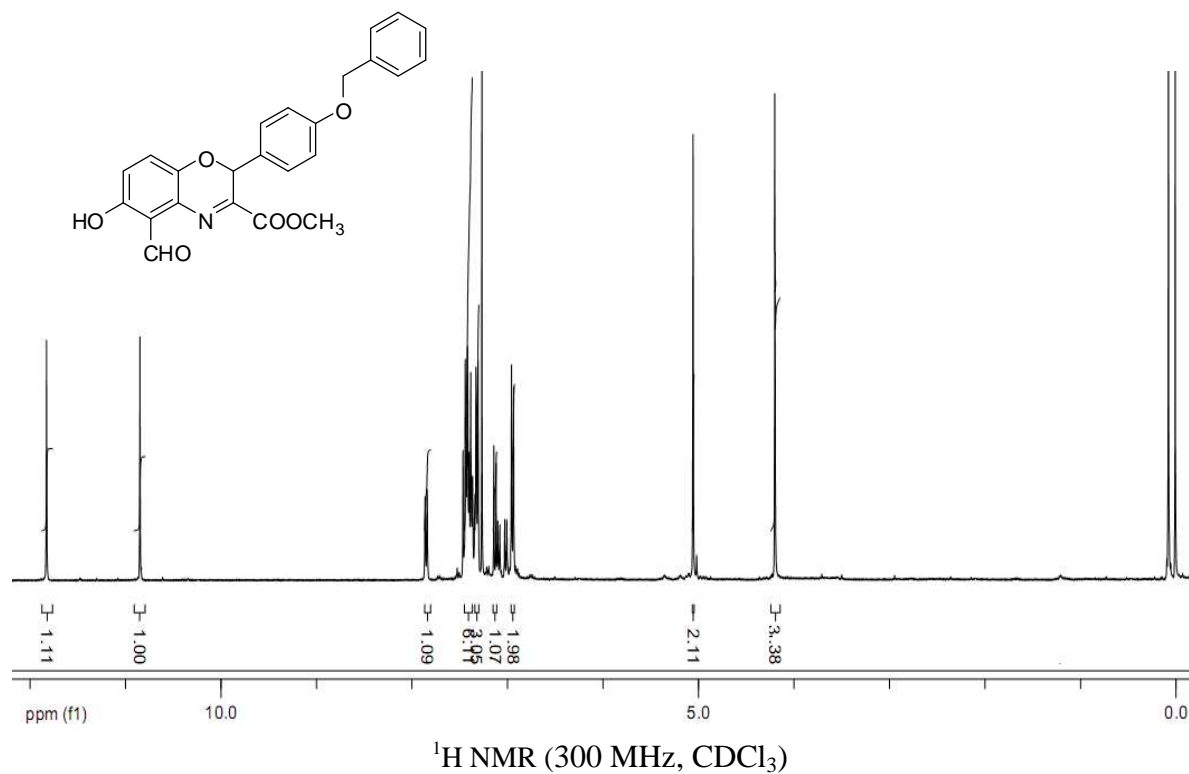


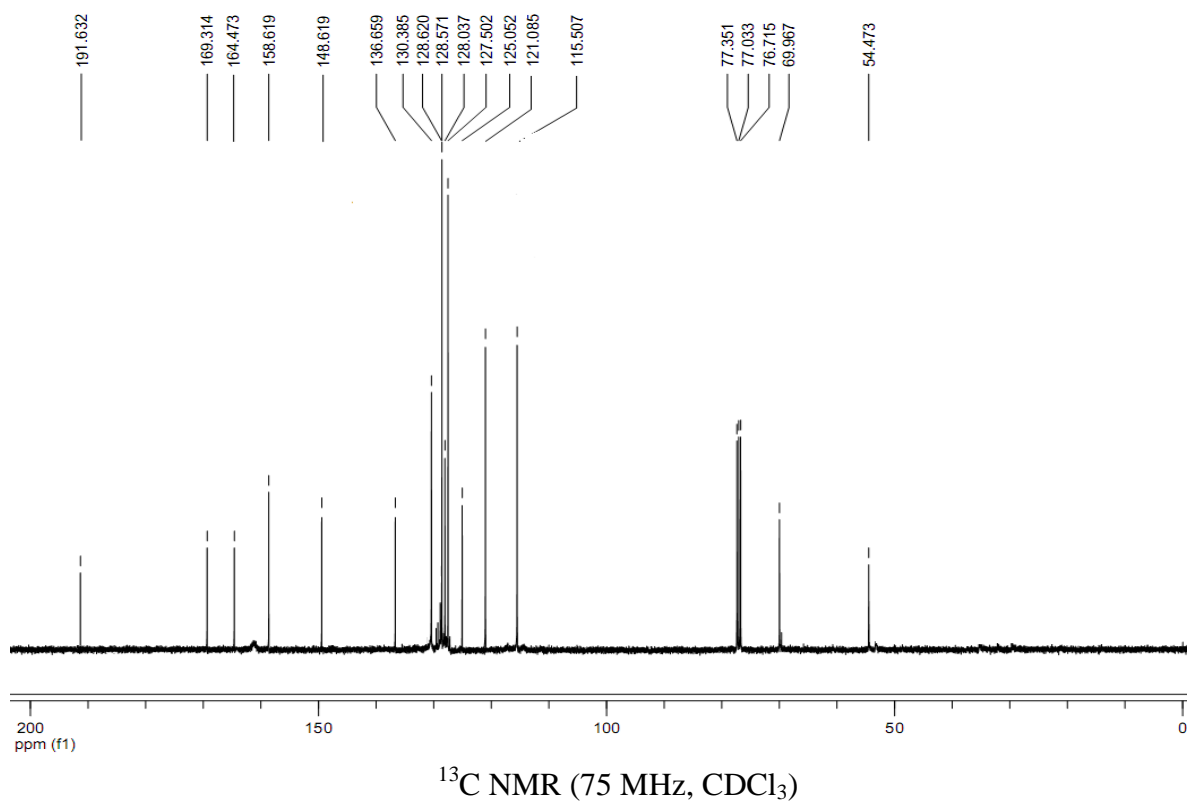
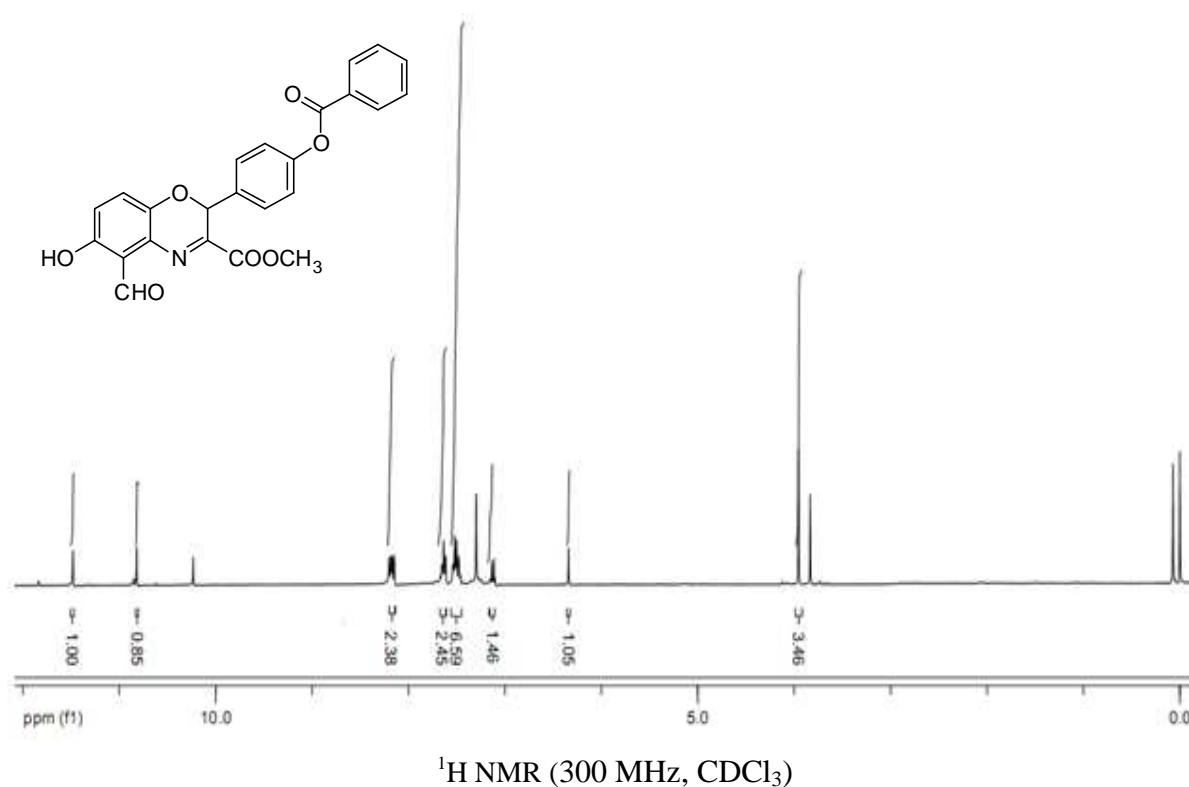
Methyl 5-formyl-6-hydroxy-2-phenyl-2H-benzo[b][1,4]oxazine-3-carboxylate (70):

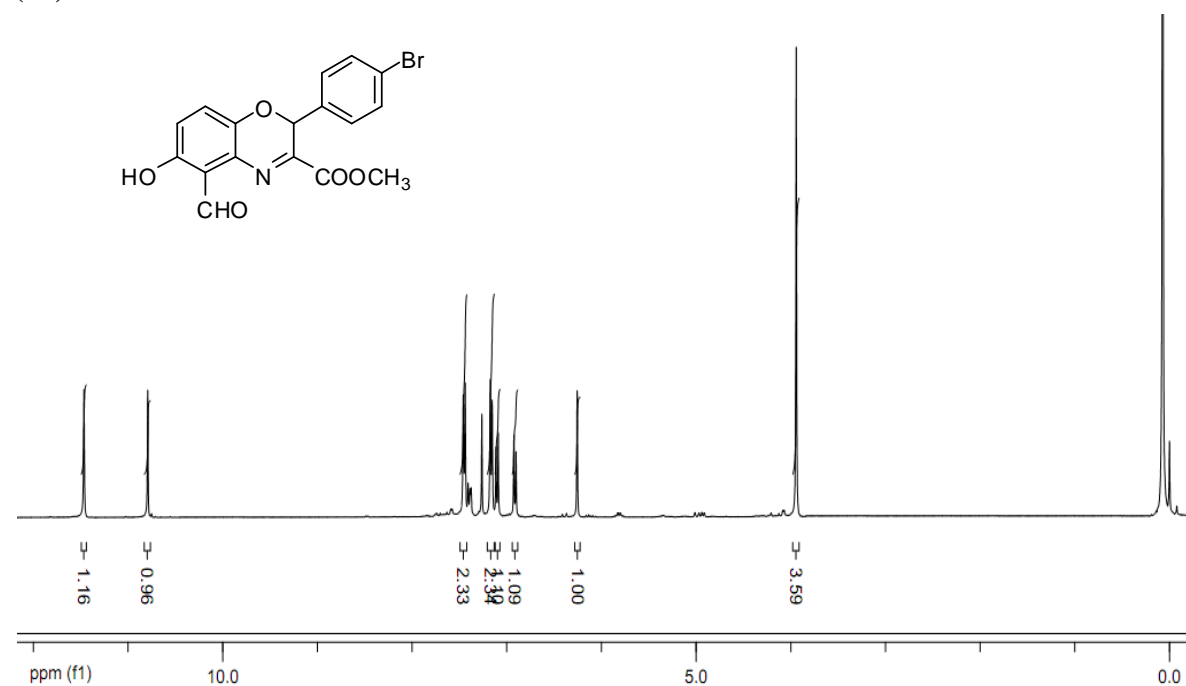
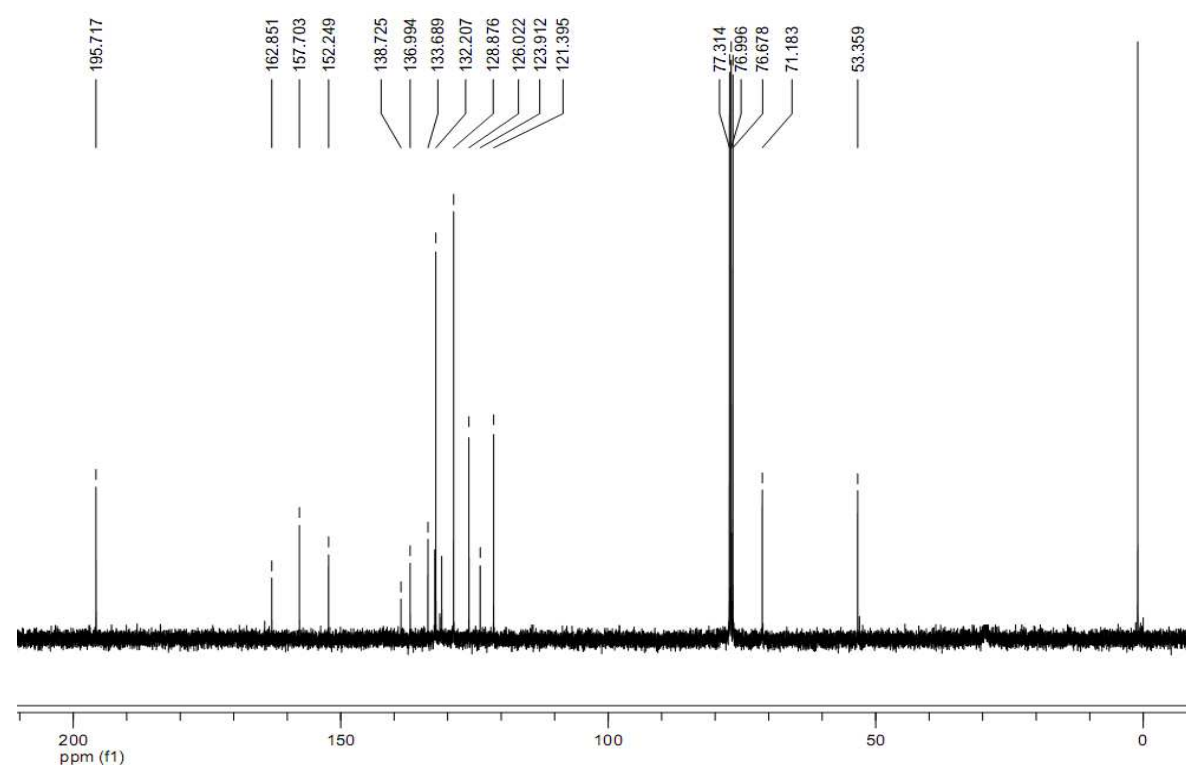
 ^1H NMR (300 MHz, CDCl_3) ^{13}C NMR (75 MHz, CDCl_3)

Methyl 5-formyl-6-hydroxy-2-(4-methoxyphenyl)-2H-benzo[*b*][1,4]oxazine-3-carboxylate (71):

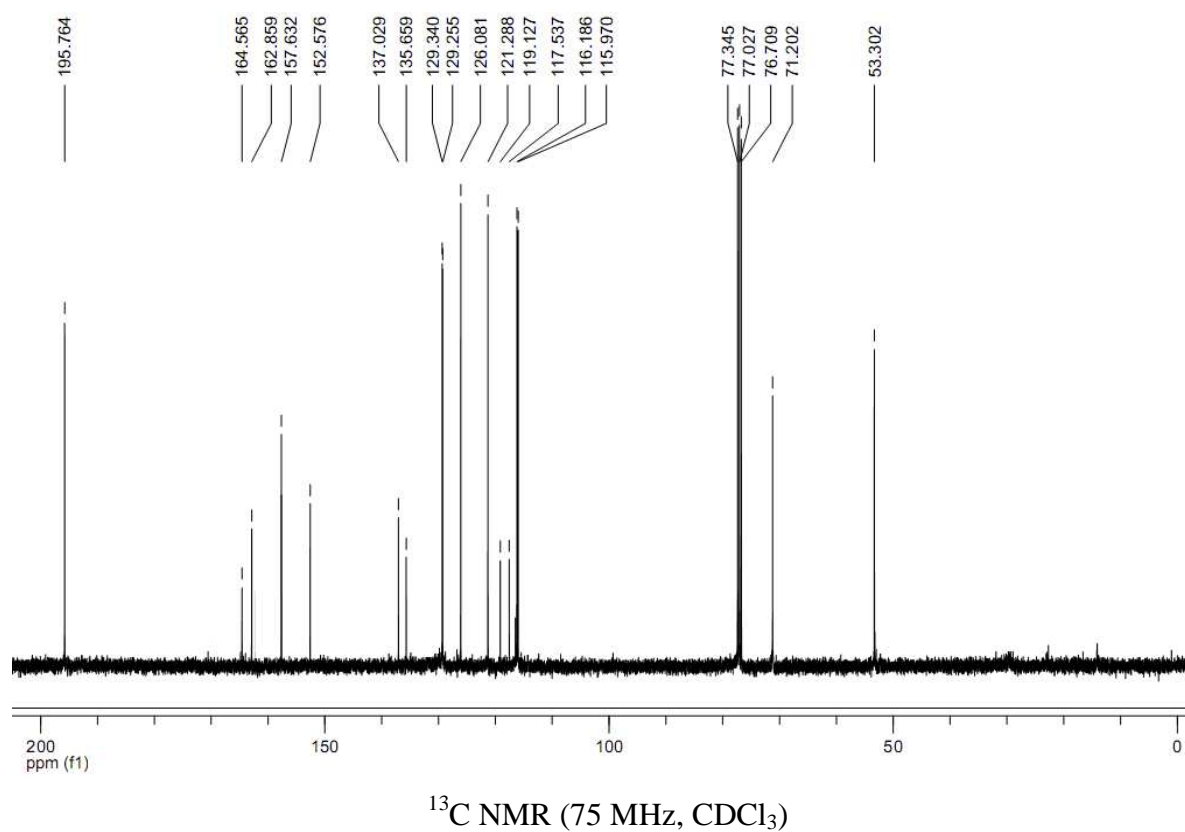
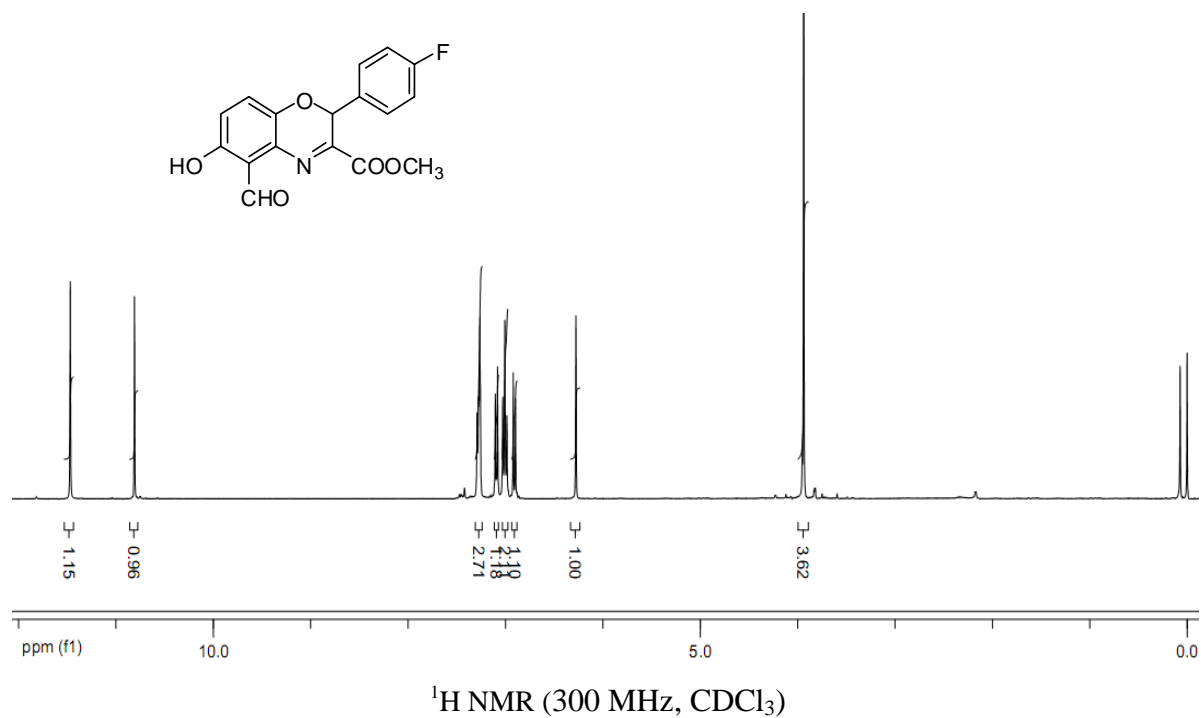
Methyl 2-(4-(benzyloxy) phenyl)-5-formyl-6-hydroxy-2H-benzo[*b*][1,4]oxazine-3-carboxylate (72):



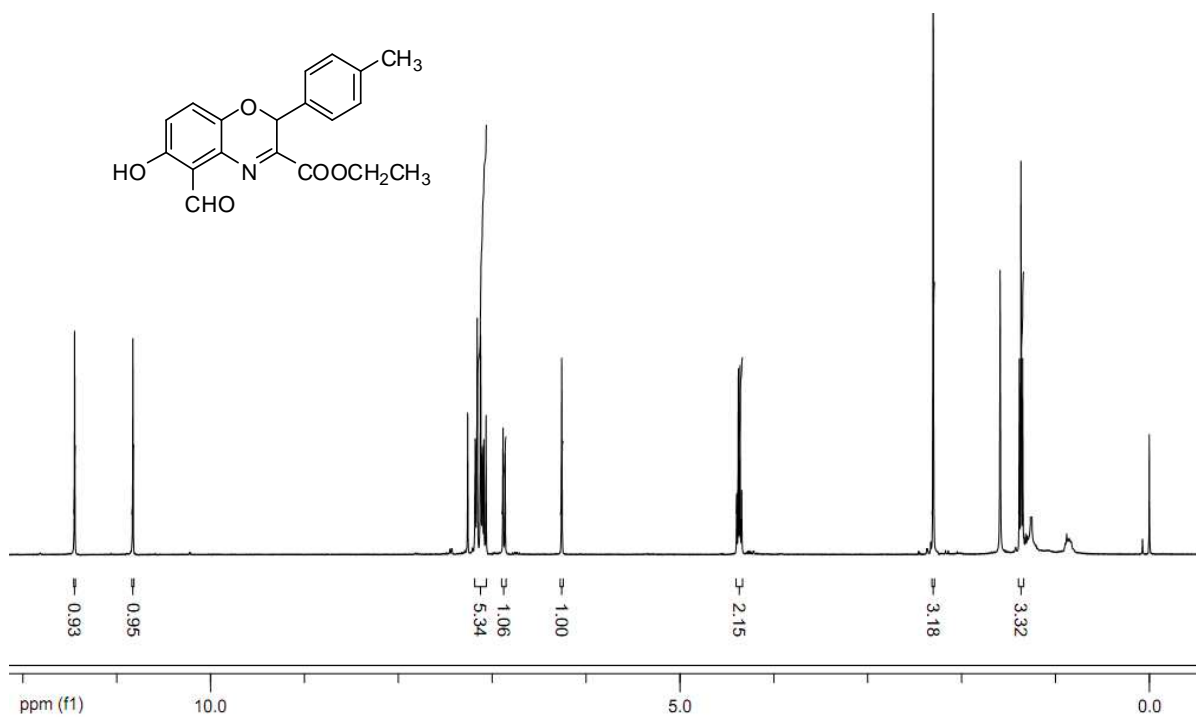
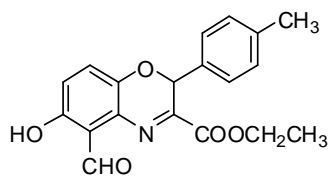
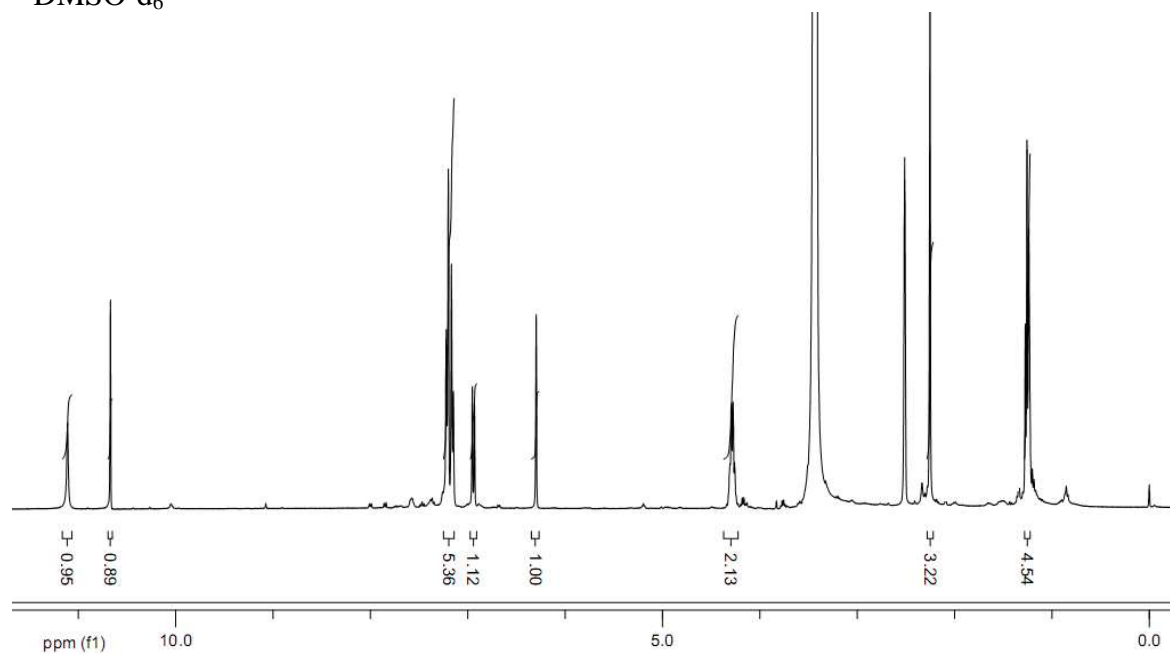
Methyl 2-(4-(benzyloxy)phenyl)-5-formyl-6-hydroxy-2H-benzo[b][1,4]oxazine-3-carboxylate (73):

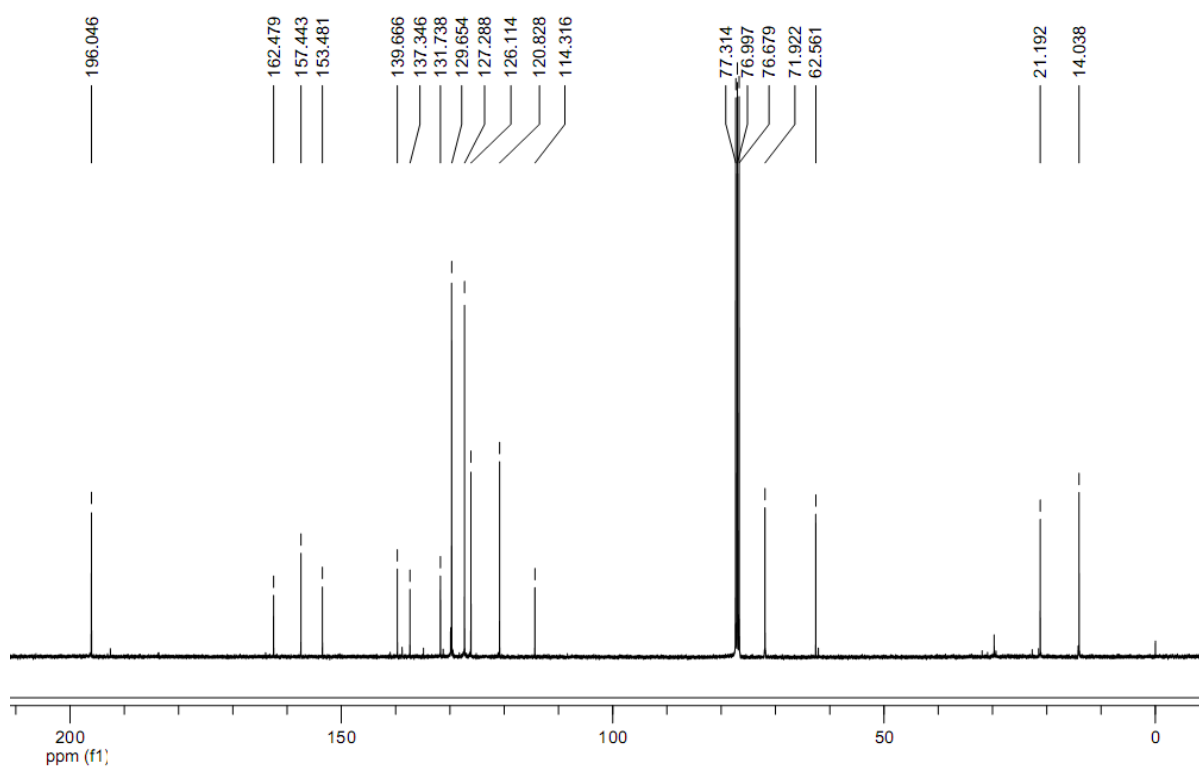
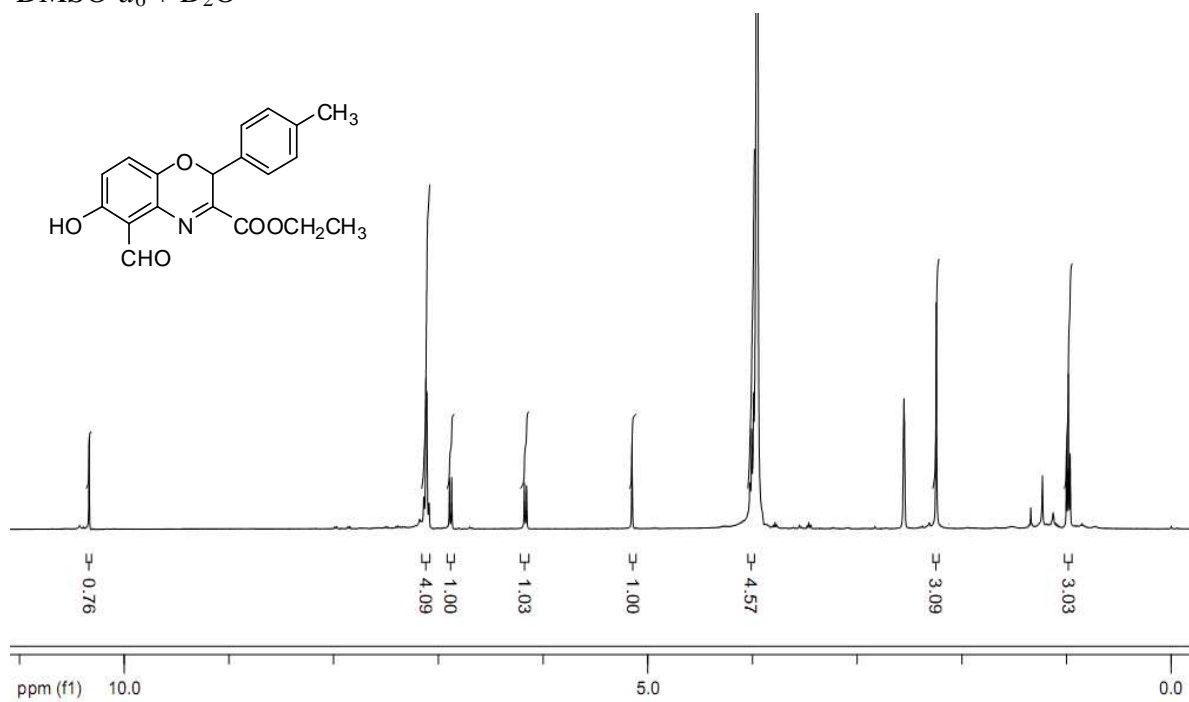
Methyl 2-(4-bromophenyl)-5-formyl-6-hydroxy-2H-benzo[*b*][1,4]oxazine-3-carboxylate (74):¹H NMR (300 MHz, CDCl₃)¹³C NMR (75 MHz, CDCl₃)

Methyl 2-(4-fluorophenyl)-5-formyl-6-hydroxy-2H-benzo[b][1,4]oxazine-3-carboxylate (75):

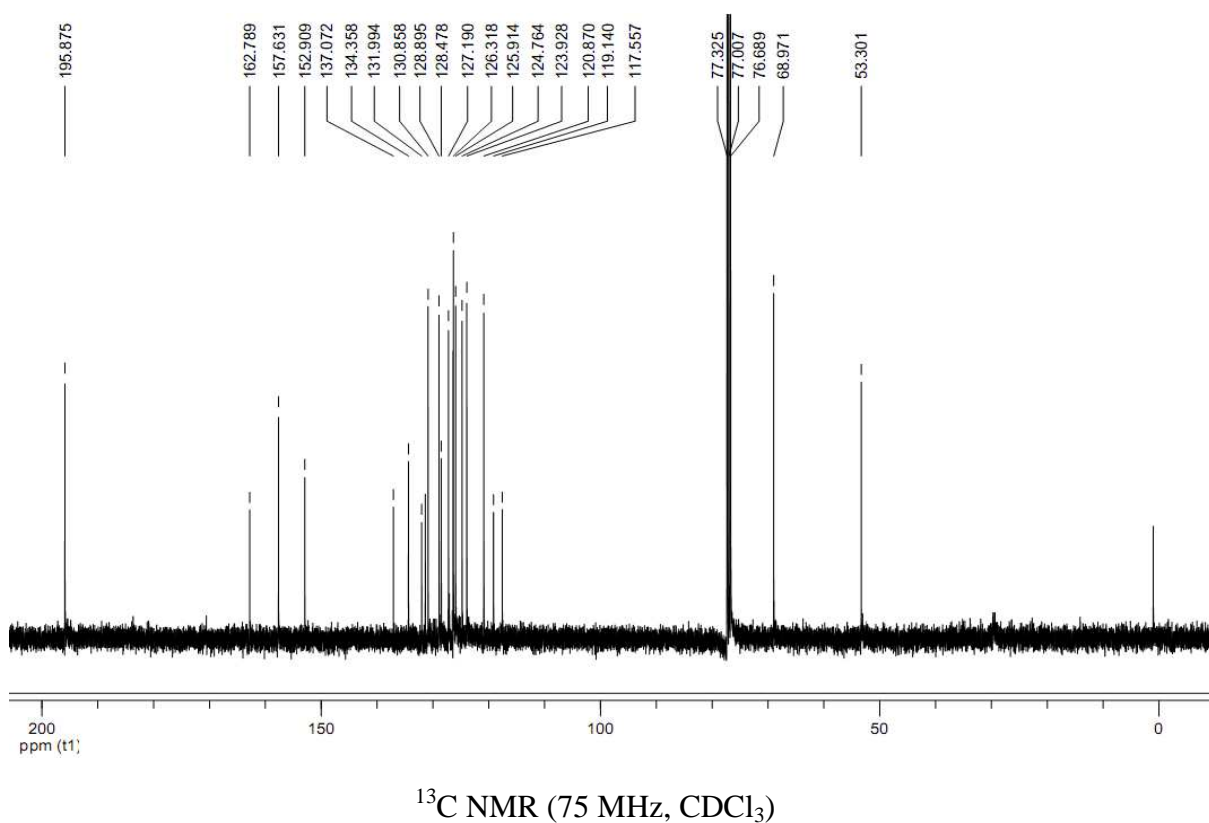
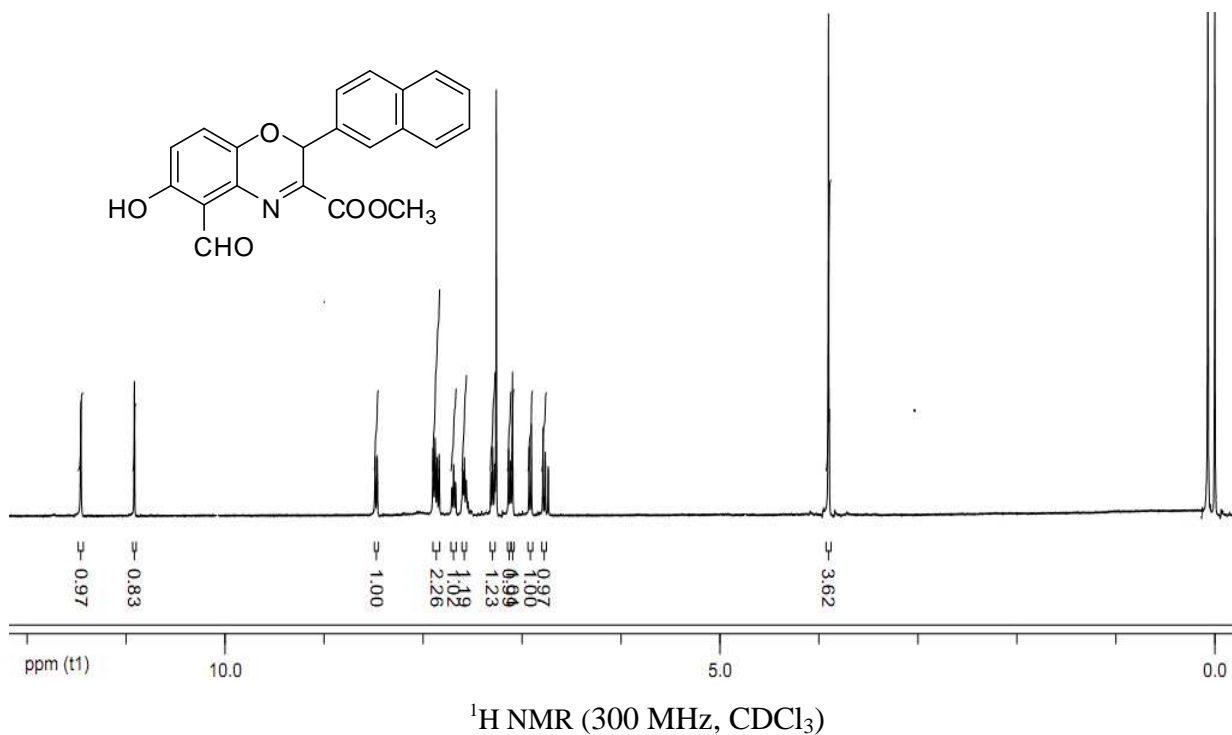


Ethyl 5-formyl-6-hydroxy-2-(p-tolyl)-2H-benzo[b][1,4]oxazine-3-carboxylate (76):

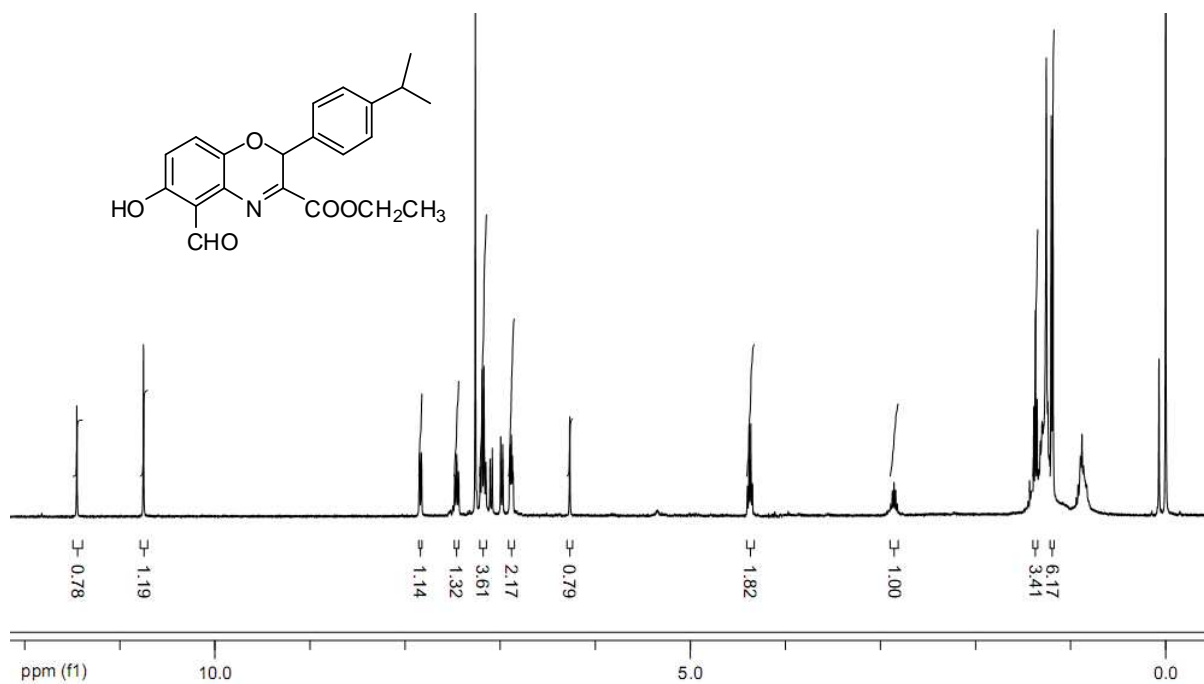
 ^1H NMR (300 MHz, CDCl_3)DMSO- d_6  ^1H NMR (300 MHz, $\text{DMSO-}d_6$)

DMSO- d_6 + D $_2$ O ^{13}C NMR (75 MHz, CDCl_3)

Methyl 5-formyl-6-hydroxy-2-(naphthalen-2-yl)-2H-benzo[b][1,4]oxazine-3 carboxylate (77)

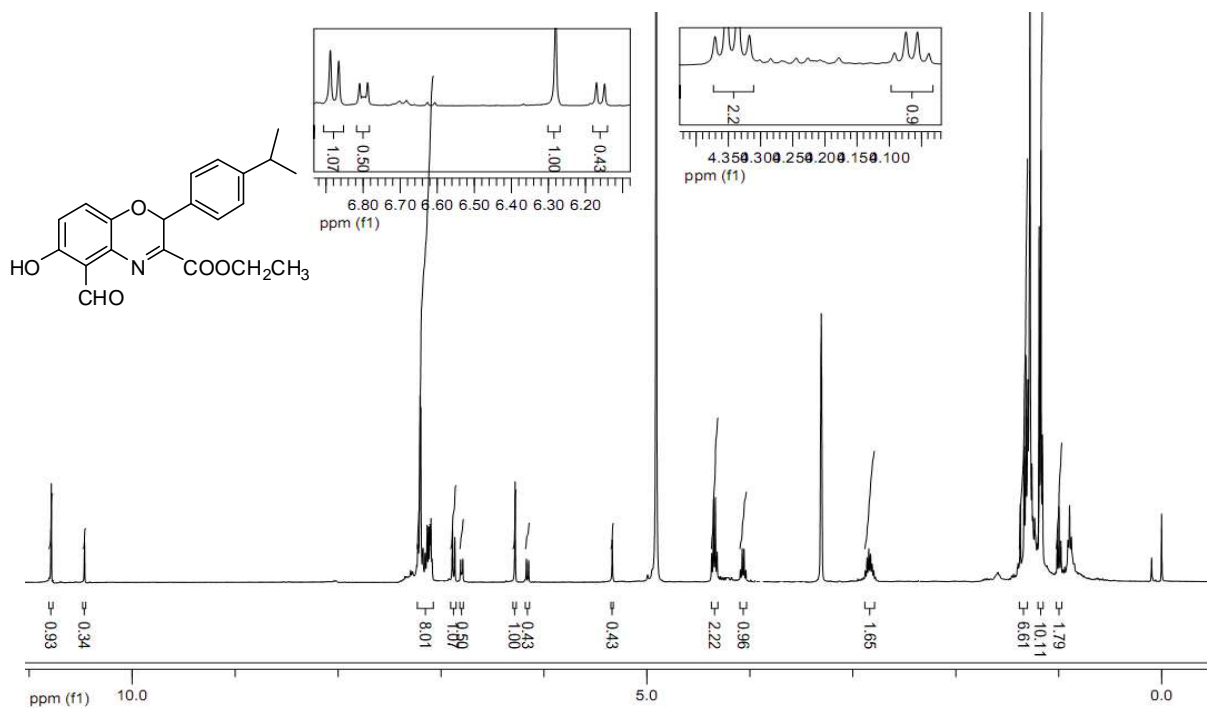


Ethyl 5-formyl-6-hydroxy-2-(4-isopropylphenyl)-2H-benzo[b][1,4]oxazine-3-carboxylate (78):

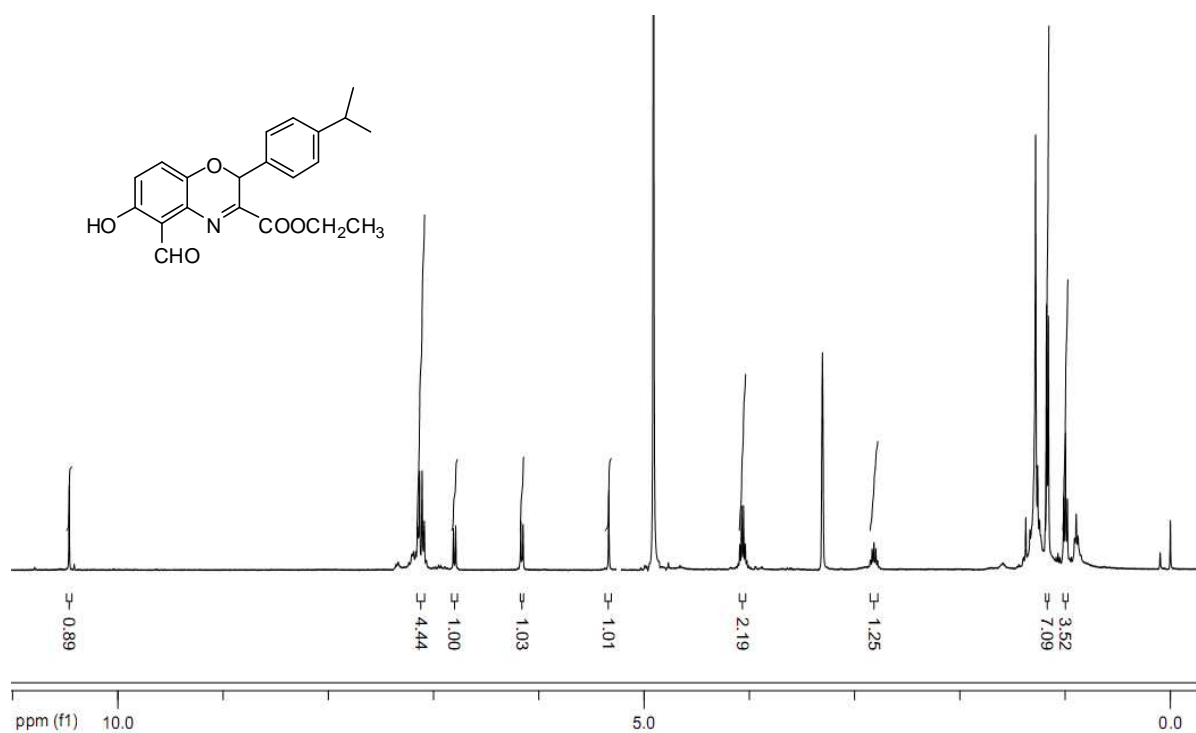
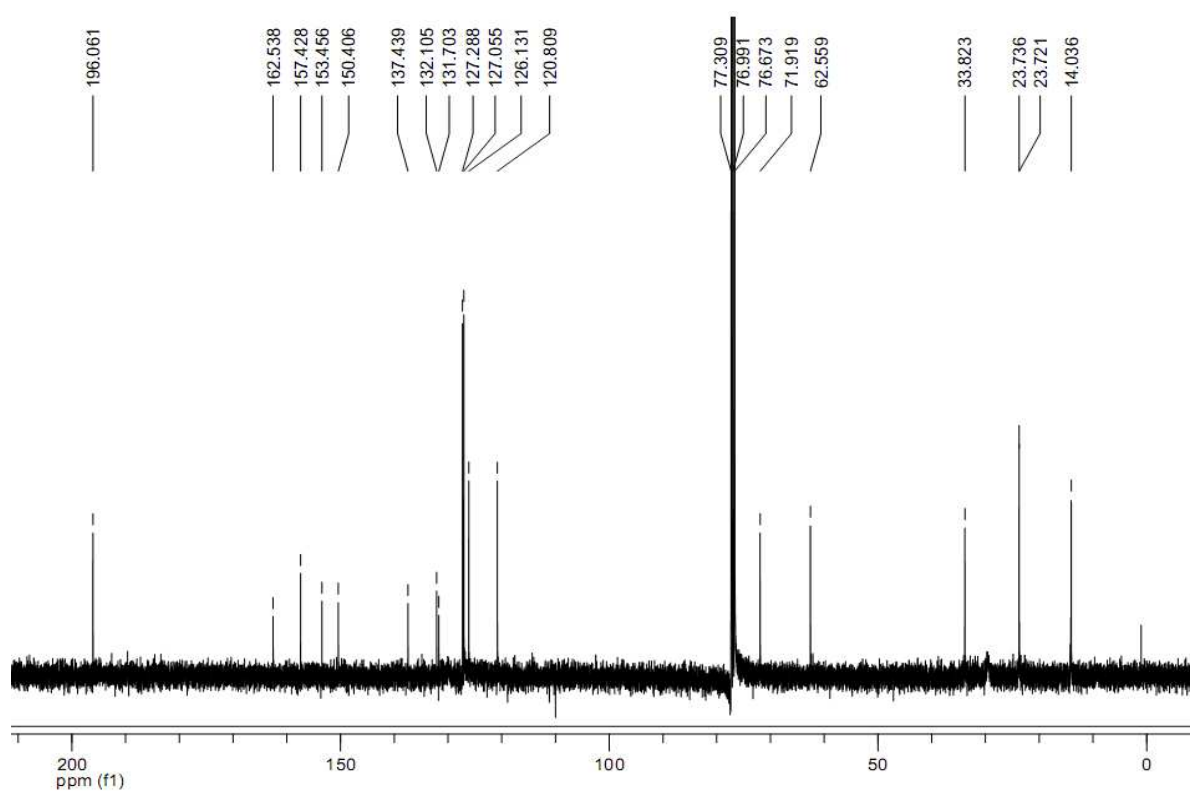


^1H NMR (300 MHz, CDCl_3)

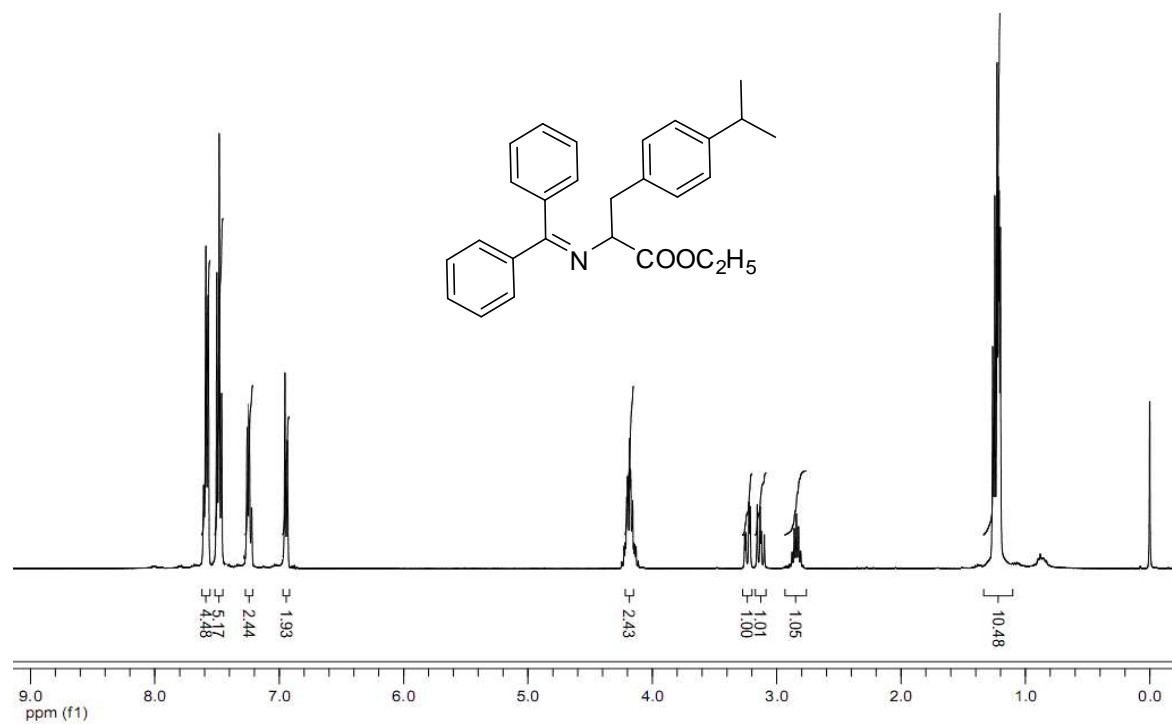
1h after the addition of CD_3OD



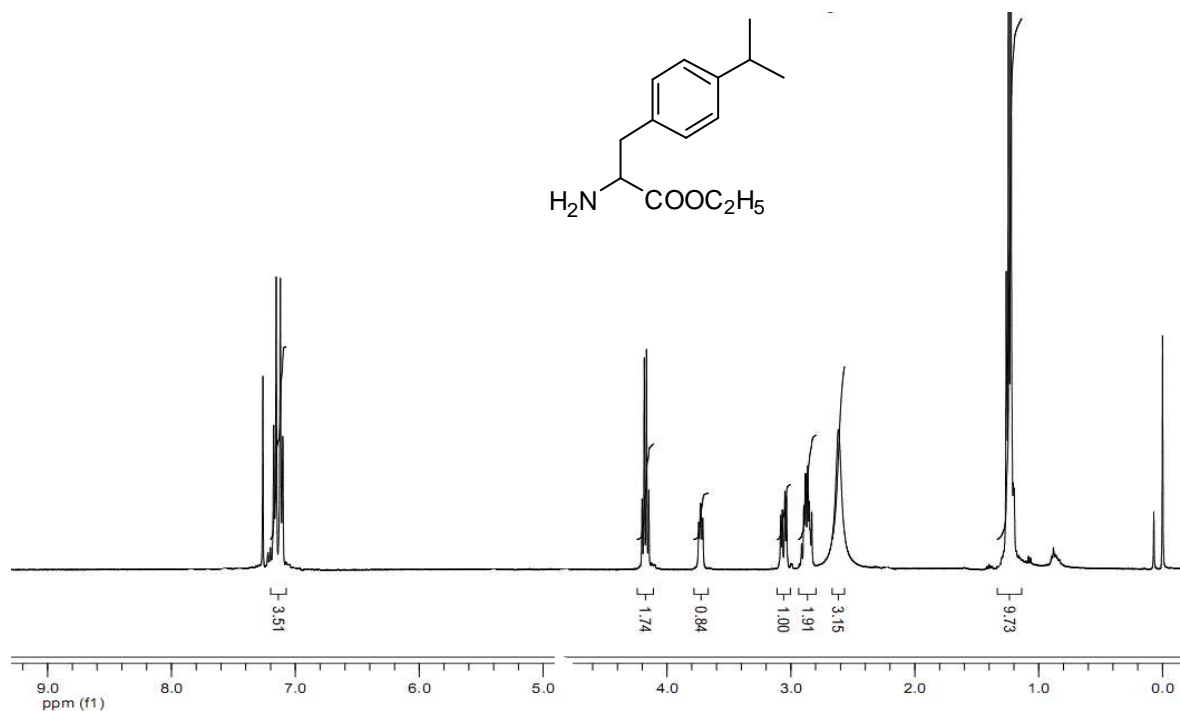
^1H NMR (300 MHz, CD_3OD)

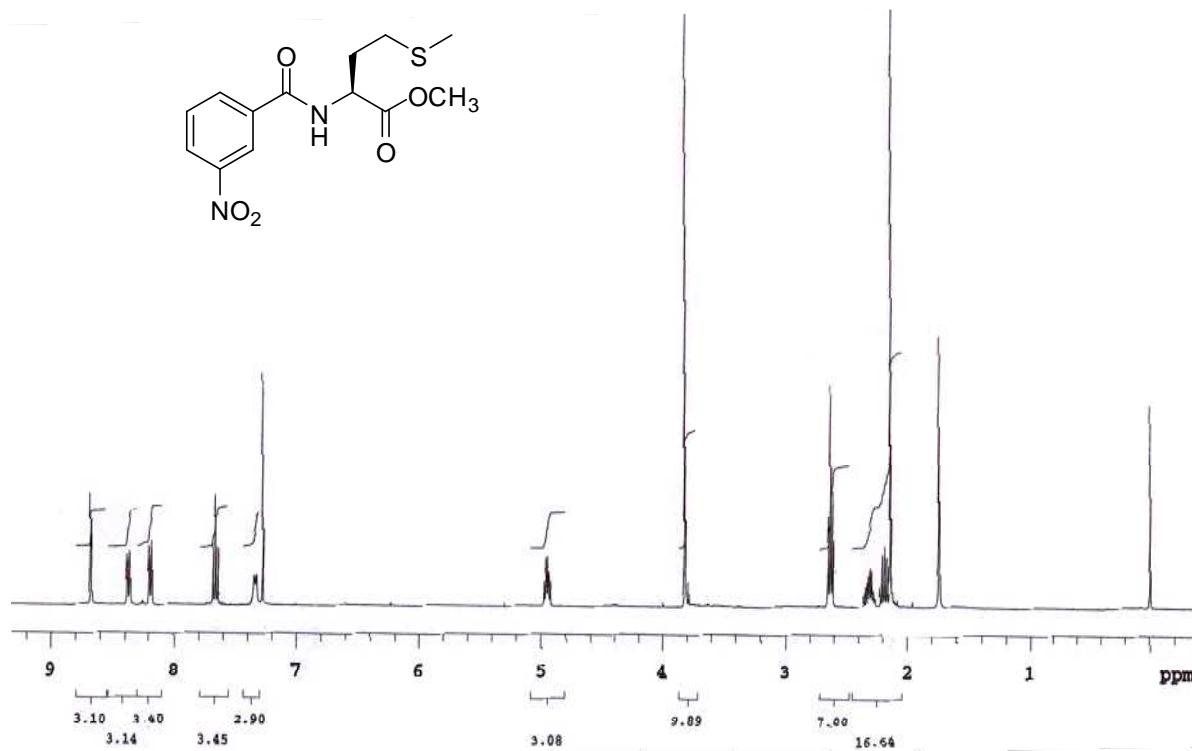
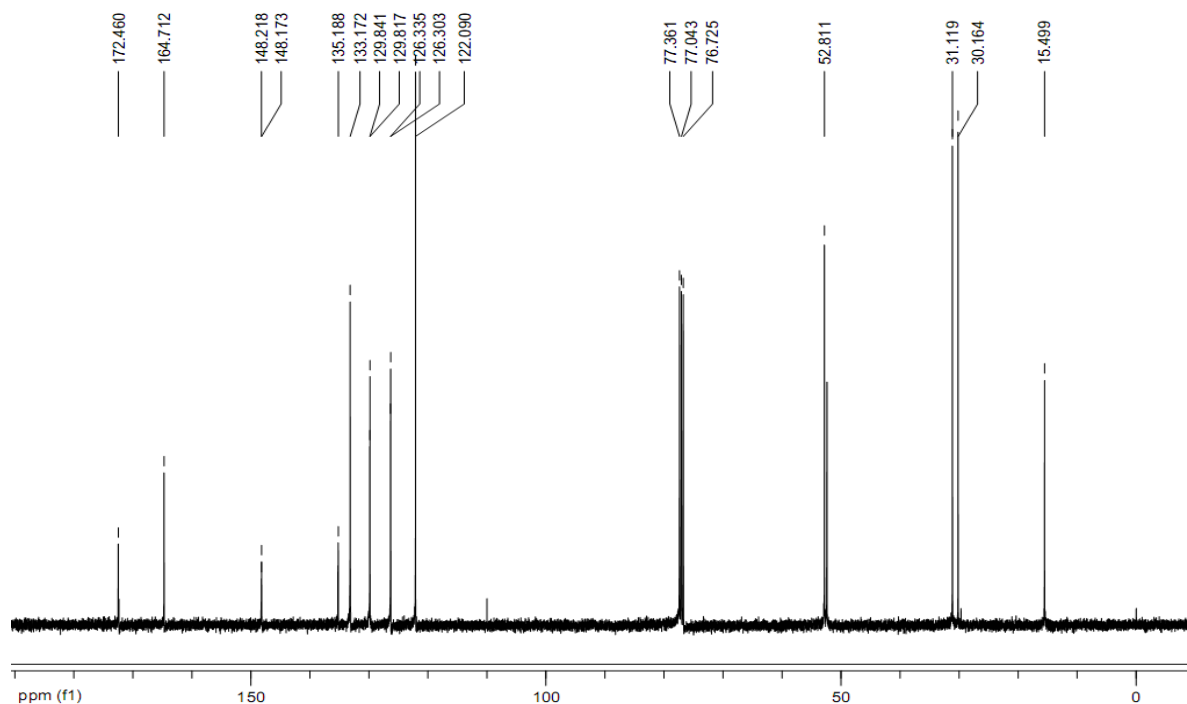
72 h after the addition of CD₃OD:¹H NMR (300 MHz, CD₃OD)¹³C NMR (75 MHz, CDCl₃)

Ethyl 2-(di phenyl methylene amino)-3-(4-isopropylphenyl)propanoate (81):

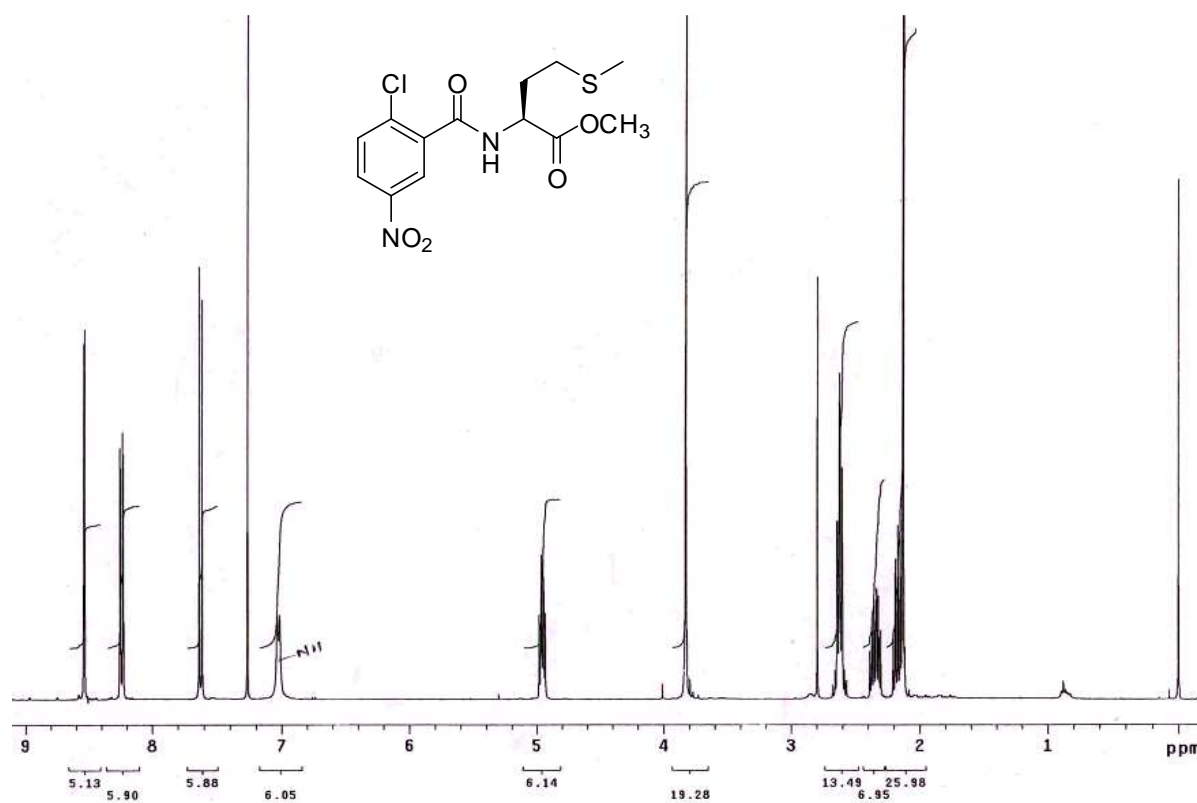
¹H NMR (300 MHz, CDCl₃)

Ethyl 2-amino-3-(4-isopropylphenyl)propanoate (82):

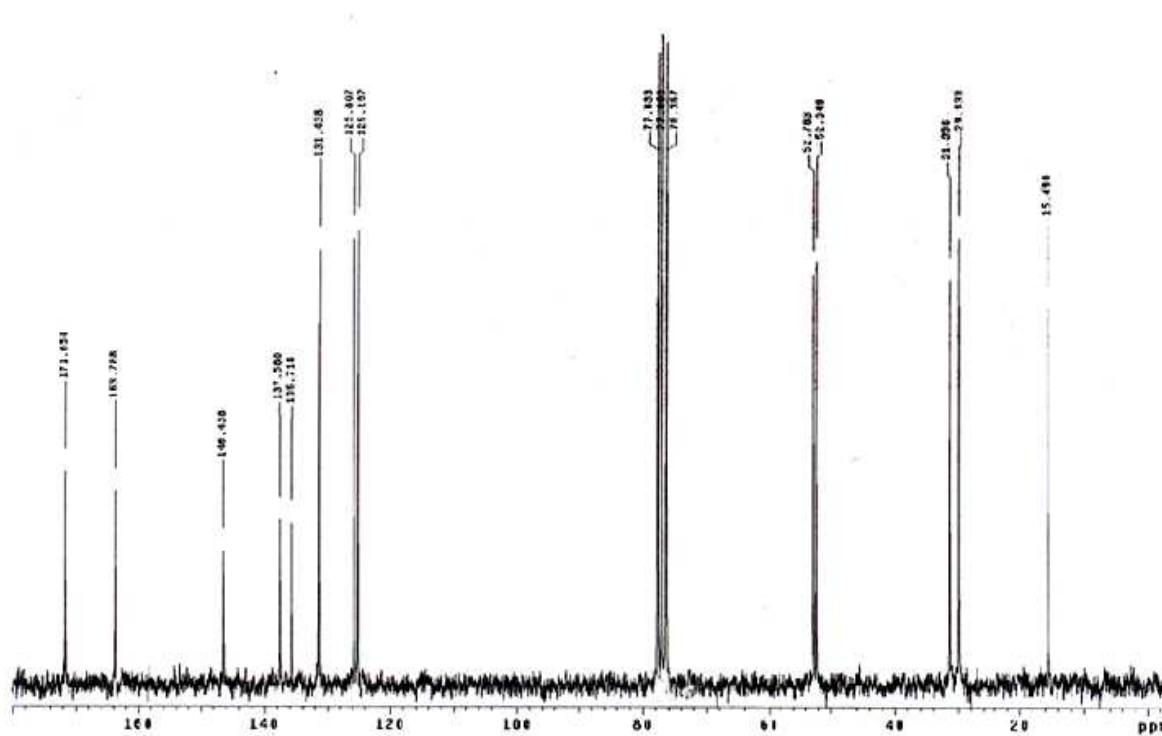
¹H NMR (300 MHz, CDCl₃)

4. Synthesis & pharmacological evolution of substituted phenyl oxazoles as a novel class of LSD1 inhibitors with anti-proliferative properties**Methyl 4-(methylthio)-2-(3-nitrobenzamido)butanoate (2a):****¹H NMR (300 MHz, CDCl₃)****¹³C NMR (75 MHz, CDCl₃)**

(S)-Methyl 2-(2-chloro-5-nitrobenzamido)-4-(methylthio)butanoate (2b):

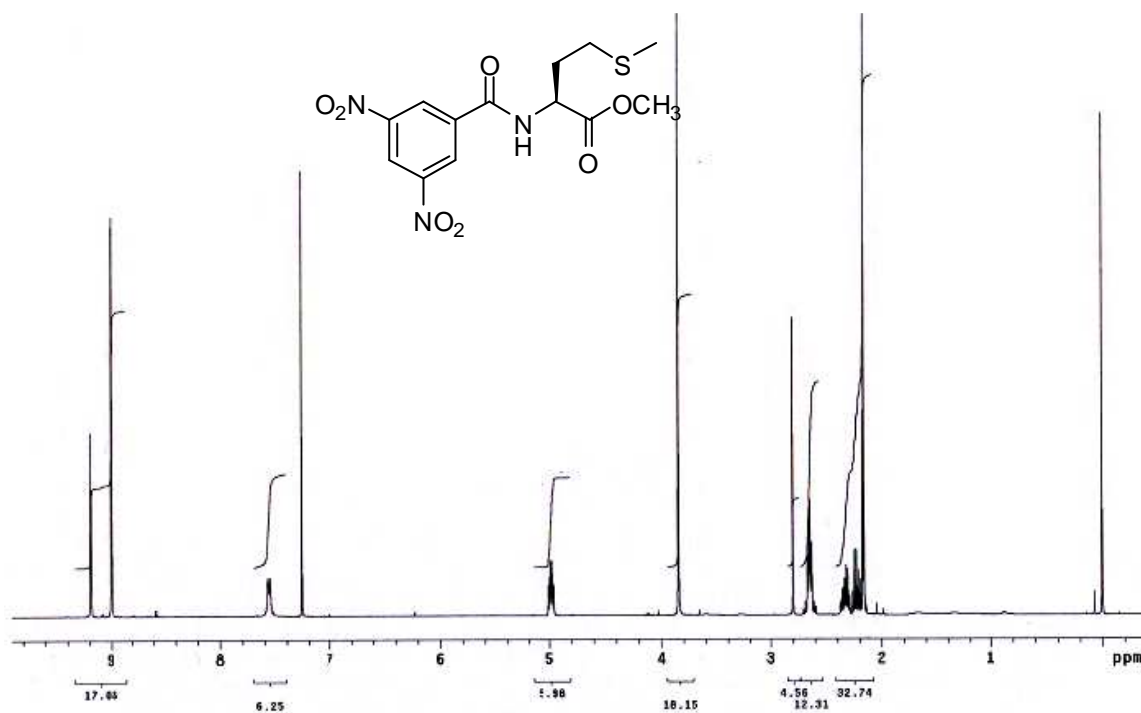


$^1\text{H NMR}$ (300 MHz, CDCl_3)

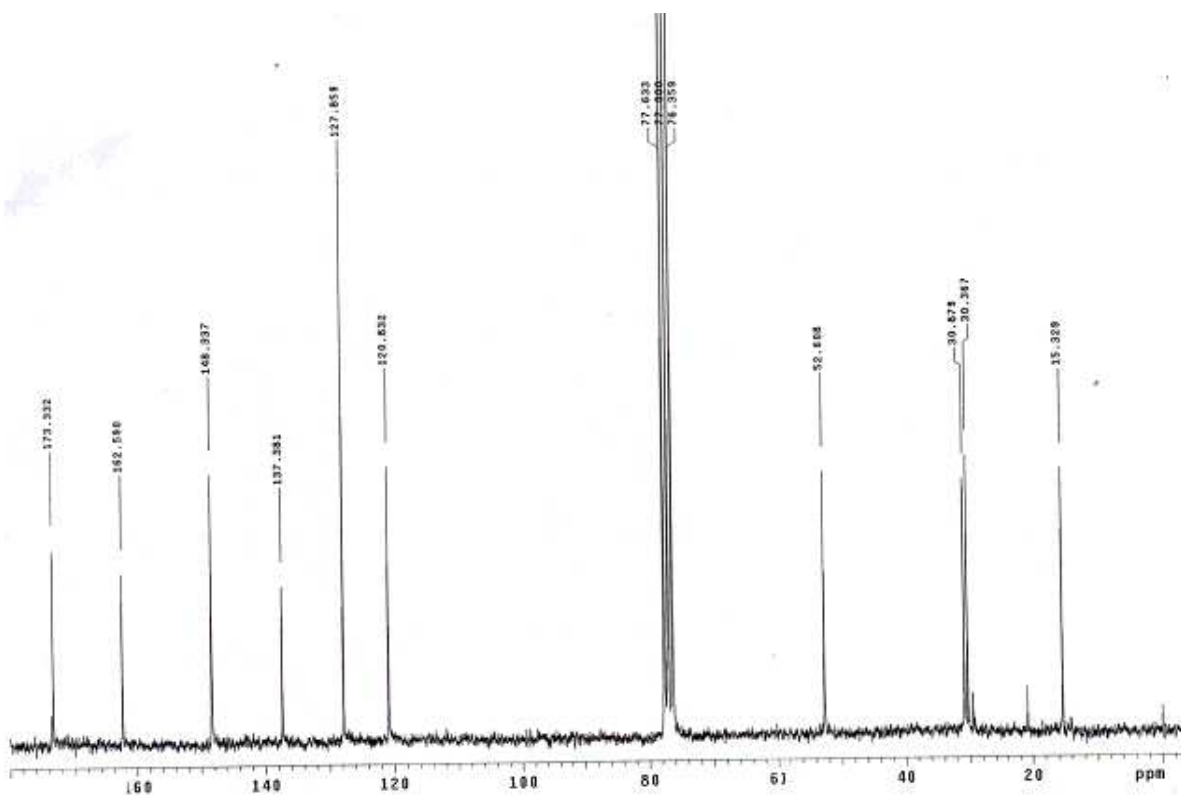


$^{13}\text{C NMR}$ (75 MHz, CDCl_3)

(S)-Methyl 2-(3,5-dinitrobenzamido)-4-(methylthio)butanoate (2c):

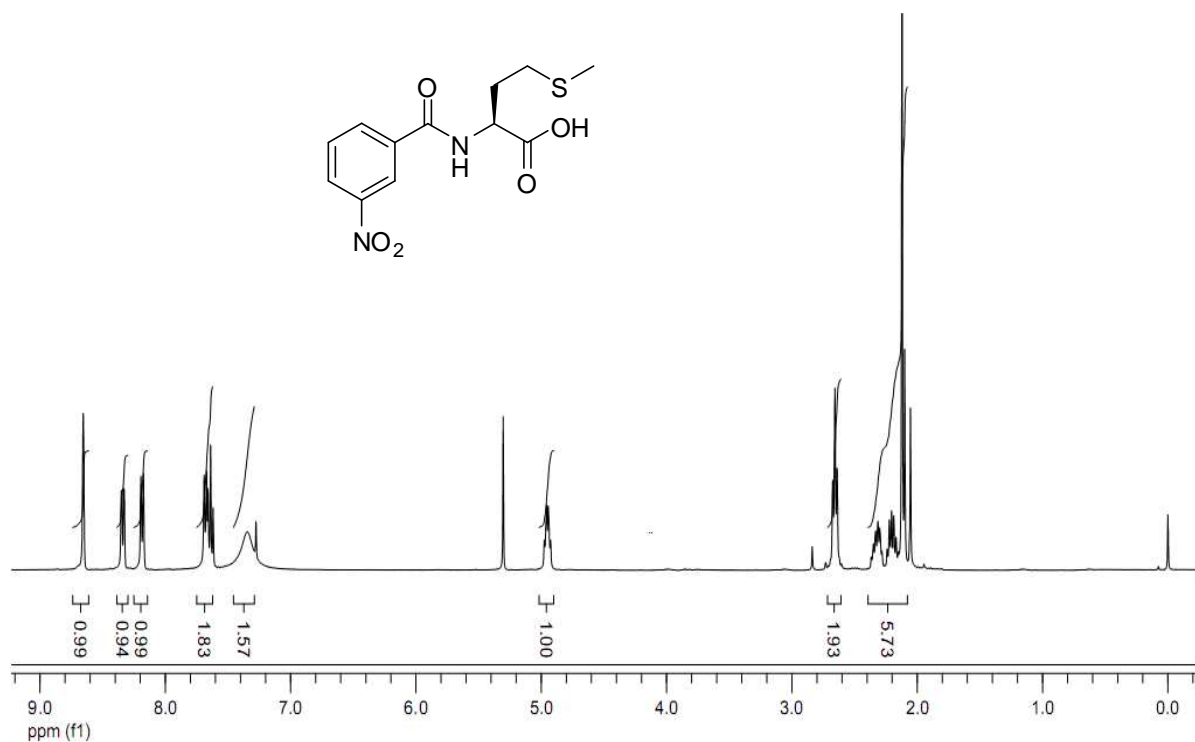
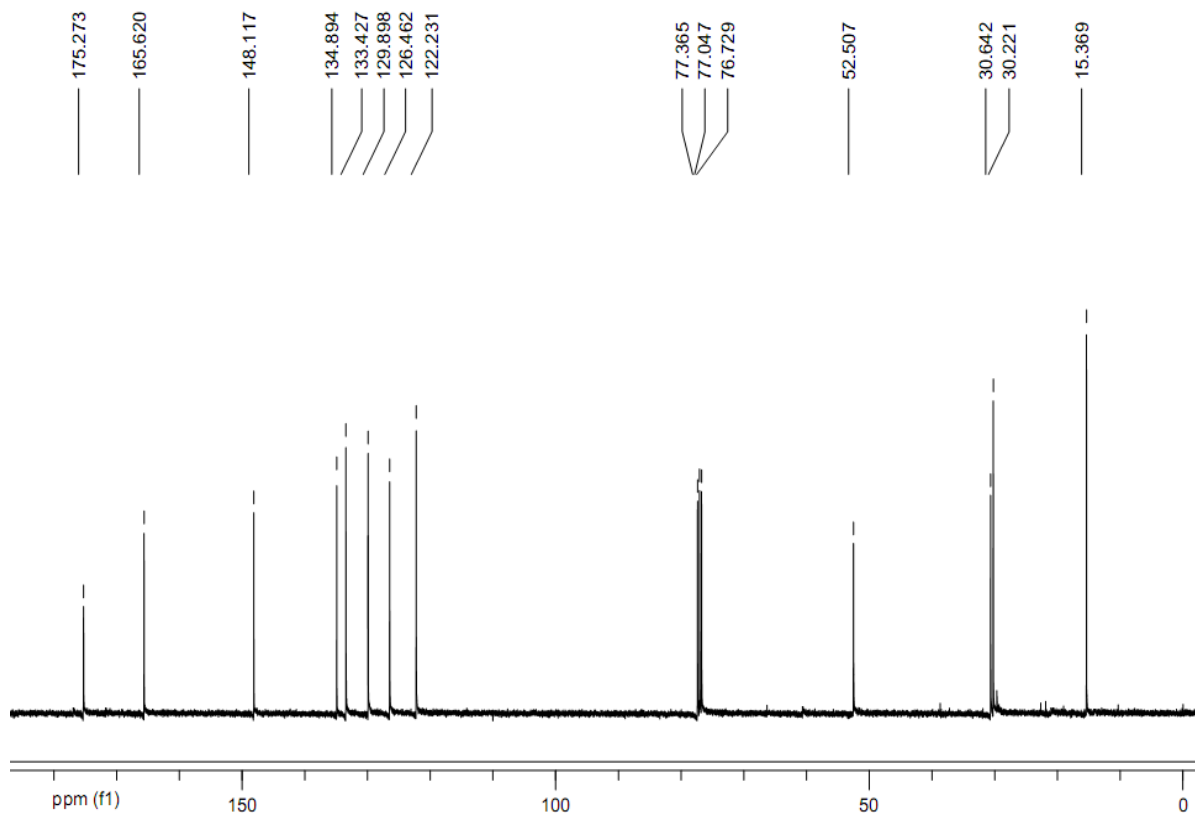


^1H NMR (300 MHz, CDCl_3)

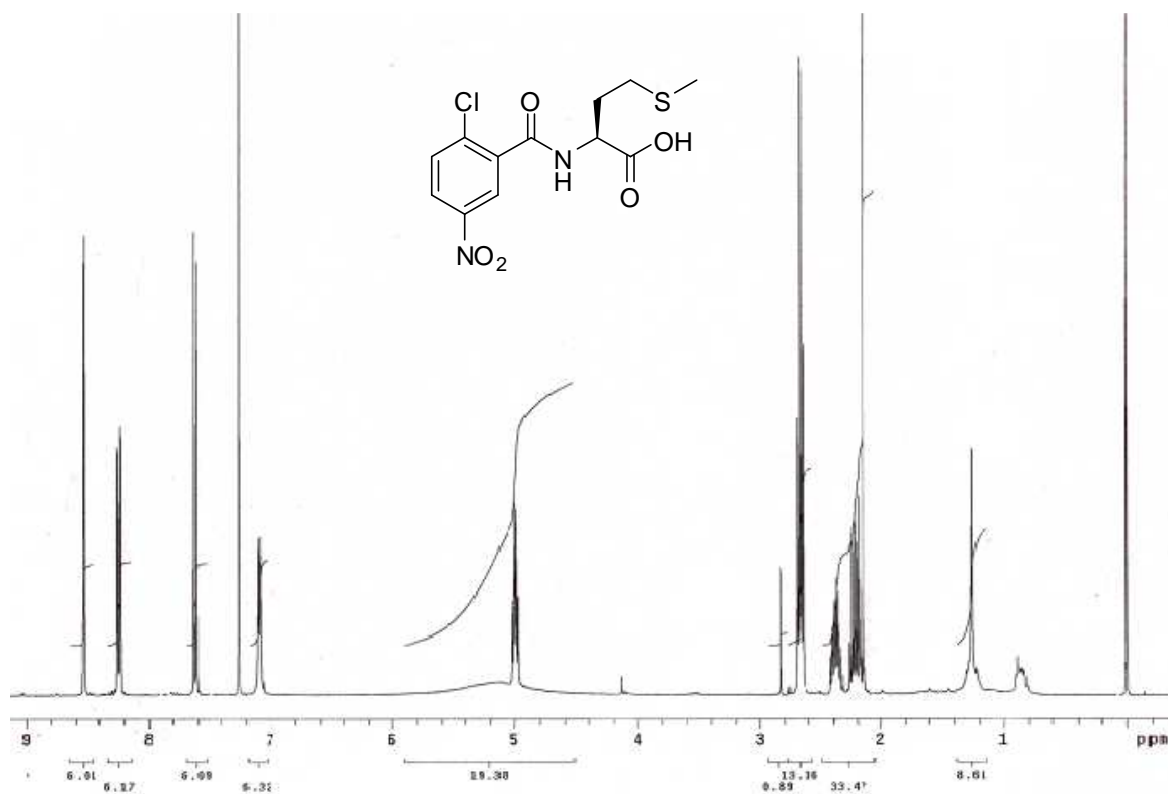


^{13}C NMR (75 MHz, CDCl_3)

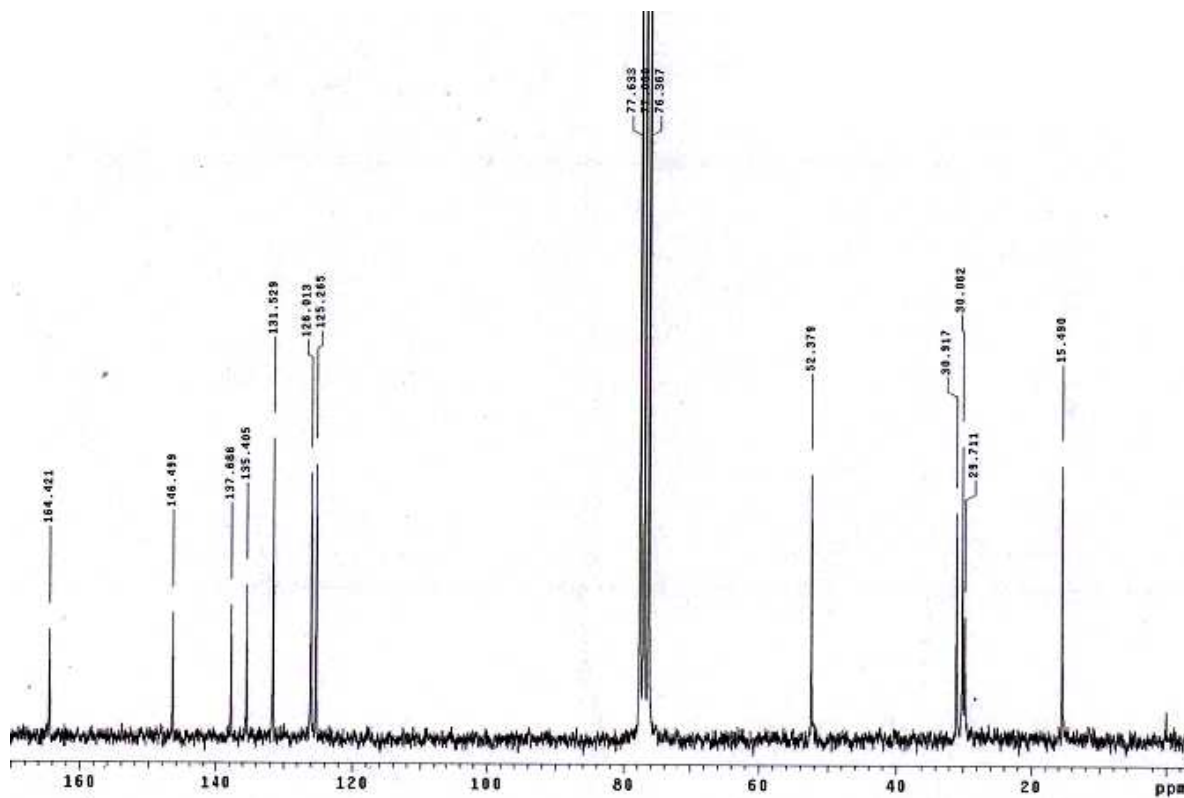
4-(Methylthio)-2-(3-nitrobenzamido)butanoic acid (3a):

¹H NMR (300 MHz, CDCl₃)¹³C NMR (75 MHz, CDCl₃)

(S)-2-(2-chloro-5-nitrobenzamido)-4-(methylthio)butanoic acid (3b):

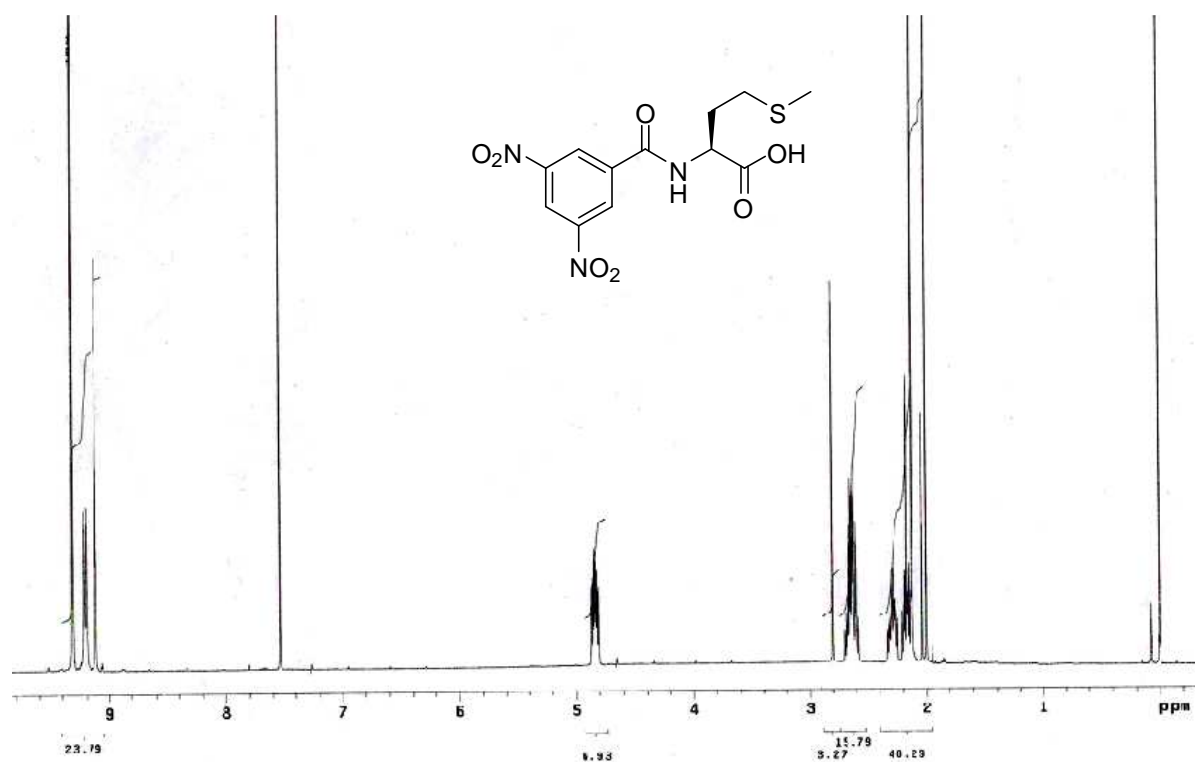


¹H NMR (300 MHz, CDCl₃)

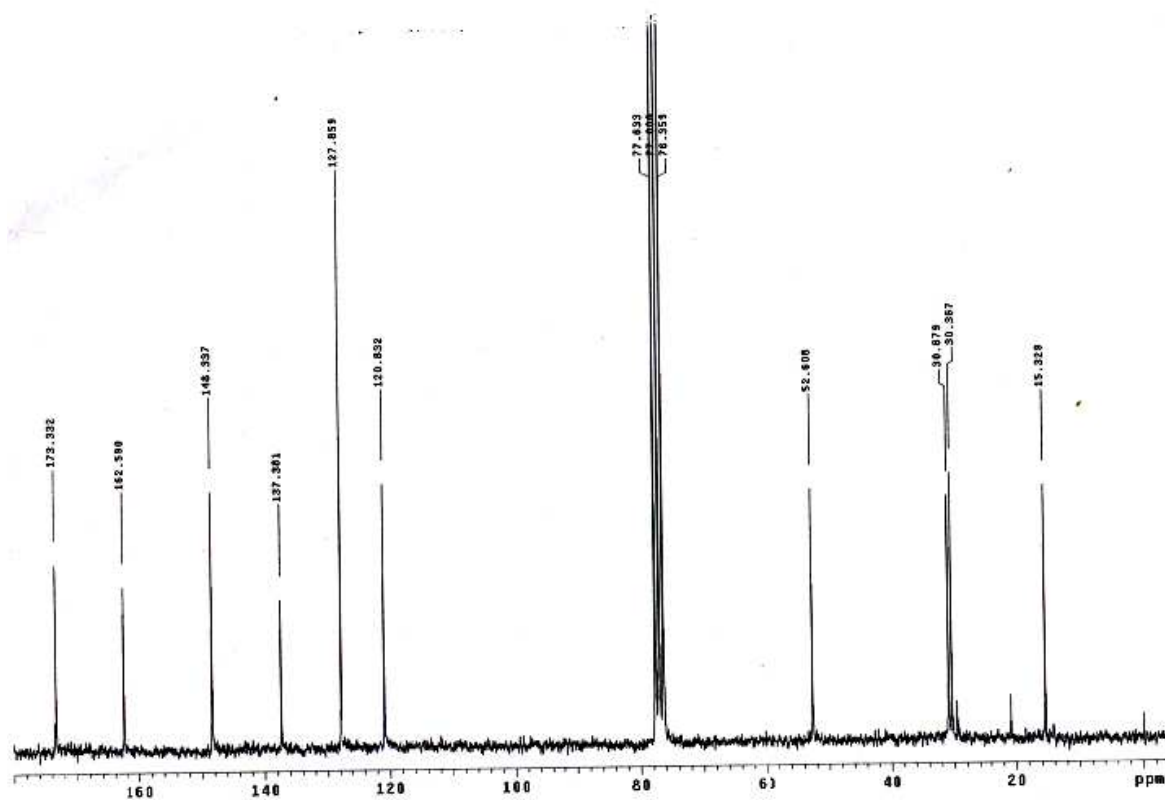


¹³C NMR (75 MHz, CDCl₃)

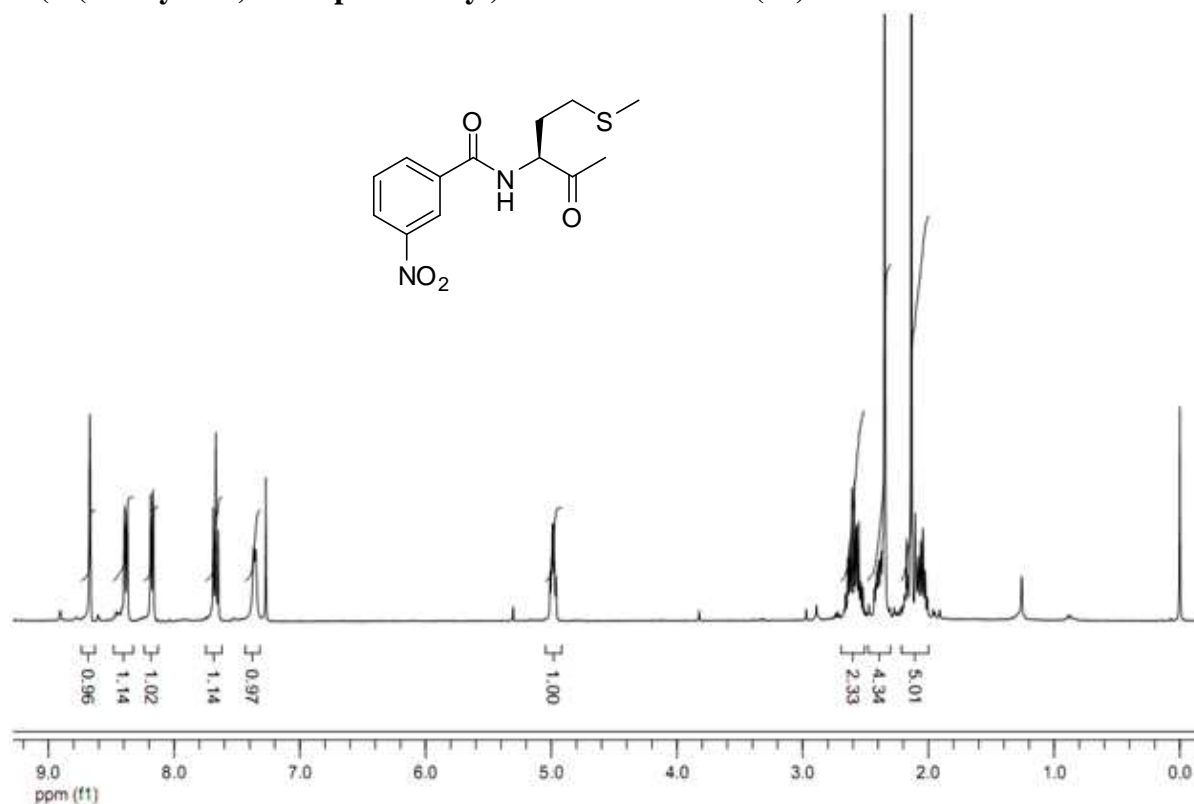
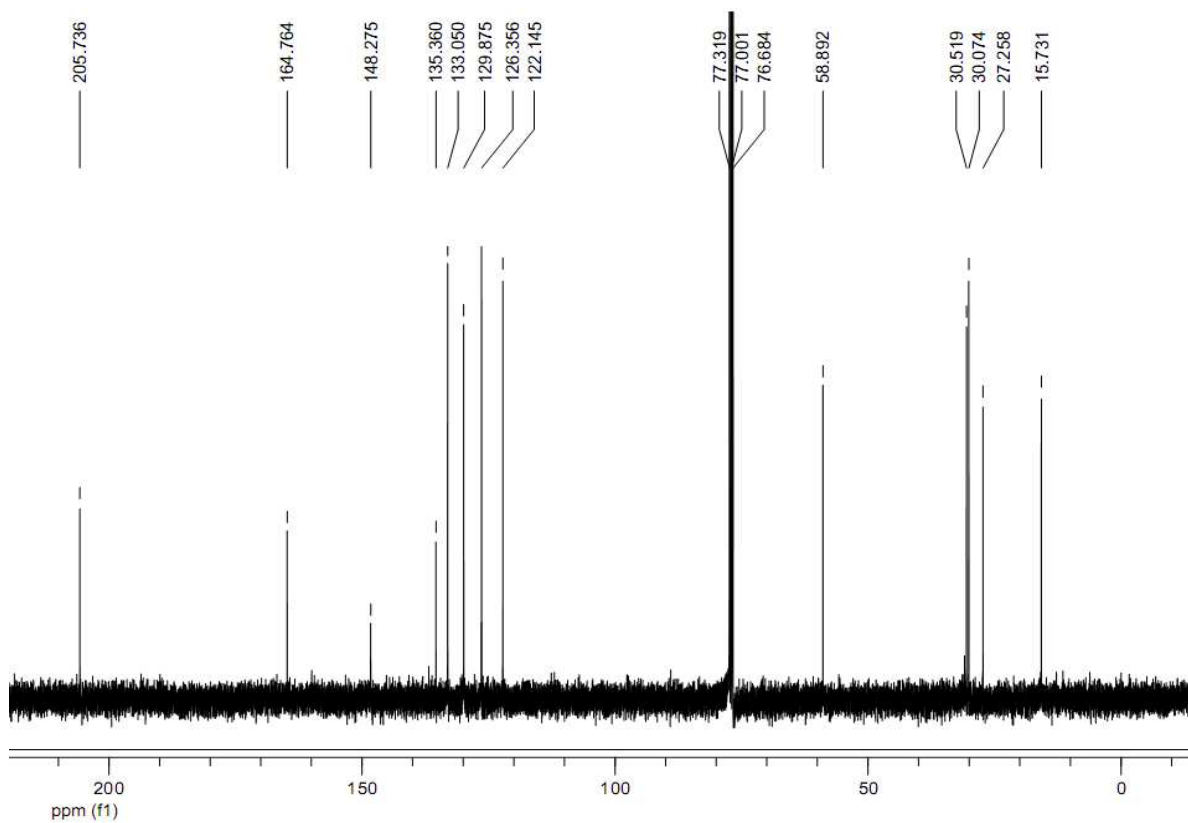
(S)-2-(3, 5-dinitrobenzamido)-4-(methylthio)butanoic acid (3c):



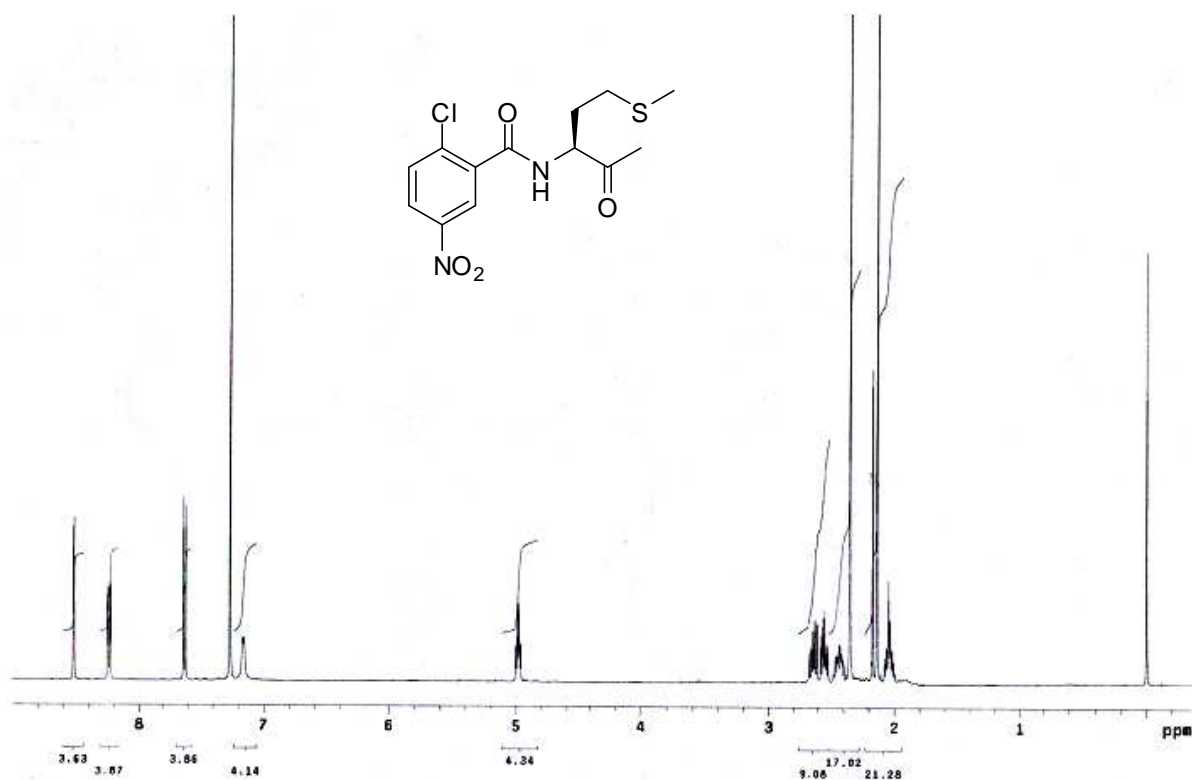
$^1\text{H NMR}$ (300 MHz, CDCl_3)



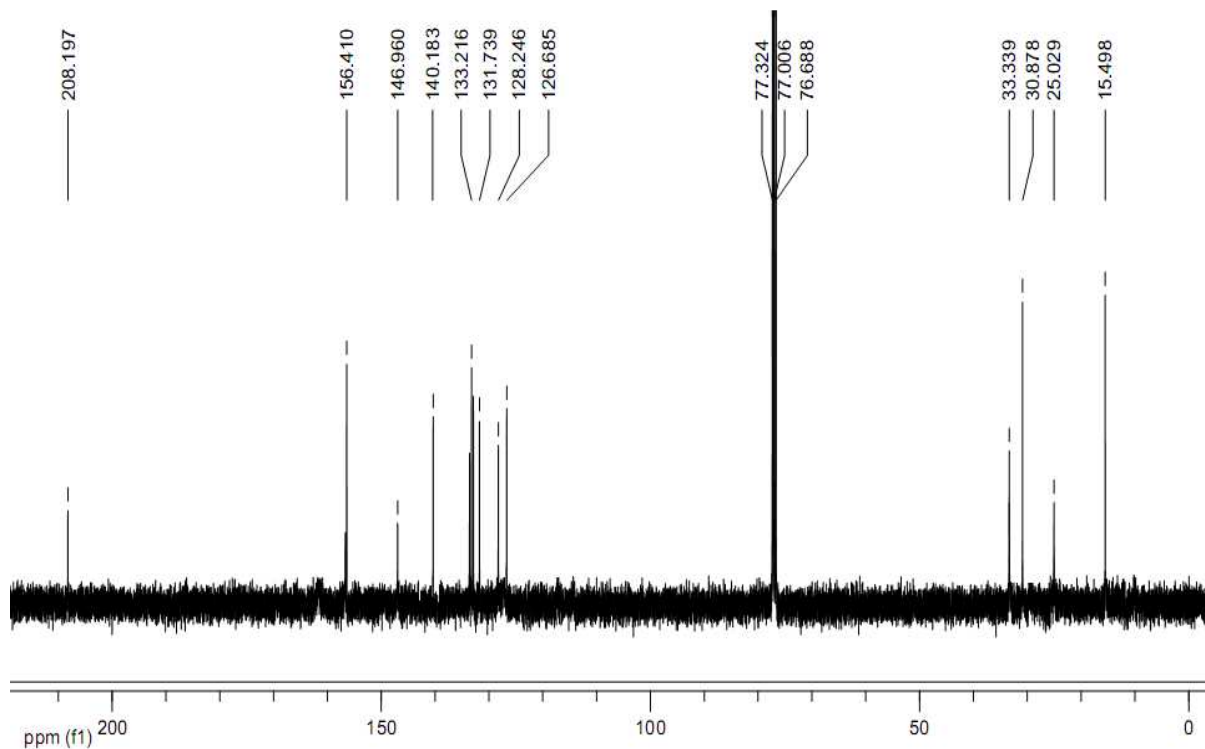
$^{13}\text{C NMR}$ (75 MHz, CDCl_3)

N-(1-(Methylthio)-4-oxopentan-3-yl)-3-nitrobenzamide(4a):**¹H NMR (300 MHz, CDCl₃)****¹³C NMR (75 MHz, CDCl₃)**

(S)-2-chloro-N-(1-(methylthio)-4-oxopentan-3-yl)-5-nitrobenzamide (4b):

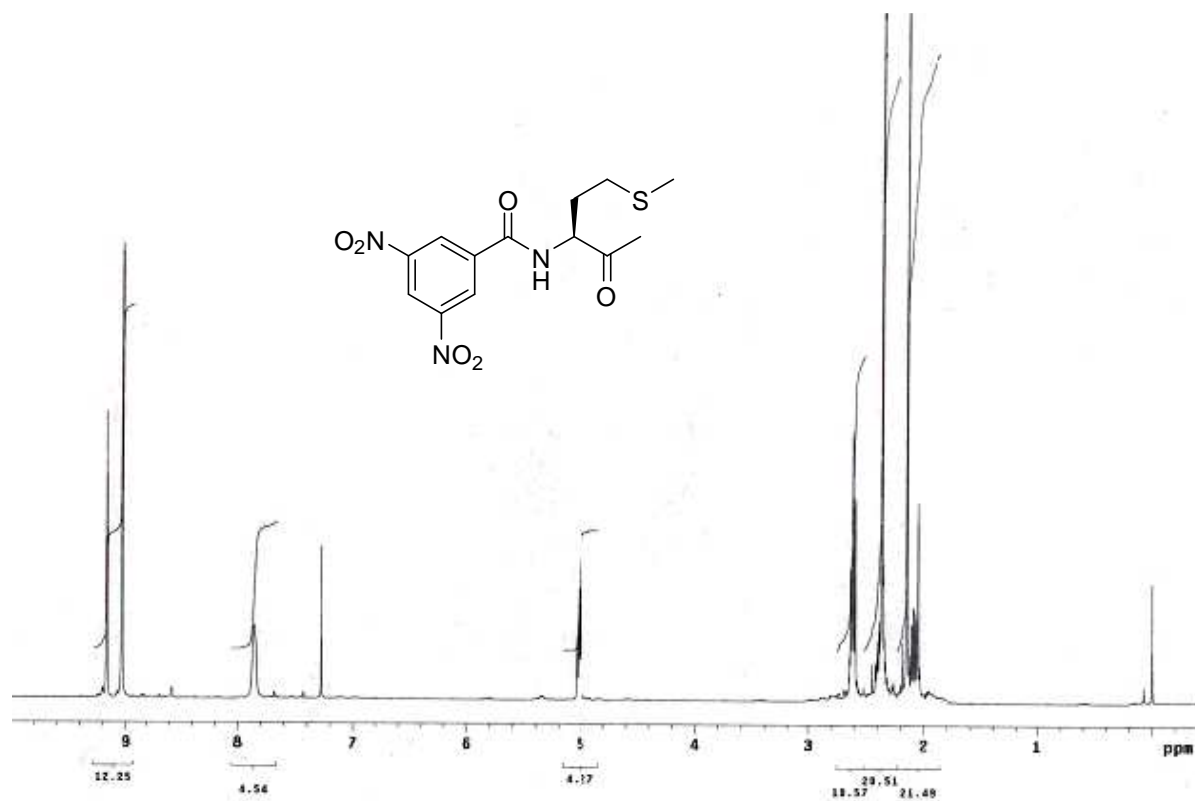


¹H NMR (300 MHz, CDCl₃)

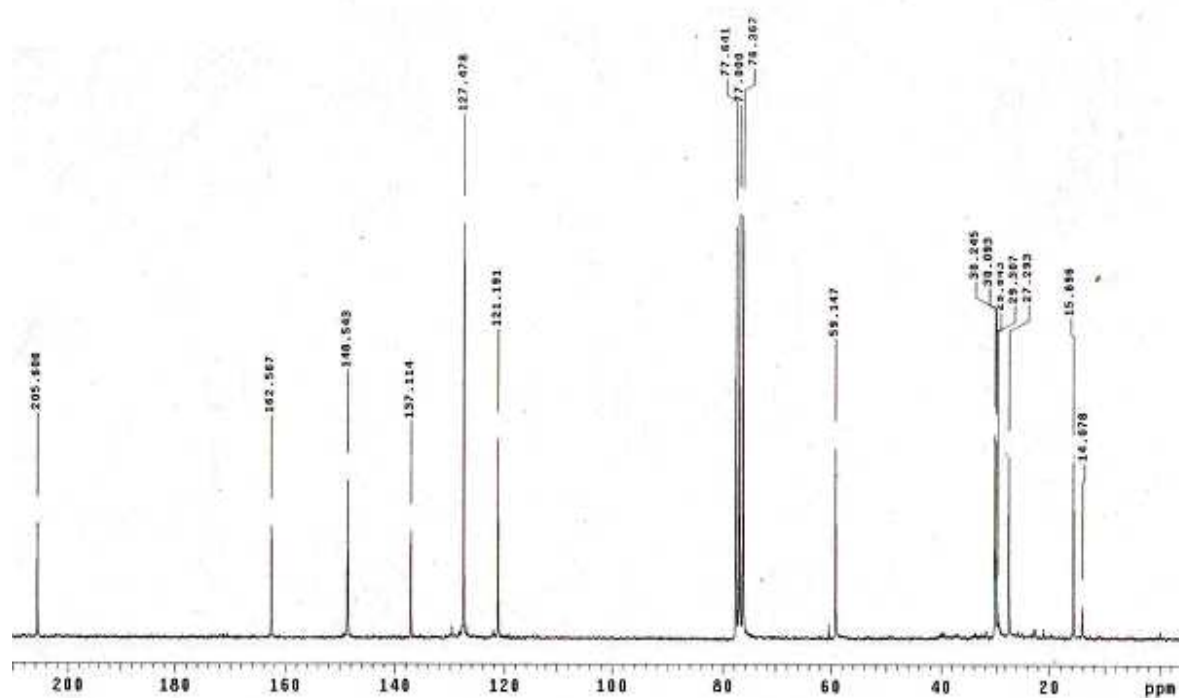


¹³C NMR (75 MHz, CDCl₃)

(S)-N-(1-(methylthio)-4-oxopentan-3-yl)-3,5-dinitrobenzamide (4c):

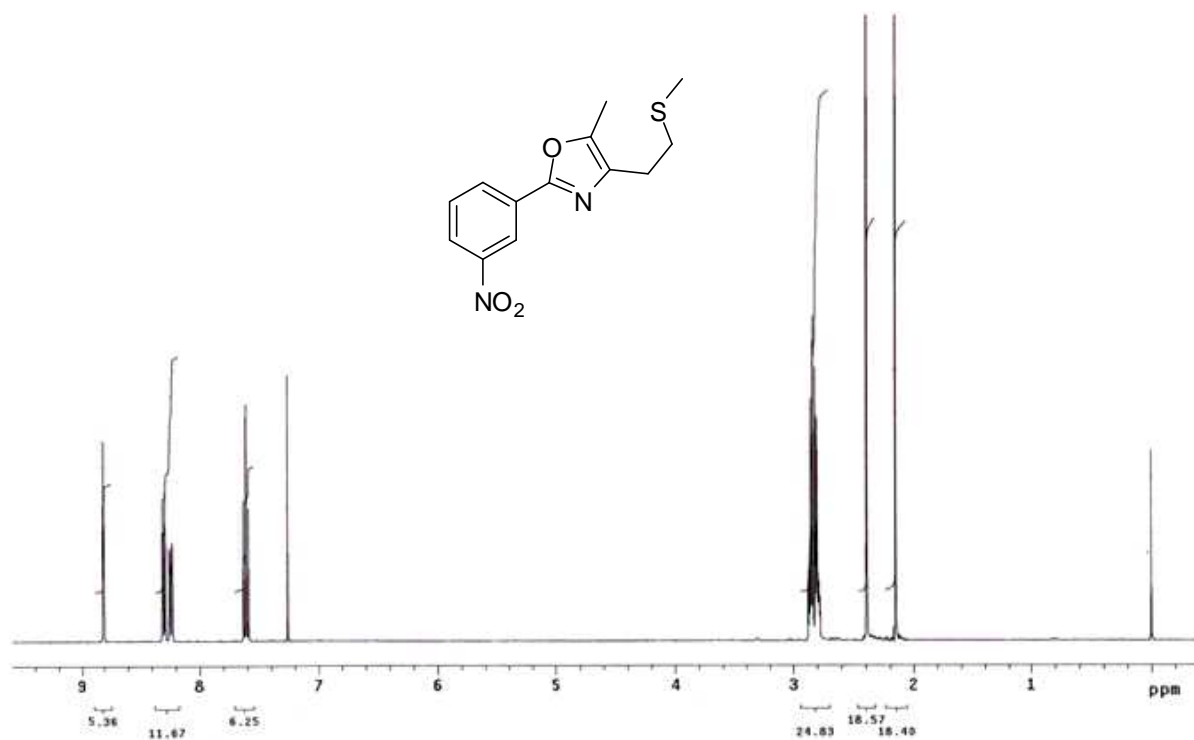
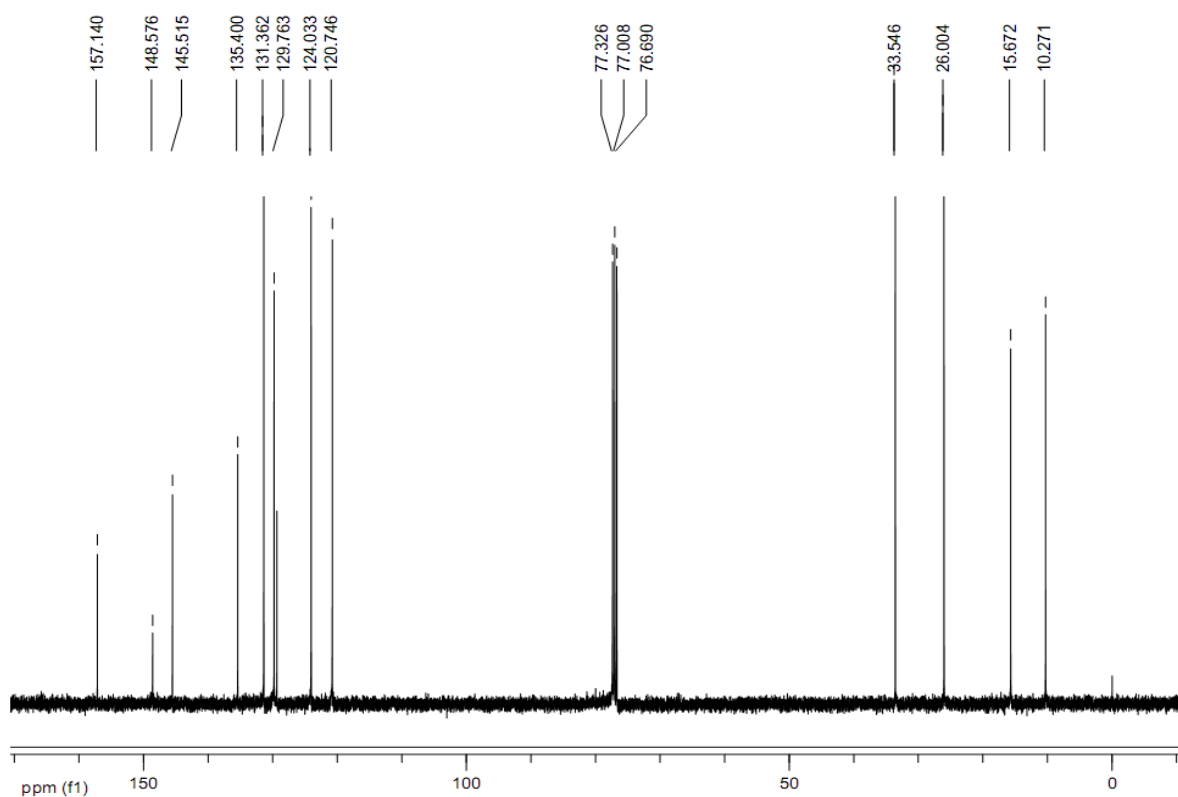


$^1\text{H NMR}$ (300 MHz, CDCl_3)

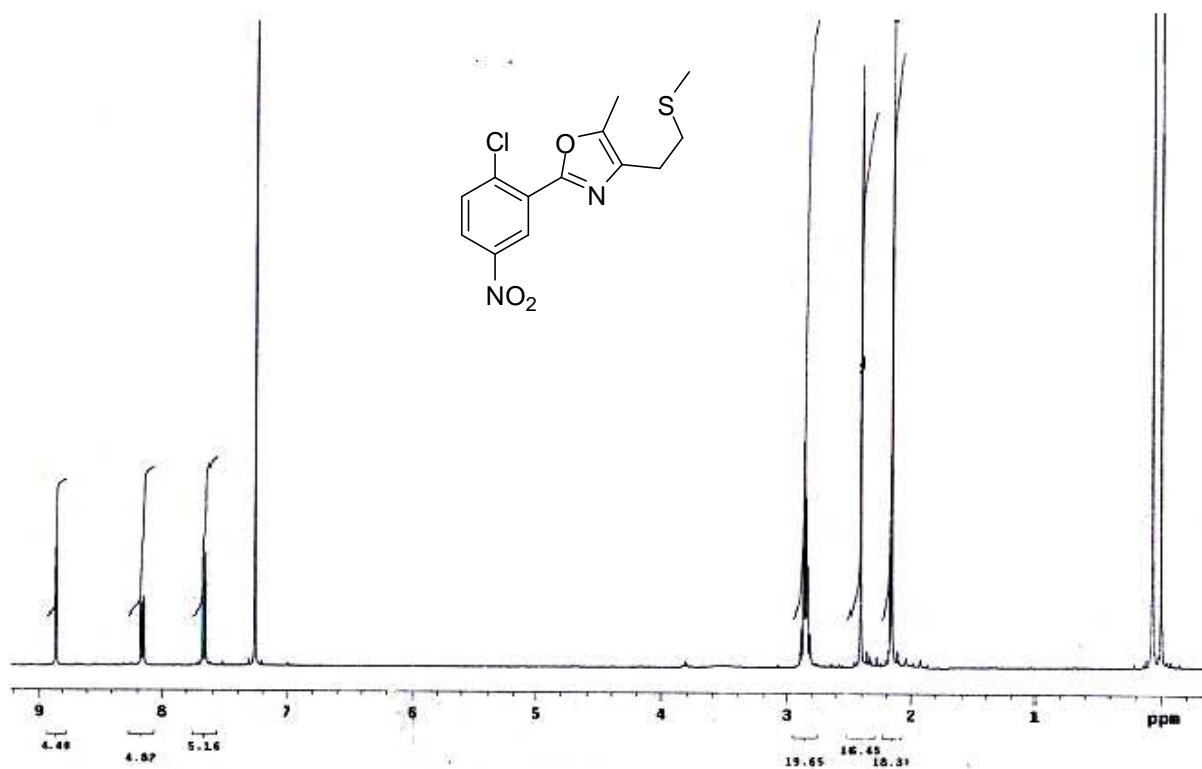
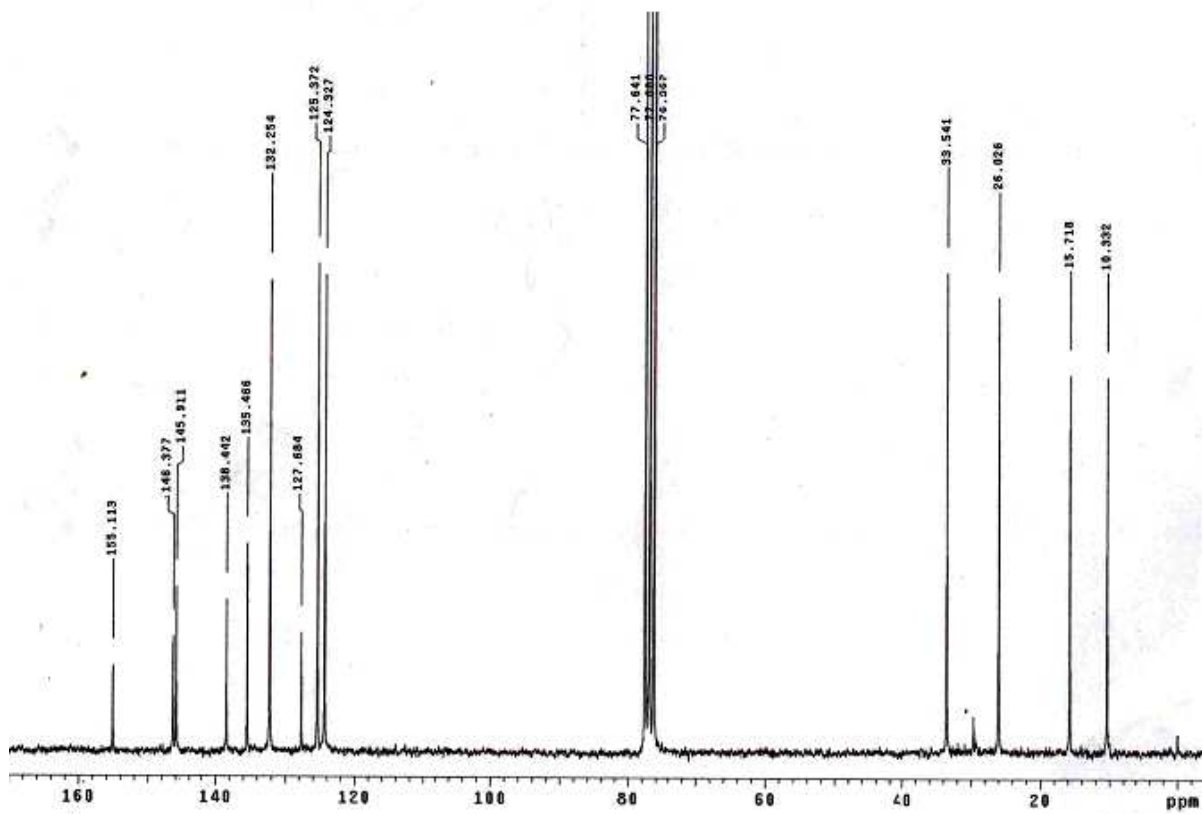


$^{13}\text{C NMR}$ (75 MHz, CDCl_3)

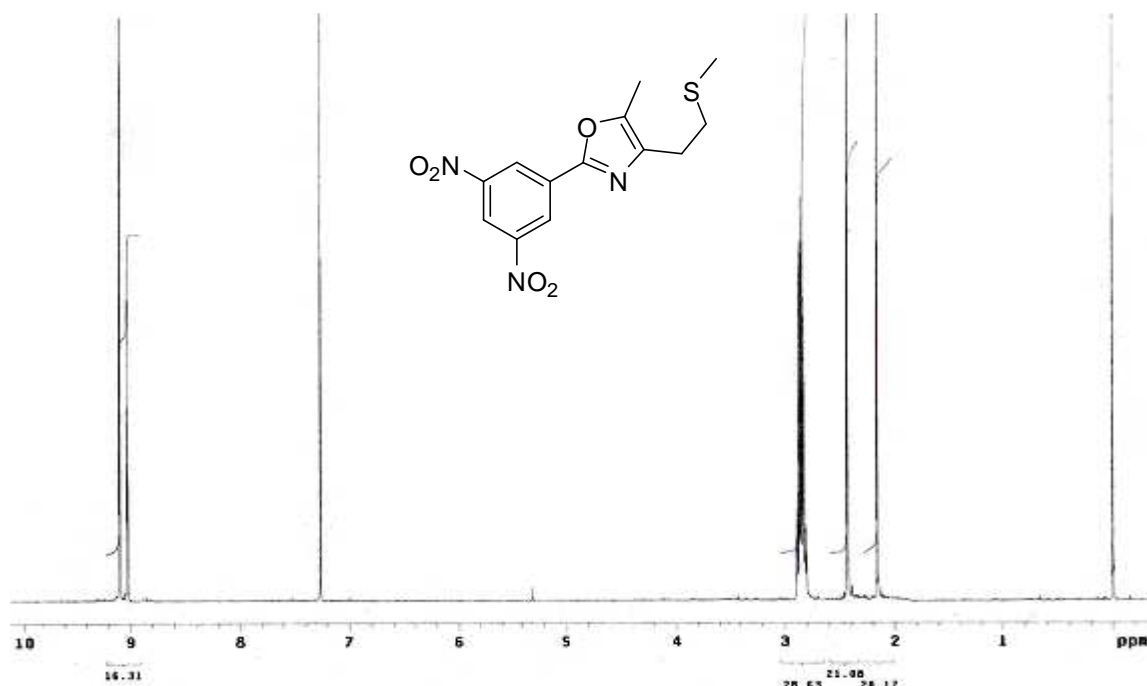
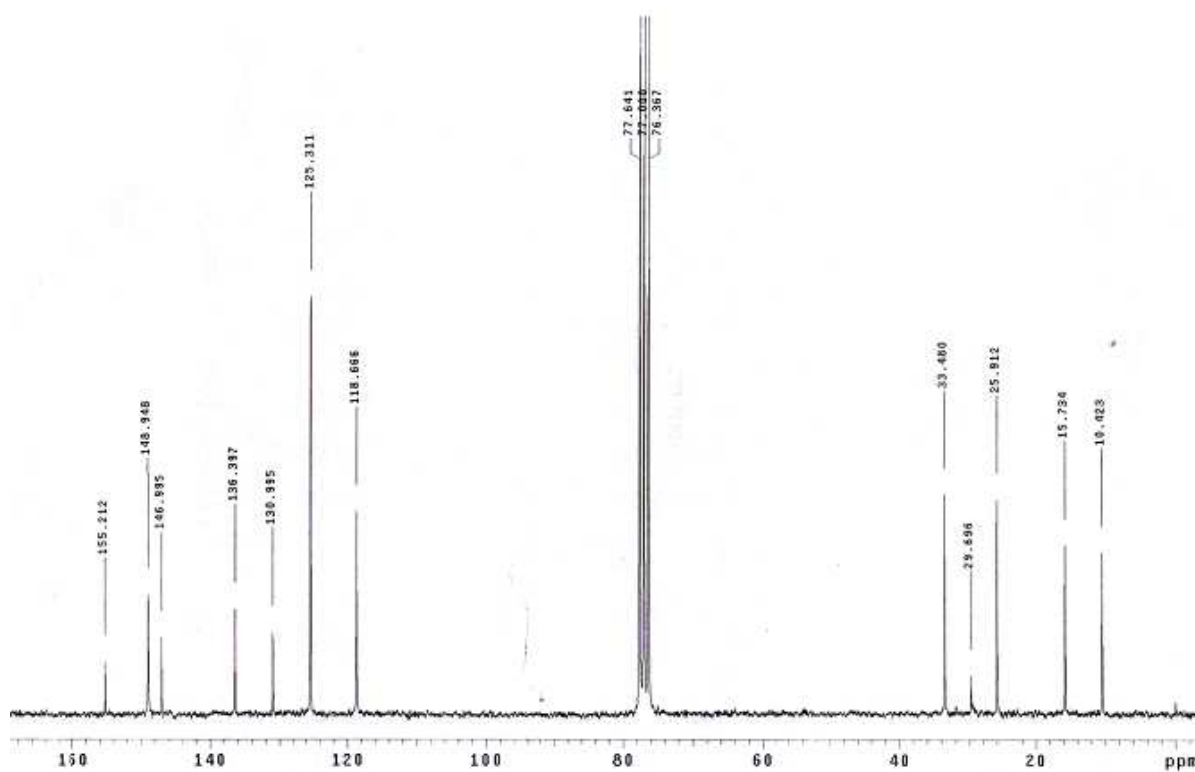
5-Methyl-4-(2-(methylthio) ethyl)-2-(3-nitrophenyl) oxazole (5a):

 $^1\text{H NMR}$ (300 MHz, CDCl_3)

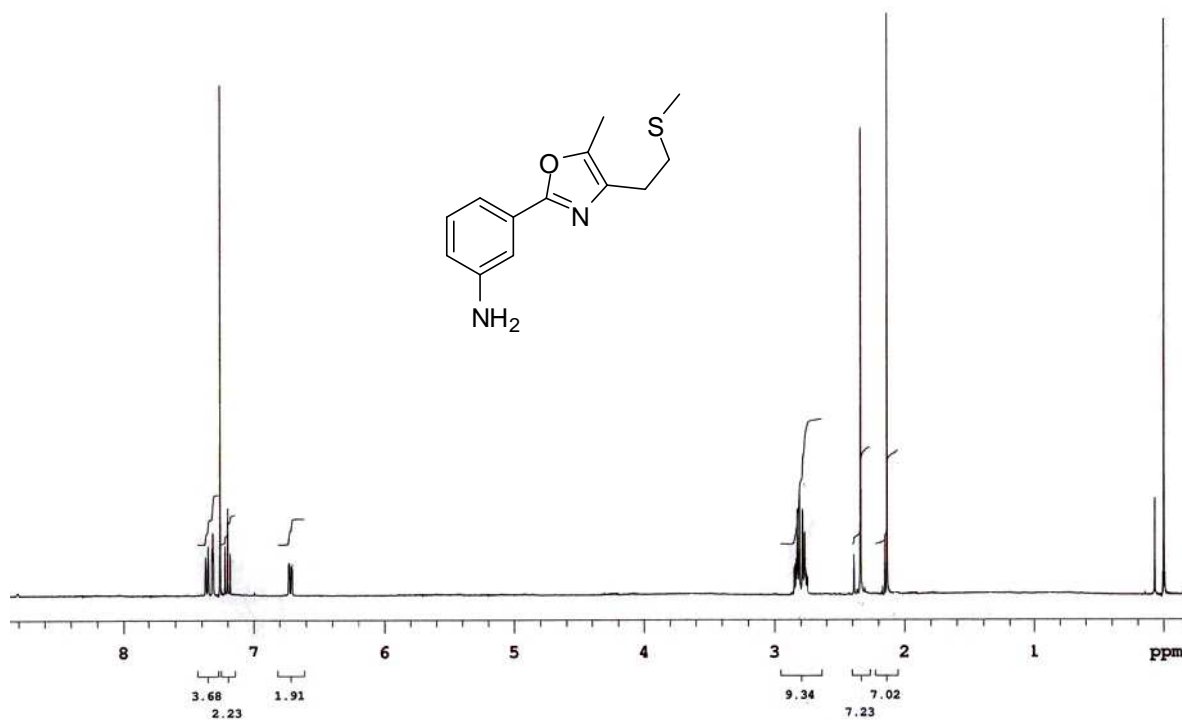
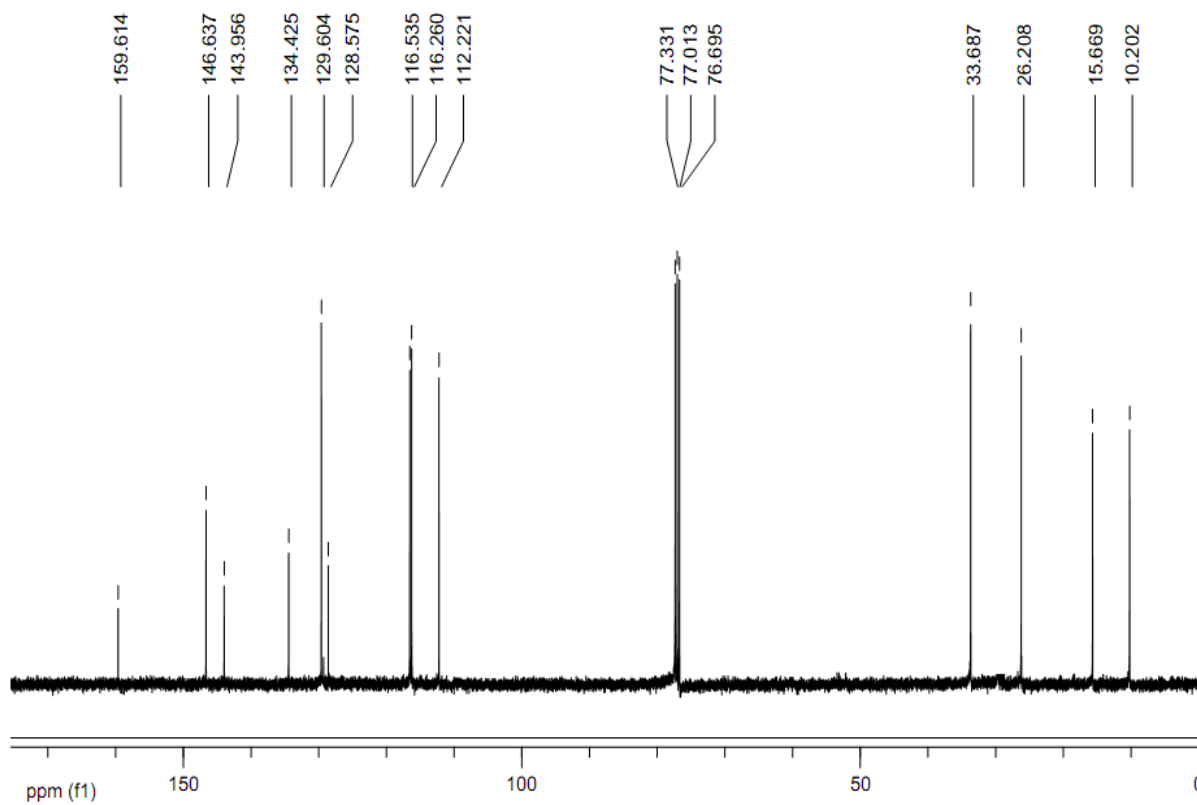
2-(2-chloro-5-nitrophenyl)-5-methyl-4-(2-(methyl thio) ethyl oxazole (5b):

¹H NMR (300 MHz, CDCl₃)¹³C NMR (75 MHz, CDCl₃)

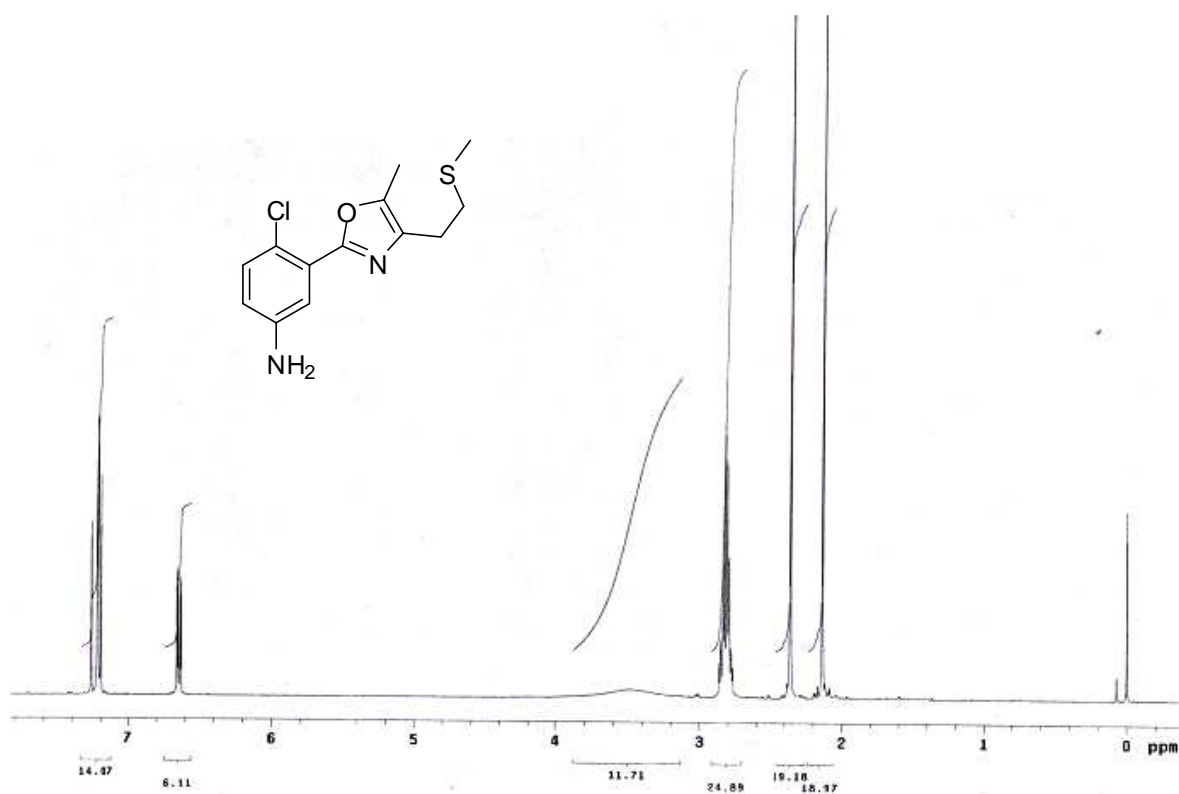
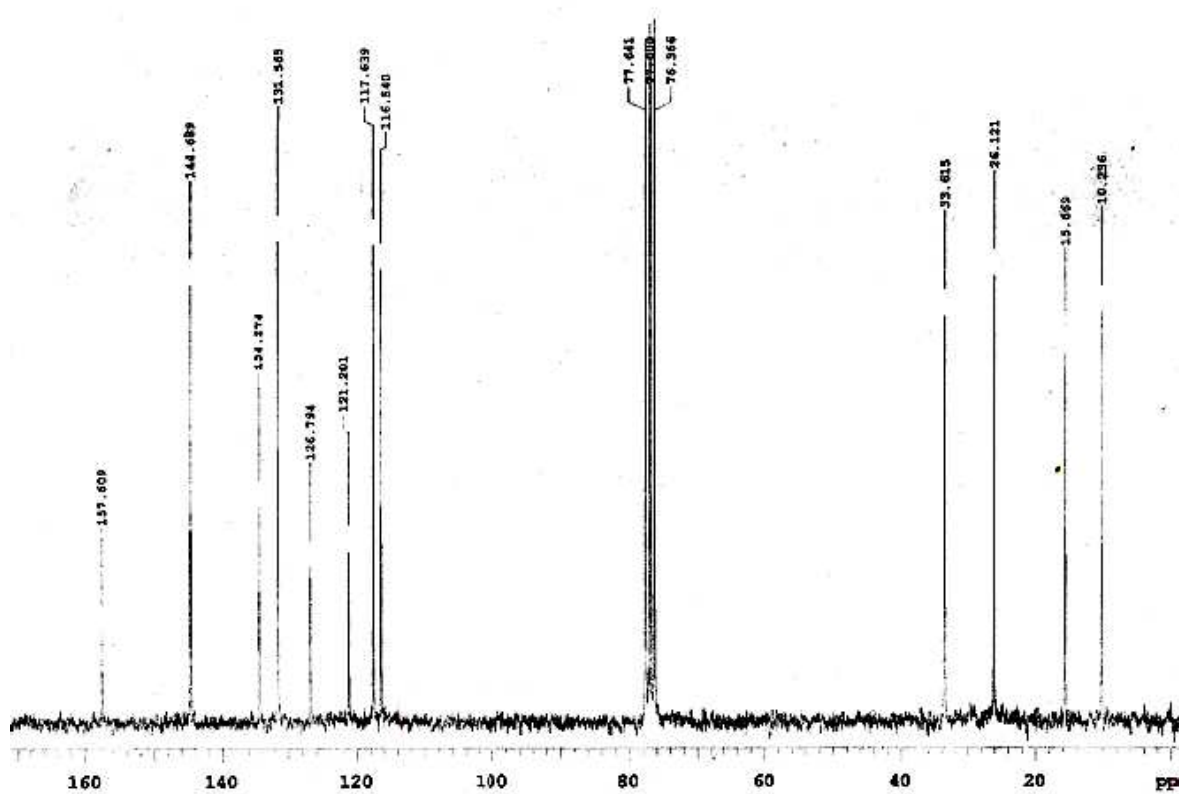
2-(3,5-dinitrophenyl)-5-methyl-4-(2-(methylthio) ethyl) oxazole (5c):

¹H NMR (300 MHz, CDCl₃)¹³C NMR (75 MHz, CDCl₃)

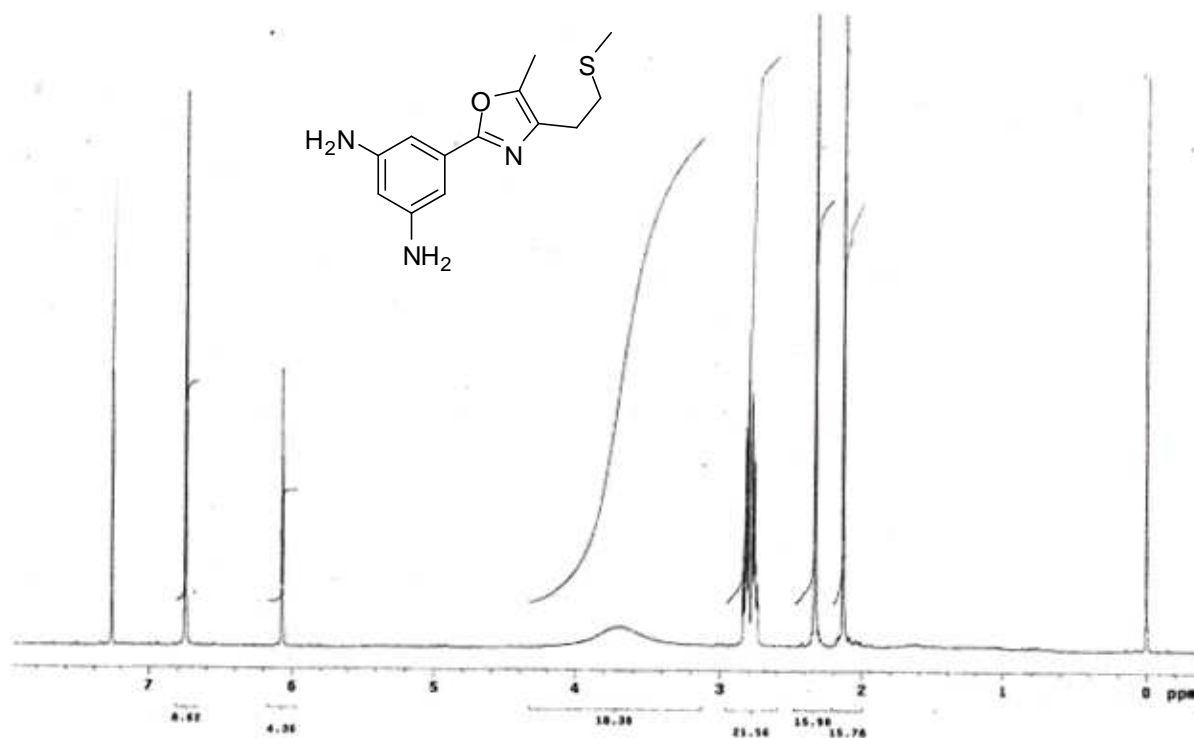
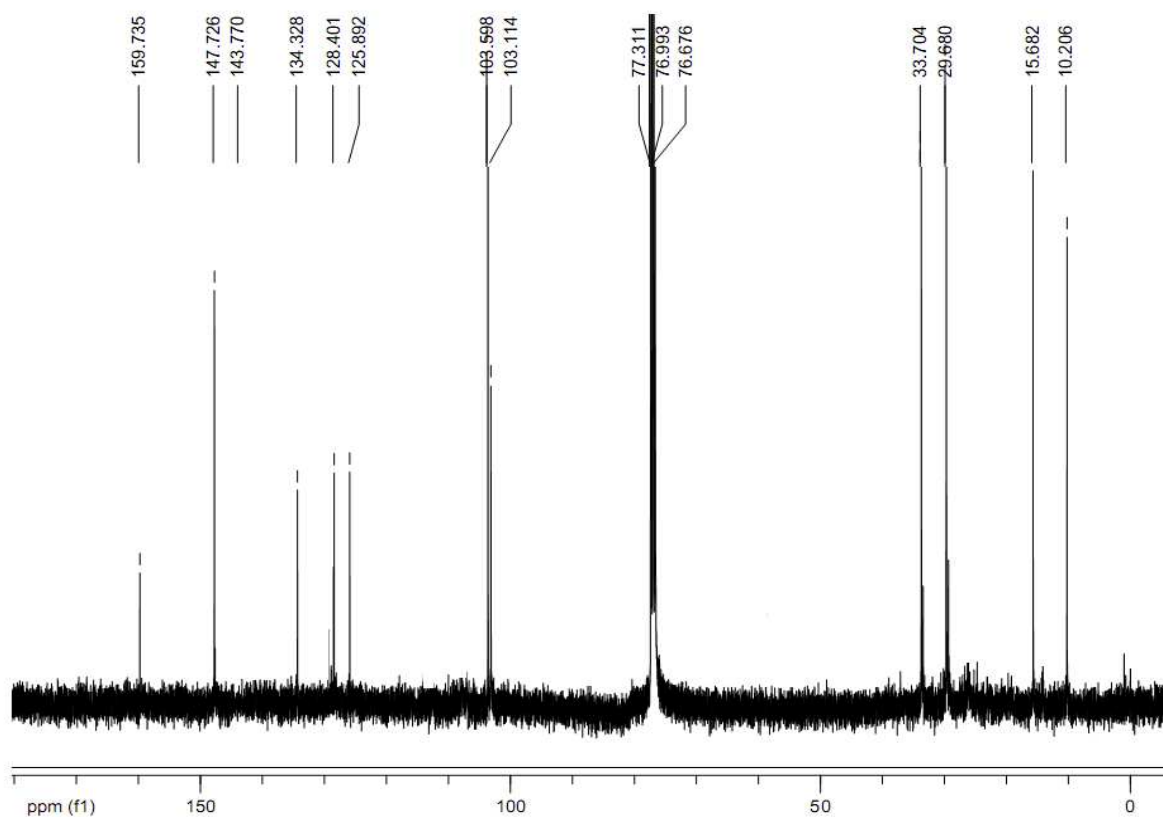
3-(5-Methyl-4-(2-(methylthio) ethyl) oxazol-2-yl) aniline (6a):

¹H NMR (300 MHz, CDCl₃)¹³C NMR (75 MHz, CDCl₃)

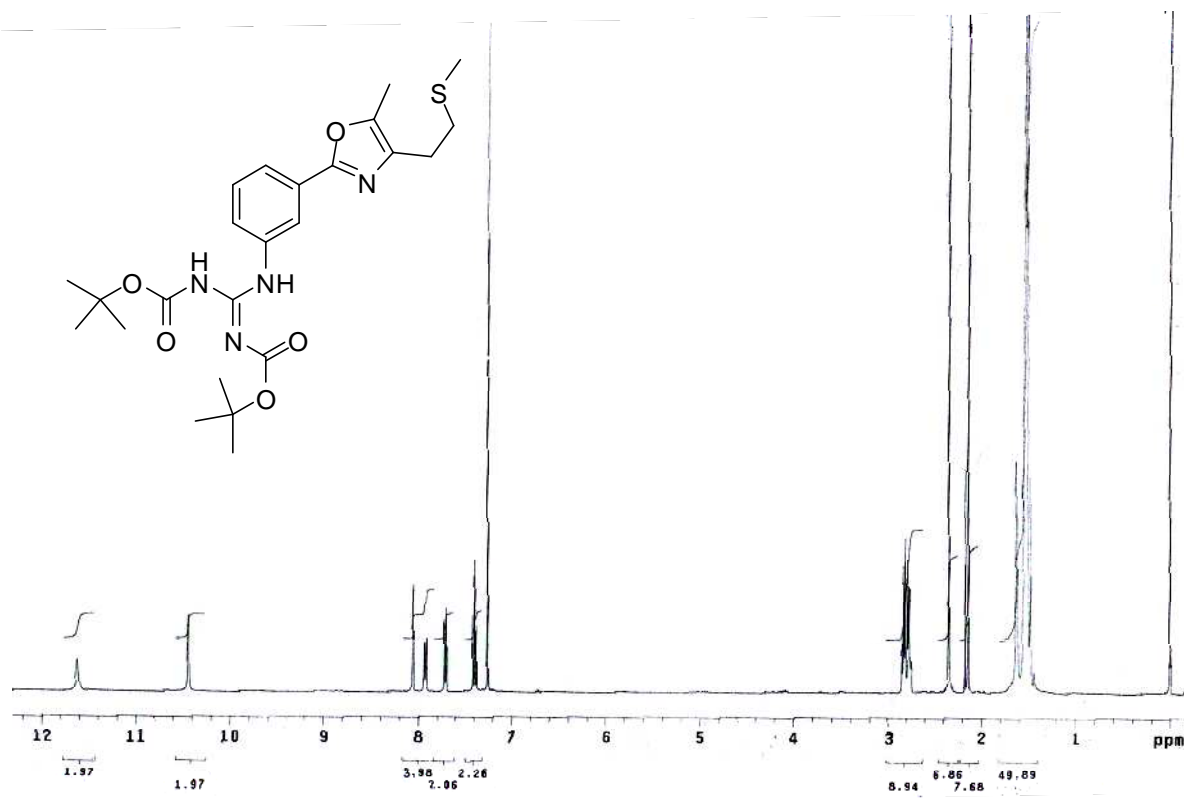
4-chloro-3-(5-methyl-4-(2-(methylthio)ethyl)oxazol-2-yl)aniline (6b):

 $^1\text{H NMR}$ (300 MHz, CDCl_3) $^{13}\text{C NMR}$ (75 MHz, CDCl_3)

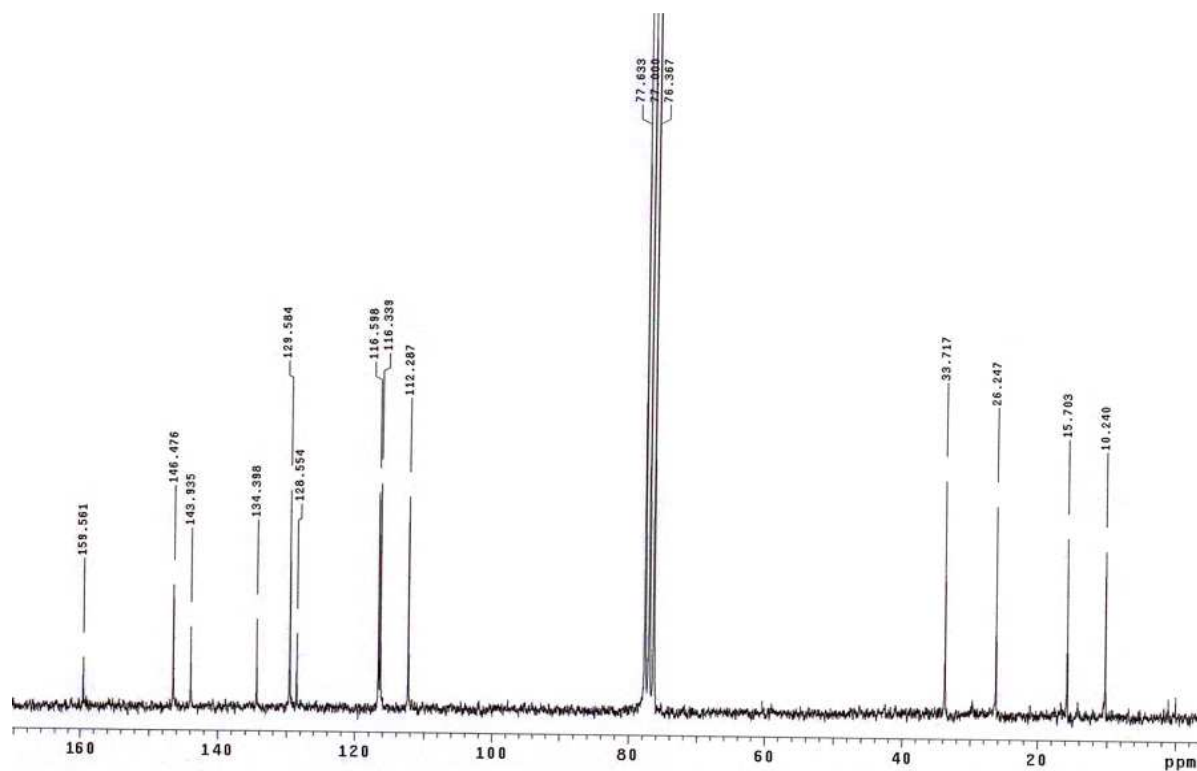
5-(5-methyl-4-(2-(methyl thio) ethyl) oxazol-2-yl)benzene-1,3-diamine (6c):

¹H NMR (300 MHz, CDCl₃)¹³C NMR (75 MHz, CDCl₃)

(E)-tert-butyl (tert-butoxycarbonylamino) (3-(5-methyl-4-(2-(methylthio)ethyl)oxazol-2-yl)phenylamino)methylenecarbamate (8a):

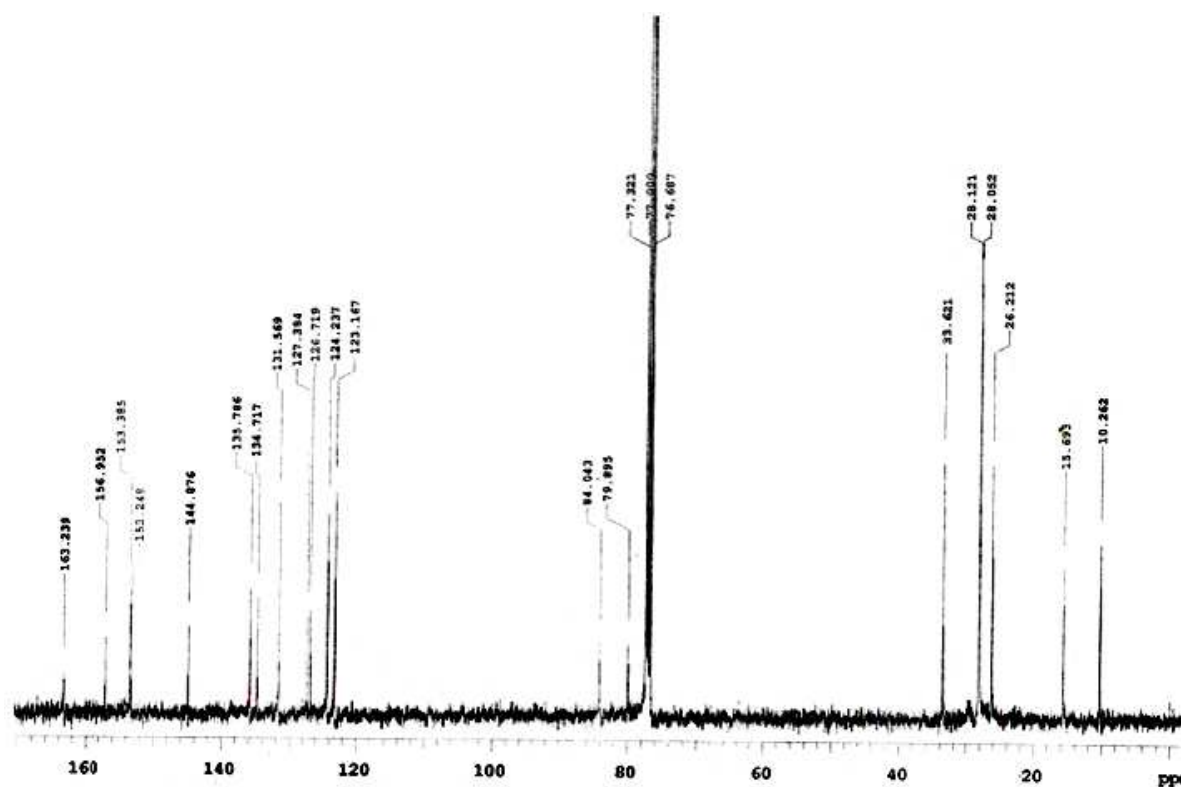
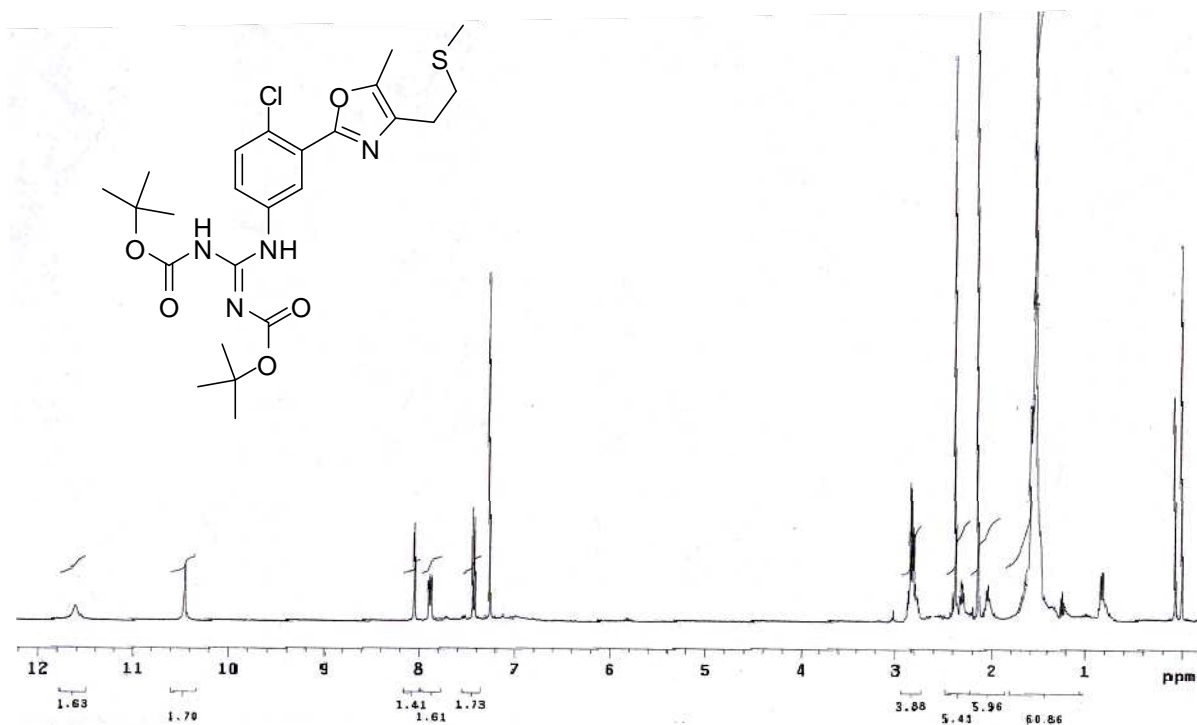


¹H NMR (300 MHz, CDCl₃)

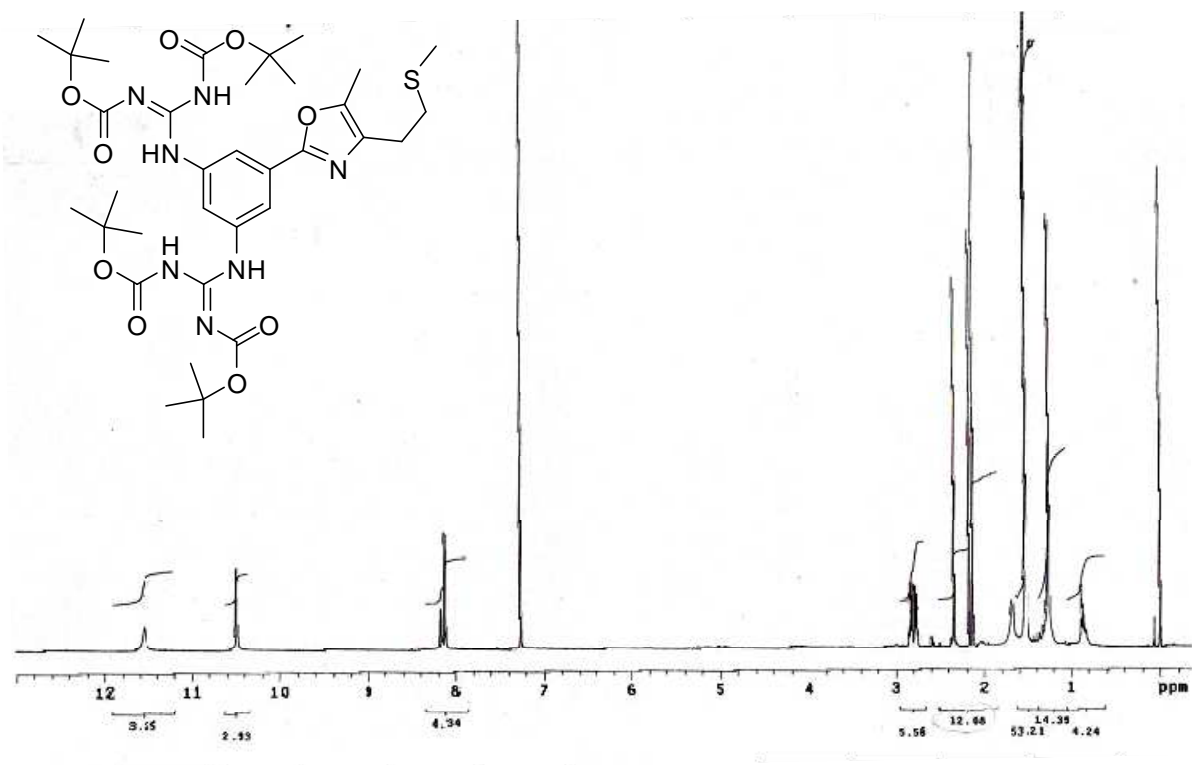


¹³C NMR (75 MHz, CDCl₃)

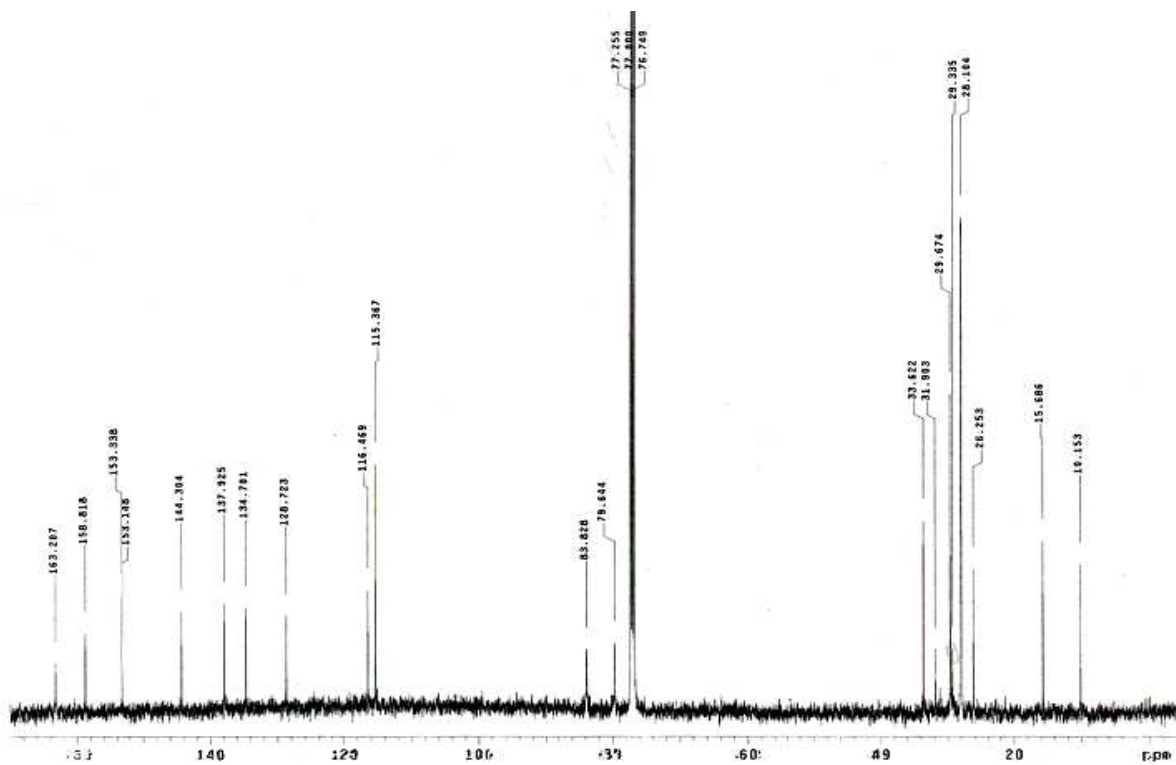
(E)-tert-butyl (tert-butoxycarbonylamino)(4-chloro-3-(5-methyl-4-(2-(methylthio) ethyl) oxazol-2-yl) phenyl amino) methylene carbamate (8b):



Tert-butyl (5-(5-methyl-4-(2-(methylthio) ethyl) oxazol-2-yl)-1, 3-phenylene) bis (azanediyl) bis ((*tert*-butoxycarbonylamino) methan-1-yl-1-ylidene) dicarbamate (8c):

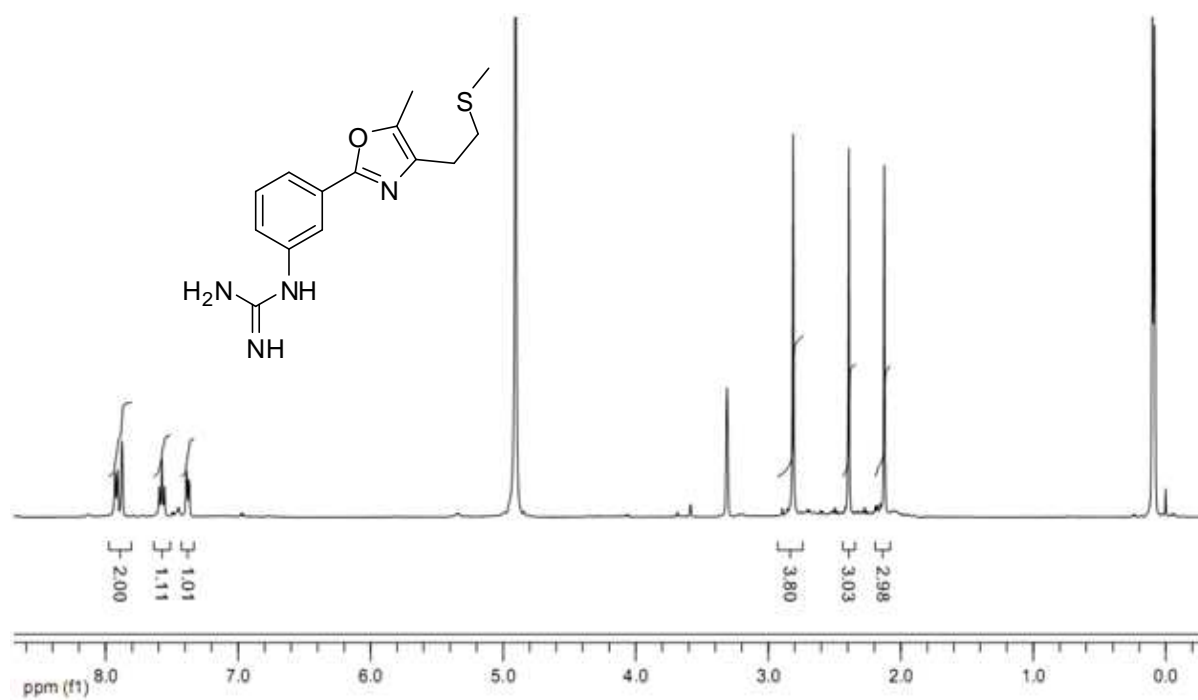
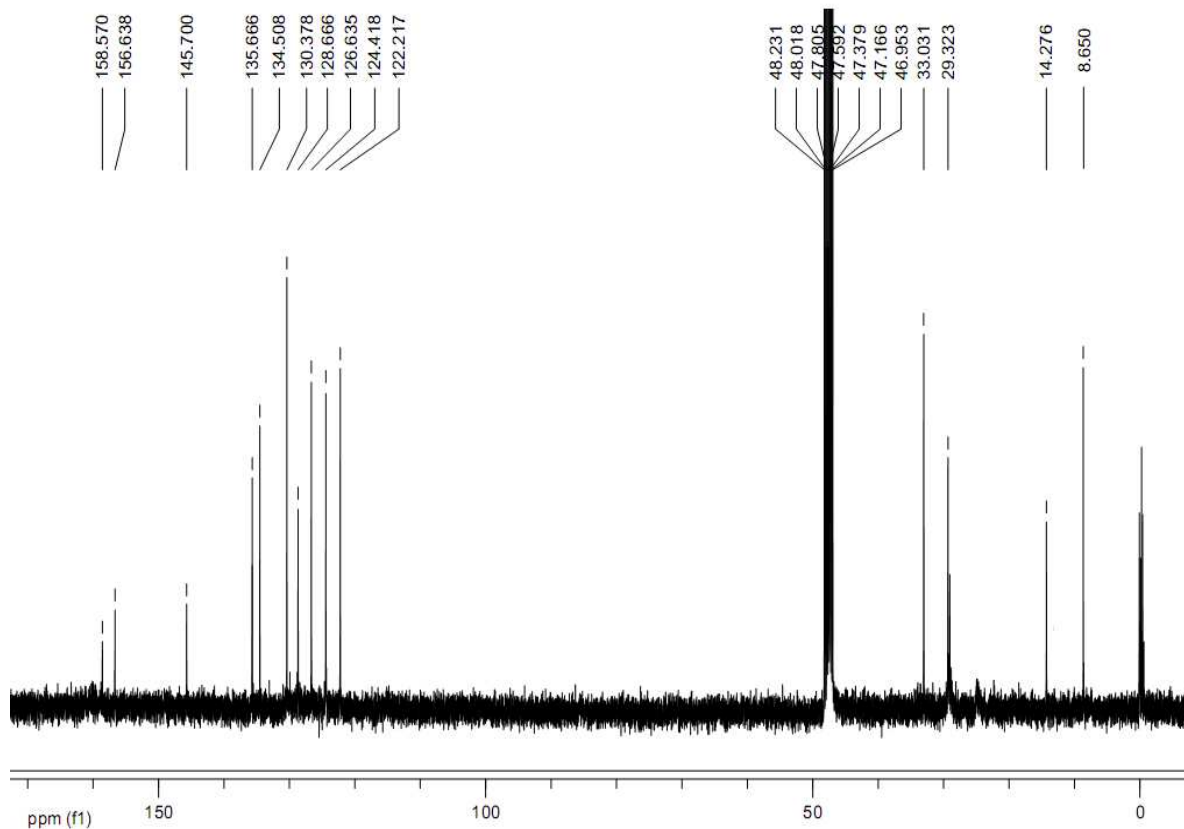


¹H NMR (300 MHz, CDCl₃)

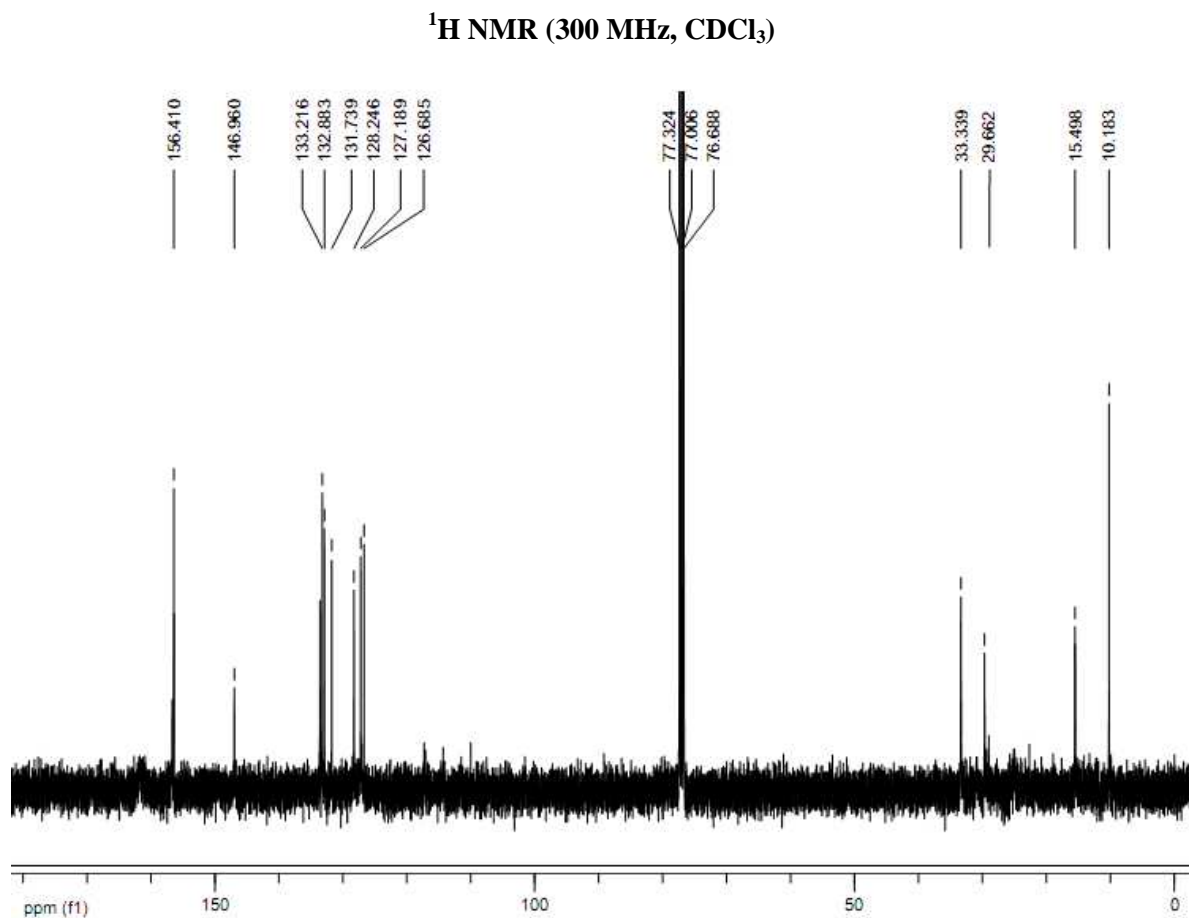
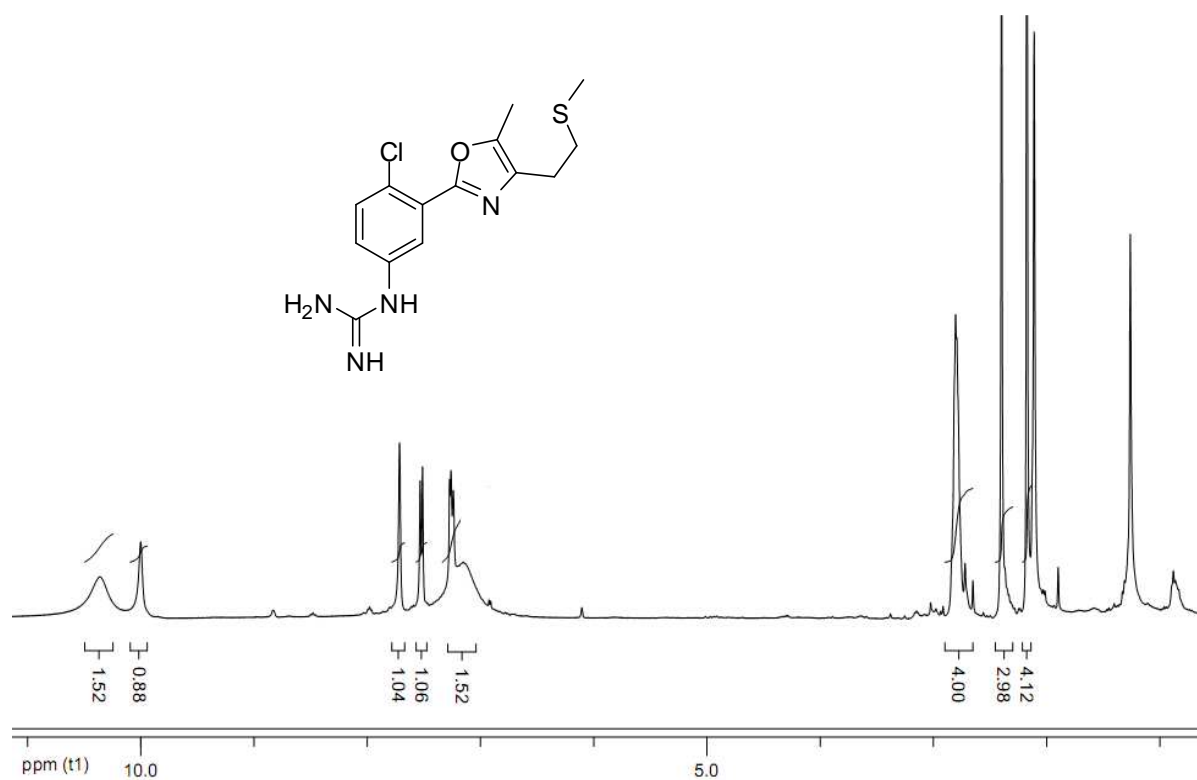


¹³C NMR (75 MHz, CDCl₃)

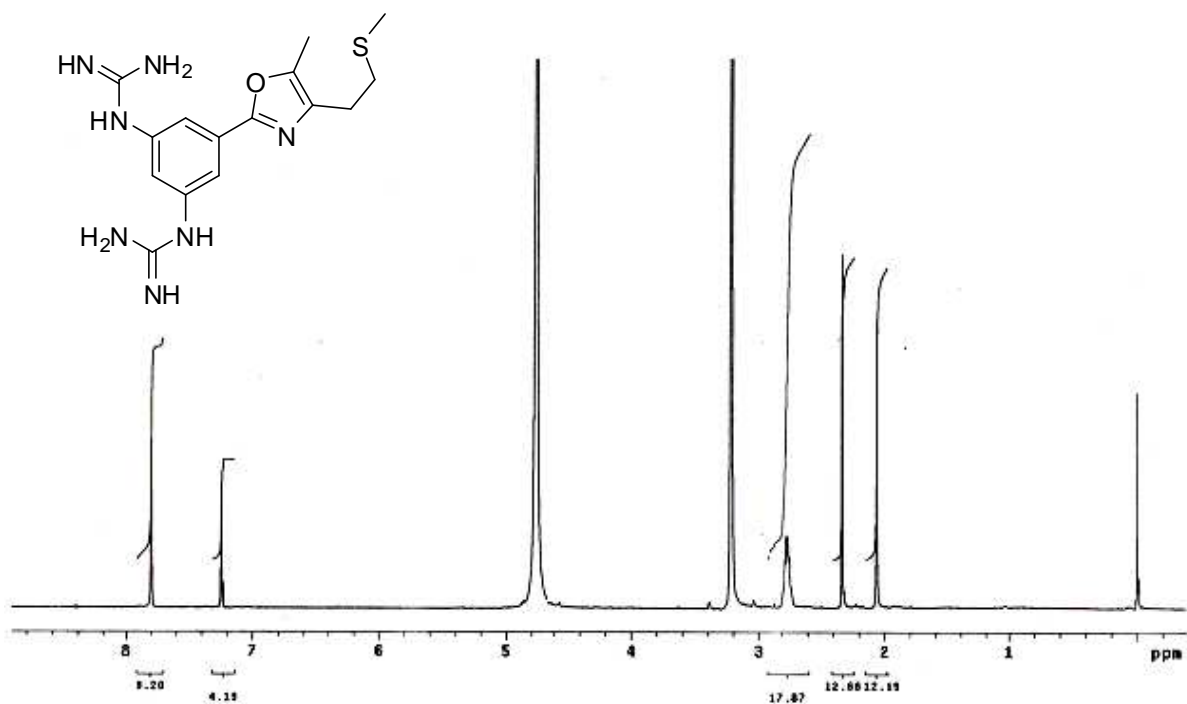
1-(3-(5-Methyl-4-(2-(methylthio) ethyl) oxazol-2-yl) phenyl) guanidine (9a):

 $^1\text{H NMR}$ (300 MHz, CD_3OD) $^{13}\text{C NMR}$ (75 MHz, CD_3OD)

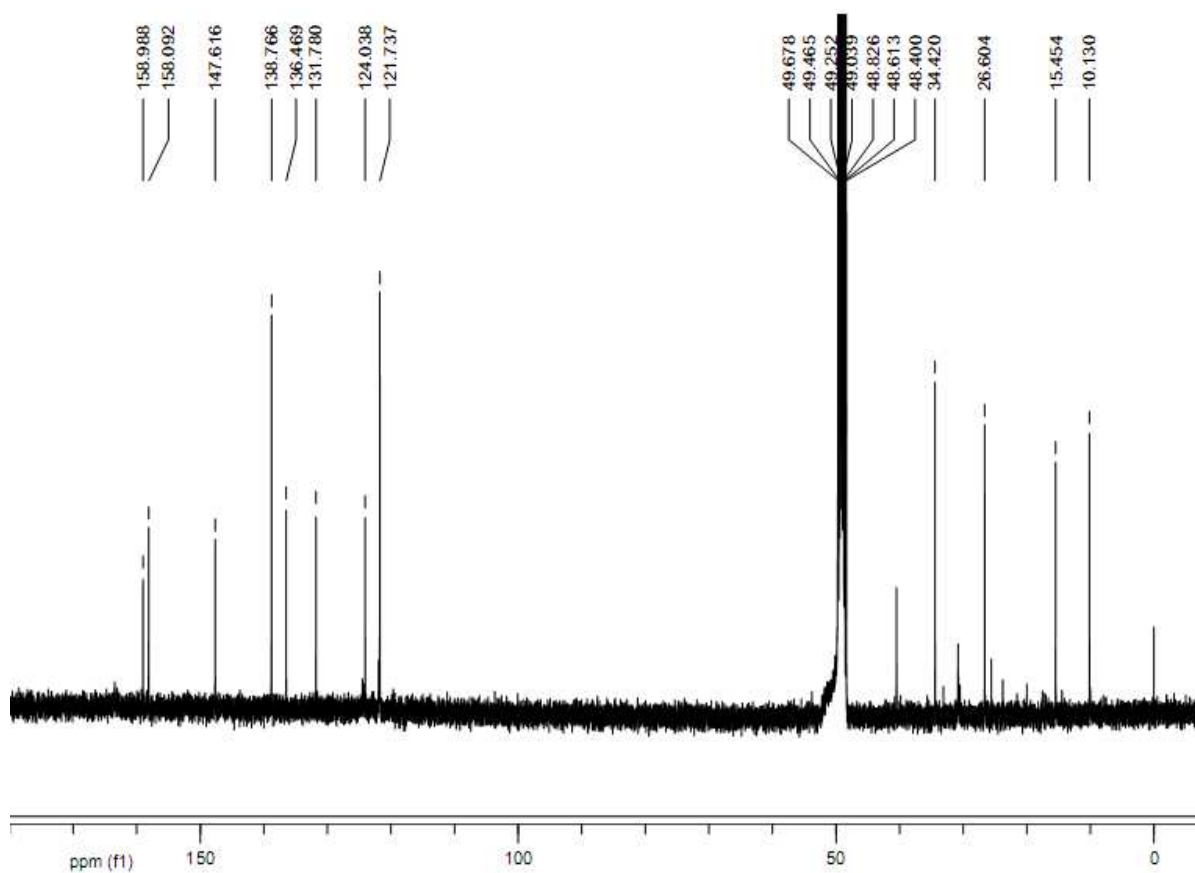
1-(4-chloro-3-(5-methyl-4-(2-(methyl thio) ethyl) oxazol-2-yl) phenyl) guanidine (9b):



1,1'-(5-(5-methyl-4-(2-(methylthio) ethyl) oxazol-2-yl)-1,3-phenylene) diguanidine (9c):

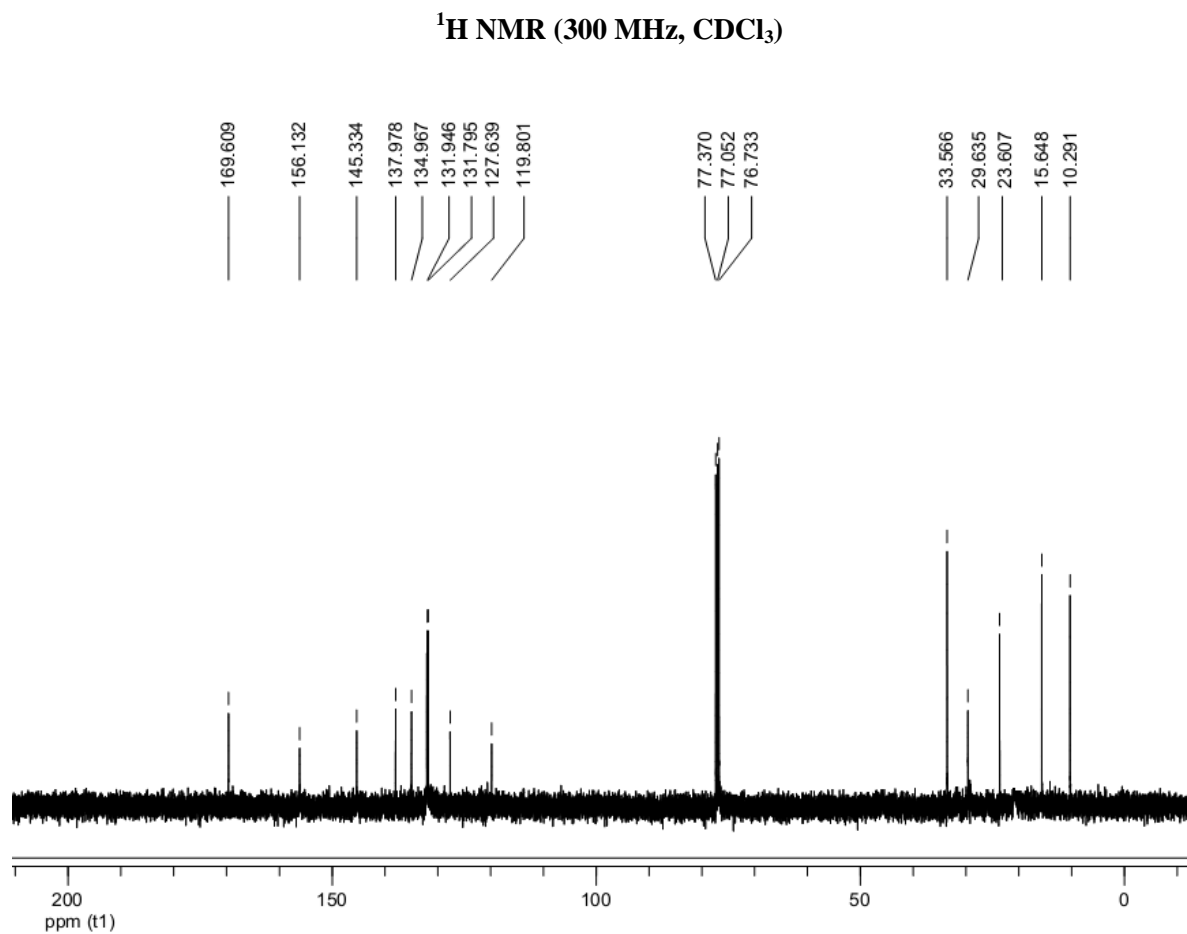
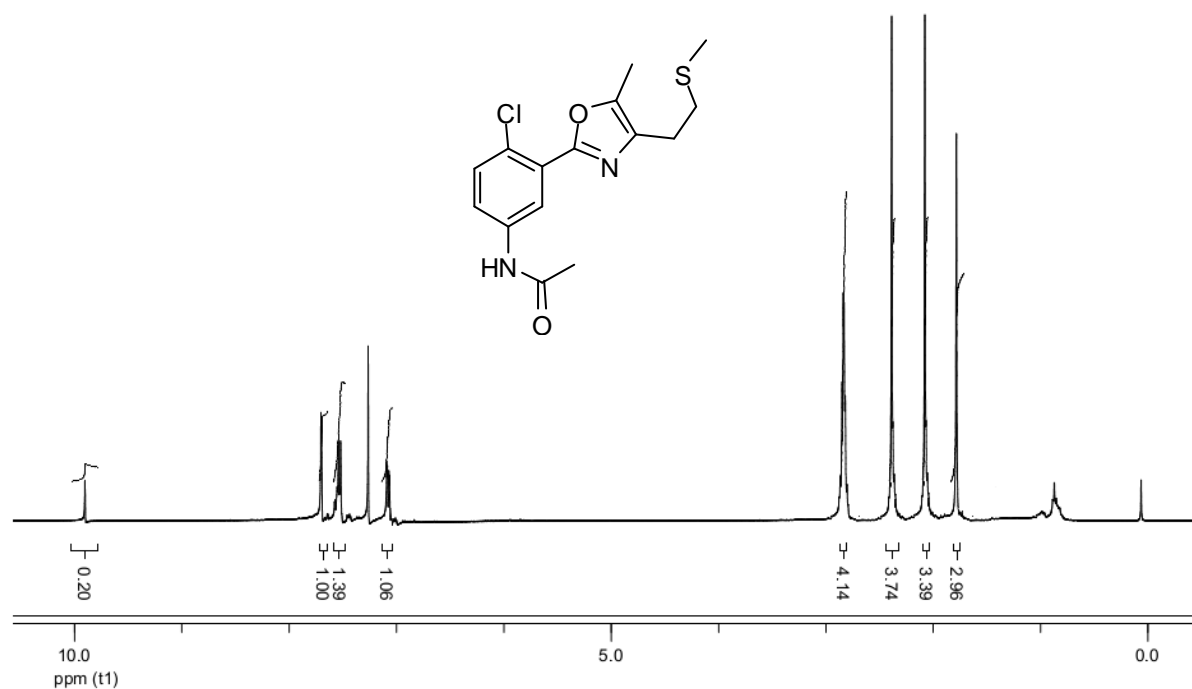


¹H NMR (300 MHz, CD₃OD)

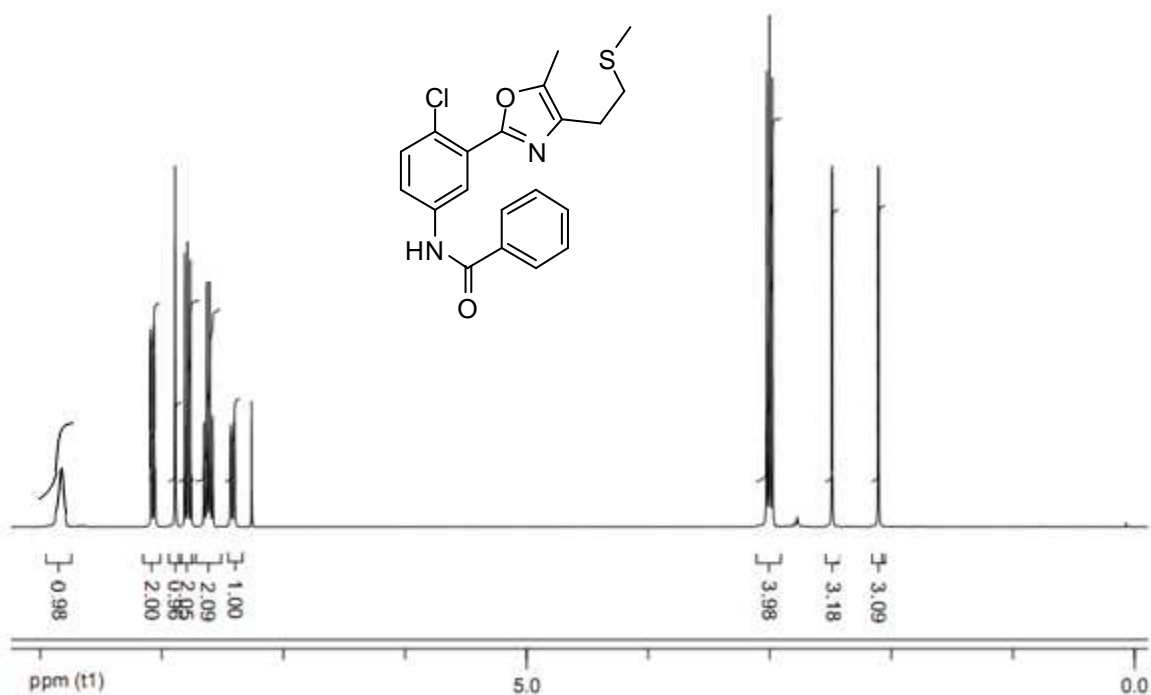


¹³C NMR (75 MHz, CD₃OD)

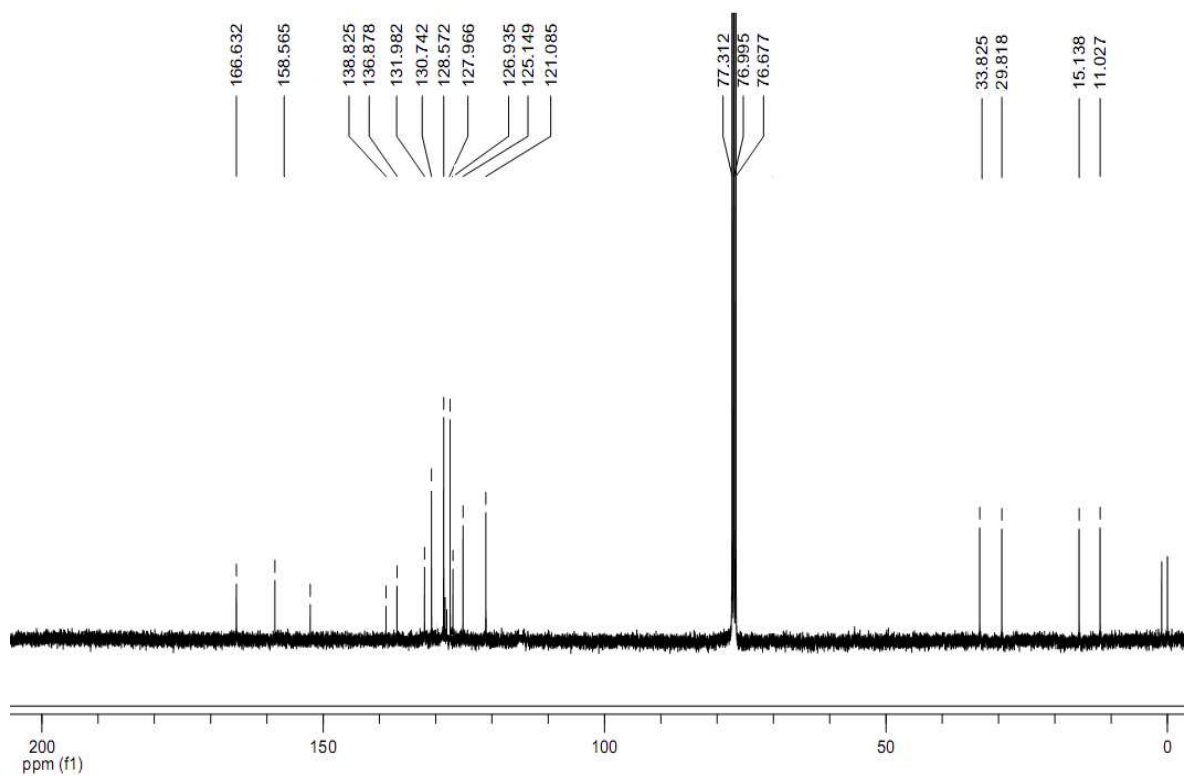
N-(4-chloro-3-(5-methyl-4-(2-(methylthio) ethyl) oxazol-2-yl) phenyl) acetamide (10):



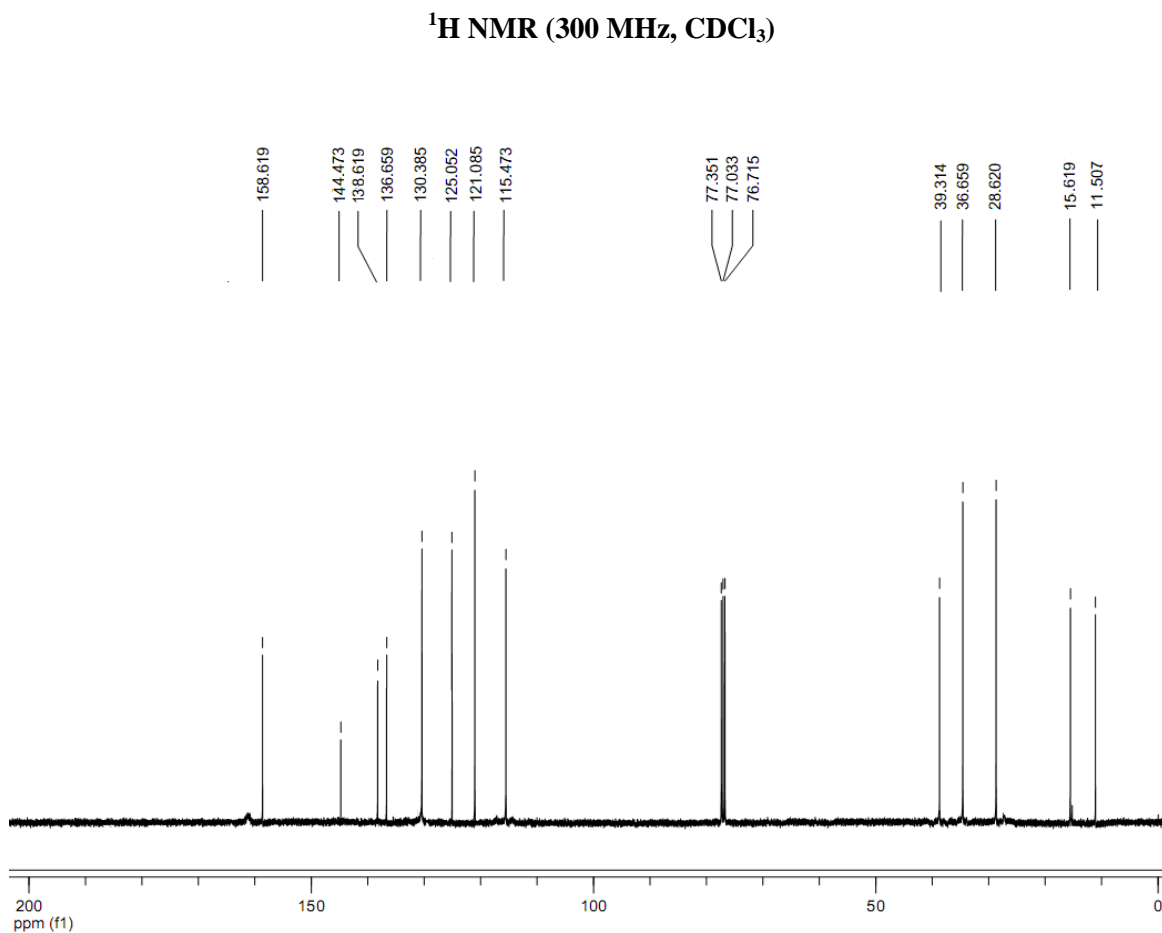
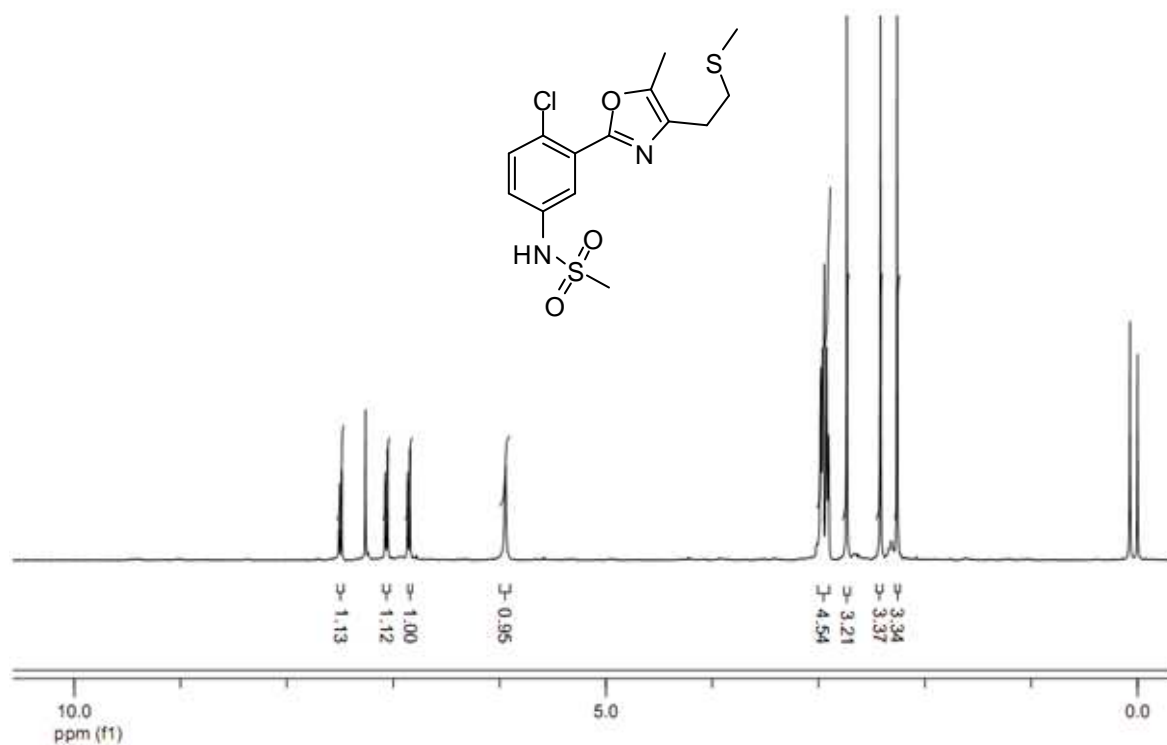
N-(4-chloro-3-(5-methyl-4-(2-(methylthio)ethyl)oxazol-2-yl)phenyl)benzamide (11):



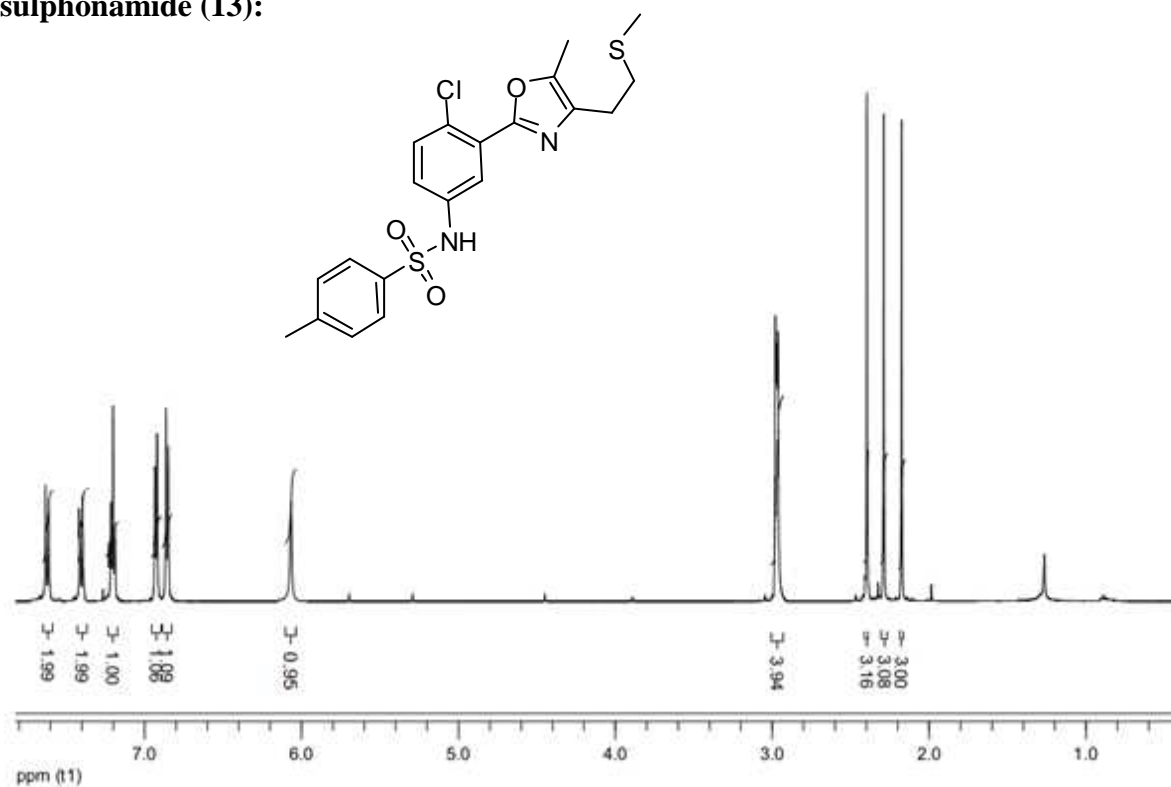
¹H NMR (300 MHz, CDCl₃)



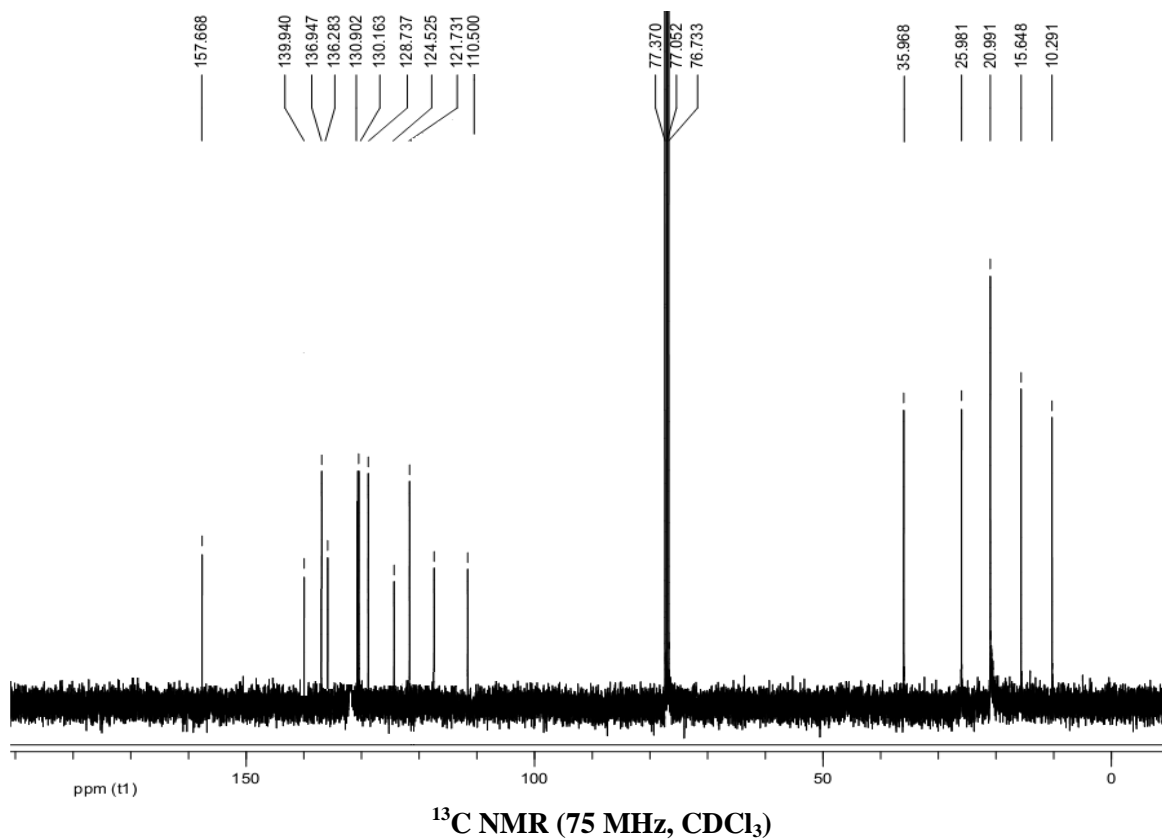
¹³C NMR (75 MHz, CDCl₃)

***N*-(4-chloro-3-(5-methyl-4-(2-(methylthio)ethyl)oxazol-2-yl)phenyl)methanesulfonamide (12)**

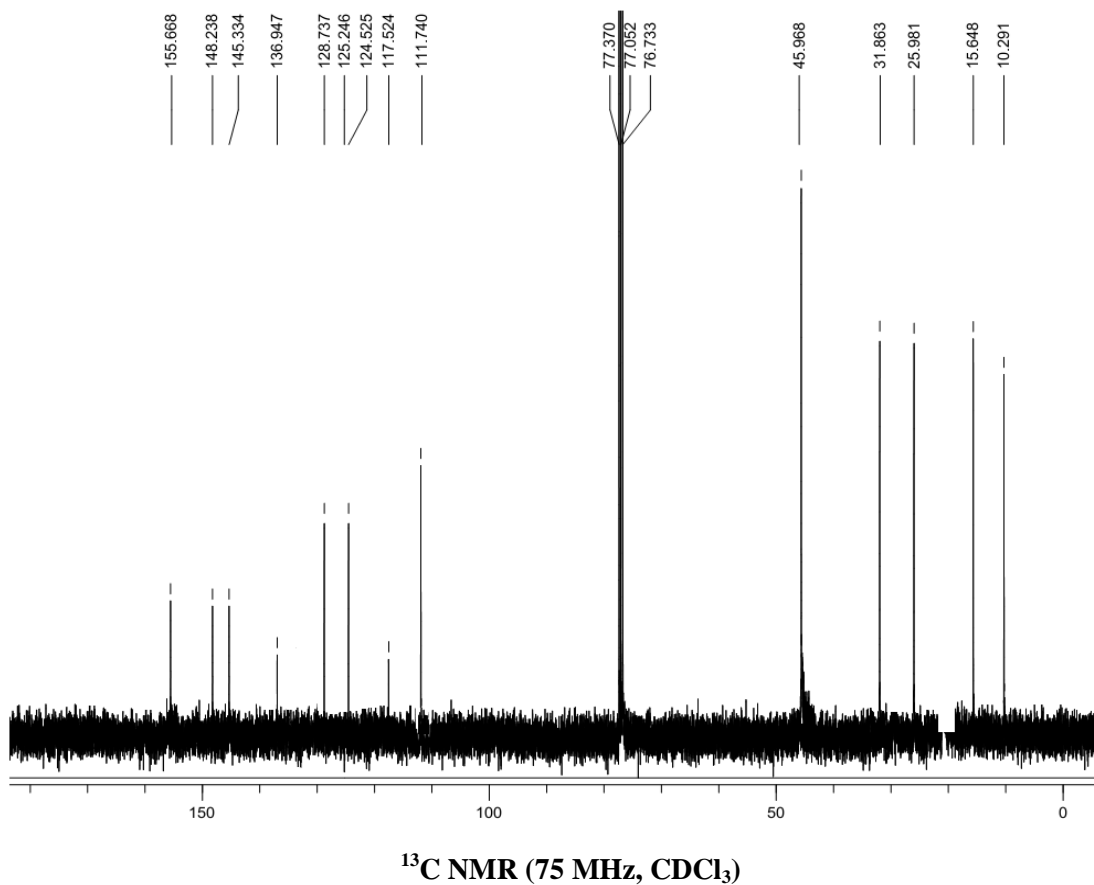
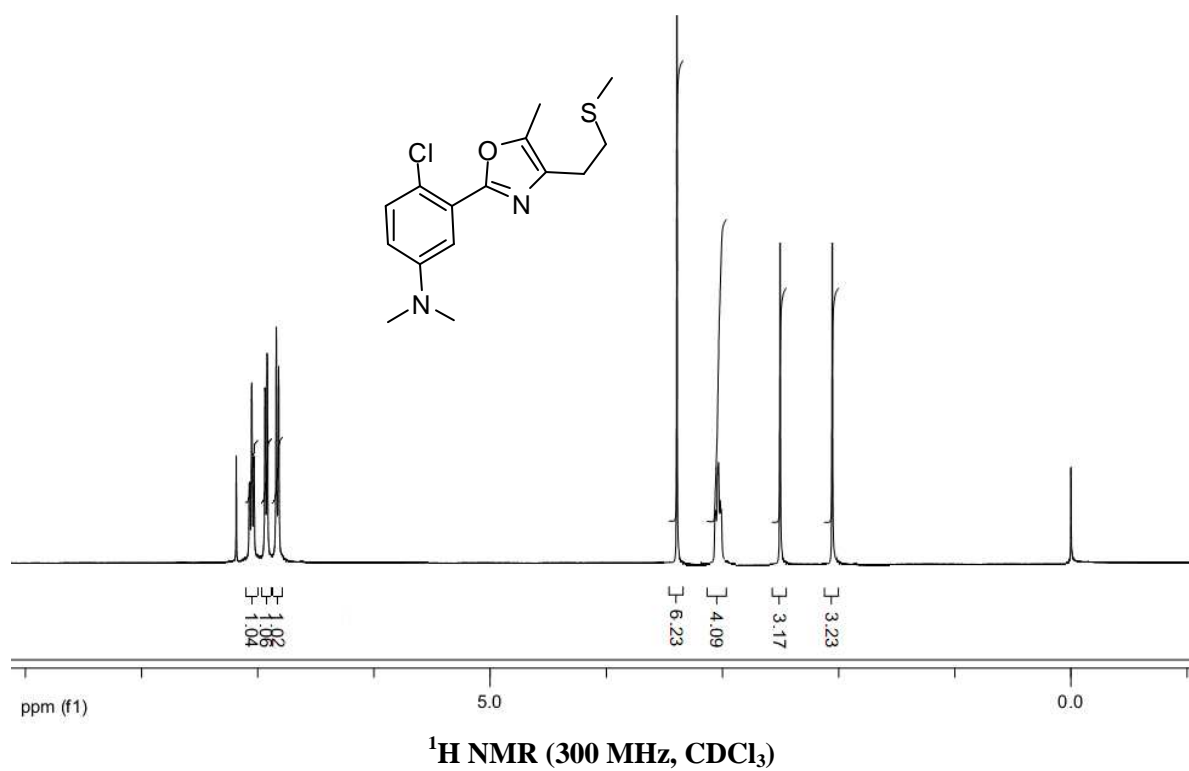
***N*-(4-chloro-3-(5-methyl-4-(2-(methyl thio) ethyl) oxazol-2-yl) phenyl)-4-methyl benzene sulphonamide (13):**



¹H NMR (300 MHz, CDCl₃)

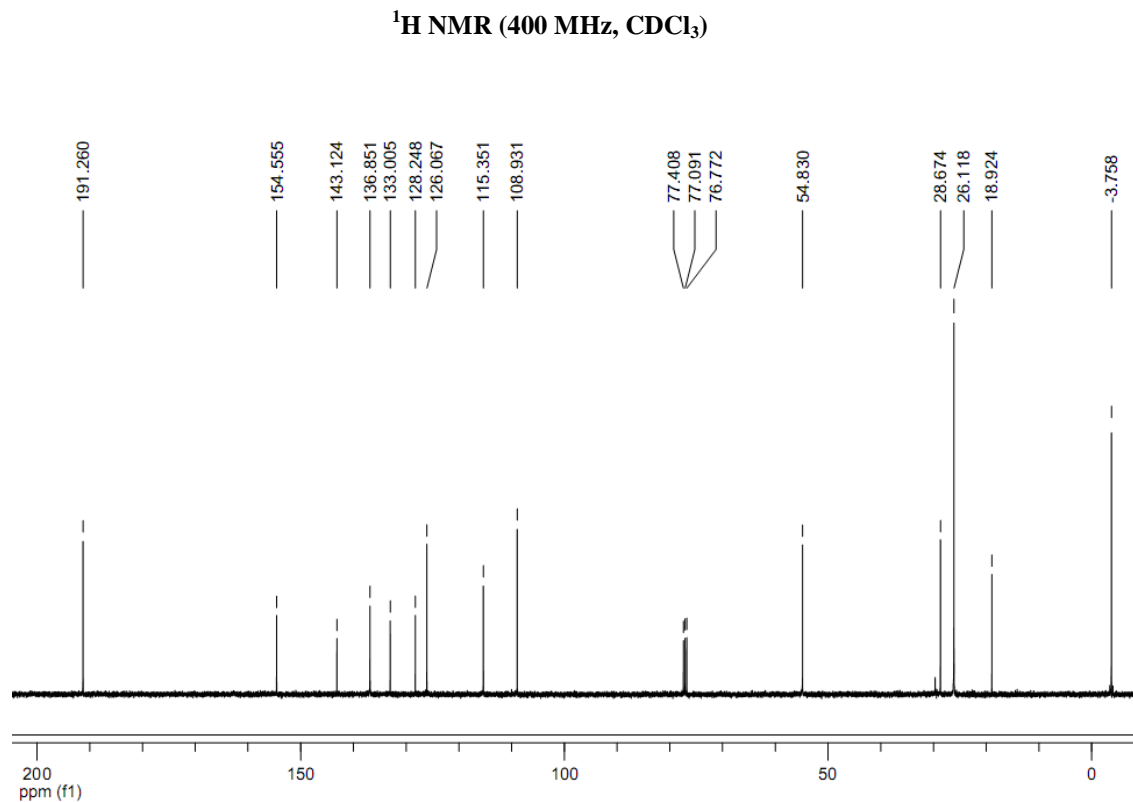
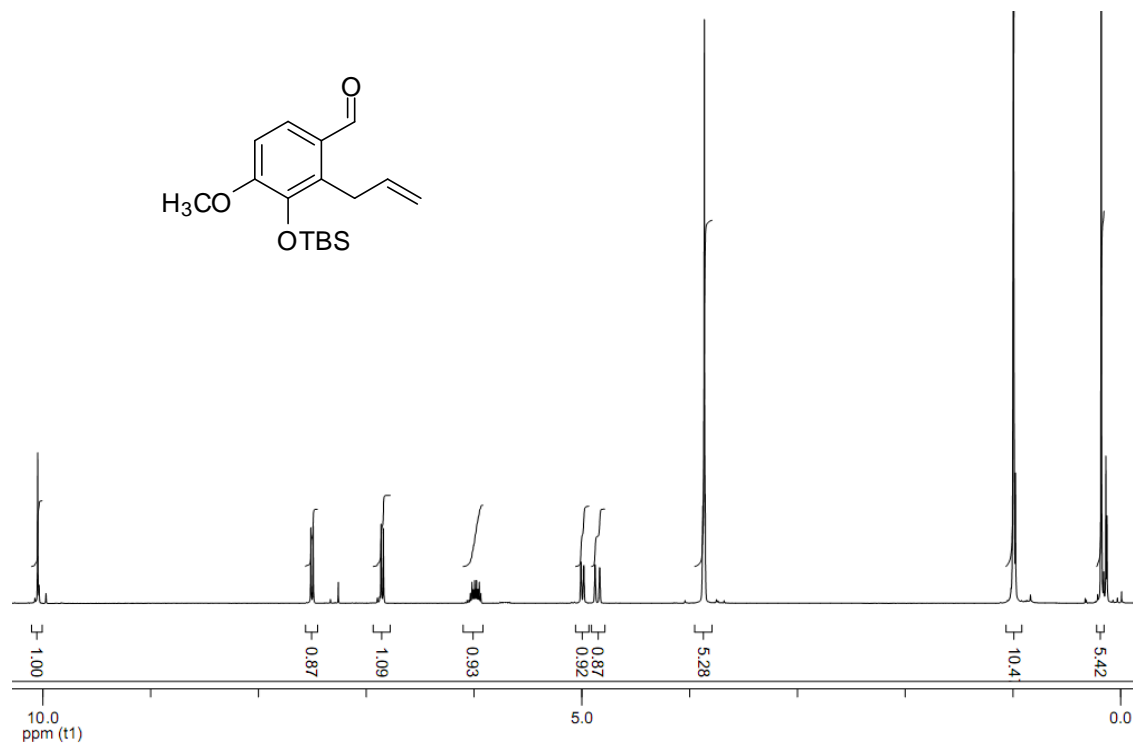


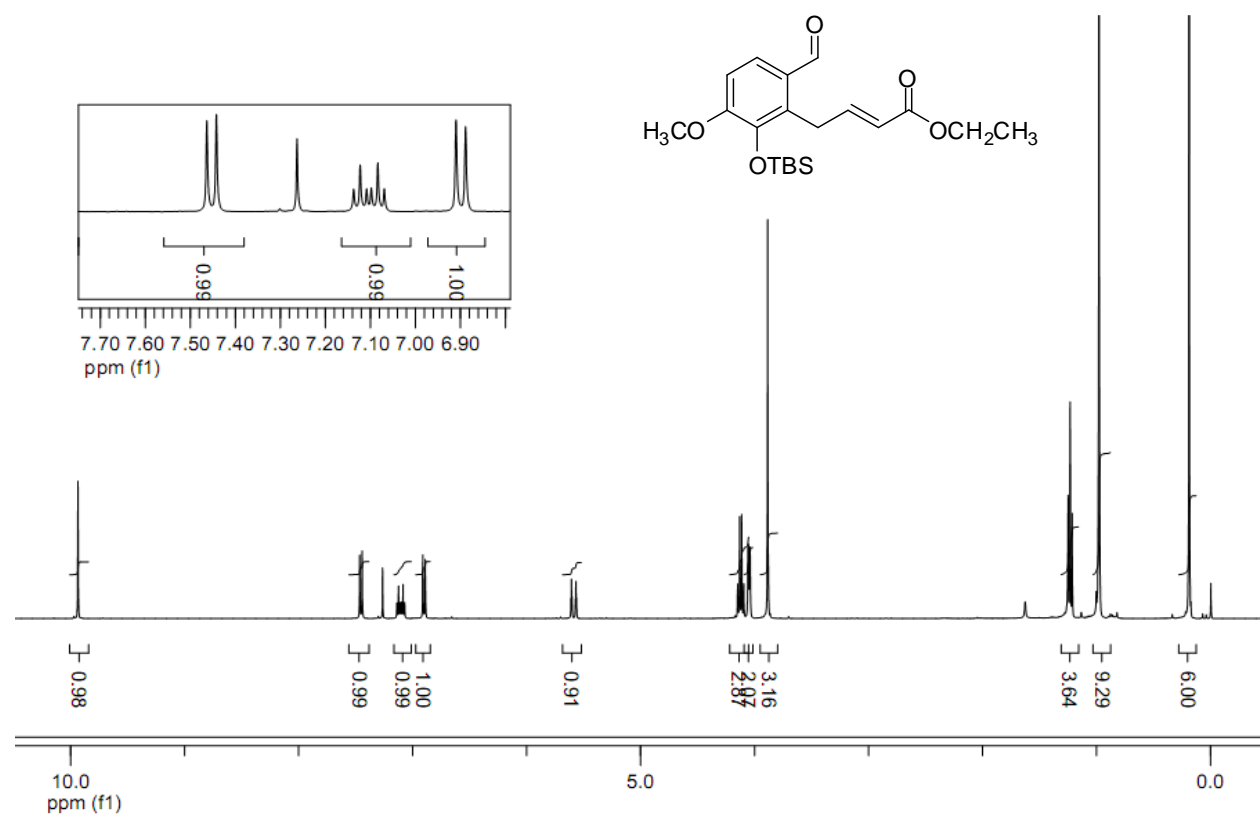
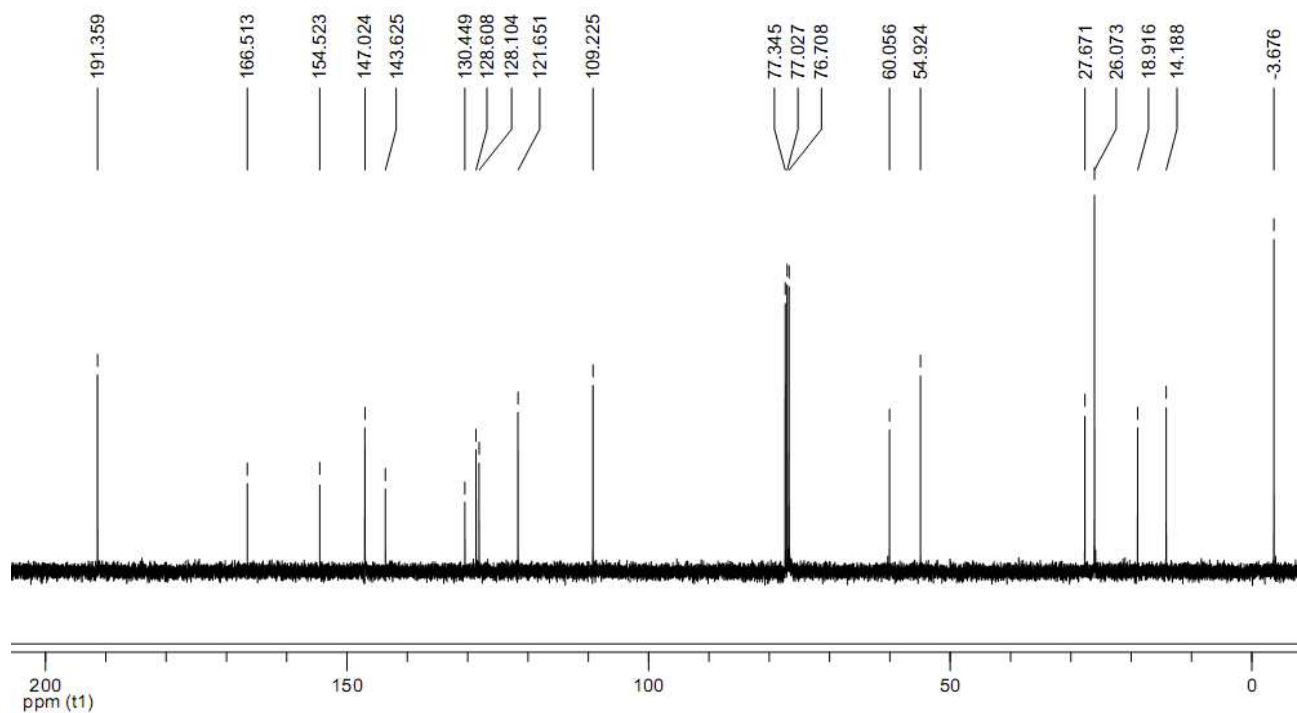
¹³C NMR (75 MHz, CDCl₃)

4-chloro-*N,N*-dimethyl-3-(5-methyl-4-(2-(methylthio) ethyl)oxazol-2-yl)aniline (14):

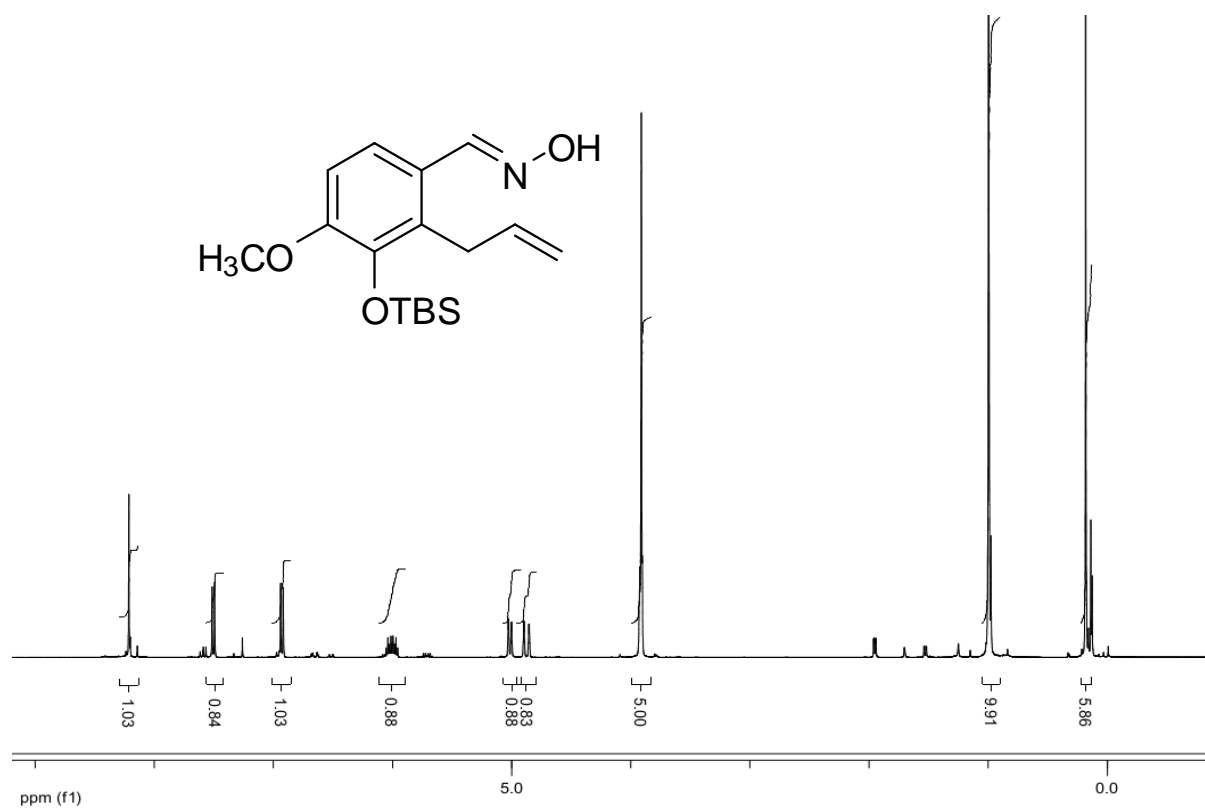
5. Design, synthesis & pharmacological evolution of isovanillin derived Isoxazolidines as potential vanilloid receptors

2-Allyl-3-(*tert*-butyldimethylsilyloxy)-4-methoxybenzaldehyde (9a):

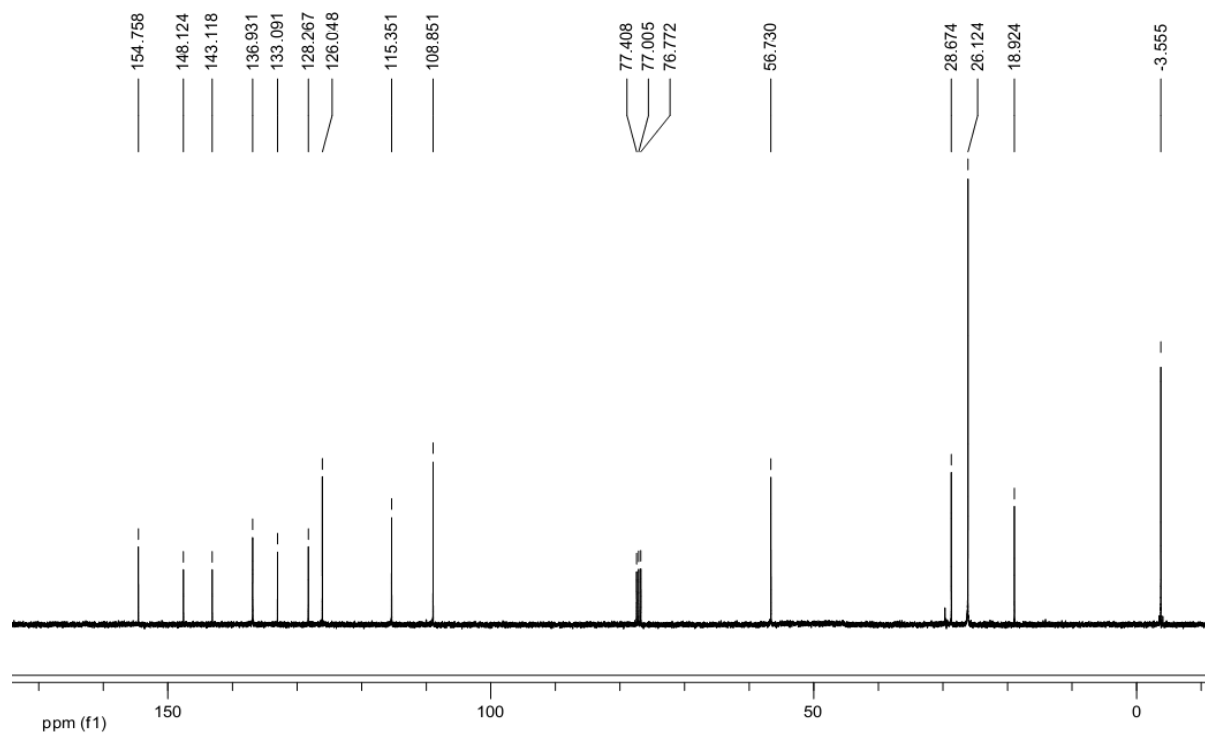


(E)-Ethyl 4-(2-(*tert*-butyldimethylsilyloxy)-6-formyl-3-methoxyphenyl)but-2-enoate (9b):**¹H NMR (400 MHz, CDCl₃)****¹³C NMR (100 MHz, CDCl₃)**

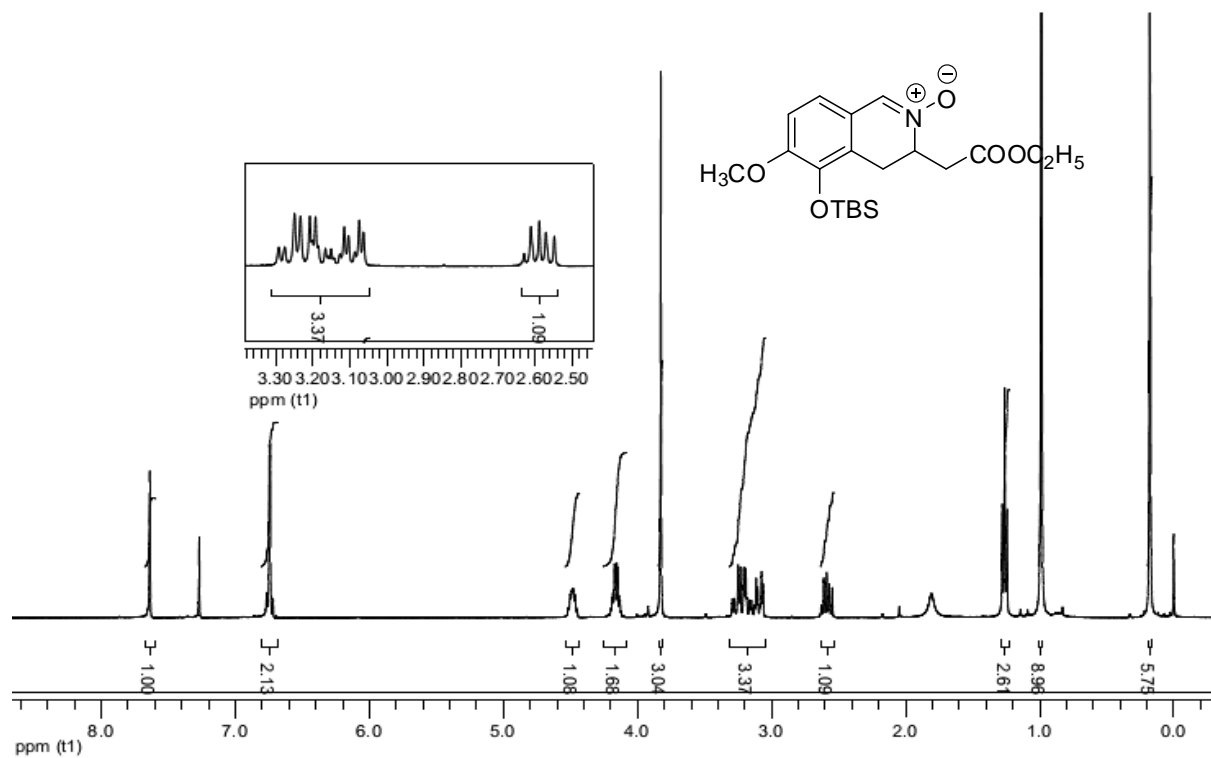
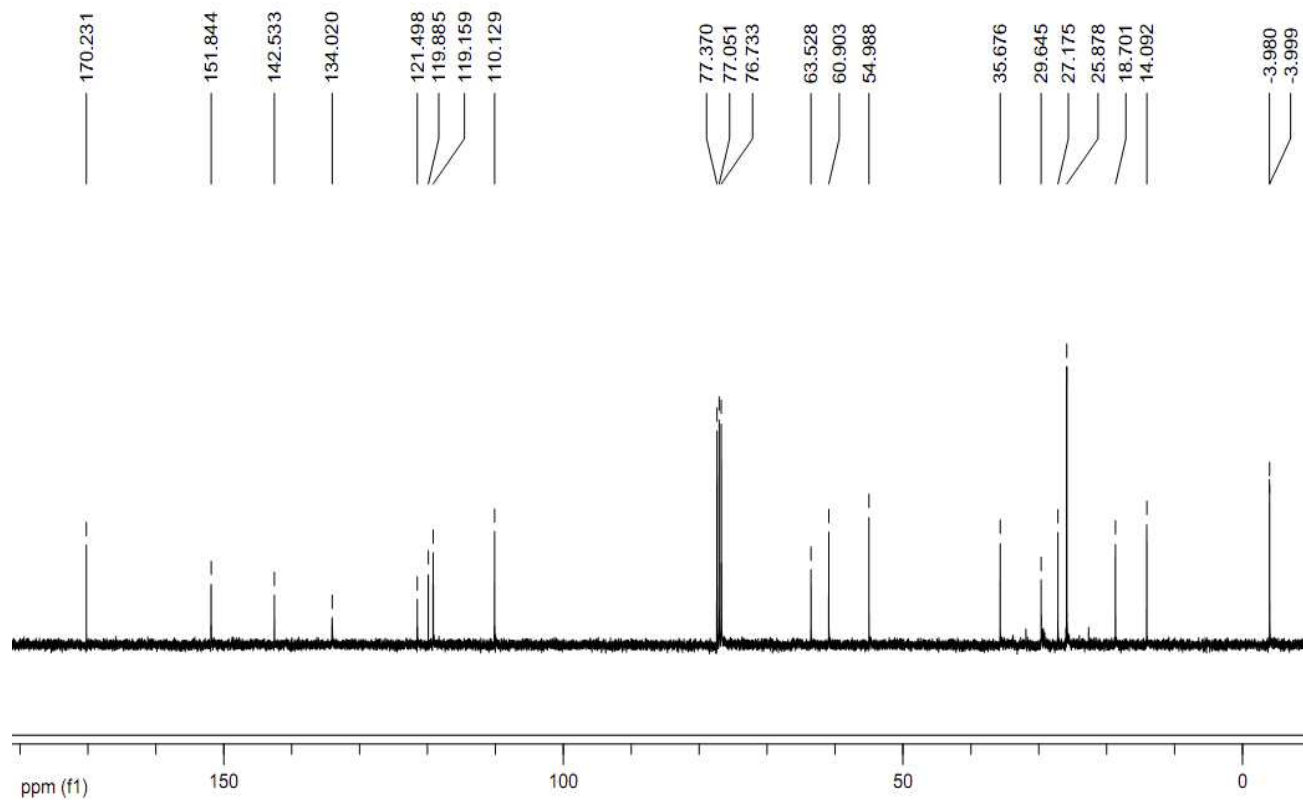
(*E*)-2-allyl-3-(*tert*-butyldimethylsilyloxy)-4-methoxybenzaldehyde oxime (10):



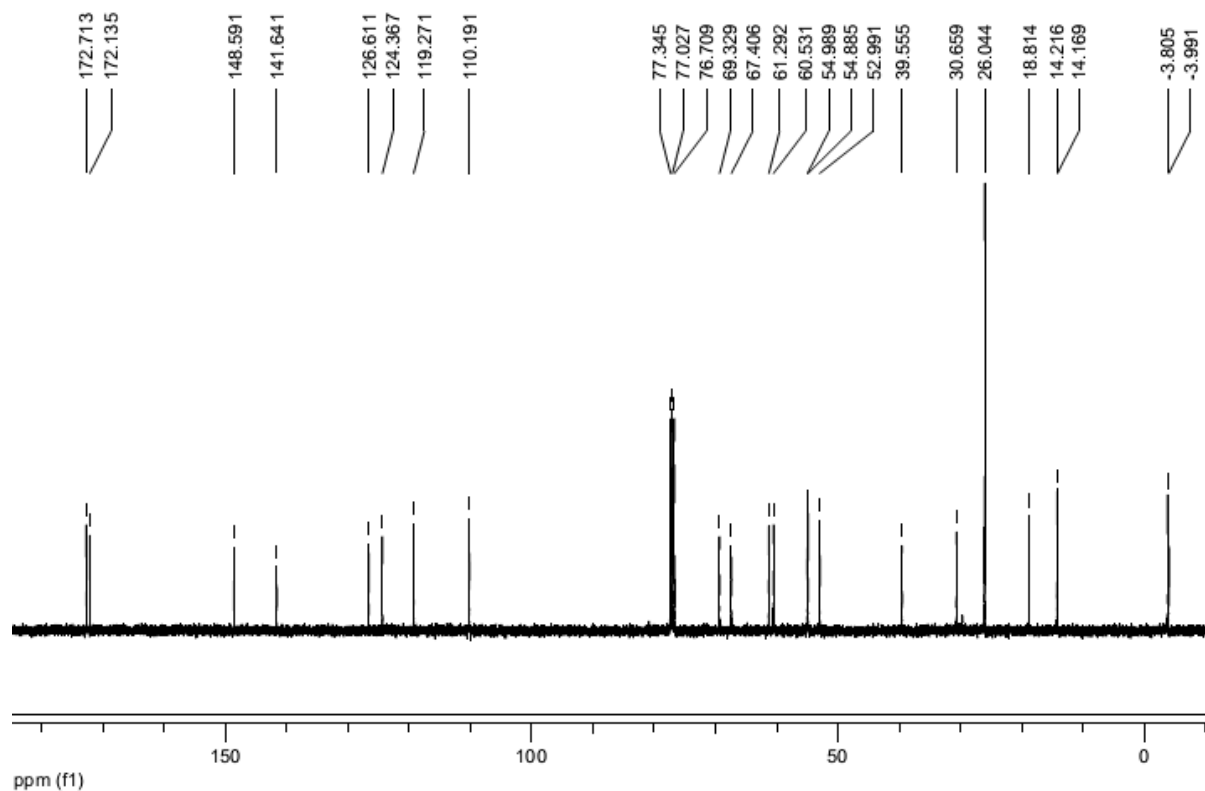
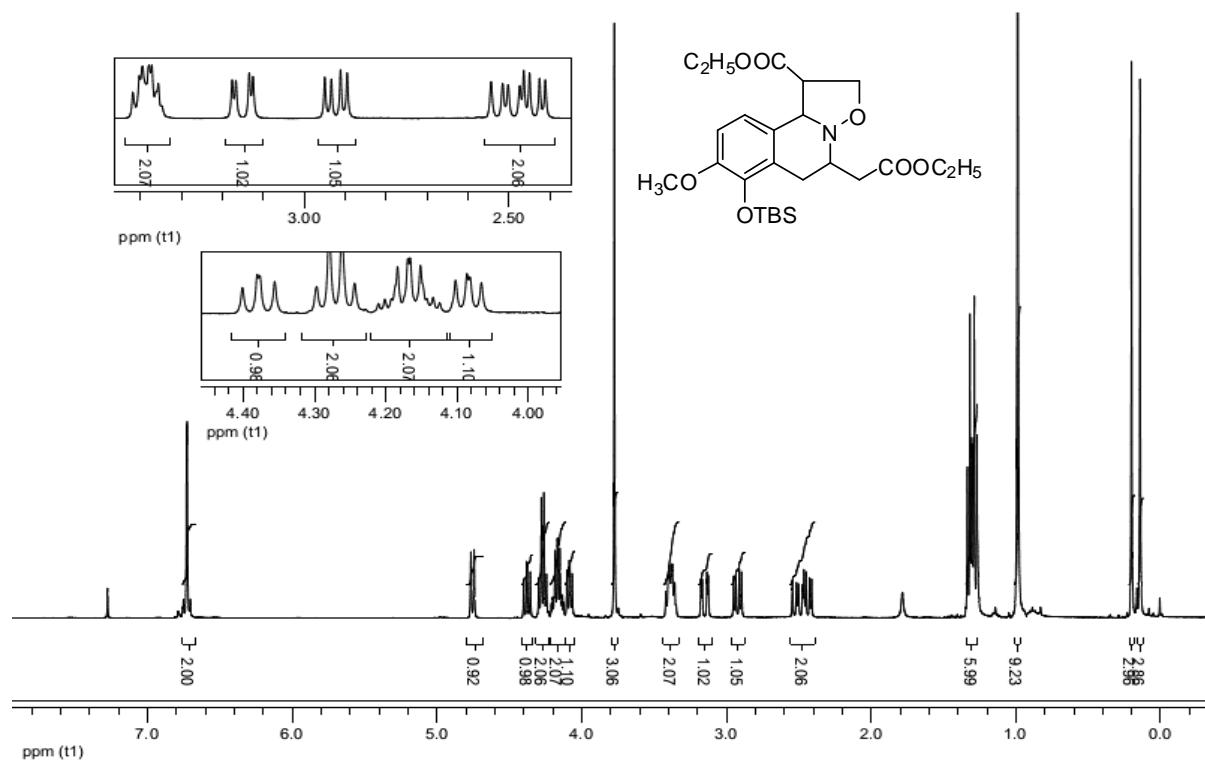
¹H NMR (400 MHz, CDCl₃)

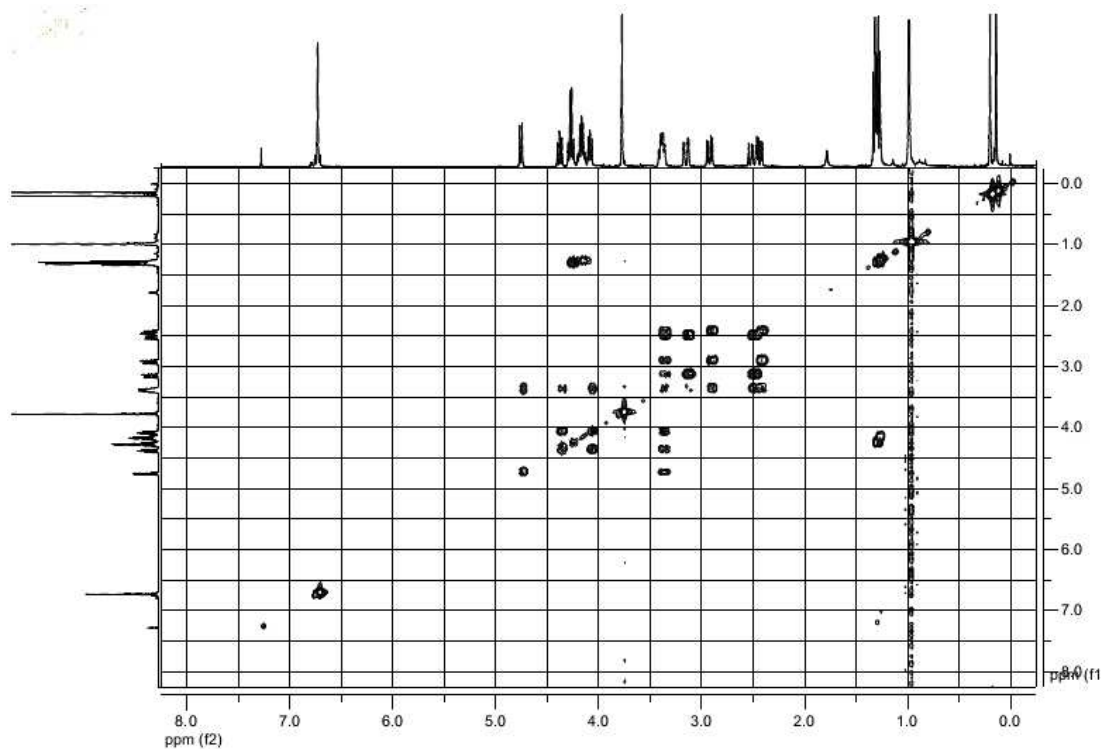
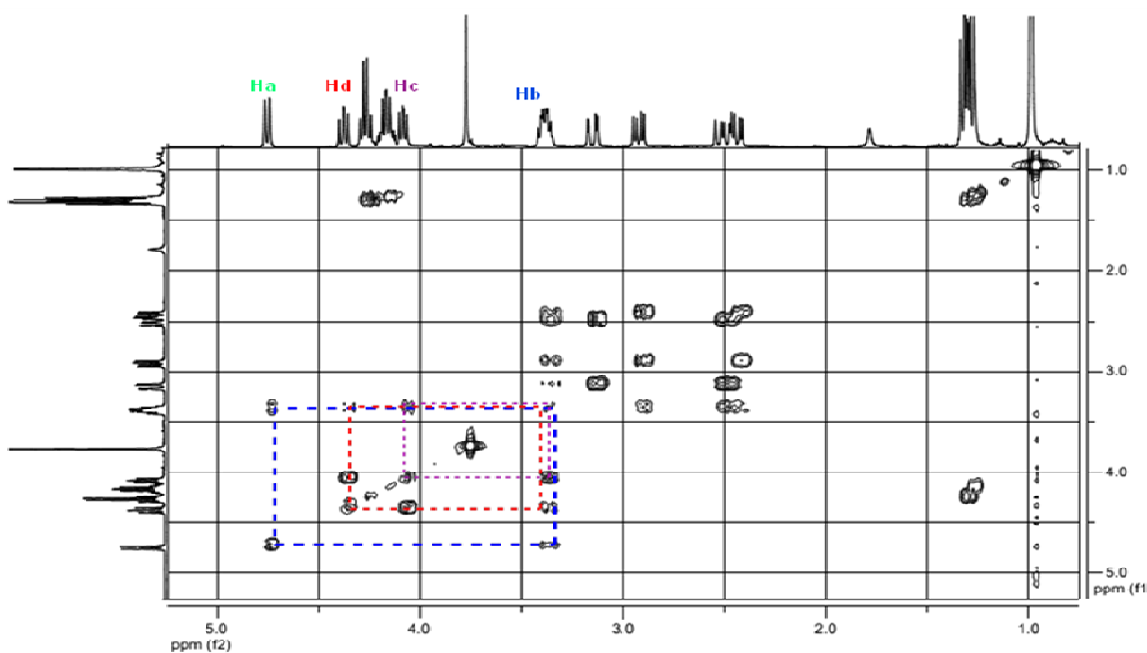
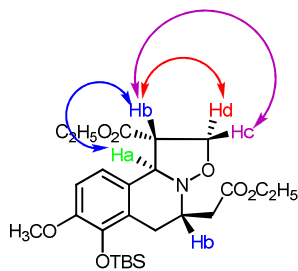


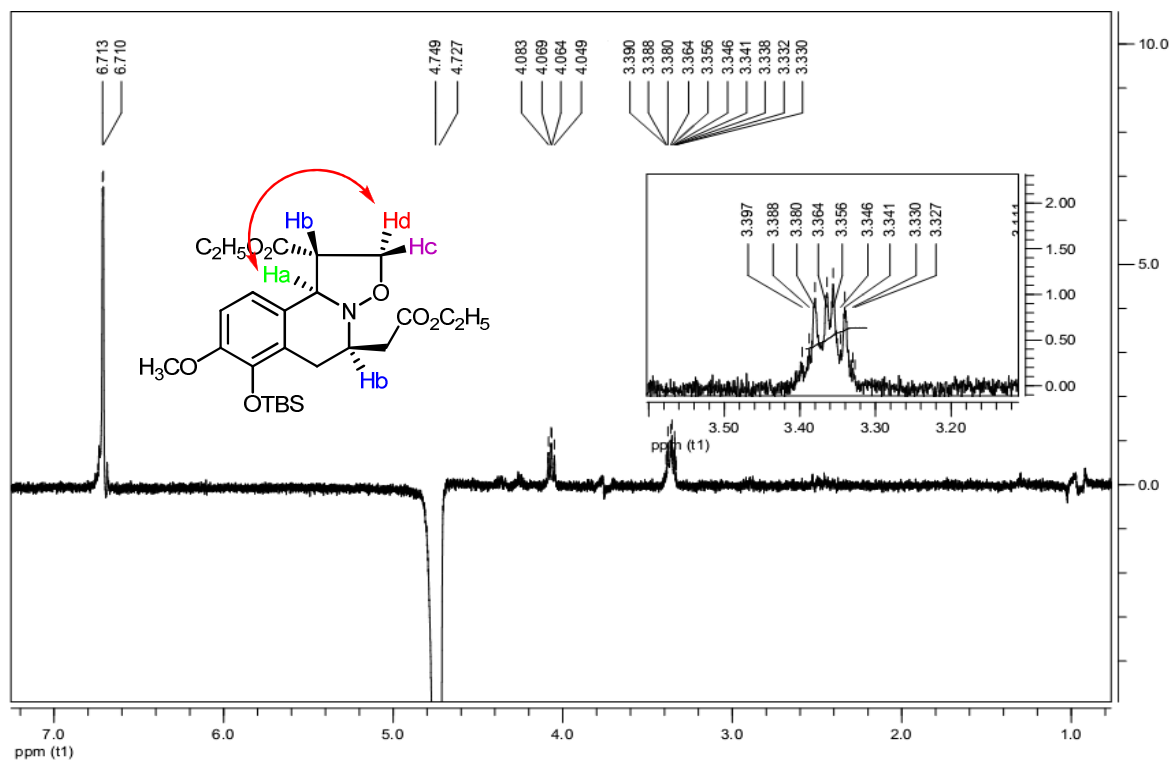
¹³C NMR (100 MHz, CDCl₃)

5-(*tert*-butyldimethylsilyloxy)-3-(2-ethoxy-2-oxoethyl)-6-methoxy-3,4 dihydro isoquinoline 2-oxide (11):**¹H NMR (400 MHz, CDCl₃)****¹³C NMR (100 MHz, CDCl₃)**

Ethyl 7-(*tert*-butyldimethylsilyloxy)-5-(2-ethoxy-2-oxoethyl)-8-methoxy-2,5,6,10b-tetrahydro-1*H*-isoxazolo [3,2-*a*] isoquinoline-1-carboxylate (12a):

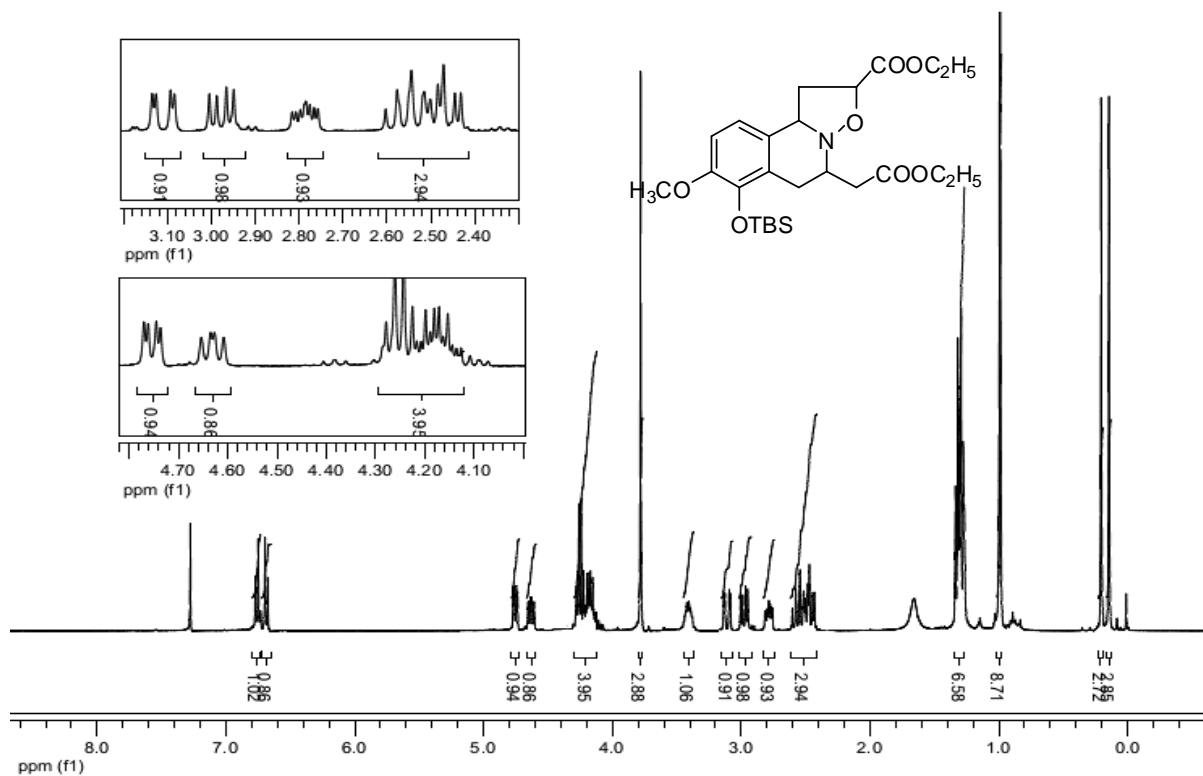


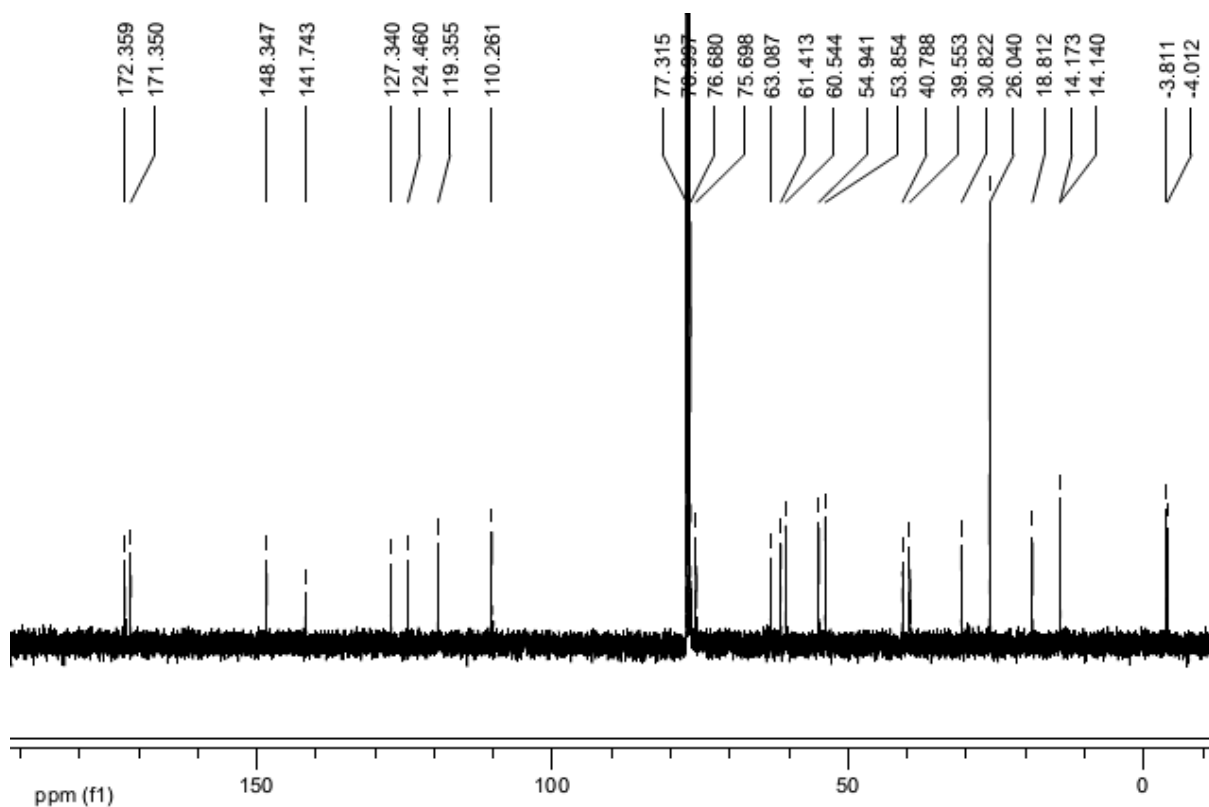
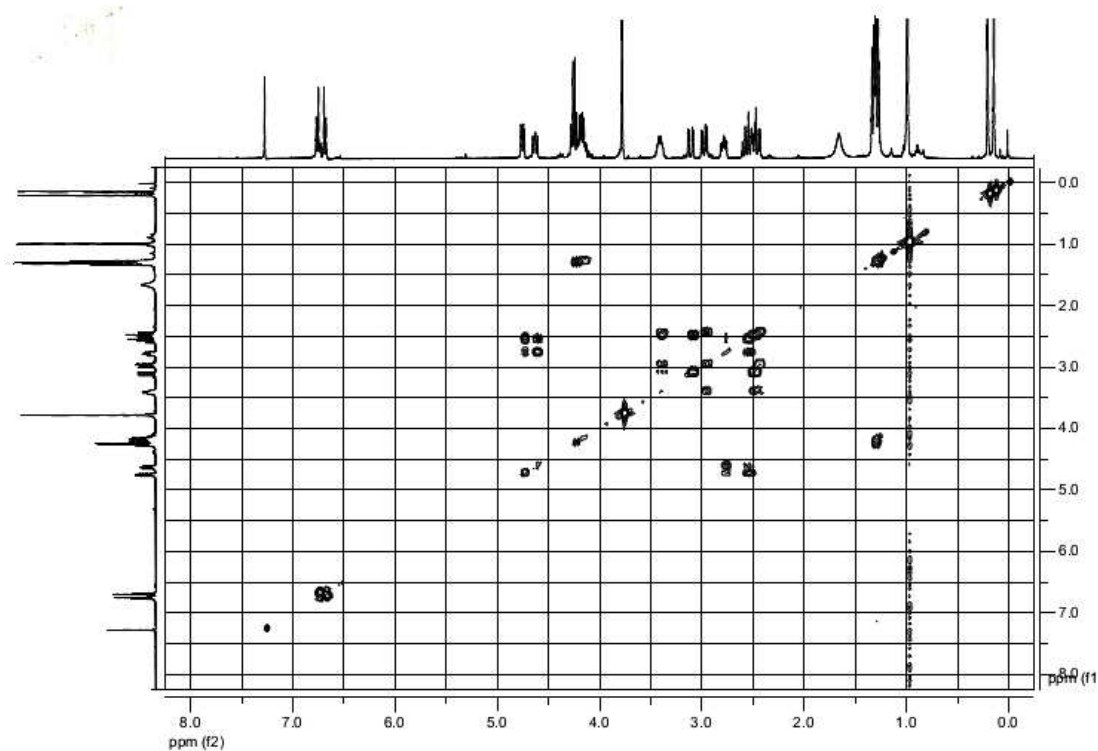
 ^1H - ^1H COSY NMR of Compound 12aExpansion of ^1H - ^1H COSY NMR of Compound 12a

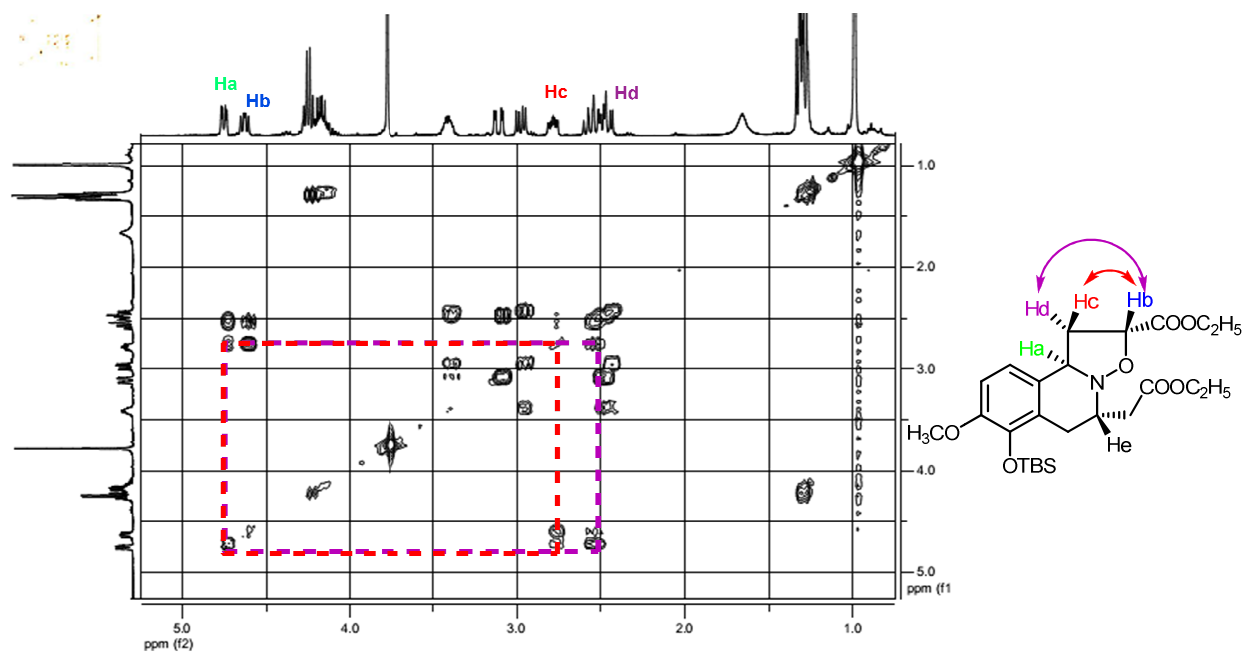
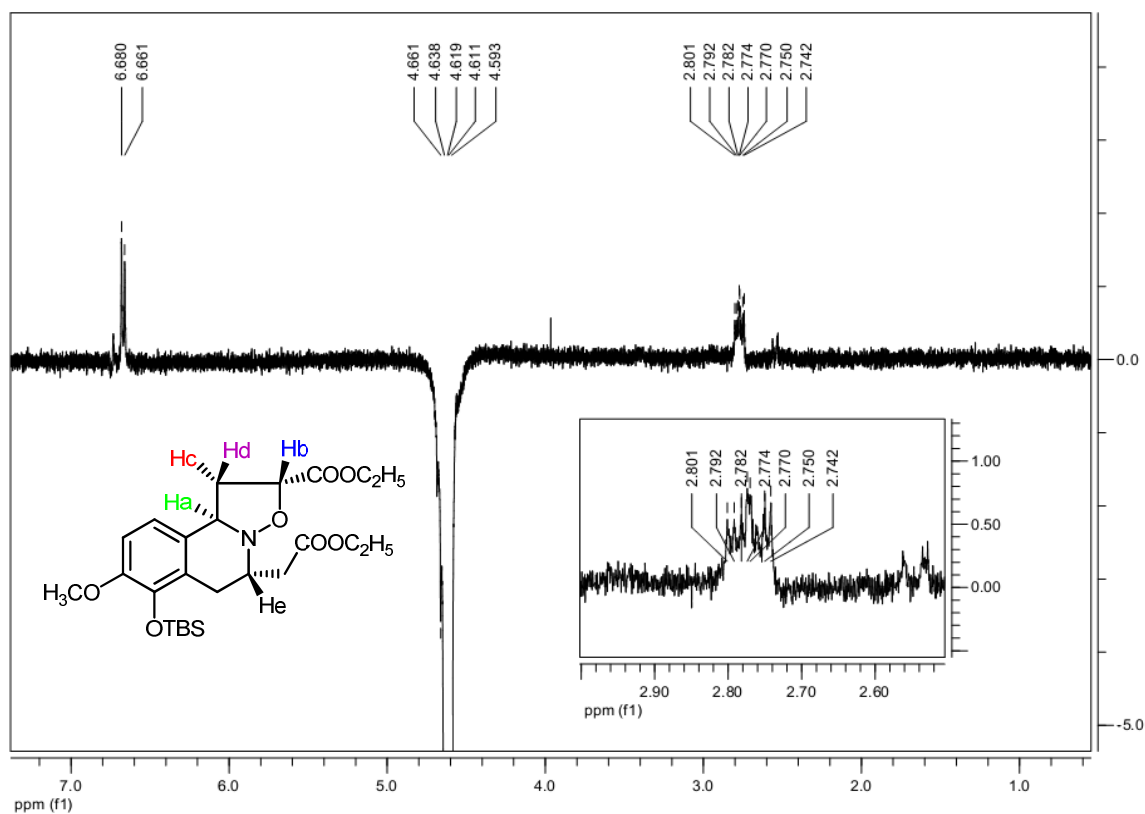


Expansion of 1D NOE of Compound 12a

Ethyl 7-(*tert*-butyldimethylsilyloxy)-5-(2-ethoxy-2-oxoethyl)-8-methoxy-2,5,6,10b-tetrahydro-1*H*-isoxazolo[3,2-*a*] isoquinoline-2-carboxylate (12b):

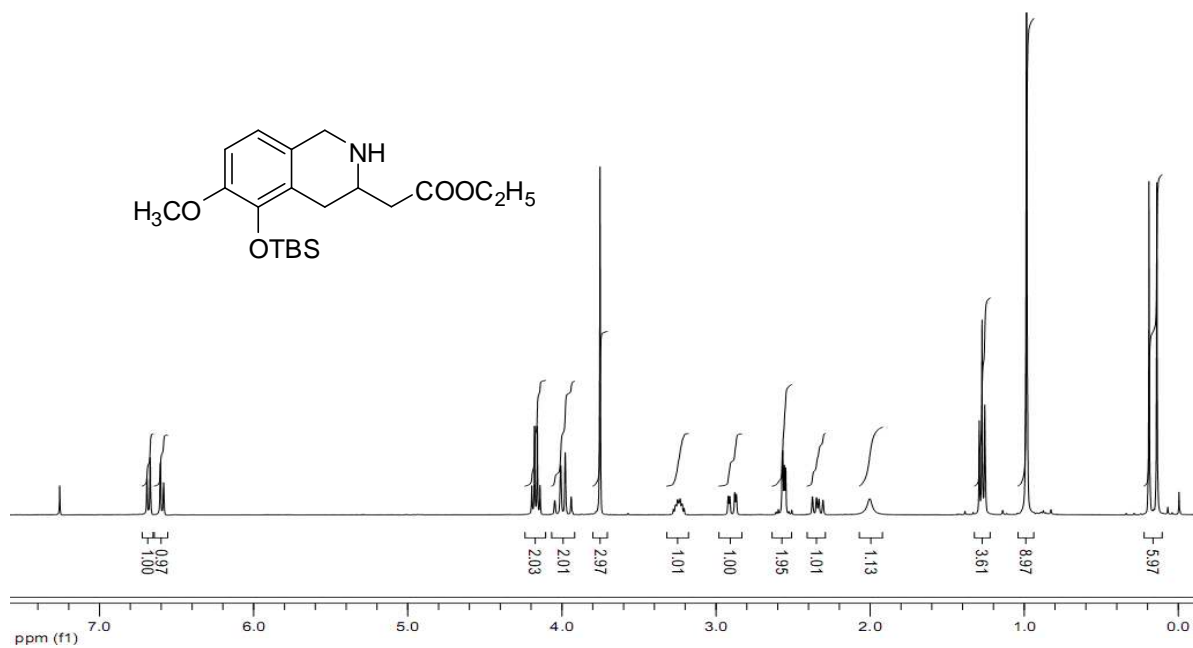
 ^1H NMR (400 MHz, CDCl_3)

 ^{13}C NMR (100 MHz, CDCl_3) ^1H - ^1H COSY NMR of Compound 12b

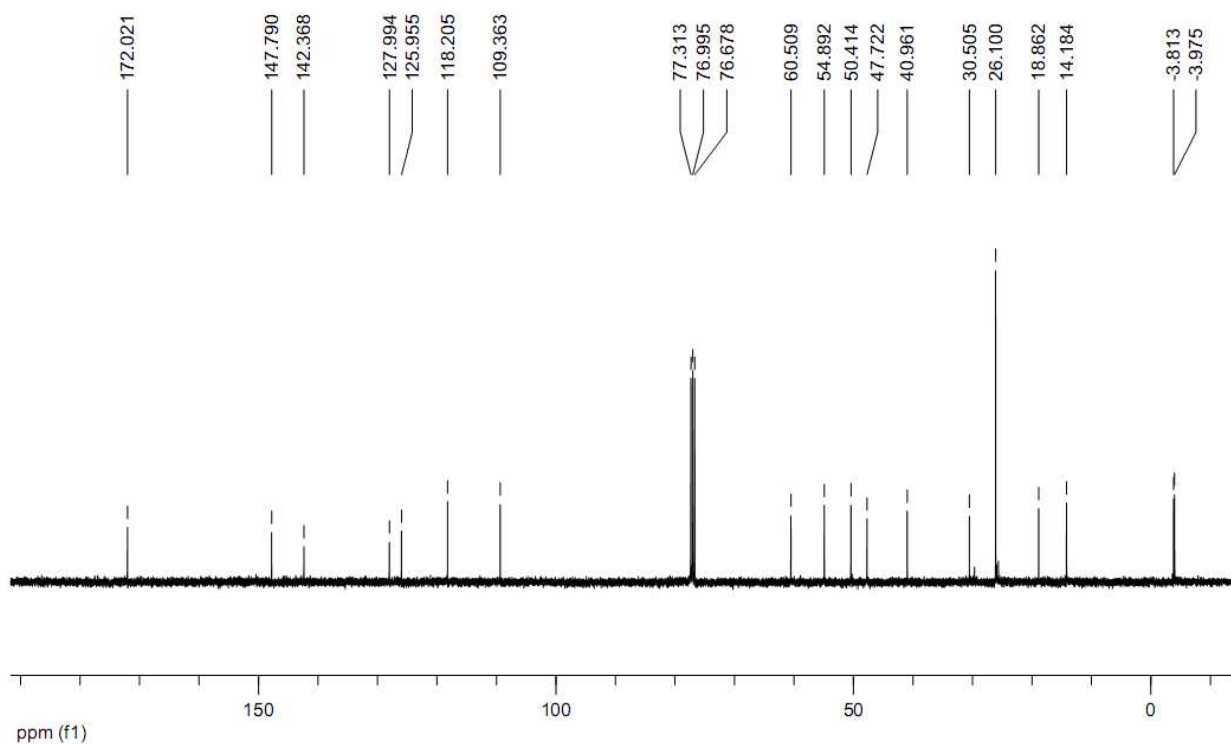
Expansion of ^1H - ^1H COSY NMR of Compound 12b

Expansion of 1D NOE of Compound 12b

Ethyl-2-(5-(*tert*-butyldimethylsilyloxy)-6-methoxy-1,2,3,4 tetrahydroisoquinolin-3-yl)acetate (13):

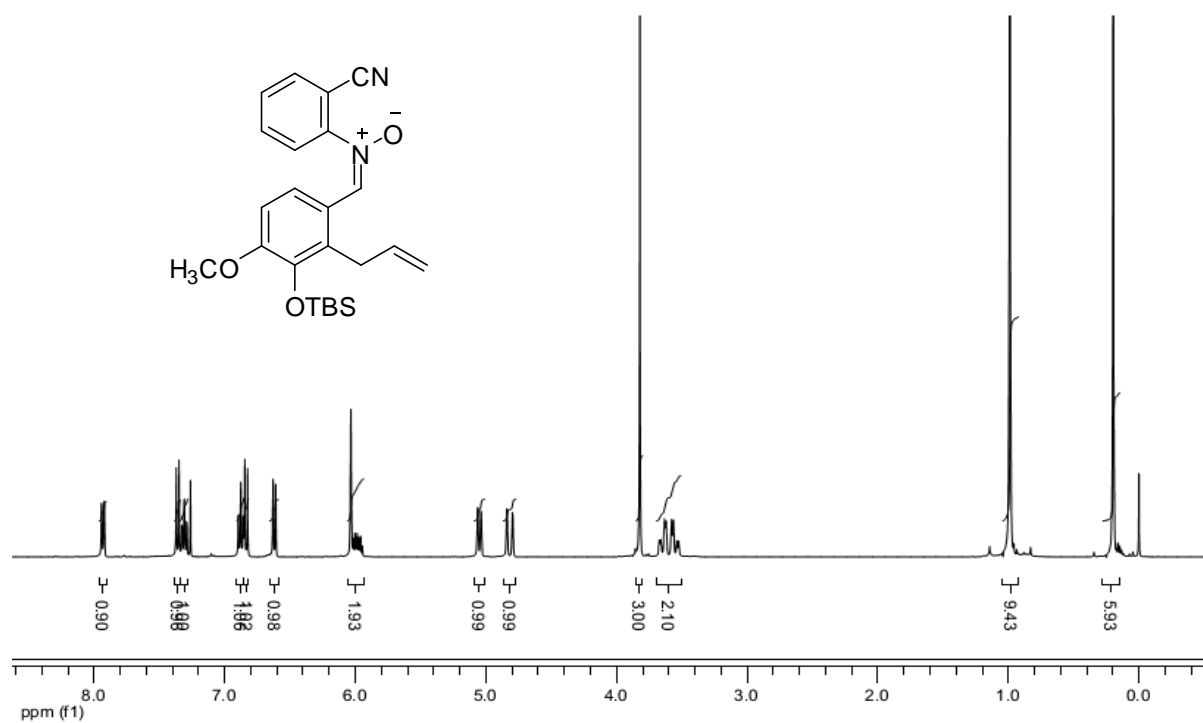


¹H NMR (400 MHz, CDCl₃)

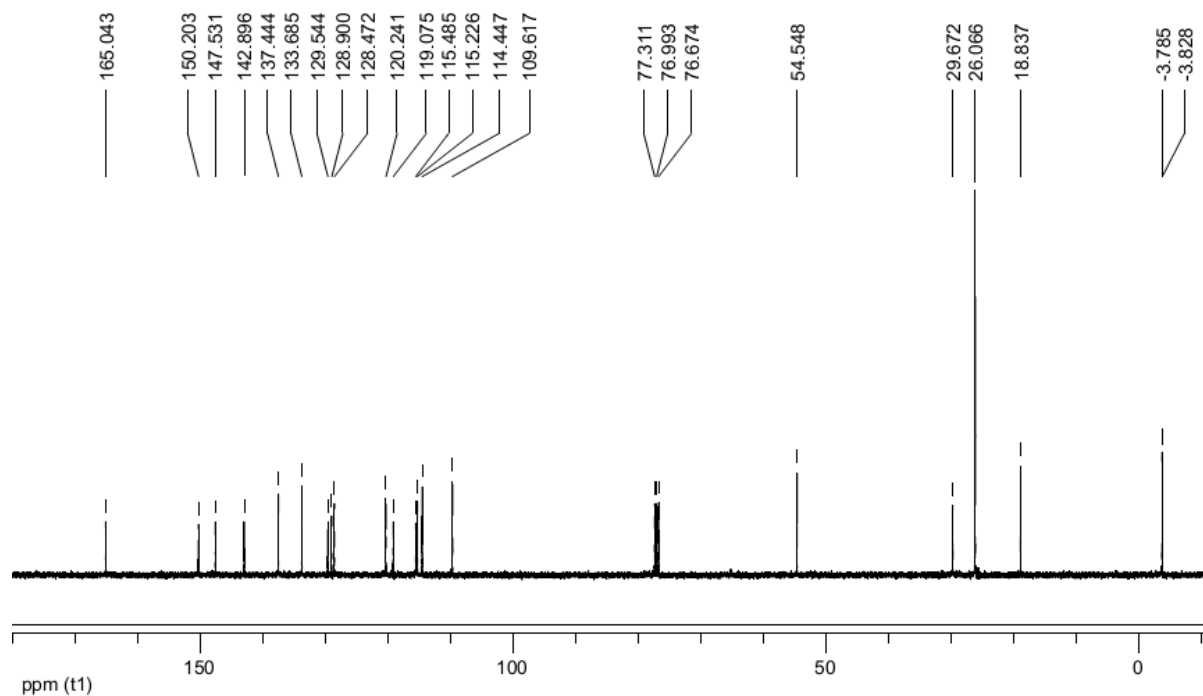


¹³C NMR (100 MHz, CDCl₃)

(*E*)-*N*-(2-allyl-3-(*tert*-butyldimethylsilyloxy)-4-methoxybenzylidene)-2-cyanoaniline oxide (15e):

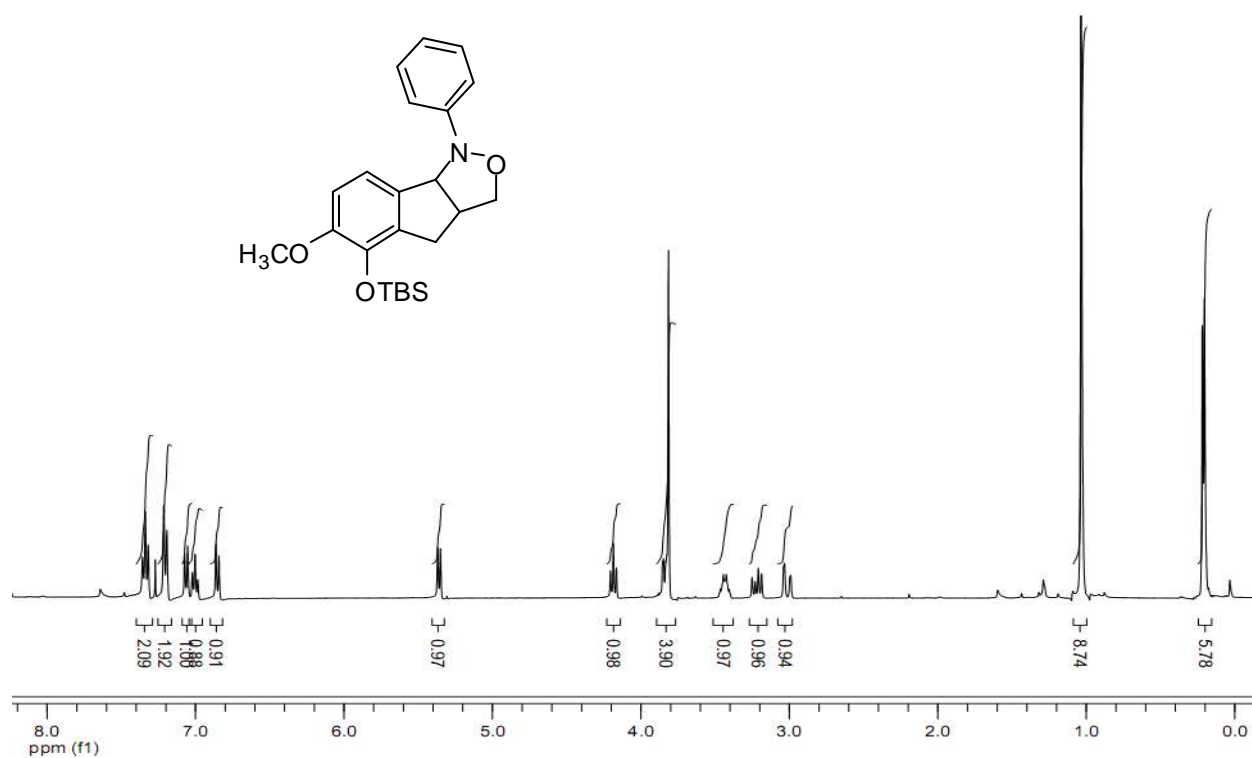


¹H NMR (400 MHz, CDCl₃)

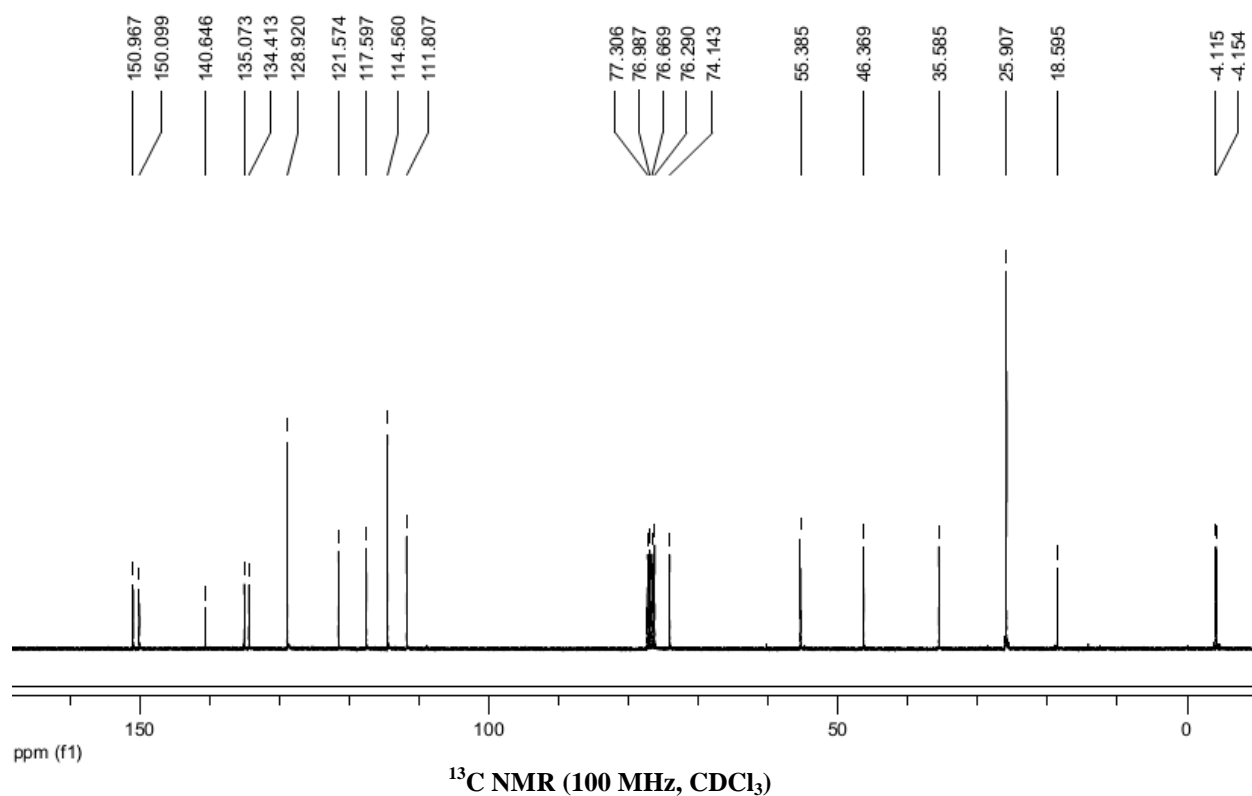


¹³C NMR (100 MHz, CDCl₃)

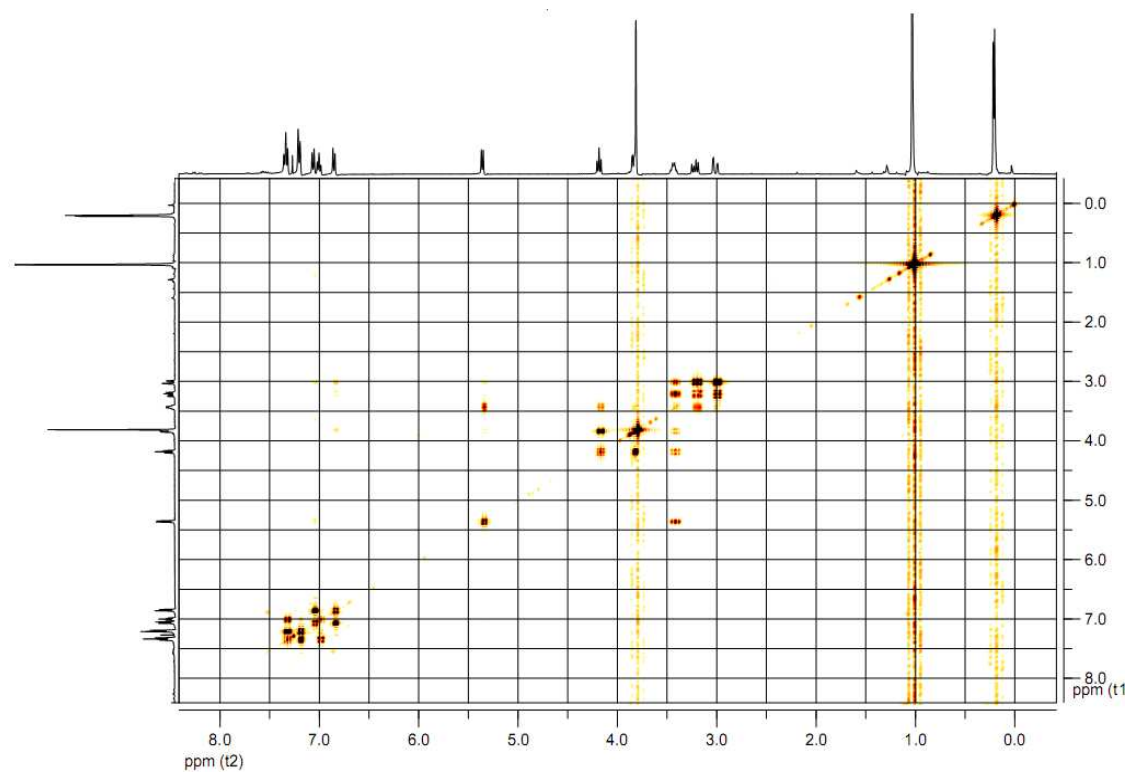
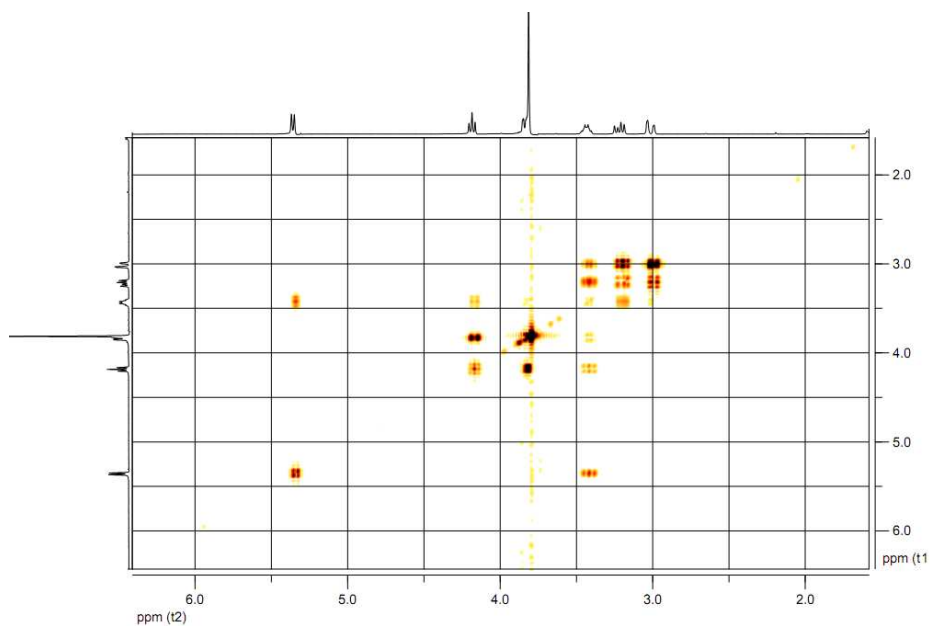
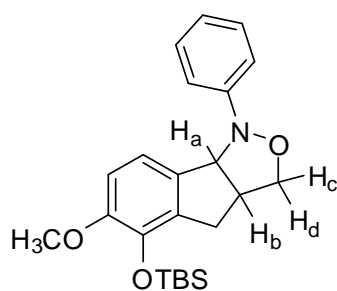
5-(*tert*-butyldimethylsilyloxy)-6-methoxy-1-phenyl-3,3a,4,8b-tetrahydro-1*H*-indeno [1,2-*c*] isoxazole (16a):



¹H NMR (400 MHz, CDCl₃)

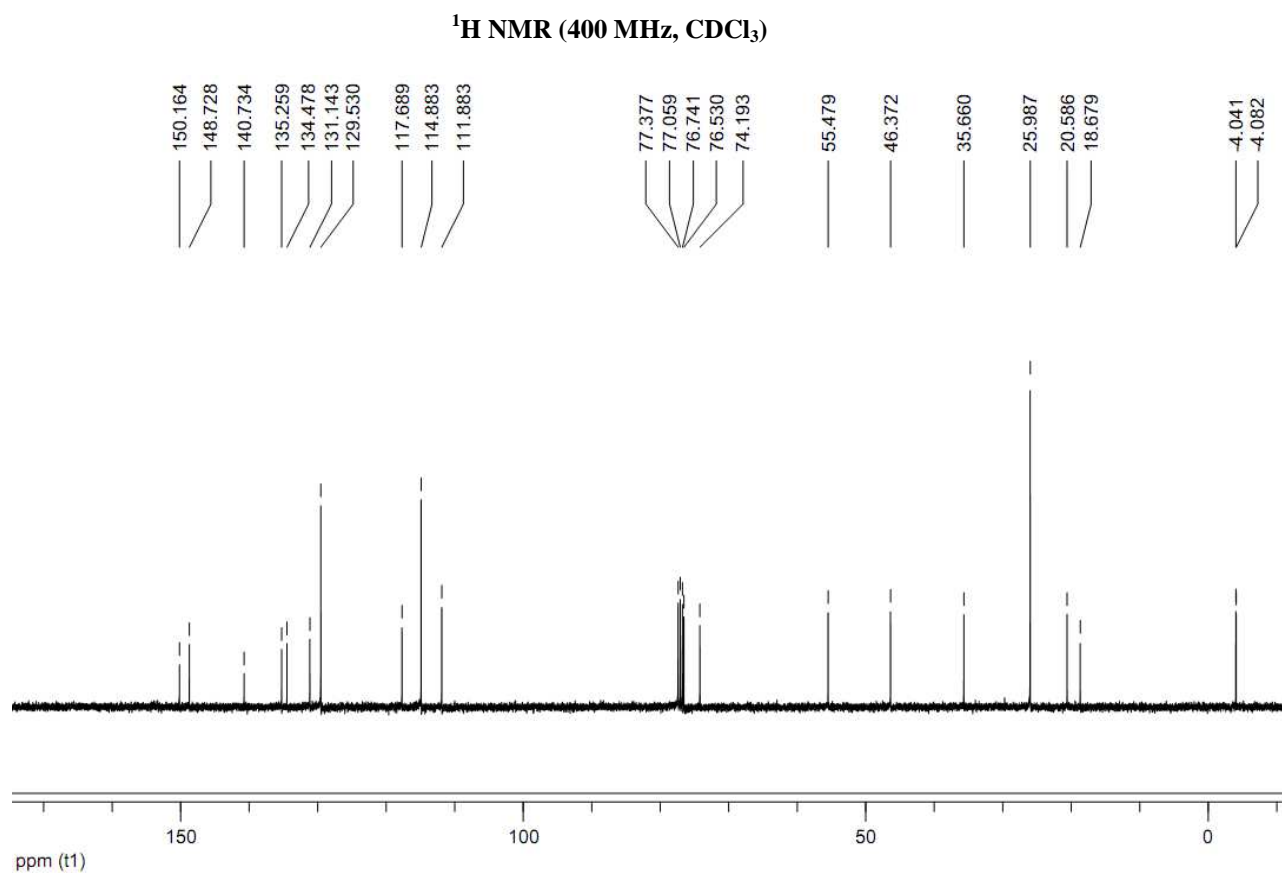
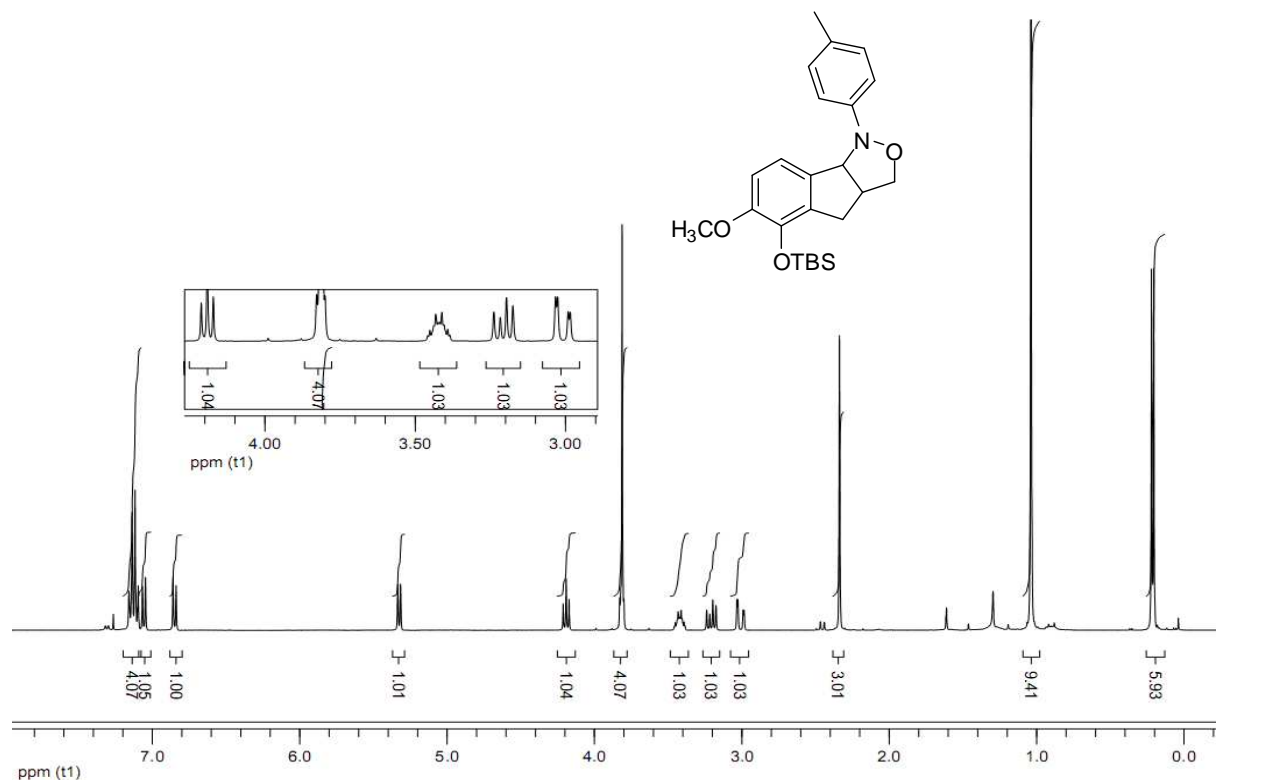


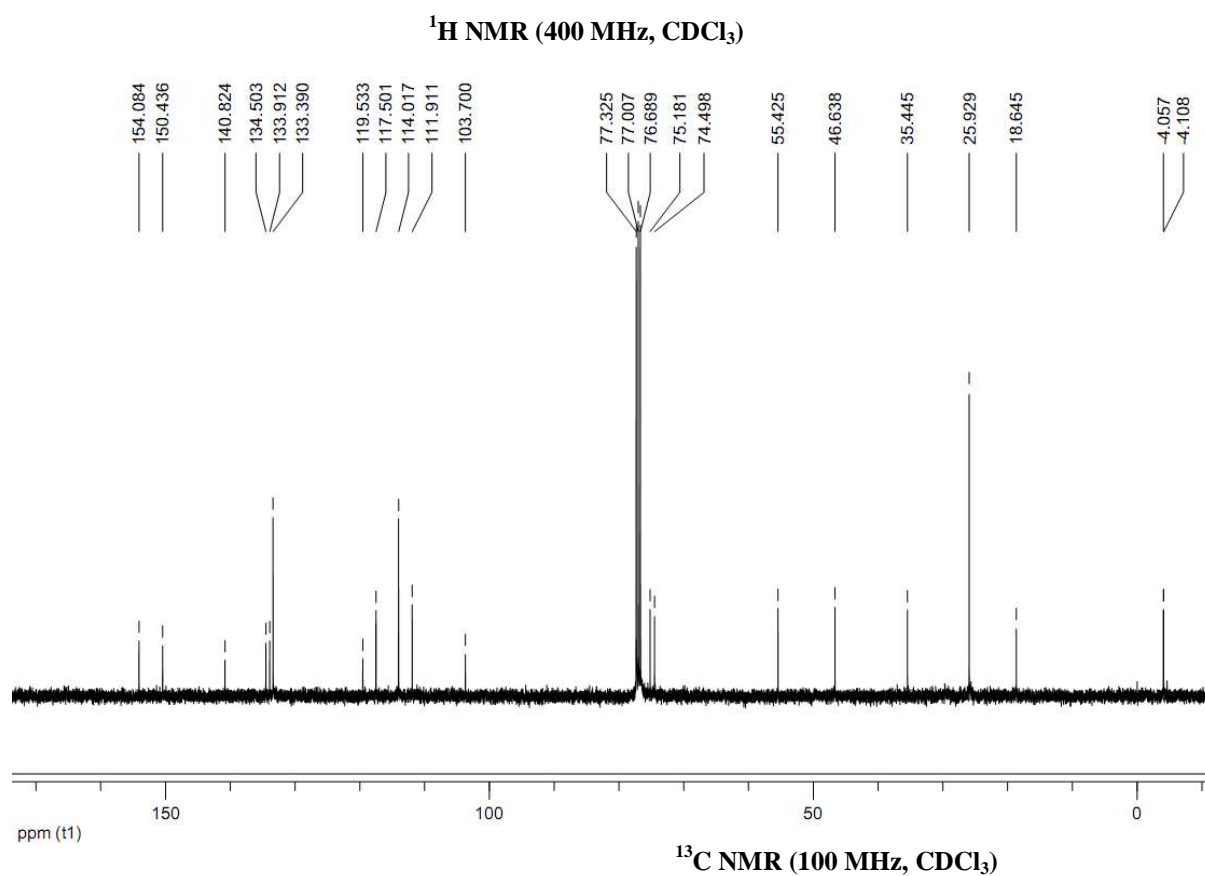
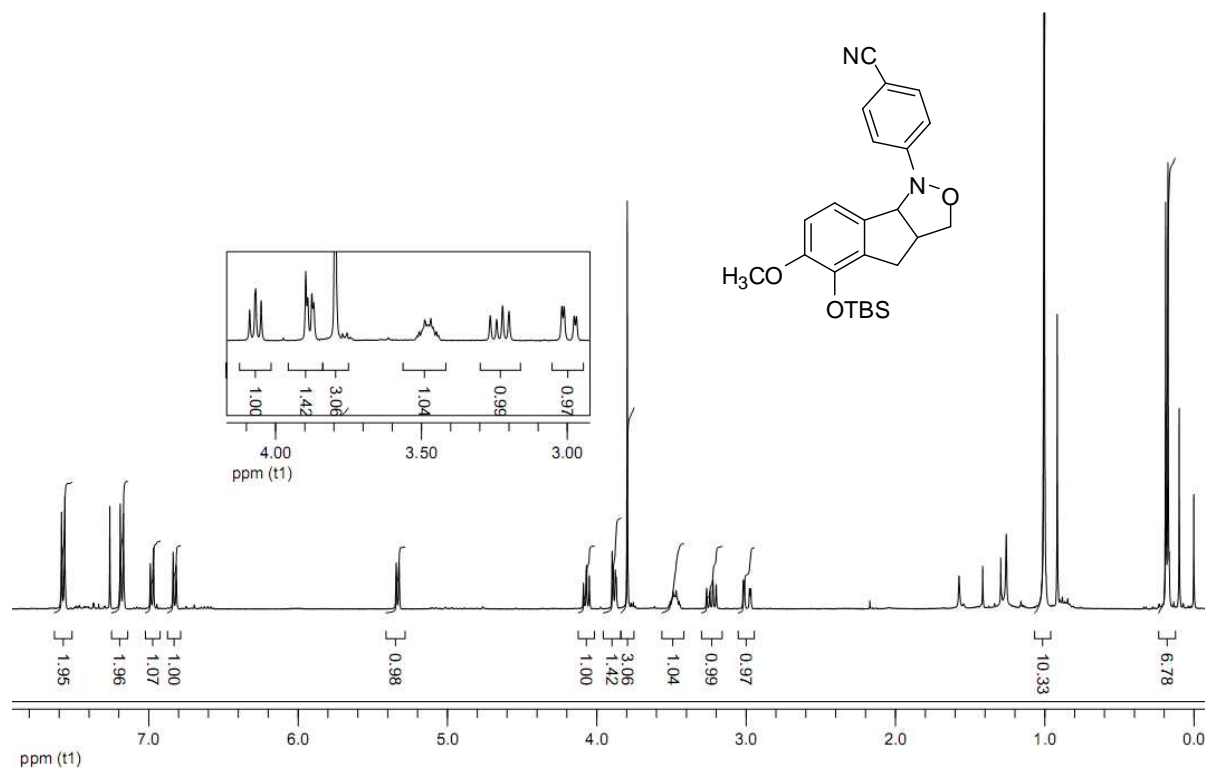
¹³C NMR (100 MHz, CDCl₃)

 **^1H - ^1H COSY NMR of Compound 16a****Expansion of ^1H - ^1H COSY NMR of Compound 16a**

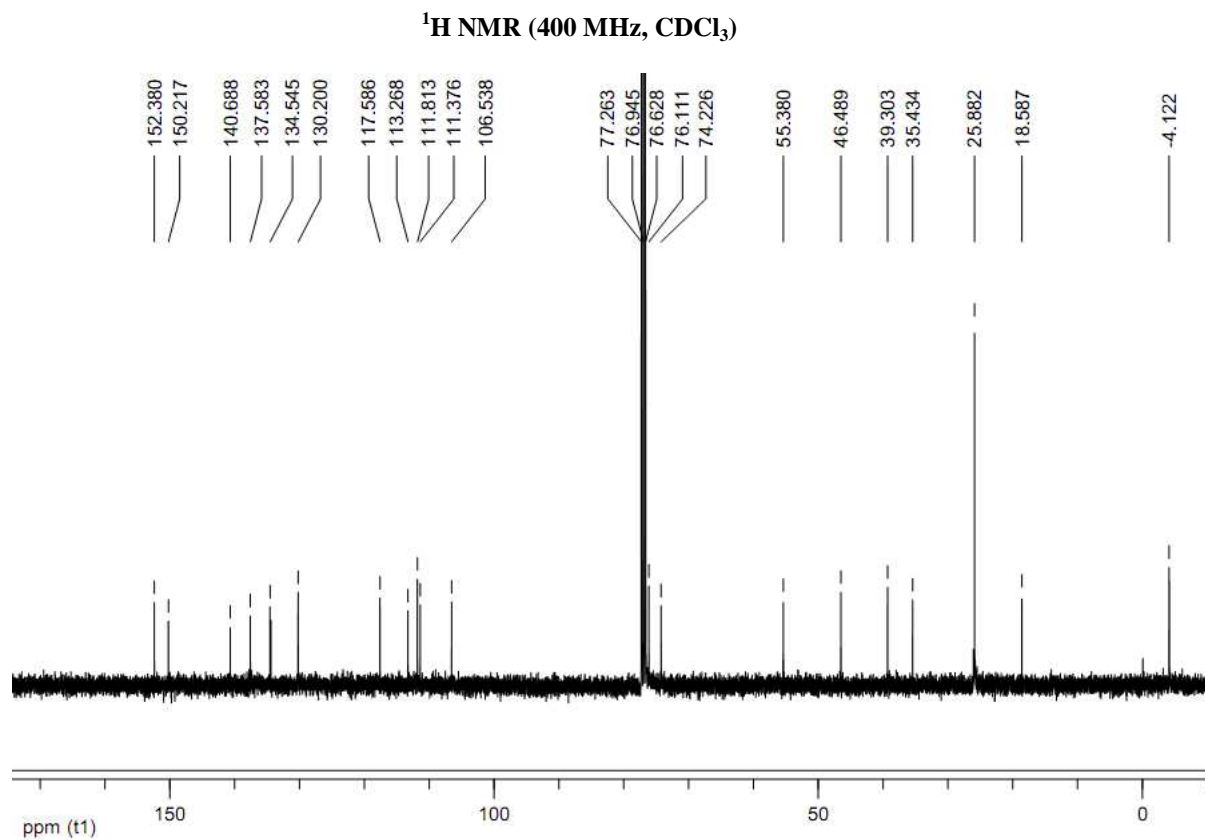
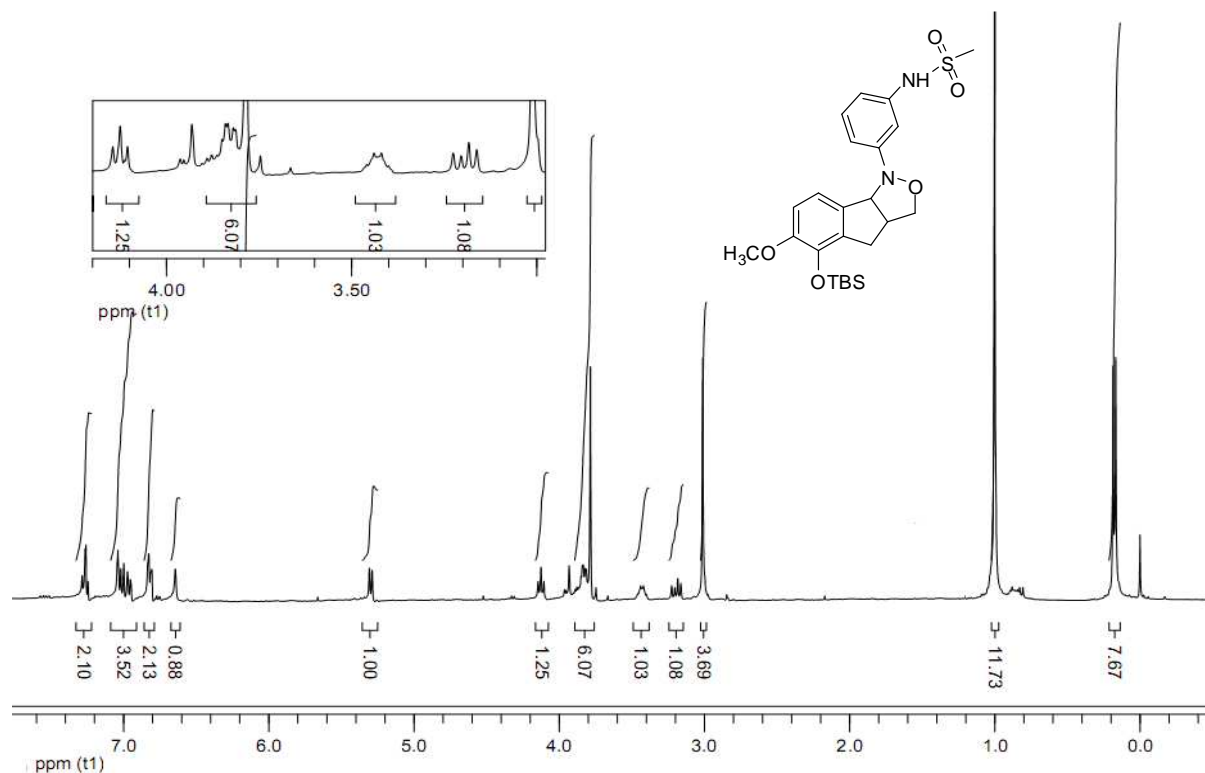
H_a : 5.36 ppm H_c : 4.18 ppm
 H_b : 3.45 ppm H_d : 3.89 ppm

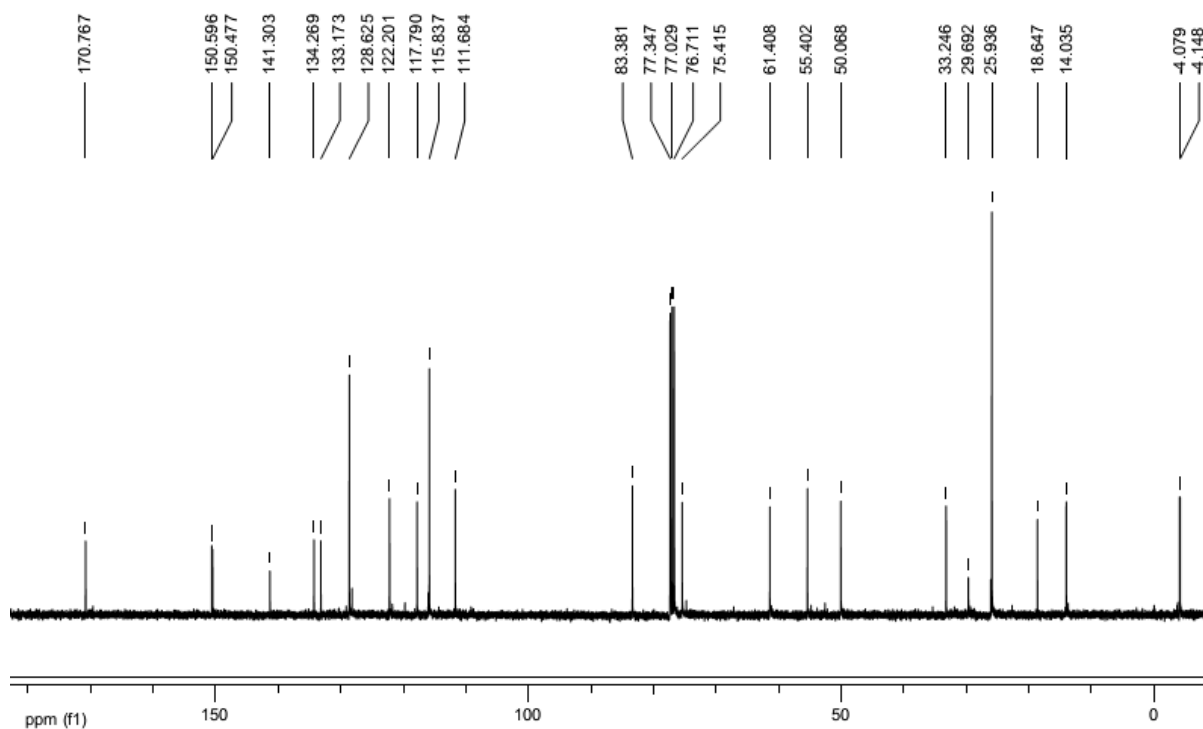
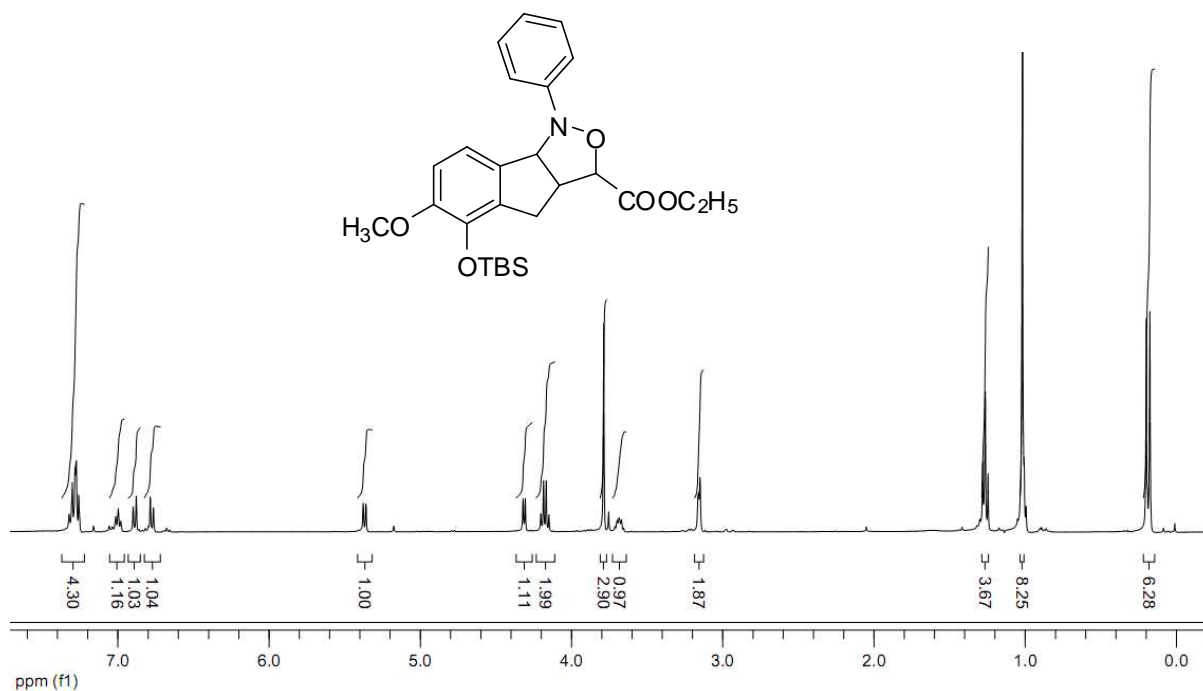
5-(*tert*-butyldimethylsilyloxy)-6-methoxy-1-*p*-tolyl-3,3a,4,8b-tetrahydro-1*H*-indeno[1,2-*c*]isoxazole (16b):

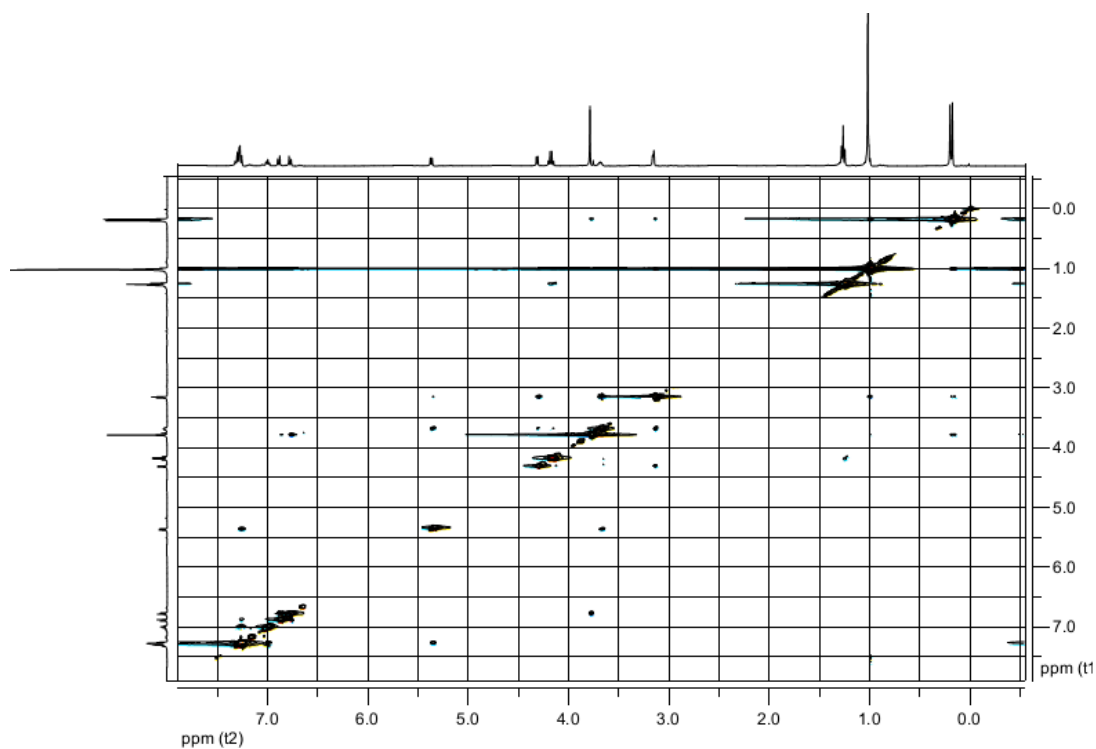


4-(5-(*tert*-butyldimethylsilyloxy)-6-methoxy-3,3a,4,8b-tetrahydro-1*H*-indeno [1,2-*c*] isoxazol-1-yl) benzonitrile (16c):

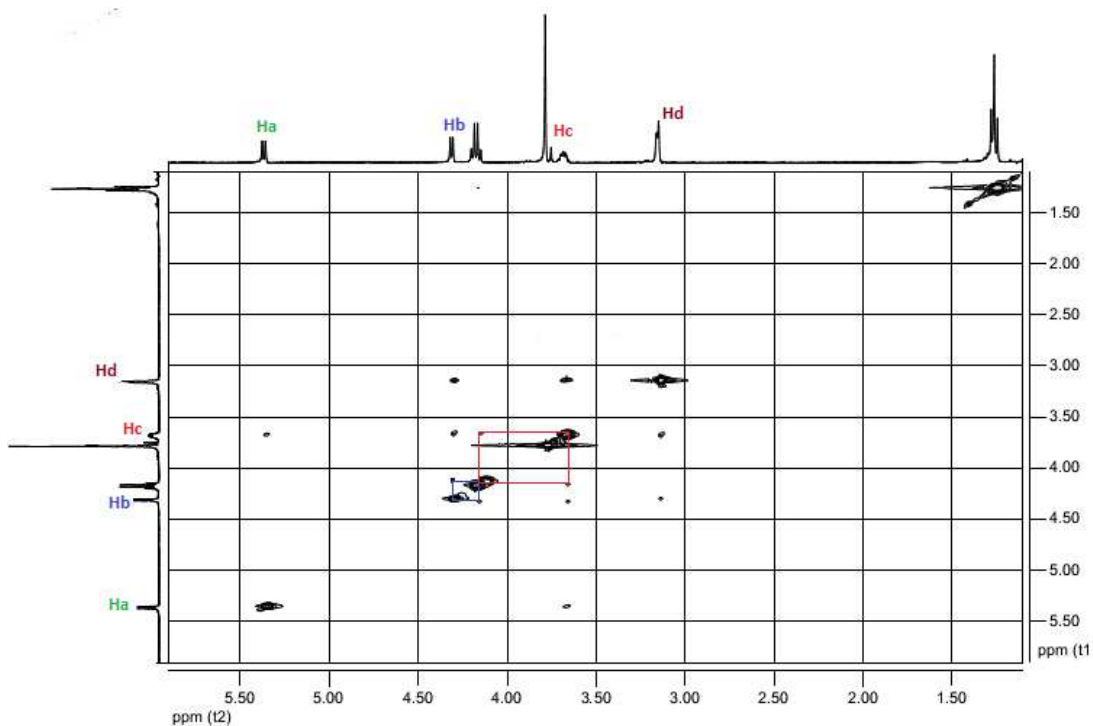
N-(3-(5-(*tert*-butyldimethylsilyloxy)-6-methoxy-3,3a,4,8b-tetrahydro-1*H*-indeno[1,2-*c*]isoxazol-1-yl) phenyl) methanesulfonamide (16d):



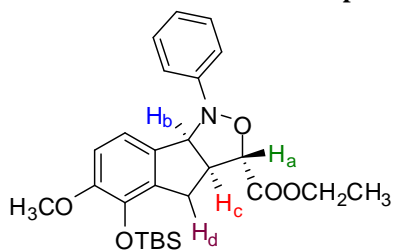
Ethyl 5-(*tert*-butyldimethylsilyloxy)-6-methoxy-1-phenyl-3,3a,4,8b-tetrahydro-1*H*-indeno[1,2-*c*]isoxazole-3-carboxylate (16f):



2D NOESY of Compound 16f

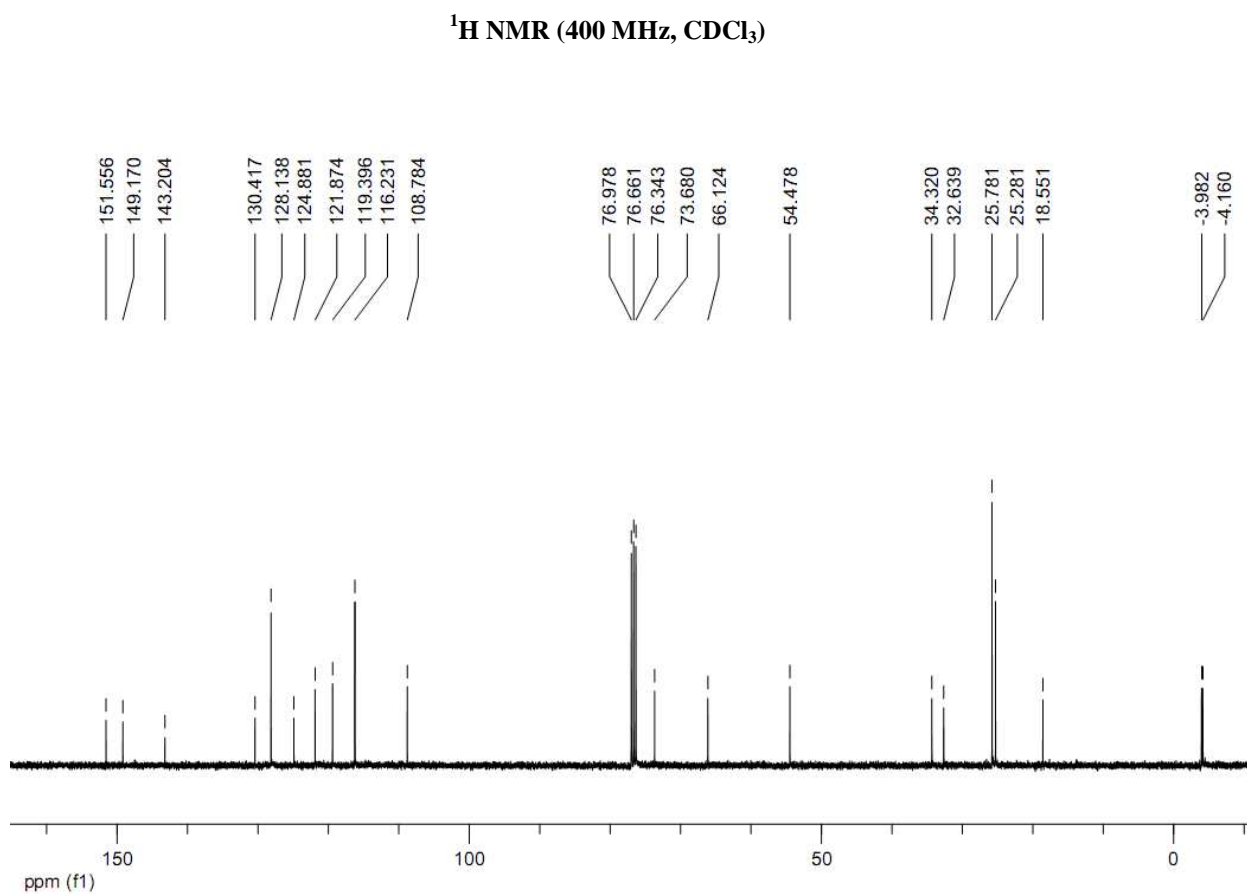
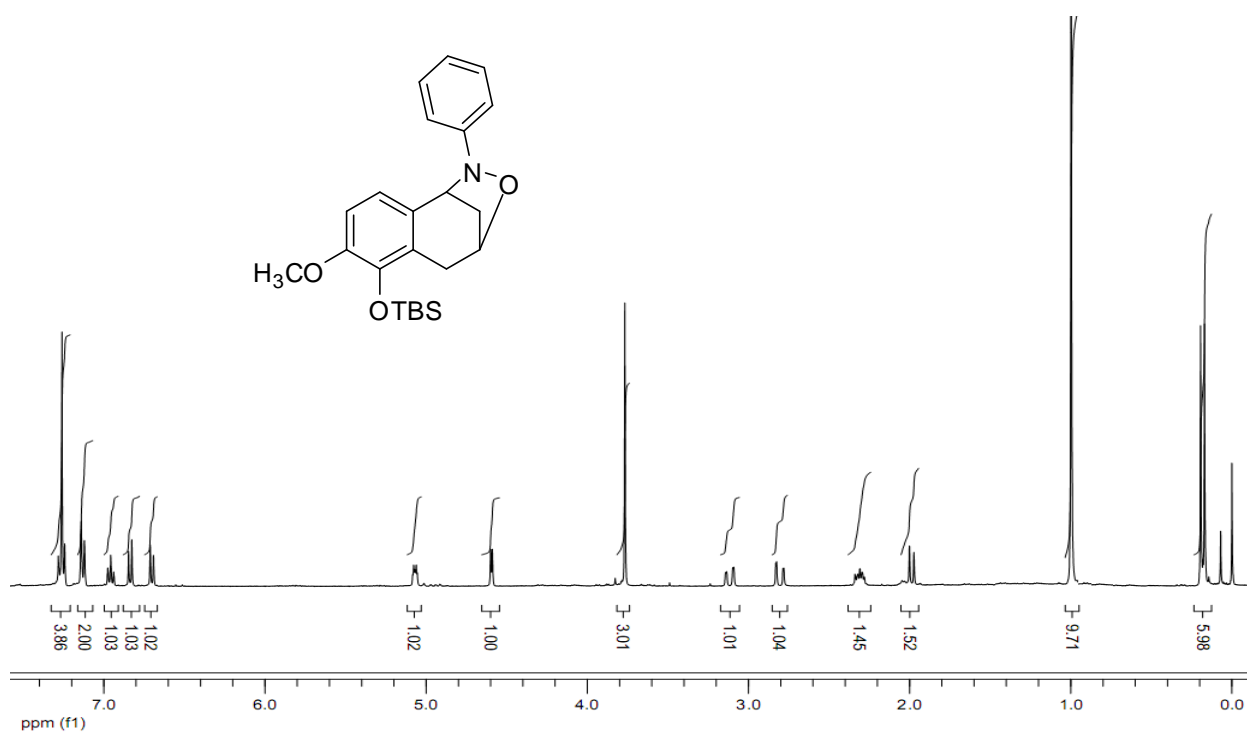


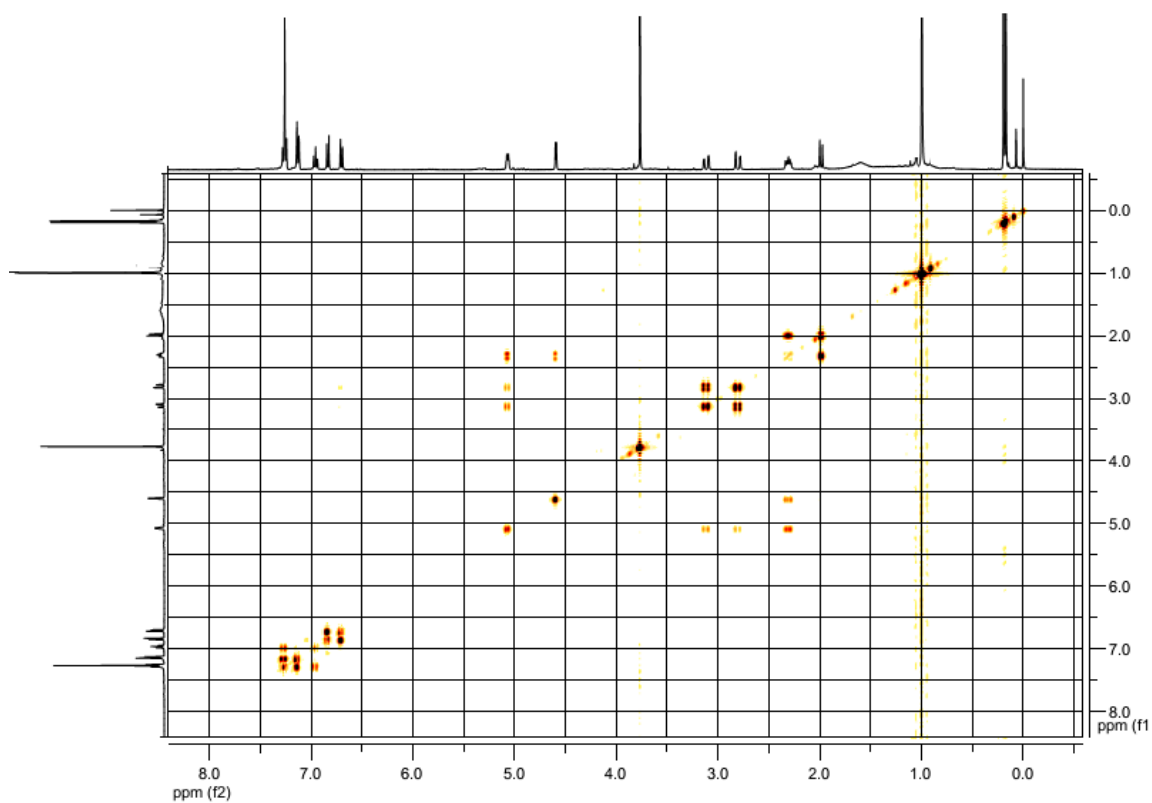
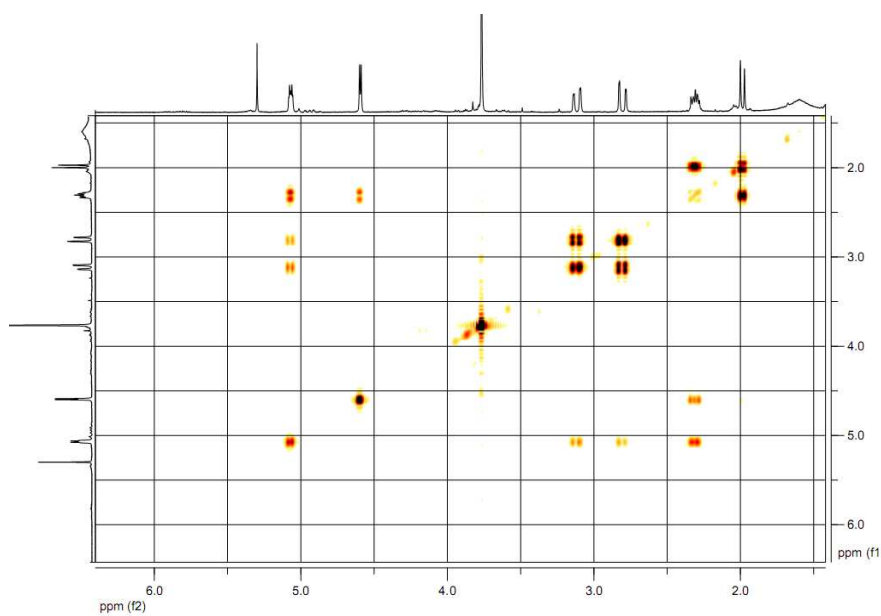
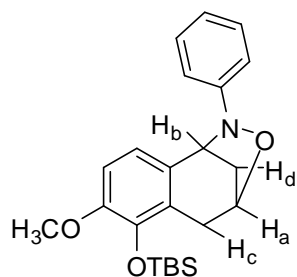
Compound 16f



-ve noe between
H_a and H_b

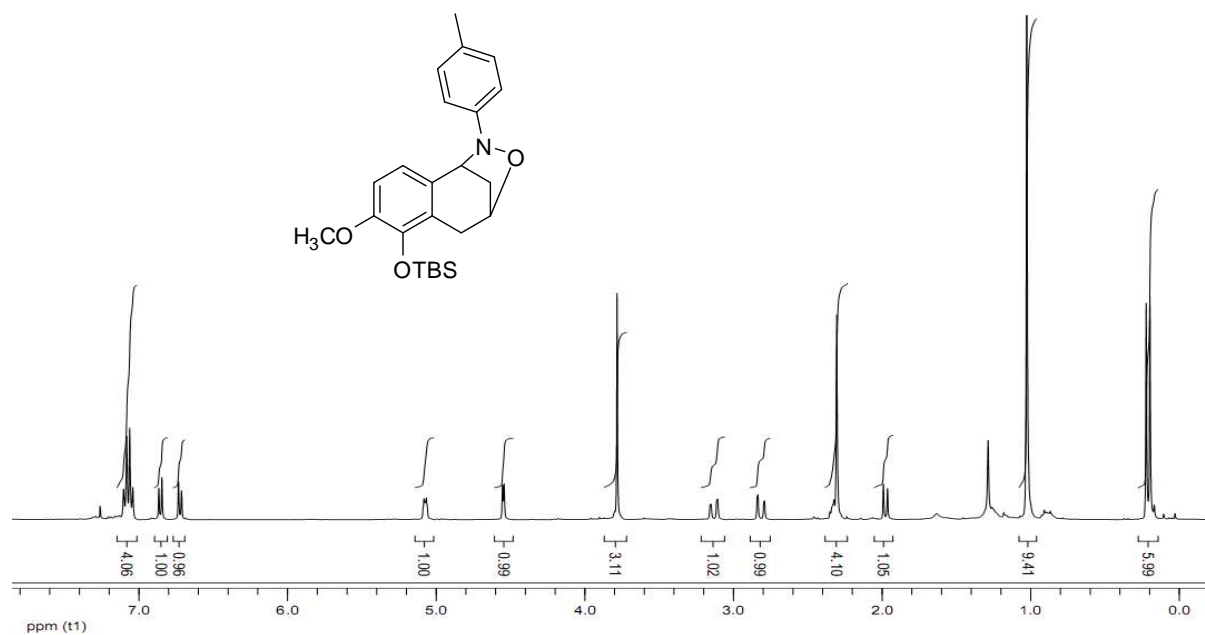
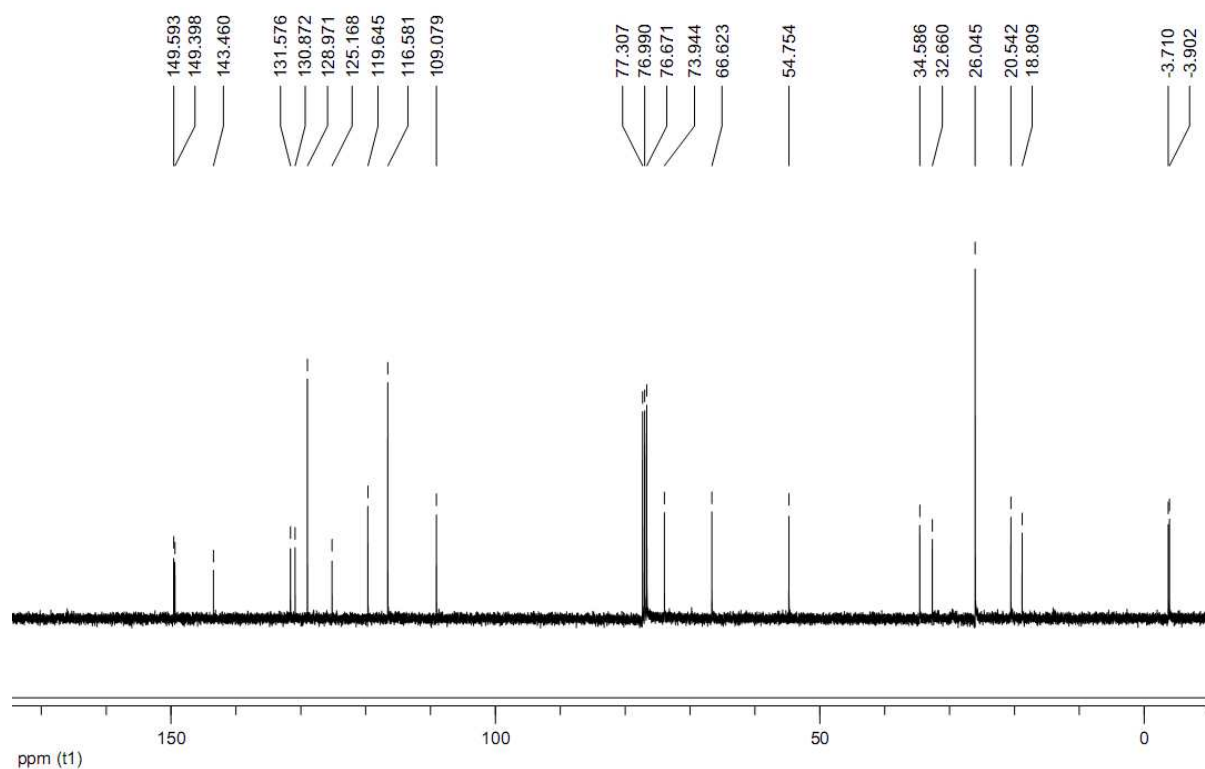
Compound 17a:



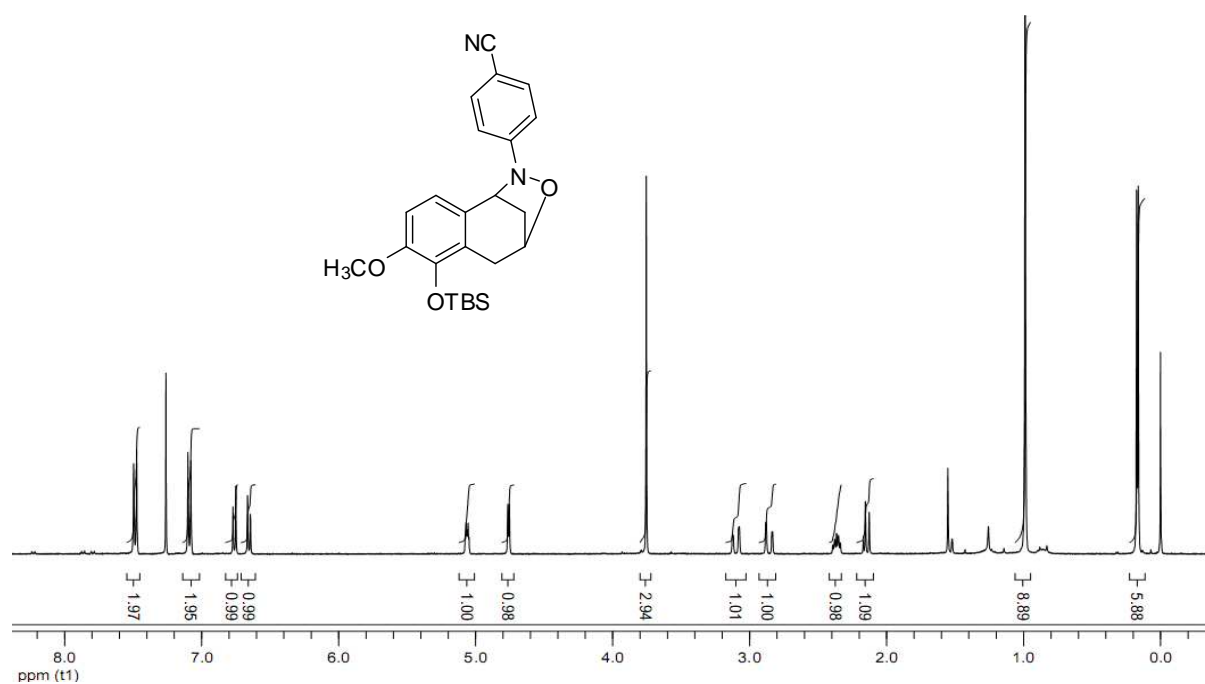
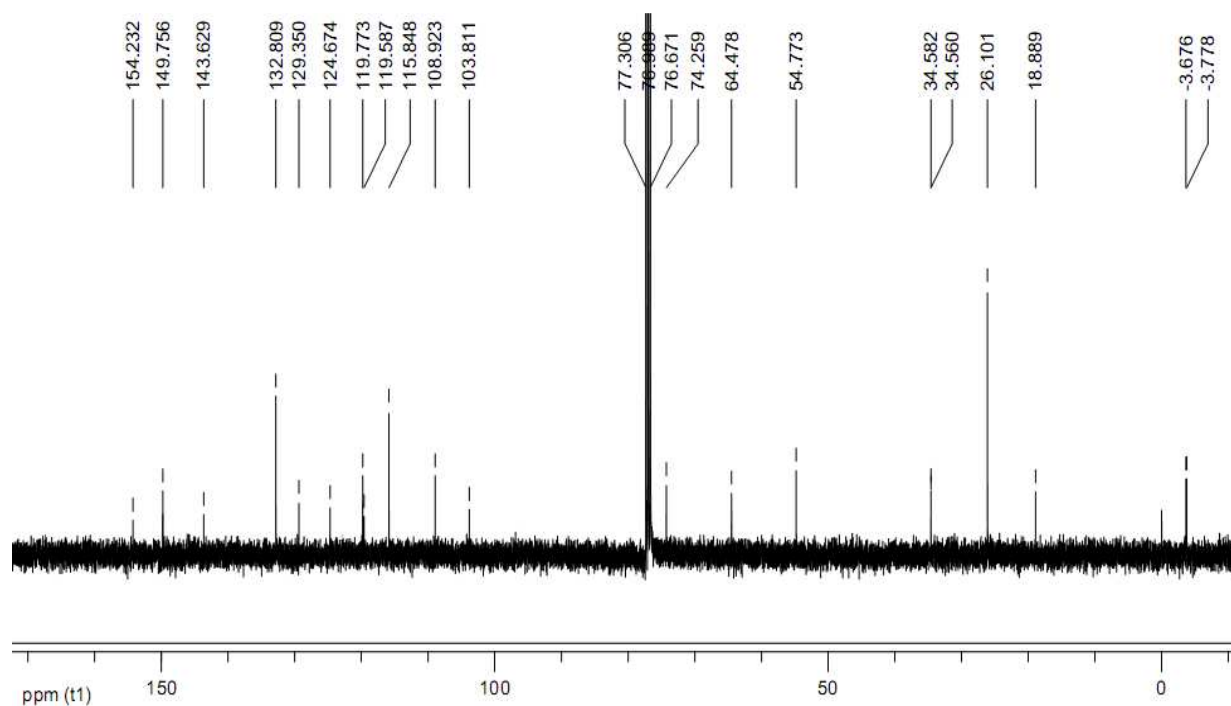
 **^1H - ^1H COSY NMR of Compound 17a****Expansion of ^1H - ^1H COSY NMR of Compound 17a**

H_a : 5.12 ppm H_c : 3.09 ppm
 H_b : 4.59 ppm H_d : 2.31 ppm

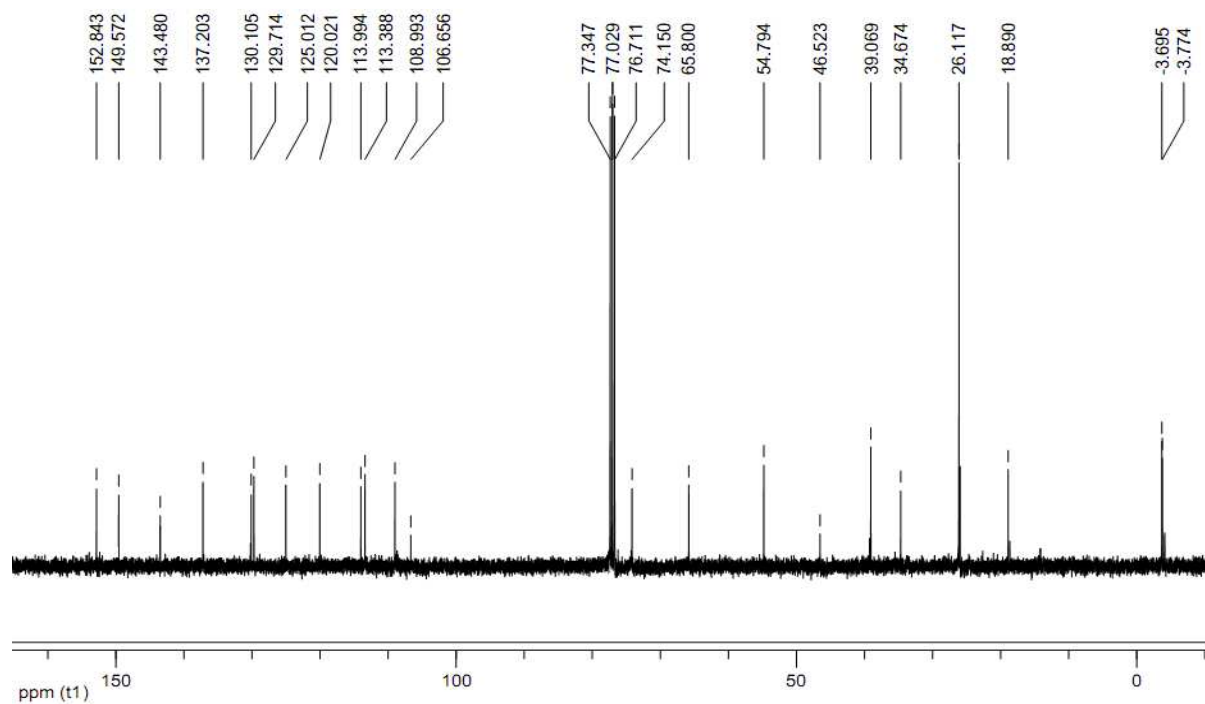
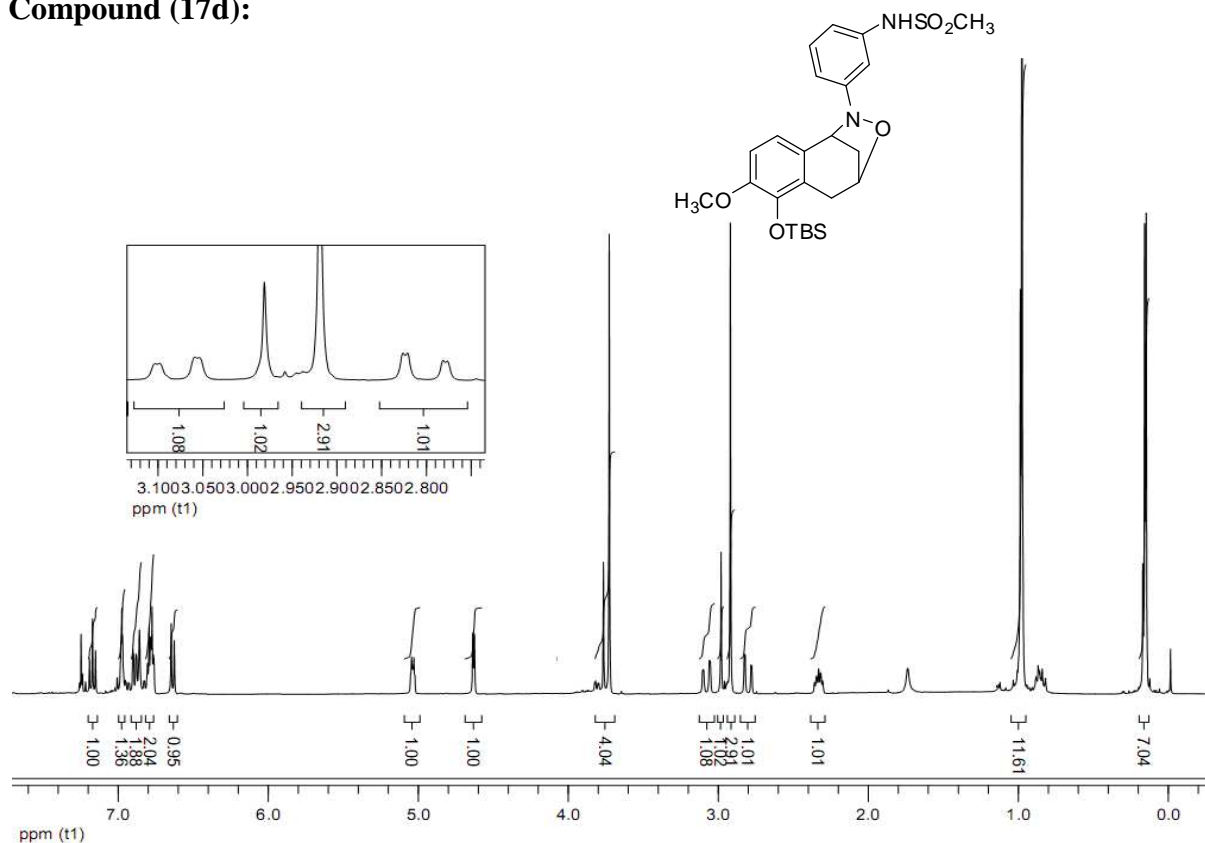
Compound (17b):

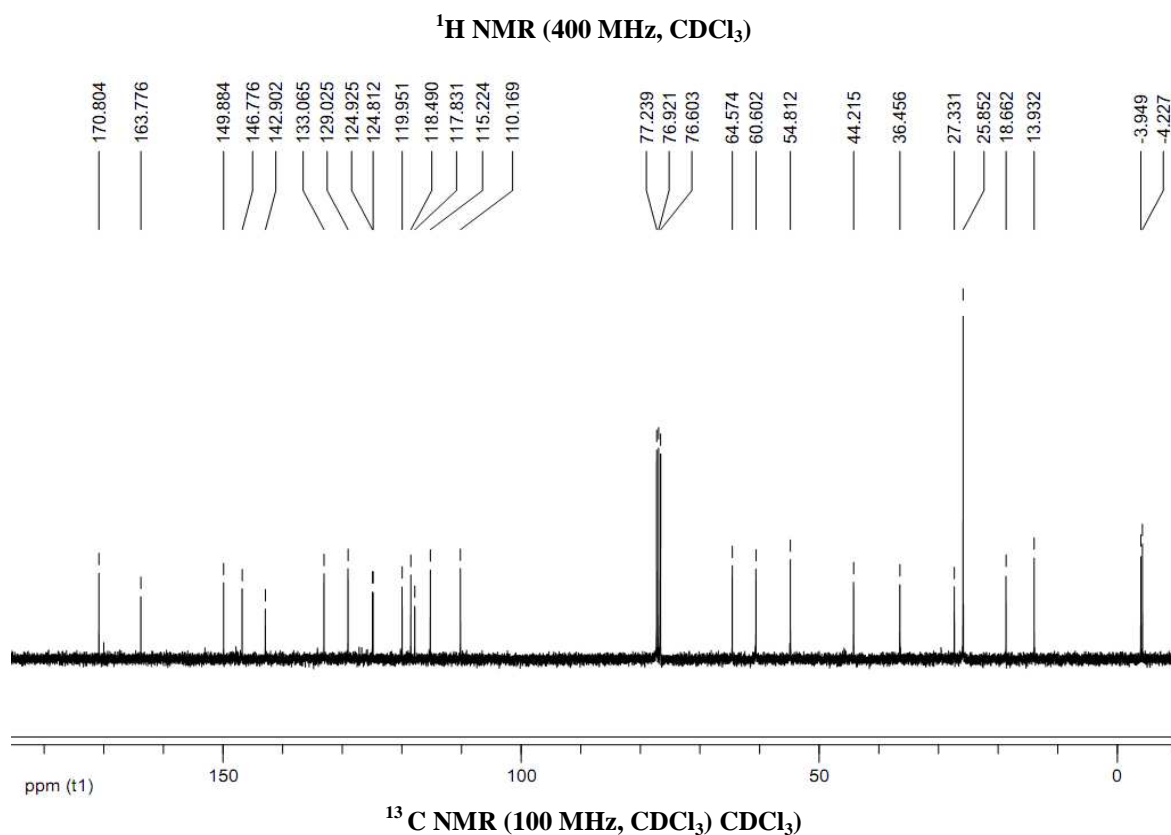
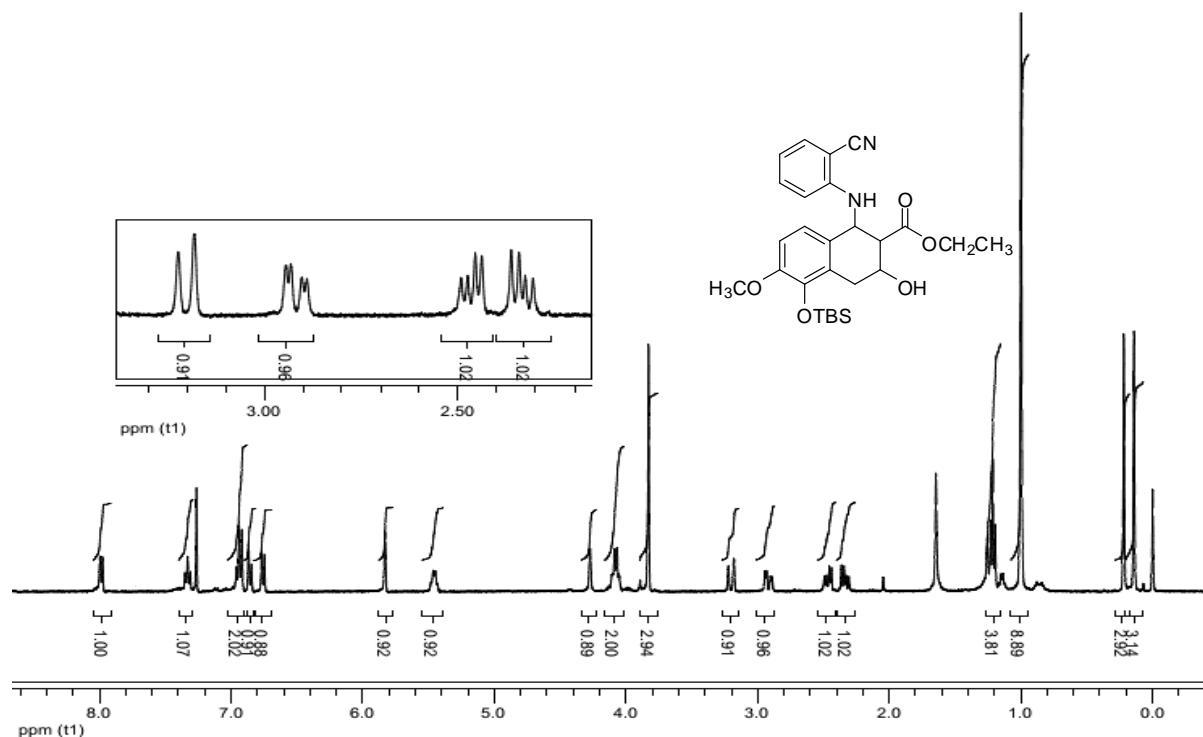
¹H NMR (400 MHz, CDCl₃)¹³C NMR (100 MHz, CDCl₃)

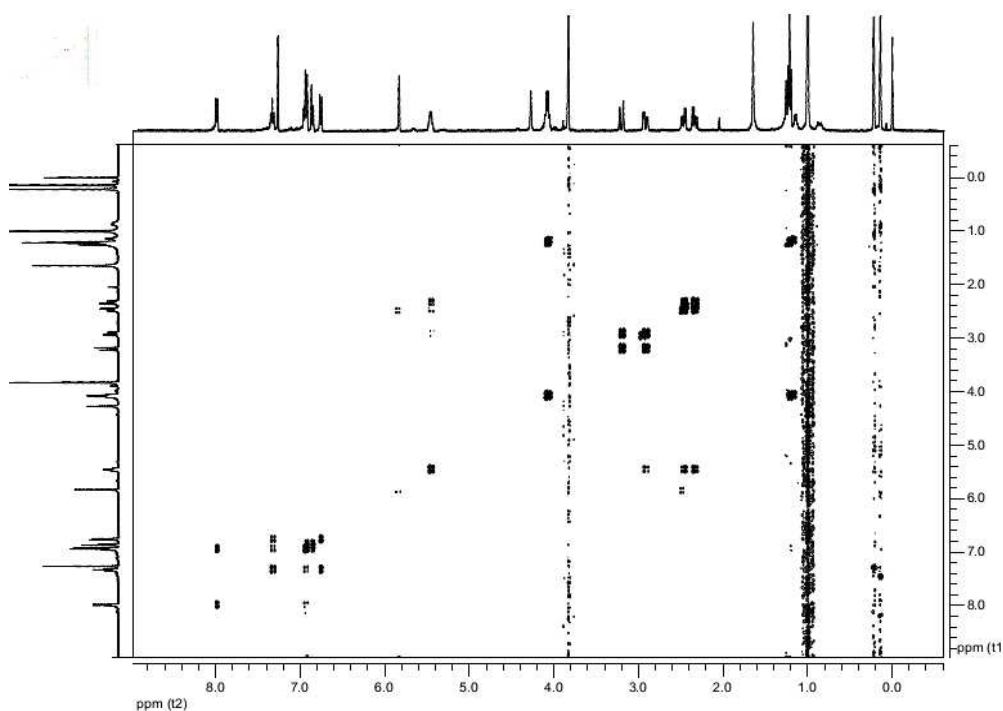
Compound (17c):

¹H NMR (400 MHz, CDCl₃)¹³C NMR (100 MHz, CDCl₃)

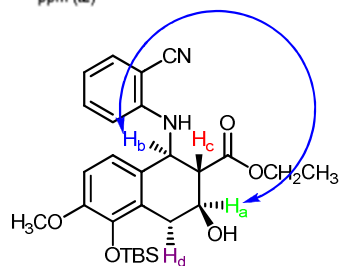
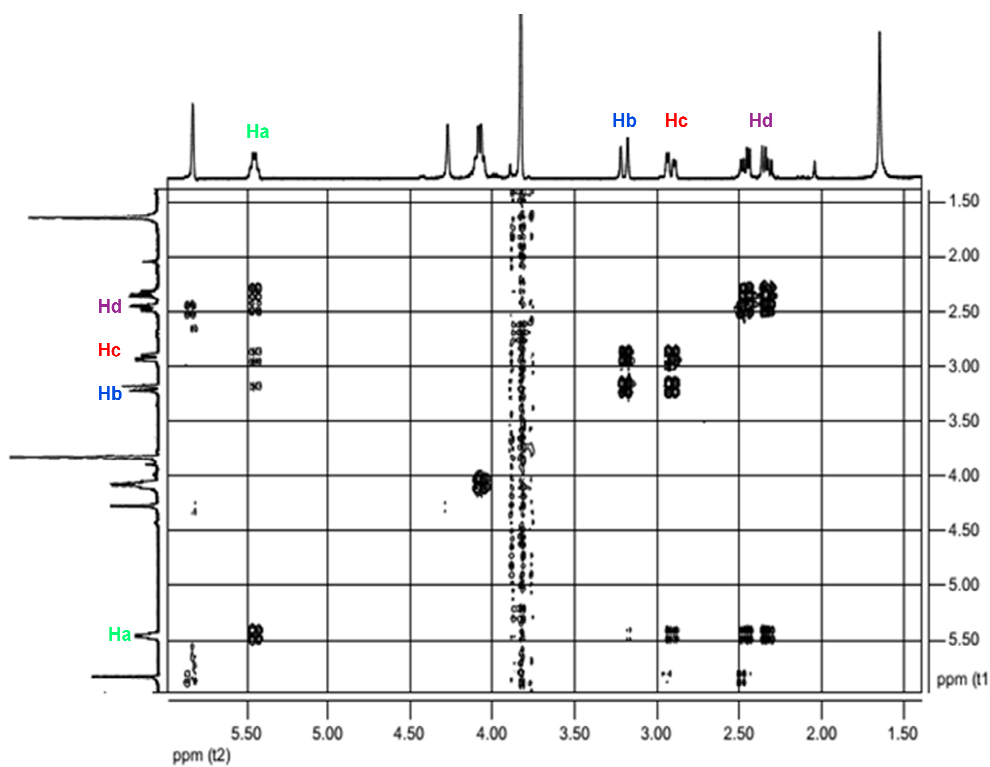
Compound (17d):



Ethyl 5-(*tert*-butyldimethylsilyloxy)-1-(2-cyanophenylamino)-3-hydroxy-6-methoxy-1,2,3,4-tetrahydronaphthalene-2-carboxylate (18):



2D NOESY of Compound 18

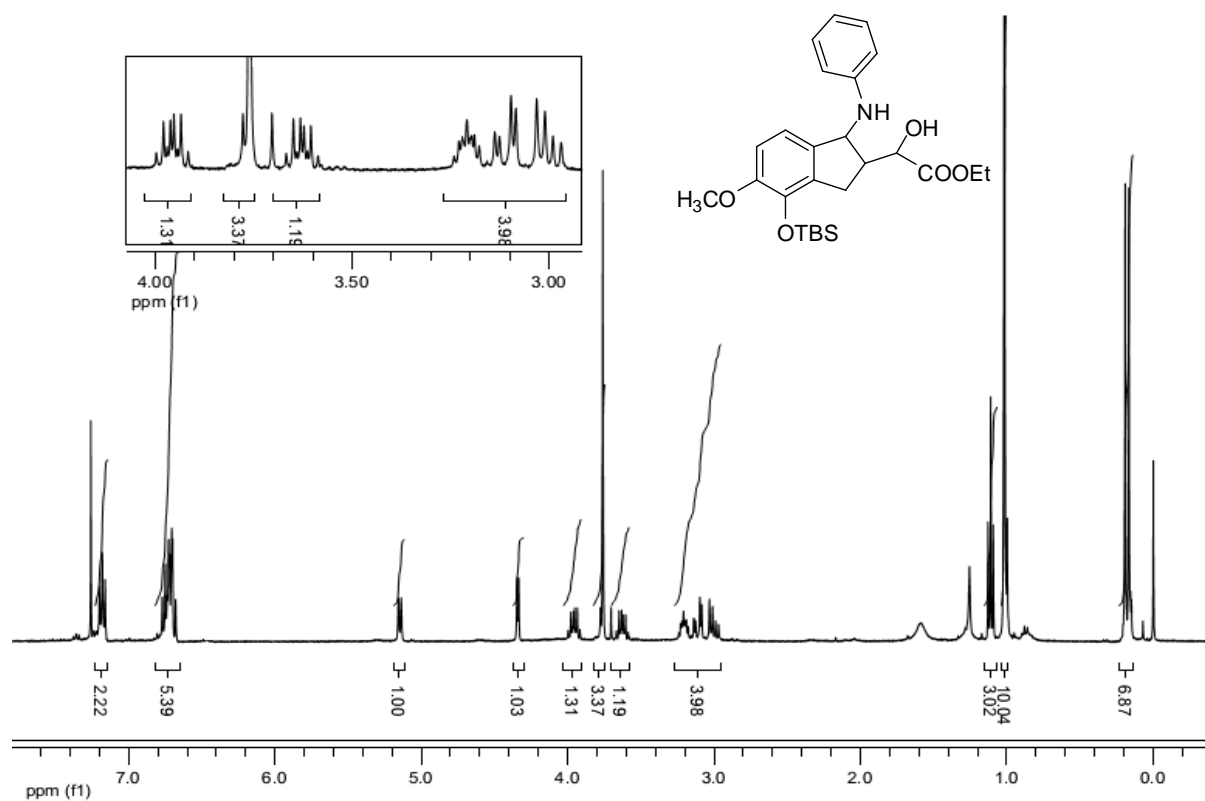


$$J_{ac} = 17.2 \text{ Hz}$$

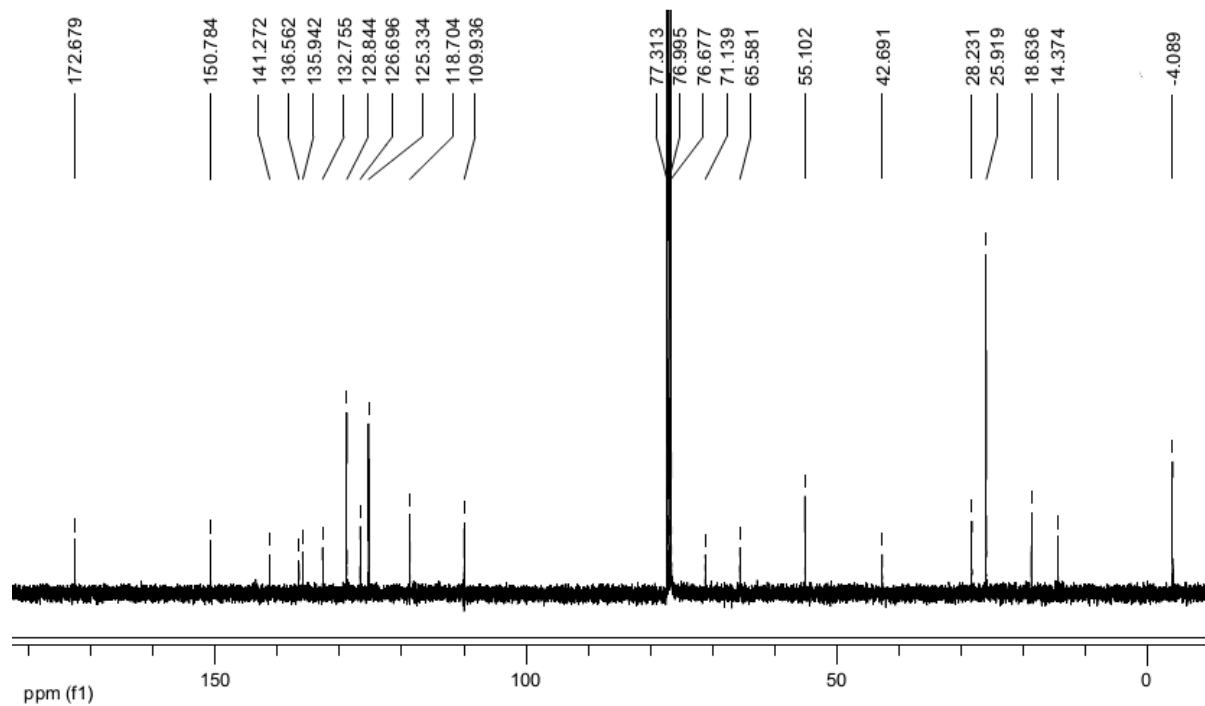
$$J_{bc} = 16.4 \text{ Hz}$$

Expansion of 2D NOESY of Compound 10

Ethyl-2-(4-(*tert*-butyldimethylsilyloxy)-5-methoxy-1-(phenylamino)-2,3-dihydro-1*H*-inden-2-yl)-2-hydroxyacetate (19):

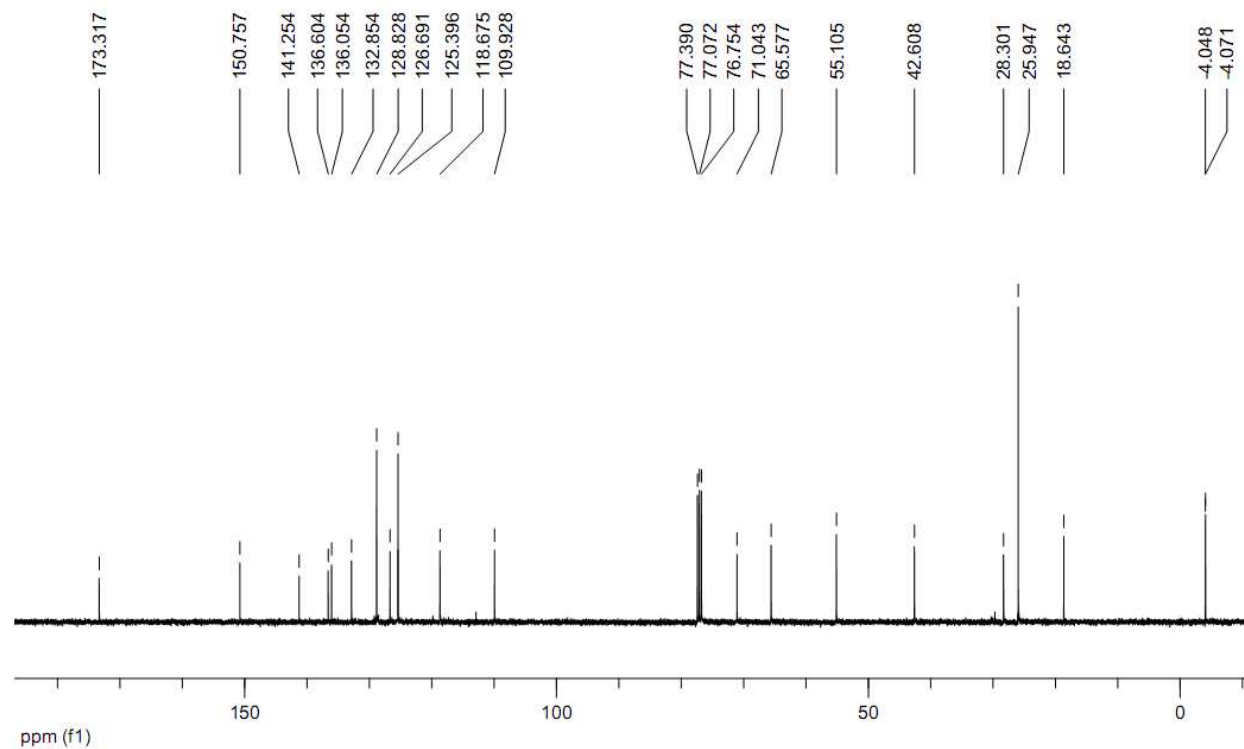
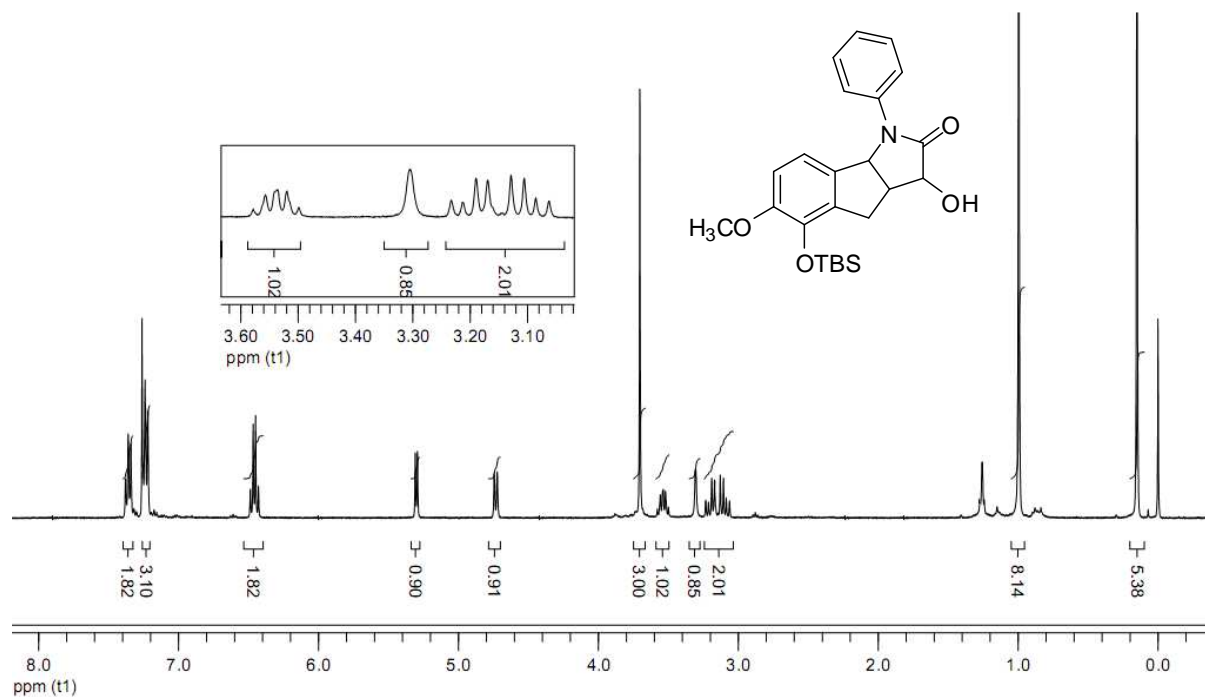


¹H NMR (400 MHz, CDCl₃)

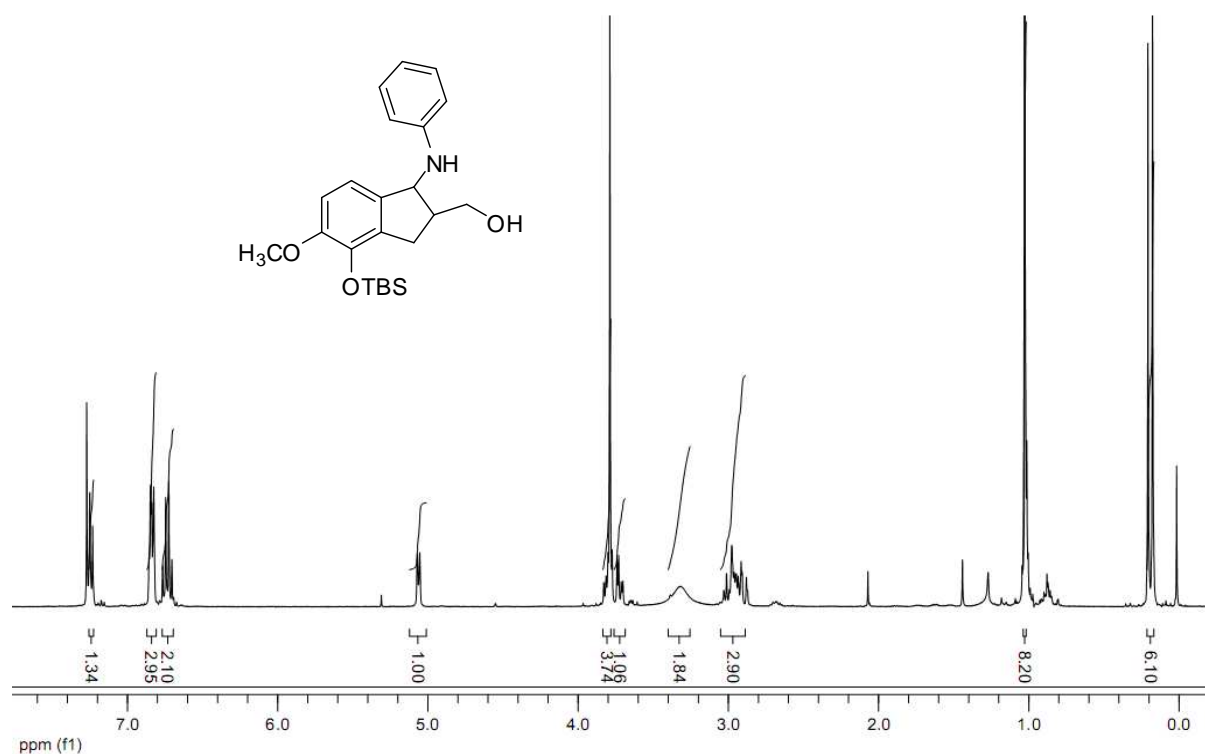


¹³C NMR (100 MHz, CDCl₃)

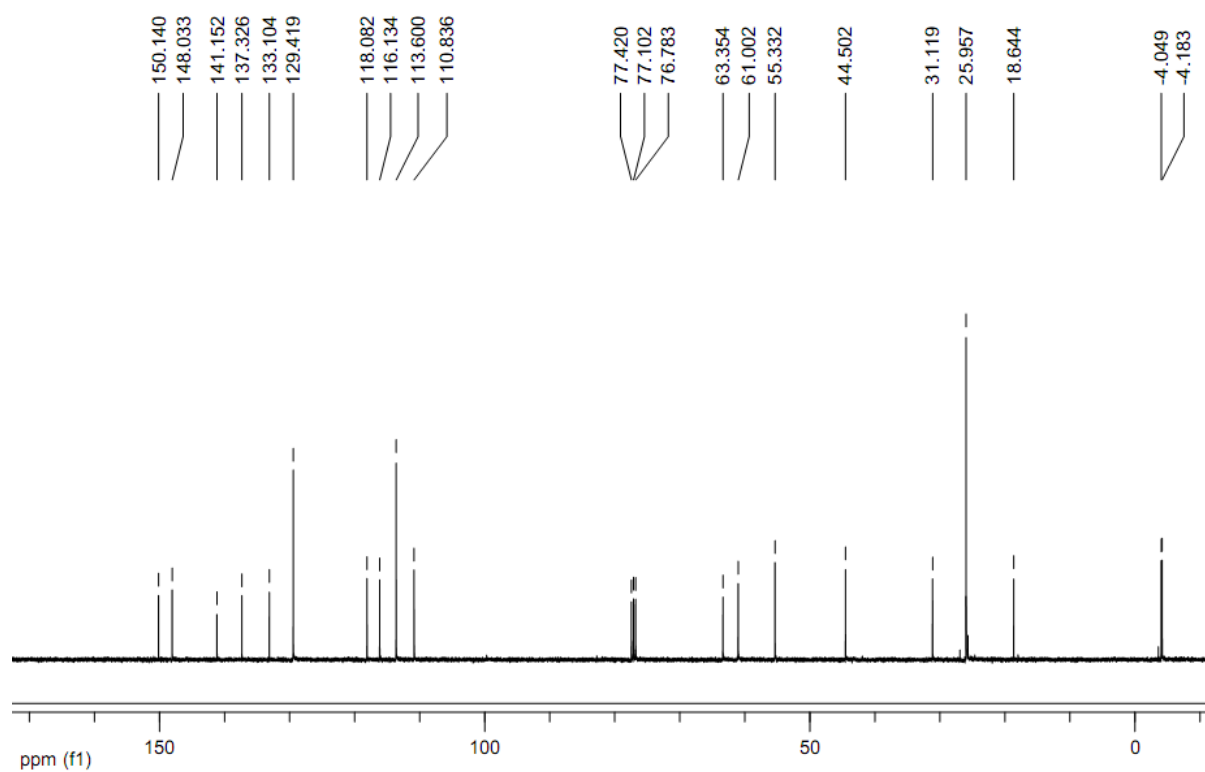
(5-(*tert*-butyldimethylsilyloxy)-3-hydroxy-6-methoxy-1-phenyl-1,3a,4,8b-tetrahydroindeno[1,2-*b*]pyrrol-2(3*H*)-one (20):



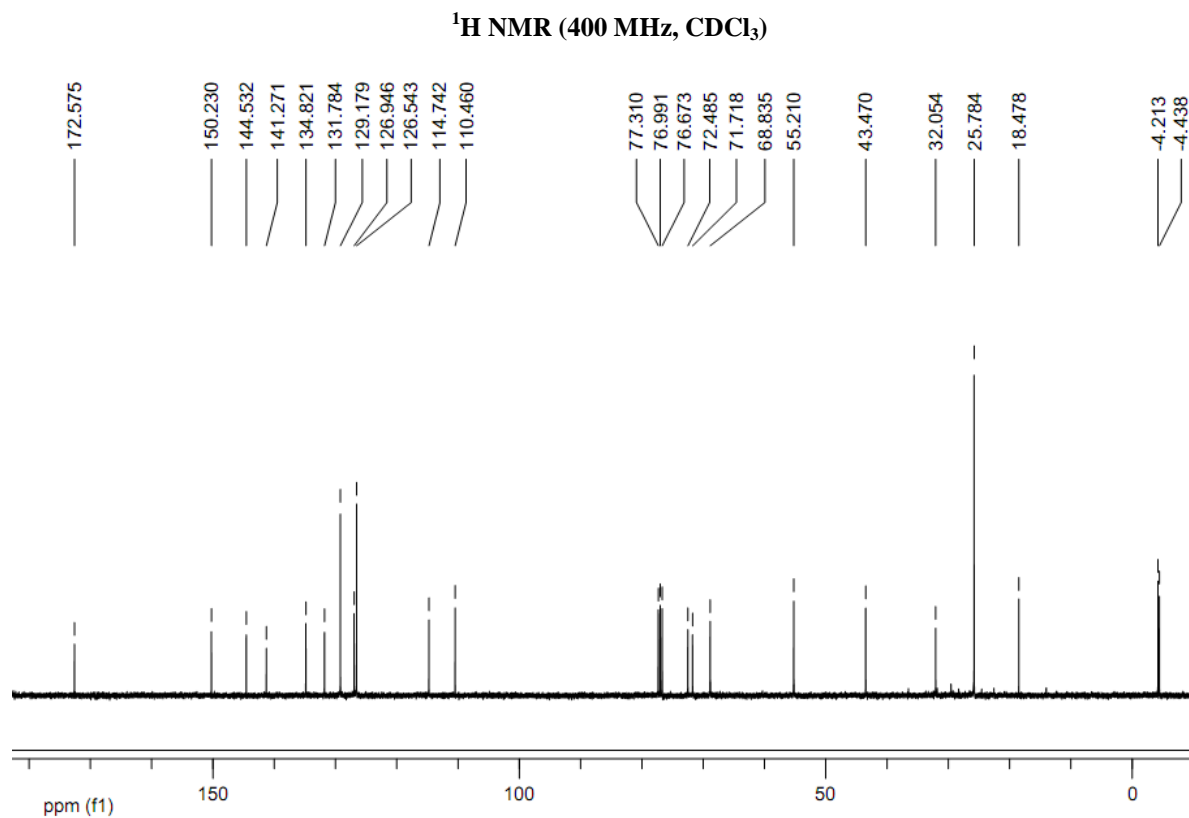
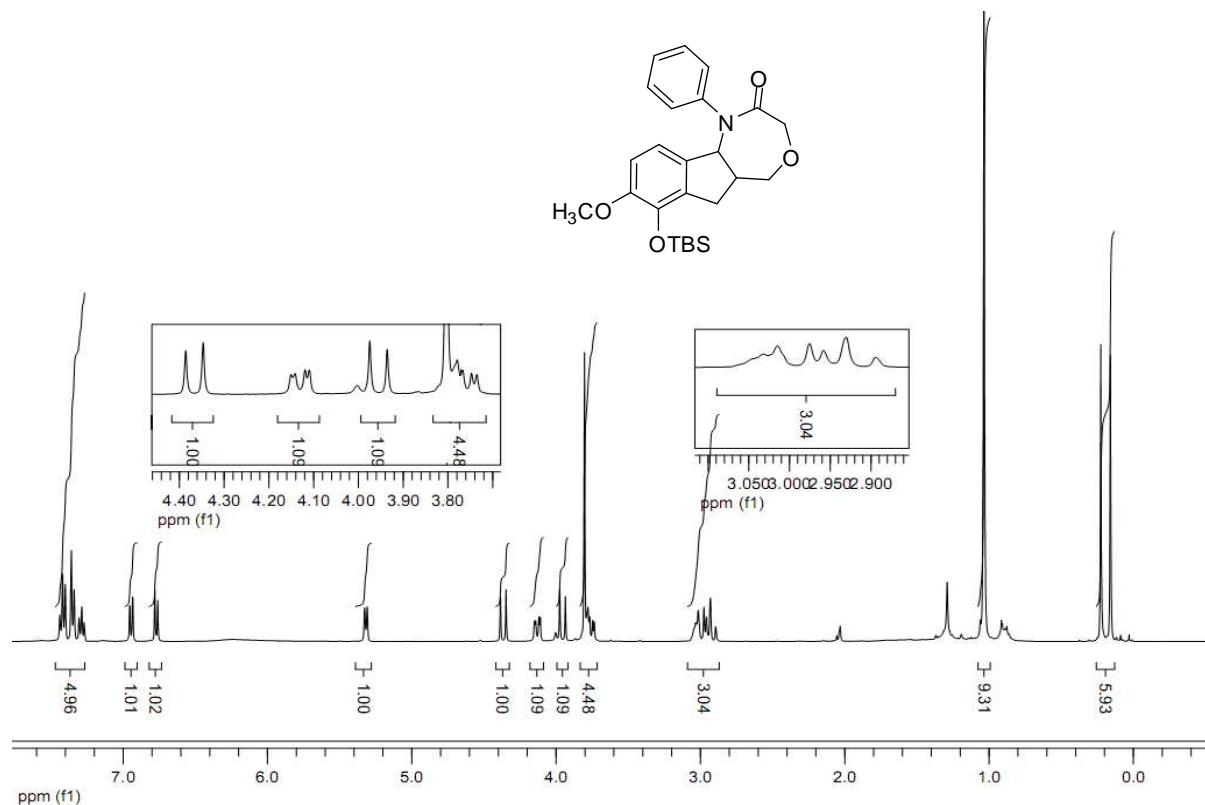
(4-(*tert*-butyldimethylsilyloxy)-5-methoxy-1-(phenylamino)-2,3-dihydro-1*H*-inden-2-yl) methanol (21):



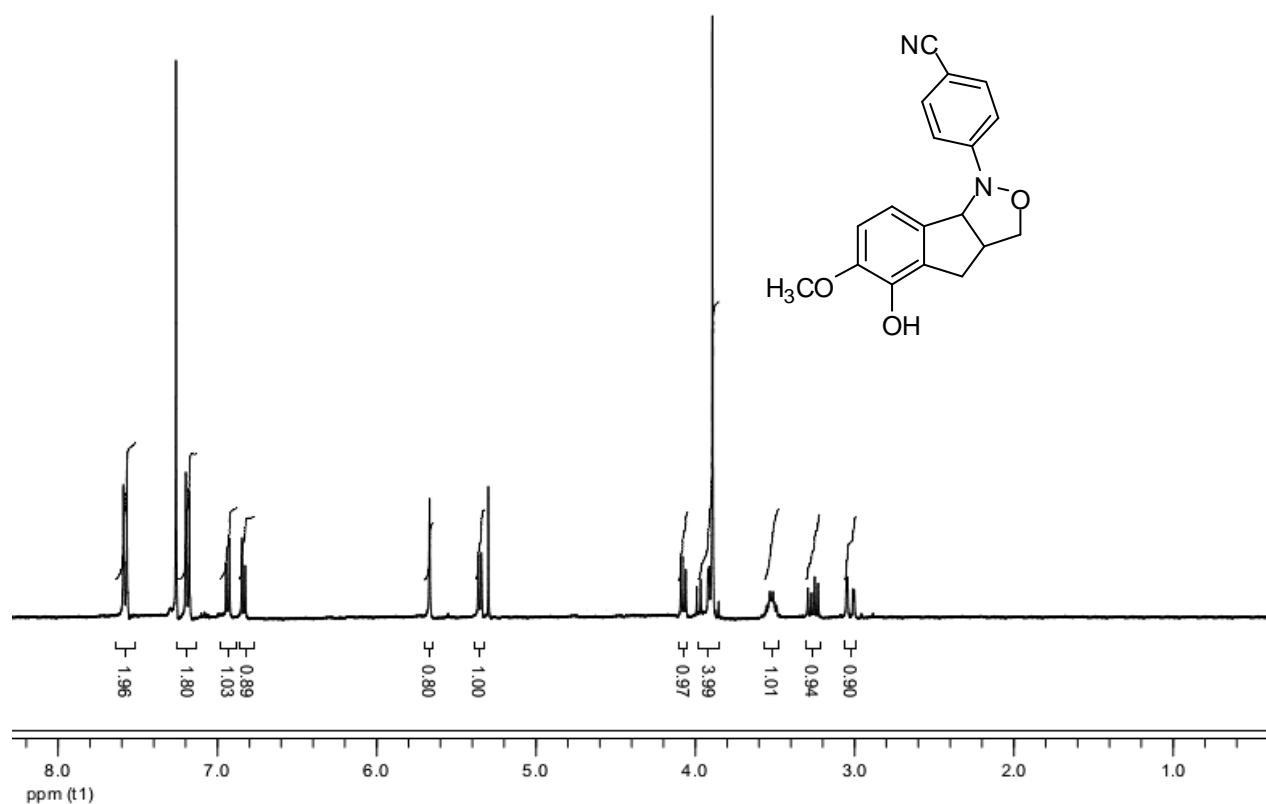
¹H NMR (400 MHz, CDCl₃)



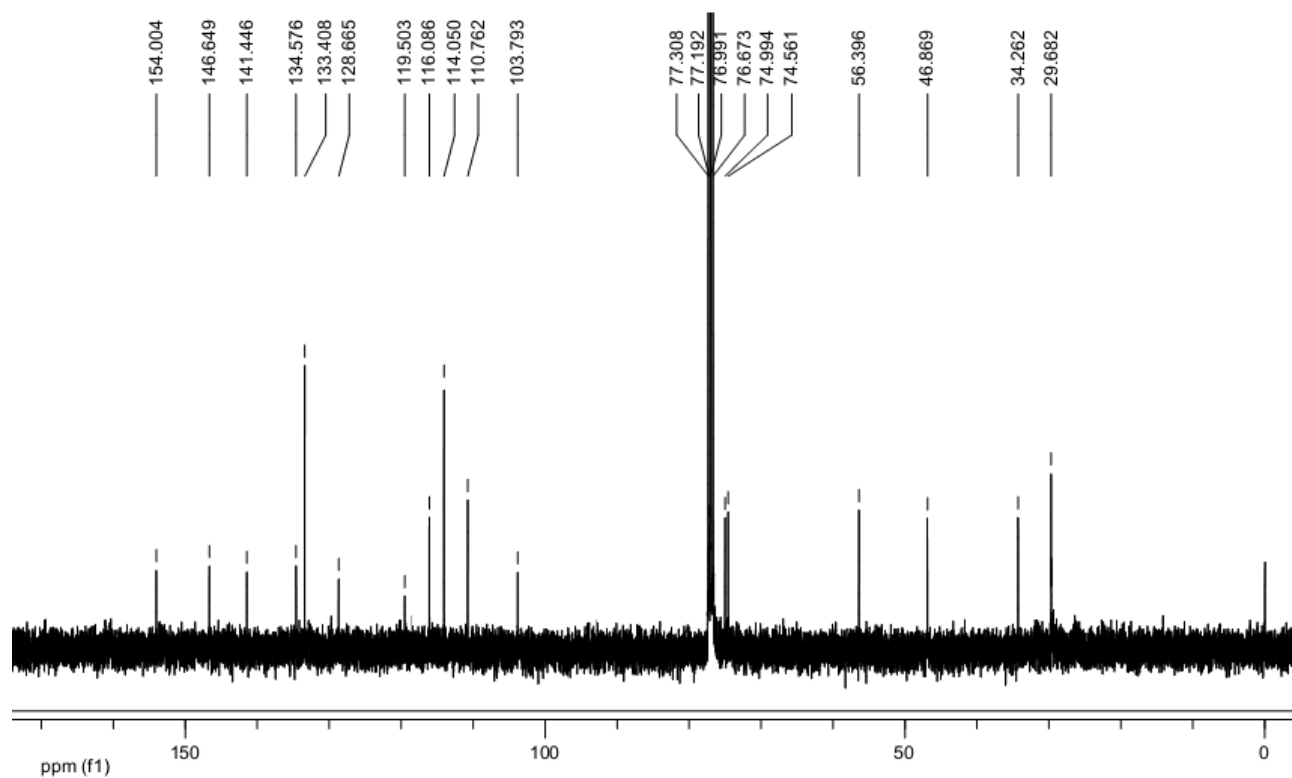
¹³C NMR (100 MHz, CDCl₃)

7-(*tert*-butyldimethylsilyloxy)-8-methoxy-1-phenyl-5,5a,6,10b-tetrahydro-1*H*-indeno[1,2-*e*][1,4]oxazepin-2(3*H*)-one (22):

4-(5-Hydroxy-6-methoxy-3,3a,4,8b-tetrahydro-1H-indeno[1,2-c] isoxazol-1-yl)benzonitrile (23):

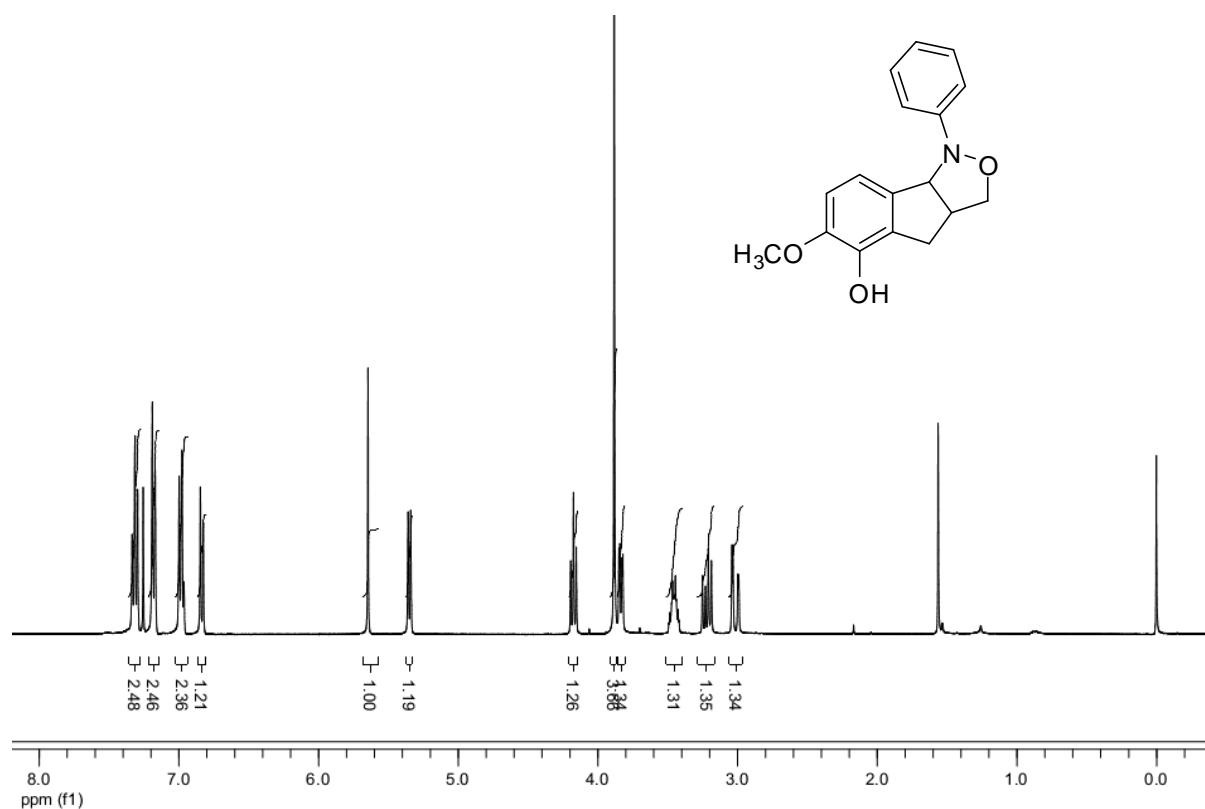
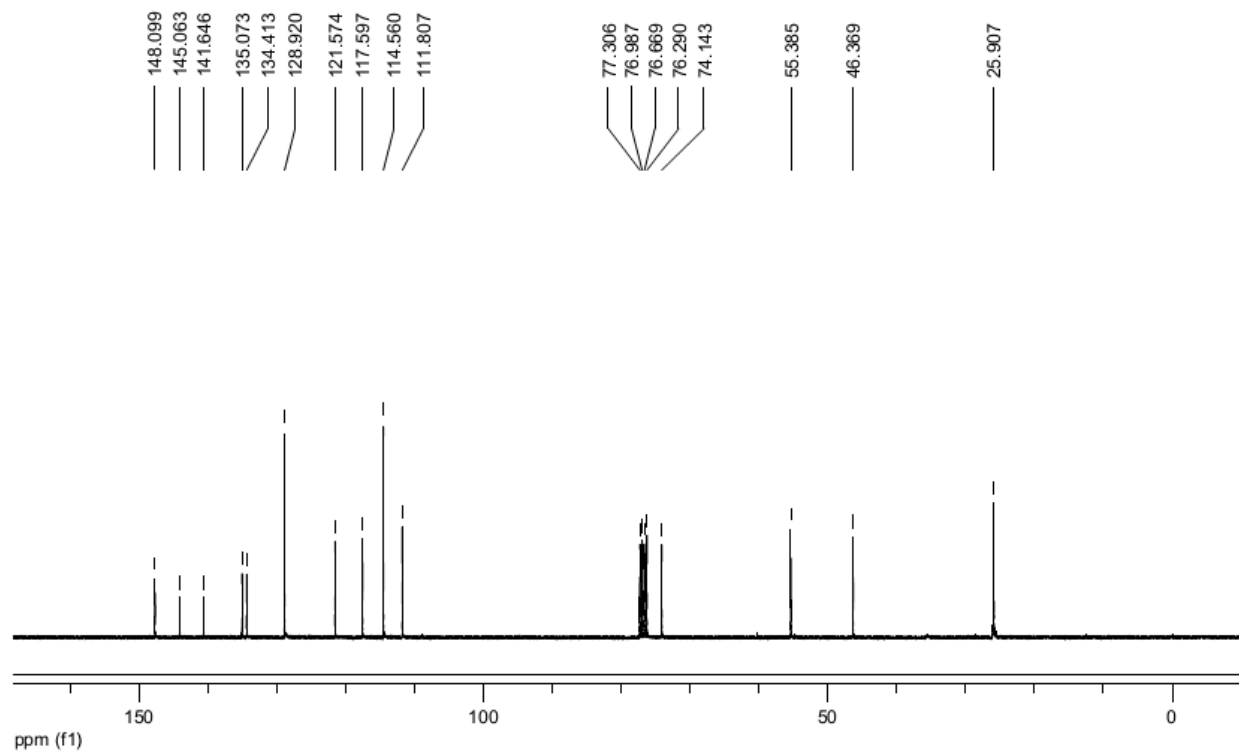


¹H NMR (400 MHz, CDCl₃)

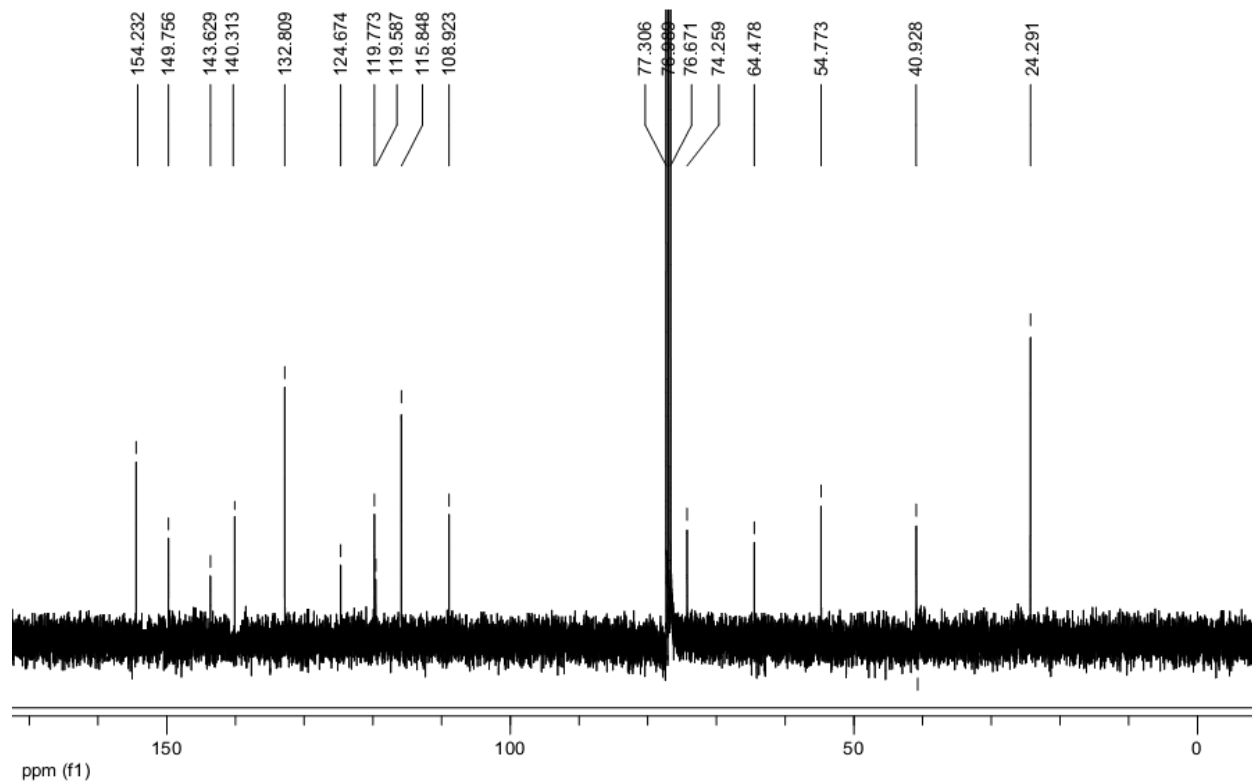
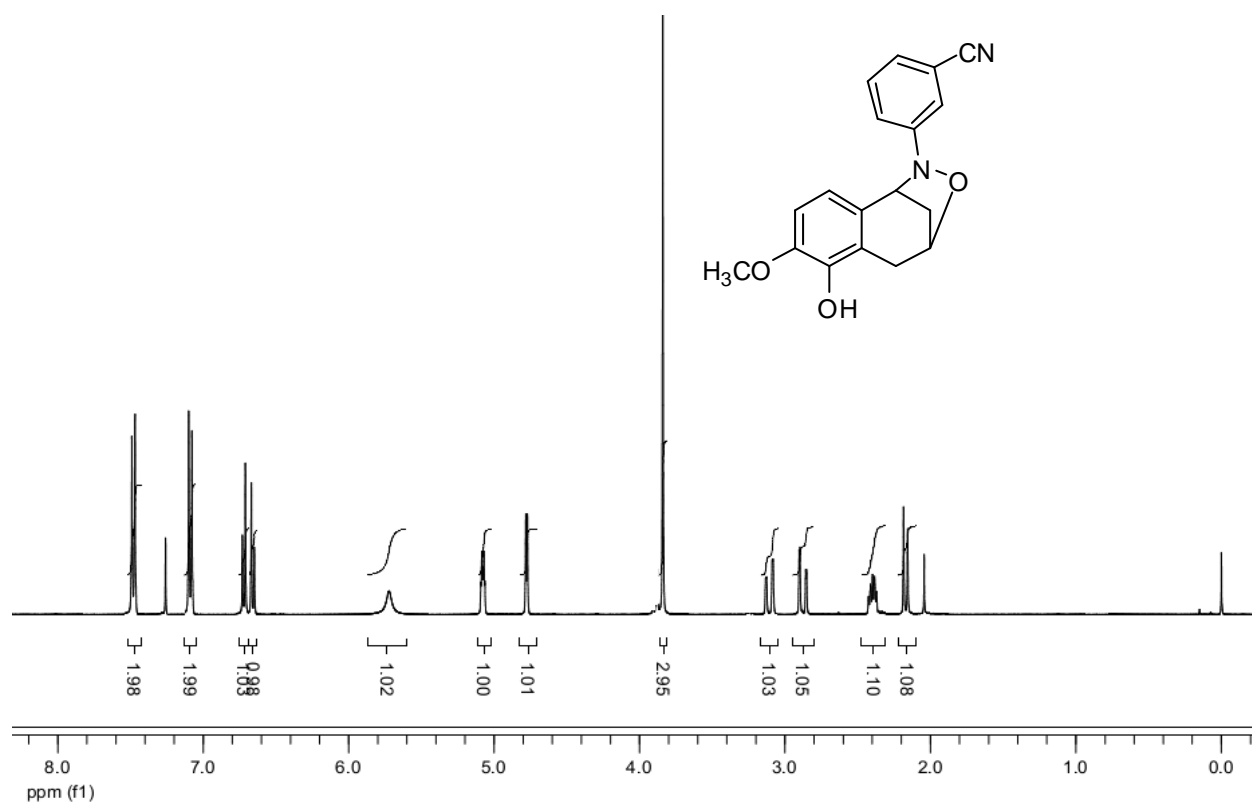


¹³C NMR (100 MHz, CDCl₃)

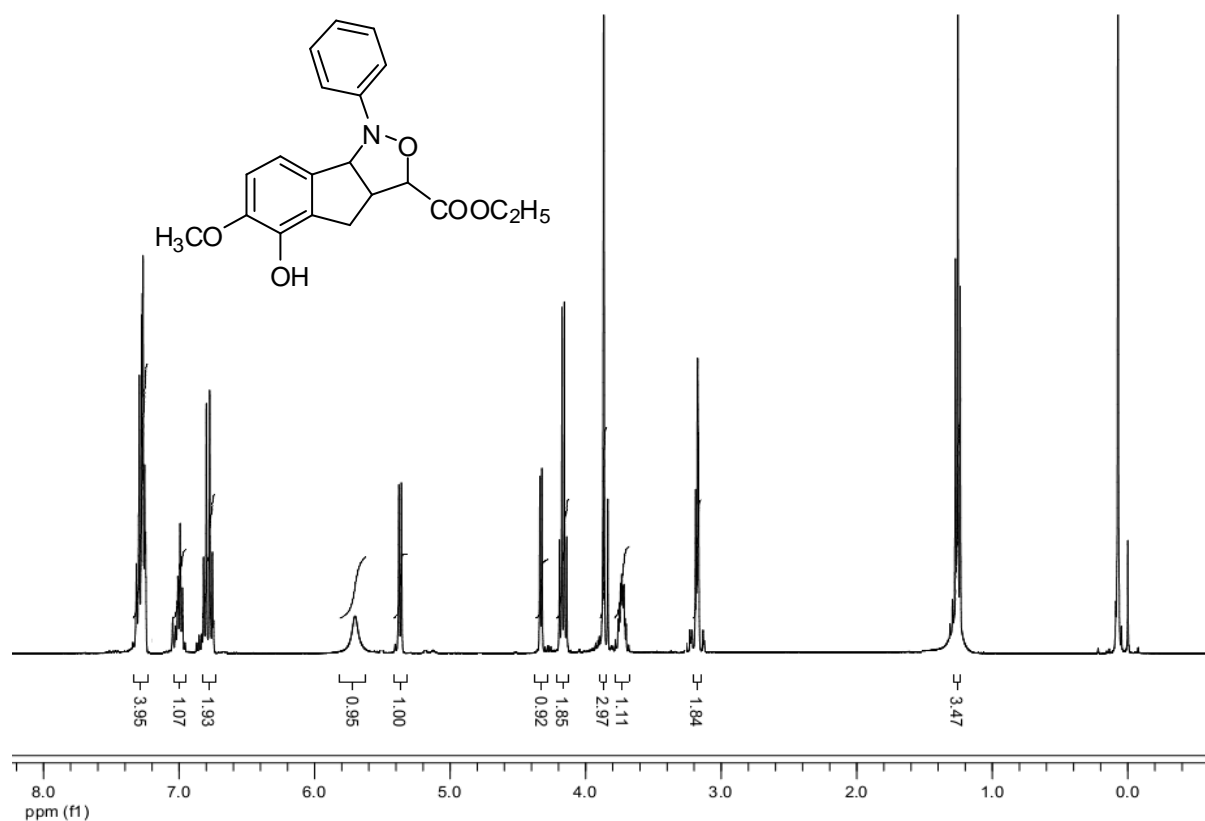
6-Methoxy-1-phenyl-3,3a,4,8b-tetrahydro-1H-indeno[1,2-c]isoxazol-5-ol (24):

¹H NMR (400 MHz, CDCl₃)¹³C NMR (100 MHz, CDCl₃)

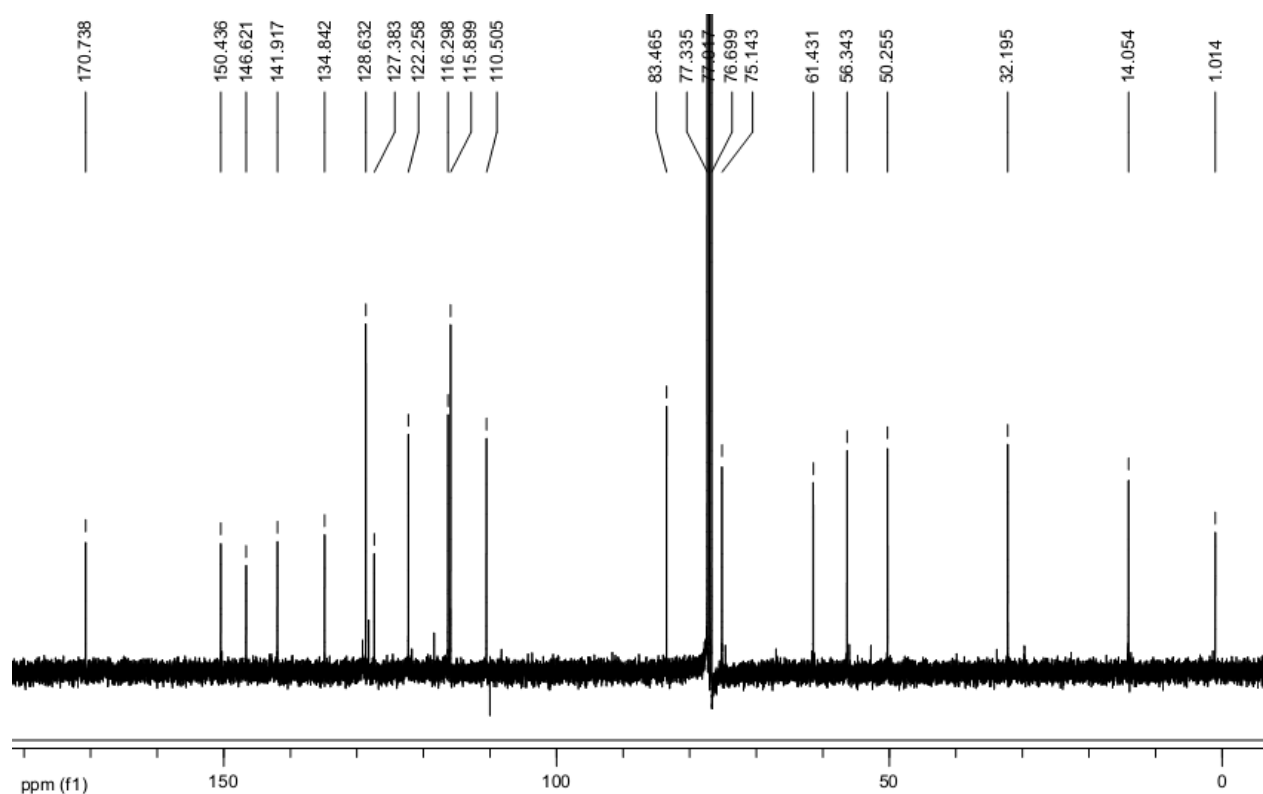
Compound 26:



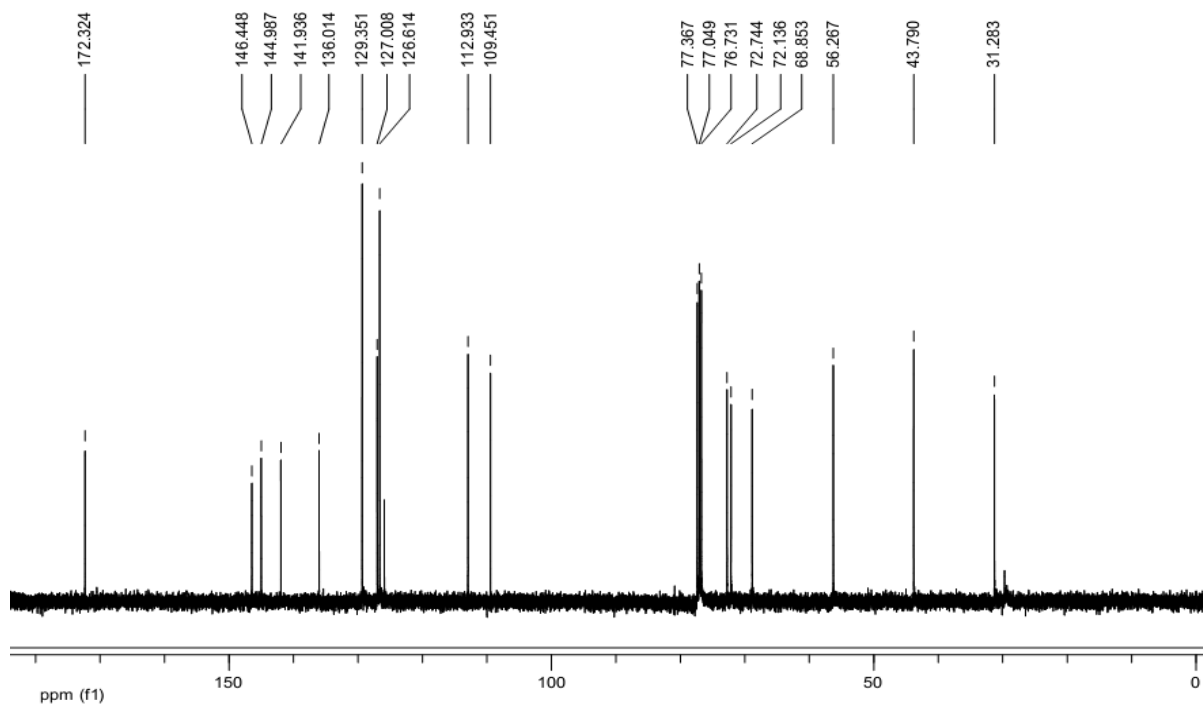
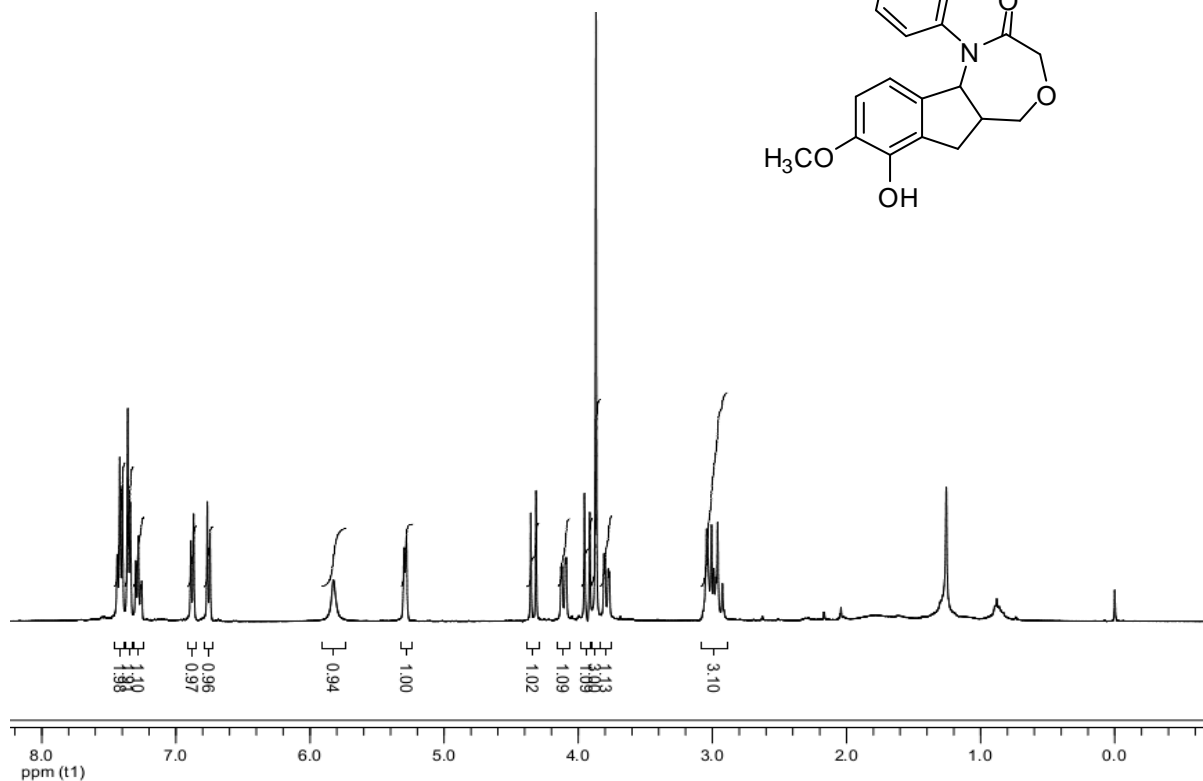
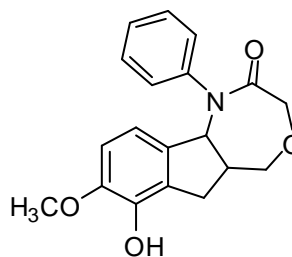
Ethyl 5-hydroxy-6-methoxy-1-phenyl-3,3a,4,8b-tetrahydro-1H-indeno[1,2-c]isoxazole-3-carboxylate (30):



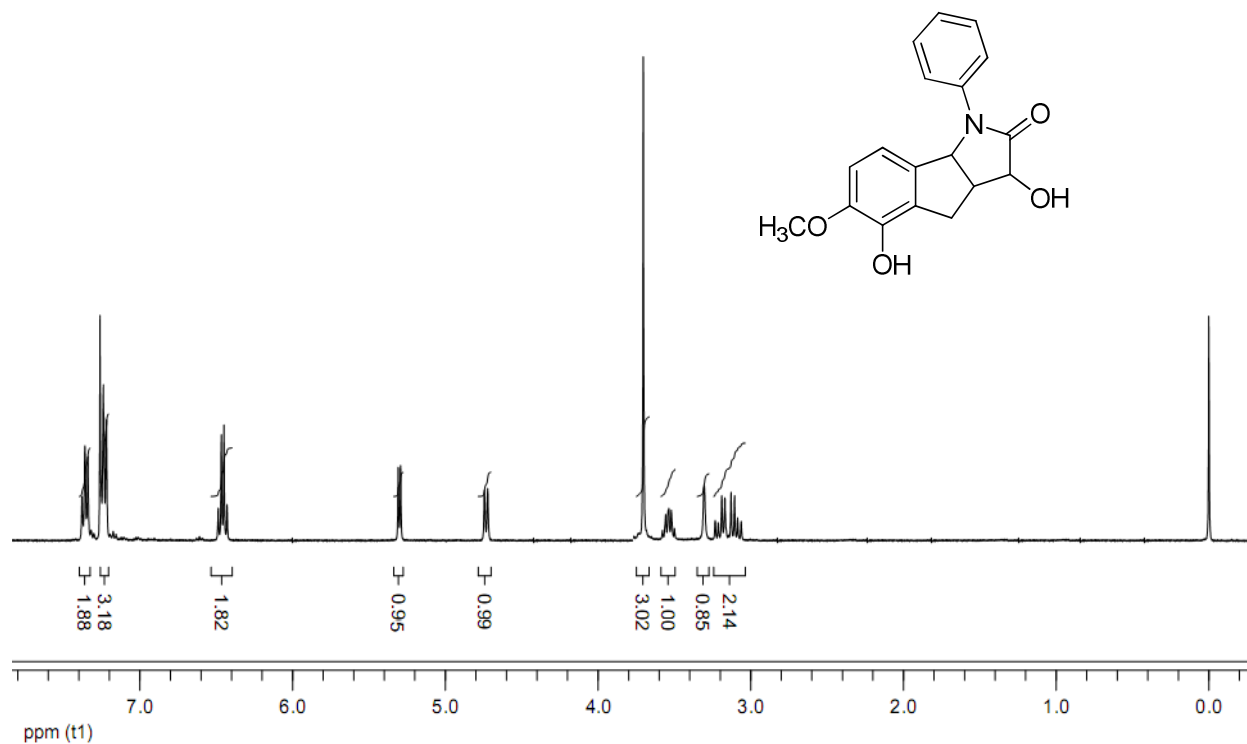
¹H NMR (400 MHz, CDCl₃)



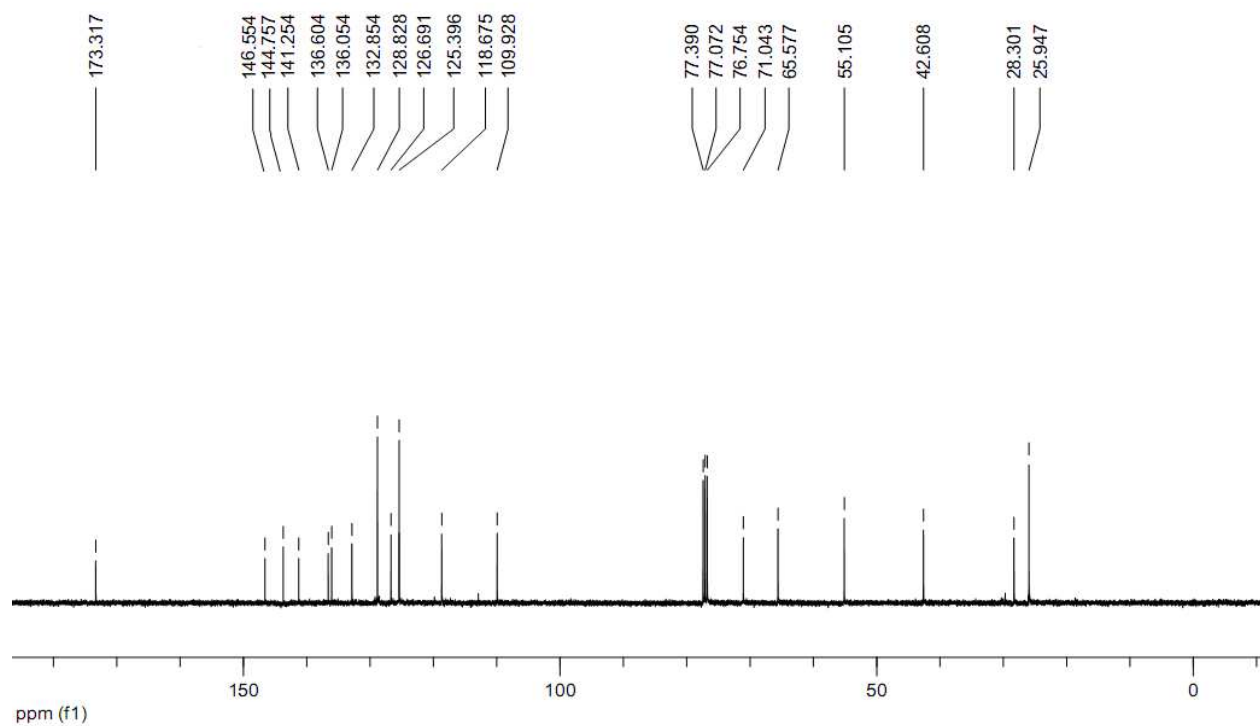
¹³C NMR (100 MHz, CDCl₃)

7-hydroxy-8-methoxy-1-phenyl-5,5a,6,10b-tetrahydro-1*H*-indeno[1,2-*e*][1,4]oxazepin-2(3*H*)-one (34):

3,5-dihydroxy-6-methoxy-1-phenyl-1,3*a*,4,8*b*-tetrahydroindeno[1,2-*b*]pyrrol-2(3*H*)-one
(35):



¹H NMR (400 MHz, CDCl₃)



¹³C NMR (100 MHz, CDCl₃)

BALAKRISHNA DULLA

Senior Research Fellow

Dr. Reddy's Institute of Life Sciences(An Associate Institute of University
of Hyderabad)

University of Hyderabad Campus

Gachibowli, Hyderabad-500 046, India

Contact+91-9885369010/9491838182

Tel: +91-4066571500 (Ext.-630)

E-mail: baludulla@gmail.combalakrishnad@drils.org**ACADEMIC QUALIFICATIONS**

-
- | | |
|---------------------|--|
| 2010 to 2013 | Ph.D. thesis submitted (Medicinal Chemistry, University of Regensburg, Germany)
Supervisor: Prof. Oliver Reiser, Prof. Javed Iqbal, Prof. Javed Iqbal |
| 2005 to 2007 | Master in Organic Chemistry (M. Sc.) (Distinction), Andhra University, India |
| 2002 to 2005 | Bachelor in Chemistry (B. Sc.) (Silver medal), Andhra University, India. |

RESEARCH EXPERIENCE (+5 years)

-
- | | |
|---|----------------------------------|
| ❖ Senior Research fellow | January 2013 to till Date |
| Dr. Reddy's Institute of Life Sciences, I am responsible for | |
| ➤ Synthesis of Fluorescent Saccharide Sensors as Potential Tool for the Diagnosis of Carbohydrate Metabolism Disorders. Project Advisor: Dr. Marina S. Rajadurai (Junior Research Scientist) | |
| ❖ Junior Research fellow | December 2010 to 2012 |
| Dr. Reddy's Institute of Life Sciences, I was responsible for | |
| ➤ Synthesis of Novel Drug-like Scaffolds by Diastereoselective Intra-molecular Aza-Diels-Alder Cyclization based on α -Amino acid and Vanillin Precursors. | |
| ➤ Regioselective Intramolecular 1, 3-dipolar Cycloadditions of Isovanillin derived Nitrones: Transformation into Oxazepine Containing Tricyclic Scaffolds. Project Advisor: Prof. Javed Iqbal (The Director of Dr. Reddy's Institute of Life Sciences) | |

- ❖ **The Indian-German Graduate School (INDIGO) Exchange student (Regensburg, Germany)** **May 2010 to September 2010**
- Design, synthesis and pharmacological evaluation of dehydroshikimic acid analogues as anti-Tuberculosis agents.
Project Advisor: Prof. Oliver Reiser (University of Regensburg, Germany)
- ❖ **Internship at BASF (Ludwigshafen, Germany) November 2010 to December 2010**
- I was responsible for-
- Organic Synthesis in the field of renewable resources
 - Purification of novel compounds
- ❖ **Research Trainee** **January 2008 to April 2010**
- Dr. Reddy's Institute of Life Sciences, University of Hyderabad, Hyderabad, India.
- I worked on followings research projects:
- Synthesis and evaluation of 3-Guanidine Phenyl Oxazole as a novel class of LSD1 inhibitors with anti-proliferative activity *in vitro* and *in vivo*.
Project Advisor: Prof. Javed Iqbal (The Director)
 - Design and synthesis of novel Indanone Indoles with anti cancer activity
 - Developing unique novel methodology for synthesis of Benzoxazole, Benzoimidazole, and Benzothiazole.
Project Advisor: Prof. Manojit Pal (Head of the Medicinal Chemistry)

RESEARCH AREA/INTEREST

- **Synthetic Medicinal Chemistry:** Developing novel chemical entities with interesting biological properties for bioorganic and medicinal chemistry investigations using conventional and modern techniques.
- **Organo catalysis:** Design of novel organo catalysts with stereo specific applications.
- **Total synthesis:** Design of novel strategies for natural products, natural inspired macromolecules

PATENTS

❖ **Novel compounds for cancer treatments.** M. Pal, U. Reddy CH, M. Auleri, **B. Dulla**, J. Iqbal; Indian patent filed in Feb-2011, Application Number: 228/CHE/2011.

PUBLICATIONS**Published:**

1. Construction and functionalization of fused pyridine ring leading to novel compounds as potential antitubercular agents; **Balakrishna Dulla**, Baojie Wan, Scott G. Franzblau, Ravikumar Kapavarapu, Oliver Reiser*, Javed Iqbal*, Manojit Pal*; **Bioorganic & Medicinal Chemistry Letters**, 2012, 22, 4629-4635. (DOI:10.1016/j.bmcl.2012.05.096).
2. Pd/C-mediated Alkynylation of Indazoles: Synthesis and Pharmacological Evaluation of Mono and Dialkynyl-substituted Indazoles; D. R. Gorja, K. Shiva Kumar, **B. Dulla**, K. Mukkanti and M. Pal; **Journal of Heterocyclic Chem**, 00, 00, (2012). (DOI: 10.1002/jhet.1602).
3. Novel synthesis of 2H-benzo[b] [1, 4] oxazines from 2, 5 dihydroxy benzaldehyde and Aminoacid precursors; Javed Iqbal*, Neelima Tangellamudi*, **Balakrishna Dulla**, Balasubrahmanyam; **Organic Letters**. 2012, Vol. 14, No. 2, 552-555.(DOI: 10.1021/ol203174).
4. Synthesis and Pharmacological evolution of novel 3- guanidine phenyl oxazoles as LSD1 protein inhibitors for the potential treatment of Cancer; **Balakrishna Dulla**, Vandana Rathore, Girdhar Singh Deora, Krishna Tulasi, Kiranam Chetti, Oliver Reiser*, Javed Iqbal*, Manojit Pal*; **Organic & Biomolecular Chemistry**, 2013, 11,3103. (DOI: 10.1039/c3ob40217g).
5. Amberlyst-15 Catalyzed synthesis of 2-substituted 1, 3-benzazoles in water under ultrasound. Rambabu Dandela, **Balakrishna Dulla**, P. Radha Krishna Murthi, M. V. Basaveswara Rao, Manojit Pal^{a,*} **Synthetic Communications**, 2013, (DOI:10.1080/00397911.2013.769605).
6. Catalyst / surfactant free chemoselective acylation of amines in water. **Balakrishna Dulla**, S. Vijayavardhini, D. Rambabu, V. Radha, M. V. Basaveswara Rao, Manojit Pal*; **Current Green Chemistry** (Accepted).

Under communication:

7. Isovanillin derived *N*-(un)substituted hydroxylamines possessing an *ortho*-allylic group: valuable precursors to bioactive *N*-heterocycles; **Balakrishna Dulla**, Neelima D. Tangellamudi, Sridhar Balasubramanian, Swapna Yellanki, Raghavender Medishetti, Pushkar Kulkarni,* Javed Iqbal,^a* Oliver Reiser,* and Manojit Pal*; **Chemical Communications** (Manuscript submitted).
8. Pd/C-mediated Alkynylation of 5, 6-dimethoxy-2-(prop-2-ynyl)-2, 3-dihydro-1H-inden-1-one: Synthesis and Pharmacological Evaluation of Mono and Dialkynyl-substituted 5,6-dimethoxy-2-(prop-2-ynyl)-2,3-dihydro-1H-inden-1-one; **Balakrishna Dulla**, Upendar Reddy. Ch, Manojit Pal*; **Beilstein Journal of Organic Chemistry** (Manuscript submitted).
9. Organic Nano-Vesicular Cargoes for Drug Delivery: Synthesis, Self-assembly, Controlling Vesicles Fusion and Terfenadine Loading/Release Studies; Ajay Kumar Botcha, **Balakrishna Dulla**, E. Ramanjaneya Reddy, Pushkar Kulkarni* Rajadurai Chandrasekar* and Marina S. Rajadurai*; **Angewandte Chemie International Edition** (Manuscript submitted)

CONFERENCES

1. **Oral presentation** on “Novel synthesis of 2*H*-benzo[*b*][1,4]oxazines from 2,5 dihydroxy benzaldehyde and Aminoacid precursors”. 3rd INDIGO Ph.D. Research Conference and Intensive Course "Sustainable chemistry", conducted by IIT Madras, Chennai, India, February 12-16, 2012.
2. Catalyst 2011- Dr. Reddy' Chemistry Conclave (International year of Chemistry), December 16-17, 2011.
3. **Oral presentation** on “Synthesis of dehydroshikimic acid analogues as novel anti-tuberculosis”. 2nd INDIGO Ph.D Research Conference and Intensive Course "Sustainable chemistry" conducted in Donaustauf near Regensburg / Germany, October 3-6, 2010.
4. The Summer School “Medicinal Chemistry” GRK 760, Regensburg, Germany, 2010

AWARDS AND FELLOWSHIPS

- Awarded “**Junior Research Fellowship**” (2010) by DST, Council for Scientific and Industrial Research (CSIR), Govt. of India.
- Summer semester 2010, “**Organic chemistry Modern Synthetic Methods**” (6. sem) (53162, 4 st.)- Secured 4.0 points, conducted by University of Regensburg, Germany.

- **INDIGO Graduate Program Fellowship** by the Indian-German Graduate School (INDIGO) for "Advanced Organic Synthesis for a Sustainable Future (Regensburg, Germany 2010).
- **GATE** (2011): 90.00 Percentile, awarded by I.I.T's and IISC
- **CSIR-NET** (2011): 0043/0970 rank in Chemical Sciences conducted by CSIR, Govt. of India
- **Gold Medal:** Master of Sciences with 78.66 % in Organic Chemistry, Rajah R.S.R.K. Ranga Rao P.G College, Andhra University, India
- **Silver Medal:** Bachelor of Sciences with 71.00 % in Chemistry, Sri. G. C. S. R Degree College, Andhra University, India

REFERENCES

Prof. Dr. Oliver Reiser

Institute of Organic Chemistry
University of Regensburg
Universitätsstr. 31, Room: CH 33.1.80
D-93053 Regensburg, Germany
E-mail: Oliver.Reiser@chemie.uni-regensburg.de
Phone +49 941 943-4631
Fax +49 941 943-4121

Prof. Dr Javed Iqbal

The Director
Dr. Reddy's Institute of Life Sciences
(An associated Institute of University of Hyderabad)
Gachibowli, Hyderabad
Andhrapradesh- 500046, India
Email: JIqbal@drils.org
Phone: +91 40 66571571

Prof. Dr. Manojit Pal

Head Organic and Medicinal Chemistry
Dr. Reddy's Institute of Life Sciences
(An associated Institute of University of Hyderabad)
Gachibowli, Hyderabad
Andhrapradesh- 500046, India
Email: manojitp@drils.org
Phone: +91 40 66571633

Acknowledgements

It's an immense pleasure to express my sincere heartfelt gratitude to my research supervisors Prof. Dr. Oliver Reiser, Prof. Dr. Javed Iqbal who gave an golden opportunity to pursue my Ph D in University of Regensburg, and for introducing me to INDIGO programme. Their constant encouragement, constructive criticisms and valuable suggestions made me to inspire to grow as a good research chemist.

I deeply acknowledge Prof. Dr. Manojit Pal, Dr Reddy's Institute of Life Sciences, University of Hyderabad for his excellent teaching and the opportunities and exceptional support he provided during my research, thesis writing, and corrections and also for being my inspiration of kindness.

I warmly thank Prof. Dr. Joachim Wegener and Prof. Dr. Javed Iqbal being the doctoral committee members and referring my thesis. I thank Prof. Dr. Robert Wolf for being Chairman in my PhD defence.

My sincere thanks to Dr. Peter Kreitmeier for his great support in ordering chemicals technical supports, etc. I would like to thank Dr. Petra Hilgers. I would like to thank Mrs. Rotermund, Ms. Ohli and Ms. Antje Weigert for helping me in official work.

I am very thankful to DR. Reddy's Institute of Life Sciences, University of Regensburg for the infrastructure. I am very grateful to DAAD (German Academic Exchange Service) and DST (Department of Science and Technology) for the financial assistance throughout my Ph.D. tenure.

I thank Dr. Neelima Tangellamudi, Dr. Marina Rajadurai for their continuous encouragement to achieve my research goals.

I am very thankful to complete analytical department of University of Regensburg for recording NMR, elemental analysis and X-Ray studies of my compounds. Special thanks to Sridhar Balasubramanian (IICT Hyderabad, India) for his valuable X-Ray studies.

I thank all of my lab colleagues and members of Reiser group for creating homely atmosphere inside and outside the lab. My special thank to Deepak, Tapan, Senthil, Tamil Selvi for their help during my stay in Regensburg. I also thank Dr. Soumita Mukherjee from Prof. Manojit Pal group for her suggestions during my thesis writing. I specially thank all my

Acknowledgements

Indian friends and Germany friends I have met during my PhD. We had nice discussions regarding chemistry and also had fun. To name few of them Ramesh, Ananta, Suva, Sudipta, Mouchumi, Sunil, Julian Bodensteiner, Quirin Kainz, Paul Khols, Allan Patric Macabeo, Victor Kais, Andy, Lalith Kumar, Narendar Reddy, Bhanu Das, Madhu, Ramu, Ratnam, Deva, Giridhar, Vandhana.

I warmly thank Prof. Scott G. Franzblau (Institute for Tuberculosis Research, College of Pharmacy, and University of Illinois at Chicago), Dr. Kishore Parsa, Dr Kiranam Chetti, Dr. Pushkar (Dr Reddy's Institute of Life Sciences) for assisting me in getting pharmacology results.

My special thanks from bottom part of my heart to my dearest friends RAMAKRISHNA MANNEPURI, RAVINDHRA CHINTHA, RAJA SEKHAR YETCHANA and DURGA PRASAD HARI for their endless support regarding my thesis submission and defence.

My thesis work wouldn't have been possible without the strong support of my parents (D. Appala Naidu, D.Triveni) and my lovely sisters (Krishnaveni, Nagamani, Krishna Kumari) and family members given by god (Kittu, Amma and family). Where I am today is due to their sacrifices and I can't acknowledge them just in one phrase for their affection.

Declaration

Herewith I declare that current thesis is a presentation of my original work single-handed. Wherever contributions from others are involved, all of them are made to indicate clearly, with due reference to the literature, licence and acknowledgement of collaborative research and discussions.

Regensburg,

BALAKRISHNA DULLA